

FOR FORTIFIED TOWN



12
act

HLH DRIVE SYSTEM

Boeing Vertol Company
P.O. Box 16858
Philadelphia, Pa. 19142

September 1977

Final Report

Approved for public release;
distribution unlimited.



Prepared for

U. S. ARMY AVIATION RESEARCH AND DEVELOPMENT COMMAND
P.O. Box 209
St. Louis, Mo. 63166

APPLIED TECHNOLOGY LABORATORY
U. S. ARMY RESEARCH AND TECHNOLOGY LABORATORIES (AVRADCOM)
Fort Eustis, Va. 23604

Reproduced From
Best Available Copy

AD A 054024

DDC FILE 6068

APPLIED TECHNOLOGY LABORATORY POSITION STATEMENT

Due to the termination of the HLH program, reports summarizing the strides made in many of the supporting technology programs were never published. In an effort to make as much of this information available as possible, selected draft reports prepared under contract prior to termination have been edited and converted to the DOD format by the Applied Technology Laboratory. The reader will find many instances of poor legibility in drawings and charts which could not, due to the funding and manpower constraints, be redone. It is felt, however, that some benefit will be derived from their inclusion and that where essential details are missing, sufficient information exists to allow the direction of specific questions to the contractor and/or the U.S. Army.

DISCLAIMERS

The findings in this report are not to be construed as an official Department of the Army position unless so designated by other authorized documents.

When Government drawings, specifications, or other data are used for any purpose other than in connection with a definitely related Government procurement operation, the United States Government thereby incurs no responsibility nor any obligation whatsoever; and the fact that the Government may have formulated, furnished, or in any way supplied the said drawings, specifications, or other data is not to be regarded by implication or otherwise as in any manner licensing the holder or any other person or corporation, or conveying any rights or permission, to manufacture, use, or sell any patented invention that may in any way be related thereto.

Trade names cited in this report do not constitute an official endorsement or approval of the use of such commercial hardware or software.

DISPOSITION INSTRUCTIONS

Destroy this report when no longer needed. Do not return it to the originator.

REPORT DOCUMENTATION PAGE		READ INSTRUCTIONS BEFORE COMPLETING FORM
1. REPORT NUMBER USAAMRDI-TR-77-38	2. GOVT ACCESSION NO.	3. RECIPIENT'S CATALOG NUMBER
4. TITLE (and Subtitle) HLH DRIVE SYSTEM	5. TYPE OF REPORT & PERIOD COVERED Final Report	6. PERFORMING ORG. REPORT NUMBER
7. AUTHOR(s) J. C. Mack	8. CONTRACT OR GRANT NUMBER(s) DAAJ01-71-C-0840 (P6A)	
9. PERFORMING ORGANIZATION NAME AND ADDRESS Boeing Vertol Company P.O. Box 16858 Philadelphia, Penn. 19142	10. PROGRAM ELEMENT, PROJECT, TASK AREA & WORK UNIT NUMBERS	
11. CONTROLLING OFFICE NAME AND ADDRESS U.S. Army Aviation R&D Command P.O. Box 209 St. Louis, Mo. 63166	12. REPORT DATE September 1977	13. NUMBER OF PAGES 425
14. MONITORING AGENCY NAME & ADDRESS (if different from Controlling Office) Applied Technology Laboratory U.S. Army Research and Technology Laboratories (AVRADCOM) Fort Eustis, Va 23604	15. SECURITY CLASS. (of this report) Unclassified	15a. DECLASSIFICATION/DOWNGRADING SCHEDULE
16. DISTRIBUTION STATEMENT (of this Report) Approved for public release, distribution unlimited. 12485p.		
17. DISTRIBUTION STATEMENT (of the abstract entered in Block 20, if different from Report)		
18. SUPPLEMENTARY NOTES		
19. KEY WORDS (Continue on reverse side if necessary and identify by block number) Helicopters Oil Cooler Transmission Clutch Bearings Titanium Gears Rotor Brakes		
20. ABSTRACT (Continue on reverse side if necessary and identify by block number) This report summarizes the total Heavy Lift Helicopter Drive System Advanced Technology Components (ATC) program. The program included the establishment of design criteria; the development testing of advanced technology components; the integration of these components into flight-weight, full-scale HLH transmissions; and the testing of the transmissions. The aft rotor and engine combining transmissions with associated drive shafting were designed,		

443 622

18

Unclassified

SECURITY CLASSIFICATION OF THIS PAGE(When Data Entered)

Block 20 - Continued.

built, and tested. The transmission required to power the forward rotor was studied in the ATC program and was detail designed and fabricated under a later HLH prototype program.

The objective of the ATC program was to define the design, the fabrication methods, the weight, and the cost of the prototype helicopter drive system. In one major area - bevel gearing - the ATC program developed analytical and experimental techniques critical to the success of all mechanical drive systems faced with similar power and weight requirements. In other areas the ATC program demonstrated design features which had not previously been evaluated in an integrated assembly. These features are described in this report. A general improvement in the characteristics of large helicopter and V/STOL drive systems can be expected from this development effort.

ACCESSION for	
NTIS	White Section <input checked="" type="checkbox"/>
DDC	Buff Section <input type="checkbox"/>
UNANNOUNCED	<input type="checkbox"/>
JUSTIFICATION	
BY	
DISTRIBUTION/AVAILABILITY CODES	
Dist.	A. B. C. D. E. F. G. H. I. J. K. L. M. N. O. P. Q. R. S. T. U. V. W. X. Y. Z. SPECIAL
A	

Unclassified

SECURITY CLASSIFICATION OF THIS PAGE(When Data Entered)

TABLE OF CONTENTS

	<u>Page</u>
LIST OF ILLUSTRATIONS.	5
LIST OF TABLES	12
INTRODUCTION	15
Objectives	15
Approach	15
SYSTEM DISCRIPTION	20
DESIGN CRITERIA AND OBJECTIVES	47
Drive System	47
Transmission Gearboxes	47
Lubrication Systems	49
Accessories	51
Rotor Brake	52
Drive Shafts	52
DRIVE SYSTEM STRUCTURAL CRITERIA	55
General Requirements	55
Loads Determination Criteria	55
Analysis Criteria	60
Allowables	62
Miscellaneous Criteria	64
Mission Profile	65
FABRICATION	66
Upper Cover	66
Rotor Shaft	66
Bevel Gears	69
Major Castings	71
Stationary Spur Ring Gear	71
Machining Vasco X-2	74
Assembly Techniques and Problems	74
BENCH DEVELOPMENT AND ENDURANCE TESTS	76
Test Equipment and Facilities	76
Aft Transmission	82
Combiner Transmission	104
Component Investigation	111
Drive Shaft Rotating Tests	121

	<u>Page</u>
DESCRIPTION OF PROTOTYPE CONFIGURATION	124
Rotor Transmission	124
Combiner Transmission	124
Combiner Gear Redesign	142
REFERENCES	147
APPENDIXES	
A Trade Studies	149
B Analyses of ATC Components	184
C Methods of Analysis	244
D Design Support Test Summaries	270
High-Speed Tapered Roller Bearings	271
Compliant Roller Bearings	278
Rotor Shaft Bearings	287
Engine Shaft Support Bearings	297
Gear Material Evaluation	306
Gear Tooth Form	316
Titanium Rotor Shaft Proximity	
Coupon Tests	326
Titanium Hardcoat Testing	332
Transmission Housing Material Evaluation	385
Overrunning Clutch	341
Oil Seals	351
Rotor Brake Development	354
Transmission Cover Photoelastic Model	
Stress and Deflection Test	383
Transmission Noise Reduction	402
Aluminum Graphite Composite Drive Shaft	
Trade Studies	405
Aluminum Synchronizing Shaft Ultimate	
and Fatigue Tests	414
LIST OF SYMBOLS	424

LIST OF ILLUSTRATIONS

<u>Figure</u>		<u>Page</u>
1	General Arrangement Model 301 HLH	17
2	HLH ATC Summary Program Phasing	19
3	Drive System Arrangement	21
4	Combiner Transmission Assembly	23
5	Lubrication Schematic HLH/ATC Combiner Transmission	28
6	Aft Transmission Assembly	31
7	Shafting Installation, Sync and Engine . . .	43
8	Rough-Sawn Forging	67
9	Machined Cover	67
10	Comparison of HLH and CH-47 Aft Rotor Shafts Shafts.	68
11	Aft Spiral Bevel Gear (301-10419) Sun Gear Being Hobbed	70
12	Machining the Forward Face	72
13	Boring the Horizontal Axis	72
14	Boring the Shaft Axis	73
15	Machined Housing	73
16	Model 301 Aft Transmission Test Stand Assembly	77
17	Combiner Transmission Test Stand	79
18	Dynamic System Test Rig	81
19	Aft Transmission Test Sequence	83
20	HLH/ATC Transmission Failure Investigation. .	87
21	Transmission Strain Survey Instrumentation. .	88
22	Aft Transmission Instrumentation Assembly . .	89

<u>Figure</u>		<u>Page</u>
23	Instrumentation Block Diagram	90
24	Typical Air Siren Gear Resonance Test Setup	91
25	Spiral Bevel Pinion Gear - Aft Transmission Tuning Ring Installation	92
26	View of HLH Aft Transmission Second Stage Planetary Subassembly with Straddle Plate . .	94
27	Rotor Shaft Bearing Locknut Comparison . . .	102
28	Aft Input Shaft Seal	103
29	Combiner Transmission Test Sequence	104
30	Modified Combiner Input Adapter	108
31	Response Frequency vs Operating Speed	116
32	Clutch Housing Acceleration at Zero Torque. .	118
33	Clutch Housing Acceleration at 50% Torque . .	119
34	Clutch Housing Acceleration with Modified Input Adapter	120
35	Aft Transmission Assembly	125
36	Forward Transmission Assembly	127
37	Prototype Aft Transmission	135
38	Combiner Transmission Assembly.	137
39	Prototype Combiner Transmission	141
40	Combiner Configuration 6, Reference Section A3-5, 301-10600, Sheet 6	145
A-1	Baseline Combiner Transmission	151
A-2	Alternate Combiner Transmission	157
A-3	Combining Transmission Basic Layout	161
A-4	Alternate Bearing Configuration, Combiner Transmission Design Study	163

<u>Figure</u>		<u>Page</u>
A-5	Clutch Assembly Field Replacement Concept Study	167
A-6	Overrun Roller Clutch Study Field Replacement	169
A-7	Second-Stage Ring Gear Diameter (3.674 Ratio)	172
A-8	Trade Study - Planetary High Contact Ratio vs Standard Growth Versions, 20,300 Horsepower	175
A-9	Rotor Shaft Comparison, Steel-Titanium. . . .	179
A-10	Cost Effectiveness of Graphite Shafting . . .	182
B-1	Hub Loads Symbols and Signs	185
B-2	Single Tooth Bending Fatigue Test Data . . .	191
B-3	Single Tooth Bending Fatigue Test Data (Probability of Survival)	192
B-4	Contact Stress Test Data	193
B-5	Contact Stress Test Data (Probability of Survival)	194
B-6	HLH/ATC Gear Tooth Form Test Results	195
B-7	BMS 7-223 Steel Rotating Beam Data	196
B-8	Detonating Gun Coating on 6AL-4U Rotating Beam Fatigue Test Results	197
B-9	Rotor Shaft-Aft Transmission	205
B-10	Gear Spiral Bevel Slant Shaft, Combine Transmission	213
B-11	Gear Helical Pinion-Central Engine Shaft Combiner Transmission	214
B-12	Gear, Spiral Bevel Pinion-Engine Shaft Combiner Transmission	215
B-13	Shaft Clutch - Inner, Combiner Transmission .	216

<u>Figure</u>		<u>Page</u>
B-14	Housing, Clutch - Engine Shaft, Combiner Transmission	217
B-15	Gear Spur - Rotor Brake, Combiner Transmission	218
B-16	Gear, Spiral Bevel Engine Drive, Combiner Transmission	219
B-17	Gear, Spiral Bevel Pinion, Aft Transmission .	220
B-18	Gear, Spiral Bevel - Aft Transmission	221
B-19	Planet Carrier - 1st Stage Aft Transmission .	225
B-20	Drive Shafts and Adapters, Typical Sections .	233
B-21	Transmission Cover Analysis	237
B-22	Bearing Housing	243
C-1	CH-47C and Stage Planet Bearings	251
C-2	Comparison of Predicted Baseline Transmission Sound Spectrum to MIL-Spec	255
C-3	Finite Element Model of HLH Aft Input Pinion	257
C-4	Tooth Loading as a Function of Tooth Mesh Position (Mean Normal Plane)	259
C-5	Schematic Showing Location of Finite Element Loads	261
C-6	Finite Element Modeling of Distribution Loads	262
C-7	Basic Meshing Principles of Standard Involute and High-Contact-Ratio Gearing . . .	264
C-8	Five-Tooth Plot of Strain Survey of High- Contact-Ratio Spar Gear	265
C-9	Comparison of Standard and High-Contact- Ratio Tooth Loading	267
C-10	Comparison of Standard and High-Contact- Ratio Bending Stress Layouts	268

<u>Figure</u>		<u>Page</u>
C-11	Comparison of Load Capacity of Heavy-Lift Helicopter (HLH) High-Contact-Ratio Spur Planetary Gearing and Equivalent Standard Design Gearing	219
D-1	HLH High-Speed Tapered Roller Bearing Test Machine, Show Driven by 700-HP Drive System	274
D-2	Typical New, Modified HM 926700 - Series Bearing with 17 Radial Holes to the Rib Face - Z Type Machined	277
D-3	Illustration of Hollow-Ended Roller Design. .	279
D-4	HLH Design Study - Planetary Bearing (Second Stage Planet)	280
D-5	Prototype Hollow-Ended Roller Bore Shape Comparison	282
D-6	Life Comparison - HLH Planet Bearing Candidates	286
D-7	Details of Test Specimen Design and Description	289
D-8	MRC High-Temperature Grease Test Spindle. . .	299
D-9	Test Rig, Version 4	301
D-10	Modified Test Bearings, Cage Design 6	303
D-11	Final HLH/ATC Engine Shaft Support Bearing Configuration	304
D-12	S-N Data Gear Material Evaluation, Room Temperature	314
D-13	S-N Data Gear Material, -350°F.	315
D-14	Final High-Contact-Ratio Gear Configuration .	317
D-15	Gear Tooth Form Test Rig.	320
D-16	Graphic Summary of Final Configuration Test Data	322
D-17	Relative Scoring Load Capacity of AISI 9310 Gear Material Compared to VASCO XBMS 7-223 Material	324

<u>Figure</u>		<u>Page</u>
D-18	Test Specimen Area Post Proximity Tests . . .	327
D-19	Titanium Smooth Specimen Results	328
D-20	Titanium Notched Specimen Results	329
D-21	Comparison of Fatigue Crack Growth Rates in 6Al-4V Titanium Alloy Forgings	330
D-22	Fatigue Strength Hard Coated Titanium	334
D-23	Average Tensile Properties for ZE41A-T5 Magnesium	337
D-24	Mean Fatigue Strength for ZE154A-T5 at a Stress Ratio of Zero	338
D-25	Crack Growth Comparisons for Magnesium Alloys at a Constant Stress Intensity Valve	340
D-26	HLH/ATC Sprag Clutch Designs	342
D-27	Dynamic Clutch-Test Facility	344
D-28	Results of Slip Test	346
D-29	Results of the Nonrotating Cyclic Torque Fatigue Test	347
D-30	Test Configurations	352
D-31	Layout-Structural Graphic Disk and Steel Disk	356
D-32	Layout-Structural Beryllium Disk Assembly . .	357
D-33	Layout-Structural Beryllium Disk and Graphite Disk Assembly	358
D-34	Cross Sections of Piston Housing Assembly . .	362
D-35	Metallic Lined Beryllium Brake Disk Assembly	364
D-36	Carbon/Graphite Lined Beryllium Brake Disk Assembly	365
D-37	Structural Carbon/Graphite Brake Disk Assembly	366

<u>Figure</u>		<u>Page</u>
D-38	Structural Carbon Brake Disk Assembly E-V Part Number 301-10683	375
D-39	Rotor Shaft Support Housing Model	385
D-40	TORRP LR-321 Model of Closed Loop Test Stand	390
D-41	Noise Spectrum - HLH-ATC Transmission Installed in Closed Loop Test Stand	391
D-42	Coupled Bevel Gear and Sun Gear HLH/ATC Transmission Model	392
D-43	Sun Gear Responding to Sun Frequency, 2,788 rpm, 75.6% Torque (Input Shaft at 7,986 rpm)	394
D-44	Bevel Gear Responding to Sun Frequency, 7,986 rpm, 75.6% Torque	395
D-45	Bevel Gear Responding to Bevel Frequency, 7,986 rpm, 75.6% Torque	396
D-46	Sun Gear Responding Frequency, 2,788 rpm, Torque (Input Shaft at 7,986 rpm)	397
D-47	Combiner Transmission Computer Model	398
D-48	Modification to HLH Mix Box Center Shaft	399
D-49	HLH/ATC Transmission Noise Levels	401
D-50	HLH/ATC Transmission Noise-Case Damping and Attenuation Evaluation Summary - 1,400 Hz	403
D-51	Composite Shaft Ultimate Torque Test	407
D-52	Rotary Wing Drive Shaft Assembly	415
D-53	HLH Sync Shaft Fatigue Test	422

LIST OF TABLES

<u>Table</u>		<u>Page</u>
1	Mission Profile	58
2	Aft Transmission Test Problems and Resolutions	84
3	Twenty-Five Hour Load Test Schedule	95
4	DSTR Load Schedule	96
5	Run Schedule - DSTR 50-Hour Endurance . . .	97
6	Run Schedule - DSTR 30-Hour Endurance . . .	98
7	DSTR Event Log (Drive System Only)	99
8	Combiner Transmission Test Problems and Resolutions	105
9	Gear Pattern Conditions	106
10	Combiner Transmission Modification	109
11	Sprag Clutch History - DSTR Testing	115
12	Prototype Design Modification - Aft Transmission	133
13	Prototype Design Modification - Combiner Transmission	139
14	Prototype Combining Transmission Configuration Summary	143
15	Revised HLH Combiner Gearing	144
16	HLH Combiner Configuration Study, Configuration Number Six, Bearing Life Summary	146
A-1	Combiner Transmission Configuration Study	160
A-2	Shaft Design Allowables	177
B-1	Cubic Mean Power	186

<u>Table</u>		<u>Page</u>
B-2	Speed/Torque Summary for Gear and Drive Shafting Loads	187
B-3	Minimum Margins of Safety	198
B-4	Helical and Spur Gear Tooth Stress Summary	199
B-5	Spiral Bevel Gear Tooth Stress Summary	199
B-6	Tapered Roller Bearing Geometry	201
B-7	Rotor Shaft 301-104011	207
B-8	Gear Shaft Analysis-Fatigue	209
B-9	First-Stage Planet Carrier 301-10413.	223
B-10	Drive Shaft Tubes	227
B-11	Drive Shaft Adapter	229
B-12	Drive Shaft Critical Speeds	234
B-13	Spline Stress Summary	235
B-14	Rotor Transmission Upper Cover 301-10456	239
C-1	Summary of HLH Transmission Bearings	248
D-1	Test Roller Crown Geometry	284
D-2	Comparison of Test Bearings and Actual HLH Transmission Bearings	292
D-3	Test Bearing Life Summary	293
D-4	HLH Rotor Shaft Bearing Life Summary	296
D-5	Summary of Test Elements and Results	307
D-6	Fracture Toughness (K_{IC}) Test Results VASCO X-2 Hot Hardness Steel Room Temperature	312

<u>Table</u>		<u>Page</u>
D-7	Summary of Cantilever Bending Fatigue Tests of VASCO and 9310 Steels	313
D-8	Metallurgical Evaluation Results	319
D-9	Summary of Statistical Analysis of HCR VASCO Scoring Data	325
D-10	Tensile Test Results	331
D-11	Chemical Analyses From Vendor Certification	335
D-12	Summary of Load-Sharing Test Results . . .	349
D-13	Comparison of Design D and Aircraft Clutch Parameters with Design Criteria . .	350
D-14	Preliminary HLH Rotor Brake Design Parameters	355
D-15	Heat Sink Material Comparison	359
D-16	Comparison Chart - Rotor Brake Designs, Boeing Vertol, HLH	360
D-17	Conventional Steel Disk Dynamic Torque Test Results	369
D-18	Structural Graphite Dynamic Torque Test Results	371
D-19	HLH/ATC Synchronizing Shaft - Failure Progression Rate	420

1. INTRODUCTION

OBJECTIVE

The objectives of the ATC Program were:

1. To demonstrate component technology to reduce development risks applicable to a 22.5-ton HLH at the lowest total HLH system cost.
2. To secure a cost data base adequate to assure that cost estimates using that data base are credible and acceptable.
3. To provide the Government with improved technology and reduced risk for program definition for large payload helicopters.
4. To advance the level of industry expertise in HLH components.

APPROACH

The purpose of the ATC Program was to seek maximum reduction of technical and cost risks associated with the Engineering Development of an HLH system through the design, fabrication, demonstration, and test of selected critical HLH components. Engineering Development or full flight qualification of any component or concept was not the purpose of this program.

The critical components of the HLH were determined to be the rotor blades, the hub and upper controls, the drive system, the flight control system, and the cargo handling system. The scope of the HLH ATC program was limited to these components, plus the interface analytical activities necessary for the ATC components to be considered suitable for subsequent integration with the complete aircraft.

The general arrangement of the HLH as described in the Prime Item Description Document (PIDD) is shown in Figure 1. The configuration is based on the U.S. Army Aircraft System Requirement Document (ASRD) for the Heavy Lift Helicopter ATC Program. The configuration is designated the Boeing Model 301.

The drive system ATC program began in July 1971 and was completed in July 1975. The general schedule is shown in Figure 2.

MAJOR CHARACTERISTICS

ROTOR

DIAMETER (FT)	92.0
TIP SPEED (F.P.S)	750.0
DISC. LOADING (R.S.F) AT DGW	8.9
BLADE AREA (8 AT 153 SQ. FT.)	1224.0
GEOMETRIC SOLIDITY RATIO	.09226
GEOMETRIC DISC. AREA (2 AT 6647.6 SQ. FT.)	13,295.0

PROPULSION

NUMBER OF ENGINES/TYPE	T731-AD-700(3) TURBOSHAFT
TRANSMISSION RATING (H.P)	17,700
MAX. SINGLE ENGINE RATING	8,079
INTEGRAL FUEL CAPACITY (GAL)	2,938
INTEGRAL FUEL CAPACITY (LB)	19,100

WEIGHT (LB)

DESIGN GROSS WEIGHT, LF+2.5	118,000
DESIGN PAYLOAD	45,000
DESIGN MISSION FUEL	11,080
FIXED USEFUL LOAD (INCLUDES 5 MAN CREW)	2,340
EMPTY WEIGHT	59,580
MAX. ALTERNATE GROSS WEIGHT	148,000
MISSION GROSS WEIGHT	118,000

GROUND ANGLES (DEGREES)

TURNOVER	GROUND LINE	34.0° @ 93,000 L
(WT. EMPTY)		
TIP BACK	GROUND LINE	30.0° FROM HOVER
(WT. EMPTY)		

CONTROL MOVEMENTS

	FORWARD	AFT
COLLECTIVE PITCH	-1.0° TO 19.7°	-2.0° TO 16.0°
DIFFERENTIAL COLLECTIVE PITCH	± 5.0°	± 5.5°
PROGRAMED LONGITUDINAL CYCLIC PITCH	-3.2° TO 12.0°	-5.4° TO 13.0°
SIDE ARM CONTROL CYCLIC PITCH	± 5.5°	± 5.0°
DIFFERENTIAL LATERAL CYCLIC PITCH	± 12.0°	± 11.0°
LATERAL CYCLIC PITCH	± 8.0°	± 7.2°

LANDING GEAR

	NGSE	MAIN
NOSE - WHEEL/TIRE SIZE	15.00 - 16	15.50 - 20
MAIN - WHEEL/TIRE SIZE	TYPE III	TYPE IV

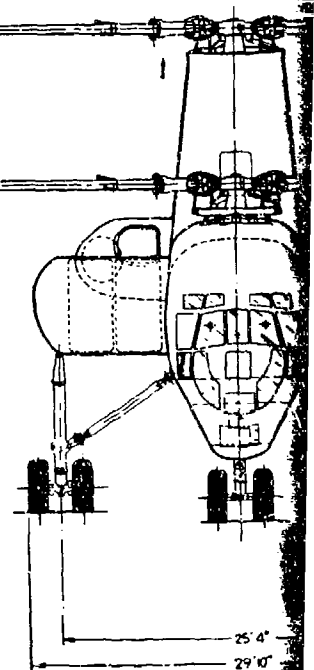


Figure 1. General Arrangement Model 301 HLH.

2 1 ISTICS

IT (LB)

ROSS WEIGHT, LF-2.5	118,000
YLOAD	45,000
SSION FUEL	11,080
UL LOAD (INCLUDES 5 MAN CREW)	2,940
IGHT	59,580
RNATE GROSS WEIGHT	148,000
GROSS WEIGHT	118,000

ND ANGLES (DEGREES)

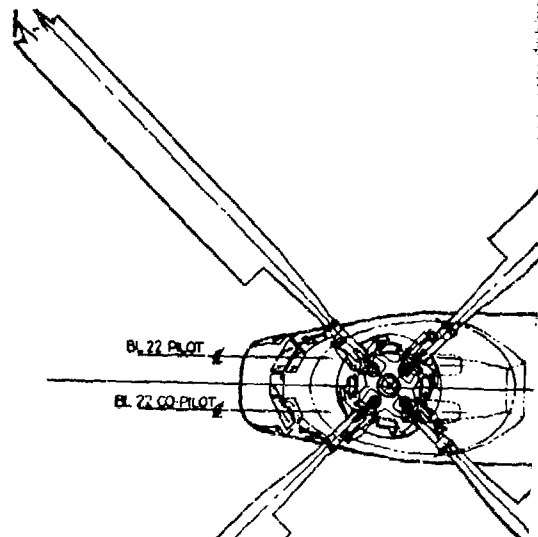
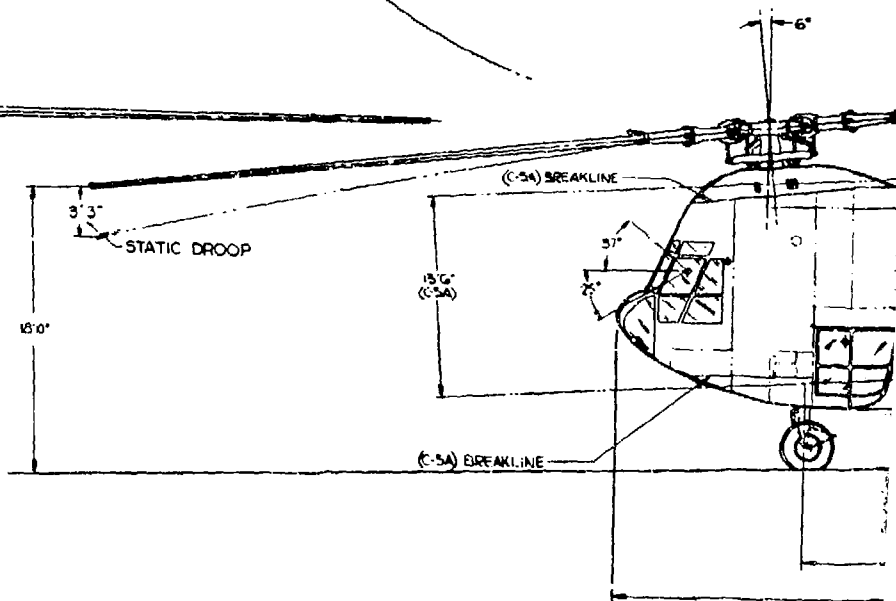
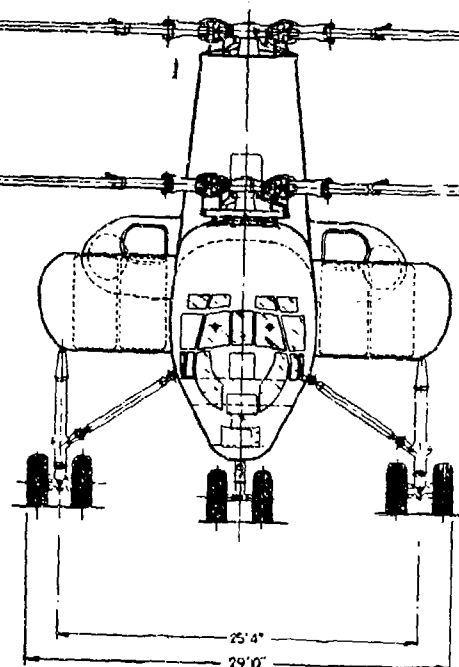
GROUND LINE	340° @ 93,000 LBS
GROUND LINE	300° FROM HOVER REF @ DESIGN GROSS WEIGHT

ROL MOVEMENTS

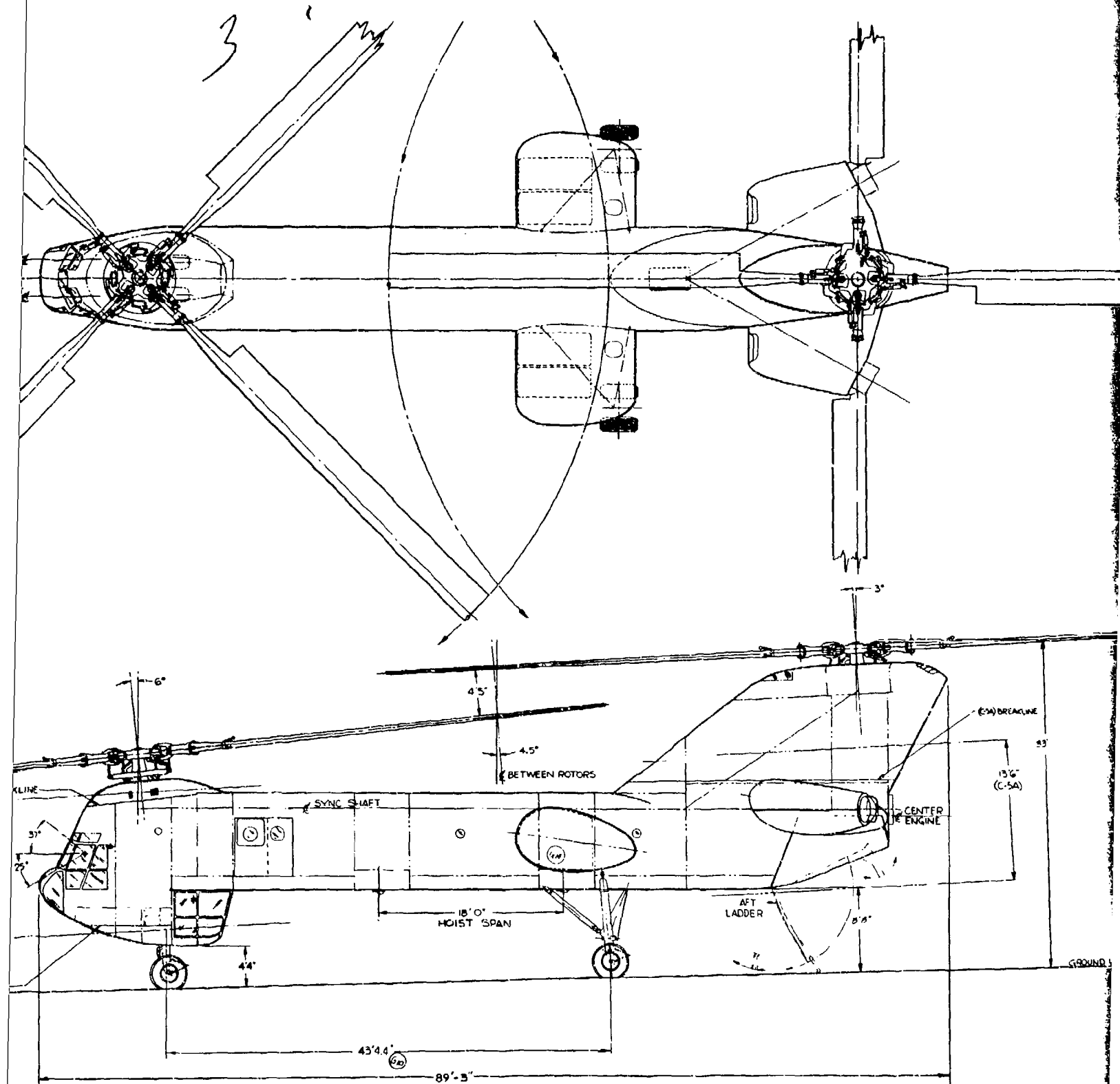
	FORWARD	AFT
VE PITCH	-1.0° TO 19.7°	-2.0° TO 16.0°
UTIAL COLLECTIVE PITCH	± 5.0°	± 5.5°
AD LONGITUDINAL CYCLIC PITCH	-5.2° TO 12.0°	-5.4° TO 10.0°
CONTROL CYCLIC PITCH	± 3.3°	± 3.0°
IAL LATERAL CYCLIC PITCH	± 12.0°	± 11.0°
CYCLIC PITCH	± 8.0°	± 7.2°

ING GEAR

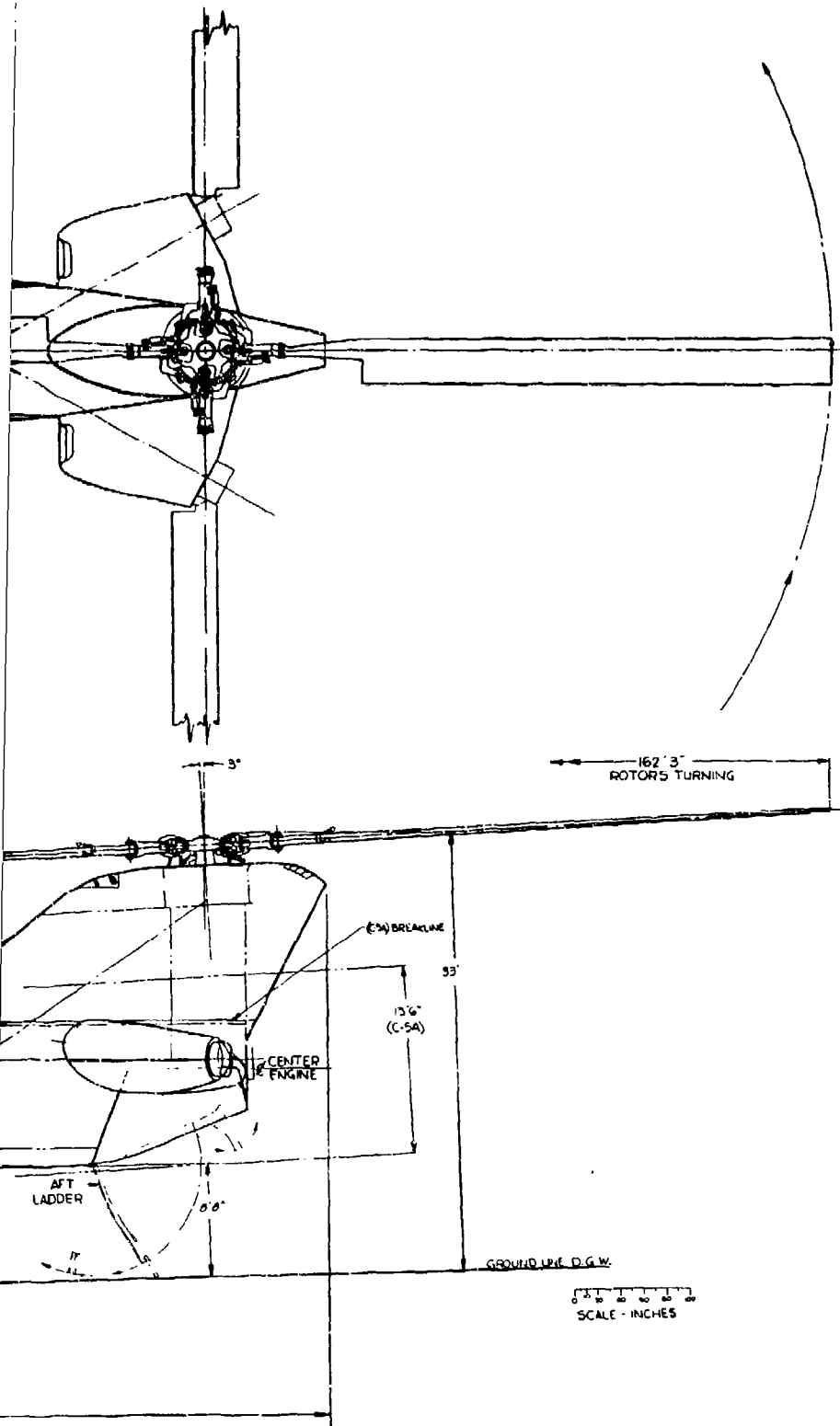
WHEEL/TIRE SIZE	1K PLY RATING	NOSE	MAIN
WHEEL/TIRE SIZE		15.00-16	15.50-20
		T-PE III	TYPE III



bl 301 HLH.



4



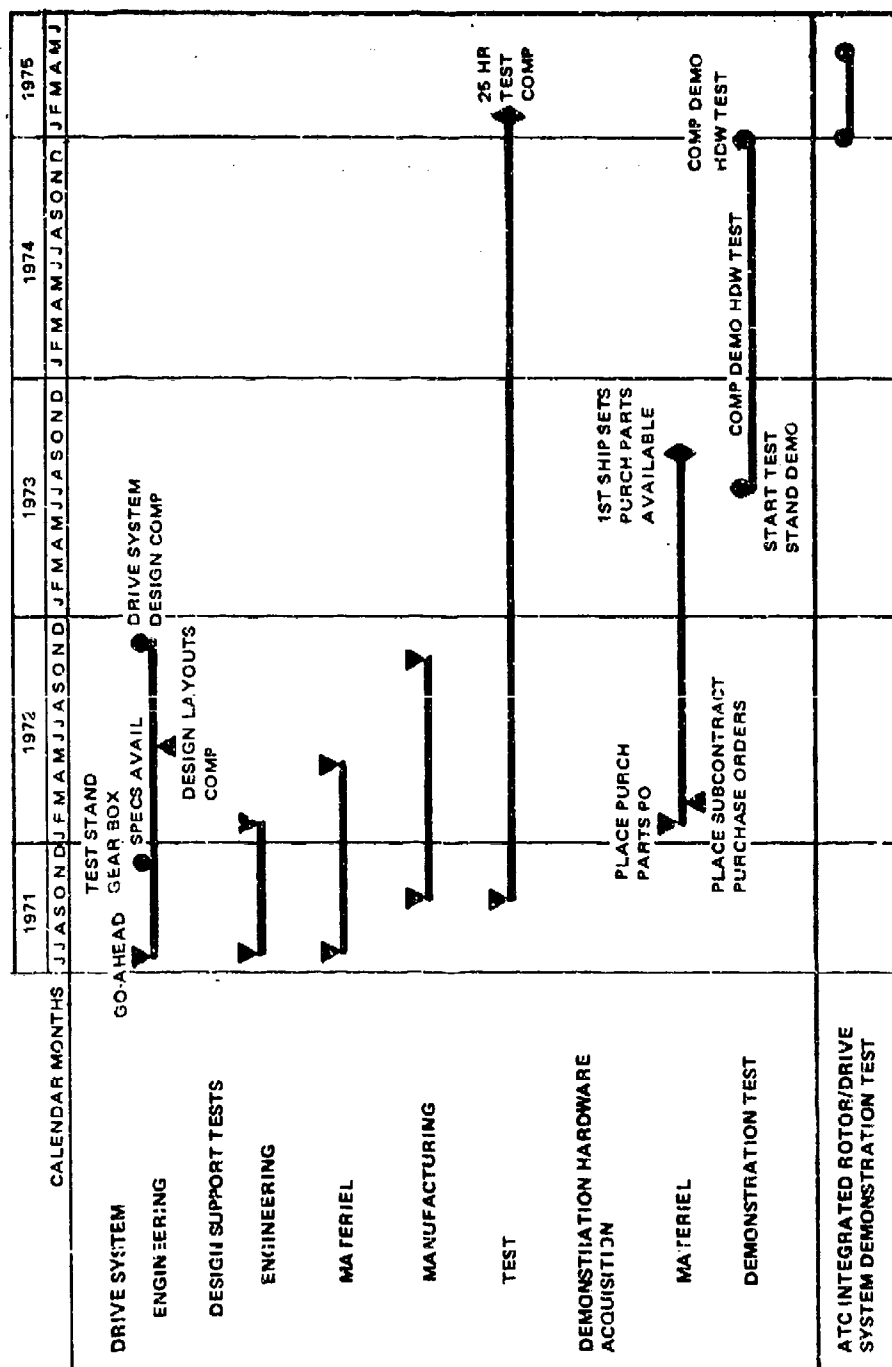


Figure 2. HLH ATC Summary Program Phasing.

2. SYSTEM DESCRIPTION

The Drive System (Figure 3) consists of three transmissions together with interconnecting shafting. The transmission design torques are determined by the following hp ratings:

1. 110% of the power required to hover OGE at design gross weight at sea level 95°F with all engines operating (17,700 hp at combining transmission output speed of 8000 rpm)
2. Maximum power of any two engines at sea level 59° with one engine inoperative (8075 hp/engine at 11,500 rpm)
3. A torque distribution of 60% to either rotor
4. Transmissions are sized for the steady torque values required by the flight envelope. The design goal for transmission removal is 2000 hours MTBR with "on-condition" removal. The transmission bearings are designed for a B₁₀ life of at least 2000 hours, using a mean load derived from the mission profile.

The combining transmission (Figure 4) combines the power from three forward drive engines, provides a 1.44 to 1 speed reduction, and directs the power to forward and aft rotor transmissions.

The three engine inputs are directed through sprag-type over-running clutches to combining gears on the centerline shaft. The clutches are spline connected to the gearing and supported within a separate housing, thus allowing field replacement if desired without major disassembly or disturbance of any gearing. The clutch inner race is connected to the rotor side of the system, thereby assuring a constant centrifugally-induced oil supply from the inner race feed. The inner face is supported within the outer by tapered roller bearings to reduce the tendency to brinell which has been shown by cylindrical or ball bearings used in this location.

The spiral bevel collector gear which combines left and right engines also serves as the driver for the slanting-shaft aft rotor takeoff. The slant-shaft bevel is supported in tapered roller bearings, as are the bevel input pinions. These bearings have inner-race lubrication directed at the major heat generation areas as well as other modifications to enable them to operate at high velocities.

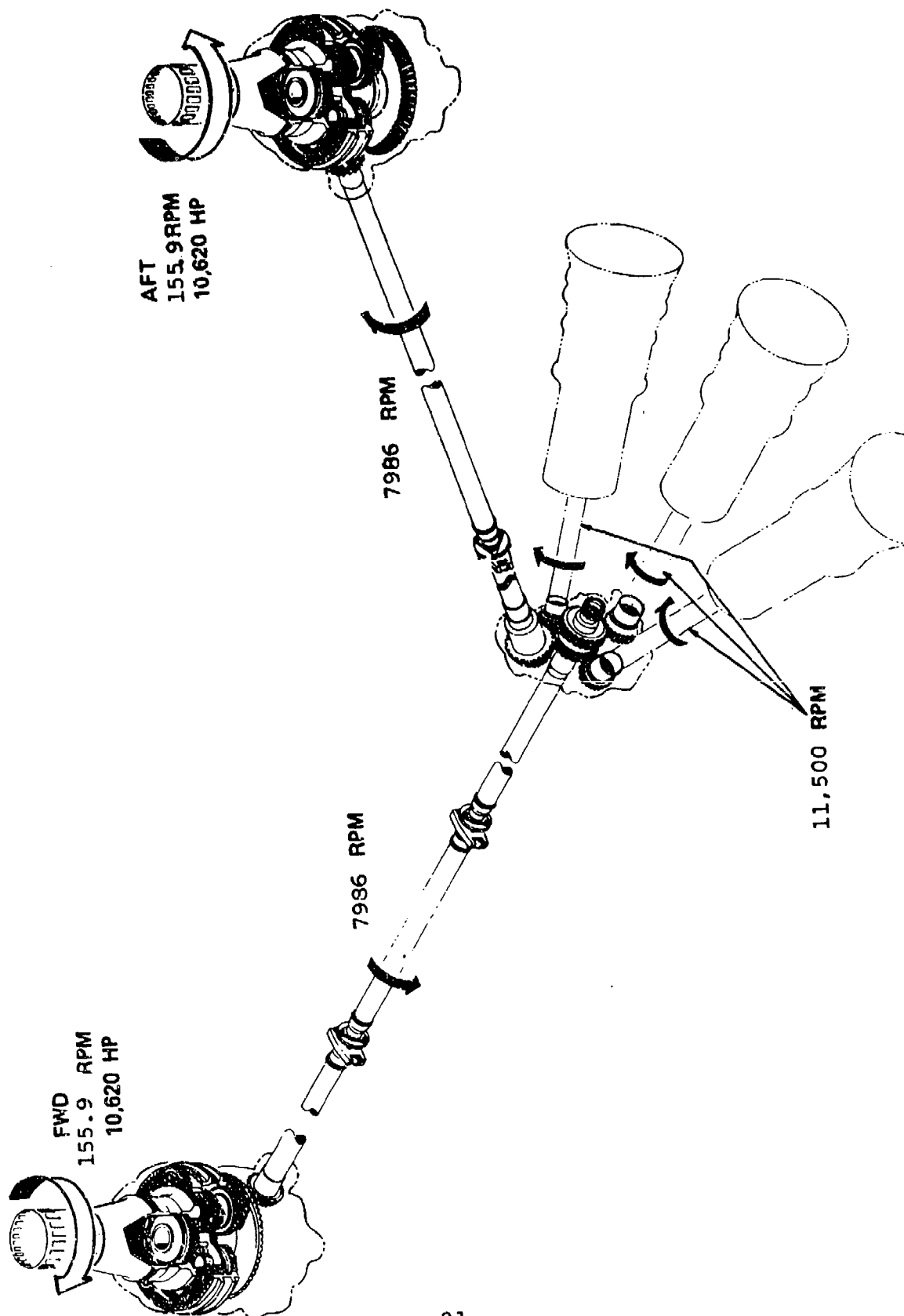


Figure 3. Drive System Arrangement.

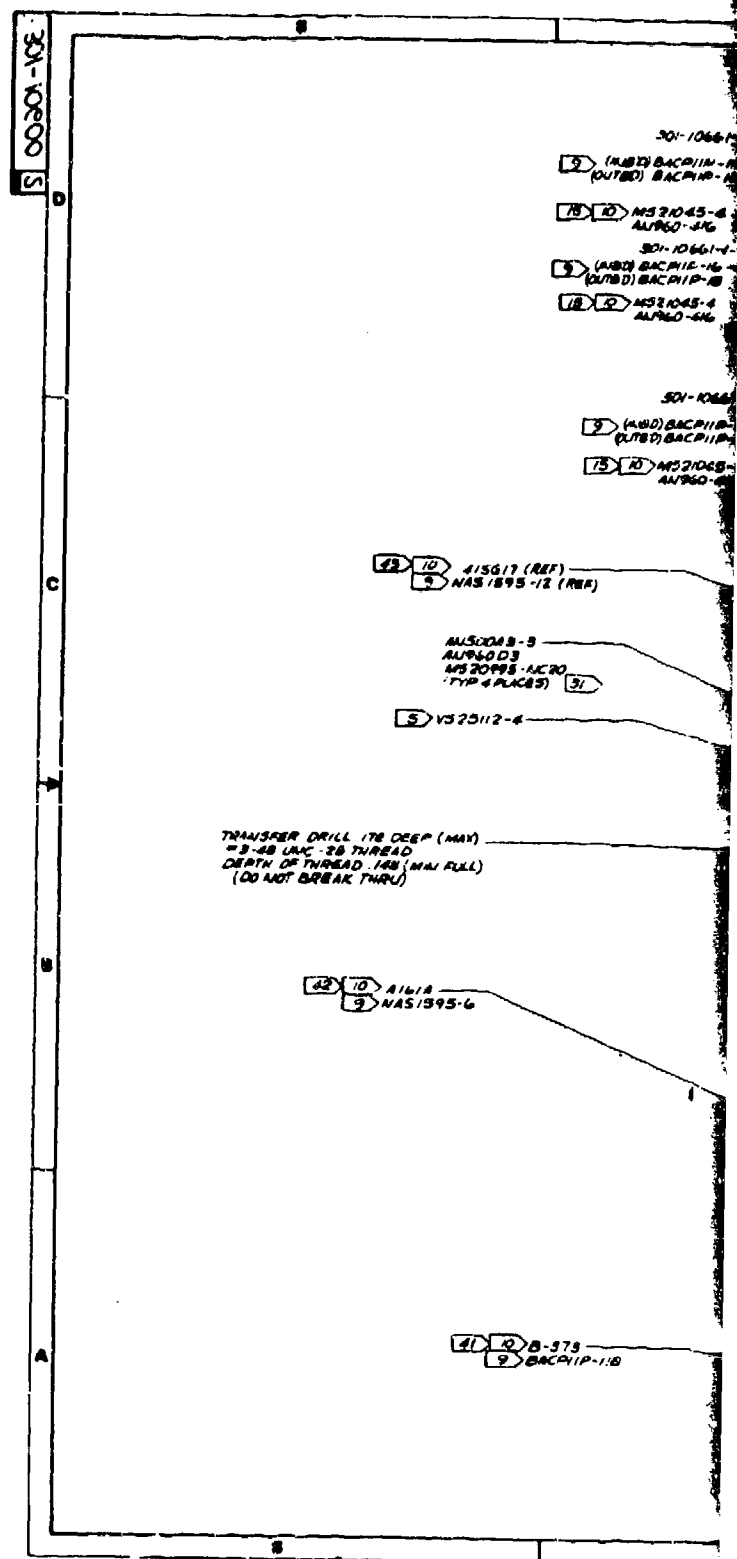
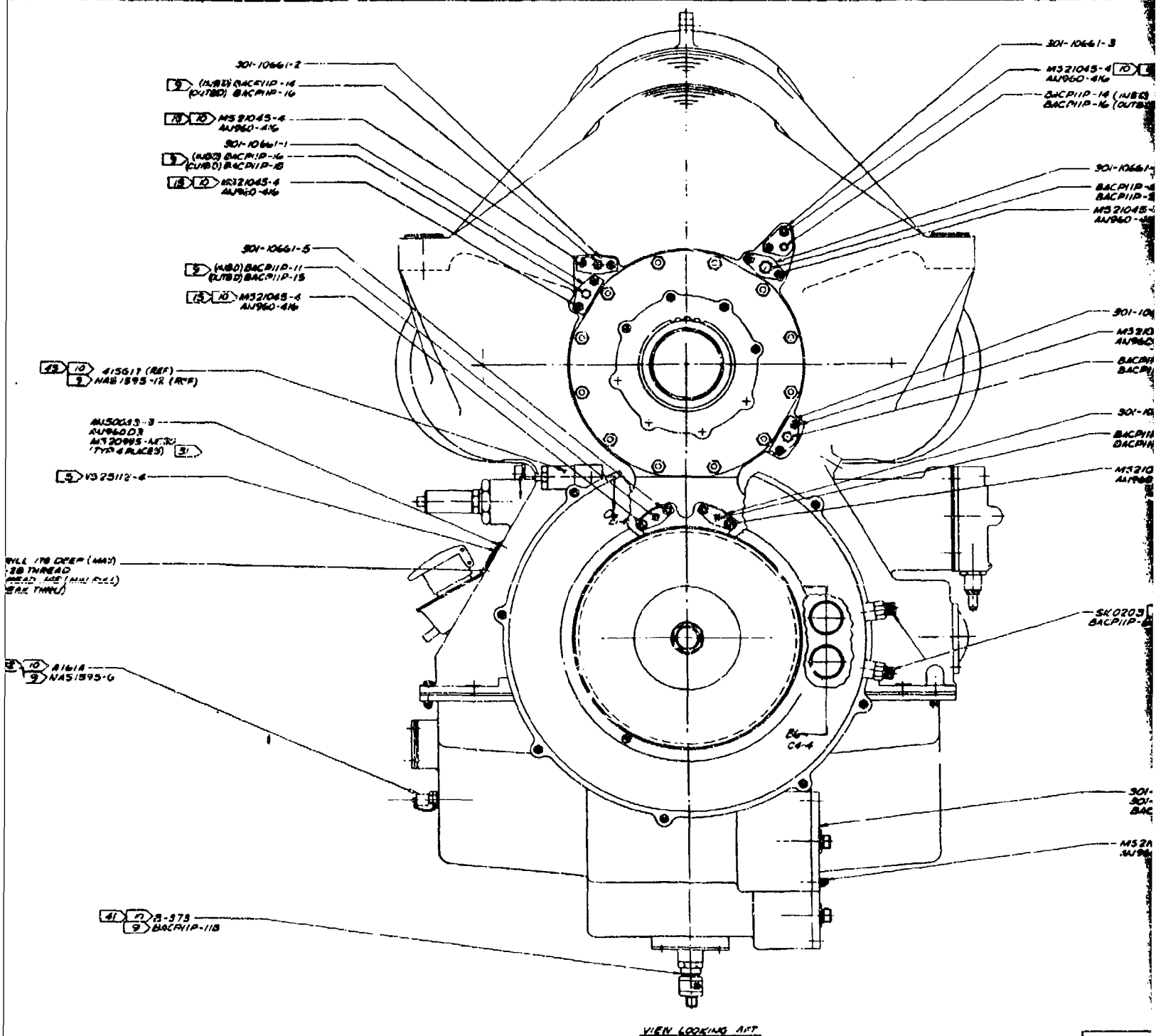


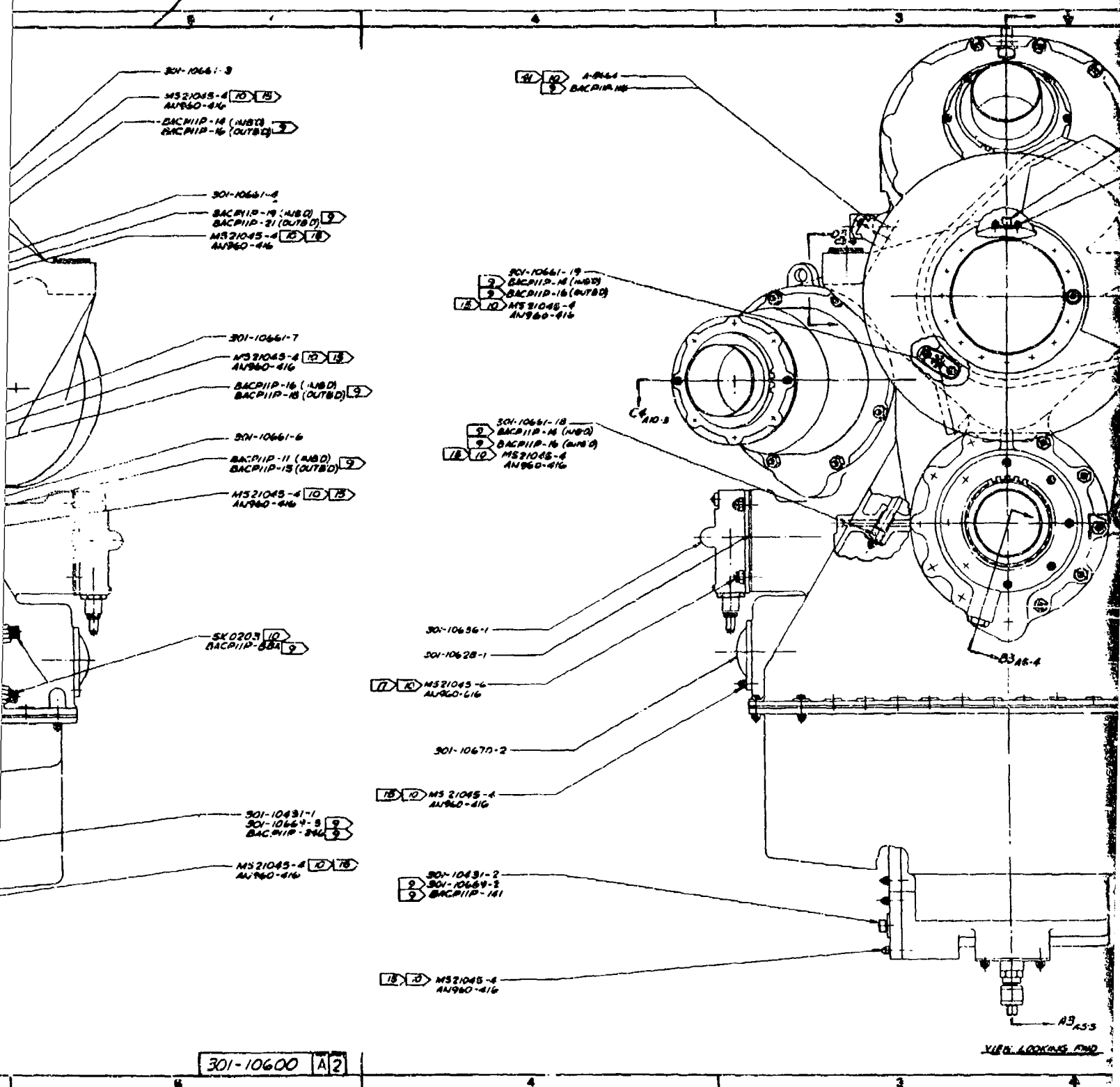
Figure 4. Combined Transmission Assembly (Sheet 1 of 2).

2



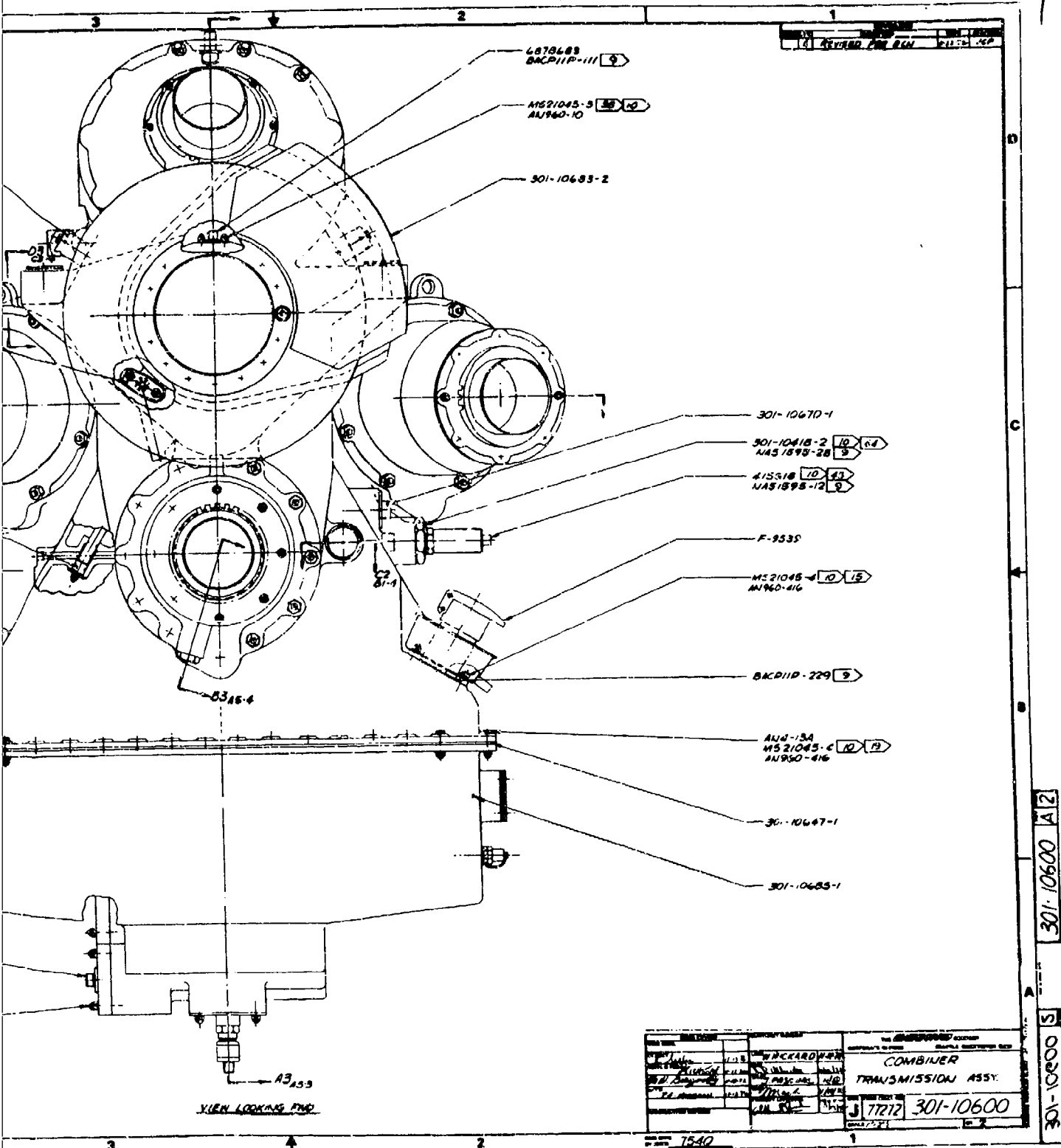
301-10661-1

3

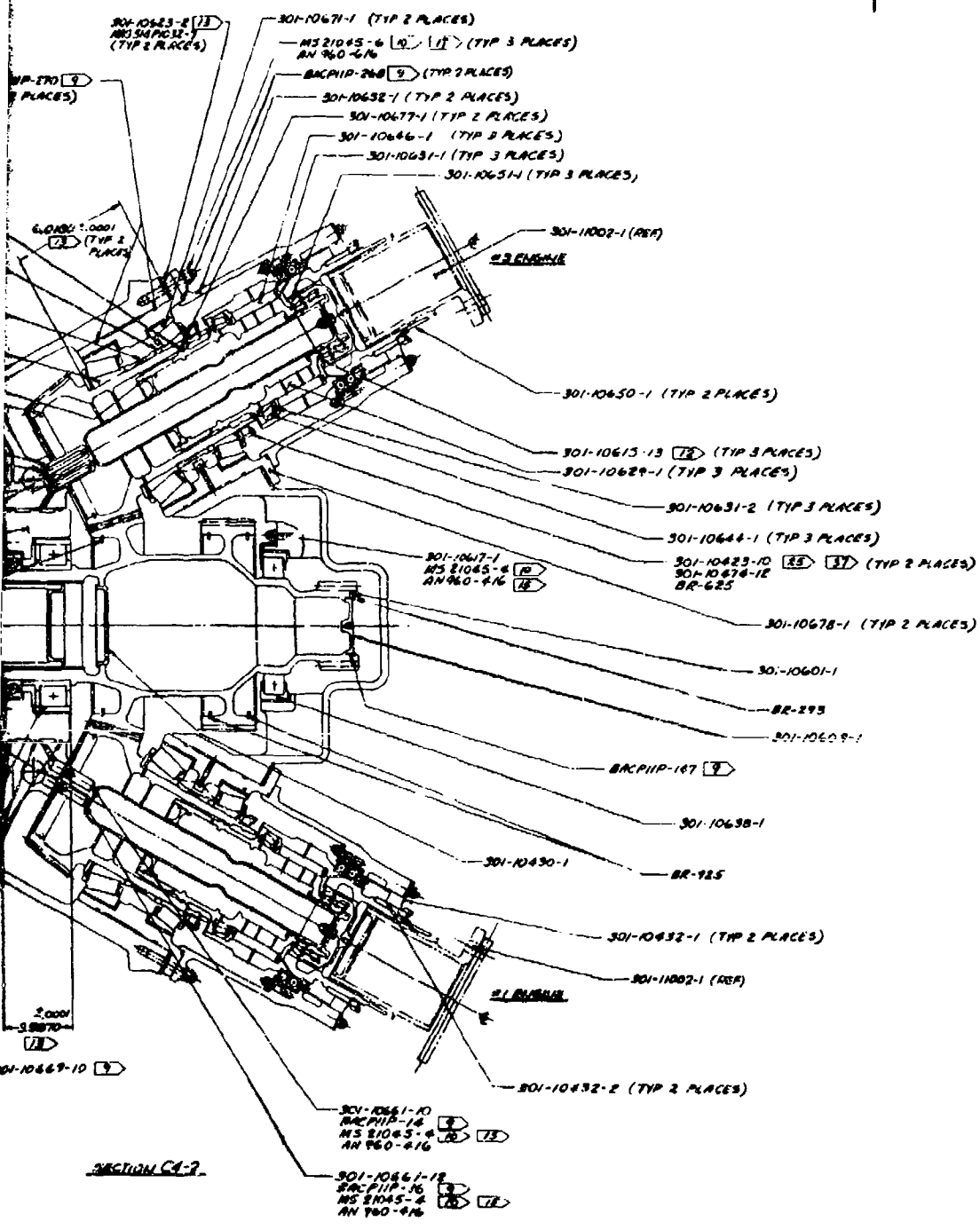


301-10600 A2

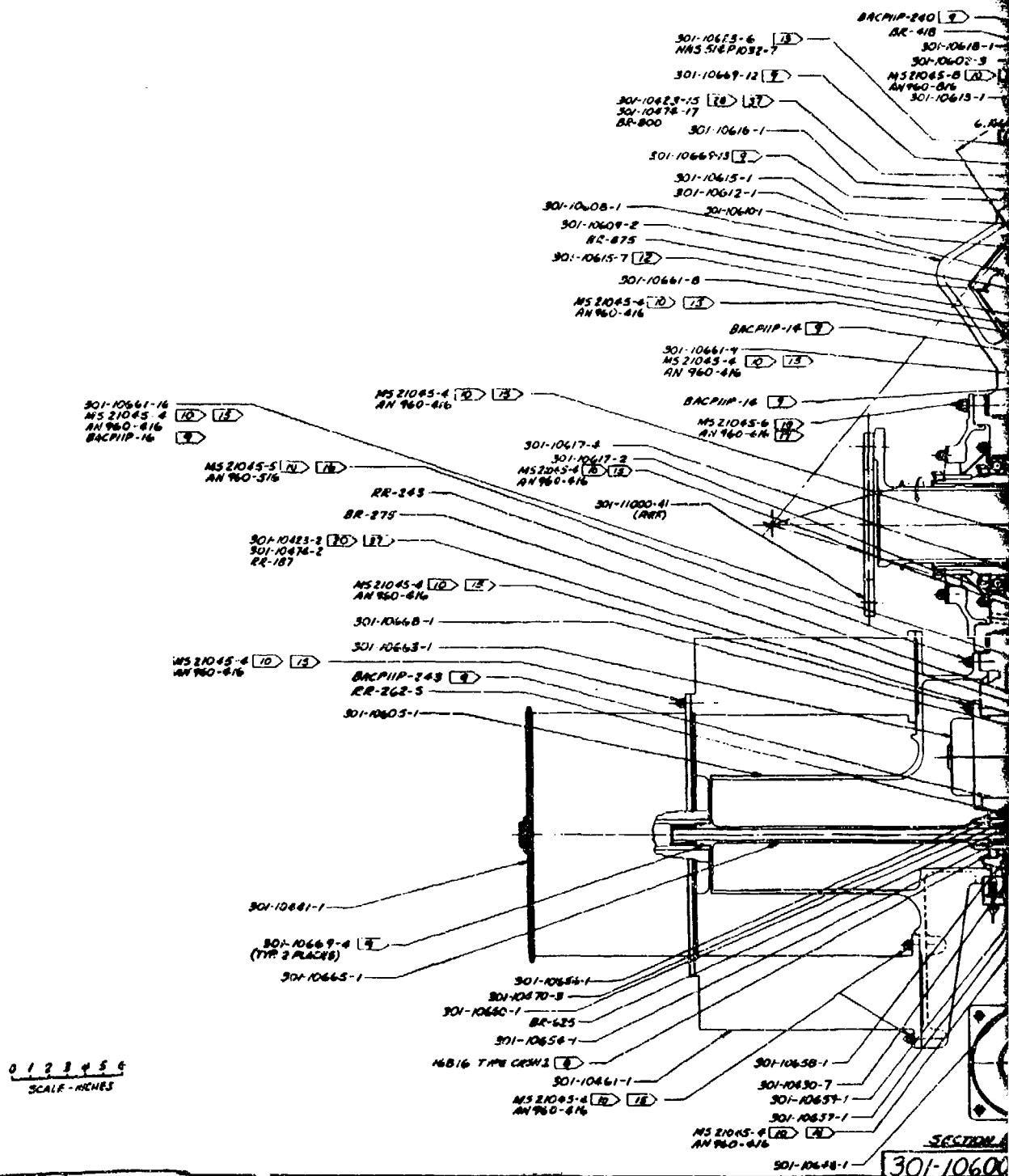
VIEW LOOKING FROM

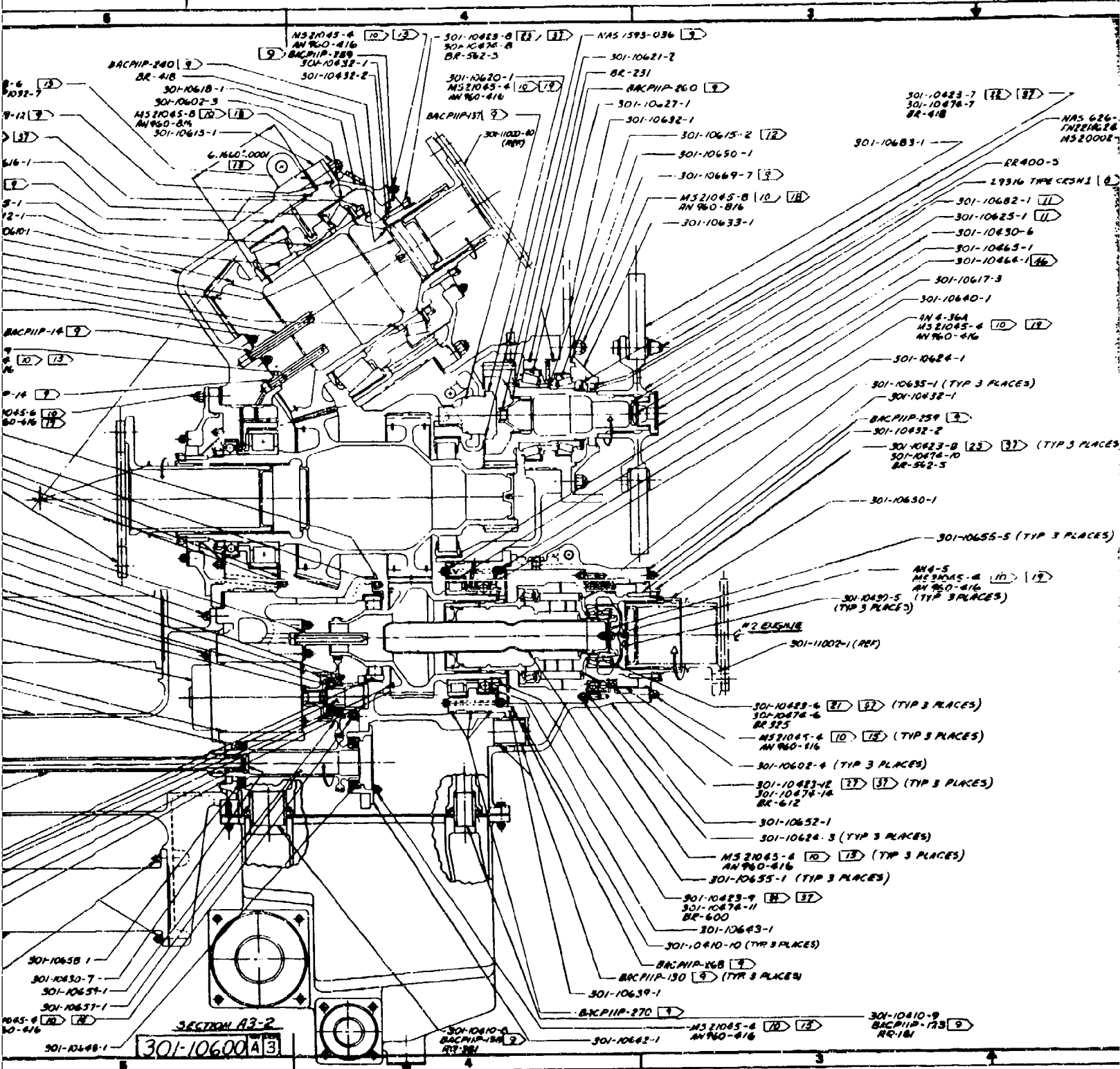


2 1



301-10600 A3





These bearings, as well as main gear meshes, are served by two separate lubrication feed systems (Figure 5), each of which incorporates its own pump, filter, passages, and jets. The main pump is located in the front of the gearbox beneath the integral blower-cooler. It draws from a level several inches above the sump floor to allow a reserve for the auxiliary system. The main pump discharges through the circular cooler, filter, and pressure relief valve to jets throughout the transmission. The auxiliary pump, which is located at the opposite end of the gearbox and driven by the brake drive, draws from the sump bottom. It does not discharge through a cooler, but goes directly to a screen and then to critical gears and bearings. The discharge capacity of the auxiliary is about 15 percent of the main system. This quantity, determined by component tests, maintains the integrity of the main drive train for a minimum of 20 minutes. Both lubrication systems have individual pressure gages so that loss of pressure on either system can be seen.

The screen-type debris detector located at the pump inlet provides warning of structural deterioration within the transmission. All of the oil flows through the detecting screen, whose mesh is sized to stop particles larger than .060 inch. Any electrically conductive material held against the screen by suction force completes an electrical continuity and activates a signal. The particle need not be magnetic. Smaller debris particles are deposited on the filter screen beyond the pump and cooler. This filter signals an accumulation of debris sufficiently heavy to activate a delta-pressure switch. As a final protection for the transmission, a further down-stream screen at the entrance to the transmission holds particles of jet clogging size that may have been left in the oil cooler passages or filter bypass. Excessive debris collection will be indicated by the oil pressure gage.

The rotor brake is mounted on and driven from the rear of the gearbox. The brake disc is a carbon composite, rotating at 5,152 rpm and running in a brake head assembly containing carbon composite linings within a caliper assembly.

The combining transmission is mounted to the structure by four bolts, with a failsafe one-joint-failed capability. There are no fluid lines connecting the transmission to the airframe. The oil system, as noted, is self-contained within the transmission. Air for the transmission-mounted cooler is brought from the aft pylon into the transmission compartment and is drawn into the outside diameter of the cooler. The hot exhaust air is drawn from the cooler inside diameter through the blower to the hoist compartment forward of the transmission and thence overboard.

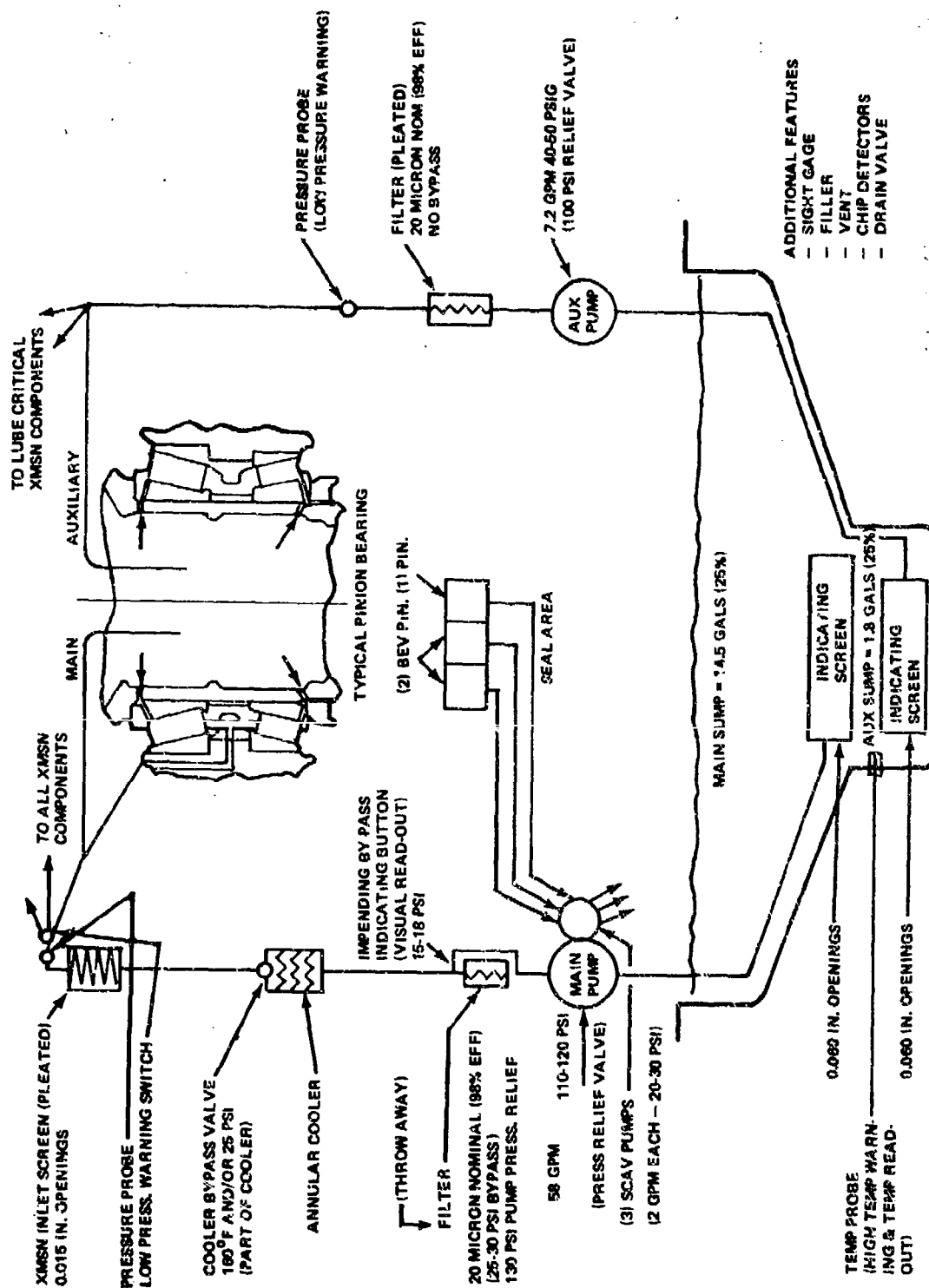


Figure 5. Lubrication Schematic HLH/ATC Combiner Transmission.

The aft transmission is shown in Figure 6. The aft and forward rotor transmissions are similar except for input bevel gear angles and orientation. Upper cover, rotor shaft, and planetary gearing are identical. The ratio of the rotor transmissions is 51 to 1, from synchronizing shaft to rotor. The bevel gear accounts for 2.86 to 1, and the two-stage planetary for 17.88 to 1.

All main drive gearing is made from carburized BMS 7-223 (Vasco X-2) high hot hardness tool steel. Bevel gears are supported in tapered roller bearings modified and lubricated for high-velocity application. Planet gears in the second (upper) stage are supported by compliant cylindrical roller bearings with hollow ends. These are designed to provide higher capacity than spherical roller bearings, while allowing a greater misalignment across the bearing than would normally be possible with solid-end cylindricals.

The rotor shaft is a titanium forging (6 AL-4V), with surface treatments at the bearing journals and at the upper spline, designed to protect the titanium from fretting and wear. The upper cover, which supports the rotor shaft and carries torque and hub loads to the airframe, is a 7075 T-73 aluminum forging. The attachment of the cover to the airframe through four bolts follows fail-safe criteria.

The lower case is a magnesium casting of ZE 41A material selected for improved properties in heavy sections typical of these large housings. Beneath the cast housing a glass reinforced epoxy sump closes the gearbox and provides pickup points for the main and auxiliary lubrication system. Glass fiber was selected for ballistic considerations, as its high-strength low-modulus properties allow it to absorb ballistic impact without large fracture areas. The sump is also designed with self-sealing compound application as a consideration for ballistic protection.

Lubrication, cooling, and condition monitoring follow the same principles as the combining transmission. The oil cooler is integrated with the transmission to eliminate fluid connections and to reduce the vulnerable area. Two lube pumps are used, with the auxiliary pump drawing from a protected deep sump, to supply critical areas in emergency conditions.

Accessory drives are arranged around the periphery of the sump at the transmission base. Two separated drive trains, beginning with a dual face central gear, supply power to duplicated accessory arrangements. Each branch has a main alternator, a flight control hydraulic pump, a flight control generator, and a transmission lube pump. Accessory drives to main alternators are designed for the use of oil cooled machines, incorporating integral oil passages.

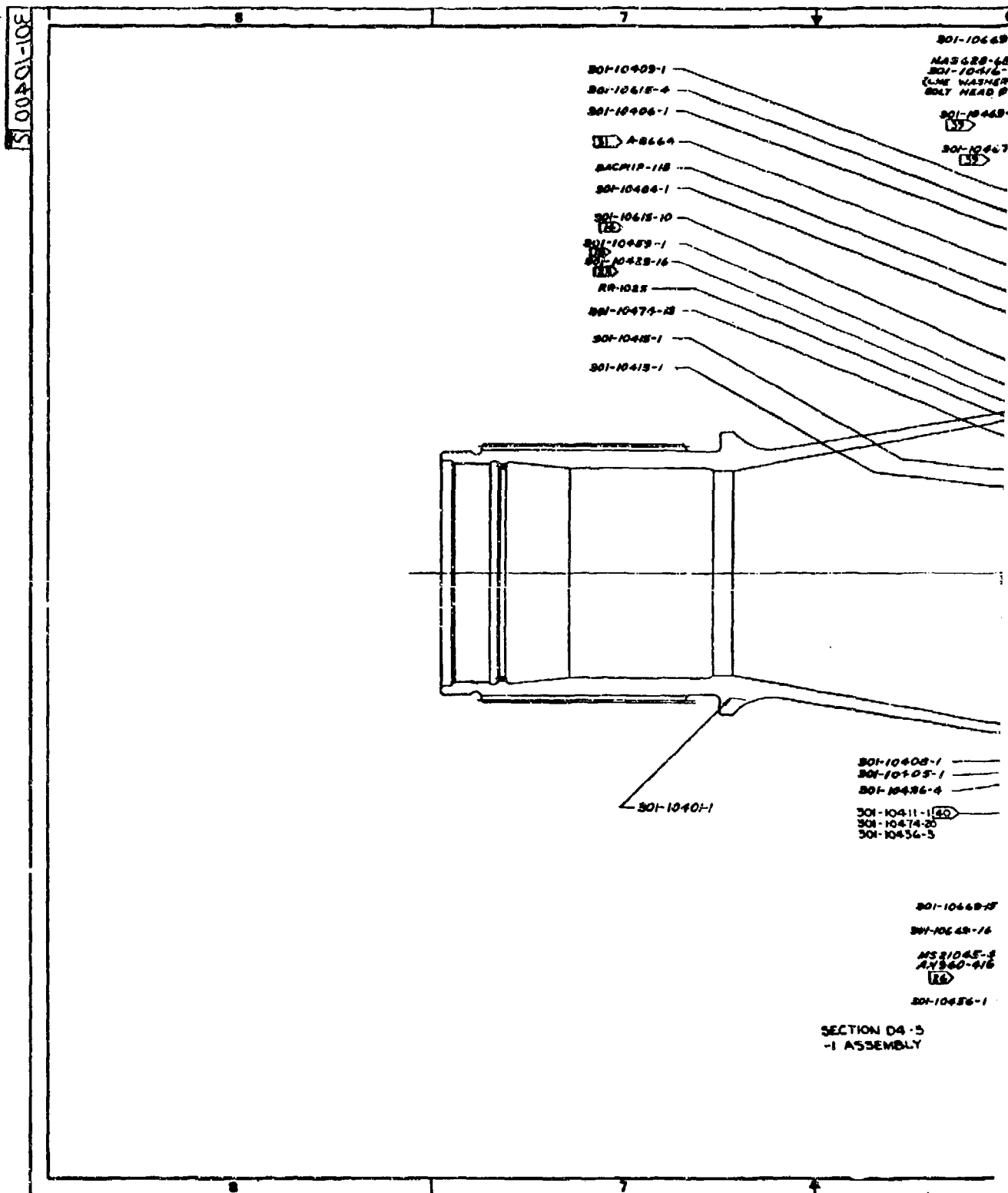
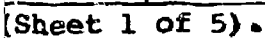
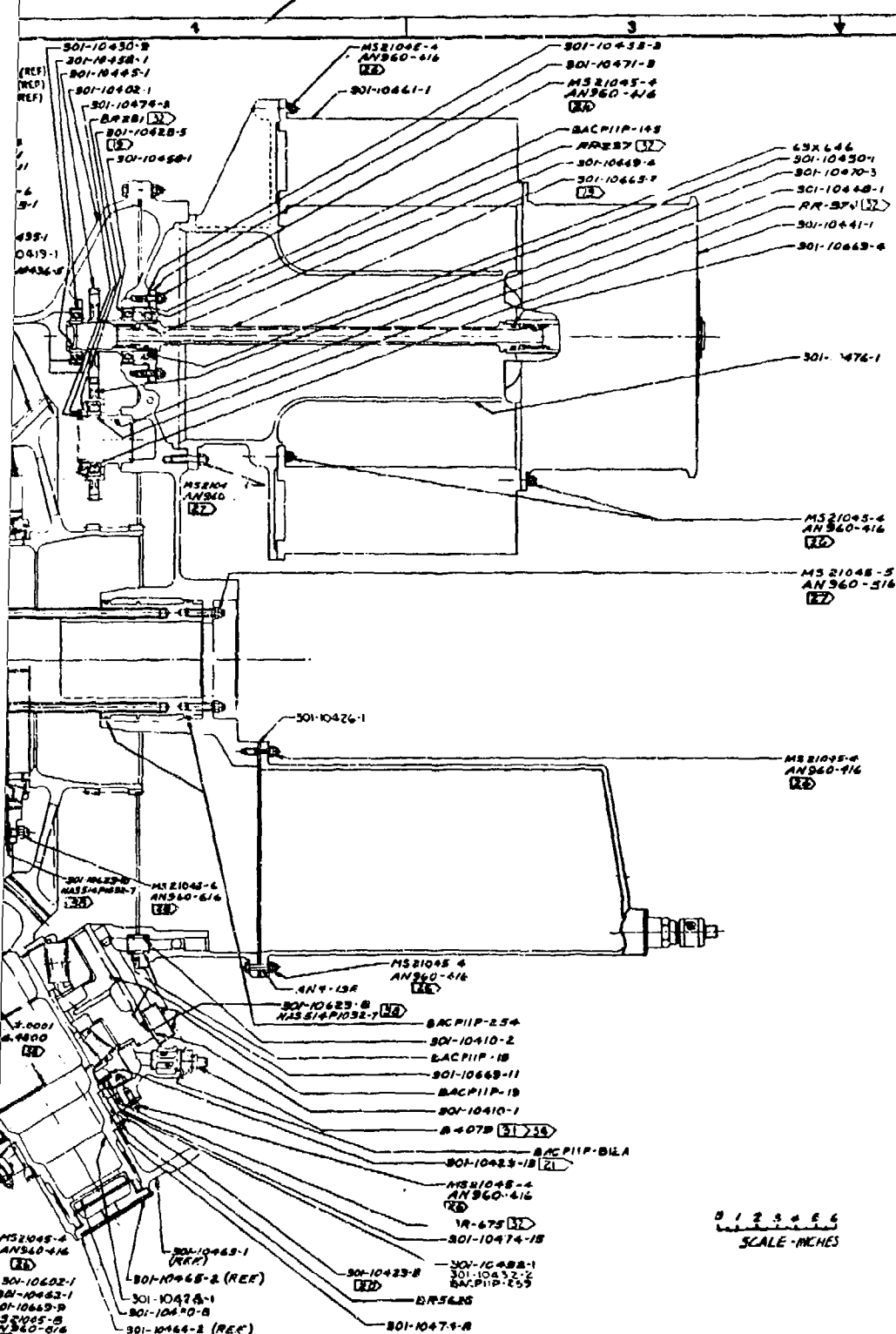


Figure 6. Aft Transmission Assembly (Sheet 1 of 5).



3



NOTES CONT

44. INSTALLATION AND REMOVAL OF BEARING RACES ON SHAFTS PER BOEING-VERTOL SPEC MS 21.06.
45. TORQUE PART TO
46. OBTAIN THIS DIMENSION BY USING MS20002-4 WASHERS UNDER NUT AS REQD.
47. TORQUE NUT TO
48. CHICAGO RAWHIDE MANUFACTURING CO. ELGIN ILLINOIS. CODE IDENT NR 00201
49. TORQUE PART TO
50. TORQUE BOLT TO 45 TO 55 IN. LBS.
51. TORQUE PART TO 50 TO 62 IN. LBS.
52. TORQUE PART TO
53. TORQUE PART TO 114 TO 140 IN. LBS.
54. TORQUE PART TO 100 TO 132 IN. LBS.
55. MEASURE & RECORD GEAR ASSEMBLY END PLAY FOR EACH GEAR ASSEMBLY BY SERIAL NO.
56. TORQUE PART TO
57. ALL BEARING RACES AND GEAR/BEARING SUPPORT CARTRIDGES TO BE INSTALLED USING OIL AS A LUBRICANT IF REQUIRED. DO NOT USE GREASE.
58. INSTALL SEAL WITH SPRING FACING OUTWARD AS SHOWN.
59. TUBE SUPPORTS TO BE INSTALLED WITH FLANGE DOWN USING HARDWARE FOR UPPER CASE AND RING GEAR AS SHOWN.
60. TUBE SUPPORTS TO BE INSTALLED WITH FLANGE UP USING HARDWARE FOR MAIN HOUSING AND RING GEAR AS SHOWN.
61. ONE (1) WASHER IS REQUIRED UNDER NUT WHEREVER 301-50325 TUBE SUPPORTS ARE REQUIRED. TWO (2) WASHERS ARE REQUIRED UNDER NUT ALL OTHER PLACES.

0 1 2 3 4 5 6
SCALE - INCHES

7540

4

NOTES CONT

44. INSTALLATION AND REMOVAL OF BEARING RACES ON SHAFTS PER BOEING-VERVOL SPEC MS 2106.

45. TORQUE PART TO

46. OBTAIN THIS DIMENSION BY USING MS20002-5 WASHERS UNDER NUT AS REQ'D.

47. TORQUE NUT TO

48. CHICAGO RAWHIDE MANUFACTURING CO.
ELGIN, ILLINOIS
CODE IDENT NO 80201

49. TORQUE PART TO

50. TORQUE BOLT TO 45 TO 55 IN. LBS.

51. TORQUE PART TO 50 TO 62 IN. LBS.

52. TORQUE PART TO

53. TORQUE PART TO 114 TO 140 IN. LBS.

54. TORQUE PART TO 100 TO 152 IN. LBS.

55. MEASURE & RECORD GEAR ASSEMBLY END PLAY FOR EACH GEAR ASSEMBLY BY SERIAL NO.

56. TORQUE PART TO

57. ALL BEARING RACES AND GEAR/BEARING SUPPORT CARTRIDGES TO BE INSTALLED USING OIL AS A LUBRICANT IF REQUIRED. DO NOT USE GREASE.

58. INSTALL SEAL WITH SPRING FACING OUTWARD AS SHOWN. TUBE SUPPORTS TO BE INSTALLED WITH FLANGE DOWN USING HARDWARE FOR UPPER CASE AND RING GEAR AS SHOWN.

59. TUBE SUPPORTS TO BE INSTALLED WITH FLANGE UP USING HARDWARE FOR MAIN HOUSING AND RING GEAR AS SHOWN.

60. ONE (1) WASHER IS REQUIRED UNDER NUT WHEREVER 301-50325 TUBE SUPPORTS ARE REQUIRED. TWO (2) WASHERS ARE REQUIRED UNDER NUT ALL OTHER PLACES.

REV	BY	DATE	REVISION
1	REVISED PER DCN	1/4/70	JEP
2	REVISED PER DCN	5-375	PCB

43X444
301-10450-1
301-10470-3
301-10448-1
R/P-374 (32)
301-10441-1
301-10443-4

301-10476-1

MS21048-4
AN360-416
(32)

MS21048-5
AN360-516
(32)

MS21048-4
AN360-416
(32)

0 1 2 3 4 5 6
SCALE - INCHES

DATE: 1/4/70		BY: JEP		THE BENDIS COMPANY	
CHECKED BY: JEP		DATE: 1/4/70		CORPORATE OFFICE	
APPROVED BY: JEP		DATE: 1/4/70		BATTLE BROS. COMPANY	
TITLE: AFT TRANSMISSION ASSEMBLY		PART NO: 301-10400		REV: 1	

301-10400B2

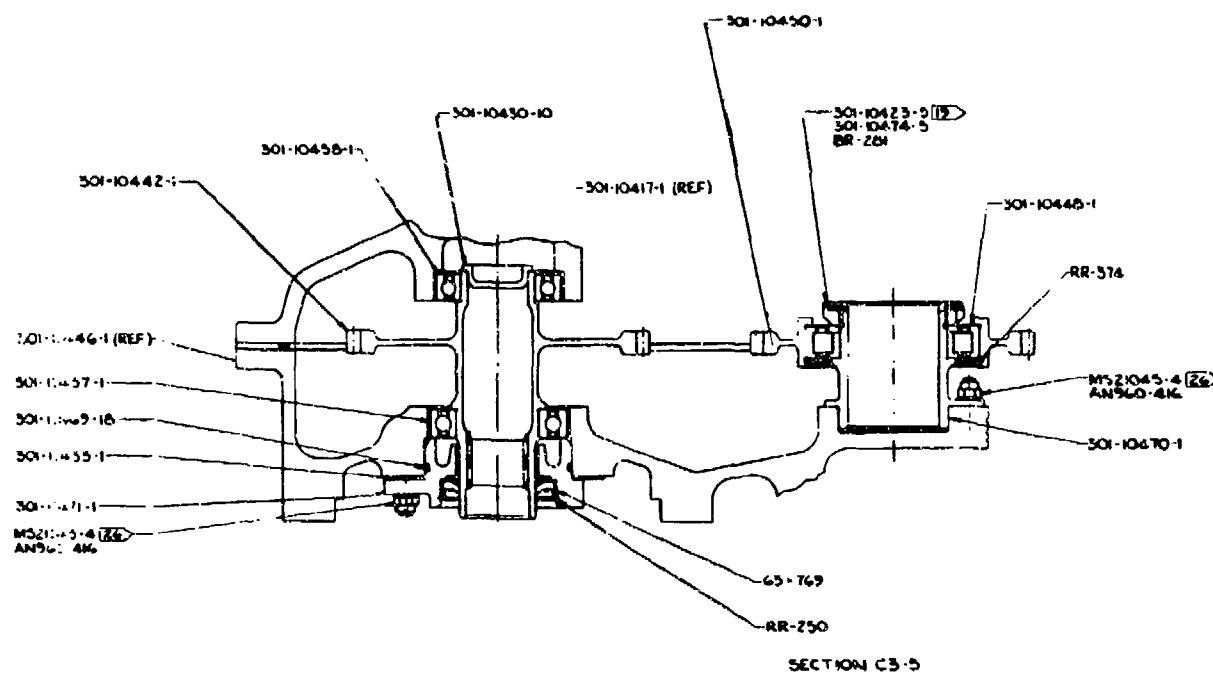
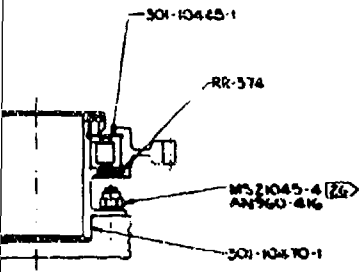


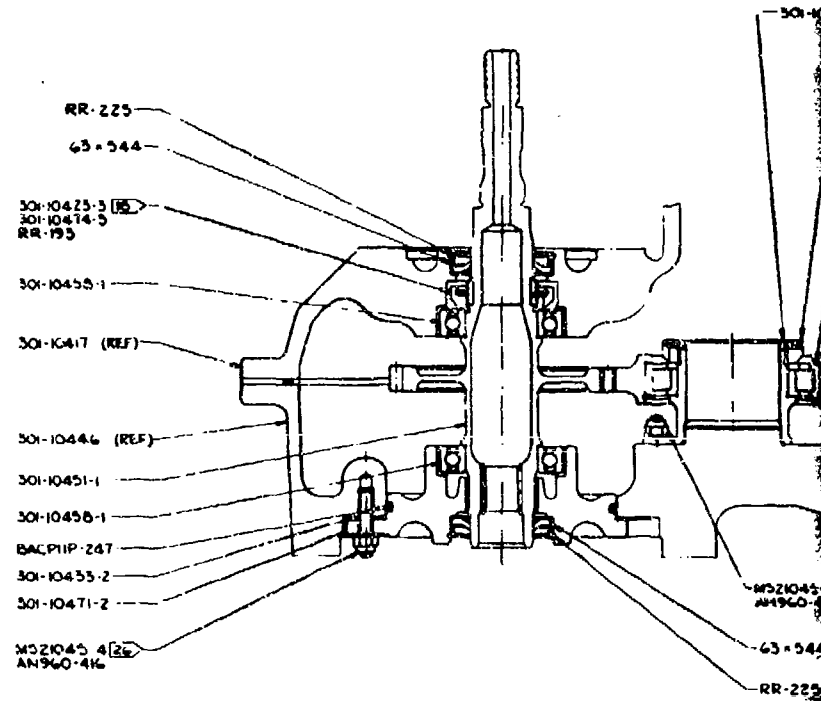
Figure 6. Aft Transmission Assembly (Sheet 2 of 5).

2 1

10423-5 (12)
10474-5
281



4 C3-5



301-10400 13

of 5).

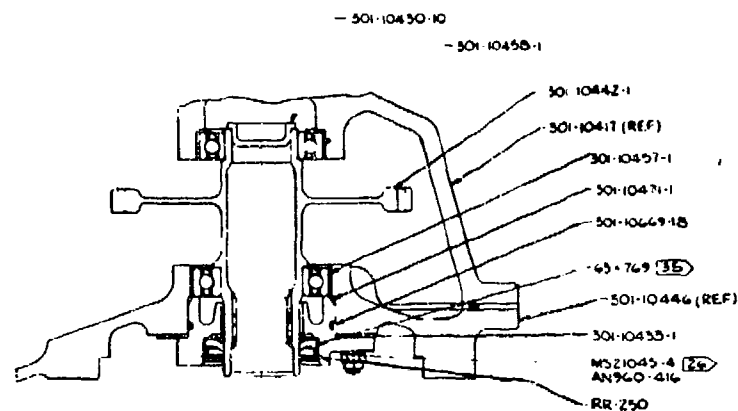
[illegible]

7540

J 77272 301-1040C

00701-105

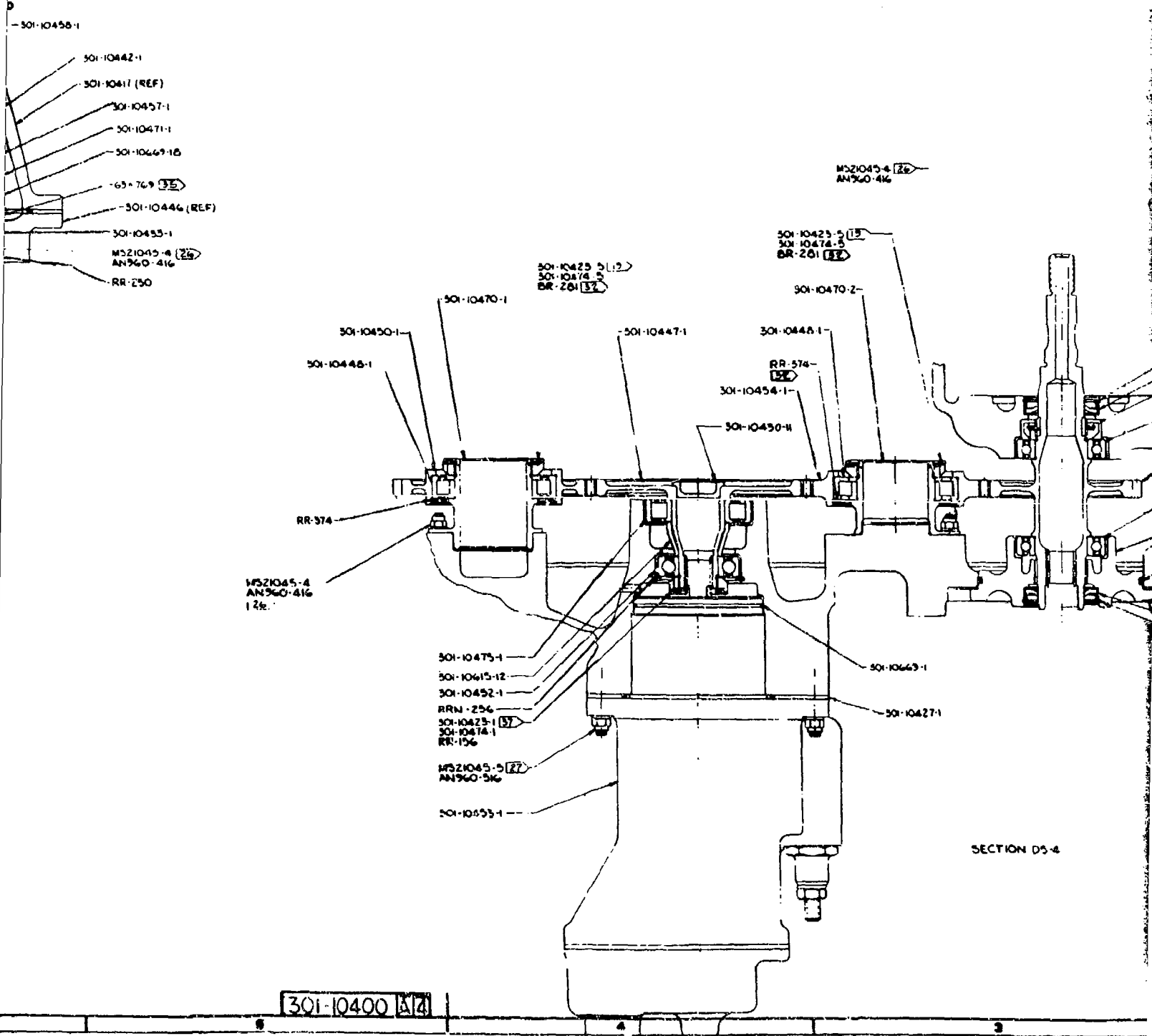
COA01-105



SECTION C6-B

Figure 6. Aft Transmission Assembly (Sheet 3 of 5).

2

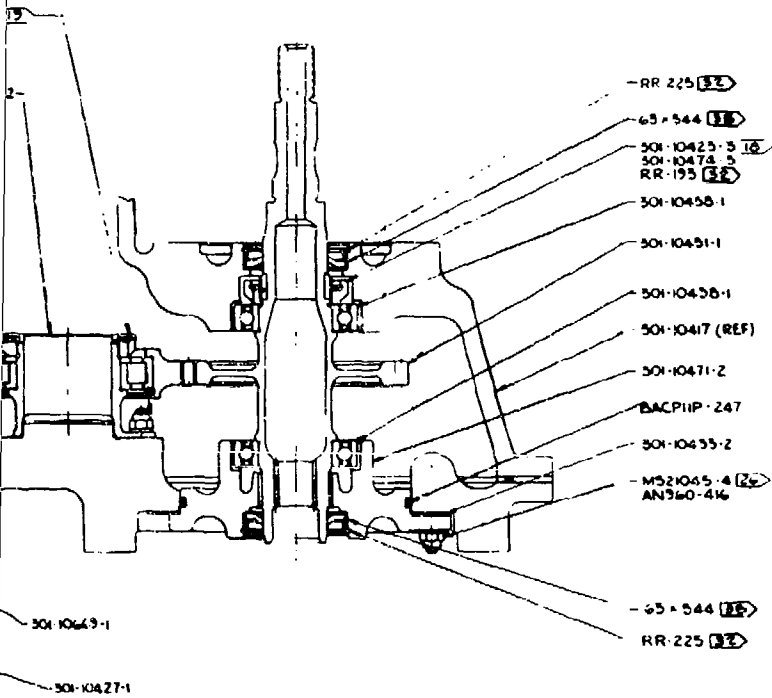


SECTION D5-4

301-10400 A74

5).

21045-4 (25)
 940-416



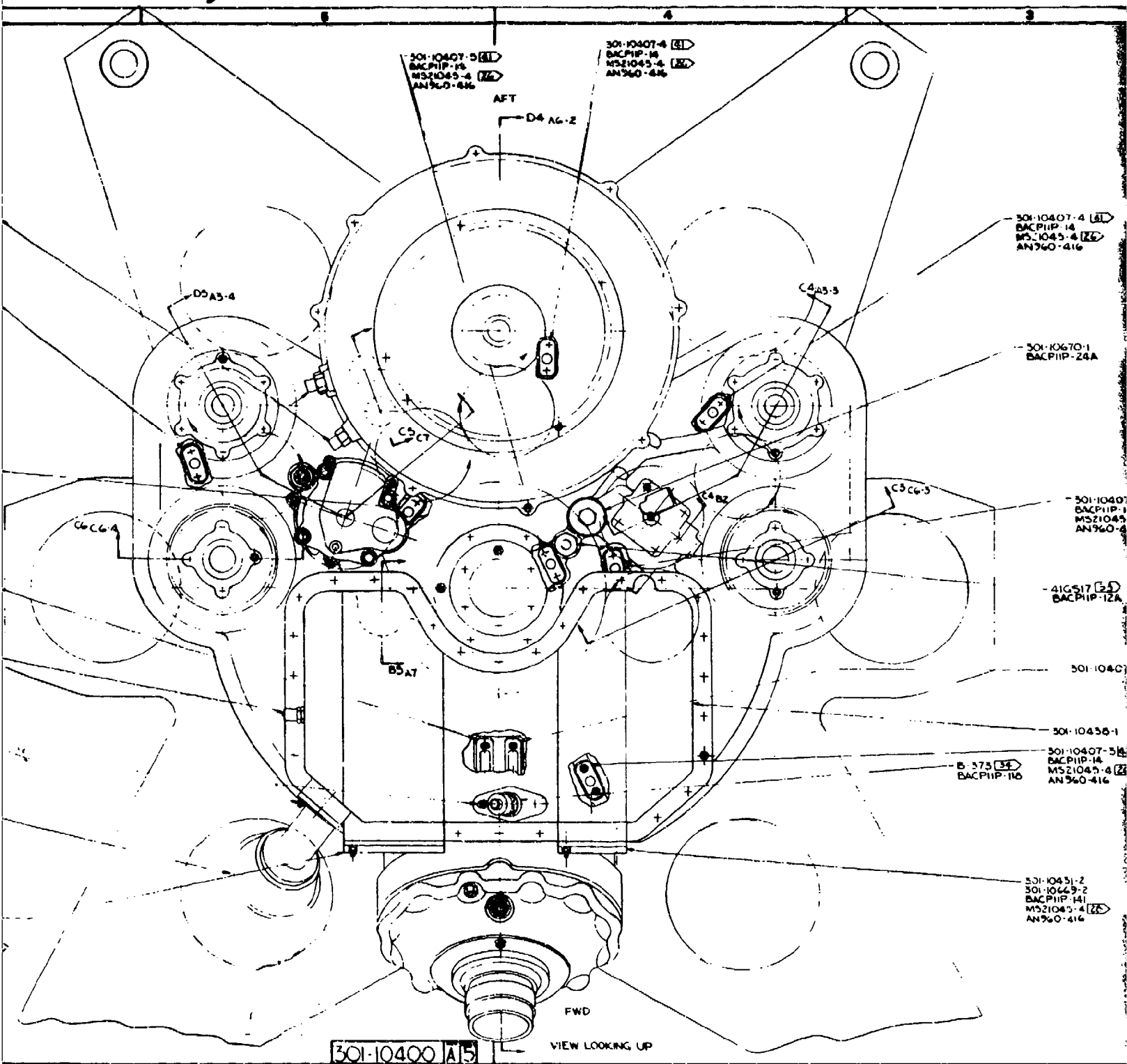
SECTION D5-4

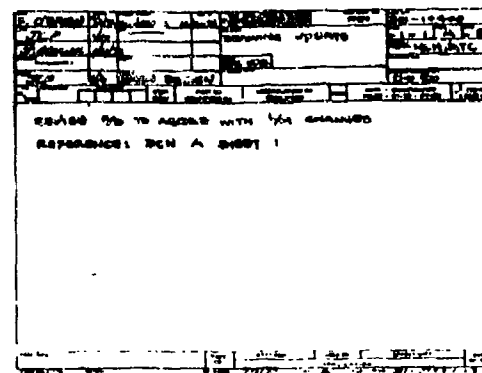
REVISION		DATE		BY	
1	REVISED PER DCN	10/10/78	10/10/78	10/10/78	10/10/78
DRAWING UPDATE					
REVISION 7/8 TO AGREE WITH 1/1 CHANGES					
REFERENCE: DCN A SHEET 1					

AFT TRANSMISSION ASSEMBLY	
301-10400	301-10400
301-10400	301-10400

301-10400 A4

2



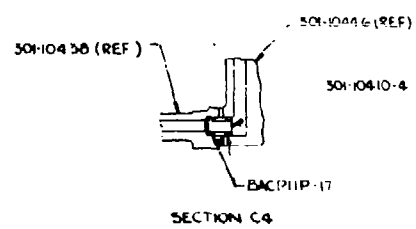


- 501-10670-1
BACP11P-24A

- 21G517 (33)
BAC.PHP-12A

301-10407-2 (REF)

- 301-10431-2
301-10449-2
BAC P11P-141
M521043-4 (28)
AN960-416



SECTION C4

SEA 050527 1 HIGH PRIORITY 1077 MAG SUPPLY		THE SECRETARY SECRETARY CHIEF OF STAFF AFT TRANSMISSION ASSEMBLY	
176 177 178 179 180 181 182 183 184 185 186 187 188 189 190 191 192 193 194 195 196 197 198 199 200	176 177 178 179 180 181 182 183 184 185 186 187 188 189 190 191 192 193 194 195 196 197 198 199 200	176 177 178 179 180 181 182 183 184 185 186 187 188 189 190 191 192 193 194 195 196 197 198 199 200	176 177 178 179 180 181 182 183 184 185 186 187 188 189 190 191 192 193 194 195 196 197 198 199 200

301-10400	2	301-10400	A5
-----------	---	-----------	----

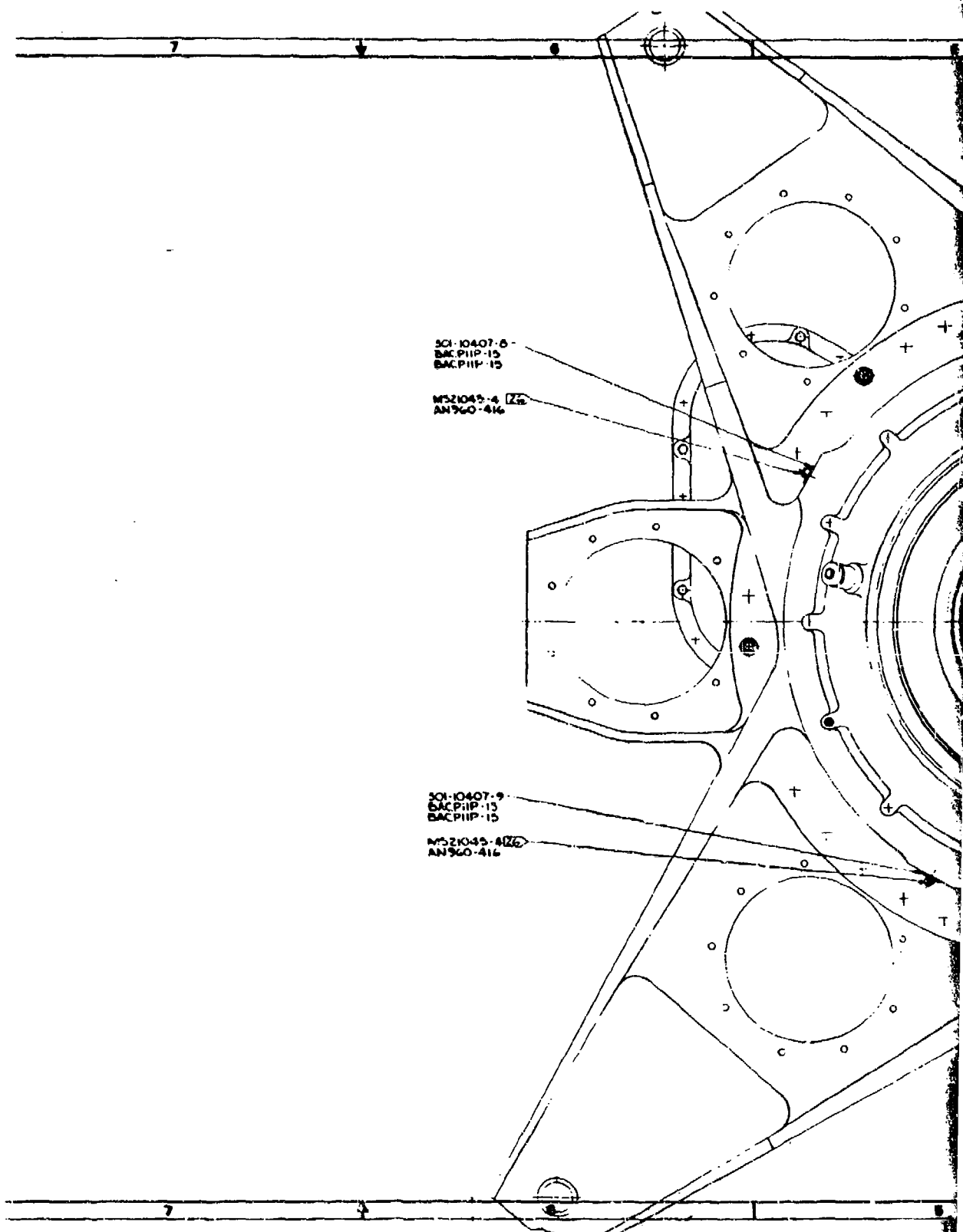
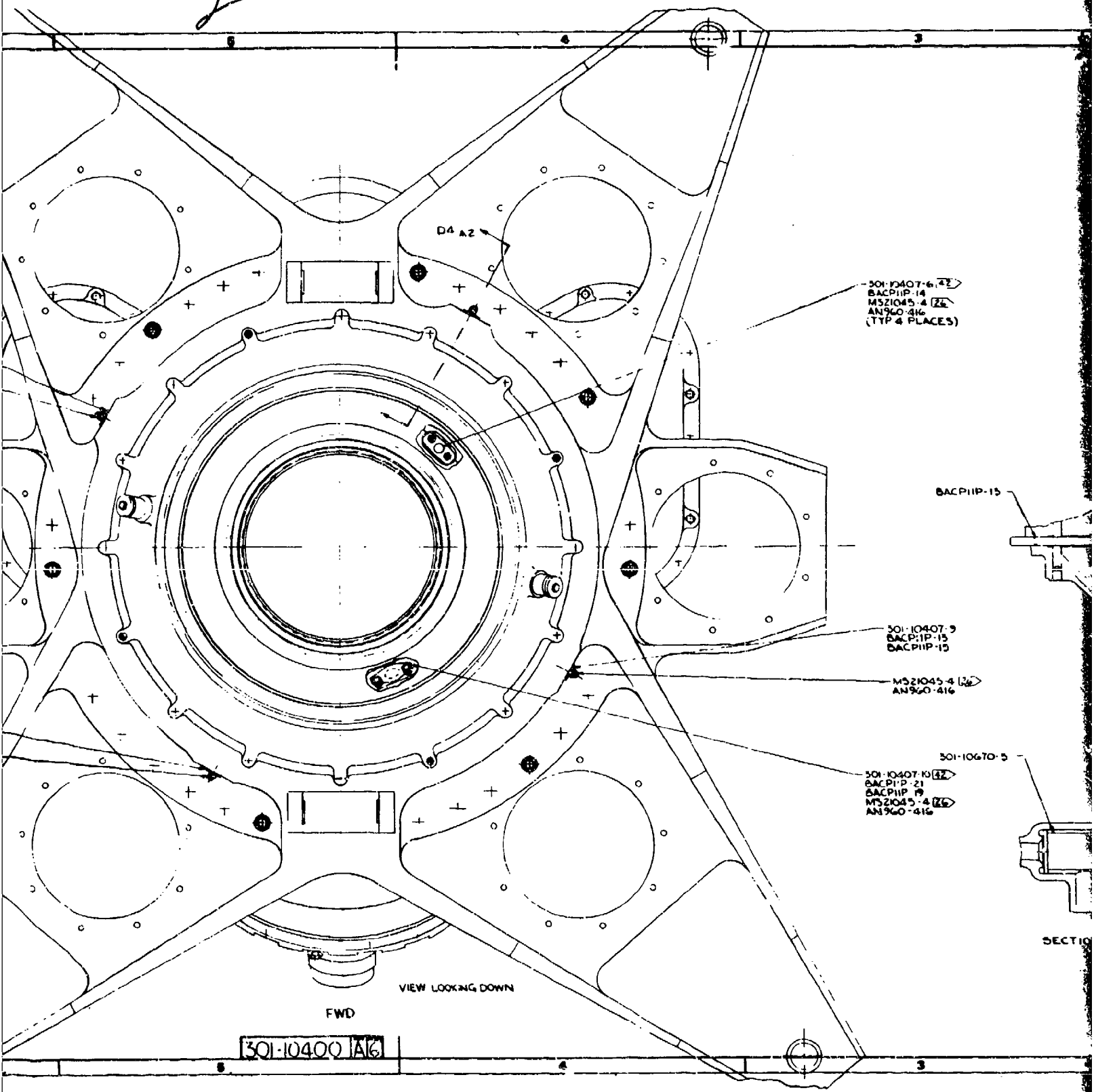


Figure 6. Aft Transmission Assembly (Sheet 5 of 5).

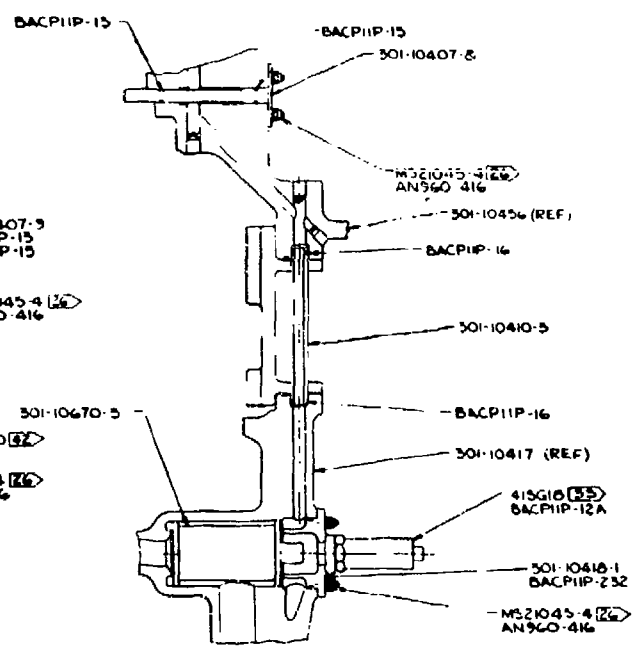
2



THIS SHEET ADDED

301-10400	
DESIGNED BY	DATE
CHECKED BY	DATE
DRAWING UPDATED	
REASON FOR UPDATE	
1. Added sheet 6 of 6.	

301-10407-6 (32)
BACP11P-14
MS21045-4 (26)
AN960-416
(TYP 4 PLACES)



SECTION D4

301-10400	
DESIGNED BY	DATE
CHECKED BY	DATE
DRAWING UPDATED	
REASON FOR UPDATE	
1. Added sheet 6 of 6.	

301-10400 (16)

AFT TRANSMISSION ASSEMBLY

301-10400

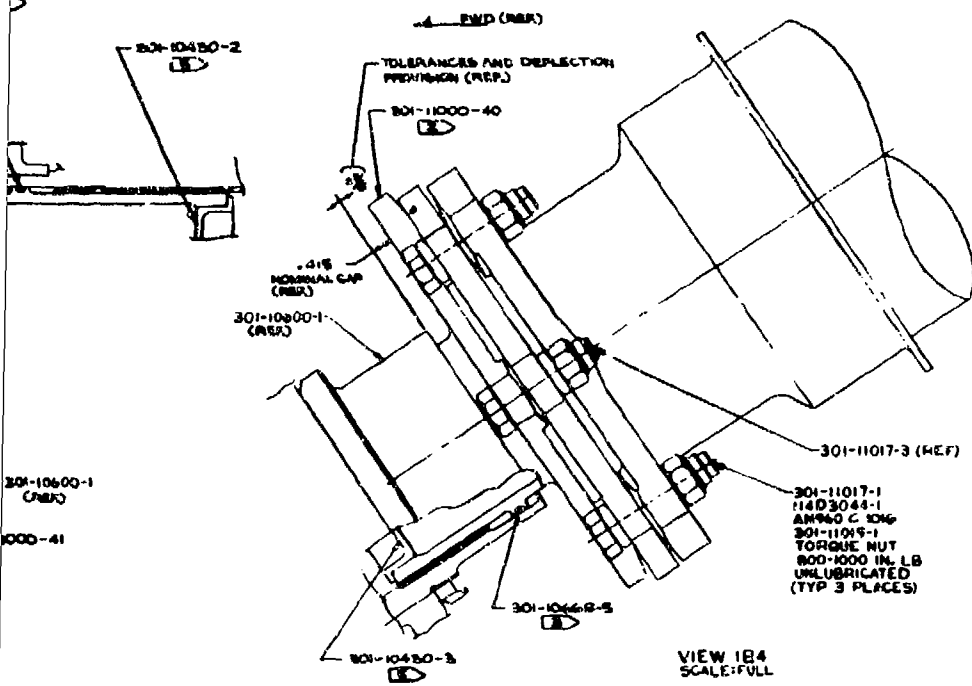
7540

Drive shafting outside the transmissions (Figure 7) is thin-wall aluminum tubing. Shaft sections are supported in grease-lubricated ball bearings at intervals to provide for subcritical operation. There are twelve sections of synchronizing shafting, nine forward and three aft, with each section approximately 60 inches long. Engine drive shafting is identical for each of the three installations. There are three shaft sections per engine, supported as the synchronizing shafting. All shafting is joined by flexible-metal-disc couplings to provide for angular misalignment. Axial location change is provided for by motion in the transmission shaft spline. Sliding splines are grease lubricated on assembly and sealed with static O-rings.

2 1

AND DEFLECTION
(REF.)

8B-6



301-10600-1
(REF.)

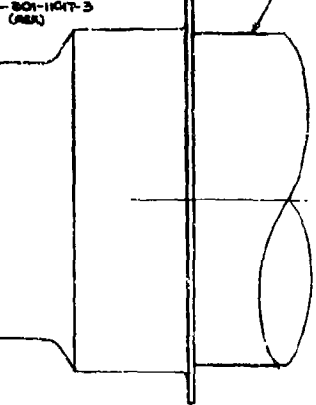
1000-41

VIEW 1B4
SCALE: FULL

301-11017-1
114D3044-1
AN 860 C 1046
301-11019-1
TORQUE NUT
800-1000 IN. LB.
UNLUBRICATED
(TYP 3 PLACES)

301-11017-3
(REF.)

301-11000-28

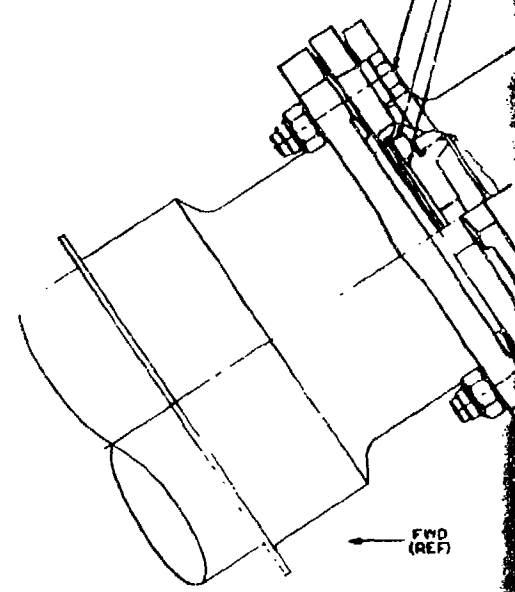


VIEW B6
SCALE: FULL

301-11017-1
114D3044-1
AN 860 C 1046
301-11019-1
TORQUE NUT
800-1000 IN. LB.
UNLUBRICATED
(TYP 3 PLACES)

301-11017-3
(REF.)

301-11017-1



FWD
(REF.)

301-11099-12

301-11017-1
114D3044-1
AN980 C 1046
301-11019-1
TORQUE NUT
800-1000 IN LB
UNLUBRICATED
(TYP 3 PLACES)

301-10464-2

301-10465-2

301-10400-1
AFT ZMSN ASSY (REF.)

301-11000-42

VIEW C3
SCALE: FULL

FWD
(REF)

301-11017-1
114D3044-1
AN980 C 1046
301-11019-1
TORQUE NUT
800-1000 IN LB
UNLUBRICATED
(TYP 3 PLACES)

301-11017-3
(REF)

GRAVE EXIT
(REF.)

CE

75
(REF)

5/32
(REF.)

COUPLING

4.33 (REF)

5.19 (REF)

VIEW B3
VIEW E3
SCALE

WL 295
(REF)

STA 201.429
(REF)

STA 199
(REF)

4 (REF)

STA 231.929 (REF)

COUPLING

STA 296.821 (REF)

COUPLING

STA 304.681 (REF)

COUPLING

STA 433.041 (REF)

COUPLING

STA 501.401 (REF)

COUPLING

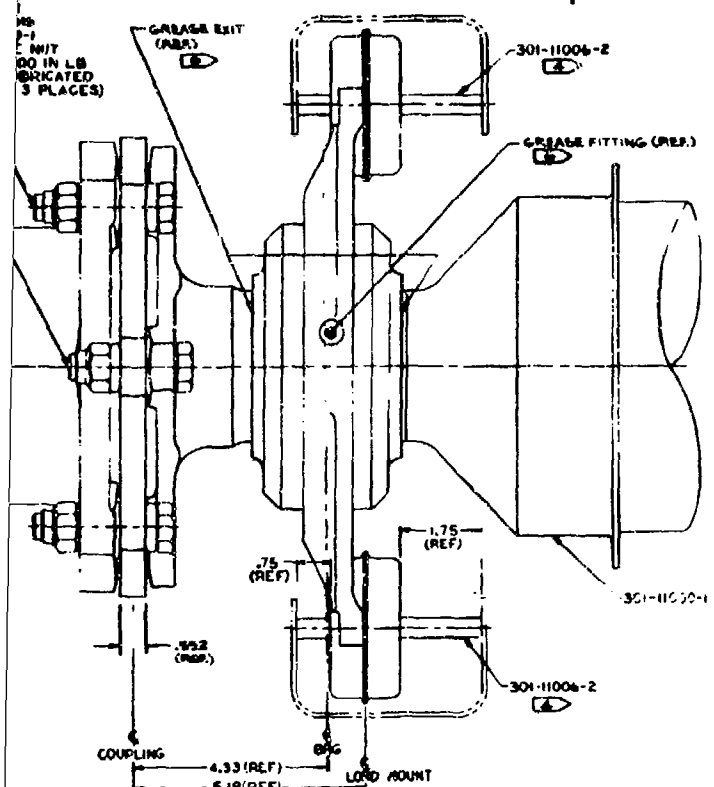
STA 547.171 (REF)

COUPLING

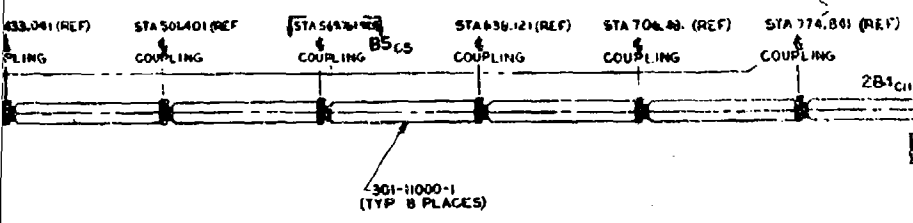
301-11000-28

SCALE: 2

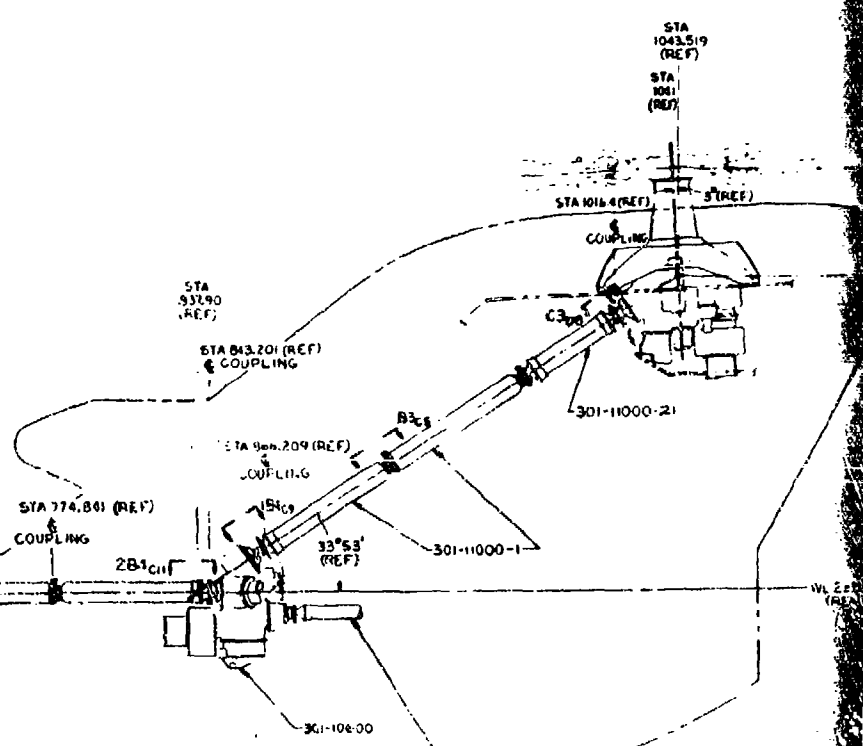
3



VIEW B5 (TYP 8 PLACES)
VIEW B3 (OPP) (TYP 2 PLACES)
SCALE: FULL



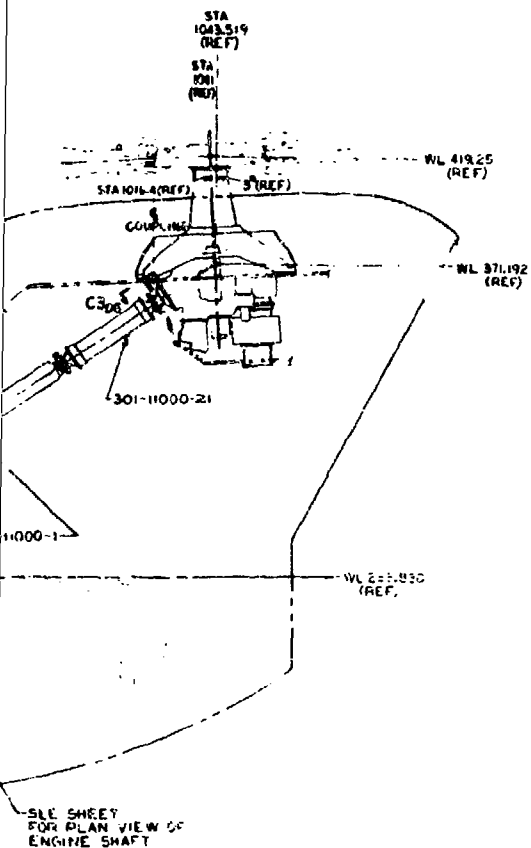
SCALE: 20:1



SEE SHEET
FOR PLAN VIEW OF
ENGINE SHAFT

301-11099 2

5



301-11099 2

<p>REVISIONS</p> <table border="1"><tr><td>1</td><td>AS SHOWN</td></tr><tr><td>2</td><td>AS SHOWN</td></tr><tr><td>3</td><td>AS SHOWN</td></tr><tr><td>4</td><td>AS SHOWN</td></tr><tr><td>5</td><td>AS SHOWN</td></tr><tr><td>6</td><td>AS SHOWN</td></tr><tr><td>7</td><td>AS SHOWN</td></tr><tr><td>8</td><td>AS SHOWN</td></tr><tr><td>9</td><td>AS SHOWN</td></tr><tr><td>10</td><td>AS SHOWN</td></tr></table>		1	AS SHOWN	2	AS SHOWN	3	AS SHOWN	4	AS SHOWN	5	AS SHOWN	6	AS SHOWN	7	AS SHOWN	8	AS SHOWN	9	AS SHOWN	10	AS SHOWN	<p>PLANS</p> <table border="1"><tr><td>1</td><td>AS SHOWN</td></tr><tr><td>2</td><td>AS SHOWN</td></tr><tr><td>3</td><td>AS SHOWN</td></tr><tr><td>4</td><td>AS SHOWN</td></tr><tr><td>5</td><td>AS SHOWN</td></tr><tr><td>6</td><td>AS SHOWN</td></tr><tr><td>7</td><td>AS SHOWN</td></tr><tr><td>8</td><td>AS SHOWN</td></tr><tr><td>9</td><td>AS SHOWN</td></tr><tr><td>10</td><td>AS SHOWN</td></tr></table>		1	AS SHOWN	2	AS SHOWN	3	AS SHOWN	4	AS SHOWN	5	AS SHOWN	6	AS SHOWN	7	AS SHOWN	8	AS SHOWN	9	AS SHOWN	10	AS SHOWN	<p>SHAFTING INST! SYNC AND ENGINE</p>
1	AS SHOWN																																											
2	AS SHOWN																																											
3	AS SHOWN																																											
4	AS SHOWN																																											
5	AS SHOWN																																											
6	AS SHOWN																																											
7	AS SHOWN																																											
8	AS SHOWN																																											
9	AS SHOWN																																											
10	AS SHOWN																																											
1	AS SHOWN																																											
2	AS SHOWN																																											
3	AS SHOWN																																											
4	AS SHOWN																																											
5	AS SHOWN																																											
6	AS SHOWN																																											
7	AS SHOWN																																											
8	AS SHOWN																																											
9	AS SHOWN																																											
10	AS SHOWN																																											
<p>77272 301-11099</p>		<p>77272 301-11099</p>																																										

7450

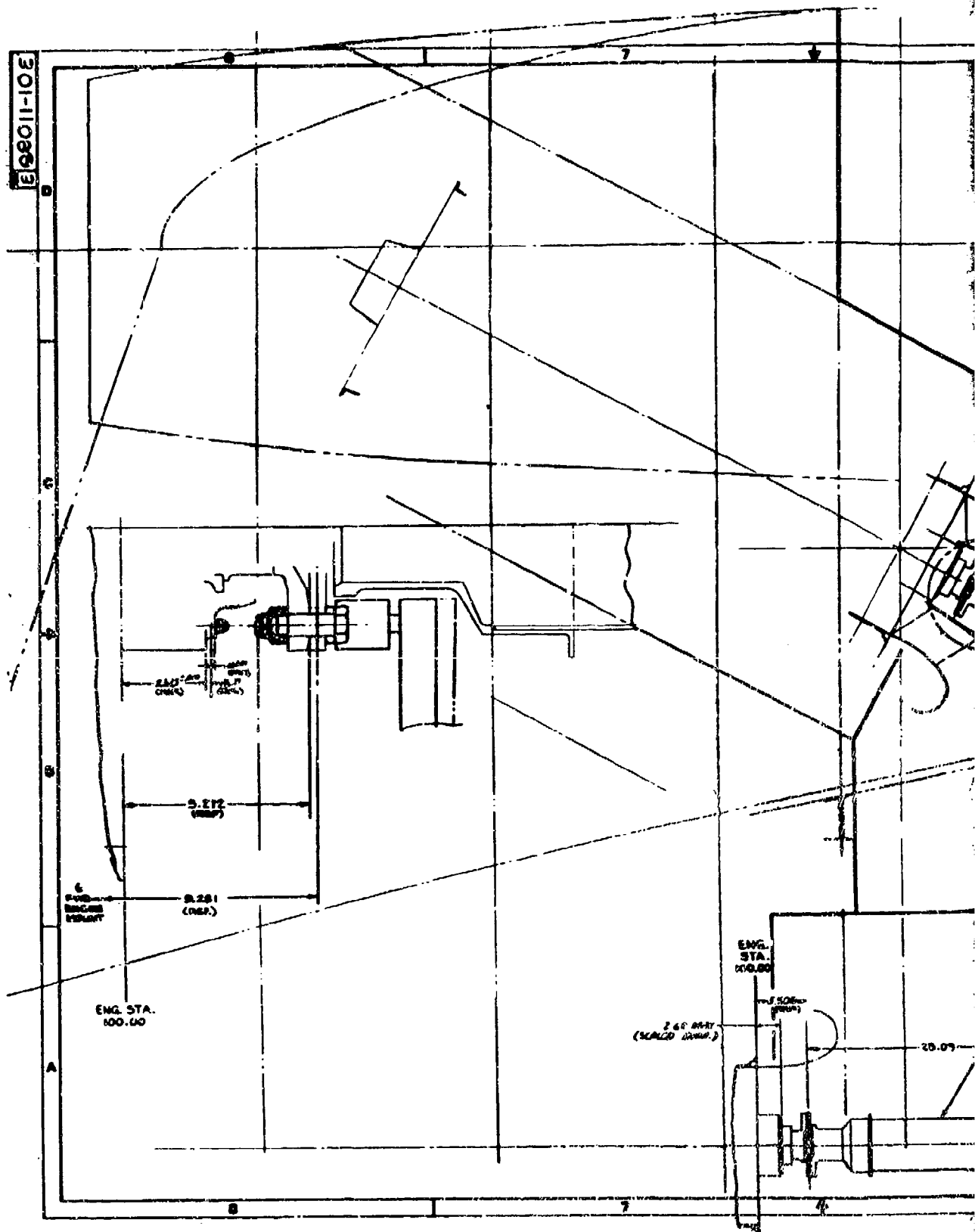
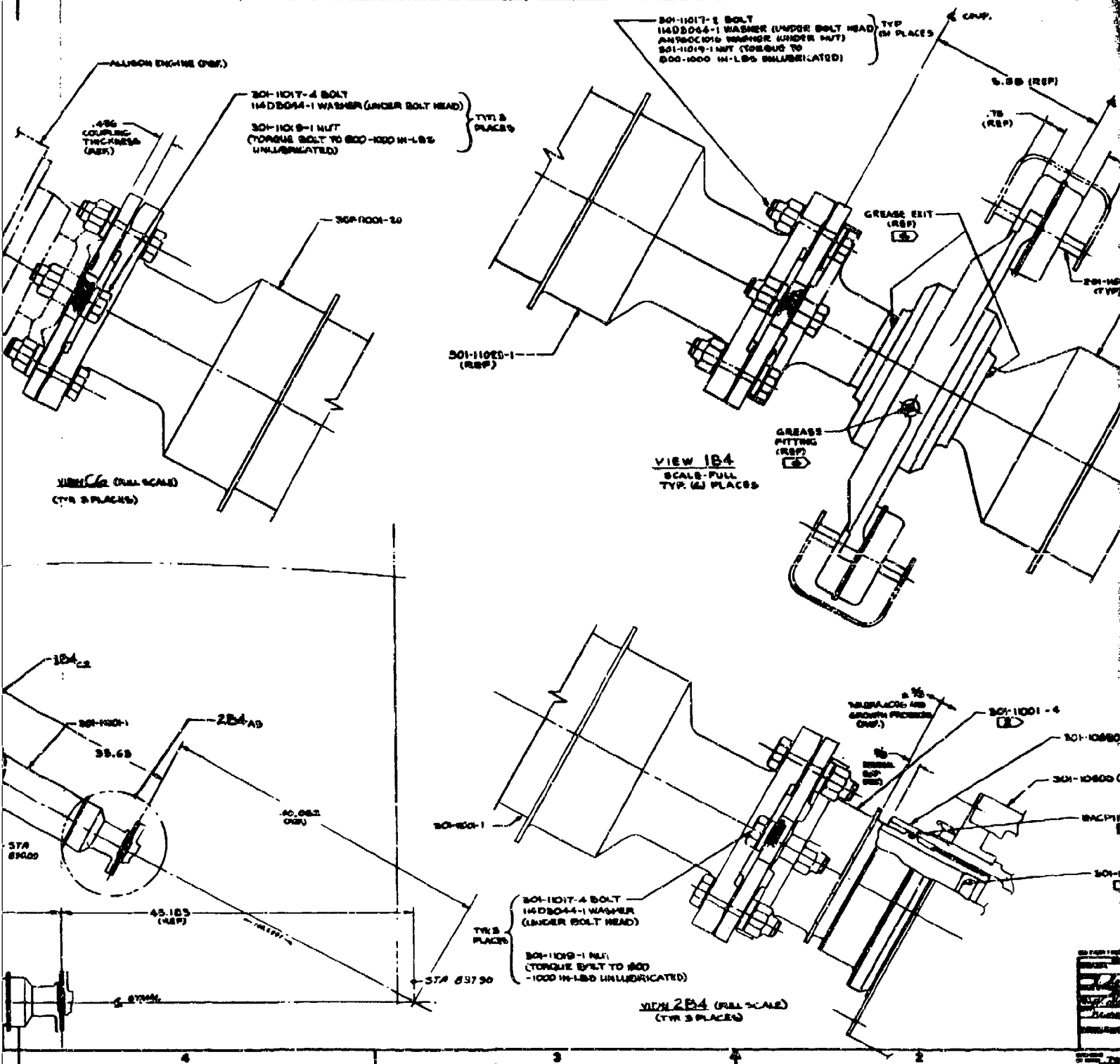
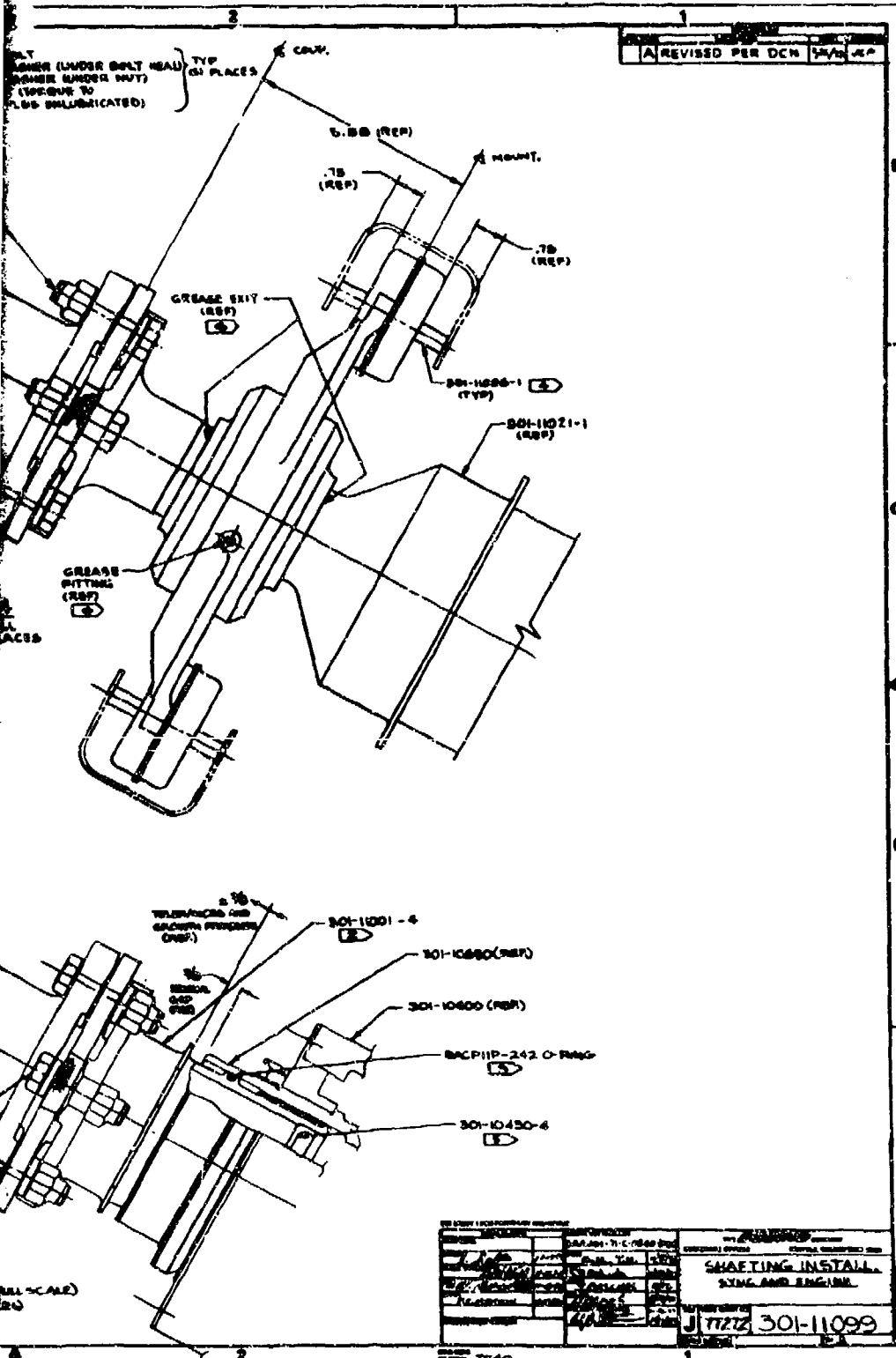


Figure 7. Shafting Installation, Sync and Engine
(Sheet 2 of 2).





4



REVISED PER DCN 1/1/64

301-11099 A3
301-11099 A3

SHAFTING INSTALL	
SYNCH AND ENGINE	
DATE	301-11099
BY	J 7722
CHECKED	
APPROVED	

3. DESIGN CRITERIA AND OBJECTIVES

DRIVE SYSTEM

The drive system shall include all parts necessary in the transmission of power from the engines to the lifting rotors. Such parts as shafting, shaft support, overrunning devices, gearboxes and speed reduction units external to the engines shall be included in the transmission system. The transmission system design shall be in accordance with the requirements of specification MIL-T-5955.

TRANSMISSION GEARBOXES

The transmission system shall include a forward rotor transmission assembly, an aft rotor transmission assembly, each of which shall contain all the accessory power takeoffs, and an engine combining gearbox assembly. Power shall be transmitted directly from each of the turbine engines into the combining gearbox. The combining gearbox shall transmit engine power to the forward and aft rotor transmissions. Gear ratios and nominal input shaft speeds shall be as follows:

<u>Gearbox</u>	<u>Gear Ratio</u>	<u>Input Speed</u>
Combining	1.44:1	11,500
Aft	51.2:1	7,986
Forward	51.2:1	7,986

The overall reduction ratio shall be 73.76:1.

Combining Gearbox Assembly

The engine combining gearbox assembly shall have spiral bevel pinion gears and helical gears receiving power from the engines. The spiral bevel input pinion gears shall mesh with a common spiral bevel collector gear, and the helical pinion shall mesh with a helical gear on a common shaft to combine three engine powers. The combined engine power shall be transmitted through shafting and flexible couplings to the forward transmission. The spiral bevel collector gear shall transmit power to the aft transmission through interconnecting shafts and couplings.

Forward Rotor Transmission

The forward rotor transmission shall be designed for power between the rotors and shall receive all rotor loads, lift, drag, and moments through the rotor shaft into the transmission. The assembly shall contain a set of spiral bevel gears driven by the interconnecting shaft and a two-stage planetary reduction gear assembly. The forward transmission shall incorporate provisions for installation of the blade deicing system slip-rings.

Aft Transmission

The aft transmission shall be similar to the forward transmission except for angle of input shaft and direction of rotor rotation.

General

- Tanks and pumps not protected by their location shall be self-sealing against 7.62 mm projectiles, or demonstration of transmission operation at normal power for 20 minutes after loss of main oil shall be required.
- Transmissions shall be sized for the steady torque values as required by the flight envelope and shall be designed for 3600 hours life. The design goal for transmission removal shall be 2000-hour MTBR with "on-condition" removal. The transmission subsystem bearings shall be designed for a B₁₀ life of at least 2000 hours.
- The natural frequency of the gear designs shall be substantially removed from gear tooth mesh frequencies and/or proper damping shall be provided.
- The design of the main transmission components shall take into consideration the growth potential of the engines. The transmission housing design shall be such that the torque carrying capacity can be increased to the design growth power without changing the transmission envelope.
- A means shall be provided for turning the drive system slowly and intermittently to enable maintenance personnel to position each rotor blade as required. A connection to

which a standard wrench or a crank can be applied shall be provided in the gear train of the forward rotor transmission to enable maintenance personnel to manually position rotors.

- Each transmission shall be capable of continuous operation in aircraft attitudes of 45° nosedown, 25° noseup, and 15° roll to either side. There will be no attitude restrictions on short duration uncoordinated aircraft maneuvers.
- Failure-detection sensors in the transmission shall include:
 - (1) Indicating Chip Detectors
 - (2) Oil Temperature
 - (3) Oil Pressure
 - (4) Clogged Filter
 - (5) Oil Screen Contamination
- The debris detector shall be located in the oil flow path and capable of inspection without oil drainage.
- Fail-safe structural mounting design shall be incorporated. In-flight failure of any single transmission mounting point shall not result in loss of the aircraft.

Lifting provisions shall be made for each applicable field-replaceable drive system component.

LUBRICATION SYSTEMS

The following requirements shall apply to all gearboxes:

- Each transmission shall have an integral lubrication and cooling system. Each oil cooler and blower shall be replaceable without removing transmission from aircraft.
- Each transmission shall have two active lubricating systems. The main system shall provide lubrication and oil cooling for all gears and bearings during normal operation. An auxiliary lubricating system, which bypasses the cooler shall supply additional oil only to the critical bearings and gears. Each system shall have a pump, filters, and monitoring devices and shall utilize separate oil transfer passages and distribution jets.

- Ground servicing with lube oil shall be accomplished by one man from inside the helicopter. The oil level gage shall be visible to the man servicing the transmission.
- The transmission filtration shall be a full-flow, single stage with a filter condition indicator. Filtration shall be 40 micron absolute. A bypass circuit shall be provided, operating on a delta-pressure principle. A down-stream screen with a .015-inch opening at the transmission shall be provided to preclude filter bypass material clogging the lube jets. This screen shall not have a bypass. Debris buildup shall be indicated by the oil pressure gage in the cockpit.
- The lubrication system shall be designed for use with oil conforming to MIL-L-7808 and MIL-L-23699.
- Transmission oil filters shall be replaceable with the transmission installed in the aircraft without draining the lubricating oil. Filter media shall be the disposable type.
- The maximum design bulk oil temperature shall be 300°F before cooler.
- Design oil heat rise shall be 50°F. A 10 percent trapped air fraction shall be used for pump and sump volume calculations.
- Oil cooler air inlet temperature shall be 125°F maximum.
- Power losses shall be calculated on the basis of:
 - Combiner Transmission - Any two engines at 8300 hp with third engine out (worst cooling case).
 - Rotor Transmissions - 60 percent power, worst case condition, to any single rotor.

Component power losses based upon experience, with the spiral bevel gears 0.60 percent to 0.50 percent per mesh depending upon velocity and planet stages 0.65 percent per stage. Accessory drives shall be 1.0 percent per mesh, based upon average accessory power.

- Pressure limits shall be:

	<u>Main</u>	<u>Auxiliary</u>
— Component Proof Pressure	400 psi	300 psi
-- Maximum Pump Pressure (Norm. Operating Temp -65°F)	160 psi max adjustable	60 psi max adjustable
— Design Operating Pressure at Oil Jets	90-100 psi	30-35 psi

- Minimum jet size shall be 0.030 inch.
- An emergency lubrication system shall be provided to enable continued transmission operation after any single 12.7 mm ballistic hit. A minimum of 20 minutes operation is required. The emergency system shall be directed to critical main power gears and bearings.
- A minimum of two jets shall be directed at main power train bearings.
- Sumps shall be sized for 15-second oil retention time (25% of flow).
- Oil passages shall be integral with the major transmission components.
- Breathers shall limit case pressure to 0.5 psig.

ACCESSORIES

- Duplicated accessories (lube pumps, hydraulic pumps, generators, auxiliary generators) shall be separated and driven by independent accessory gear trains.
- The following units shall be driven by the forward and aft rotor transmissions:

	<u>Forward</u>	<u>Aft</u>
Lube Pump (Main and Auxiliary)	2	2
Blower	1	1
Main Generators	} Identical Drive Pads	0
Deicing Generators		2
Hydraulic Pumps	2	2
Flight Control Generators	2	1

- Accessories shall be easily accessible for maintenance or removal and replacement with the transmission mounted in the helicopter.
- Failure of an accessory shall not result in replacement of transmission (i.e., accessory jamming shall not be transmitted to main transmission as spline quill will fail in shear).

ROTOR BRAKE

The rotor brake shall include the support housing, caliper assembly, shaft and disc. The brake shall be hydraulically actuated. The rotor brake disc and/or head assembly shall be replaceable without removing the transmission from the aircraft. The head assembly shall be replaceable without disturbing the disc.

- A rotor system brake shall be incorporated in the combining gearbox assembly separate from any synchronizing device shafting.
- The rotor brake assembly shall be capable of a minimum of 400 normal service stops without replacement of components with the total rotor stopping time not to exceed 60 seconds with the engines off.
- In the event of a rotor brake caliper or disc failure, the system shall preclude damage to critical dynamic components.
- The rotor brake shall be capable of one emergency stop from 156 rotor rpm within 30 seconds with the engines off.
- The rotor brake actuation system shall provide an interlock to prevent brake actuation when the engine control levers are advanced beyond the ground idle position.
- The rotor brake shall prevent rotor rotation on engine start-up and with engines at ground idle power.

DRIVE SHAFTS

The forward, aft and combining transmission shall be interconnected by drive shafting operating at approximately 8000

rpm. The engine to combining gearbox shaft shall operate at 11,500 rpm. The shafting shall consist of sections of aluminum tubes, supported by grease lubricated bearings and interconnected with flexible steel couplings. Shaft connection (coupling) bolts shall be self-retaining against loss or omission of nut.

- The drive shafting shall be designed for static strength in conjunction with the appropriate structural factors as specified in Section 4.
- Shafting bearings shall be designed with the objectives of 300-hour intervals between periodic inspections.
- The drive shafting shall be capable of transmitting limit rated torque for 30 minutes after sustaining any random hit from a 7.62 mm projectile.
- Structural clearances around the shaft shall be arranged to prevent the entrapment of loose objects which could damage the rotating shaft. A minimum of one-inch clearance shall be provided.
- Drive-shaft mounts shall be replaceable without requiring removal of shaft sections or flexible couplings.
- Shaft-flexible couplings shall accommodate angular misalignment of 1/4 degree across each coupling.
- Shaft mounts shall be protected from environmental deterioration.
- All transmissions shall have provisions for alignment at installation and for checking alignment without removal from the helicopter.
- Misalignment of shaft couplings shall not exceed 0.25 degree at full power.
- Unbalance forces on rotating shafting and gears shall not exceed 25 pounds.
- The combining gearbox shall contain the overrunning clutches. A one-way overrunning clutch shall be provided for each engine. It shall be located between the engine

and the first gear stage. The overrunning clutches shall be designed to withstand 1.5 times the single-engine torque rating without permanent deformation or yielding of the shaft, sprags or cage. The overrunning clutches shall be designed for continuous operation should one engine be shut down. Positive lubrication shall be provided to the clutch with oil dams to keep sprags submerged in oil during operation. The clutch assembly shall be field replaceable as a unit or as part of a larger sub-assembly. Clutch shall be capable of continuous operation at full overrun and at any differential speed.

4. DRIVE SYSTEM STRUCTURAL CRITERIA

GENERAL REQUIREMENTS

Design Rating

The basic drive system design rating shall be 17,700 hp. This value represents 110 percent of the power required to hover Out of Ground Effect (OGE) at sea level, 95°F at a gross weight of 118,000 pounds. The One-Engine-Inoperative (OEI) rating shall be 8075 hp per engine, which is the maximum power available at sea level, 59°F.

Design Speeds

The design engine output and rotor speeds shall be 11,500 rpm and 155.9 rpm, respectively.

Life Requirements

Component Life

All components, except bearings, shall have a retirement life of not less than 3600 hours.

Bearing Life

Bearings shall be designed for a B-10 life of not less than 2000 hours at cubic mean loads.

Rotor Brake

The rotor brake system shall be designed for not less than 400 normal stops between component replacements.

LOADS DETERMINATION CRITERIA

Torque Distribution Between Rotors

The distribution of torque between rotors shall be 60 percent of the total to either rotor for all loading conditions.

Ultimate Loads

The ultimate loads shall be obtained by applying an ultimate factor of safety of 1.50 to the limit loads.

Limit Flight Loads

Torque

The limit torque loads shall be obtained by applying a limit torque factor of 1.50 to the steady component of the fatigue torque loads.

Rotor Shaft Loads

The limit rotor shaft loads shall be obtained by considering a limit flapping angle of 20 degrees and a limit load factor of 2.5 g's.

Limit Landing Loads

The limit rotor shaft loads shall be obtained as specified in Reference 1.

Limit Ground Loads

The limit rotor shaft loads shall be obtained by considering a 60-knot wind, from any horizontal direction, acting on a stationary rotor system with the blades either folded or extended. The aircraft shall be considered to be level.

Fatigue Loads

Steady Torque

The steady torque loads shall be equivalent to the basic design or growth rating. The more critical of the AEO or OEI condition shall be employed.

Alternating Torque

The alternating torque loads shall be +12 percent of the steady torque loads.

Bearing Fatigue Torque

The cubic mean torque loads shall be obtained on the basis of the mission profile defined in Table 1, the power requirements for the conditions in the profile shall be evaluated at sea level, 50°F.

Steady Rotor Loads

The steady rotor loads shall be obtained from the following equations. A flap angle of 8 degrees shall be employed.

$$\text{Thrust} = .56 \text{ (GW) (BASED ON EXTREME C.G. POSITION)} \quad (1)$$

$$\text{Shear} = \frac{3}{2} \text{ (T) (A)} \quad (2)$$

$$\text{Moment} = \frac{B}{2} \text{ (CF) (e) (A)} \quad (3)$$

Where GW = Gross Weight
B = Number of Blades per Rotor
T = Rotor Thrust
CF = Blade Centrifugal Force
e = Horizontal Hinge Offset
A = Flap Angle

The following values shall be employed for the above parameters:

Gross Weight	118,000 pounds
Number of Blades	4
Centrifugal Force	170,000 pounds
Hinge Offset	26 inches

Alternating Rotor Loads

The alternating rotor loads shall be the following percentages of the corresponding steady rotor loads:

Thrust	10 percent
Longitudinal Shear	20 percent
Pitching Moment	20 percent

Rotor Shaft Bearing Loads

The cubic mean rotor shaft bearing loads shall be obtained from Equations (1), (2), and (3) in conjunction with the mission profile and the flap angle spectrum shown in Table 1.

Crash Loads

The crash loads for drive system components shall be obtained by applying the following ultimate crash load vectors:

Forward	20 g
Vertical	20 g
Lateral	10 g

TABLE 1. MISSION PROFILE

Conditions	Percent of Time per Occurrences	
	ASRD Profile (Ref. 7)	Modified for Cubic Mean Power
Ground Conditions	1.0	1.0
Takeoff	(400)	-
Steady Hovering	30.0	30.0
Turns Hovering	(2000)	-
Control Reversals Hovering	(2000)	-
Sideward Flight	2.0	2.0
Rearward Flight	1.0	1.0
Landing Approach	(750)	-
Forward Flight: 20% V _H	5.0	5.0
40% V _H	2.0	2.0
50% V _H	2.0	2.0
60% V _H	5.0	5.0
70% V _H	8.0	9.0
80% V _H	9.0	11.5
90% V _H	16.0	18.0
100% V _H	1.0	1.0
115% V _H	1.0	1.0
Takeoff Power Climb	3.0	3.0
Full Power Climb	4.0	4.0
Partial Power Descent	(500)	-
Right Turns	2.5	-
Left Turns	2.5	-
Control Reversals	(300)	-
Pullups	(250)	-
Power to Autorotation	(40)	-
Autorotation to Power	(40)	-
Autorotation - Steady	0.5	2.0
Autorotation - Left Turn	0.2	-
Autorotation - Right Turn	0.2	-
Autorotation - Control Reversal	0.3	-
Autorotation - Landing	0.3	-
Autorotation - Pullup	(40)	-
Power to OEI	(20)	-
OEI to Power	(20)	-
OEI to Steady	0.6	-
OEI - Left Turn	0.1	-
OEI - Right Turn	0.1	-
OEI - Control Reversal	0.1	-
OEI - Landing	0.1	-
OEI - Pullup	(20)	-
Ground-Air-Ground	(100)	-
Power Dives	2.5	2.3
Gross Weight	Percent Time	Note: 1. Parentheses are maneuvers per 100 flight hours. 2. No RPM, altitude, or CG split is taken.
78,000 lb	45	
118,000 lb	50	
147,500 lb	5	

The crash loads shall be considered to act separately in their respective directions.

Rotor Starting Loads

A rotor starting procedure shall be developed to prevent the torque from exceeding the specified design steady torque during rotor starting.

Rotor Braking Loads

Design Requirements

The rotor brake system shall be designed to accomplish the following:

- Hold the rotors stationary against the application of ground idle torque from the engines.
- Stop the rotors in a total of 45 to 60 seconds from hover rpm with the engines off.
- Hold the rotors stationary in 45 knot winds with the engines off.
- Stop the rotors in a total of 30 seconds from hover rpm with engines off, under emergency conditions without catastrophic failure of the brake assembly.

Limit Loads

The limit rotor braking loads shall be obtained by applying a limit factor of 2.0 to the loads resulting from application of the design rated torque of the brake system.

Fatigue Loads

The rotor braking fatigue loads shall be the loads resulting from application of the design rated torque of the brake system. A total of 10,000 brake application cycles shall be considered.

Sprag Clutch Loads

Design Torque

The clutch design torque shall be obtained by applying a factor of 2.0 to the steady component of the fatigue torque loads.

Limit Torque

The clutch limit torque shall be obtained by applying a factor of 1.50 to the clutch design torque.

Accessory Loads

Design Loads

The design loads applied to accessory drive components shall be those corresponding to the maximum design rating for the particular accessory.

Limit Loads

The accessory drive limit loads shall be obtained by applying a factor of 1.50 to the design loads.

ANALYSIS CRITERIA

Only special analysis methods are defined herein. Standard structural analysis procedures shall be applied to all other components.

Gear Teeth

The gear-tooth bending and contact stresses and flash temperatures shall be analyzed by the following procedures:

Spur	Computer Program R-23
Helical	Computer Program R-23
Spiral Bevel	Computer Program R-20

The torque employed for the gear-tooth analysis shall be the steady component of the fatigue torque loads. The analyses are in accordance with AGMA Standards (References 2, 3, 4, 5, 6 and 7).

Bearings

Ball Bearings

Ball bearing lives shall be analyzed by the procedure of Computer Program S-04. A factor of 5.0 shall be applied to the calculated life for Consumable Electrode Vacuum Melt (CEVM) M-50 and CEVM carburized steels. Analysis is based on methods presented in References 8, 9 and 10.

Cylindrical Roller Bearings

Cylindrical roller bearing lives shall be analyzed by the procedure of Computer Program S-04. A factor of 5.0 shall be applied to the calculated life for CEVM M50 and CEVM carburized steels. Analysis is based on methods presented in References 8, 9 and 10.

Planetary Bearings

Cylindrical and spherical roller planetary bearing lives shall be analyzed by the procedure of PLANET 1 Computer Program (Reference 11). An experience factor of 3.06 shall be applied to the calculated life for CEVM M50 and CEVM carburized steels.

Tapered Roller Bearings

Tapered roller bearing lives shall be analyzed by the procedure of TAPER 1 Computer Program (Reference 12). A factor of 3.0 shall be applied to the calculated life for CEVM carburized steel.

Planetary Gears

The stresses in the ring sections of planetary gears shall be analyzed by the following procedures:

Sun Gears	Computer Program RNGANL 51-1
Planet Gears	Computer Program PLANET 2
Ring Gears	Computer Program RNGANL 51-1

The analyses are based on standard elastic ring equations.

ALLOWABLES

Gear Teeth

Stresses

The main drive gear-tooth stresses shall not exceed the following at the basic design rating:

<u>Gear Type</u>	<u>Bending Stresses</u>	<u>Contact Stress</u>
Spur & Helical	47,000 psi	188,000 psi
Spiral Bevel	47,000 psi	260,000 psi

Tooth Backup

The gear tooth backup thickness shall not be less than the tooth height. In the case of high contact ratio gears, the height of a standard tooth at the same diametral pitch shall be used.

Gear Shafts

The deflections of gear shafts at the bearings shall not exceed the following for the three-engine operation condition:

<u>Bearing Type</u>	<u>Maximum Slope</u>
Ball	0.0010 inch per inch
Roller	0.0004 inch per inch

Spline Teeth

Stresses

The spline tooth bearing stresses shall not exceed the following at the basic design rating:

<u>Spline Type</u>	<u>Steel Splines</u>	<u>Titanium Spline (Hub)</u>
Fixed	12,000 psi	5,000 psi (Nylon Coated)
Working (Nonlubricated)	4,000 psi	---
Working (Lubricated)	6,000 psi	---

L/D Ratio

The spline contact length to pitch diameter ratio shall not exceed the following in the rotor drive system:

<u>Spline Type</u>	<u>Maximum L/D</u>
Fixed	1.00
Working	0.50

Aluminum Drive Shafts

The alternating torsional stress at the riveted end connections of aluminum drive shafts shall not exceed a net section, unconcentrated level of ± 2000 psi.

Torsional windup between rotors (including transmissions) shall not exceed 3.75 degrees at rated power.

Torsional stiffness of the shaft system shall be such that undesirable torsional amplifications do not appear within the operating range.

Lateral stiffness shall be such that first elastic mode shall be at least 10 percent above maximum operating rpm, power on or off.

The shaft mount stiffness shall be such that the first rigid body mode will not be excited by 1/rev, 4/rev, or 8/rev frequencies.

Planetary Components

Ring Stresses

The planetary gear concentrated alternating ring stresses shall not exceed the following at the basic design rating:

<u>Gear Type</u>	<u>OD Stress (R = -1)*</u>	<u>ID Stress (R = -1)*</u>
Sun	$\pm 33,500$ psi	$\pm 22,000$ psi
Sun-Carrier	$\pm 19,500$ psi	$\pm 12,500$ psi
Planet	$\pm 47,500$ psi	$\pm 47,500$ psi
Ring	$\pm 44,000$ psi	$\pm 44,000$ psi

*These values represent the CH-47C experience level at 6800 hp.

Carrier Post Stresses

The planet carrier post concentrated steady bending stresses shall not exceed the following at the basic design rating.

<u>Stage</u>	<u>Bending Stress (Steel)*</u>
First	7,700 psi

*These values represent the CH-47C experience level at 6800 hp.

Ring Gear Deflection

The radial deflection of ring gears shall not exceed 0.005 inch at the basic design rating.

Carrier Post Deflection

The slope of the planet carrier posts shall not exceed 0.005 inch per inch at the basic design rating.

Sprag Clutches

Stresses

The contact stresses in the sprag clutch shall not exceed the following: (OEI Torque = 44,250 in-lb)

<u>Clutch Torque</u>	<u>Contact Stress</u>
200 Percent OEI Torque	450,000 psi
300 percent OEI Torque	600,000 psi

Deflections

The combined radial deflection of the clutch components shall not exceed 80 percent of the available cam rise at 200% OEI torque.

Slippage

No slippage, overturning, or structural failure shall occur at 300 percent OEI torque.

MISCELLANEOUS CRITERIA

Bolt Torque

Where maximum preload is required at bolted connections, the installation torque shall provide a preload of 80 percent of the bolt yield strength.

Fail-Safe Transmission Mounting

The rotor transmission mounting system shall, in addition to the other criteria defined herein, be designed and analyzed for the following conditions with any one of the four mounting points eliminated.

Ultimate Loads

The ultimate loads shall be obtained by applying an ultimate factor of safety of 1.0 to the limit loads.

Fatigue Loads

The fatigue loads shall be identical to those defined under Fatigue Loads.

Life Requirement

The transmission mounting system shall be capable of operating for 100 hours with any one of the four mounting points failed.

MISSION PROFILE

The mission profile is presented in Table 1.

HLH FLAPPING ANGLE SPECTRUM FOR ROTOR BEARING CUBIC MEAN LOADS

<u>Flapping Angle (Degrees)</u>	<u>Occurrence (Percent)</u>	<u>Flapping Angle (Degrees)</u>	<u>Occurrence (Percent)</u>
3.2	3.75	5.2	1.3
3.4	4.90	5.3	3.4
3.7	3.25	5.4	0.5
4.0	10.00	5.5	3.9
4.1	3.55	5.6	0.8
4.2	8.30	5.7	1.8
4.3	3.75	5.8	2.3
4.4	5.35	6.0	9.9
4.5	3.80	7.0	1.0
4.7	1.75	8.0	1.0
4.8	7.60	9.0	1.0
5.0	11.60	10.0	1.0
5.1	4.50		

5. FABRICATION

Techniques used to manufacture major components are described in this section. Machining and heat treatment of major components was performed at the Speco Division of Kelsey Hayes, Springfield, Ohio. Major castings were supplied by Hitchcock Industries, Inc., Minneapolis, Minn. Rotorshaft titanium forgings were supplied by ALCOA, Cleveland, Ohio.

UPPER COVER (P/N 301-10456)

This part was made from a 7075-T411 aluminum hand forging. The forging was a rectangular billet that was formed into a partial hemisphere in a hydraulic press. The outer contour and center hole were created by band sawing (Figure 8). The result was a large (7000 lb) crude partial forging. To allow for the runout of the band saw cut of some four inches in the sixteen-inch thickness of forging, the part was considerably oversize from drawing requirements. As a result, the part would not clear the Omni Mill tape controlled machine used to contour mill the part. Many extra hours were required on a Lucas boring mill to rough out the forging to drawing forging size.

A wood model (Figure 9) was made and used to check out the tapes for control of the Omni Mill. Considerable time was taken to debug the tapes using the wood model. This time was considered excessive relative to the few number of parts (four) to be made.

As a result of the time taken to debug the numerical control tapes on the above ATC cover, the decision was made on the new prototype cover (P/N 301-65025) to make a wood model and finish the part to size on a Keller duplicating mill. This part was made from a forged rectangular billet weighing approximately 11,000 pounds, which was nearly the limit of Alcoa capacity. The part was essentially machined from the solid.

In production, the part could be made from a contour die forging. However, in these large sizes that approach the vendor limit to even produce a billet, a true contour forging would require three or more stages at a cost of \$80,000 or more per stage. Only large quantity production could justify the tooling cost.

ROTOR SHAFT (P/N 301-10401) (Figure 10)

The rotor shaft was made from a 6Al-4V titanium alloy forging. The bearing support journal was coated with tungsten carbide by detonation flame spray method. The output spline was silver plated. Titanium requires some coating or plating for mating surfaces to avoid fretting.

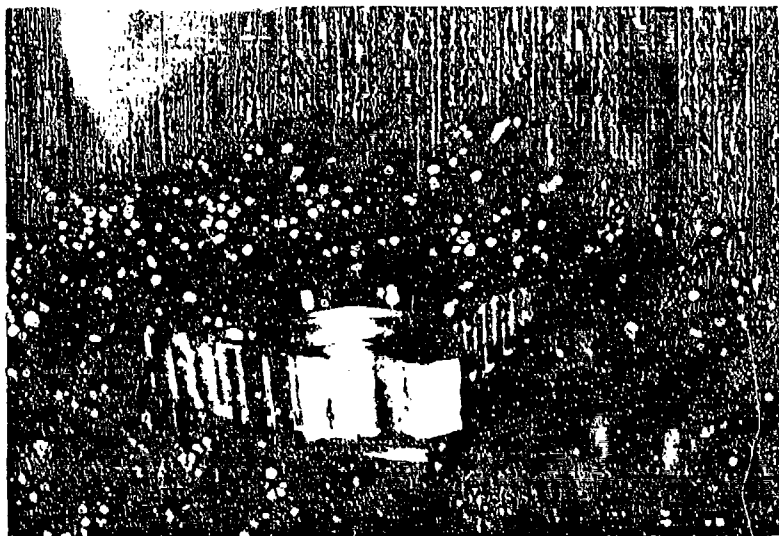


Figure 8. Rough-Sawn Forging.

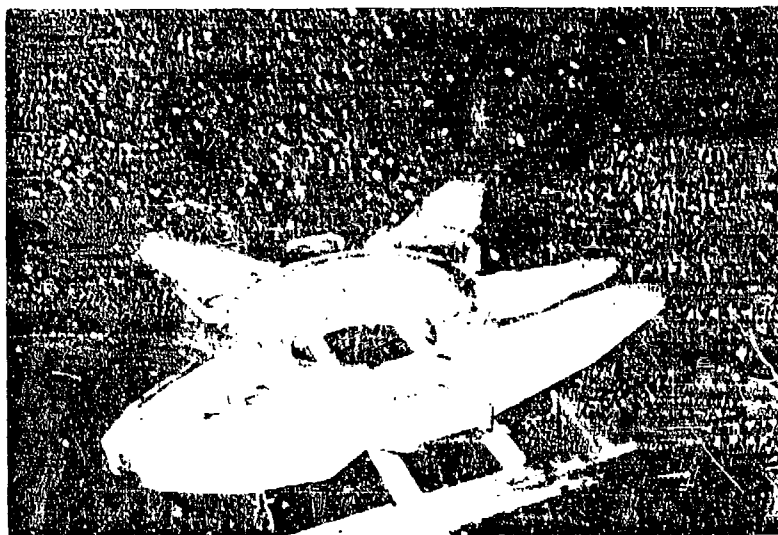


Figure 9. Machined Cover.



Figure 20. Comparison of HLH and CH-47 Aft Rotor Shafts.

Silver plating the shaft spline was a problem as anticipated. Titanium requires special cleaning and treatment prior to plating to secure proper bonding. The procedures as finally evolved included glass bead cleaning, alkaline cleaning, electrochemical etching in an acid solution, and a nickle strike before the silver plating. The final inspection criteria was that the plating should resist a mechanical scrape-off test.

The bearing journal was tungsten carbide coated by the detonation (D-gun) process to provide a hard surface as on interface to the mating bearing. Grinding the coating requires a diamond wheel. The shaft was designed with undercuts so that diamond wheel ground only on diameters and hence did not require corner radius on wheel.

Improper setup resulted in grinding through the carbide coating. There was a distinct sudden red burst that made grinding into the titanium shaft obvious. It was then necessary to have the vendor (Linde) electrochemically strip the coating completely. The carbide coating cannot be added to a coated surface.

The prototype rotor shaft posts were protected by silver plating the mating planet bearing inner ring. Initially, coated steel sleeves were shrunk on and finished at assembly; however, the sleeves worked off during running. Carbide coating of the posts was desired but tooling cost was prohibitive. For carbide coating, the part must be rotated about the center of each post since the detonation gun cannot be rotated about the part.

It was necessary to perform Zyglo inspection by using aerosol application of penetrant due to size and weight of the part.

Spline inspection for involute and spacing was achieved only on a dummy piece made at each shaft and set up on the hobber. Lead check was made in the hobber using the machine for axial motion and an indicator attached to the machine.

BEVEL GEARS (P/N 301-10677 AND 301-10419)

The shaft diameter of the bevel pinion gears exceeded the Gleason work head spindle hole. The pinion was mounted ahead of the spindle with a special adapter. The adapter length plus the pinion mounting distance exceeded the normal work head maximum mounting distance. The Gleason 27 machine capacity was extended by removing the workhead stops and moving the head to partially overhang the machine base. Additional hold-down bolts were added to secure the work head column.

The aft sun-bevel gear (Figure 11) was ground in the Gleason 137 grinder with the gear mounted in an adapter ahead of the

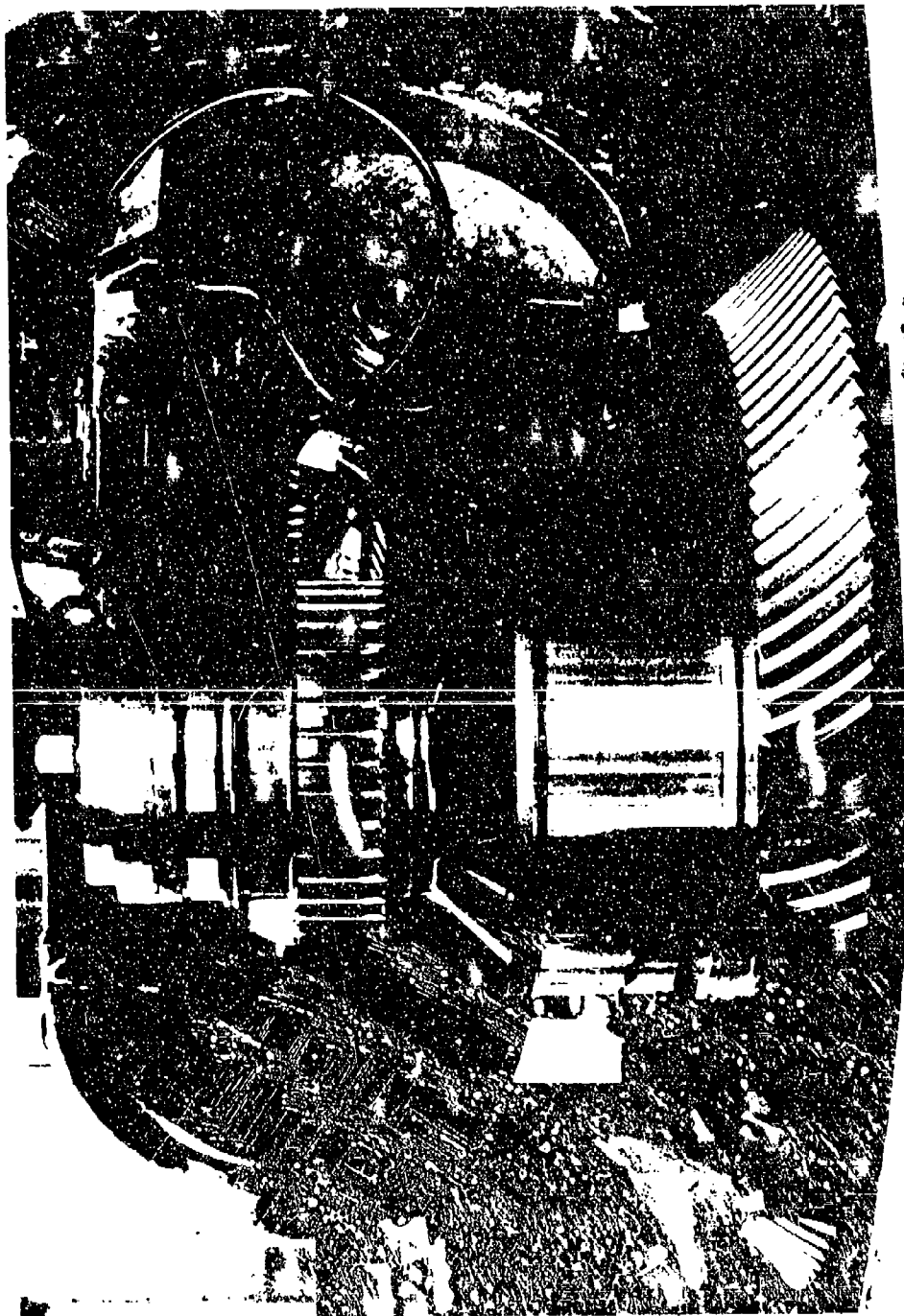


Figure 11. Aft Spiral Bevel Gear (301-10419) Sun Gear
Being Hobbed.

work head spindle because of the large shaft size. The two spur gears were ground in the Michigan 36 Helical Grinder. The large capacity was required only to clear the bevel gear blank, not for the spur gear size.

The most difficult problem was the quenching of the sun bevel gear for hardening. The limiting feature was not the diameter on the gear (27 inch), which is well below the Gleason 36 press capacity. Rather, it was the gear shaft length of approximately 21 inches, which is beyond the normal 8-inch vertical throat opening of the quench press with dies in place. It was necessary to assemble the dies and hot part outside the press and then move the entire assembly into the press. By making several trial runs, the vendor achieved this assembly in 2 minutes.

In quenching, the gear section distorted excessively in relation to the shaft section until the quench die assembly was modified to provide pilots to center quench plugs at each end. The pilots held the shaft square to the large flat bevel gear section.

MAJOR CASTINGS (P/N 301-10417 AND 301-10608)
(Figures 12 through 15)

The major castings were cast from ZE-41 magnesium alloy by Hitchcock Industries. The combiner housing casting (301-10608) weighed 250 pounds when cleaned up. Approximately 1000 pounds of magnesium were poured for each casting. Seventy-five percent of this was in risers, gates, and other areas necessary to distribute and vent the molten magnesium.

Cored holes for filters and screens were off location, requiring machining cast bores to clear the screen assembly. Future parts would provide these cavities with machining stock to permit machining the entire cavity. Similarly, threaded plug bosses required snifting of hole locations to match the final part.

Small-diameter, long-length, cored holes were irregular, resulting in thin wall areas or actual contact of parallel cores. Future parts should have all passages drilled if possible to control the location and the size, and to provide clean full-size passages for oil.

STATIONARY SPUR RING GEAR (P/N 301-10412)

The ring gear was successfully die quenched in the Gleason 36-inch Quench Press. However, the part grew approximately 0.0050 inch in diameter, necessitating added allowance on gear teeth to provide grind stock after hardening.

The gear teeth were ground on a Michigan 36-inch Helical form grinder with no special problems except that the original grinding wheel support arm had to be stiffened to reduce deflection under grinding load.

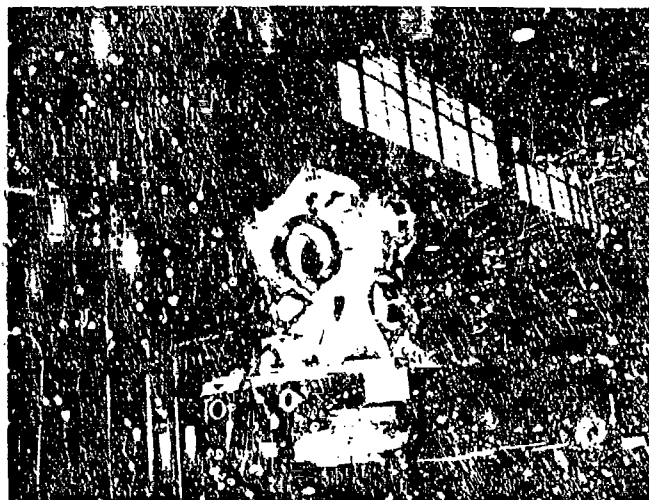


Figure 12. Machining the Forward Face.

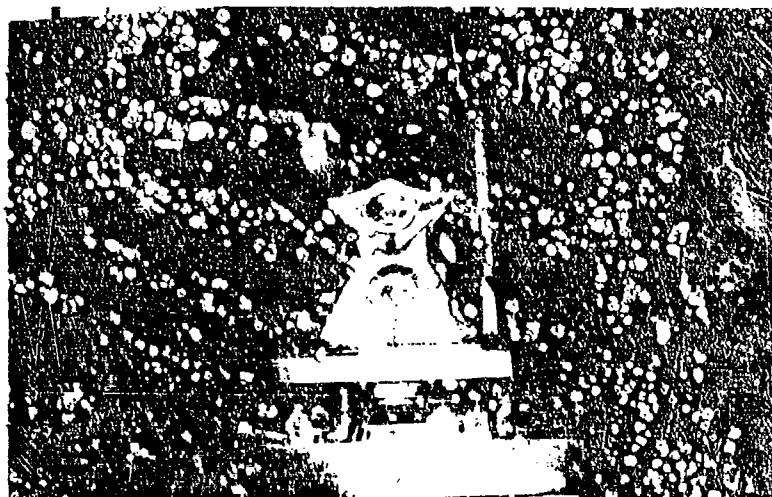


Figure 13. Boring the Horizontal Axis.

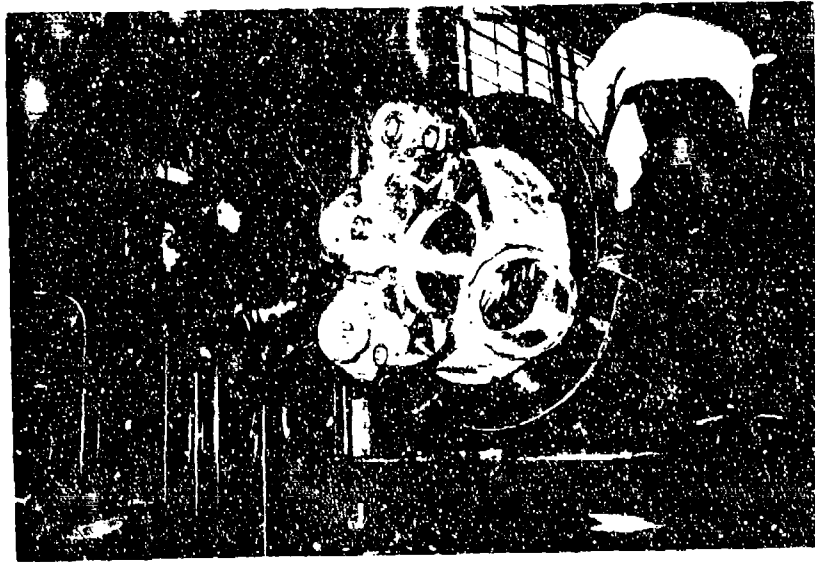


Figure 14. Boring the Shaft Axis.

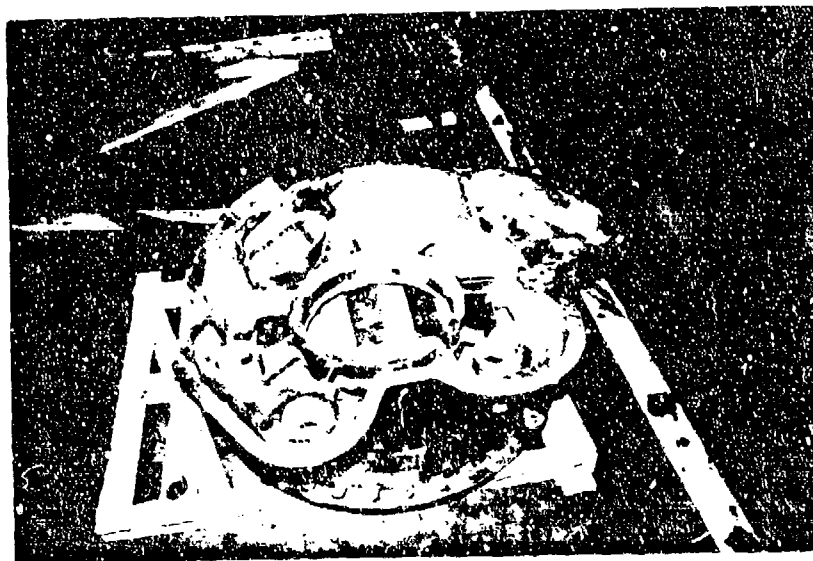


Figure 15. Machined Housing.

The gear teeth were inspected for involute form on an Illinois machine. A special arbor was made to provide a ring of balls for support of the heavy (260 LB) gear in the checking machine. It is necessary to slide the part in relation to the machine spindle to set up the check.

MACHINING VASCO X-2

In turning and grinding operations, Vasco was found to be similar to 9310 steel. Although some abusive grinding tests showed Vasco to be superior, in actual practice grind burns occurred on Vasco as frequently as they did on 9310.

The only true problem occurred in machining bores of gears after heat treat. Typically on prototype parts, excess stock is left on gear webs and in shaft bores. Vasco core areas quench out at approximately five Rockwell C points higher than 9310. The result is that it is more difficult to remove stock by turning, particularly in bores where tooling size is limited, and thus chatter and tool bit breakage occurs. Speeds and feed rates must be reduced for the harder material.

ASSEMBLY TECHNIQUES AND PROBLEMS

The rotor shaft bearing nut required a special gearbox adapter to a Sweeney wrench. A mechanical advantage of approximately 10,000 to one was needed to install the nut with a torque of 15,000 lb-ft. The wrench was satisfactory for normal tightening. However, in cases of a tight fitting nut it required nearly four hours to remove the nut using the high ratio mechanical wrench. A two-speed device would be desirable for rapid turning at lower torques.

Bearing-to-shaft assembly was accomplished by heating the bearing in an oven and dropping onto a room temperature shaft. The assembly was then held in a hydraulic press until cool.

Assembly of the rotor brake gear into the combiner housing revealed a blind assembly problem. The spline coupling in the end of the rotor brake gear engages the spline shaft of the auxiliary lube pump already installed in the housing. The pump offered no drag to rotation; rotating the gear to seek engagement moved the pump shaft as well. An extra long quill on the pump would solve this problem by allowing engagement of the pump spline prior to engagement of the gear assembly cartridge to the combiner housing.

The jacking screw inserts in the bearing cartridge supports proved to be far too small. The large bearing supports took greater loads to remove than similar smaller parts. Inserts stripped or jacking screws buckled from the excessive loads.

applied to remove the parts. Future large parts should have larger thread size inserts.

Installation of the low shaft angle (29°) input bevel pinions into the combiner assembly was marginal due to the design that required the mating combiner gear be installed from the opposite side. In future designs, if the mating gear cannot be installed from the same side (Apex first), then dummy gears should be made and checked for axial assembly of pinion in the Gleason tester.

6. BENCH DEVELOPMENT AND ENDURANCE TESTS

The purpose of these tests was to identify problems that might develop during operation of the advanced technology transmission under various loading conditions. Identified problems were to be corrected and the design solutions were to be evaluated to the extent possible within the ATC program. Verification of the final design was to be done under the prototype aircraft program.

The original plan called for 201 hours of operation of the aft and combiner transmissions at design and overload torques with (for the combiner transmission) various combinations of engine inputs. These tests were to be performed in regenerative test stands, with further testing to be done in the Dynamic System Test Rig (DSTR) using gas turbines and an HLH rotor system. The original plan was changed to reflect limitations in the ATC hardware and to accommodate a failure of the regenerative stands drive system. The ATC program was completed in the DSTR.

Transmission test specimens were complete assemblies, including integral lubricating and cooling system and accessories. The transmissions were connected to the test stands through representative lengths of HLH drive shafting and flexible couplings.

TEST EQUIPMENT AND FACILITIES

In the aft transmission test stand, Figure 16, the Model 301 aft transmission is inserted in one corner of the square loop with the rotor shaft connected to an overhead helical gearbox and the synchronizing shaft connected forward to a bevel gearbox. The bevel gearbox vertical shaft connects to the overhead helical gearbox completing the loop.

Torque is applied in the overhead helical gearbox hydraulically by axially shifting a compound helical gear set which drives the mating gears in opposite directions to lock in the desired torque.

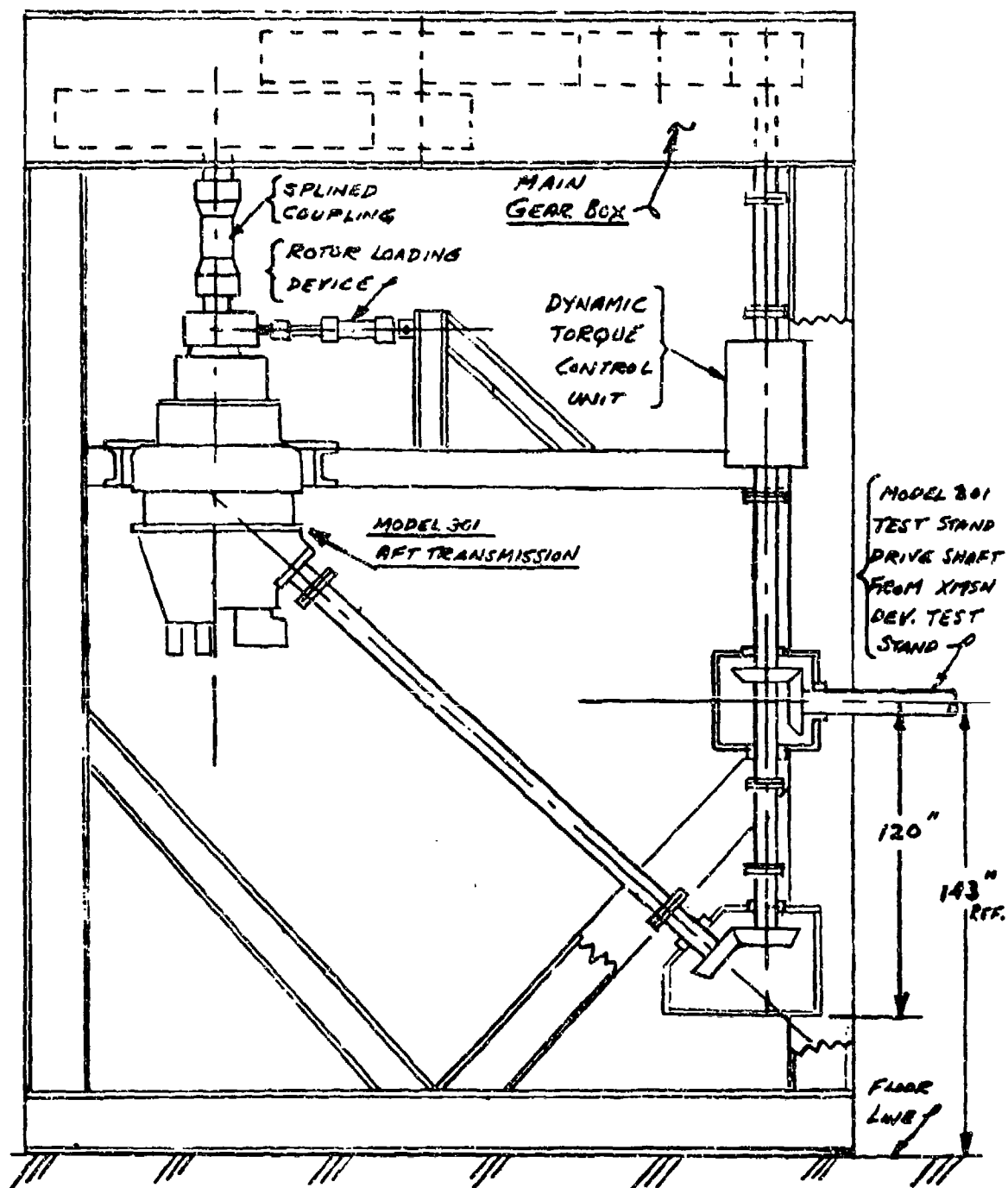


Figure 16. Model 301 Aft Transmission Test Stand Assembly.

Rotor loads are applied to the rotor shaft through hydraulic actuators simulating lift, pitching moment, and drag. The accessory loads are induced by the use of aircraft alternators and pumps.

The aft transmission test stand as designed is capable of loading the transmission as follows:

	<u>Percent of Design</u>
● Rotor shaft speeds up to 170 rpm	110
● Rotor shaft torque up to 6,350,000 in-lb	150
● Rotor shaft lift up to 102,000 lb	150
● Rotor side load (drag) up to 28,300 lb	200
● Pitching moment up to 1,510,000 in-lb	125

In the combiner transmission test stand, Figure 17, the Model 301 combiner transmission is inserted into a system consisting of four connected closed loops. Each engine shaft input to the combiner is a complete closed-loop system, utilizing the forward and aft synchronizing shafts as common shafts for all three inputs. With this system, the power applied to the forward and aft transmission shafts can be varied to duplicate torque distribution associated with the different flight regimes.

Torque is applied to each loop through individual torque systems by hydraulically shifting a compound helical gear set in the same manner described above for the aft stand.

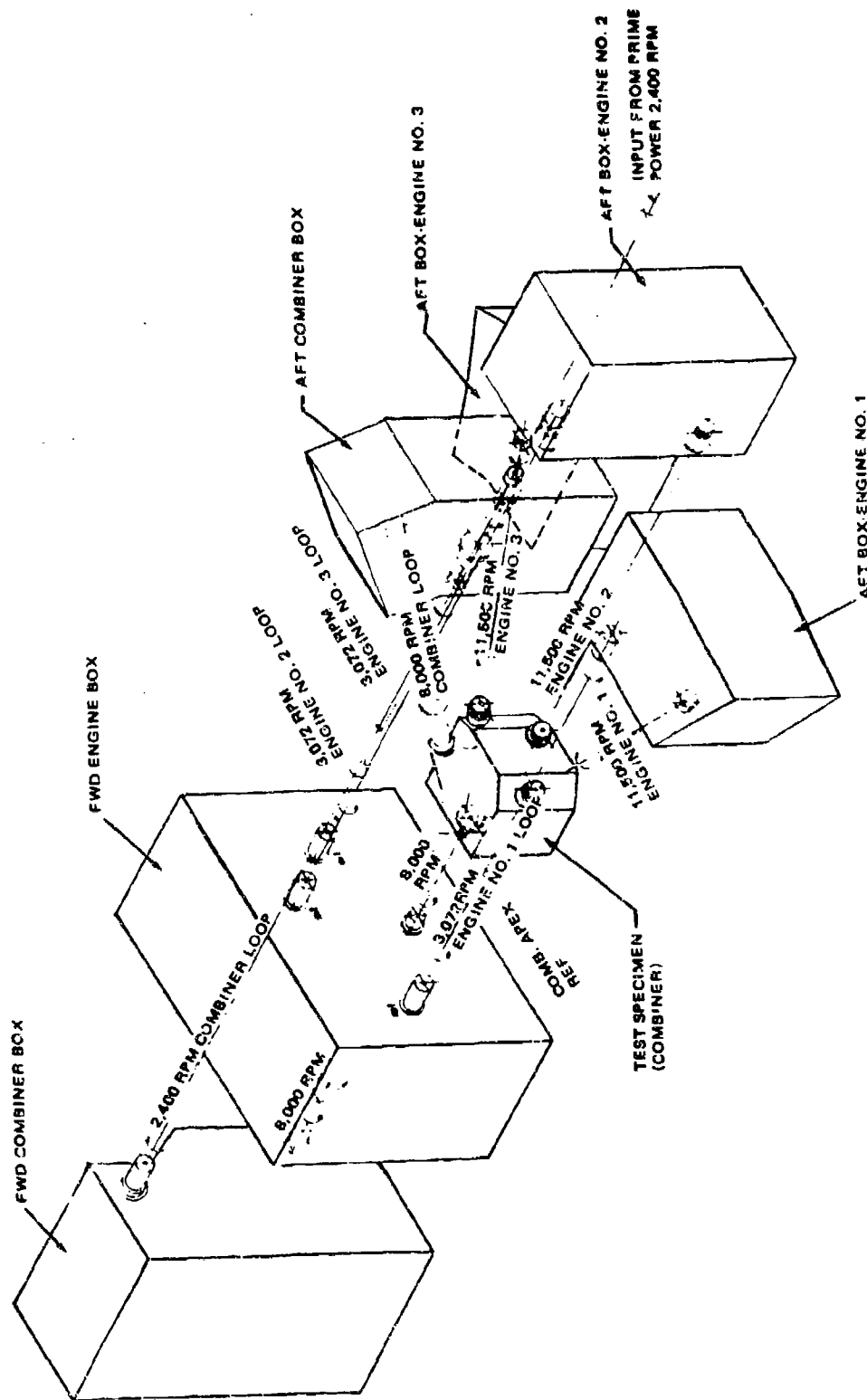


Figure 17. Corbiner Transmission Test Stand.

The combiner transmission test stand is capable of loading the transmission as follows:

	<u>Percent of Design</u>
• Engine input speeds up to 13,225 rpm each	115
• Engine shaft torques up to 71,500 in-lb each	160
• Synchronizing shaft torque up to 123,700 in-lb each	160

In both stands, the dynamic torqueing units are capable of applying and removing torque with the test stand at rest or with it running at operating speeds. All controls for applying torque and rotor loads and for running the stand are located outside the test cell.

The Dynamic System Test Rig (DSTR) shown in Figure 18 provided a means for integrating and testing the aft and combiner transmissions, the aft rotor, three gas turbines, and aircraft drive shafting. The forward rotor was simulated to a limited extent by a water brake mounted at the combiner forward output shaft.

The DSTR gas turbines, designated 501-M62B, were dynamically similar to the XT701-AD-700 engines to be used in the prototype aircraft. Their maximum power output was approximately 90% of the flight engines. Engine-mounted torque meters were supplied.

The forward-mounted water brake had a rated capacity of 1800 hp at 8000 rpm. A torquemeter monitored the power absorption.

Drive shaftings from engines to combiner and from combiner to aft were essentially duplicates of the aircraft installation. Provision was made for offsetting the shaft support bearings to simulate aircraft misalignments.

The DSTR was able to supply drive system related information difficult or impractical to obtain in the closed-loop stands. This included simulation of hub to rotor shaft interface conditions, rotor brake operation, engine to transmission torsional dynamics and clutch overrun operation.

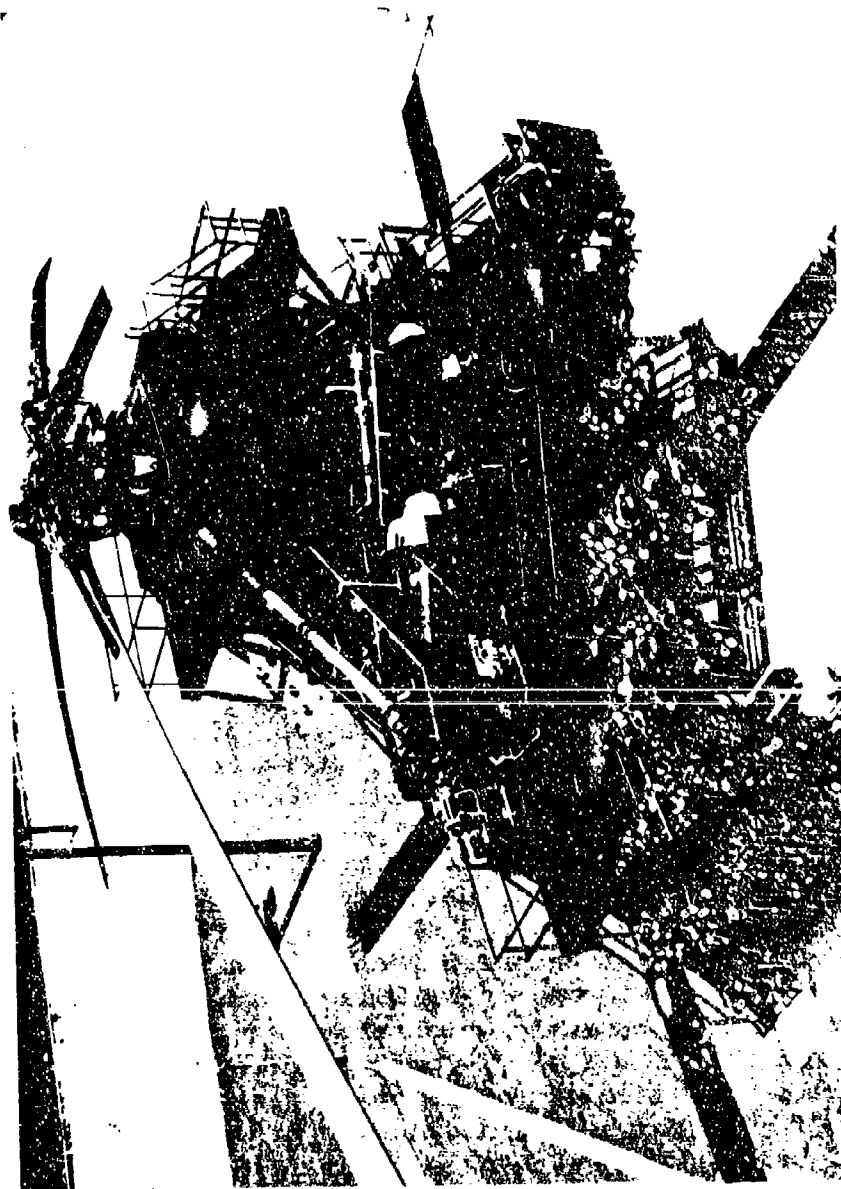


Figure 18. Dynamic System Test Rig.

AFT TRANSMISSION

Summary

A total of 128 hours of load testing was accumulated on the aft transmission assembly. The sequence of development testing and modification is shown in Figure 19. Test problems and resolutions are outlined in Table 2. Technical solutions beyond the scope of the ATC Program were developed under the prototype program. In the important area of bevel gear capability, completed effort includes a partial verification of the Prototype hardware as described in Section 7. In other areas as well, the ATC program was able to develop data to substantiate the adequacy of the Prototype technical approach.

Test Specimen

The initial test specimen was defined by Drawing 301-10400-1. Latter test specimens were modified as defined in this report.

Pretest Preparation

Spiral bevel gear tooth bearing patterns were taken and the pinion was adjusted for what was judged to be an optimum pattern. Previous experience was used as a guide. The HLH procedure differed from the past practice of tooth pattern development. Smaller test stands had allowed torque loads to be varied while the stand was stationary. After torque application, patterning was performed by rolling the teeth through mesh at a constant torque. The HLH test stand size and design precluded this practice; the stands were started up at zero torque and torque was increased while rotating. Load patterns were necessarily a composite of the selected load level and all lower loads that had been seen on the way up. This problem was finally overcome by building static-torque stands for the HLH transmissions, which provided for first setting a torque and then for a slow, controlled rotation of the bevel pinion. Latter development of bevel gears during this program used gear tooth strain gages to provide better information on tooth stresses than is possible by using load footprint location relative to toe, heel, top, and bottom features of the tooth.

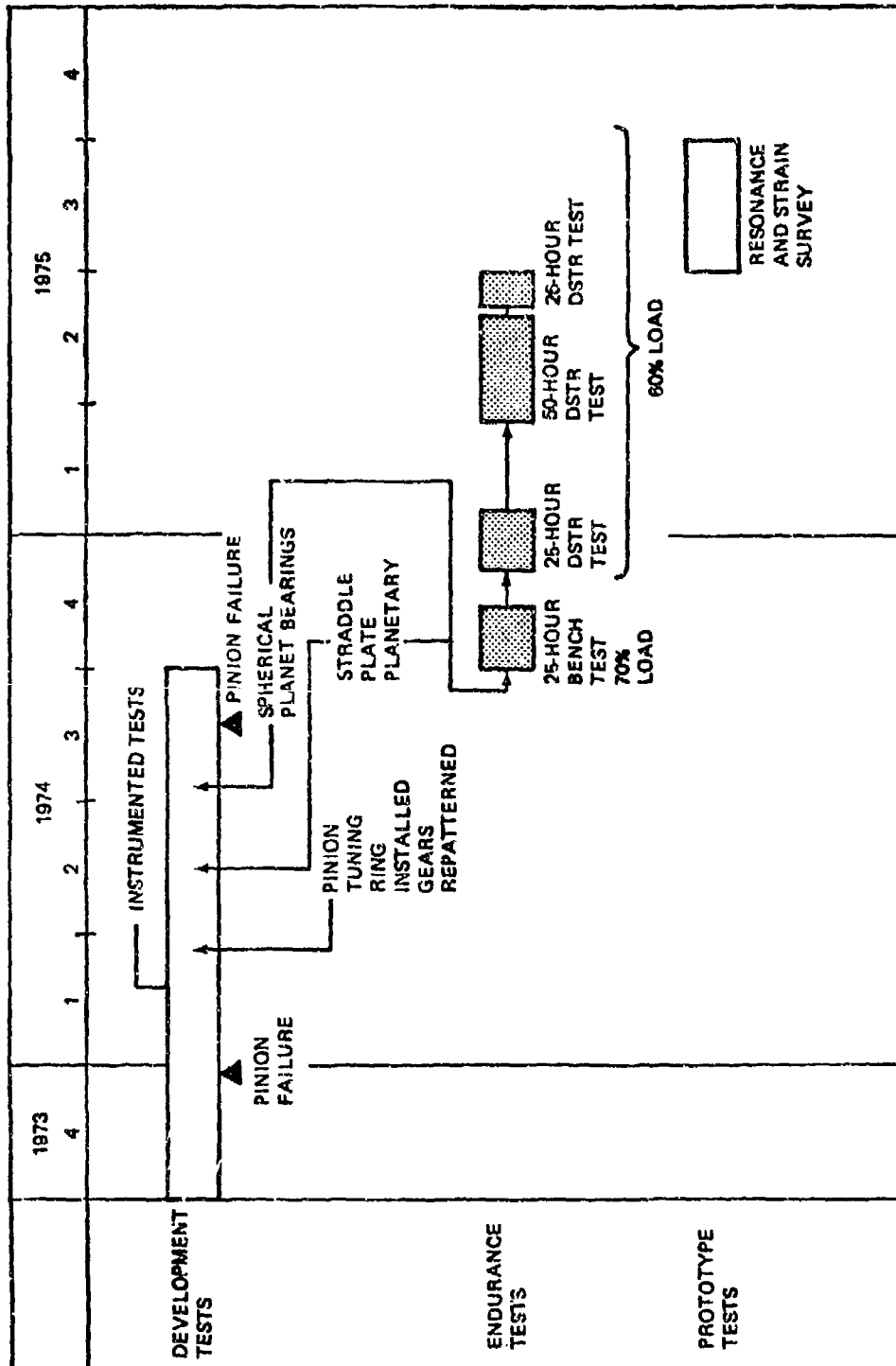


Figure 19. Aft Transmission Test Sequence.

TABLE 2. AFT TRANSMISSION TEST PROBLEMS AND RESOLUTIONS

PROBLEM	ATC RESOLUTION	PROTOTYPE RESOLUTION
Pinion Stress Above Allowables	<ol style="list-style-type: none"> 1) Repattern Pinion to Develop Optimum Load Distribution 2) Investigate Add-on Stiffening of Rim 3) Operate at Reduced Torque 	<ol style="list-style-type: none"> 1) Increase Thickness of Pinion and Gear Rims 2) Further development of Optimum Load Distribution
Resonant Frequencies Leading to Damaging Stresses in Pinion and Gear	<ol style="list-style-type: none"> 1) Develop and Apply Analytical and Experimental Methods to Predict and Measure Stresses 2) Detune with Add-on Stiffening Rings 3) Add Damping to Criteria Developed in ATC Program 	<ol style="list-style-type: none"> 1) Apply Analytical and Experimental Methods 2) Detune by Redesign 3) Maintain Added Damping
Planet Gear Scuffing	<ol style="list-style-type: none"> 1) Change from Cylindrical to Spherical Roller Bearings 2) Improve Lubrication 	SAME AS ATC
Planet Post Stresses Above Allowables	<ol style="list-style-type: none"> 1) Add Outboard Support Plate to Second-stage Carrier 	<ol style="list-style-type: none"> 1) Increase post strength by Redesign 2) Improve Material Allowables. $\propto \beta$ to β_{STOA}

TABLE 2. Continued

PROBLEM	ATC RESOLUTION	PROTOTYPE RESOLUTION
Rotor Shaft Bearing Locknut Loosening	Periodic Inspection During Test	1) Increase Strength and Stiffness of Both Locknut and Lockwasher by Redesign 2) Add Buttress Threads
Rotor Shaft Hub Nut Excessive Deflection	Periodic Inspection	1) Increase Stiffness of Nut and Local Area of Shaft 2) Add Buttress Threads
Input Oil Seal Leak	Increase Seal Drainage	SAME AS ATC
Output Oil Seal Wore Shaft	Bond Seal O.D. to Housing	SAME AS ATC
Output Oil Seal Allowed Water Ingress	Add Rain Seal above Oil Seal	SAME AS ATC
Planet Post Bushing Loosened	Periodic Inspection	Eliminate Bushing and Silver Plate Bearing I.D.

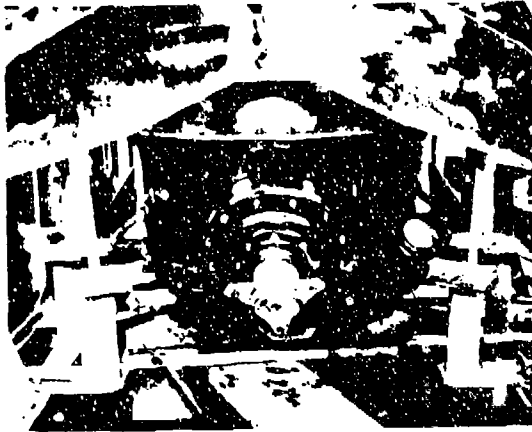
Development Testing

In Sept. 1973, the 301-10400-1 aft transmission was first run under torque. After performing check-out runs and a strain survey of the planetary system, endurance testing was initiated at 100% torque and full rotor thrust. After a total of 2 hours, 29 minutes, under these conditions, and over 15 hours total operation, a mechanical failure of the test specimen occurred. Coincident with the noise of the failure, debris indication lights illuminated and the test stand shut down automatically. It was determined that the primary failure occurred in the 301-10428 spiral bevel pinion, with the fatigue origin occurring in the bevel tooth root fillet area (Figure 20). The cause for this failure was ascribed to a resonant condition of the pinion gear. As gear tooth strain surveys were made later in the testing sequence, an improved understanding of gear and rim stresses served to modify the opinion that resonant stresses were primarily responsible for the failure.

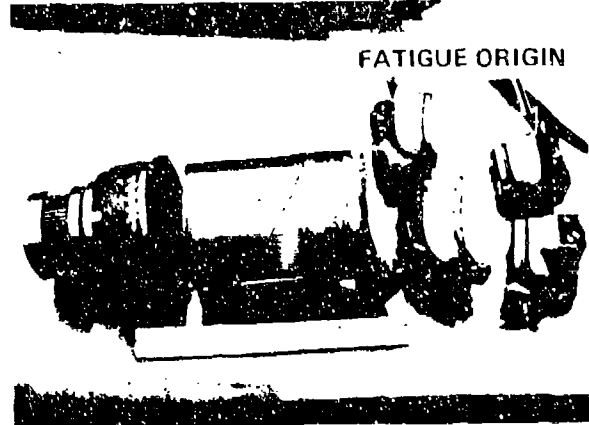
Strain gages were applied to the spiral bevel gears and other components and telemetry packages were designed to bring the signals out through the rotating system (Figures 21, 22 and 23). The transmission went back into test in essentially the same configuration as initially. Minor changes included reduction in tapered bearing axial play, increased strength in the rotor shaft locknut locking device, and increased clearance in the first-stage carrier support bearing to prevent rotor shaft deflections from loading this bearing (P/N 301-10403-1).

Analysis of pinion stress data verified the resonant response frequencies predicted in tests of the pinion alone, excited by an electromagnet or air blast (Figure 24). The highest stress response on the pinion occurred in the area of the fatigue failure. Stress levels were not sufficiently high to explain the fatigue failure as resonance-induced, assuming the pinion damping ring was properly in place during the load test. Thus, the primary cause of the failure was more probably due to overload of the tooth.

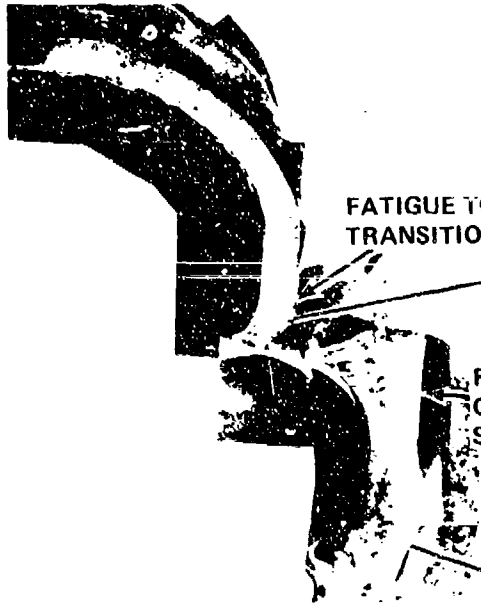
To eliminate the possibility of gear response as a failure mechanism, a tuning or stiffening ring was fabricated and fitted into the mouth of the pinion bore (Figure 25). The ring raised the exciting frequency of the pinion outside the operating rpm.



AS RECEIVED PHOTOGRAPH OF
FAILED AFT TRANSMISSION



FATIGUE ORIGIN
FAILED INPUT PINION P/N 301-10428-1
WITH ARROW INDICATING FATIGUE INITIATION
SITE

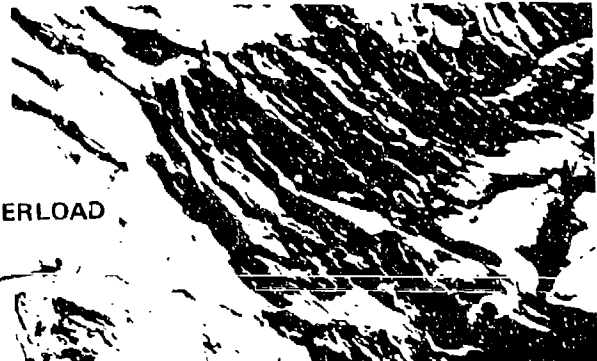


PANORAMIC VIEW OF INPUT PINION
FRACTURE SURFACE INDICATING
FATIGUE ORIGIN IN TOOTH ROOT
FILLET RADIUS P/N 301-10428
PINION GEAR

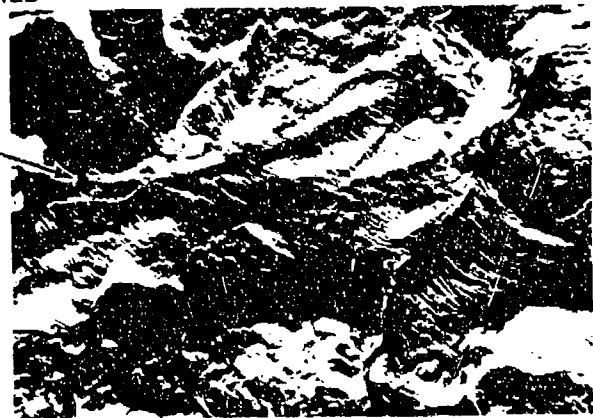
FATIGUE TO OVERLOAD
TRANSITION

FATIGUE
ORIGIN
SMEARED

.9X



FATIGUE AREA B -
SECONDARY FATIGUE ZONE 10,000X



PRIMARY FATIGUE ZONE A 7,500 X

Figure 20. HLH/ATC Aft Transmission Failure Investigation.

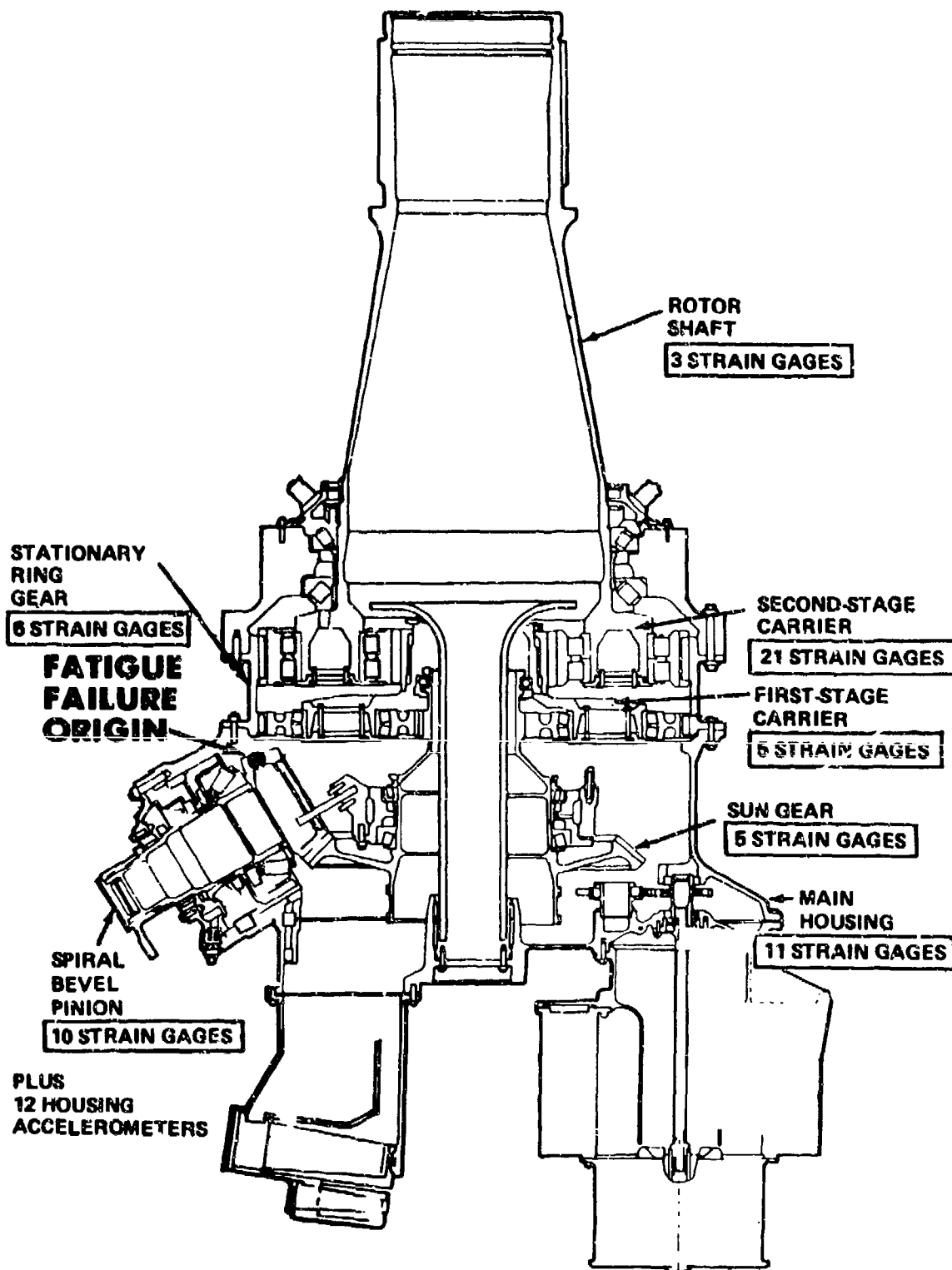


Figure 21. Aft Transmission Strain Survey Instrumentation.

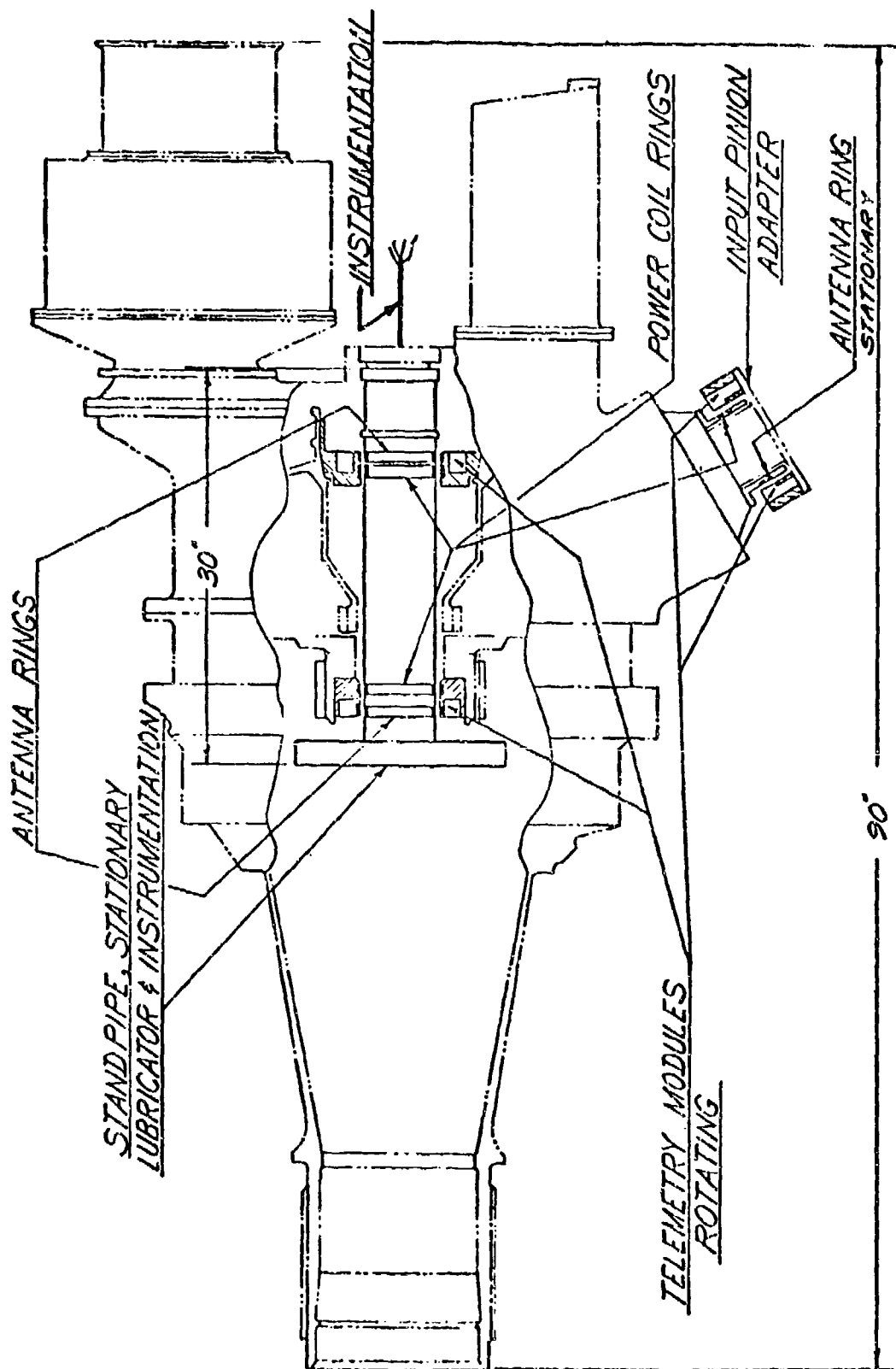


Figure 22. Aft Transmission Instrumentation Assembly.

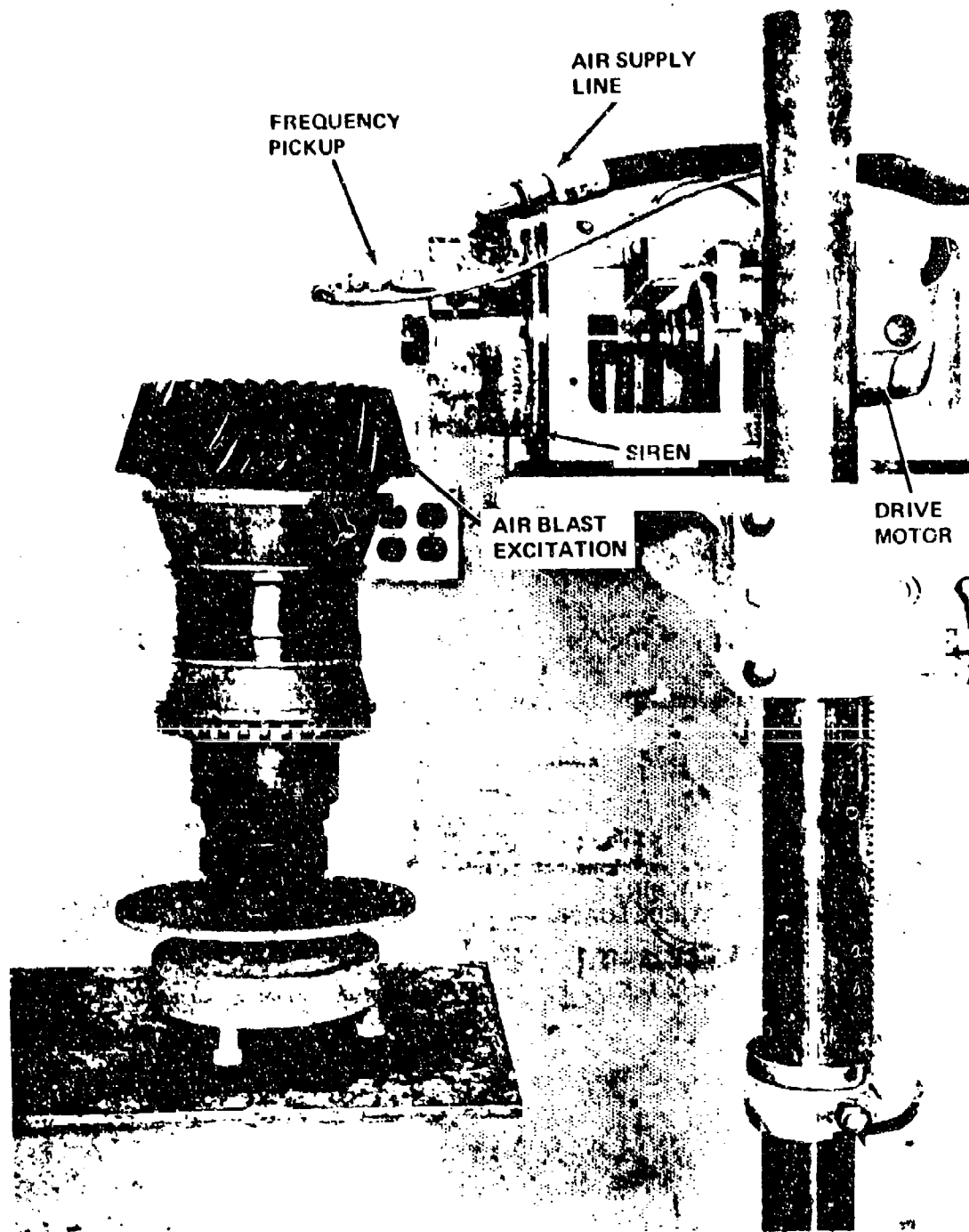


Figure 24. Typical Air Siren Gear Resonance Test Setup.

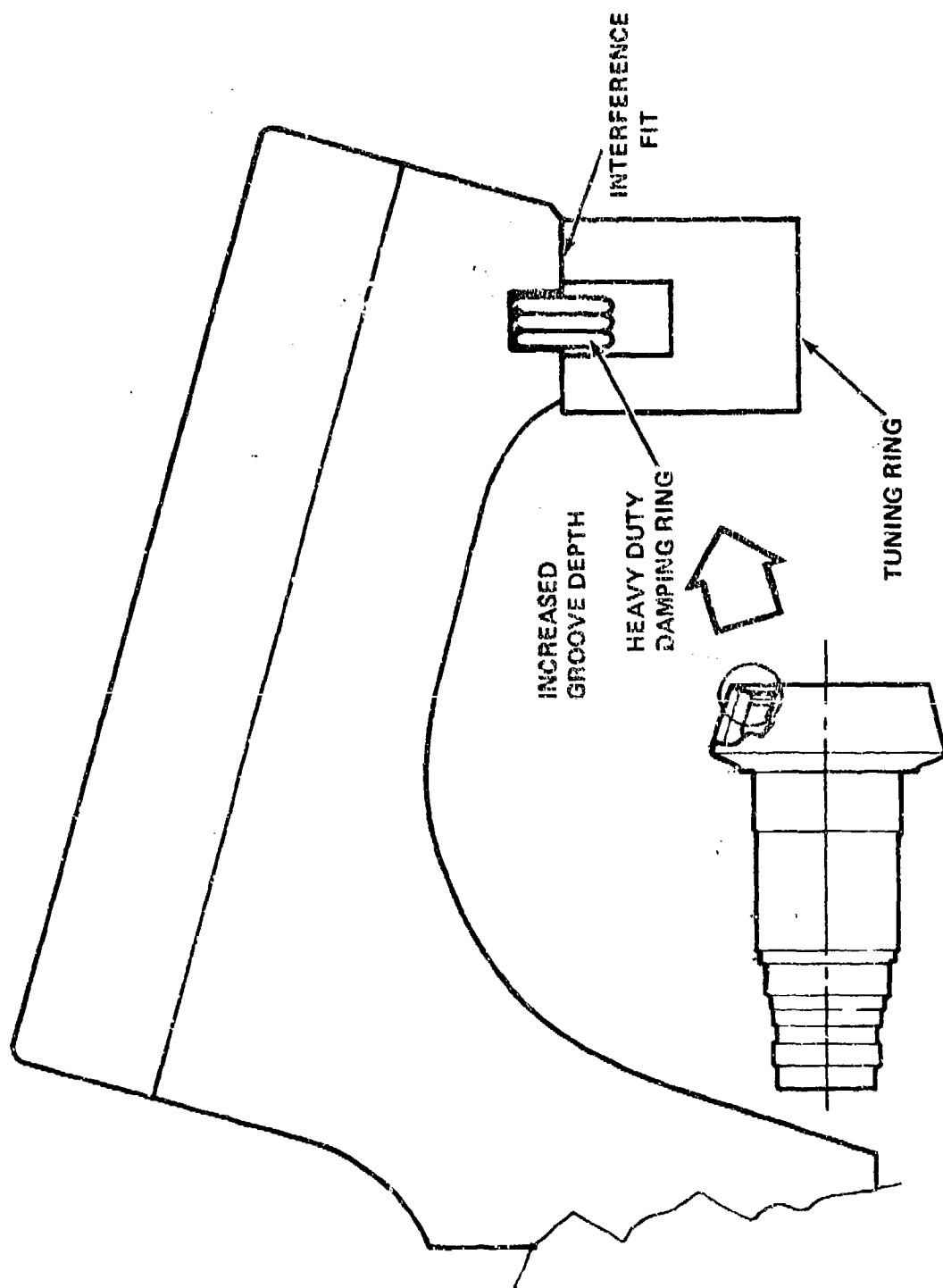


Figure 25. Spiral Bevel Pinion Gear - Aft Transmission Tuning Ring Installation.

To reduce tooth stress levels, a second input pinion was modified by regrinding in order to change the tooth load pattern.

Stress survey testing of the transmission was then conducted to establish a configuration satisfactory for further load tests. At this point, it was believed that satisfactory pinion stress levels could be achieved with the aid of the second development pattern and the tuning ring. High planet post stresses in the second stage (rotor shaft) were encountered, however. To reduce these, a straddle plate was designed and attached to the lower end of the posts (Figure 26).

A short 100% torque load run was made in this configuration. Inspection after operation showed second-stage planet to sun-gear scuffing. This was attributed to a combination of unfavorable lead tolerances between sun and planets and also to the rigidity of the planet gears as mounted on compliant cylindrical roller bearings. The compliant bearings in the second-stage planets were replaced with self-aligning spherical bearings which had been procured as backups. A new second-stage sun with more favorable tooth lead was installed. Another load run and inspection showed that the second-stage planet scuffing problem had been eliminated.

While this transmission testing was in progress, the static gear deflection test rig had been completed and was used to evaluate pinion regrinds to determine if the load distribution could be improved by pattern changes.

The transmission reentered load testing with the following major configuration changes:

- Straddle plate
- Spherical planet bearings
- Tuning ring in pinion
- Heavy damping ring in pinion and sun/bevel gears
- Added damping ring in sun/bevel gear

A strain survey was performed. The sun/bevel gear showed marked improvement of its gear response with no apparent amplification from gear resonance. Following the strain survey and teardown inspection, the endurance test was restarted. After 4.5 hours of test (approximately 9 hours total transmission time, and 13.5 hours total pinion time), the pinion

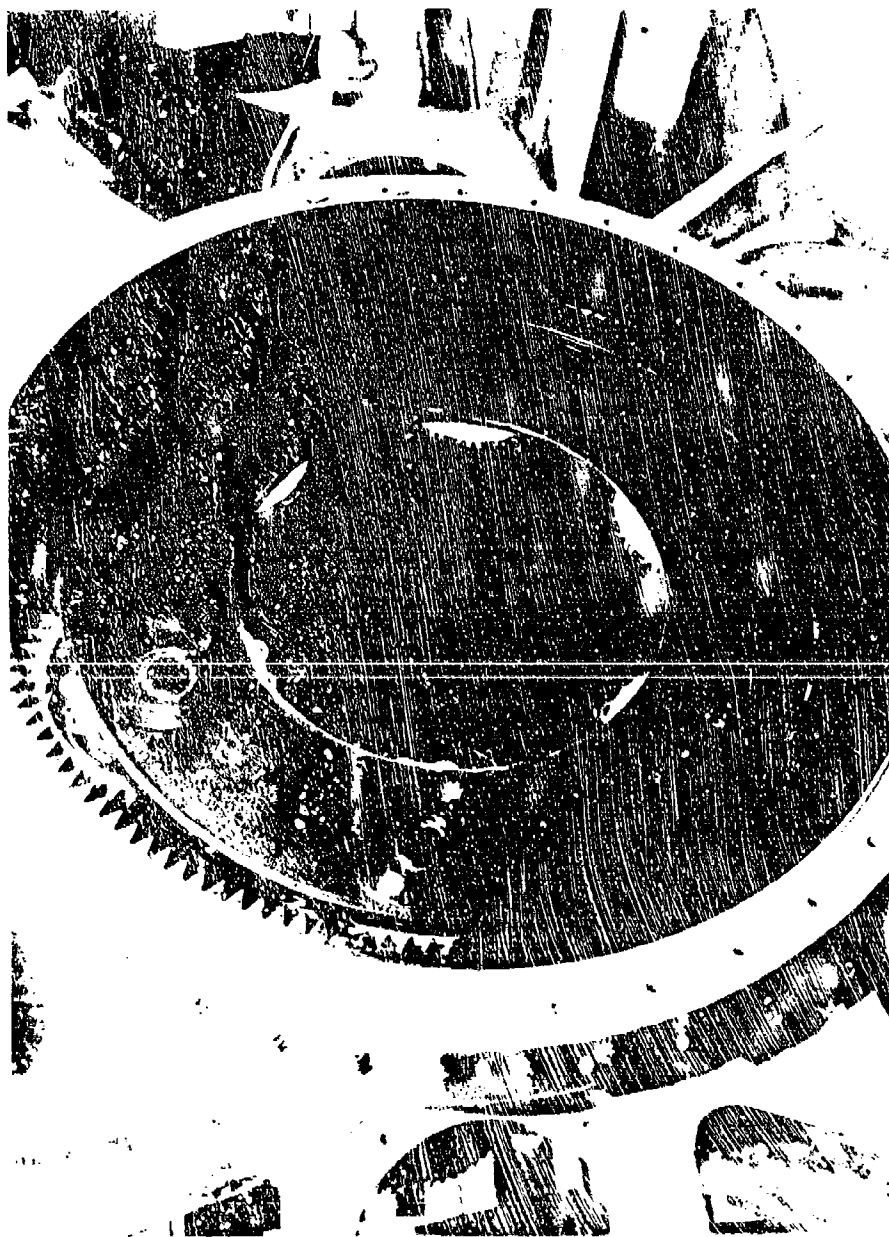


Figure 26. Aft Transmission Second-Stage Planetary Subassembly
with Straddle Plate.

failed. Operating conditions were 100% design torque and speed and 50% applied rotor loads. The failure mode was similar to that which occurred earlier in the program.

The effectiveness of the tuning ring under the influence of temperature and dynamic load conditions was questioned. As a result, the ring was removed and additional tests were performed to evaluate other configurations. At the same time, an increase in damping ring mass was incorporated. Analysis of the gear stresses showed that with the ATC configuration of pinion and gear, a maximum safe level of operation was 70% of design torque. Consequently, all further testing of the aft transmission was held to this level, or below. Comparable analysis of the combiner showed a maximum safe level of 60%. When both transmissions were run together, as in the DSTR, the lower torque was used. The gear and pinion were redesigned at this time for the prototype.

Endurance Testing

Limitations of the ATC hardware resulted in a planned reduction in test time, with the full testing reoriented to the prototype hardware. A 25-hour load test at 70% torque was successfully conducted on the aft transmission in the load run stand. Conditions were as shown in Table 3. The transmission testing was then moved to the DSTR.

TABLE 3. TWENTY-FIVE HOUR LOAD TEST SCHEDULE				
ROTOR TORQUE (IN-LB)	ROTOR LOADS			ROTOR SPEED (RPM)
	MOMENT (IN-LB)	DRAG (LB)	THRUST (LB)	
3,005,000	590,000	6600	66,000	156

A 105-hour planned test of aft and combiner concurrently was conducted in the DSTR according to Tables 4 through 7. The aft transmission was inspected at intervals during the test period. Three problems occurred during this testing. The first was rotation of the bearing locknut on the rotor shaft. The lockwasher remained keyed to the shaft while the nut turned in the tightening direction, shearing off nut-locking tangs in the process. At 76 hours, the nut rotation approached the point at which it was feared the nut would expand radially over the shaft threads. A partial disassembly was performed and the nut and washer were changed and reassembled.

TABLE 4. DSTR LOAD SCHEDULE

25-HOUR COMBINEE TRANSMISSION ENDURANCE RUN

Run Time - Hours	4.75	0.5	0.5	0.5	0.5	0.5	0.5	0.5	0.5	0.5	0.5	0.5	0.5	0.5	0.5	0.5	0.5	0.5
% Rotor Speed	100	100	100	100	100	100	100	100	100	100	100	100	100	100	100	100	100	100
Aft Xman HP	6385	5585	5585	5585	5585	5585	5585	5585	5585	5585	5585	5585	5585	5585	5585	5585	5585	5585
No. 1 Engine Torque lb Ft	1246	2154	0	1219	1246	2154	0	1219	1246	2154	0	1219	1246	2154	0	1219	1246	2154
No. 2 Engine Torque lb Ft	1246	1219	2154	0	1246	1219	2154	0	1246	1219	2154	0	1246	1219	2154	0	1246	1219
No. 3 Engine Torque lb Ft	1245	0	1219	2154	1246	0	1219	2154	1246	0	1219	2154	1246	0	1219	2154	1246	0
Water Brake HP	1800	1800	1800	1800	1800	1800	1800	1800	1800	1800	1800	1800	1800	1800	1800	1800	1800	1800

NOTE: 1246 lb ft engine torque is equivalent to 2728 hp at 155.9 rotor rpm.

2154 lb ft engine torque is equivalent to 4716 hp at 155.9 rotor rpm.

1219 lb ft engine torque is equivalent to 2669 hp at 155.9 rotor rpm.

TABLE 5. PUN SCHEDULE - DSTR 50-HOUR ENDURANCE

Test Condition No.		1	2	3	4	5	6	7	8	9	10	11	12	13	14	15	16	17	18	19	20	21	22	23	24
Run Time - Hours & Mins.		1:00	1:15	2:23	2:23	3:22	2:22	2:22	2:23	2:23	2:22	3:57	3:57	1:0	1:13	2:23	2:23	2:23	2:23	2:23	2:23	2:23	2:23	2:23	2:23
Cur. Load Engine- Hours & Mins.		1:00	2:18	4:41	7:04	9:27	11:50	14:13	16:36	18:59	19:26	15:54	20:59	22:17	24:40	27:03	29:26	31:49	34:12	36:35	38:58	39:28	39:58	40:16	
Motor Speed RPM		156	156	156	156	156	156	156	156	156	156	156	156	156	156	156	156	156	156	156	156	156	156	156	
#1 Engine Torque Lb Ft		1553	A9	1244	1244	1244	1244	1244	1244	1244	1244	AR	1244	GI	AR	1244	1244	1244	1244	1244	1244	1244	1244	1244	
#2 Engine Torque Lb Ft		1553	AB	1244	1244	1244	1244	1244	1244	1244	1244	AR	1244	1553	AB	1244	1244	1244	1244	1244	1244	1244	1244	1244	
#3 Engine Torque Lb Ft		GI	AB	1244	1244	1244	1244	1244	1244	1244	1244	AB	1244	1553	AB	1244	1244	1244	1244	1244	1244	1244	1244	1244	
AFT X-ray Input Power HP		5000	Min	6372	6372	6372	6372	6372	6372	6372	6372	Min	6372	5000	Min	6372	6372	6372	6372	6372	6372	6372	6372	6372	
CYCLIC PITCH																									
60°																									
60°																									
20°																									
Pitch																									
a																									
b																									
c																									
d																									
e																									
f																									
g																									
h																									
i																									
j																									
k																									
l																									
m																									
n																									
o																									
p																									
q																									
r																									
s																									
t																									
u																									
v																									
w																									
x																									
y																									
z																									
AA																									
AB																									
AC																									
AD																									
AE																									
AF																									
AG																									
AH																									
AI																									
AJ																									
AK																									
AL																									
AM																									
AN																									
AO																									
AP																									
AQ																									
AR																									
AS																									
AT																									
AU																									
AV																									
AW																									
AX																									
AY																									
AZ																									
BA																									
BB																									
BC																									
BD																									
BE																									
BF																									
BG																									
BH																									
BI																									
BJ																									
BK																									
BL																									
BM																									
BN																									
BO																									
BP																									
BQ																									
BR																									
BS																									
BT																									
BU																									
BV																									
BW																									
BX																									
BY																									
BZ																									
CA																									
CB																									
CC																									
CD																									
CE																									
CF																									

DOWNWASH, NOISE, AND EXPRESS SURVEYS

Rotor Brake Stop No. (Scheduled)																									
Rotor Brake Hi																									
Rotor Brake Ni																									
#1 Alternator Load - KVA																									
#2 Alternator Load - KVA																									
#3 Alternator Load - KVA																									
#1 Hyd. Pump - GPM @ 3000 PSI																									
#2 Hyd. Pump - GPM @ 3000 PSI																									

2008

1264 lb ft engine torque is equivalent to 2724 hp at 153.9 rotor rpm.

1533 14 TRANS TORQUE IS EQUIVALENT TO 3400 HC AT 135.0 RPM TORQUE 240.

this test accumulated 51 hours, 21 minutes total time.

TABLE 6. RUN SCHEDULE - DSTR 30-HOUR ENDURANCE

Test Condition No.	1	2	3	4	5	6	7	8	9	10	11	12	13	14	15	16	17	18	19	20	21	22
Run Time - Hours & Mins.	8.0	1.0	1.0	1.0	1.0	1.0	1.0	1.0	1.0	1.0	1.0	1.0	1.0	1.0	1.0	1.0	1.0	1.0	1.0	1.0	1.0	2.0
Cum Load Endure - Hours & Mins.	8.0	9.0	10.0	11.0	12.0	13.0	14.0	15.0	16.0	17.0	18.0	19.0	20.0	21.0	22.0	23.0	24.0	25.0	26.0	27.0	28.0	30.0
Rotor Speed RPM		155	156	156	156	140	155	156	156	156	156	162	156	156	156	156	156	156	156	156	156	
#1 Engine Torque Lb Ft		1244	1244	1244	1244	AR	1553	1244	1244	1244	1244	AR	GI	1244	1244	1244	1244	1553	1244	1244	1244	
#2 Engine Torque Lb Ft		1244	1244	1244	1244	AR	1553	1244	1244	1244	1244	AR	1553	1244	1244	1244	1244	GI	1244	1244	1244	
#3 Engine Torque Lb Ft		1244	1244	1244	1244	AR	GI	1244	1244	1244	1244	AR	1553	1244	1244	1244	1244	1553	1244	1244	1244	
Aft Zmen Input Power HP		6372	6372	6372	6372	MIN	5000	6372	6372	6372	6372	MIN	5000	6372	6372	6372	6372	5000	6372	6372	6372	
8.0 HOURS RUNNING FOR SPECIAL TESTS																						
CYCLIC PITCH DBN Item																						
TIME, MINS. AT EACH CYCLIC PITCH SETTING																						
6°																						
2°																						
0°																						
Pos																						
Aft																						
Zero																						
Right																						
Left																						
Chg.																						
Rotor Brake Stop No. (Scheduled)		1	2	3	4	5	6	7	8	9	10	11	12	13	14	15	16	17	18	19	20	
Water Brake HP		1500	1500	1500	1500	MIN	1500	1500	1500	1500	1500	1500	0	1500	1500	1500	1500	1500	1500	1500	1500	
#1 Alternator Load - KVA		30	60	60	30	30	30	60	60	30	30	30	30	60	60	30	30	60	60	30	60	
#2 Alternator Load - KVA		30	60	30	60	30	30	60	60	30	30	30	30	60	60	30	30	60	60	30	60	
#1 Hyd. Pump - GPM @ 3000 PSI		7.5	15	7.5	15	MIN	7.5	15	7.5	15	7.5	7.5	7.5	15	15	7.5	7.5	7.5	15	7.5	15	
#2 Hyd. Pump - GPM @ 3000 PSI		7.5	15	15	15	7.5	15	15	15	7.5	7.5	7.5	7.5	15	15	7.5	7.5	7.5	15	7.5	15	

NOTE: The hub-mounted camera will be left in position for the duration of the 30-hour test.

1244 lb ft engine torque is equivalent to 2724 hp at 155.9 rotor rpm.
1553 lb ft engine torque is equivalent to 3400 hp at 155.9 rotor rpm.
This test was concluded after 26 hours, 32 minutes.

TABLE 7. DSTR EVENT LOG (DRIVE SYSTEM ONLY)

Event	CUMULATIVE TEST RIG TIMES			Event	CUMULATIVE TEST RIG TIMES		
	Total Rig	Total Endur- ance	Toward Test		Total Rig	Total Endur- ance	Toward Test
1) <u>December 2, 1974</u> Endurance test transmissions installed in rig ready for 25-hr combiner endurance test.	6:17	0	0	19) <u>April 30</u> Removed #1 input pinion cartridge for Timken bearing replacement.	87:45	47:18	22:18
2) <u>December 3</u> Aft xmen drained and refilled for water contamination of lube oil.	6:34	0	0	20) <u>May 1</u> Installed #1 & #3 input pinion cartridges. Made backlash & pattern check.	87:45	47:18	22:18
3) <u>December 6</u> Drained and refilled aft xmen for water contamination of lube oil.	7:20	0	0	21) <u>May 5</u> Found filter element crushed in comb. xmen. Found last chance screen disintegrating in aft xmen.	104:24	65:21	40:41
4) <u>December 16</u> Checked for rotation of thrust bearing and retention nut.	17:59	4:45	4:45	22) <u>May 8-June 2</u> Conducted post 50-hr. test teardown inspection. Replaced 2 of 3 clutches with ground sprag versions.	116:36	76:21	51:21
5) <u>December 17</u> Drained and refilled aft xmen for water contamination of lube oil.	20:23	6:15	6:15	23) <u>June 3</u> Investigated aft xmen input seal performance. Cavity pressure unchanged but no detectable leakage during running and only very slight weepage at shutdown.	117:26	76:38	00:17
6) <u>December 18</u> Performed in-rig inspection of combiner xmen to identify source of metal particles. No damage found. Combiner xmen removed and shipped to plant for further teardown and inspection.				24) <u>June 10</u> Thrust bearing retention nut found to have rotated 5 tangs. Decision made to cut off nut and replace with new nut and lock washer.	117:26	76:38	00:17
7) <u>January 6, 1975</u> Combiner reinstalled. No damage or distress found. Aft xmen oil changed for water contamination.	20:40	6:15	6:15	25) <u>June 12</u> Removed rotor shaft thrust bearing retention nut by drilling & splitting. Cleaned up threads and shaft prior to installation of new nut.	117:26	76:38	00:17
8) <u>January 7</u> Removed and cleaned combiner sump and last chance filters.	25:54	9:38	9:38	26) <u>June 13</u> Installed new nut and lock washer. Prepared to run 30-hr. test.	117:26	76:38	00:17
9) <u>January 11</u> Replaced #1 clutch cartridge for failed duplex bearing.	40:52	20:30	20:30	27) <u>June 18</u> Thrust bearing retention nut rotated approx. 2" due to wear in keyways in rotor shaft. Lockwasher reassembled engaged with shaft and nut.	126:54	84:48	7:50
10) <u>January 15</u> Completed 25-hr. endurance test. Total time on this combiner xmen = 40:55 mins, including 69 rig starts.	47:15	25:00	25:00	28) <u>June 19</u> Checked thrust bearing retention nut and found no rotation after 30 mins. of running, on condition but with no cyclic pitch. #3 shaft on #1 engine shows bearing wear.	127:23	84:48	8:25
11) <u>January 17</u> Accomplished first rotor brake stop (15 sec. stop time).	48:3	25:00	25:00	29) <u>June 20</u> Some accumulation of debris in comb. xmen.	131:52	88:48	12:26
12) <u>January 18 - March 7</u> Tear-down inspection of combiner xmen.	48:28	25:00	25:00	30) <u>June 23</u> Small amount debris in comb. xmen.	135:34	91:48	15:26
13) <u>March 13/14</u> Started running 50-hr. test. Replaced #3 clutch cartridge for oil leak.	49:11	25:00	0	31) <u>June 24</u> Some accumulation of debris in comb. xmen.	141:11	97:03	20:41
14) <u>March 15</u> Heavy oil leak #3 clutch cartridge. Pulled out input pinion cartridge to change transfer tube "O" rings.	50:05	25:14	01:14	32) <u>June 25</u> Some accumulation of debris in the comb. xmen.	143:57	99:36	23:14
15) <u>April 25</u> Some accumulation of bronze debris in aft xmen. Accessory housing removed for inspection of gear clusters. No damage found.	71:42	38:21	13:21	33) <u>June 26, 1975</u> Shut down for comb. xmen chip detector and aux. screen light. Removed combiner sump for xmen inspection and search for further debris. Test terminated.	147:49	102:54	26:32
16) <u>April 27</u> Picked up 6 Timken bearing roller stake dimples in combiner.	73:23	39:39	14:39				
17) <u>April 28</u> Endurance running. Two more bearing stake dimples in combiner.	82:41	47:18	22:18				
18) <u>April 29</u> Picked up 7 more bearing stakes and one interroller spacer from Timken taper roller bearing. Removed #3 input pinion for shipment to plant for examination & replacement of inboard Timken taper roller bearing.	82:45	47:18	22:18				

A second problem encountered was leakage from the input pinion oil seal. Analysis indicated that the seal wind-back was flooding. Drain holes were incorporated in the seal. Further testing demonstrated this solution substantially eliminated the leakage.

The third problem was water ingestion caused by moisture collecting at the base of the rotor shaft and passing into the transmission through the upper seal. This problem was eliminated by attaching a rainshield to the rotor shaft.

Following 102 hours and 54 minutes of DSTR testing, and 25 hours of bench testing, the aft transmission was disassembled and a complete inspection was made. ATC testing was concluded at this point.

Component Investigation

This section describes investigation and design changes of major components. These include:

- Rotor Shaft Bearing Locknut and Lockwasher Modification
- Oil Seal Modifications Leading to Satisfactory Performance

Rotor Shaft Bearing Locknut

The function of this nut is to maintain the axial position of the two tapered roller bearings that react rotor loads. Forces on the nut include differential axial loading generated from rotor shaft moment and carried out at the bearings by a combination of shear and axial loads. The installation torque of the nut was set by the requirement of seating the bearings against shaft interference friction. Resulting torque was 200,000 inch pounds. A torque multiplying, geared spanner wrench was used for assembly and disassembly.

The nut itself is a large (21.25 pitch diameter), thin wall cylinder with wrenching contours on the outside diameter and a recess bore in the upper side. Into this cavity is set a locking washer with tangs to keyslots in the shaft and the nut. The locking washer is retained by a multi-turn snap ring. Further space is made available for a wave washer to prevent looseness and wear in the locking washer.

The nut and lockwasher material is 4340 steel treated to 34-38 Rc. The nut is silver plated to reduce the tendency to gall on the titanium rotor shaft.

During initial testing on the closed loop test stand this nut moved in a tightening direction, breaking the two inner tangs of the washer. The washer thickness was increased from .050 to .250 for DSTR testing. Figure 27 shows the major features and dimensions of the assembly and illustrates the design progression.

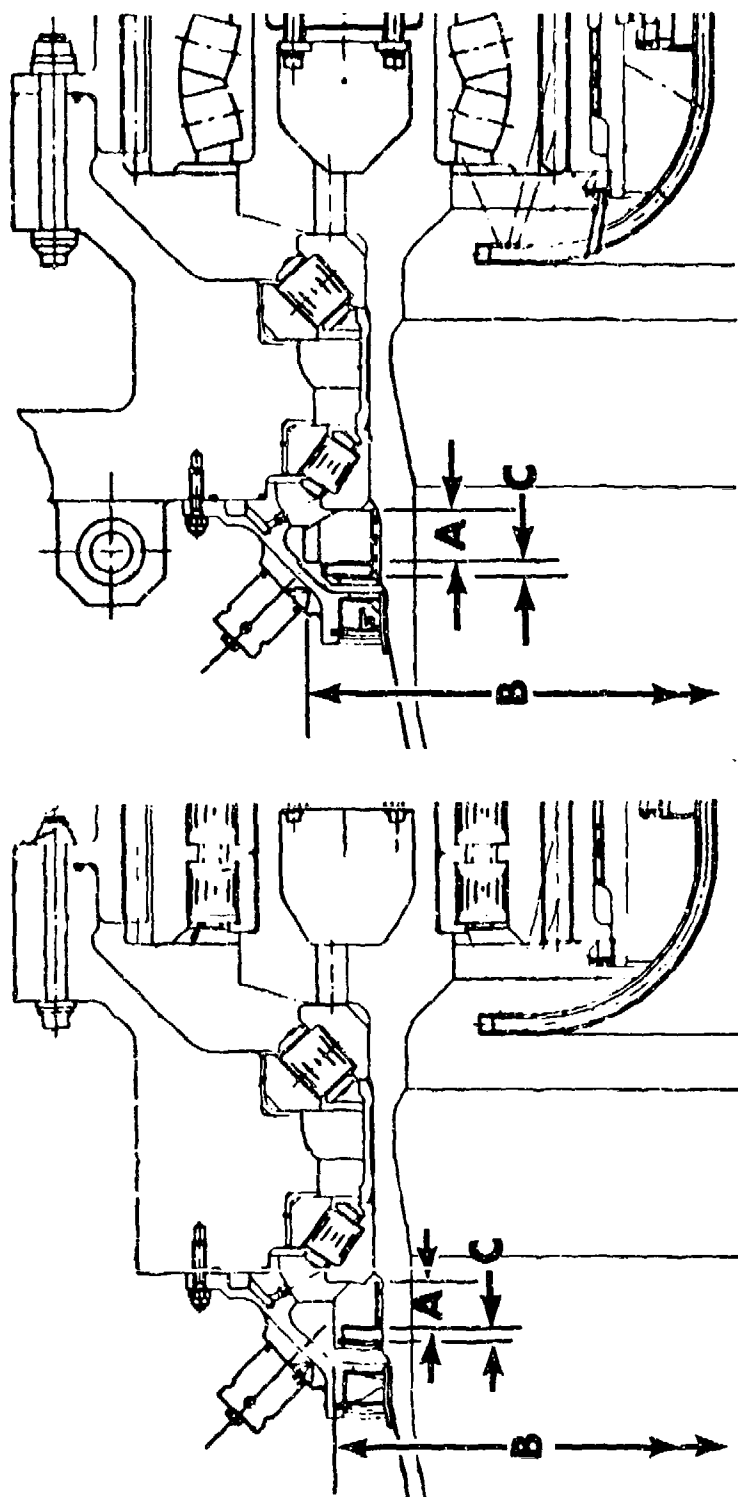
During DSTR testing the nut continued to move in a tightening direction, this time breaking the nut tangs rather than the washer. It was apparent that the failure mechanism was not purely shear, but rather that an outward radial expansion of the washer was loading the tangs in their weaker axis and causing their failure. This outward expansion was explained by wear at the shaft keyway to inner tang interface, creating a radial component along the wear slope created there. In consequence of the DSTR nut locking failure some of this testing was run without a lockwasher. When the nut tightened beyond permissible limits, established by measured expansion of the thread diameter, it was replaced with another like part.

The prototype nut and locking assembly was redesigned as a result of the DSTR experience. The criterion for the locking devices was that they should accept twice the installation torque, using conservative assumptions of load sharing among tangs. As Figure 27 shows, the lockwasher thickness remained at .25 inch but the number of tangs increased, as did their depth of penetration into the shaft. The nut slots were redesigned for a significant increase in strength.

In addition, the threads were redesigned for lower expansive forces by changing to a nonsymmetrical form. A 7° flank angle is used on the loaded side and a 45° angle on the opposite side. This change is calculated to reduce nut hoop expansion by 90%. The pitch of the thread was reduced from 8 t.p.i. to 6, to further assure that the nut would not expand over the thread diameter. Finally, the width of the nut was increased by 20% to better react the rolling moment created by the offset of the centroid of axial forces from the thread diameter. The material, heat treat and silver plating of the ATC nut were continued unchanged in the prototype design.

Shaft Oil Seal (301-10432)

This is a segmented circumferential carbon seal manufactured by the Stein Seal Company. A carbon seal was required due to the relatively high rubbing speed (10,450 FPM) at the seal/shaft contact in the aft and 16,600 FPM at the combining transmission inputs. The seal is used at the input bevel pinion



	ATC DESIGN	PROTOTYPE DESIGN
Nut Width. A	1.096	1.315
Nut Dia. B	23.350	24.500
Thread Dimen. C	21.250-8 UNJS-3A	21.250-6 (N BUTT-3) Flank Angle = 7°
Lockwasher	.05(Initial); .25(Final)	.25
Internal Tangs	2 (.490 Wide)	6 (.490 Wide)
External Tangs	4 (.275 Wide)	8 (.490 Wide)

Figure 27. Rotor Shaft Bearing Locknut Comparison.

on the aft and at five positions on the combiner transmission. In the aft transmission the seal cavity was scavenged by a mechanically driven pump. A similar approach was used at the combining transmission engine-input location. The seal design (Figure 28) incorporates a coarse thread in the housing and a slotted sleeve on the rotating shaft. This feature, called a windback, acts as a pump to force oil away from the seal as an aid to the primary carbon sealing elements. The hand of thread changes with direction of rotation; different dash numbers were used for clockwise and counter-clockwise positions.

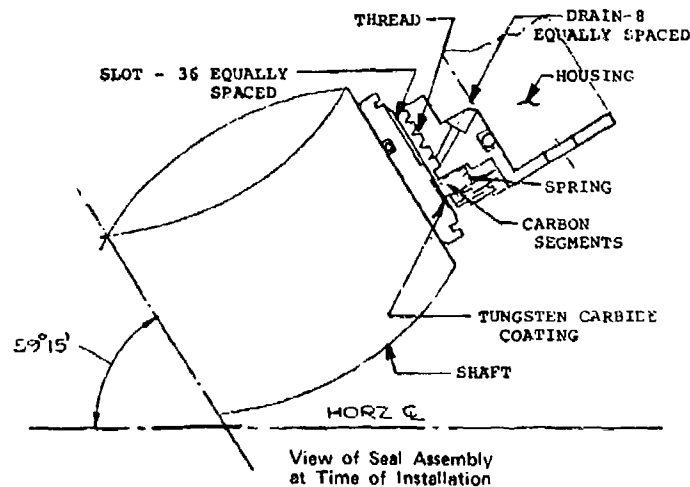


Figure 28. Aft Input Shaft Seal.

Initial leakage problems were masked by assembly damage caused by driving the pinion support housing into the main housing and breaking the carbon elements by the impact. This was corrected by installing the seal after the pinion assembly was installed.

Leakage in the aft transmission continued at an excessive rate (1 quart/hr versus a desired limit of 2cc/hr).

A review of the hardware and installation with the vendor concluded that the leakage was in part due to the seal being at the low point of the box and filling up with oil at shutdown.

The solution was to add internal oil drain holes in the seal housing to allow oil to drain out of the seal windback area at shutdown.

The final 30 hour test at the DSTR incorporated eight holes added by rework by the seal vendor. Seal leakage was within limits for the final 30 hours test.

COMBINER TRANSMISSION

Summary

The combiner transmission development program is outlined in Figure 29. Following the failure of the bevel portion of the collector gear, the maximum torque was limited to 60% of the original design. A 103-hour test of the combiner was conducted at this and other lesser torque conditions, and with various engine input combinations in the DSTP. Evaluation of strengthened gears for prototype use was made at the end of the ATC program. Results of this investigation are found in Section 7. Problems that were not power related were defined and corrected during the ATC program, as will be seen in Table 8. The ATC development, therefore, provided a measurable increase in confidence in the final design.

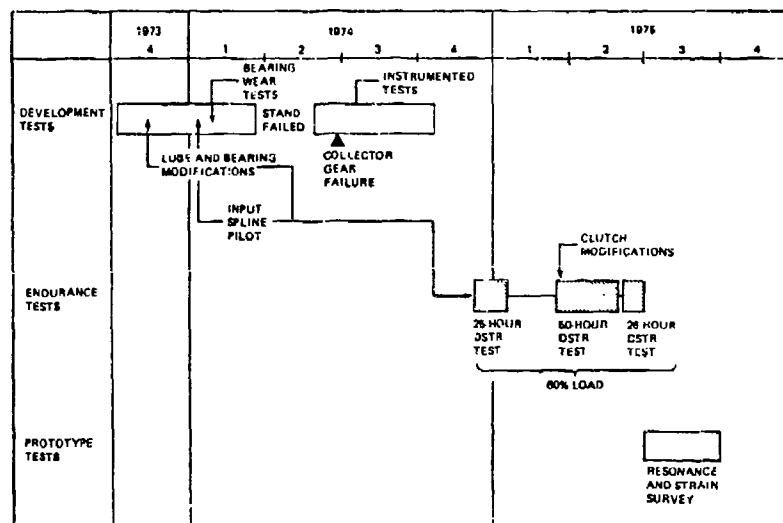


Figure 29. Combiner Transmission Test Sequence.

Test Specimen

The initial test specimen was as defined by Drawing 301-10600-1. Latter test specimens were modified as defined in this report.

Pretest Preparation

Spiral bevel gear tooth bearing patterns were taken as described under aft transmission. The scope of this effort was necessarily larger and more complex because of the number of gears involved (4), and the interactions between gears. Table 9 describes the conditions for gear patterning before the initial load run.

**TABLE 8. COMBINER TRANSMISSION TEST PROBLEMS
AND RESOLUTIONS**

PROBLEM	ATC RESOLUTION	PROTOTYPE RESOLUTION
Gear (Combiner, Slant Bevels) Stresses above Allowables	1) Repattern to develop optimum load distribution 2) Investigate Add-on stiffening of rim 3) Operate at reduced (60%) torque	1) Increase thickness of gear rims 2) Increase face width and coarsen pitch
Resonant Frequencies Leading to Damaging Stresses in Pinion and Gear	1) Develop and apply analytical and experimental methods to predict and measure stresses 2) Detune with add-on stiffening rings 3) Add damping to criteria developed in ATC program	1) Apply analytical and experimental methods 2) Detune by redesign 3) Maintain added damping
Tapered Roller Bearing Roll-End Wear	1) Reduce axial play to eliminate skidding 2) Improve lube distribution 3) Improve oil (Aeroshell 555) 4) Temper at 500°F and phosphate coated	SAME AS ATC
Tapered Roller Bearing Cage Failure	Increase cage pocket corner radius	SAME AS ATC
Tapered Roller Bearing Retainer Tang Failures	Do not rebend tangs	SAME AS ATC
Clutch Support Bearing Outer Race Wear	Bond outer to housing	Mechanical key - Outer to housing
Clutch Housing Crack	Eliminate source of load by improved piloting of input shaft (centering rings)	SAME AS ATC, except add integral pilots
Sprag Clutch Wear	1) Improve lube distribution and retention 2) Modify sprag design	SAME AS ATC
Cylindrical Roller Bearing Roll-End Wear	Decrease internal axial clearance	SAME AS ATC
Fretting of Bearing Seats (Various Shafts)	NONE	PHOSPHATE INNER RACES

TABLE 9. GEAR PATTERN CONDITIONS

Test Sequence	Engine Input Condition	Engine Power %	Engine Torque In-Lb	Temperature °C	Fwd/Aft Output Torque Split - %
1	1, 2, 3	50 AEO	16, 150	99°	40/60
2	1, 2, 3	75 AEO	24, 225	99°	40/60
3	1, 2, 3	110 AEO	35, 500	99°	40/60
4	1, 3	100 OEI	44, 250	99°	50/50
5	1, 2	100 OEI	44, 250	99°	50/50
6	2, 3	100 OEI	44, 250	99°	50/50
AEO - All Engines Operative					
OEI - One Engine Inoperative					

Development Testing

Load testing began in October 1973 under the schedule shown in Table 9. Inspection after 4 hours and 39 minutes of operation revealed heavy roller-end wear of the tapered roller bearings on the engine bevel pinions and light-to-moderate wear of cylindrical roller bearings supporting the helical pinion and the collector gear.

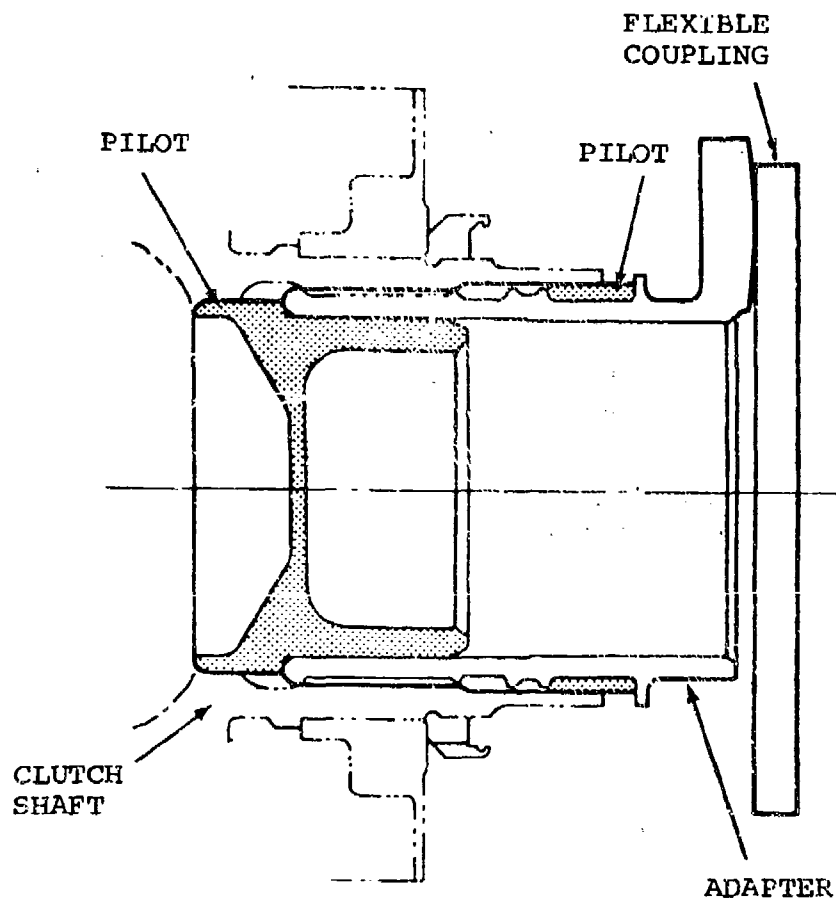
Pinion-area lubrication was improved by providing added breather area and by improving oil distribution and drainage. It was found that oil was not distributing properly from the rotating lube tubes in the pinion bores. These rotating tubes were replaced by longer, nonrotating jets, pressure fed from the main lube system. Oil was thus supplied through metering holes to each area that required lubrication. Additionally, more lubricant was supplied to critical areas and the lubricant was changed to Aeroshell 555.

Modification to the roller bearings was also made to eliminate end-wear. As-mounted axial clearance of the taper bearings was reduced to eliminate roller skewing. Additionally, the bearings were retempered at 500°F, and the inner races and rollers phosphate finished to improve scuffing resistance. Internal geometry changes were made to the cylindrical roller bearings.

Broken studs and severe fretting and wear were noted in the clutch housing area. It was initially believed that test stand shaft misalignment was responsible. Alignment was rechecked and corrected where necessary. In later tests, the clutch housings cracked after a few hours of running. With instrumented shafts, it was then determined that a nonsynchronous whirl was primarily responsible for these failures. The condition was corrected by addition of piloting surfaces to the adapter (Figure 30).

At this point in the program, the failure of the aft transmission input pinion occurred and a strain gage survey of all gearing was introduced to the program. Load testing of the combiner was delayed for installation of strain gages and telemetry read-out equipment. Gear resonance tests were begun as well.

When the transmission reentered strain survey and load testing, the configuration had been modified as shown in Table 10. Beyond the changes previously noted, the auxiliary oil supply was now filtered to eliminate a suspected cause of dirt denting.



PILOTS MINIMIZE ANGULAR
MOTION ACROSS SPLINE

Figure 30. Modified Combiner Input Adapter

TABLE 10. COMBINER TRANSMISSION MODIFICATIONS

ITEM	ORIGINAL CONFIGURATION	NEW CONFIGURATION 2/1/74
Input Pinion - Tapered Bearings Clearance Tempering Temp Lubrication	.004 - .005 in. 300°F Rotating Internal Tube	.002 - .003 in. 500°F Stationary Internal Jet (Ref 301-10600 Sheet 6)
Finish	None	External Oil to Heel End of Inboard Bearing Phosphate (Inner Race & Rollers)
Oil Filtration (Aux. System)	.015 in. Opening Inlet Screen	20/40 Micron Filter at Inlet
Input Adapter - Splined Connection	Unpiloted Splines - Radial Play Controlled by Spline Backlash	Piloted Splines - Radial Clearance .002 in.
Rotor Brake Gear	No Damping	Spirolox Damping Ring
Slant Shaft Pinion - Tapered Bearings		
Clearance	.0086 - .0096 in.	.005 - .006 in.

During operation, dynamic responses were verified on the main drive gears. These closely matched those predicted from excitation testing. In addition, testing of the piloted input adapters revealed no whirl mode at the previously noted 139 Hz or any other frequency. No shaft resonant responses were seen and vibration levels were well within acceptable limits. Following the reduction of the tapered bearing axial play, no evidence of roller end wear was noted.

The strain survey testing recorded acceptable stress levels on the input pinions, helical input pinion and the helical portion of the collector gear. No data were recorded on the slant shaft or the bevel portion of the collector due to loss of instrumentation.

During these strain survey tests under load, a failure of the collector gear (P/N 301-10601) occurred. The failure origin was in the tooth root. The mode of failure was fatigue.

Extensive static strain surveys and resonance testing were conducted to determine the configuration of each combiner gear to provide optimum tooth stress distribution and to eliminate high-stress resonant conditions in the operating range. Strain surveys were conducted at room and elevated temperatures and at a variety of torque levels. All gears incorporated increased damping ring mass. A transmission was then assembled for endurance testing.

Endurance Testing

The DSTR testing began with 25 hours of load running to the schedule of Table 3. Maximum torque was limited to 60% based on bevel gear tooth stresses. After 20.5 hours of running, a failure warning occurred in an overrun clutch cartridge assembly. Teardown and inspection revealed a broken cage in the duplex ball bearing. A spare clutch cartridge assembly was installed for the remainder of the test.

A clutch wear problem was noted. The cause of this was an over-large radial clearance in the oil dams on each end of the sprag assembly. This led to inadequate oil wetting of the clutch inner race, and consequent wear of both inner race and sprags.

A further 50-hour test on the DSTR was conducted following the schedule of Table 5. The combiner was inspected with the following results:

- 1) Cage cross-bar failure of an input pinion bearing (P/N 301-10676). This occurred and was detected after 22 hours of running. Corrective action was to modify the cage design to enlarge the corner radius and incorporate peening.
- 2) Filter cartridge top plate failed and allowed debris to migrate to the filter protecting screen. The cause was overtightening of the filter mounting stud. An axial stop was to be incorporated to prevent this.
- 3) Sprag wear was noted. Two of the three clutches were replaced. Gear and bearing condition was satisfactory for continued running.

A further 30-hour test was begun following the load schedule in Table 6. Near the conclusion of this test, a cage failure of the outboard tapered roller bearing carrying the rotor brake was detected and the test was stopped at this point. Analysis of the failure indicated that the end play of the taper roller support bearings should be decreased to prevent misalignment through the bearing when a load is applied from rotor brake. This adjustment can be made by change of shim size.

Total DSTR running time on test conditions was 102 hours, 54 minutes. The rotor brake was applied 44 times during DSTR running.

COMPONENT INVESTIGATION

This section describes investigation and design changes of major components. These include:

- Bearing wear - tapered rollers and cylindrical rollers
- Overrunning clutch wear problems

- Input shaft - whirl problem and its solution
- Bevel gears - stress measurements and resonant analysis and tests including final prototype configuration

Roller Bearing End Wear

End wear was characterized by removal of material from roller ends and race guiding ribs. In addition, there were areas of skid damage on the inner race of the tapered roller bearings. There was also moderate wear of the cage pockets with heavy wear in the corners.

Bearings that showed end wear problems are listed below. All were from the combining transmission.

<u>Location</u>	<u>Part No.</u>	<u>Type</u>	<u>Degree of Wear</u>
Input pinion (Spiral Bevel)	301-10676-1	Taper Roller	Heavy
	301-10671-1	Taper Roller	Heavy
Input Pinion (Helical)	301-10656-1	Cyl. Roller	Light
	301-10640-1	Cyl. Roller	Light to Moderate
Collector	301-10666-1	Cyl. Roller	Moderate
	301-10638-1	Cyl. Roller	Light to moderate

Timken Roller Bearing Company examined six tapered bearings from combiner tests. Their conclusions are summarized as follows:

Cause of damage was skidding. Skidding is caused by slippage of the cage and roller set relative to the cone (inner race).

- The primary damage was remelting, rehardening, and tempering.
- The remelted areas were raised above the original surface to become asperities. These subsequently spalled away and provided very hard abrasive particles to cause a machining type wear of the mating surfaces.
- Pitting seen on the cone race, ribs, and roller ends was caused by this spalling.

- Skidding was initiated and propagated by system vibrations.
- Skewing occurred as a consequence of damage to the roller guiding surfaces and excessive axial play.

Corrective actions for the tapered bearings included the following:

- Reduction in axial play from the .004-.005 inch prescribed for the original design to .000 to .001 inch preload. The purpose of this reduction was to increase the roller driving force to prevent skidding. It served also to increase roller guidance to prevent skewing. The skewing of the rollers produced the corner wear in the cage.
- Increasing the amount of oil delivered by increasing the size and number of jets.
- Changing oil from MIL-L-23699 Rev. B Specification to an oil with an improved load capacity rating which also meets a proposed Rev. C of the Specification. This oil was Aero Shell 555.
- Phosphate coating the cone (inner race) and rollers to provide a degree of break-in lubrication.
- Tempering at 500°F to improve scoring resistance by reducing retained austenite.

Roller end wear in the cylindrical roller bearings was examined by the Rollway Bearing Company and SKF Industries, Inc., the manufacturers of cylindrical roller bearings. It was concluded that insufficient roller guiding was suspected as a main cause of the problem. Bearing channel clearance (the axial space between roller ends and race flanges) is critical to the prevention of roller skewing. Recommendation for the application was to reduce the channel clearance to .0005-.0017 inch. The problem bearings had .002-.004 inch clearance. Bearings with lower-limit clearances appeared to have suffered less damage in the first tests. In addition, the angle of the flange is important for oil film generation and supply. Final recommendations were to taper the flange outward by 30 minutes for 50% of flange height, and then to increase to $3 \pm \frac{1}{2}$ degrees to the outside diameter.

To further increase roller guidance, the end face diameter of the rollers were enlarged by decreasing both the break point dimension and the roller corner radius.

The modifications enumerated, together with a change in lubricant to provide increased surface capacity (Aero Shell 555), eliminated the roller end wear problem in both cylindrical and tapered roller bearings as evidenced by further testing.

Overrunning Clutch (301-10646-1)

An overrunning clutch is at each of the three engine inputs to the combiner. The clutch is a two-row, tandem-cage, full-phasing sprag-type clutch made by Borg-Warner.

During initial checkout of the system at the DSTR, clutch slip occurred on one engine as the clutch engaged after slipping and suddenly brought the system up to speed. Instrumentation on subsequent runs with the same parts disclosed engine torsional resulting from resonance of a spring in the engine fuel control. An immediate fix for the problem was a hydraulic accumulator in the fuel system.

During ATC bench testing of HLH clutches, it was determined that cyclic torque variation above $\pm 39\%$ steady torque resulted in clutch slip. In the above testing, the torque variation was close to $\pm 100\%$ of steady torque. It was, therefore, to be expected that the clutch would slip.

Inspection of the clutches during the DSTR tests (Table 11) showed wear of the inner sprag contact and inner clutch shaft-mating surface. Investigation revealed that the oil dams on either side of the clutch, which normally retain oil in the clutch, were oversize in internal diameter. The oversize dams allowed the oil to flow out of the clutch to the inner race contact area. New dams were made for the 50- and 30-hour tests. Input location three, which incorporated the new dams and an unworn clutch assembly, demonstrated the improvement potential of the new dams during the 50-hour test.

Inspection of the clutch, following completion of 26½ hours of the final 30-hour DSTR test, revealed wear on the number one and number three position clutches similar to the wear observed during the 50-hour test, but somewhat more severe relative to tearing of surfaces. Also, wear occurred on the

TABLE 11. SPRAG CLUTCH HISTORY - DSTR TESTING				
INPUT LOCATION	CLUTCH S/N	SPRAG WEAR (FLAT WIDTH-INCHES)		
		25-HOUR TEST	50-HOUR TEST	30-HOUR TEST
#1	XBW 100	.060	.090	--
	XBW 103	--	--	.080
#2	XBW 108	.070	.100	--
	XBW 116	--	--	0
#3	XBW 107	.050	--	--
	XBW 101	--	0	--
	XBW 104	--	--	.060

input adapter pilots in the same clutch positions. The clutch and pilots in the center position (number two position) were not worn.

The prototype clutch assembly would have incorporated improved adapter pilots with integral pilot surfaces, the proven dam configuration for adequate lubrication, and modified sprags. With these changes, and with normal continued development, it is expected that clutch sprag wear could be reduced to meet the requirements.

Input Shaft Whirl

During initial testing of the HLH Combiner Transmission, fatigue cracks were observed (after only a short period of operation) at the base of the magnesium castings which house the input pinion/clutch assemblies. The units were replaced, and subsequent runs with the housings instrumented revealed both high vibration and stress levels over a broad range of operating speeds. It was further established that the problem only existed below 50% torque and was most severe at zero torque.

Examination of the overall vibration levels indicated that the problem area was confined to the engine shaft speed range from 134 to 172 Hz (8040 to 10,320 RPM). An analysis of the frequency content of an accelerometer mounted at the free end of the cantilevered housing is shown in Figure 31 for the zero torque condition. During run-up, the frequency of vibration coincides with the engine shaft (combiner input shaft) operating speed up to approximately 134 Hz. For speeds between 134 and 172 Hz, the predominant frequency of vibration remains nearly constant at 134 Hz, and above 172 Hz the frequency shifts abruptly to approximately 90 Hz. During the

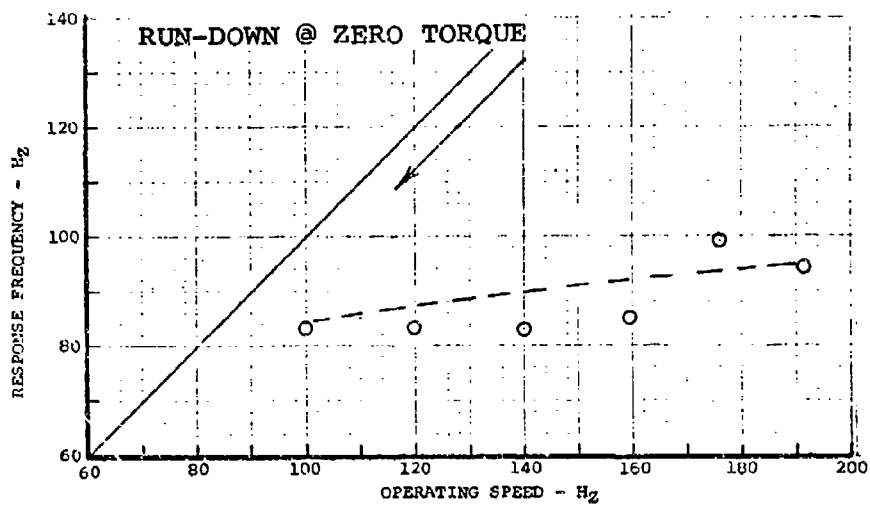
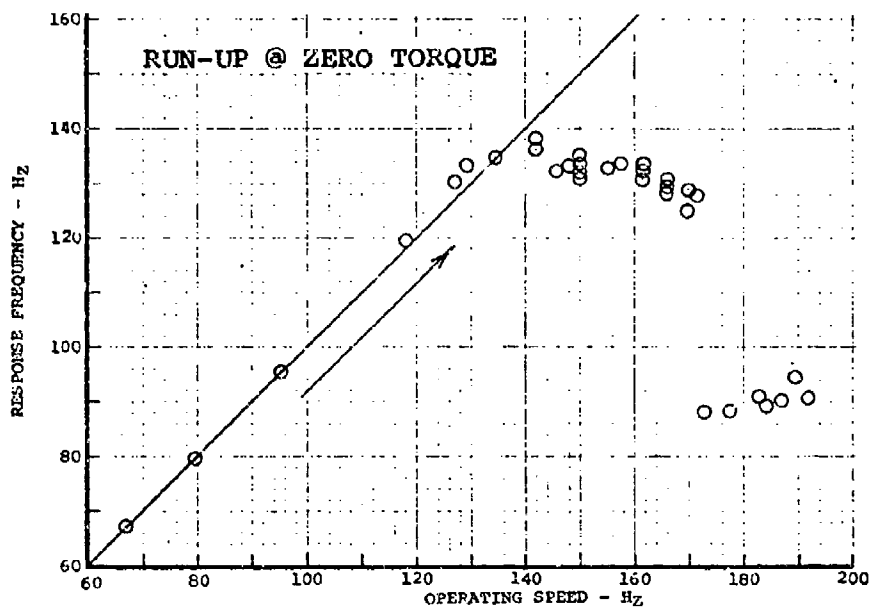


Figure 31. Response Frequency vs Operating Speed.

subsequent deceleration, the low-frequency component, 83 to 95 Hz, persisted down to operating speeds below 100 Hz.

Filtered acceleration response plots for the zero torque condition are shown in Figure 32. The upper plot illustrates the vibratory component at the engine shaft operating speed and indicates a peak response centered at an engine shaft speed of approximately 8040 RPM (134 Hz). The lower plot shows the vibratory component at 134 Hz, and significant response at this frequency is observed over the engine speed range from slightly below 8040 RPM (134 Hz) up to 10320 RPM (172 Hz). Note also that within this range, the magnitude of the response at 134 Hz is generally greater than the response at the operating speed.

An acceleration response plot displaying the vibratory component at the engine shaft operating speed with 50% torque is shown in Figure 33. The maximum level is only 5G's compared to 20G's observed for the zero torque condition.

Together, the plots of Figures 31 and 32 point to a phenomenon referred to as nonsynchronous whirl; i.e., a whirling motion which does not correspond to the speed of rotation. Published literature on the subject of nonsynchronous whirl is limited; however, the material of References 13 and 14 appears applicable. Briefly, this document indicates that nonsynchronous whirl is a frictionally excited instability associated with large angular motions (bending) of splined joints. Implicit in this situation is the proximity of a critical speed with a bending mode shape displaying large angular deflections at the spline.

It was theorized that the splined input adapter represented the most probable source of excitation due to the angular freedom permitted by the adjacent flexible coupling. The mitigating effect of torque also suggested the presence of a low-frequency critical speed due to low initial stiffness of bearings and splines in the input pinion/clutch/shaft assembly. In this regard, the splined input adapter was again believed to be one of the major contributors.

On the basis of the above, the modified input adapter of Figure 30 was designed for test evaluation. The addition of pilot surfaces on each end of the spline restricts the angular bending motion across the spline. Axial freedom of the spline, which is a principal design requirement, is not impaired. Response at the engine shaft operating speed with the piloted spline is presented in Figure 34. There is no indication of any resonance, and comparison with the original adapter configuration shows a dramatic reduction in the response level.

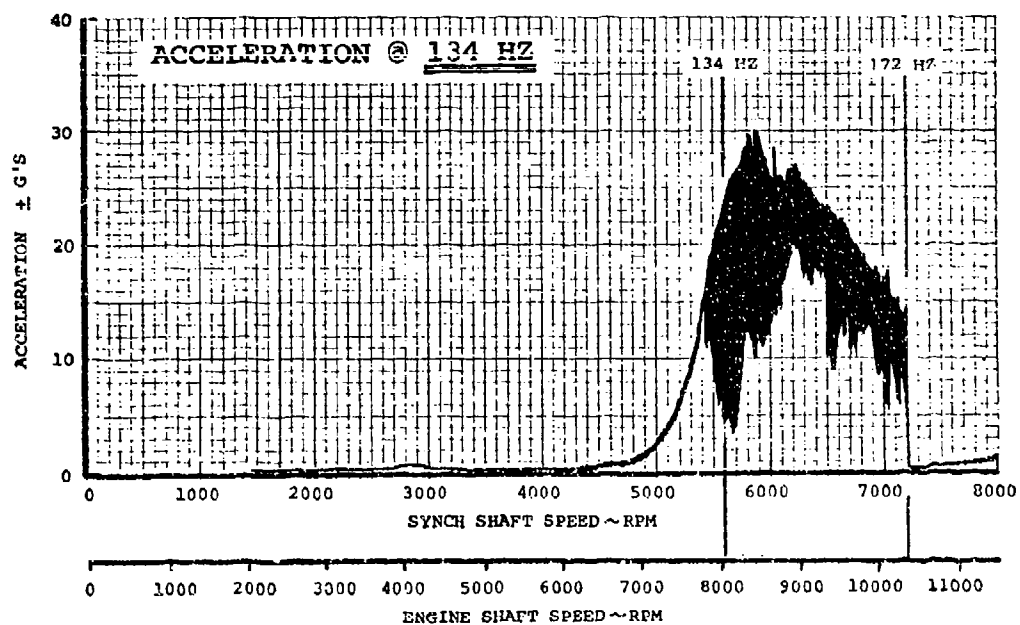
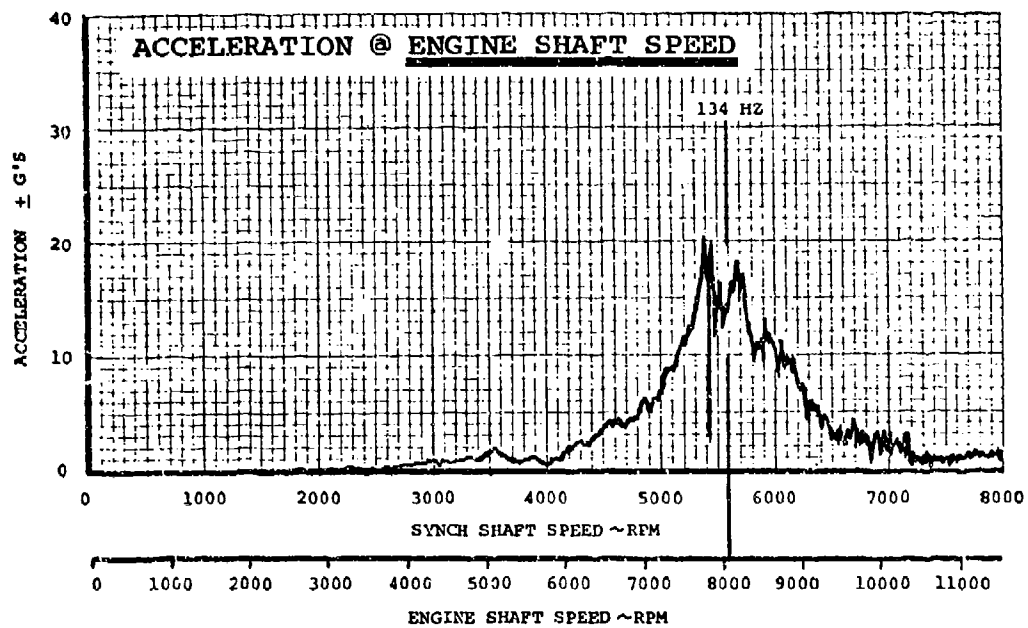


Figure 32. Clutch Housing Acceleration at Zero Torque.

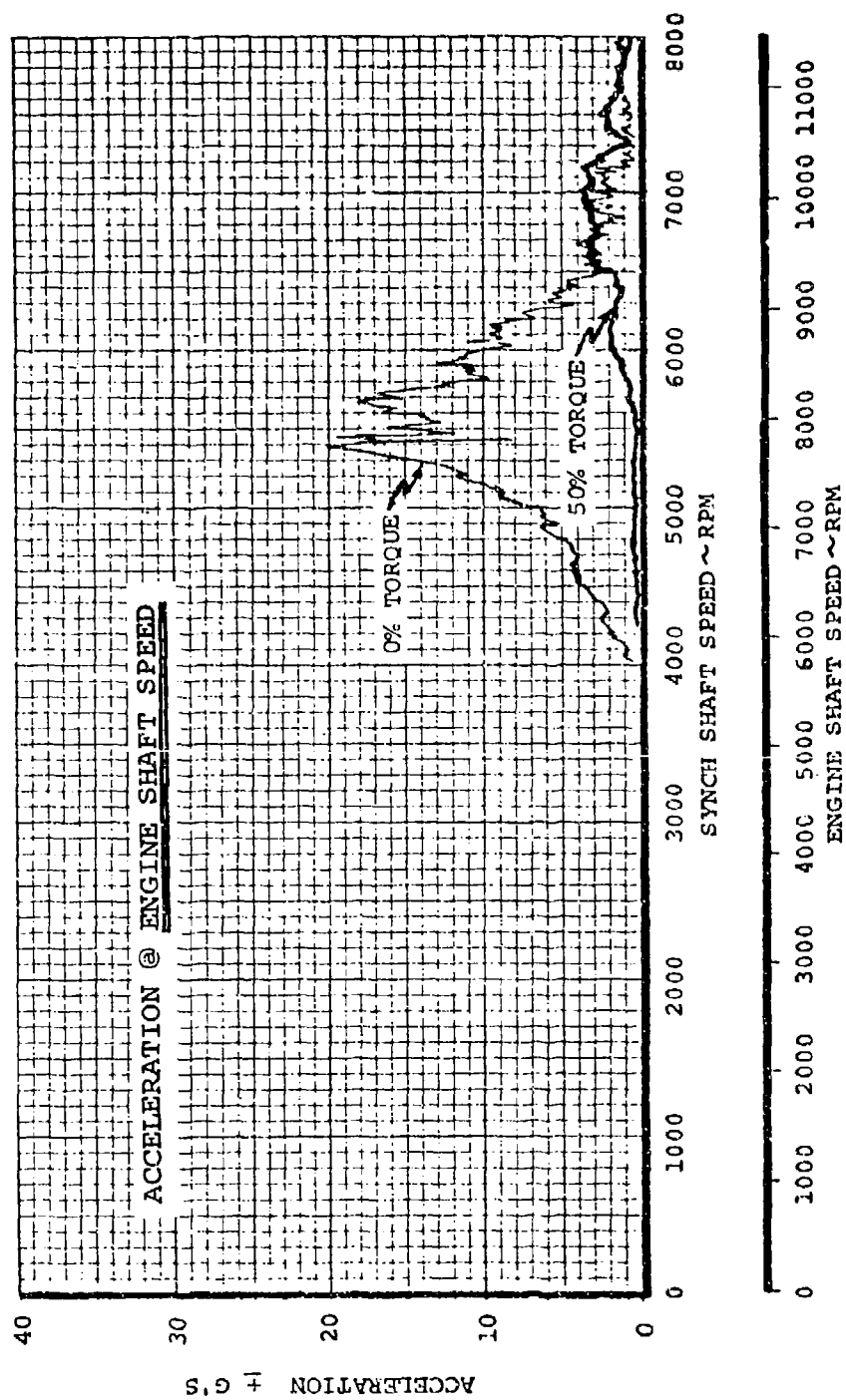


Figure 33. Clutch Housing Acceleration at 50% Torque.

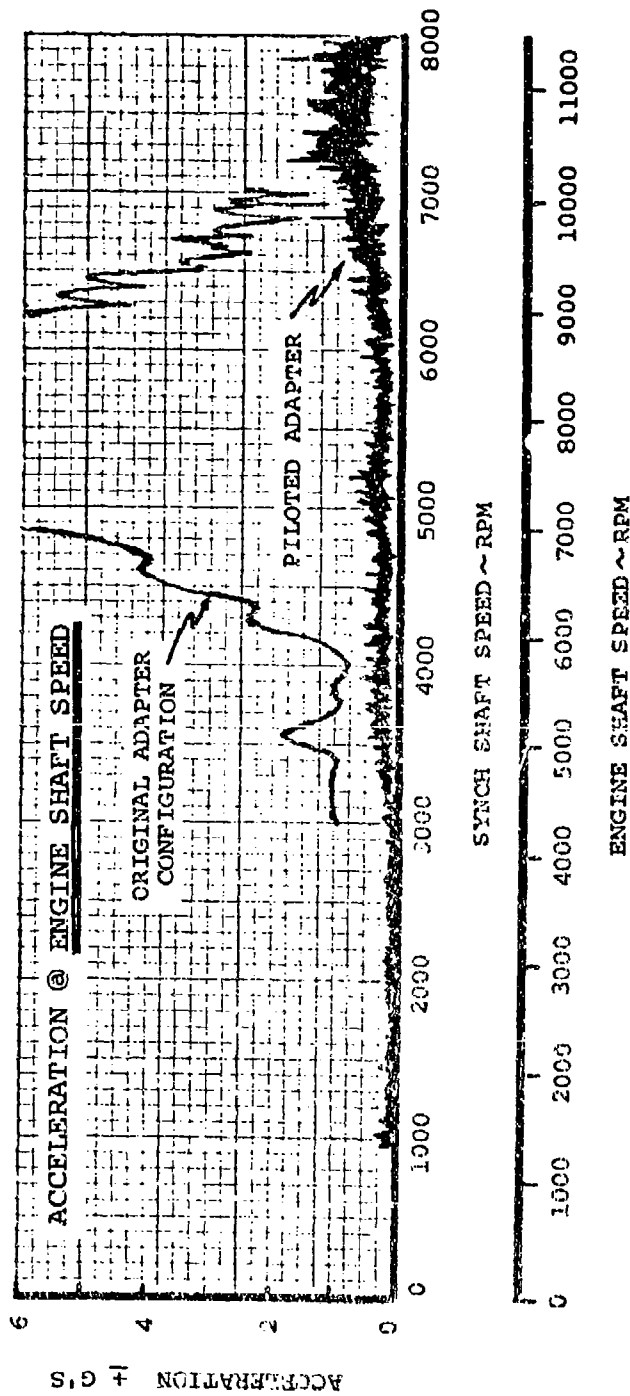


Figure 34. Clutch Housing Acceleration With Modified Input Adapter.

DRIVE SHAFT ROTATING TESTS

Test Specimen

Both the load test stands and the DSTR used HLH design drive shaft sections, couplings, and adapters. Input shafts were each in three sections with two support bearings following the design shown in Figure 7. The load stand had one representative synchronizing shaft section attached to the combiner aft drive and one attached to the forward drive; one shortened synchronizing shaft segment was attached to the aft transmission input. The DSTR differed from the load stand in that the combiner aft drive incorporated the full aircraft complement of three shaft sections and two support bearings. In addition to these test facilities, an input shaft section was also run at DDA in order to connect the T-701 engine to a dynamometer.

Test History

The only shafting problem encountered in the load stand testing was the nonsynchronous whirl phenomenon described in the combiner section. As noted, the problem was localized to the input adapter to pinion spline joint and corrected.

Testing of the engine shaft section at DDA resulted in a failure of the coupling adapter (similar to P/N 301-11023-1). This failure resulted in a reappraisal of loads and forces on the lug and bolt area of the HLH adapters. These connections operate at higher peripheral speeds than were encountered in previous experience. Following reanalysis of the adapters for both engine and synchronizing shafts, the decision was made to improve material allowables and eliminate or reduce the fretting seen in the bolt-lug and lug-coupling path interfaces. This corrective action was implemented for the prototype aircraft.

Engine Shaft Support Bearing (P/N 301-11018-1).

Three failures of this bearing occurred during the DSTR Program. On no occasion did the bearing actually break up or fail to operate; but on all occasions the bearing overheated and exuded melted grease and/or evidenced sufficient looseness that further operation was considered to be impractical.

The first occurrence was discovered on the number one engine shaft forward hanger during a walk-around inspection of the rig after approximately 5 hours of rig time. Initial analysis

concluded that the condition was due to lack of grease lubricant. However, a subsequent similar occurrence during UTTAS drive system testing indicated that the cause was misalignment through the bearing. This misalignment is a result of the end faces of shafting being out of parallel as assembled. The shaft assembly comprises steel end fittings riveted to aluminum tubes. Initial design depended on diameter fit and seating parts against shoulders for alignment. Measurement of finished shafts revealed an excessive out of parallel condition that was not limited by the tolerances of subassembly but depended on the tolerances of details. An assembly parallelism requirement was established; subsequently all rig shafting was removed and inspected to the requirement, reworked as necessary, and reinstalled on the rig.

This condition occurred a second time at the same hanger location and was discovered during a post-run inspection after approximately 110 hours of rig operation. The condition again was initially attributed to loss of grease and all rig shaft bearings were regreased before the next rig start. However, examination of the removed bearing revealed heavy case wear, several broken rivet heads, and balls worn undersize by 0.006 in. It was concluded later that this failure was probably again due to misalignment, and all DSTR shafting was removed and the bearings were visually inspected as part of the post 50-hour tear-down inspection (116 hours total rig time).

During the late stages of the 30-hour endurance test, the bearing at the forward hanger location on the number one engine shaft again began to emit grease. The bearing was regreased and inspected for looseness at all subsequent rig inspections. At approximately 141 hours rig time, that bearing was running hot and appeared much looser than the other shaft hanger bearing, and it was decided to replace the bearing. All rig testing was terminated approximately six and a half hours rig time later.

Examination of the third replaced bearing was not accomplished due to program termination. Cause of the overheated condition has not been established; however, the following facts are known:

- All malfunctions occurred at the same bearing location (number one engine shaft, forward hanger).
- Optical alignment verification of combining transmission mount points, shaft hanger bearing locations, and engine mount points was performed only at the number two engine location during the course of DSTR testing, and those only during the course of repairs required to rig structural damage caused by freezing of trapped water.

- Misalignment induced at other shaft hanger bearing locations throughout the course of the DSTR Program did not result in any bearing malfunctions or unsatisfactory conditions, nor did inspection of any of the other hanger bearings give indication of any unsatisfactory condition.
- Hanger bearing regreasing intervals on the DSTR ranged from 25 to 50 hours - far below the 300-hour design objective.

An apparent cause of the bearing overheat problem is rig misalignment; however, this has not been substantiated due to the termination of the program.

7. DESCRIPTION OF PROTOTYPE CONFIGURATION

ROTOR TRANSMISSION

Prototype rotor transmission configurations are shown as Figure 35 (Aft) and Figure 36 (Forward). These incorporate the changes developed as a result of the ATC program. Significant changes are defined in Table 12 and Figure 37.

The bevel gears designed and fabricated for the prototype were subjected to static strain surveys in which they were rolled through mesh and tooth root and fillet stresses recorded. Compared to the ATC configuration, the Prototype gears exhibited an increase in root tension and a large decrease in root compression. This was because the increased backup material in the rim reduced the ring bending stresses.

Fillet stresses in the pinion were found to limit allowable torque. Allowable torque was defined as 93% of the design rating of 83,800 inch-pounds at the pinion. Because the pinion pattern ran off the tip of the tooth, a grinding improvement to bring the pattern onto the tooth can be expected to reduce the pinion fillet stresses sufficiently to allow prototype operation at 100% of the design rating. The aft bevel gears were, therefore, considered satisfactory for Prototype flight. The forward bevel gears, although not tested, are similar in design so that their torque capacity is likely to be comparable to the aft.

COMBINER TRANSMISSION

The prototype combiner transmission is shown in Figure 38, with significant changes defined in Table 13 and Figure 39. The bevel gears shown are designed with increased rim thickness, but with identical face width and dimetral pitch, compared to the ATC program.

These gears were fabricated and evaluated in the same type of static strain survey as the rotor transmission bevel gears received. The measured stress levels would not have permitted operation at full torque in the prototype aircraft. It was evident that further design would be required to allow the combiner to operate at its design point. The possible approaches were explored and a satisfactory approach was defined as explained below. The new design was not tested because of the limits of program termination.

125

301-10668-17
NAS630-6-3
301-10416-5
(ONE UNDER BOLT HD
(ONE UNDER NUT)
EWSN22-10 (2)

ANY-21A
ANS60-7/6
MS21045-7
301-50325-4 (REF)
301-10412-3
301-10414-1
301-10425-2

301-10428-21
301-10436-1
301-10474-10
NAS626-30
MS20002-6
FN22-624 (2)

301-10607-6 (REF)
MS21045-4 (REF)
ANS60-8/6 (REF)
BACPIIP-14
301-10648-14
301-10440-4
301-10615-11

301-10430-3
301-10458-1
301-10445-1
301-10402-2
301-10474-5
301-10428-5
301-10458-1

MS21045-4
ANS60-4/6
301-10441-2

301-10440-1

46-084
167

301-10428-1
301-10435-4
301-10435-1
301-10436-9
301-10419-5
301-10434-5

8265 RPM

MS21045-8
ANS60-8/6
(2)

10678 RPM
2700 RPM
(2)

301-10426-1

301-10408-1
301-10405-1
301-10436-4
301-10411-3 (2)
301-10474-25
301-10474-50
301-10436-5

301-10668-15
301-10648-16
MS21045-4
ANS60-4/6
(2)
301-65025-1

RR-775
301-10423-M
(2)

EWSN22-30
301-10416-1
301-50325-4 (REF)
301-10423-100
301-10474-100
301-10436-2

MS21045-7
ANS60-7/6
(2)

NAS626-20
301-10416-5
(ONE UNDER BOLT HD
(ONE UNDER WASHER)
FN22-624 (2)

BACPIIP-M
MS21045-4
ANS60-4/6
(2)
301-10436-7 (2)

301-10407-17

SECTION D4-10
-2 ASSEMBLY

301-10400 (2)

1.0001
64500 (3)

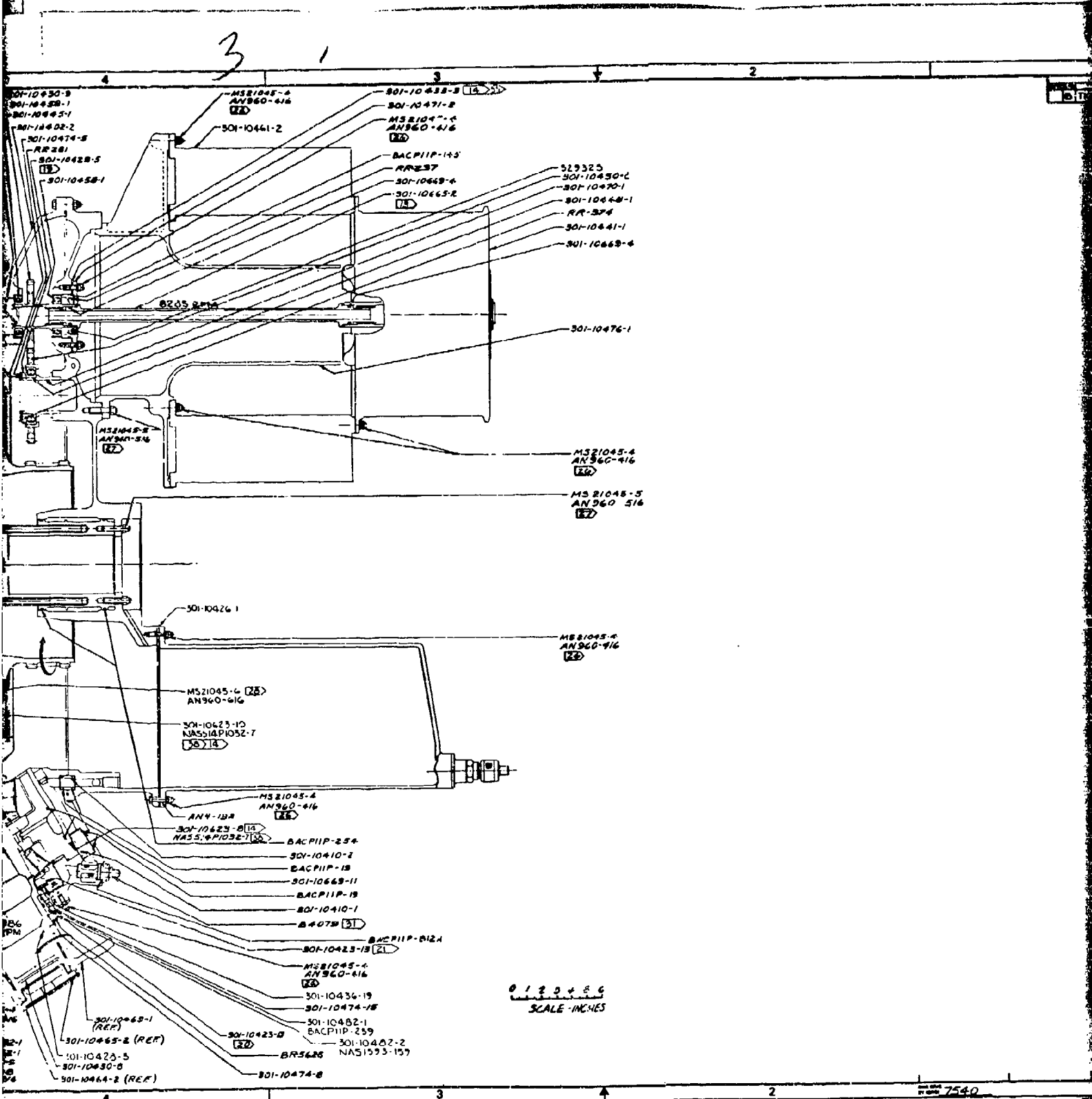
1756 RPM

MS21045-4
ANS60-4/6
(2)
301-10602-1
301-10448-1
301-10449-5
MS21045-8
ANS60-8/6
(2)

301-10465-1 (REF)
301-10425-5
301-10430-5
301-10464-2 (REF)

301-10422-6
(2)

301-10422-6
(2)



4

NO.	REV.	DATE	BY
1	1	20-15	20
THIS SHEET ADDED			

0

C

B

A

301-10400B7

7540

1

2

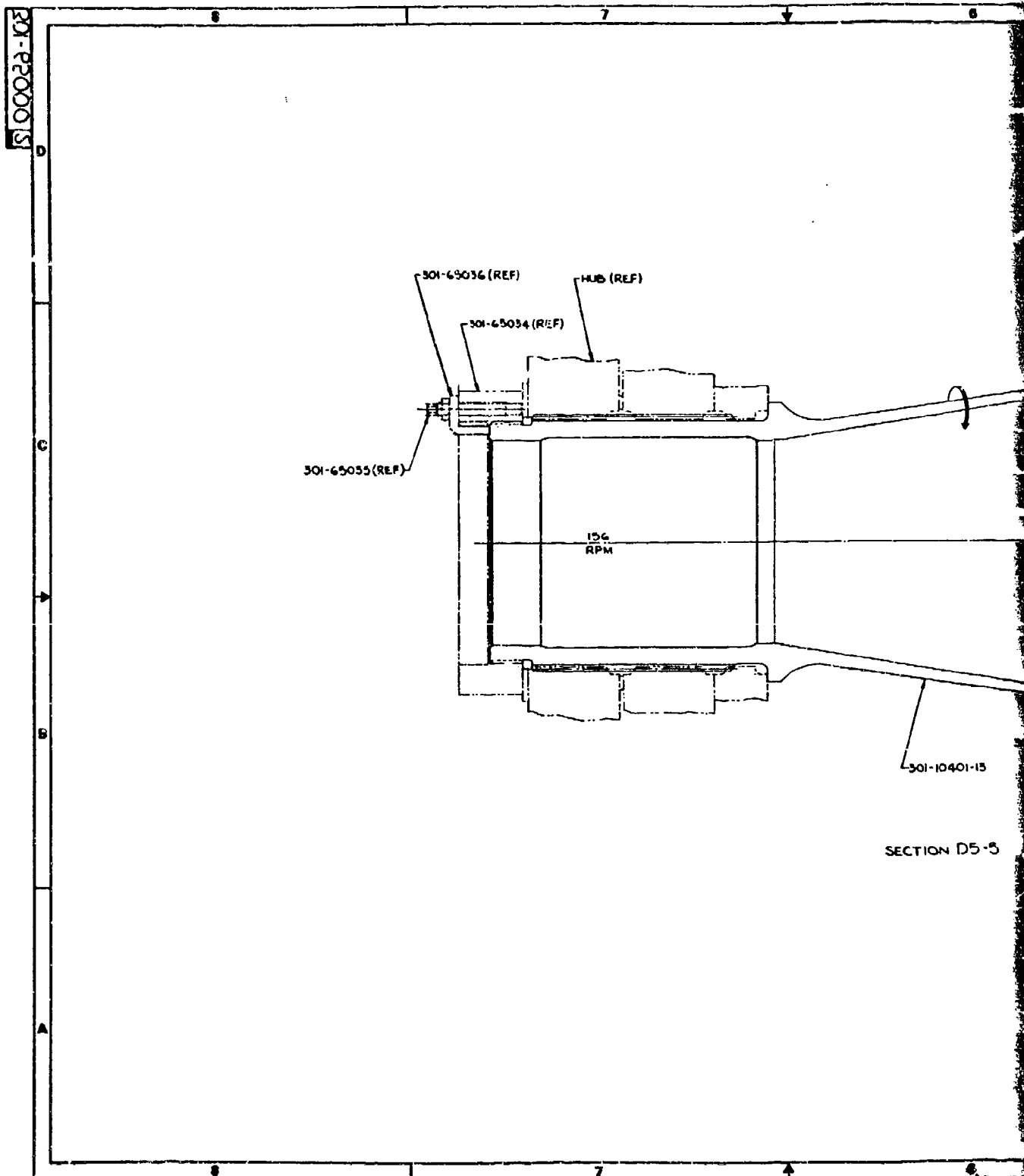
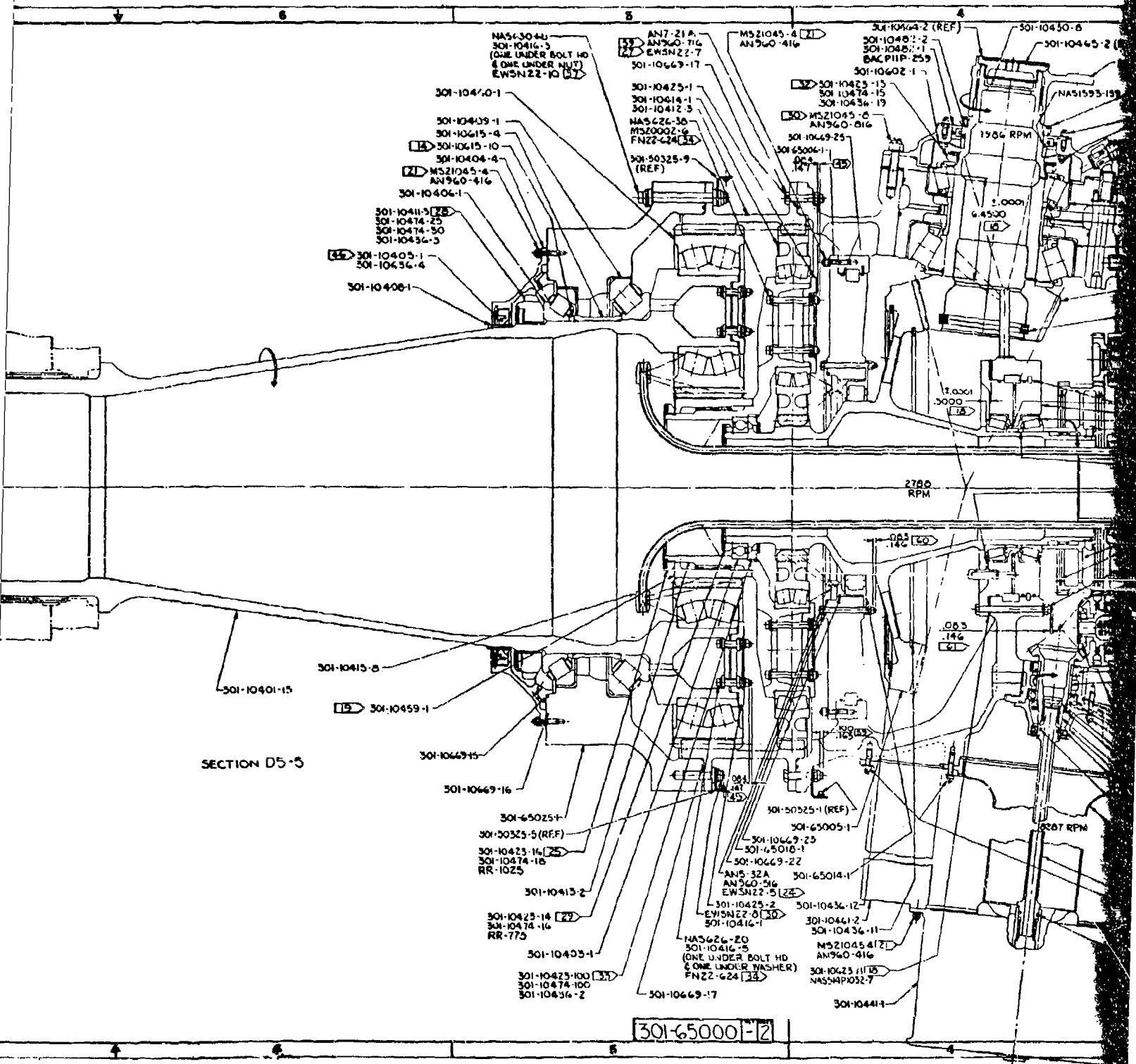
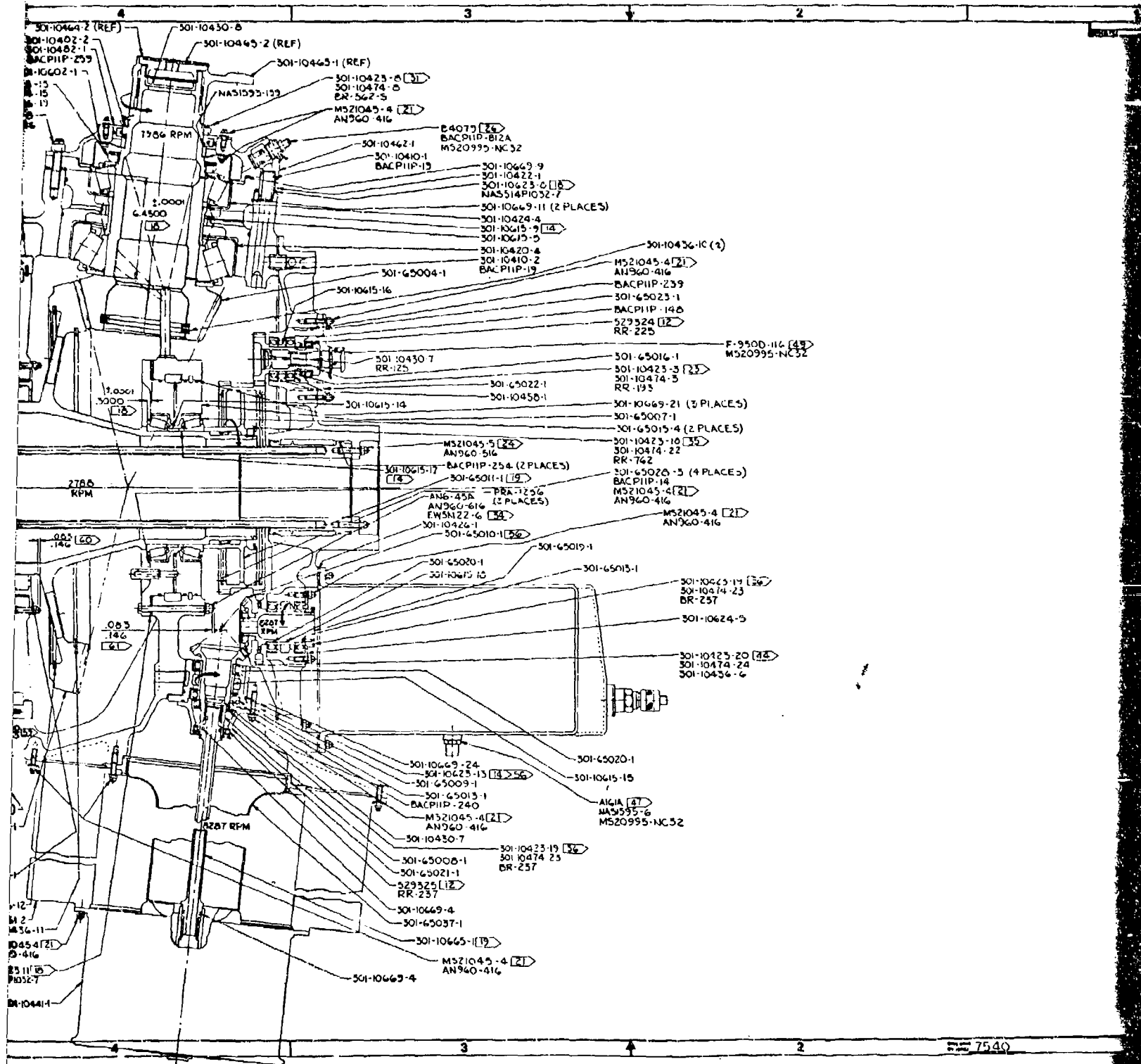


Figure 36. Forward Transmission Assembly (Sheet 1 of 3).



3 1



4

2		1	
F-550D-116 (33)		M320995-NC52	
CES)		CES)	
CES)		CES)	
21		21	
23-19 (36)		24-23	
24-5		25-20 (34)	
74-24		36-6	
2		1	
7540		301-62000 [S]	
		301-65000 [2]	

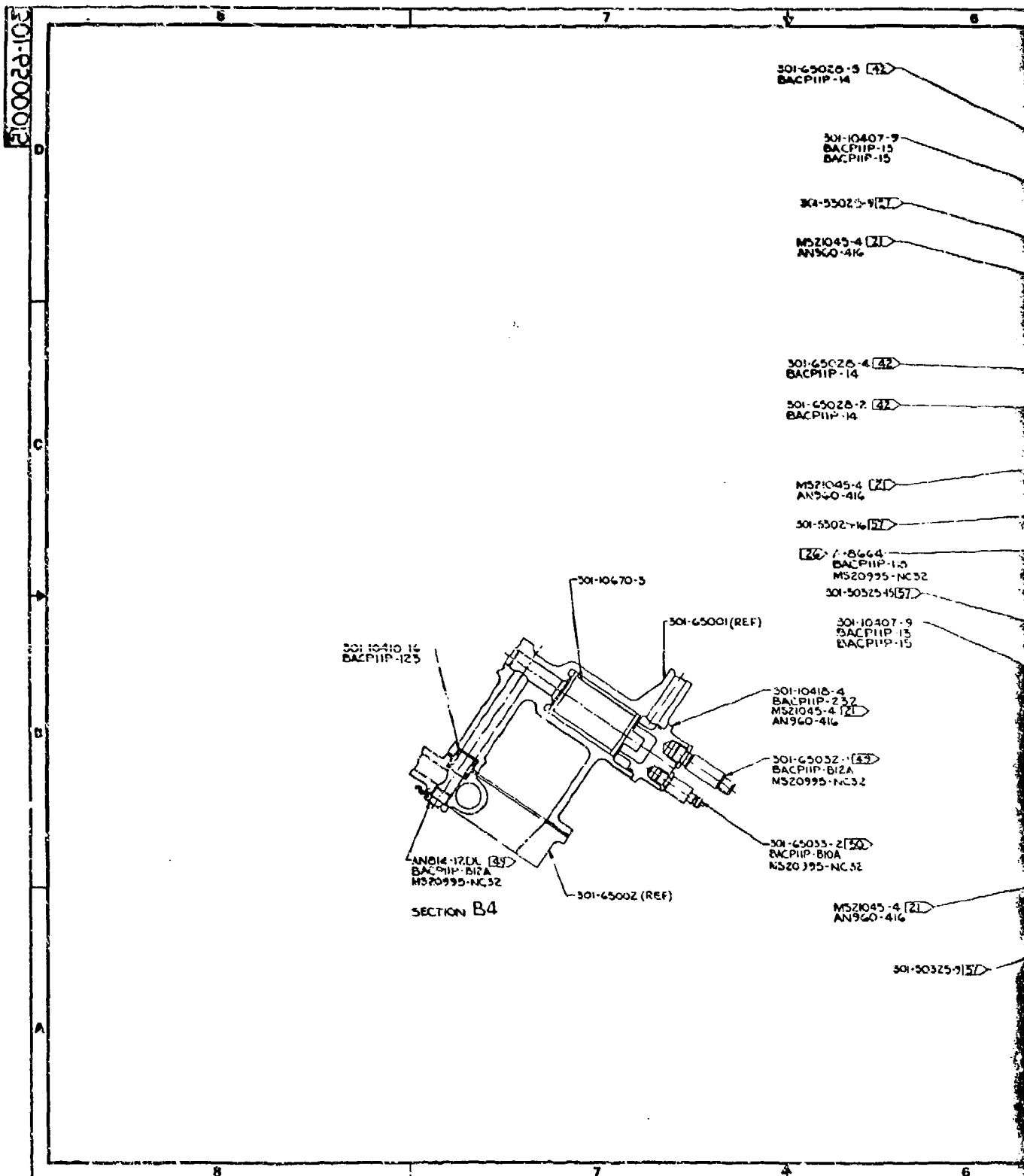
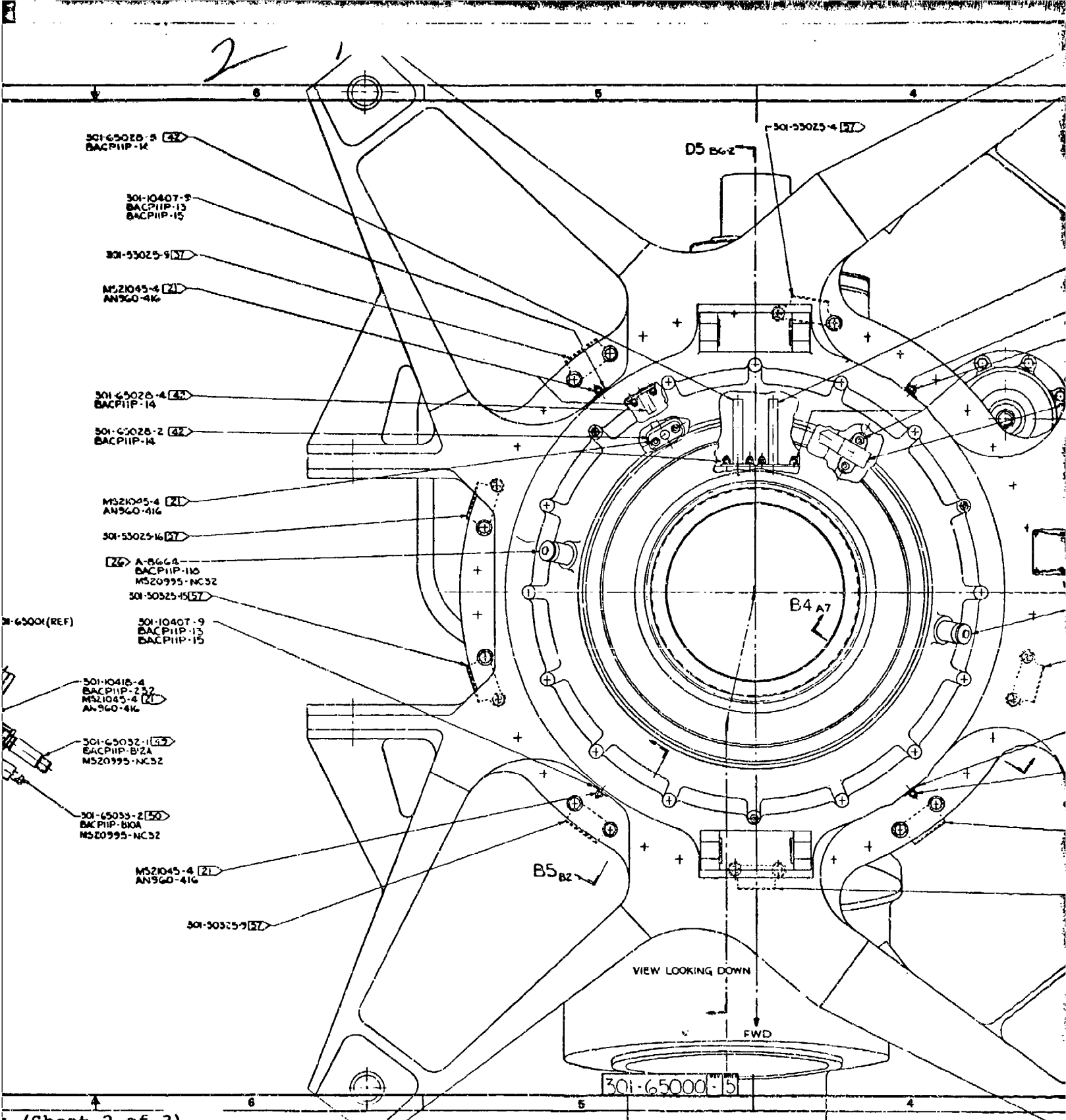


Figure 35. Forward Transmission Assembly (Sheet 2 of 3).



301-65026-12 [42]
BACP11P-14

301-10407-9
BACP11P-13
BACP11P-15

M521045-4 [21]
AN960-416

301-65026-1 [42]
BACP11P-21

BACN12MLVU [1]
DEPTH OF TAP DRILL 19±02
TAP N° 3-48UNC-2B (4 PLACES)
AN50025-5
AN960-3
M520995-NC20
(USE NAMEPLATE FOR TEMPLATE)

1.75±.06

1.10±.06

A-8664 [23]
BACP11P-110
M520995-NC32

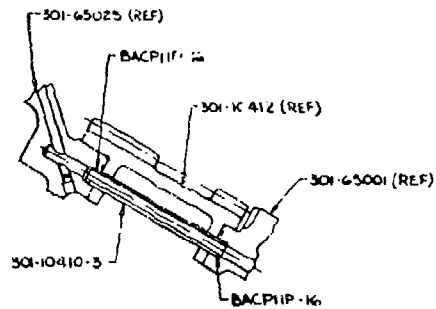
301-50525-5 [57]

301-10407-9
BACP11P-13
BACP11P-15

M521045-4 [21]
AN960-416

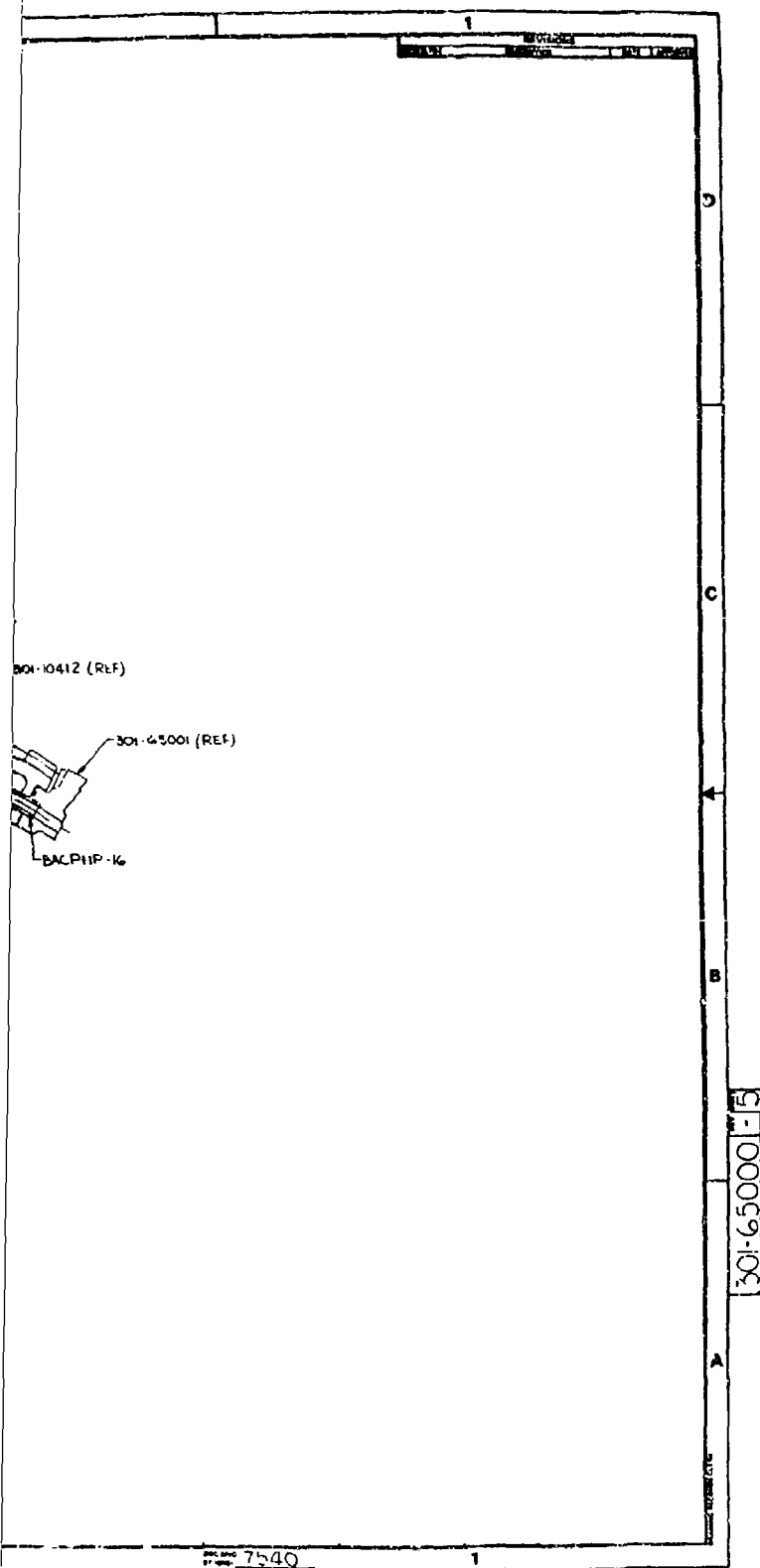
301-50525-9 [57]

301-50525-5 [57]



SECTION B5

4



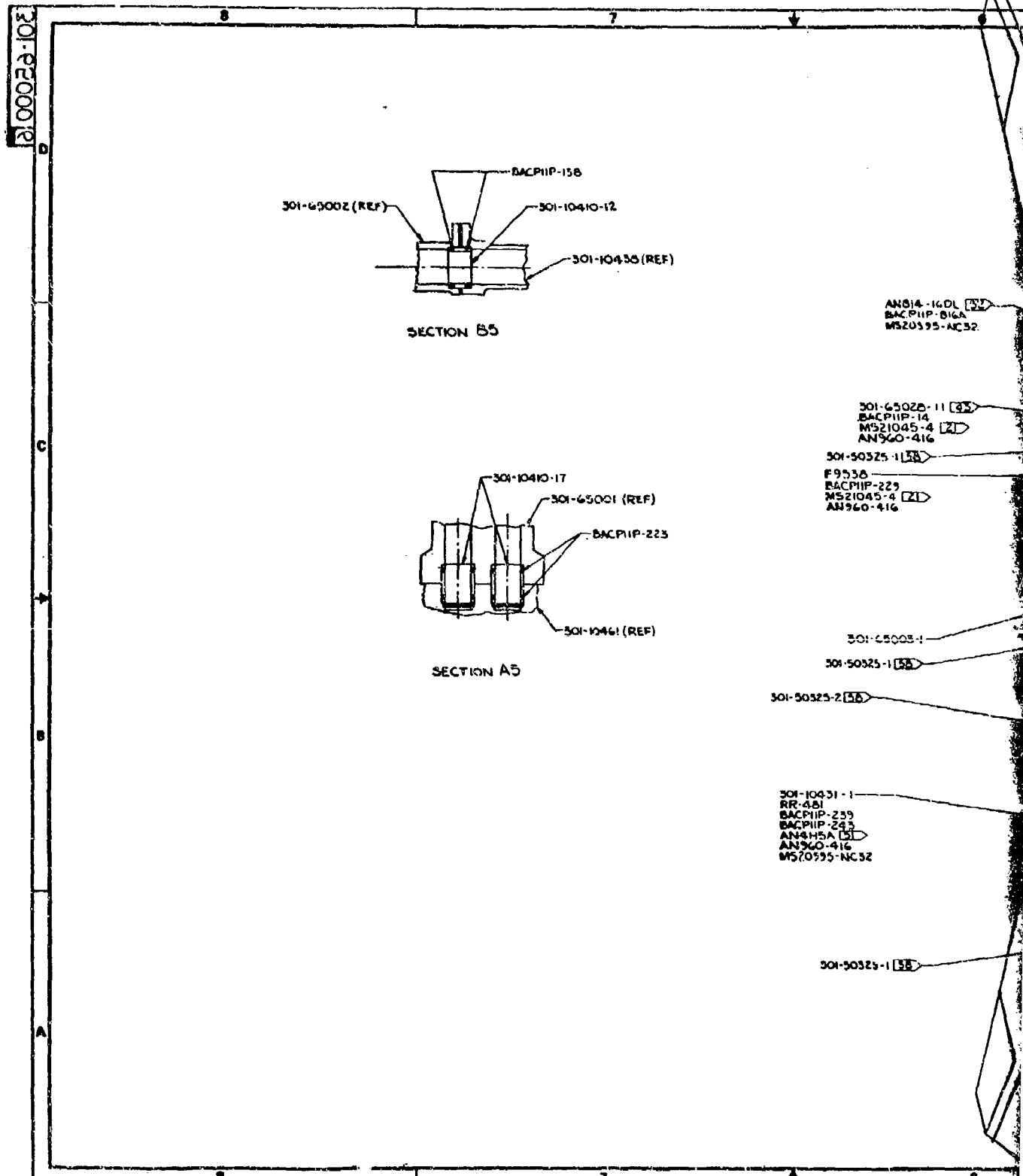
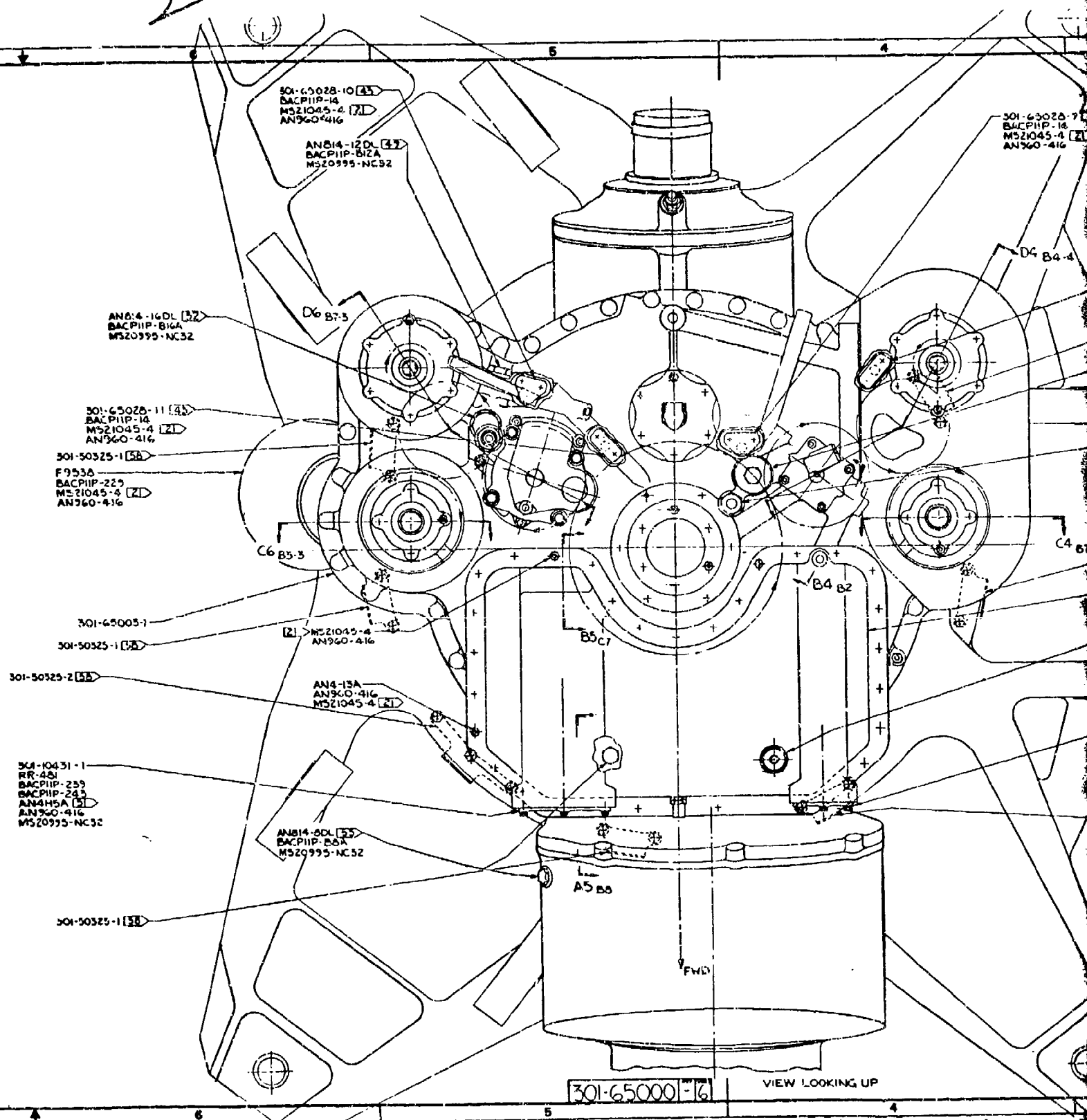
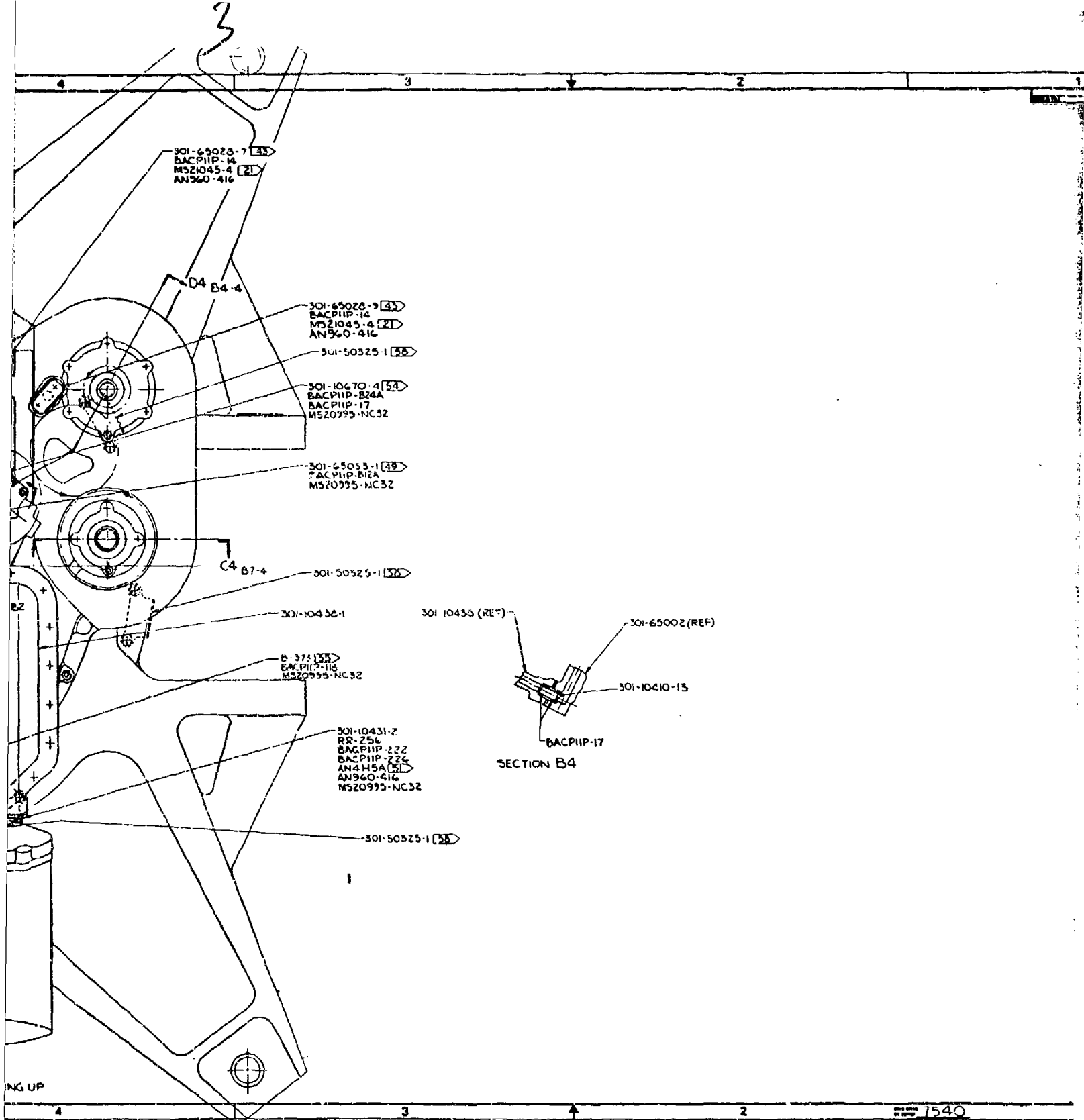


Figure 36. Forward Transmission Assembly (Sheet 3 of 3).

2





4

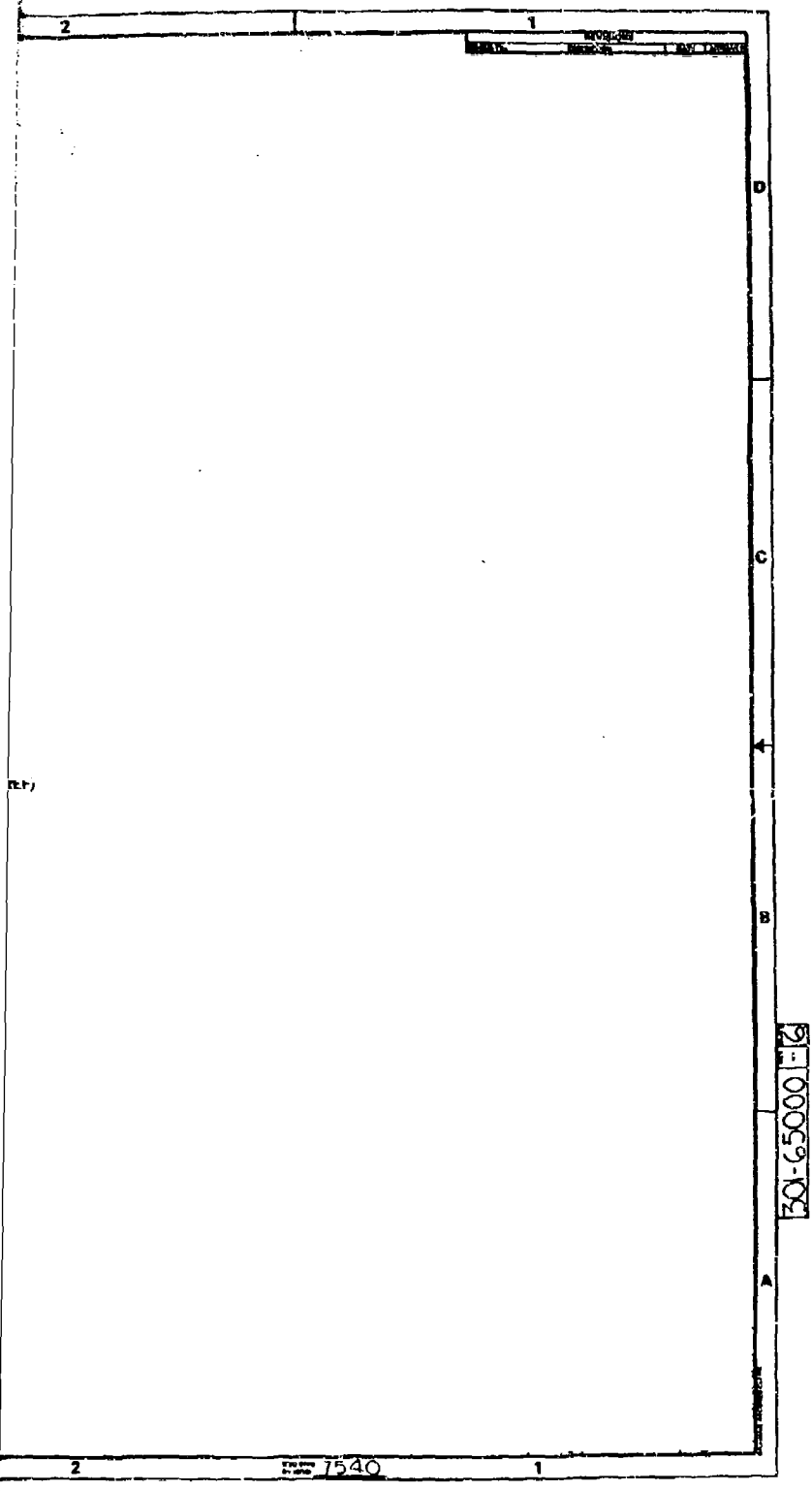


TABLE 12. PROTOTYPE DESIGN MODIFICATION - AFT TRANSMISSION	
AREA/COMPONENT	MODIFICATION
BEVEL PINION 301-10428-3	<ul style="list-style-type: none"> - Increased shaft wall thickness - Increased rim thickness - Increased damping ring mass - Increased chamfer at ends of teeth
BEVEL GEAR 301-10419-3	Same as pinion plus increased web thickness
FIRST STAGE CARRIER 301-10413-2	Added Peening
ROTOR SHAFT 301-10401-13	<ul style="list-style-type: none"> - Changed rotor hub and bearing locknut threads to buttress profile - Increased wall thickness under threads - Increased planet post and flange thickness - Changed to 8 forging solution treated and overaged - Eliminated straddle plate
BEARING LOCKNUT 301-10411-3	<ul style="list-style-type: none"> - Changed to buttress thread - Increased diameter and thickness - Incorporated increased strength lockwasher
UPPER COVER 301-65025-1	<ul style="list-style-type: none"> - Changed actuator mounting system - Changed mount hole location - Changed arm design

TABLE 12. Continued

AREA/COMPONENT	MODIFICATION
RING GEAR 301-10412-3	<ul style="list-style-type: none"> - Increased bolt hole size to .625 in. - Chamfered ends of teeth
TAPERED ROLLER BEARINGS 301-10420-4 301-10443-4 301-10440-4 301-10424-4	Added phosphate coating to cone and rollers
ACCESSORY DRIVE SECTION	Changed to accommodate oil cooled generators

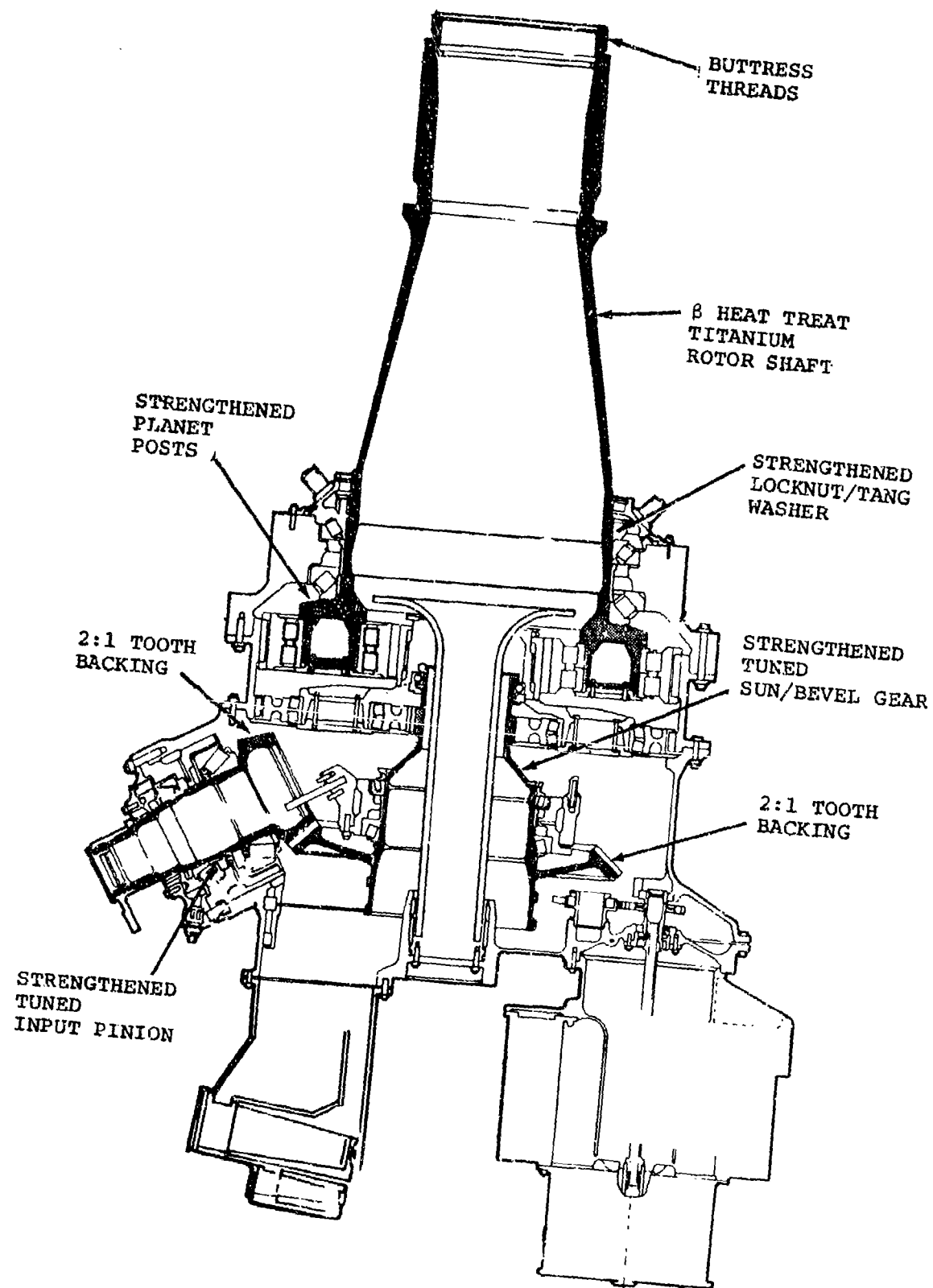
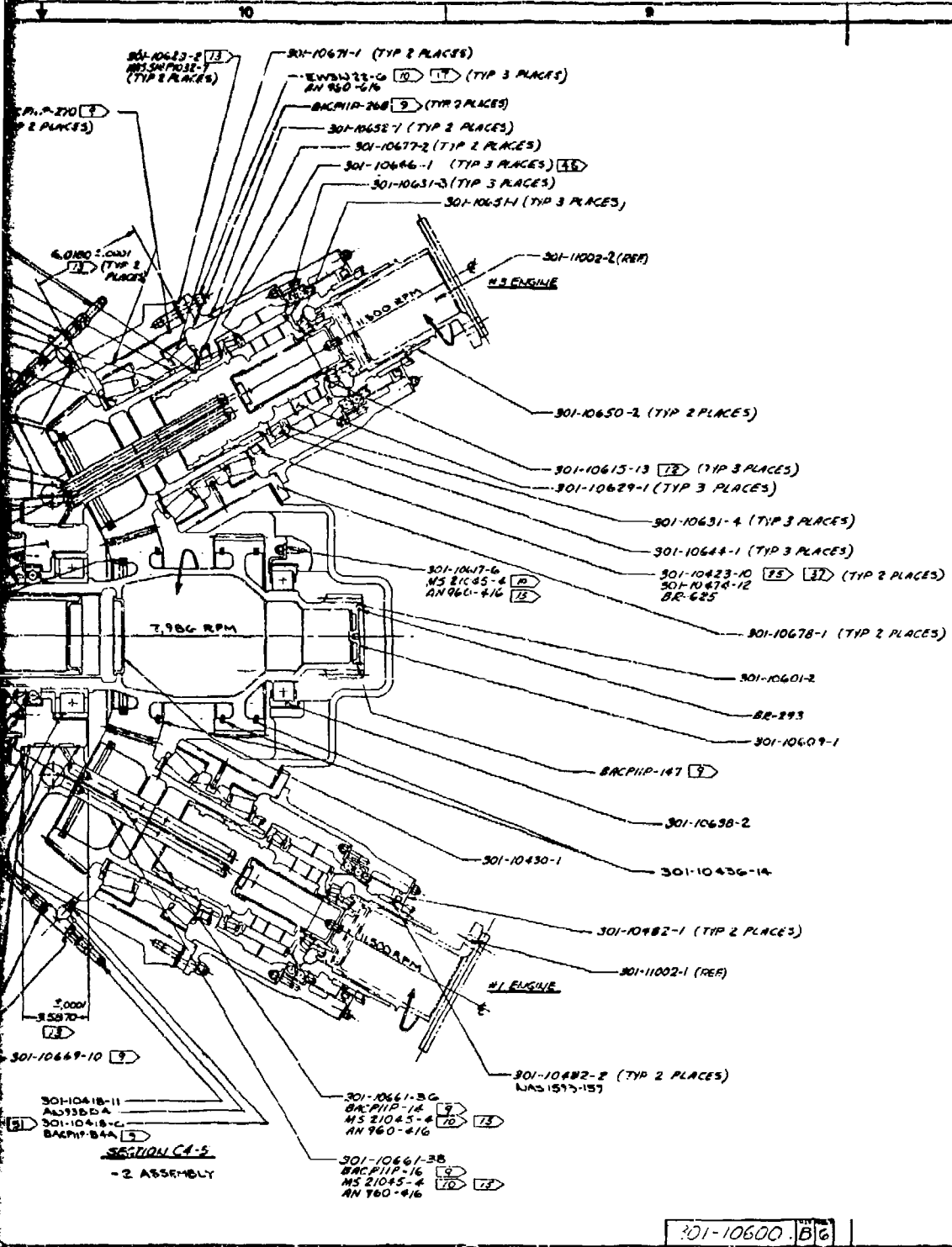


Figure 37. Prototype Aft Transmission.

Figure 38. Combiner Transmission Assembly.

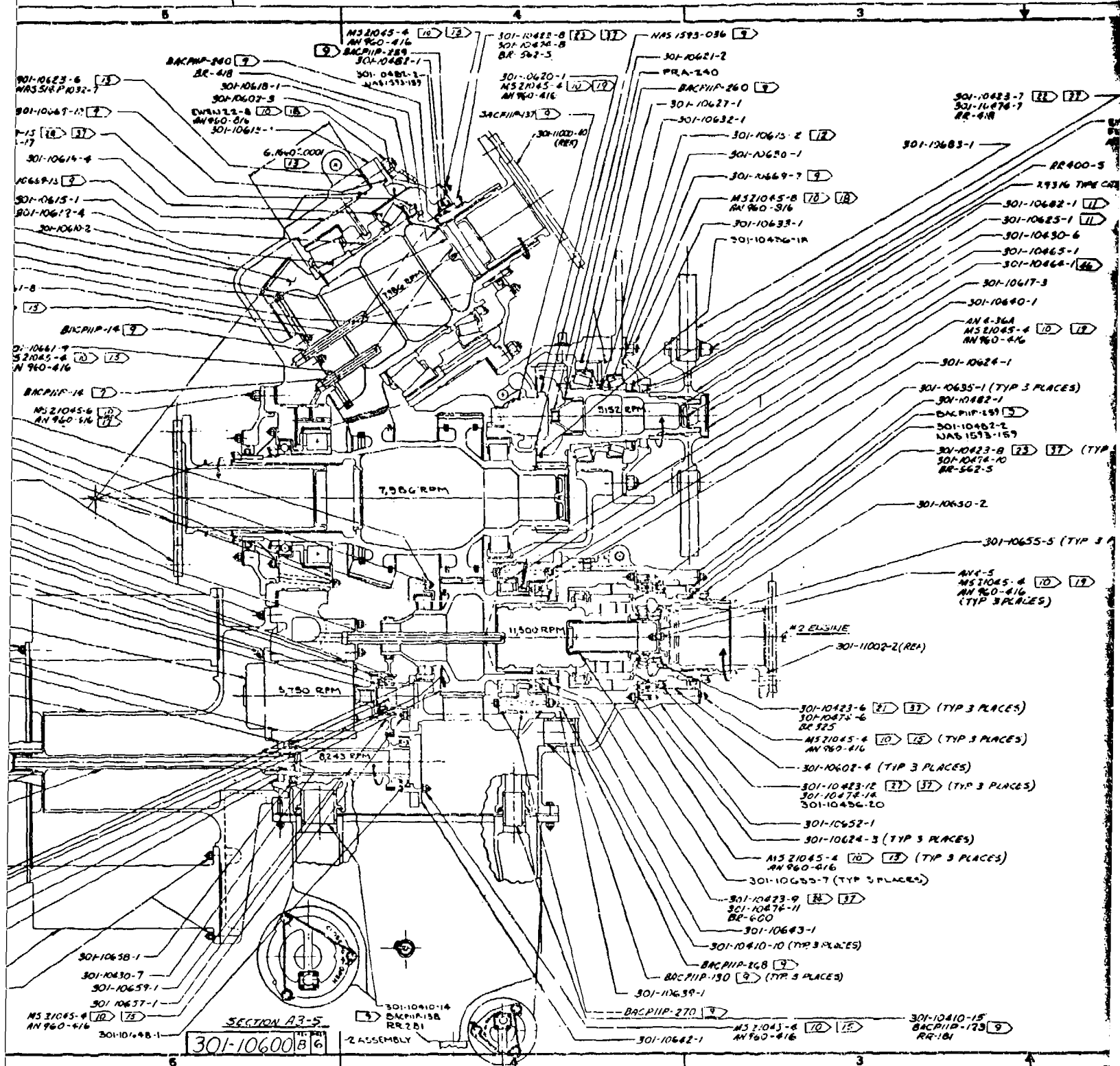
2 1



6

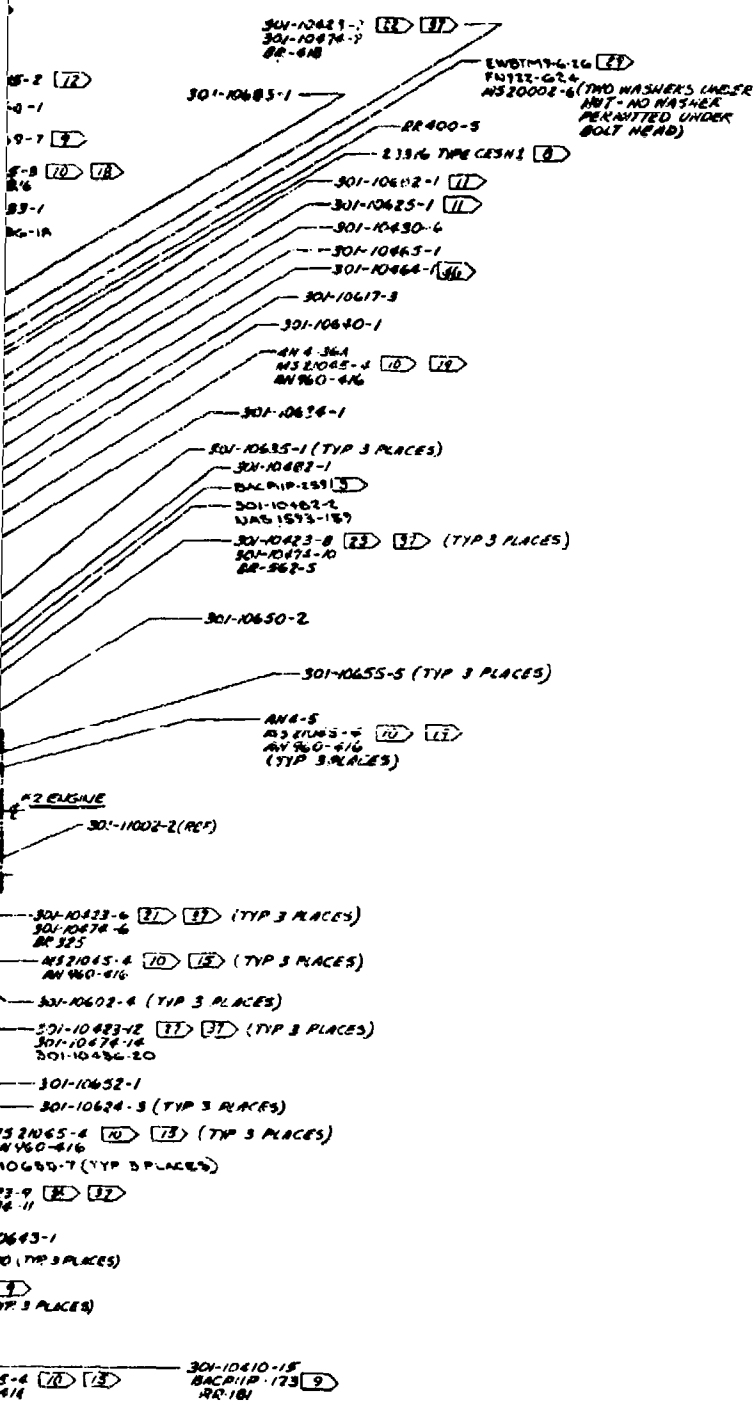


301-106



5

REV	DESCRIPTION	DATE	BY	CHKD
1	THIS SHEET ADDED	5/1/78	EDS	



301-106000816

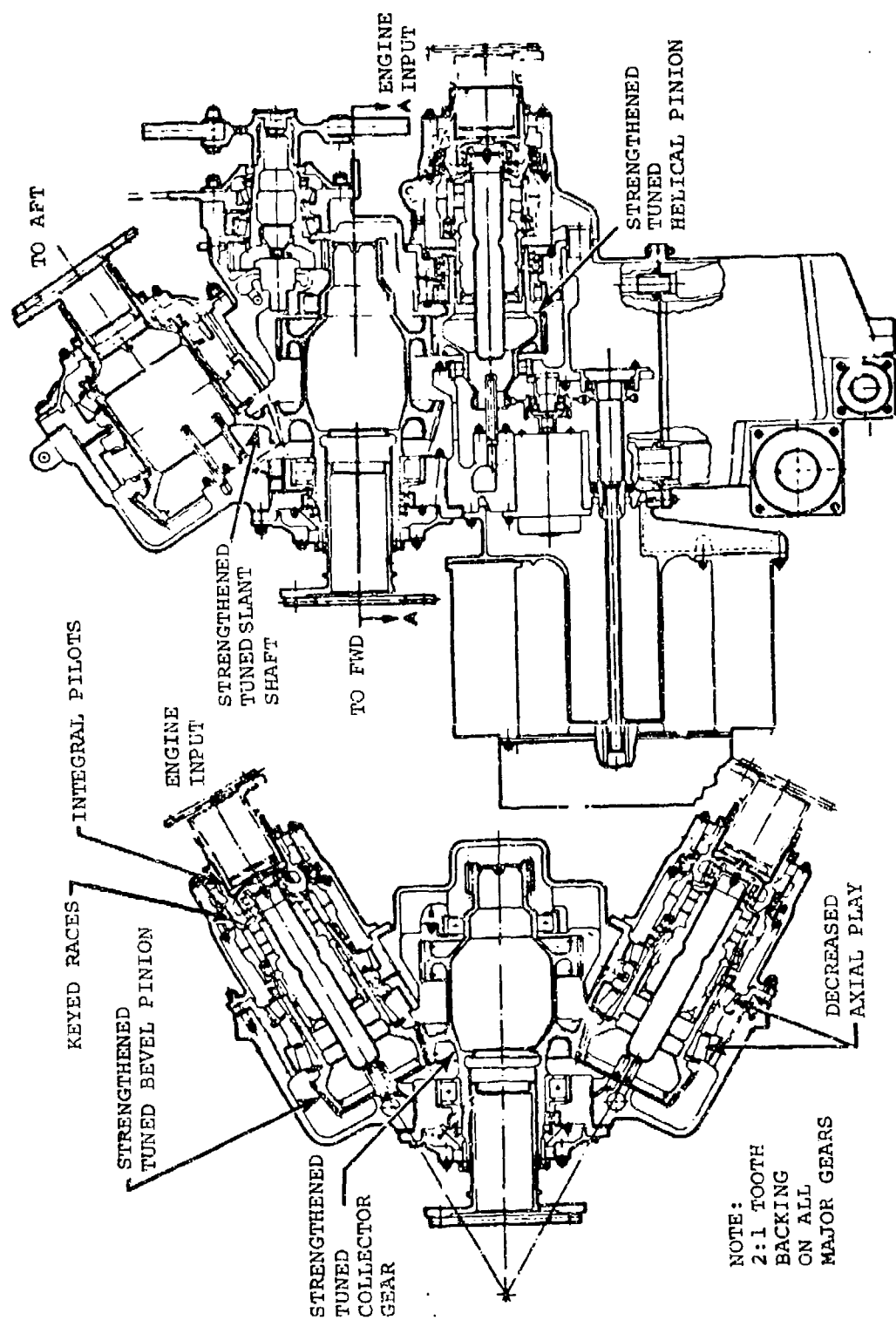
7540

TABLE 13. PROTOTYPE DESIGN MODIFICATIONS - COMBINER TRANSMISSIONS

Area/Component	Modification
COLLECTOR GEAR 301-10601-2	<ul style="list-style-type: none"> - Increased wall thickness - Increased rim thickness - creased damping ring mass - creased chamfer at ends of teeth
BEVEL PINION 301-10677-2	
SLANT GEAR 301-10610-2	
HELICAL PINION 301-10654-2	
CLUTCH HOUSING 301-10650-2	<ul style="list-style-type: none"> - Added pilot diameters for adapter
LUBRICATORS 301-10655-7 301-10661-36, -38, -40	<ul style="list-style-type: none"> - Changed for improved distribution of clutch area lube
INPUT PINION BEARINGS 301-10676-1 301-10671-1	<ul style="list-style-type: none"> - Added lube jet

TABLE 13. Continued

Area/Component	Modification
BEARINGS 301-10612-4 -10616-4 -10638-2 -10671-1 } -10676-1 } -10635-1 -10656-1 -10640-1 -10666-1	<ul style="list-style-type: none"> - Added phosphate coating to cone and rollers - Added phosphate coating to cone and rollers - Decreased channel clearance and increased width of race - Added phosphate coating to cone and rollers and tempered at 500°F. - Added outer race key - Decreased channel clearance - Decreased channel clearance - Decreased channel clearance



VERTICAL SECTION THROUGH COMBINER TRANSMISSION

Figure 39. Prototype Combiner Transmission.

COMBINER GEAR REDESIGN

There were three objectives of redesign. The first was to reduce gear stresses below the mean-minus-three sigma allowable, preferably to a point which would allow a margin for less than optimum tooth bearing patterns. The second was to fit within the physical confines of the existing combiner housing. The third was to maintain the exact gear ratio so that the existing regenerative test stand could be used.

Two possibilities were presented. The combiner gear face could be widened in relation to the slant shaft and input pinions. These could then be staggered so that the alternating stresses on the combiner gear (the idler gear effect) would be minimized at any given axial position along the collector tooth. The second possibility was to halve the numbers and the diametral pitch of teeth in all gears, thus increasing the beam strength of the teeth; to maintain or slightly increase the pitch diameters; and to uniformly increase the face width of all the gears.

Both possibilities were analyzed (Table 14), as well as a third alternative which intermixed one and two. While the staggered system with half the number of teeth could provide theoretically satisfactory tooth stresses, problems in manufacturing the extended face width collector gear were foreseen. Therefore, the selected approach was to increase all gear face widths to 3.55 inches and to change to 3.025 diametral pitch (Table 15); with this configuration, the maximum gear stresses (fillet and root) were calculated. The collector gear stresses are 15% below the mean-minus-three sigma allowable under both AEO and OEI design condition. Slant shaft and input pinion stresses are below collector stresses. Gearing is shown in Figure 40.

A summary of bearing lives are shown in Table 16. Calculated lives for the selected configuration (Configuration 6) are in excess of requirements and with two exceptions are greater than the original configuration.

The conclusions of this study are that the selected Configuration 6 will meet the redesign objectives. A confirmatory finite element analysis would be performed prior to committing to manufacture.

TABLE 14. PROTOTYPE COMBINING TRANSMISSION CONFIGURATION SUMMARY					
CONFIG	DESCRIPTION	CRITICAL AREA			STRESSES WITHIN ALLOWABLE
		PINION	COLLECTOR	SLANT	
1	Tested (301-10600-2)	Fillet	Fillet	Fillet & Root	No
5	Increased Collector Face. Staggered Meshes.	Fillet	Root	Both	No
4	Same as 5 above but half number of teeth	Fillet	Root	Both	Yes
6 (Selected)	Increased all faces. Gears in line. Half number of teeth	Fillet	Root	Both	Yes

TABLE 15. REVISED HLH COMBINER GEARING						
	PITCH	COLLECTOR	COLLECTOR	SLANT		
Number of Teeth	25	36	36	36		36
Diametral Pitch			3.025			
Face Width	3.55	3.55	3.55			3.55
Pressure Angle			20.			
Spiral Angle			25.			
Shift Angle		28.5		33.75		
Contact Ratio:						
Face		1.75		1.78		
Profile		1.33		1.37		
Modified		2.21		2.23		
Pitch Diameter	8.2645	11.9008	11.9008			11.9008
Torque	44,255	63,726	83,812			83,812
Power		8675.		10,620.		
Speed	11,500	7,986	7,986			7,986
Bending Stress, KSI	29.7	18.3	22.5			37.2
Contact Stress KSI		215.7	(226.7)*	220.9		(231.3)*
Flash Temperature, °F.		500	(322)*	407		(298)*
Bearing Loads:	LR/CM	RR/CM	RR/CM	LR/CM		
Cubic Mean Power	4203			7710		
Tangential	6103			11,195		
Separating	1827	3171	2787			5818
Thrust	3281	-2012	6301			-3690
Thrust Moment	12,385	-10,935	34,245			-20,058
Existing HLH Bearing Loads:						
Tangential		6026		11,381		
Separating	2486	3499	4202			6606
Thrust	2751	-1234	5602			-2325
Thrust Moment	10,163	-6,583	29,953			-12,432

* Value in () are for current configuration.
Allowables: $P_c = 260,000$ psi; Flash Temp. = 550°F.

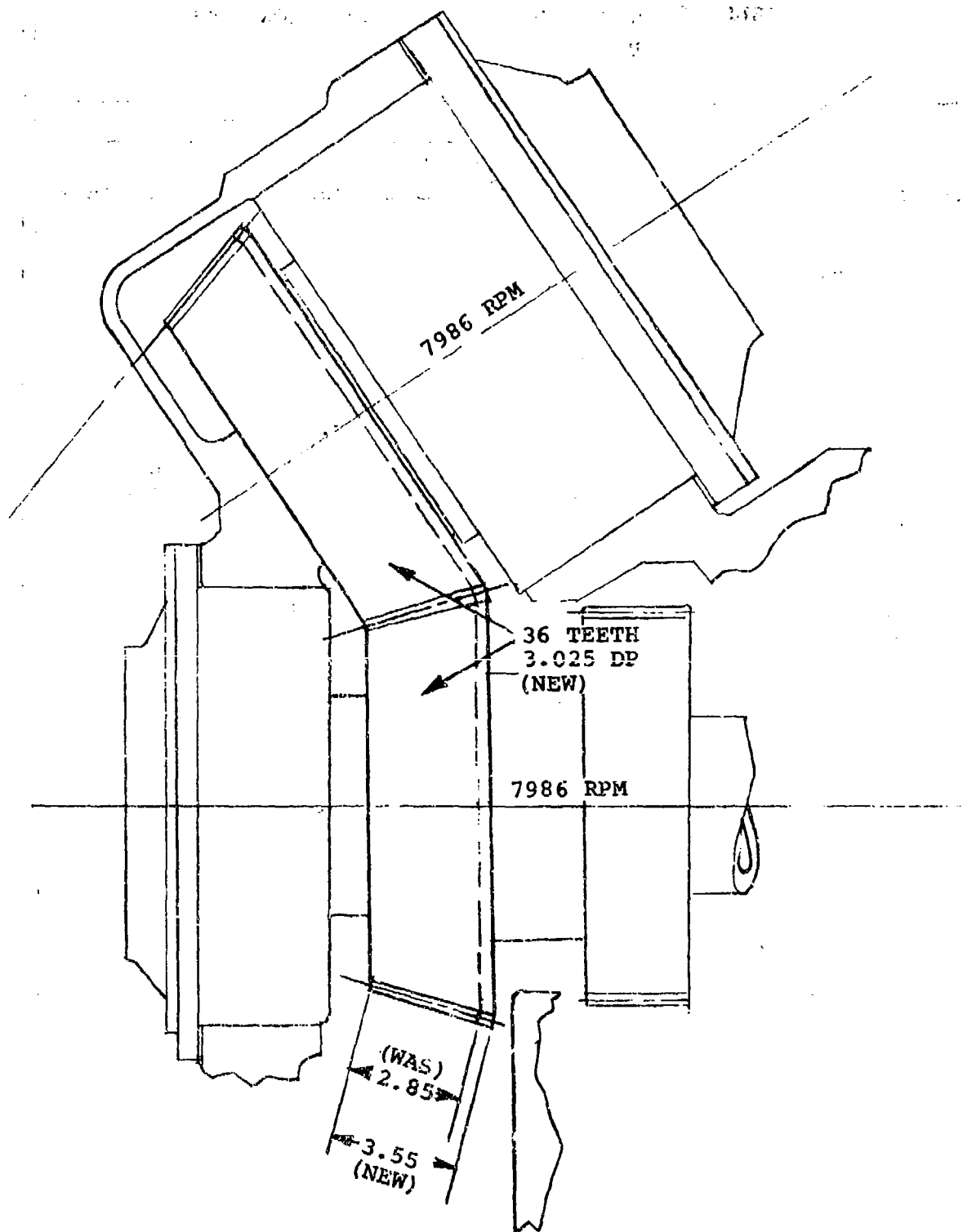


Figure 40. Combiner Configuration 6, Reference Section A3-1, 301-10600, Sheet 6.

**TABLE 16. HLH COMBINER CONFIGURATION STUDY
BEARING LIFE SUMMARY**

Location & Type	P/N	L ₁₀ Life, Hours	
		301-10600-2 Configuration	-6 Configuration
S.B. Pinion			
Inboard - Taper	301-10676	2840	3040
Outboard- Taper	301-10671	31400	48400
Collector Gear			
Forward-Roller	301-10666	7800	7635
Aft - Roller	301-10638	3280	3550
Thrust - Ball	301-10667	3620	15570
Slant Gear			
Inboard - Taper	301-10612	4260	5300
Outboard-Taper	301-10616	46900	23900

Notes:

Ball and Roller Bearing Lives per S-04, Mat'l. Factor = 5.

Taper Roller Bearing Lives per Taper 1, Mat'l. Factor = 4.

* At CMP = 12850 HP, 155.9 Rotor RPM, AEO

REFERENCES

1. HELICOPTER STRUCTURAL DESIGN REQUIREMENTS, AR-56, February 17, 1970.
2. SURFACE DURABILITY (PITTING) OF SPUR GEAR TEETH, AGMA Standard 210.01.
3. SURFACE DURABILITY (PITTING) OF HELICAL AND HERRINGBONE GEAR TEETH, AGMA Standard 211.02.
4. SURFACE DURABILITY (PITTING) FORMULAS FOR SPIRAL BEVEL GEAR TEETH, AGMA Standard 216.01.
5. RATING THE STRENGTH OF SPUR GEAR TEETH, AGMA Standard 220.02.
6. RATING THE STRENGTH OF HELICAL AND HERRINGBONE GEAR TEETH, AGMA Standard 221.02.
7. RATING THE STRENGTH OF SPIRAL BEVEL GEAR TEETH, AGMA Standard 223.01.
8. Lundberg, G., and Palmgren, A., DYNAMIC CAPACITY OF ROLLING BEARINGS, ACTA Polytechnical Journal, 1947.
9. Lundberg, G., and Palmgren, A., DYNAMIC CAPACITY OF ROLLING BEARINGS, ACTA Polytechnical Journal, 1952.
10. Jones, A. B., A GENERAL THEORY FOR ELASTICALLY CONSTRAINED BALL AND RADIAL ROLLER BEARINGS UNDER ARBITRARY LOAD AND SPEED CONDITIONS, ASME Paper 59-LUB-10, 1959.
11. Jones, A. B., and Harris, T. A., ANALYSIS OF A ROLLING-ELEMENT IDLER GEAR BEARING HAVING A DEFORMABLE OUTER-RACE STRUCTURE, ASME Journal of Basic Engineering, June 1963.
12. The Timken Engineering Journal, Timken Roller Bearing Company, 1963.
13. R. Trent and W. R. Lull, DESIGN FOR CONTROL OF DYNAMIC BEHAVIOR OF ROTATING MACHINERY, ASME Paper 72-DE-39.
14. R. Williams and R. Trent, THE EFFECTS OF NONLINEAR SUPPORTS ON TURBINE ROTOR STABILITY, SAE Paper No. 700320.
15. Figge, Sr., I.E., STATIC, BALLISTIC, AND IMPACT BEHAVIOR OF GLASS/GRAPHITE DRIVE SHAFTING, USAAMRDL Technical Memorandum 1, Eustis Directorate, U.S. Army Air Mobility Research and Development Laboratory, Ft. Eustis, Va., June 1972, AD 743938.

16. Lemanski, A. J., and Rose, H. J., EVALUATION OF ADVANCED GEAR MATERIALS FOR GEAR BOXES AND TRANSMISSIONS, D210-10345-1 September 1971.
17. Alberti, J. P., and Lemanski, A. J., EVALUATION OF ADVANCED GEAR MATERIALS FOR GEAR BOXES AND TRANSMISSIONS, D210-10103-1 October 1970.
18. ADVANCED TECHNOLOGY COMPONENT PROGRAM. 6th Quarterly Summary Report, D301-10100-6 January 25, 1973.
19. Boeing Vertol Report 114-ET-047-1, TEST PROCEDURE - CH-47C 1,500 HOUR BENCH ENDURANCE TEST PROGRAM FOR FORWARD, AFT, ENGINE, AND COMBINING TRANSMISSIONS, SRD-57.
20. Lenski, Jr., J. W., TEST RESULTS REPORT AND TECHNOLOGY DEVELOPMENT REPORT HLH/ATC COMPLIANT ROLLER BEARING DEVELOPMENT PROGRAM, The Boeing Co., USAAMRDL TR-72-62, Eustis Directorate, U.S. Army Air Mobility Research and Development Laboratory, Fort Eustis, Virginia, November 1972, AD 755535.
21. Lemanski, A.J., Lenski, Jr., J.W., and Drago, R.J., DESIGN, FABRICATION, TEST, AND EVALUATION OF SPIRAL BEVEL SUPPORT BEARINGS (TAPERED ROLLER), Boeing Vertol Co., USAAMRDL TR-73-16, Eustis Directorate, U.S. Army Air Mobility Research and Development Laboratory, Fort Eustis, Virginia. June 1973, AD 769064.
22. Lenski, Jr., J.W., TEST RESULTS REPORT AND DESIGN TECHNOLOGY DEVELOPMENT REPORT - HLH/ATC HIGH-SPEED TAPERED ROLLER BEARING DEVELOPMENT PROGRAM, Boeing Vertol Co., USAAMRDL TR 74-33, Eustis Directorate, U.S. Army Air Mobility Research and Development Laboratory, Fort Eustis, Virginia, June 1974, AD 78651.
23. Lenski, Jr., J.W., TEST RESULTS REPORT AND TECHNOLOGY DEVELOPMENT REPORT - HLH/ATC DRIVE SYSTEM AFT ROTOR SHAFT BEARING TEST, Boeing Vertol Co., USAAMRDL TR 73-92, Eustis Directorate, U.S. Army Air Mobility Research and Development Laboratory, Fort Eustis, Virginia, January 1974, AD 775897.

APPENDIX A

TRADE STUDIES

COMBINING TRANSMISSION CONFIGURATION STUDIES

Combining Gear Fabrication

The starting-point combining transmission is shown in Figure A-1. Its general arrangement includes a collector gear for combining the power of the two side-mounted engines and a helical gear mesh for the center engine. A separate bevel mesh is used to transfer power to the aft transmission.

To permit gear fabrication, the aft shaft gear must have no obstruction at the toe end that extends beyond the root diameter of the teeth. To accomplish this, the combiner shaft assembly (Figure A-1, sheets 2 and 3) consists of two spiral bevel gears, one helical gear, one spur gear, and two spanner nuts. This assembly has conventional spline joints for the bevel and helical gear. The estimated weight is 156 pounds. This design was estimated to cost \$19,881 per unit plus \$18,700 for tooling.

An alternate design is shown on Sheet 1. This assembly incorporates an EB weld between the two bevel gears. The two spline joints are eliminated. The estimated weight is reduced by 45 pounds. This design was estimated to cost \$15,600 per unit plus \$12,000 for tooling.

The one-piece design presents certain disadvantages for prototype manufacture and development. If any problem occurs during welding, the entire assembly may be lost. The slant-shaft bevel gear cannot be reground to salvage the gear in case of gear scuffing. Having two bevel gears on the same shaft makes it impossible to shim one of the gears for pattern thus forcing a very close control on the gear-to-shaft location.

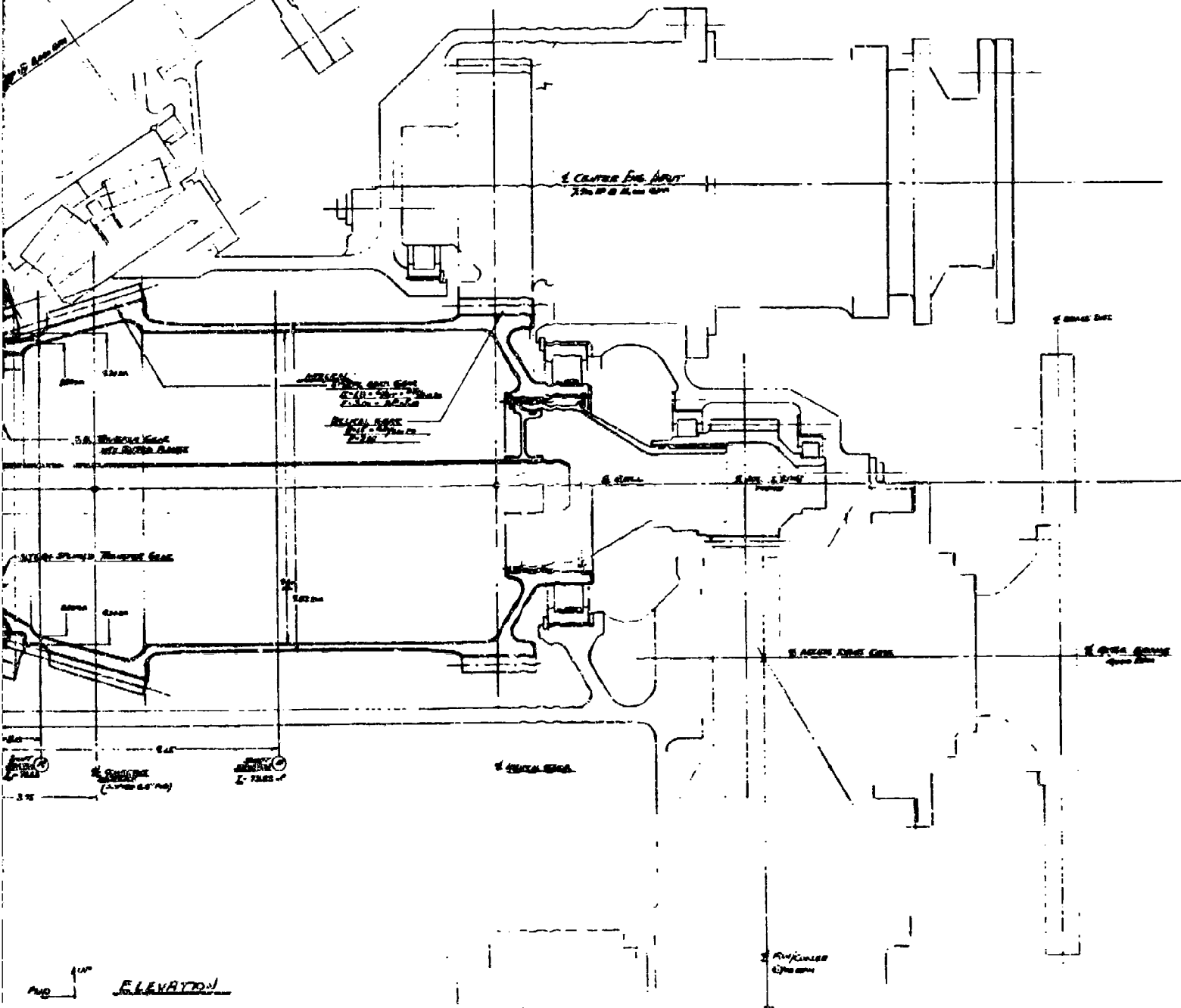
Gear Arrangement

In pursuing this trade study, it became evident that another configuration could eliminate a gear mesh and also weigh less. The gearbox configuration shown in Figure A-2 evolved. This configuration has the two side engine input bevel pinions and the bevel pinion to transfer power to the aft transmission meshing with one gear. In addition, the center engine helical mesh was rotated 180 degrees and moved forward. These changes

1



153



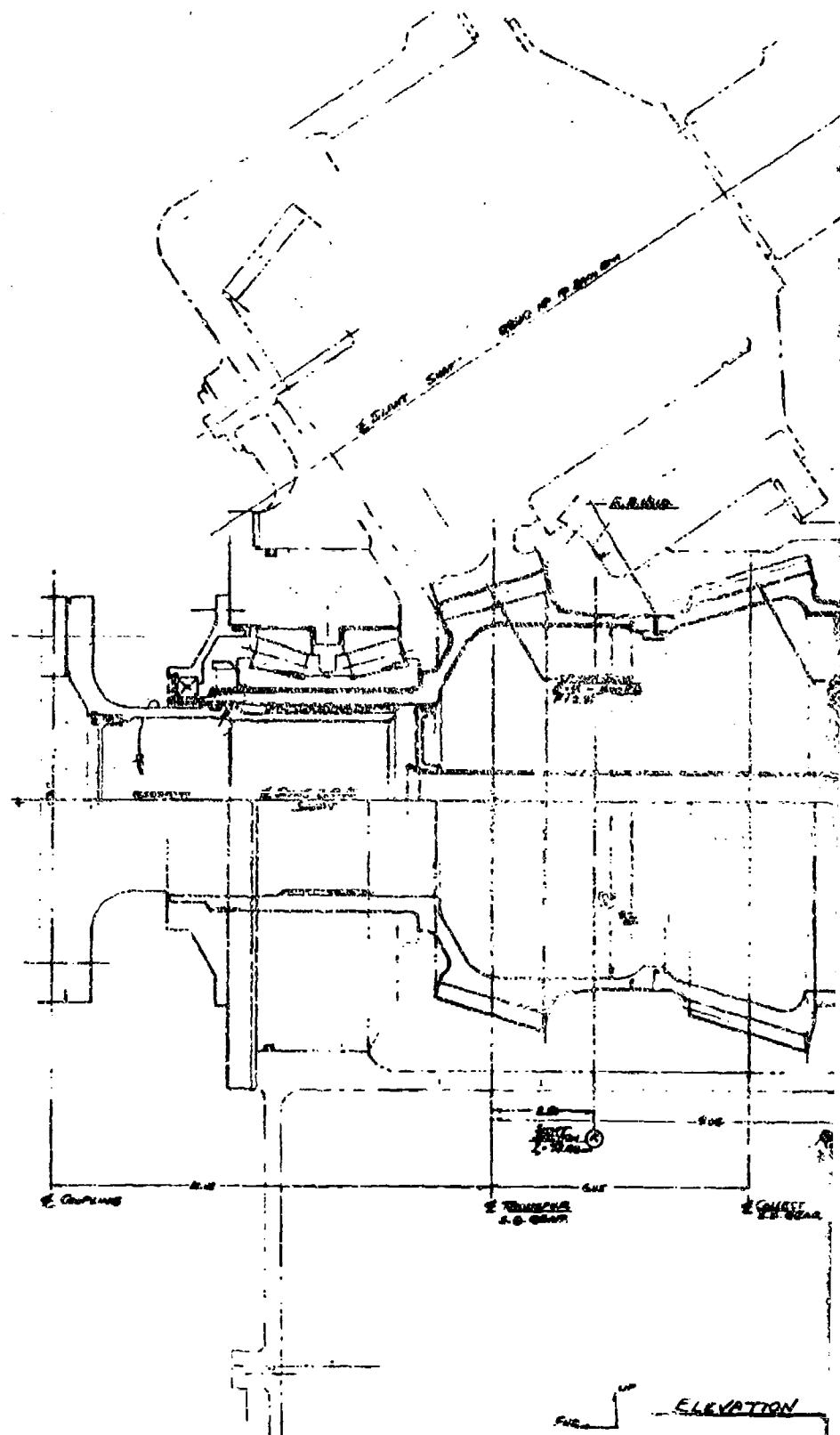
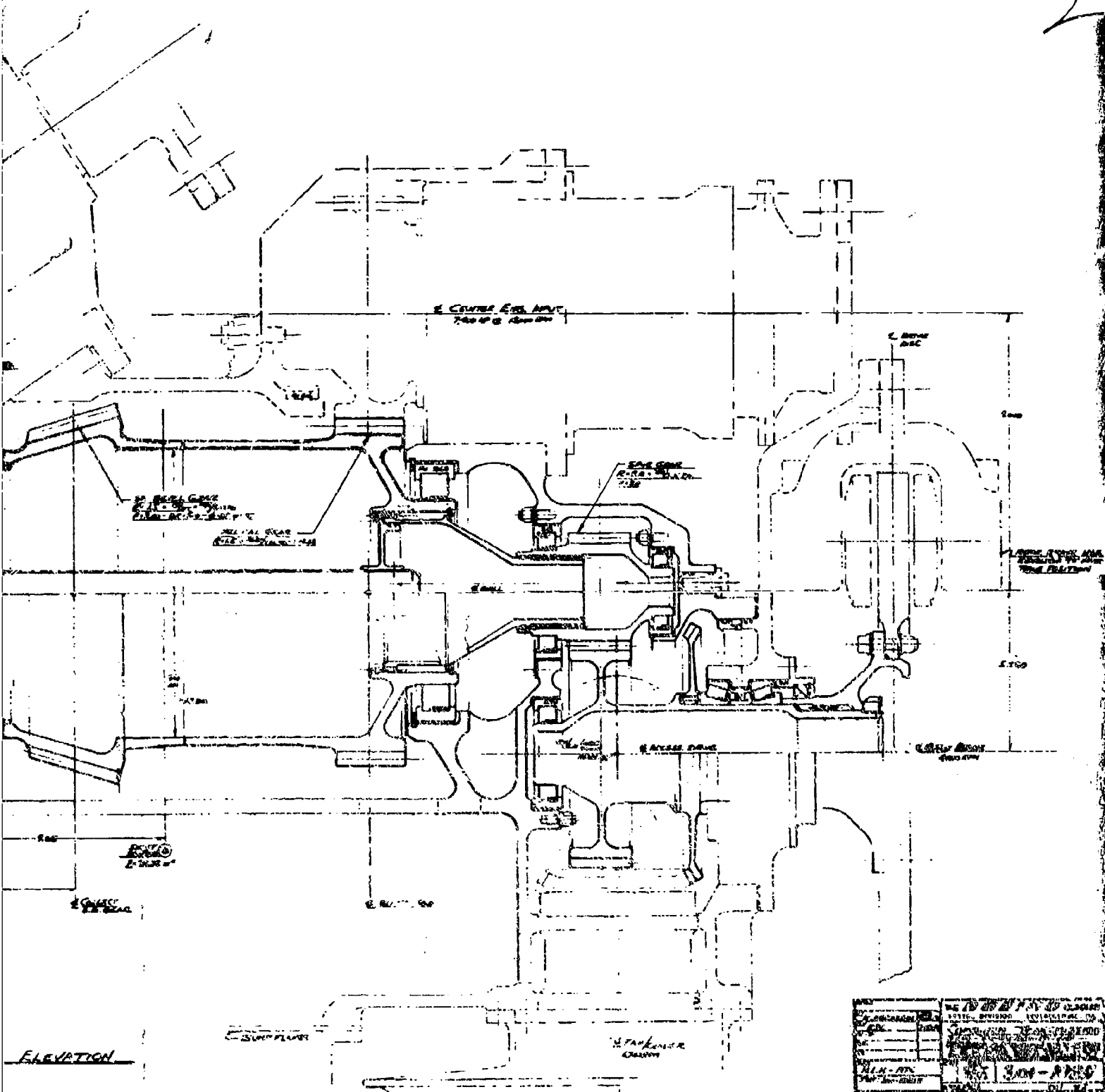


Figure A-1. Baseline Combiner Transmission (Sheet 3 of 3).



result in a weight savings of 150 pounds. A comparison of the two configurations is shown in Table A-1.

As further design interaction, Figure A-3 shows the basic layout of the combining transmission configuration selected for development. Since the chosen configuration entailed meshing three bevel pinions on a common gear, Gleason Gear Works was consulted concerning its technical feasibility. They indicated that no additional risk was involved. Instead, they feel that it might be slightly more advantageous than the original configuration with regard to gear-mesh patterning.

One major airframe problem considered in lowering the center engine was the loss of carry-through structure in the rear spar for the outboard engines support structure. A layout was made to show what is required to maintain adequate airframe strength with the lower engine and indicates an approximate 25-pound increase in airframe weight. Part of this same general problem is the removal of the combiner transmission through the rear passageway. In order to maintain adequate clearance, it became necessary to revise the engine firewall arrangement. In addition, the engine IR suppressor blower must be removed before transmission removal.

A center-engine inlet-configuration study was also made to evaluate any major differences in overall inlet system pressure losses. This data is reflected in trade study document D301-10054-1. In summary, it indicated that if the C5A splice was raised and the inlet separator lowered below the splice, an acceptable or superior air inlet system could be attained.

A review of the preliminary layouts indicates that lowering the center engine 18 inches below the baseline engine location had no adverse effect on maintainability. The requirement to remove the IR suppressor blower in order to provide clearance for combiner box removal is compensated for by allowing the mechanic to reach the top of the engine without using a work platform.

Alternate Bearings

The selected combiner-transmission configuration incorporates tapered roller bearings for all the main bevel and helical shaft supports. Alternate support arrangements utilizing ball and roller bearings were investigated and are shown in Figure A-4. These two transmission configurations have equivalent bearing B₁₀ lives except in the area of the bevel input pinion supports. Equivalent lives in this location would have meant an enlargement of the basic transmission housing along with increases in the gear diameters to accept larger-capacity bearings. A weight analysis of the two transmissions indicates

TABLE A-1. COMBINER TRANSMISSION CONFIGURATION STUDY

	Separate Engine/Transfer Gears + High Center Engine (Proposal)	Common Engine/Transfer Gears + Low Center Engine
Weight	W	W - 150 pounds
Depth below Sync Centerline	D	D + 2 inches
Length	L	L - 14 inches
Number of Gears	7	6
Number of Bearings	12	12
Number of Gear Joints	2 mechanical or 1 weld	None Required
Bevel Gear Risk	Comparable to CH-47 Combining Transmission	No additional risk (Gleason) Both sides of tooth must be developed, however
Effect of sync due to rotor brake failure (brake disc failure in direction of sync)	Brake disc must first pass through center engine shaft Loss of engine would result	Brake disc could pass through sync shaft if not shielded, center engine shaft not hit
Blower/Cooler Location	Brake disc debris or wear products could impact cooler/blower (shielding might be needed)	Cooler/blower and brake have good separation. Additional drive hardware needed for blower, however
Reliability	Joints could adversely affect reliability	Improved
Maintainability	Acceptable	Probably improved when center engine location is considered

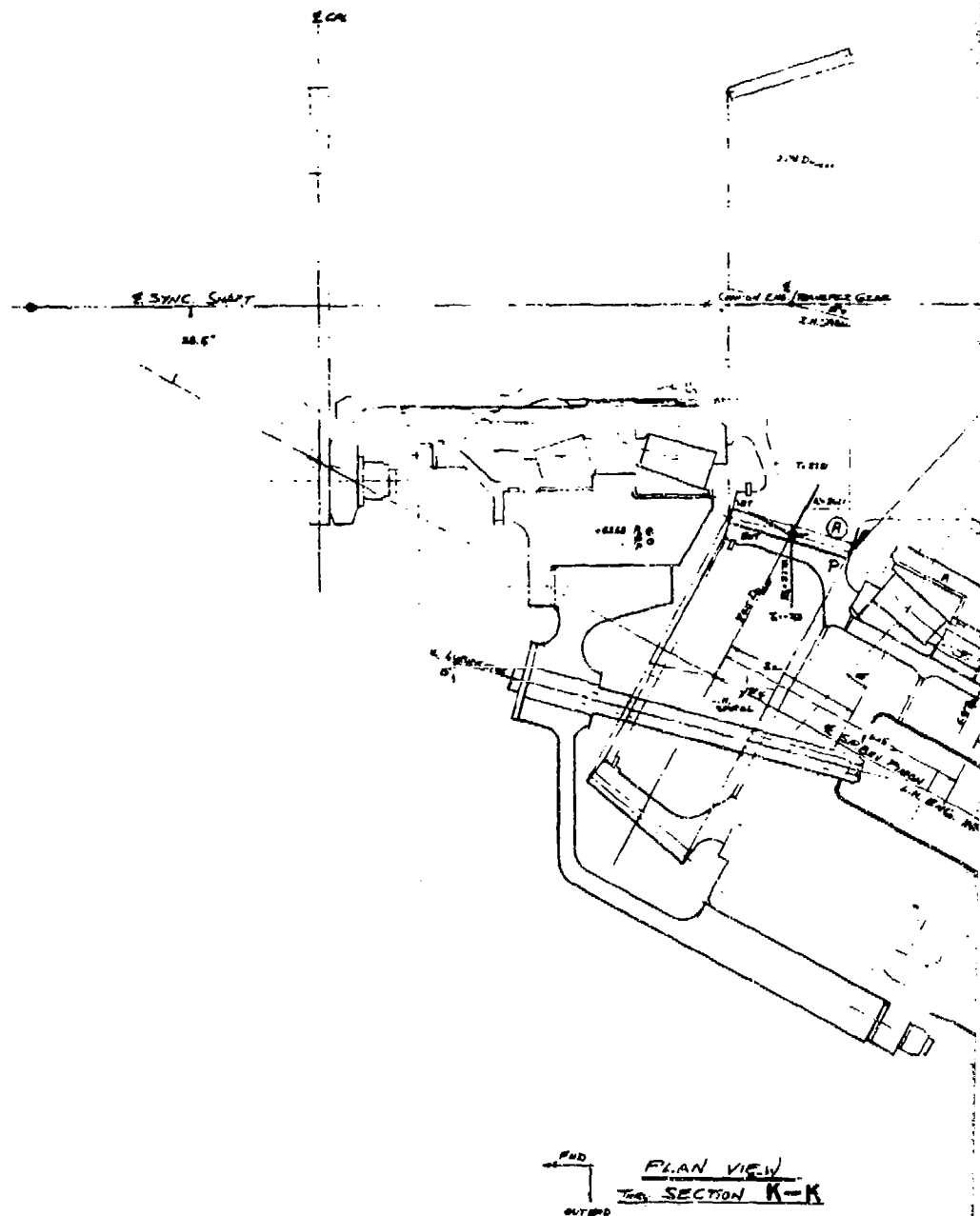
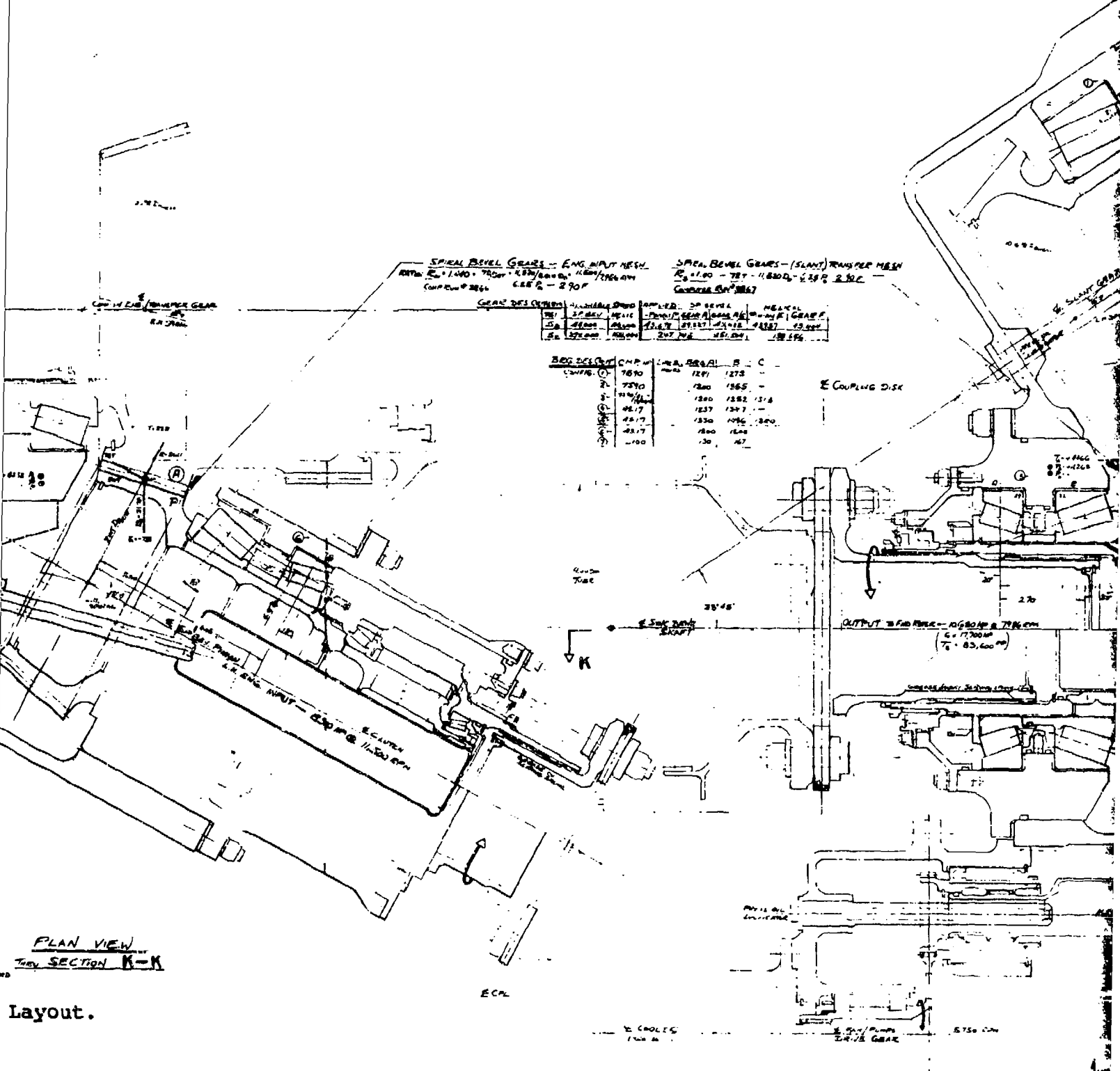


Figure A-3. Combining Transmission Basic Layout.

2



SPIRAL BEVEL GEARS - ENG. INPUT MESH
 R₁ 1.440 - 750P - 4.82/1000 - 11.60/1000
 C.P. 2.000 - 2.90P

SPIRAL BEVEL GEARS - (SLANT) TRANSFER MESH
 R₂ 1.100 - 75P - 11.800 - 2.30P
 C.P. 2.000 - 2.90P

GEAR DES. CHECK

GEAR	DES. CHECK	APPROX. SP. BEVEL	APPROX. SP. BEVEL	APPROX. SP. BEVEL
1	750P	12.00	12.00	12.00
2	750P	12.00	12.00	12.00
3	750P	12.00	12.00	12.00
4	750P	12.00	12.00	12.00
5	750P	12.00	12.00	12.00

GEAR DES. CHECK	C.P. 2.000	APPROX. SP. BEVEL	APPROX. SP. BEVEL	APPROX. SP. BEVEL
1	750P	12.00	12.00	12.00
2	750P	12.00	12.00	12.00
3	750P	12.00	12.00	12.00
4	750P	12.00	12.00	12.00
5	750P	12.00	12.00	12.00

E COUPLING DISK

PLAN VIEW
 SECTION K-K

Layout.

[illegible]

4

4. BUREAU T-15K

2 ROTOR BEARS HSG
(REMOVED 90° FROM
TRAIL FAC FOR PDS)

- SP. & GEAR DRIVE
R₁ : i₁ = 10

2. COUPLER BRAKE SHAFT

၂၅၀၆၁

- ALTERNATE WORK METHOD
(BRIEF POWER REVIEW)

PART 3: ON
 LAMBERT'S THEORY

κ↓

90406.C.D

HELIX: GRASS - FINE HAYST PRAIRIE
 $E_0 = 1400 = T_{EST} = 26.09\% \text{ } 27.2\% = 11.5\% \text{ } 100\% \text{ } 100\%$
 COND PLAN 57-5 6477 P. - 275

[illegible]

4 5/8

KORAWI CLUTCH

E CENTRAL ENG SWIFT
830 AM @ 1.600 RPM - INPU
 $T_m = 45,562^{\circ}$

[illegible]

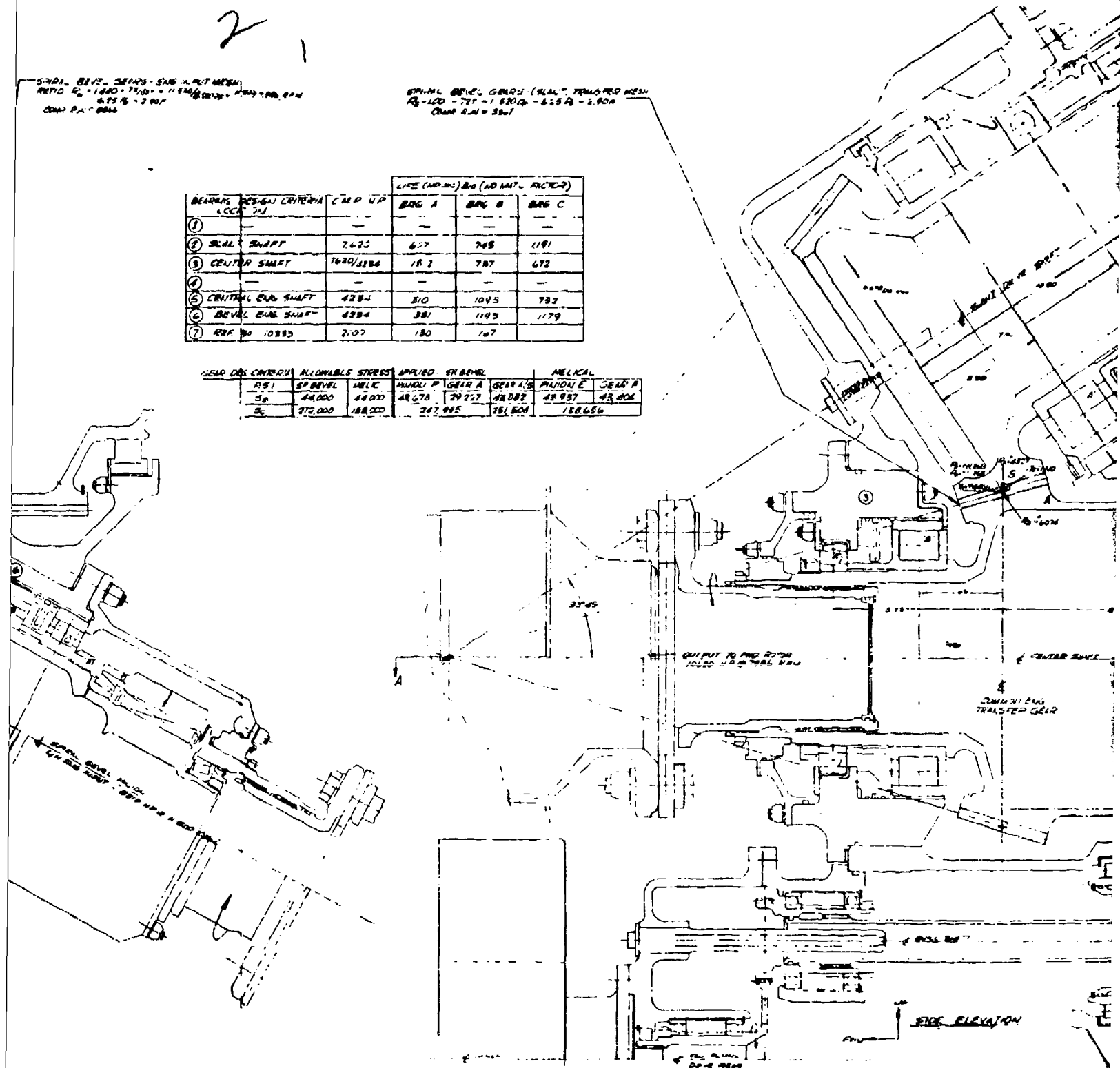
21

5701. BEVEL GEARS - SHAFT MOUNT
 RATIO $E_1 = 1.640 \times 75/10 = 11.925$
 575 1/2 - 3 9/16
 CON. P.A. 0000

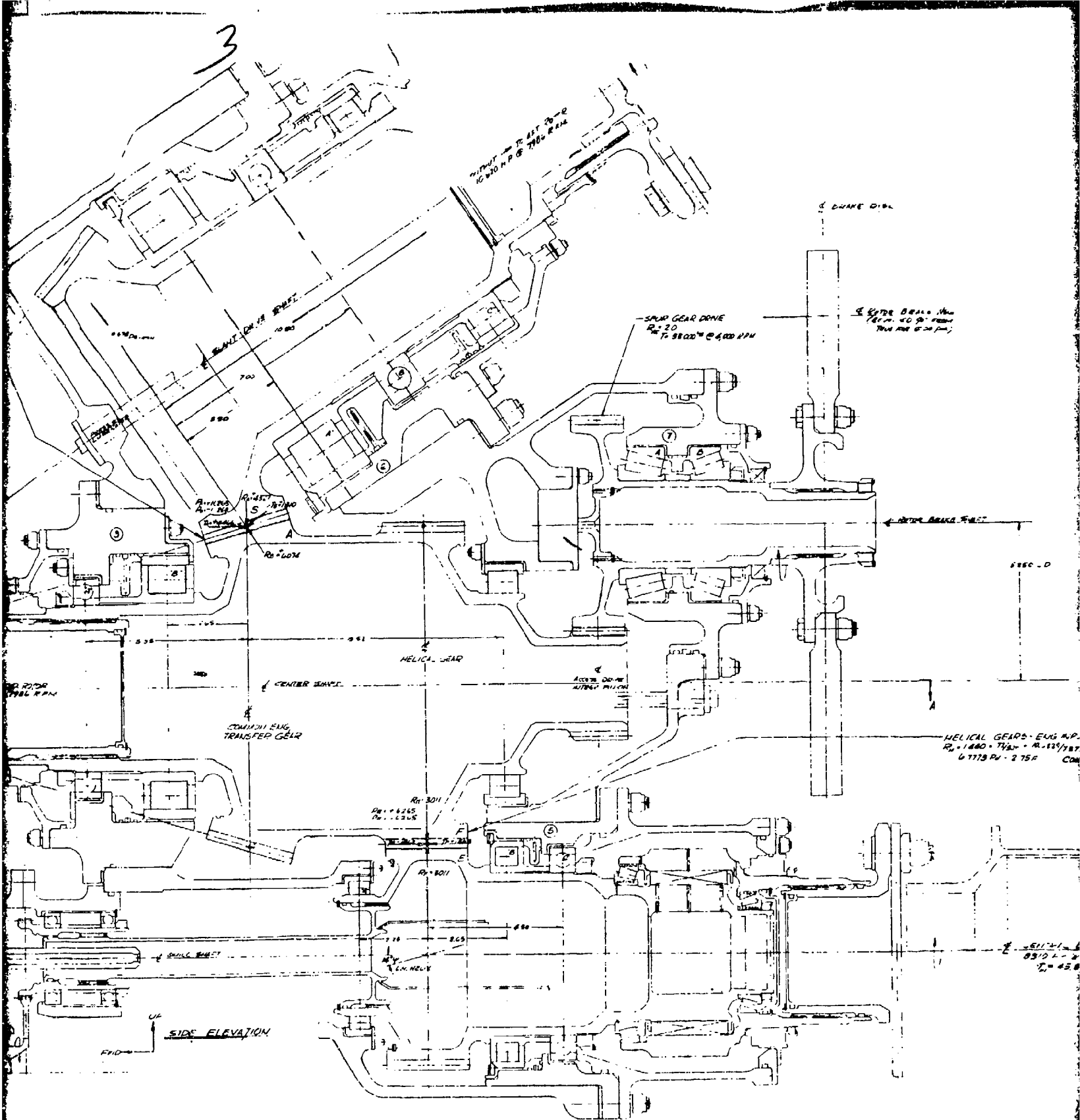
SPINAL BEVEL GEARS (SLAL) TYPICAL MESH
 $R_2 = 1.00 - 75/10 = 1.820$
 $R_3 = 1.00 - 6.25/10 = 1.900$
 CON. P.A. 0000

BEARINGS	DESIGN CRITERIA	C.M.P. UP	LIFE (HOURS) B_0 (ADJUSTED FACTOR)		
			BAG A	BAG B	BAG C
1	—	—	—	—	—
2	SHAL. SHAFT	7.625	627	745	1191
3	CENTER SHAFT	7620/1184	181	787	672
4	—	—	—	—	—
5	CENTRAL END SHAFT	4284	310	1043	782
6	BEVEL END SHAFT	4284	381	1193	1179
7	REF. NO. 10883	2.07	180	147	—

GEAR ORS CRITERIA		ALLOWABLE STRESS		APPLIED STRESS		MELICAL	
R.S.	SP. BEVEL	MELICAL	MINIMUM P	GEAR A	GEAR B	MINIMUM E	GEAR P
5a	44,000	48,000	48,678	24,727	48,082	48,987	43,806
5c	97,000	188,000	247,925	75,504	188,656	—	—



Inner



4

DRIVE SHAFT

DRIVE
W/ CARD PIN

5 PITCH BALLS ALN
181.75 - 40.50 INCHES
SHAFT DIA 1.25 INCH

NOTES: BRAKE FLUCT

6850 - D

HELICAL GEARS - ENG INPUT MESH
P_H = 1.640 - 7150 - 16.833/58770 - 11.0007106 RPM
6.7778 RV - 2.75R COMP RUN #3145

5111111 ENG SHAFT - INPUT
6510 L - 1.25 INCH
V₁ = 45.842 IN

THE GEORGE COMPANY	
SERIAL DIVISION PHILADELPHIA, PA.	
CONSUMER VMSL DESIGN STUDY	
ALTERNATE BEARING CENTER	
(REF. BOX 128.8)	
DATE	301-10393
BY	11/71
CHKD	
APPROVED	
NLH ATC	

savings of approximately 20 pounds in favor of the tapered-roller-bearing configuration.

In some locations, ball and cylindrical-roller-bearing combinations provide a better support arrangement. The center collecting shaft and helical pinion supports are two of these locations. The center collecting shaft requires a cylindrical roller at the right-hand end to allow for thermal motion. With a tapered-roller pair at the opposite end to take thrust in either direction, there is no reduction in bearings or weight advantage compared to cylindrical roller and ball thrust. Also, the lubrication of the tapered bearings through the inner race presents a special problem at this location because of the spline and the distance from the accessible end. Therefore, tapered bearings were not used here.

The helical-input-pinion straddle-mount ball and cylindrical design was selected because of slightly less weight and complexity than the tapered design. In the remaining locations (slant-shaft and bevel-input pinions), analysis showed that tapered bearings have significantly longer fatigue life within the same envelope as ball and roller bearings, are less complex, and weigh slightly less.

OVERRUNNING CLUTCH STUDY

A design objective was to make the overrunning clutch assembly a modular design that could be replaced without removal of the transmission. As a result, the design shown in 301-10221 evolved from the integral clutch-pinion shown in 301-10333.

Figure A-5 shows a typical aircraft configuration for the sprag-type clutch. Note that the inner clutch shaft is connected to the output or rotor drive and therefore is rotating when the rotors are turning. Oil is supplied by a fixed jet to the inside of the clutch shaft and is forced through holes in the shaft by centrifugal action or rotation. Lubrication to the clutch elements and bearings is positive at all times and not impaired when an engine is shut down (as is the roller clutch).

Figure A-6 shows a typical aircraft configuration for the roller-type clutch. Note that the outer clutch shaft is connected to the output or rotor drive. When an engine is shut down, the clutch inner shaft stops turning; therefore, lubrication depends on additional fixed jets to provide positive oil to the clutch elements and bearings. The inner shaft could be pressurized to improve the lubrication system but would require a rotating union or transfer tube involving rubbing parts.

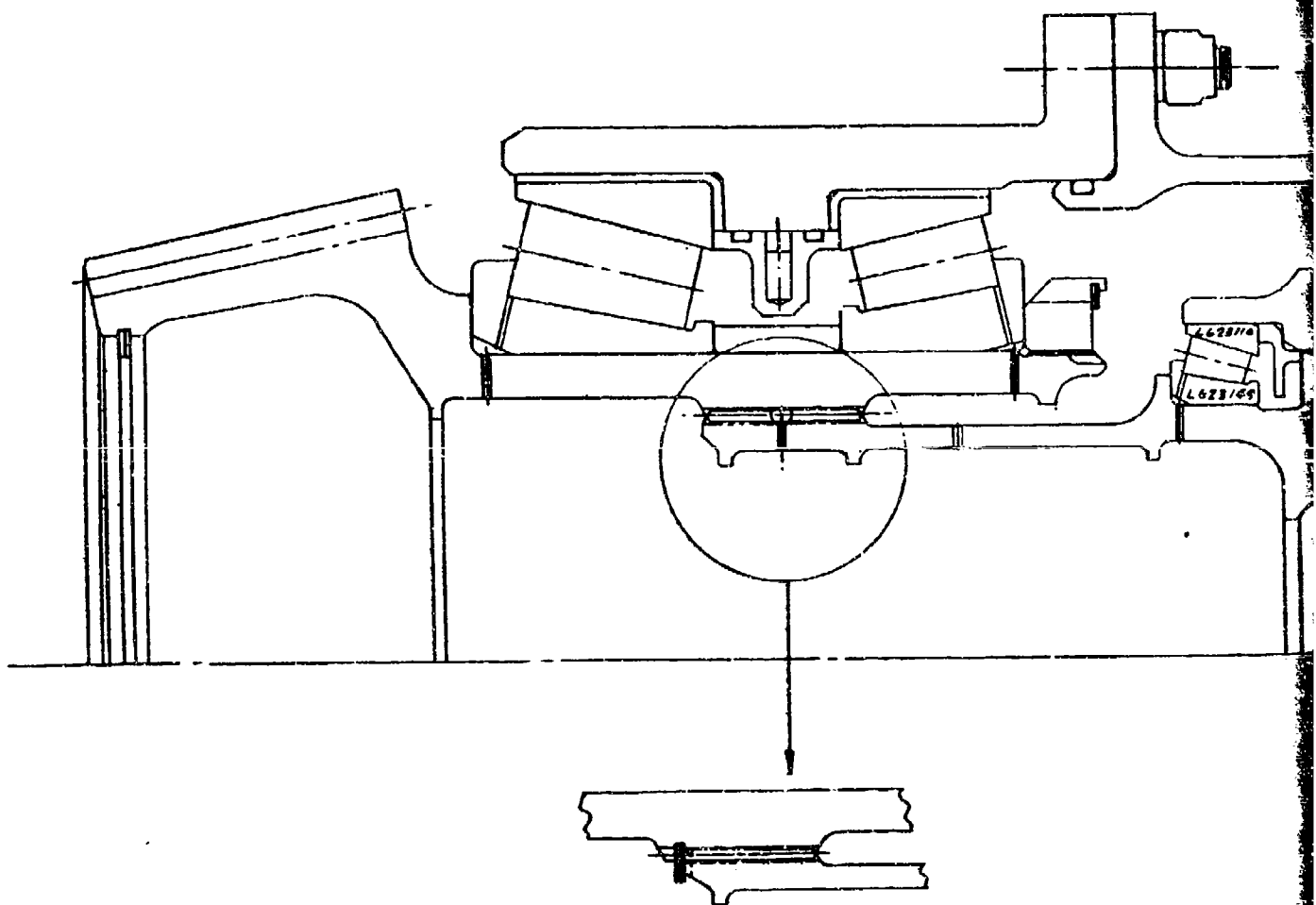
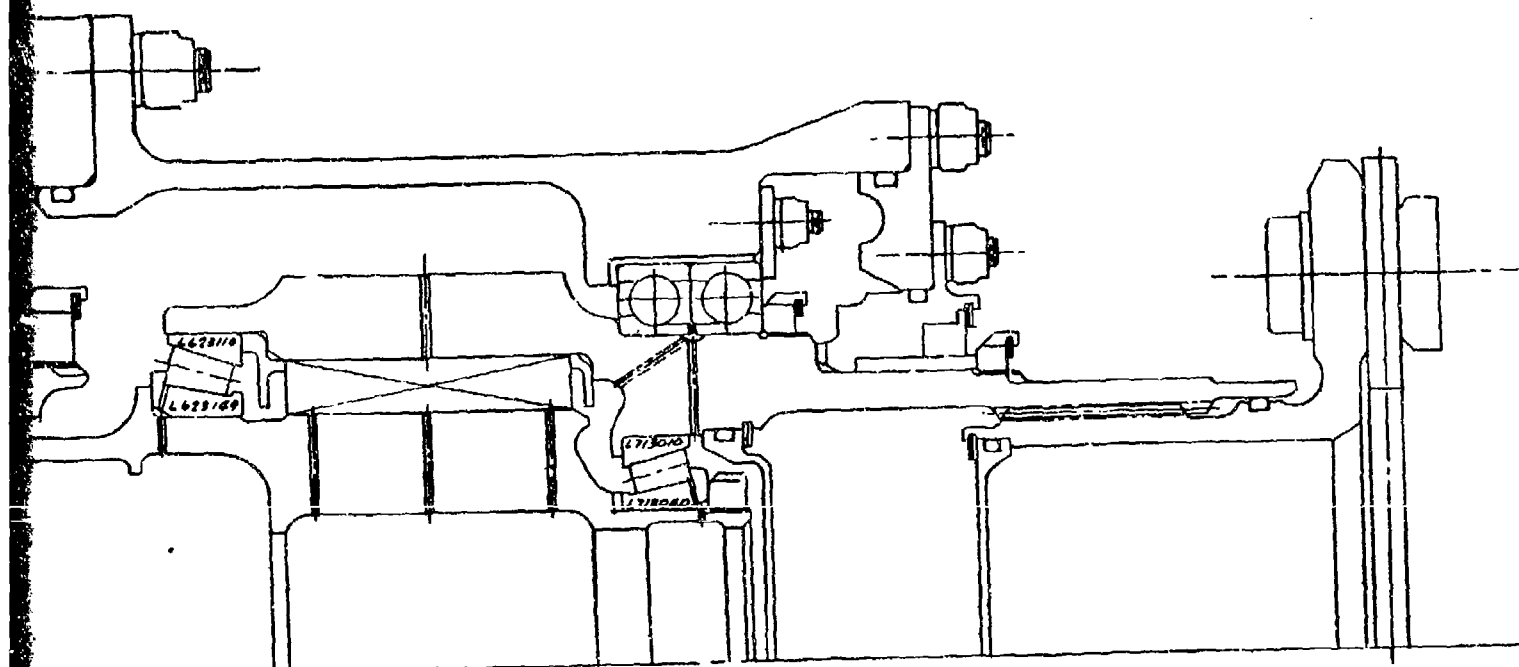


Figure A-5. Clutch Assembly Field Replaceable Concept Study.



dy.

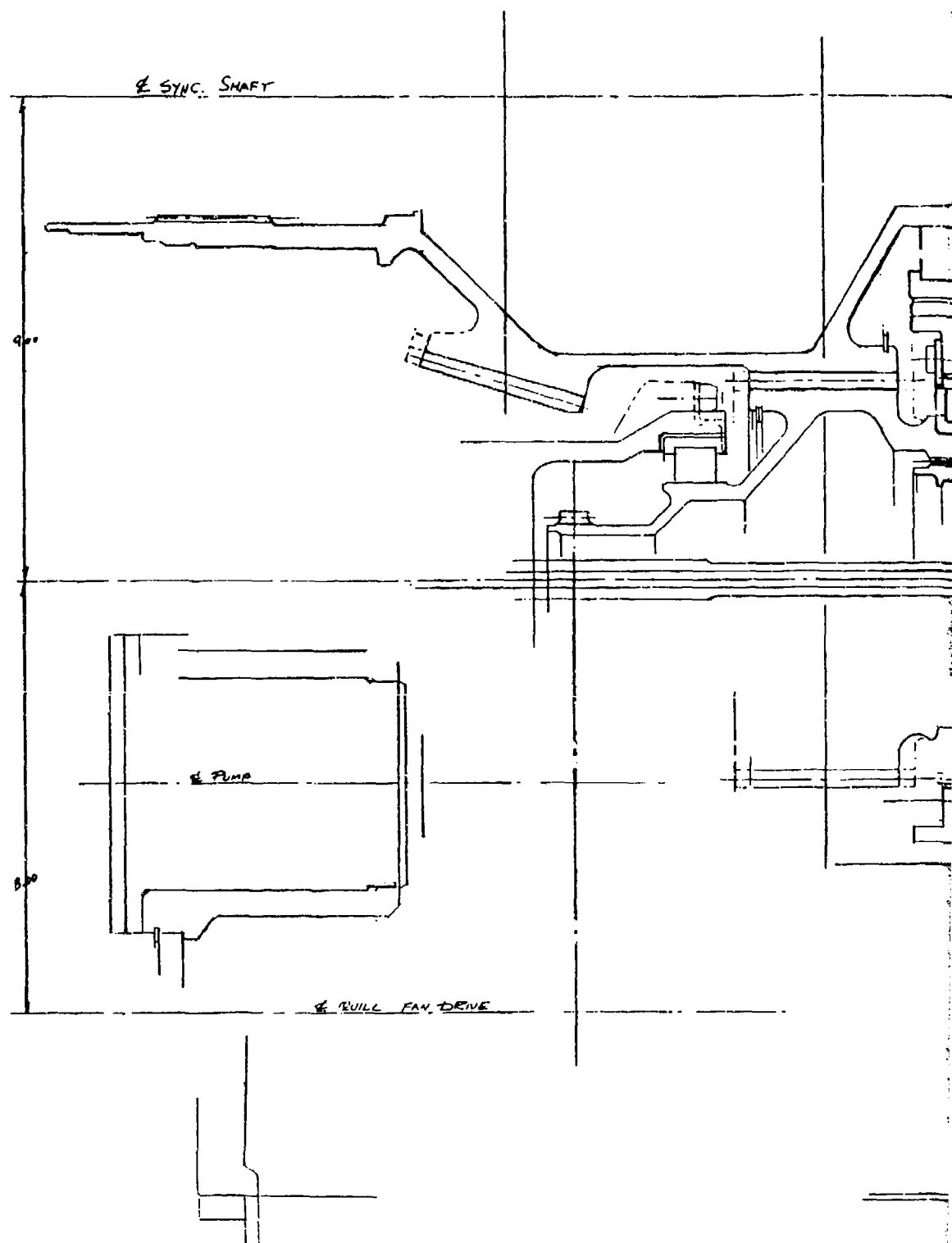


Figure A-6. Overrun Roller Clutch Study Field Replacement.

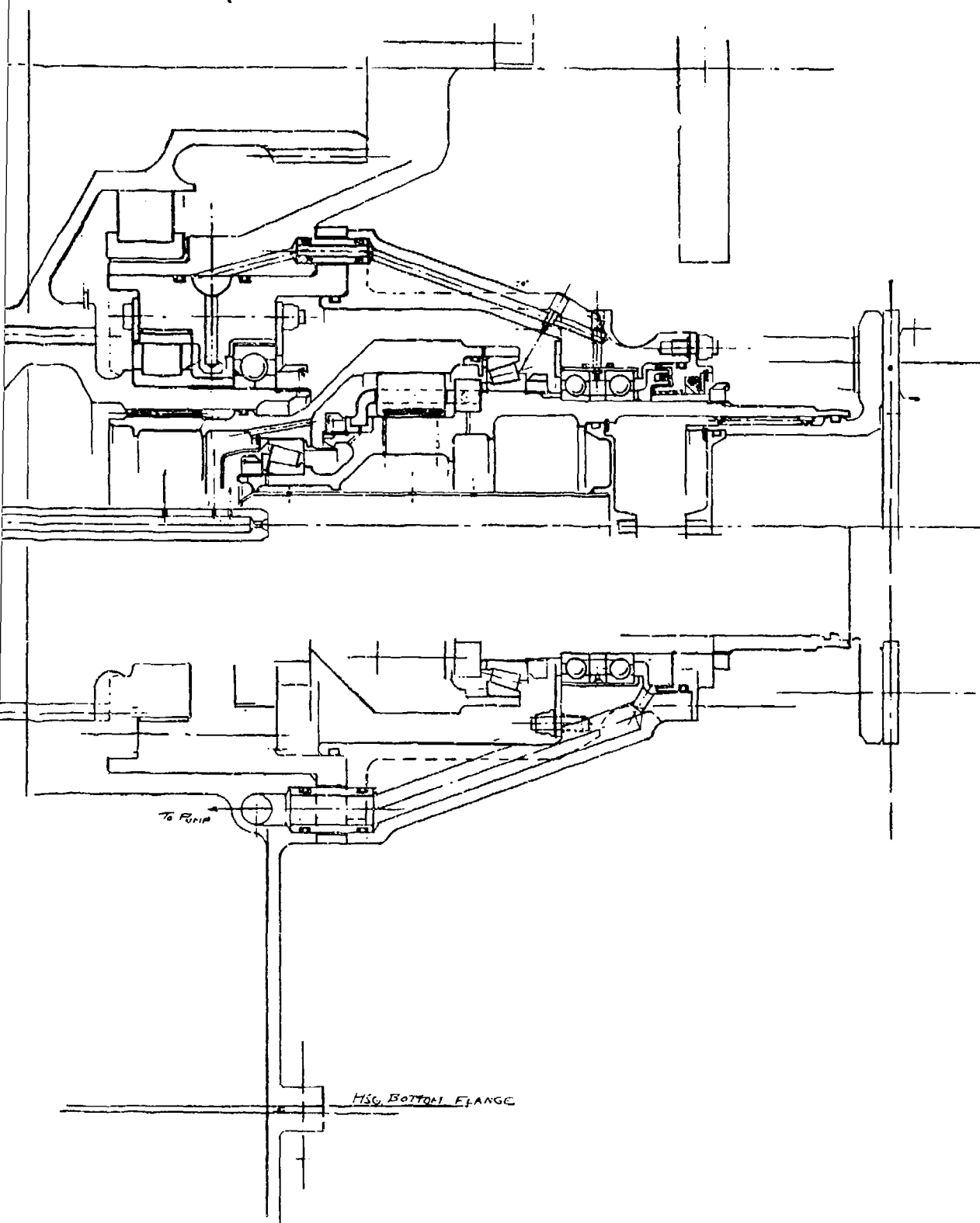
L BRAKE

2

4 CENTRAL ENG. SHAFT

TO FURIP

HSG. BOTTOM FLANGE



The HLH roller-clutch design would have a rubbing speed of over 18,000 feet per minute and relatively high roller loading from centrifugal force at speed. Another investigator has recently completed testing of a roller-type clutch aimed at application for the UTTAS. During that testing, the required speed was 26,500 RPM, which resulted in a rubbing speed at overrun of approximately 21,000 feet per minute. Differential testing was not successful due to excessive wear, even though hollow rollers were used to reduce loading and flame plating was used to eliminate wear.

The decision was made to continue with design and development testing of the sprag-type clutch with three different concepts for sprag energization. The results of this program will be reported at a later date. The test plan (D301-10118-1) has been completed and submitted. This test plan includes testing three initial designs for overrunning evaluation only. Results of testing will be used to define an optimum clutch which will be procured and tested. Testing on the optimum clutch will include static overload and cyclic fatigue, in addition to overrunning tests.

PLANETARY SIZING STUDIES

Planetary weight is 30 percent of the rotor transmission weight. Sizing of this major component assembly is dependent upon such considerations as:

- Tooth bending and contact stresses,
- Flash temperature allowed at the mesh,
- Back-up stresses, and
- Planet gear bearing capacity.

In the ATC Program, each of these considerations was subject to trade studies and several to supporting test programs.

Planet-gear bearing size, as determined by the gear loads and bearing capacity, influences planetary-ring-gear diameter. Figure A-7 shows the relationship between calculated fatigue life and ring-gear diameter, with cutoff points based on gear backup stresses and bearing internal geometry. Figure A-7 which is constructed for a spherical roller bearing, indicates that the minimum design point for gear diameter is just below 33.0 inches.

In the ATC Program, the possibility of increasing planet-gear-bearing capacity was investigated by analysis and bench tests of the compliant cylindrical roller bearing. These tests are

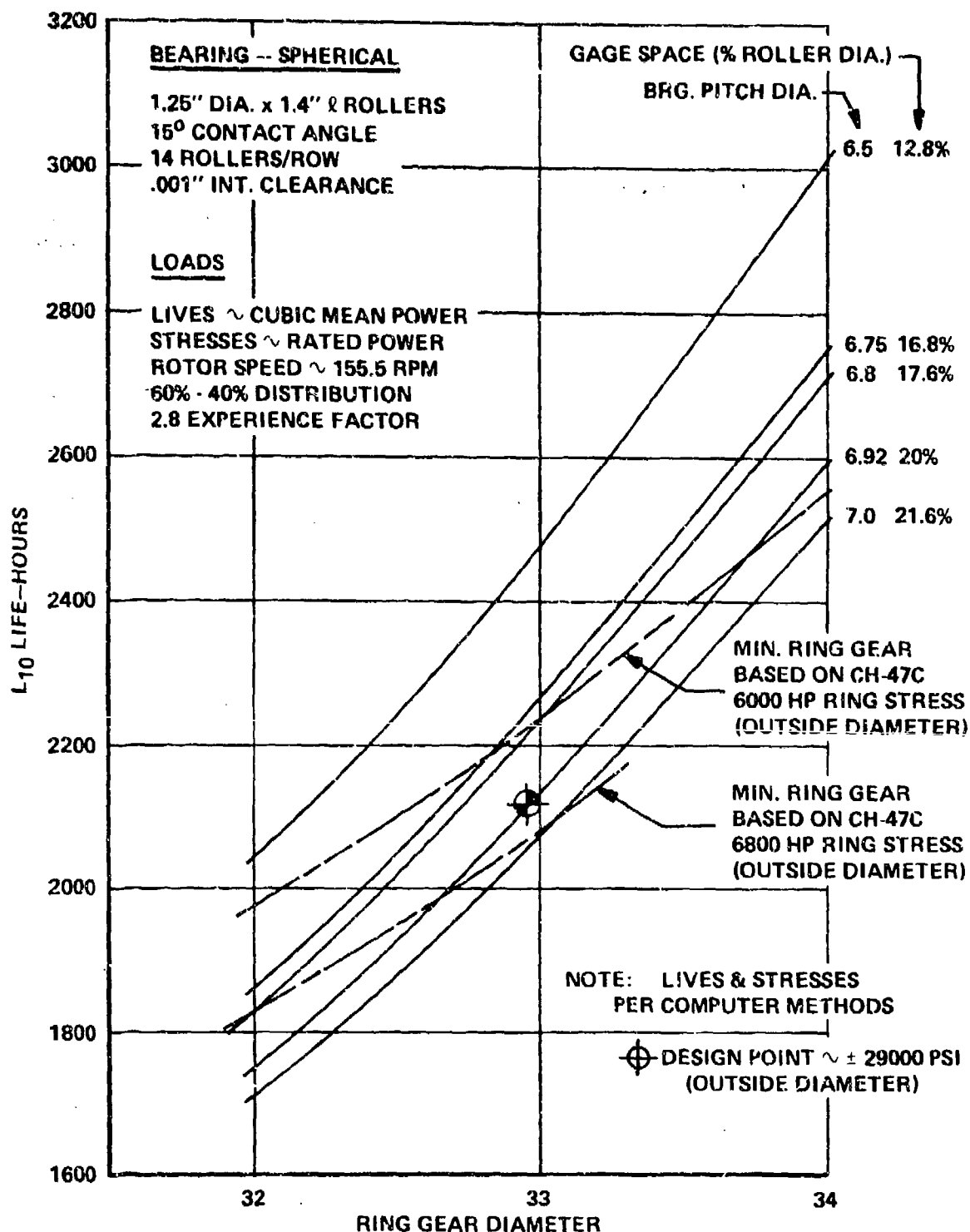


Figure A-7. Second-Stage Ring Gear Diameter (3.674 ratio).

reported in Reference 20, HLH-ATC Compliant Roller Bearing Development Program. The conclusions drawn were that the hollow-end rollers would have 50 percent greater life than the spherical-roller alternate bearing under the deflected conditions estimated to exist in the planetary. This calculated life increase was kept as reserve capacity for increased reliability. The studies and the final design were based upon a 2,000 hour B₁₀ fatigue life for spherical bearings in the planet gears. Transmission tests using both spherical and hollow-end roller bearings will verify the analytical predictions.

Gear-tooth geometry and advanced material were also investigated by a test program to evaluate high-contact-ratio gear tooth form and BMS 7-223 steel. These tests evaluate gearing of high contact ratio (over 2.0 profile overlap) against conventional contact ratio (approximately 1.6 profile overlap). BMS 7-223 steel (Vasco X-2 modified) is also compared using 9310 steel as the baseline. More than 28 data points have been obtained from this program. Results show that BMS 7-223 high-contact-ratio gears survived test-stand flash-temperature conditions which are more severe than those calculated for the rotor transmission in the trade study analysis.

The design studies compared gear contact ratios, gear materials, and bearing designs. Four candidate designs are shown in Figure A-8, wherein the ring-gear diameter is fixed by the bearing envelope and gear-tooth parameters are compared. The design objective of this study was minimum system weight, consistent with reliability objectives. Each candidate system was sized (face width) to meet the bending stress allowable. The calculated contact stresses were at or below the allowable for all designs; thus all were judged to be safe from a durability standpoint. Boeing-Vertol spur-gear geometry, strength, and surface durability computer programs were used to evaluate the strength and durability of all candidate designs.

The 4.522-pitch High Contact Ratio (HCR) system contact stress was 12 percent to 15 percent below the allowable, indicating a good margin in durability.

The scoring probability of the 3.429-pitch HCR design was in excess of 90 percent as compared to less than two-tenths of one percent (0.20 percent) for the other three designs (based on Vertol testing with the VASCO material). This design was therefore eliminated from further consideration.

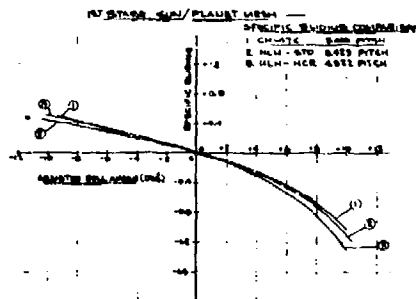
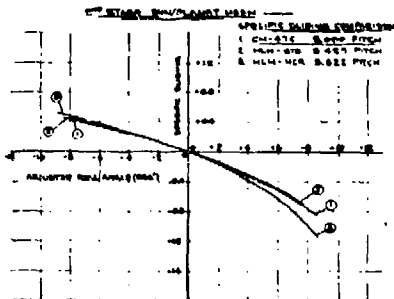
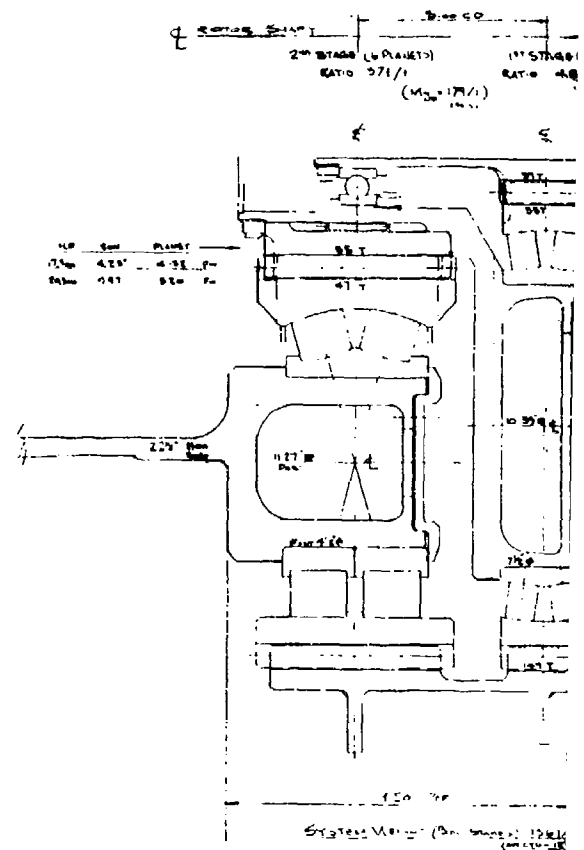
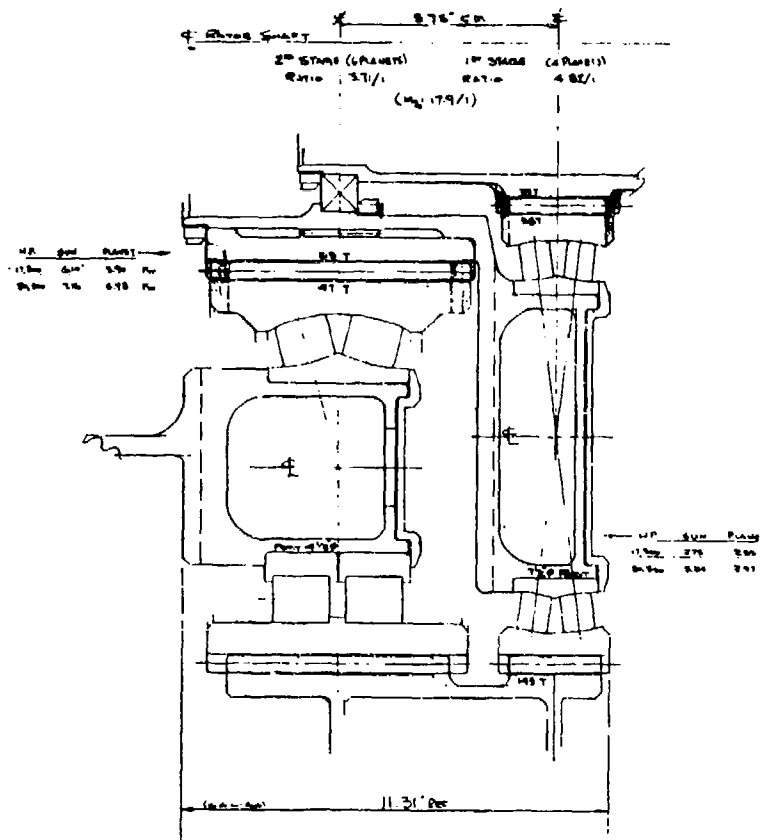
The 4.522-pitch standard configuration is significantly heavier; therefore, it was eliminated.

A comparison of the specific sliding velocity ratio (ratio of sliding to rolling velocities at an instantaneous contact

COMPARISON I: 4522 P₁

A-STANDARD TOOTH FORM (INVOLUTE)
 4522 P₁ WHOLE DEPTH 0.4168" (0.01059 in)
 17,300 H.P. STRESS LEVEL
 2P S₁ = 44,000 PSI S₂ = 161,148 PSI
 1P S₁ = 43,989 PSI S₂ = 171,000 PSI

B-HIGH CONTACT RATIO TOOTH FORM
 4522 P₁ WHOLE DEPTH 0.6335"
 17,300 H.P. STRESS LEVEL (600/100)
 2P S₁ = 44,000 PSI S₂ = 169,000 PSI
 1P S₁ = 43 S₂ = 167



BRINELL DESIGN CRITERIA FOR HLM (60% 100%)
 LIFE D₁₀ = 1000 HRS (1000 HRS) (1000 HRS)
 MATE FACTOR = 2.0
 GAGE WIDTH = 0.01 in
 MTD INT CLEAR = 0.01 in
 CHG LOADS = 75% of RATED
 L/D = 0.50
 L/D = 0.50
 PLANET RATIO = 4.25/3.75
 STRESS LEVEL = 16,000 PSI
 PLANET RATIO (M₂) = 179/1

Figure A-8. Trade Study-Planetary High Contact Ratio vs. Standard Growth Versions, 20,300 Horsepower.

ST. RATIO TOOTH FORM (INVOLUTE)
 SHAPE DATA 0.6315
 17.3mm HP 0.182mm HP
 20 45,940 psi 10 44,000 psi
 25 107,100 psi 15 107,100 psi

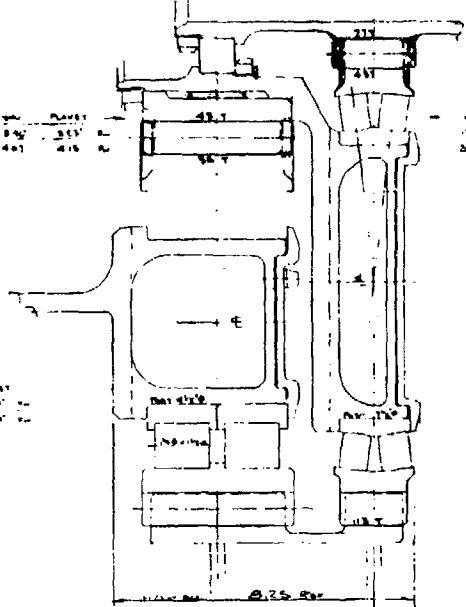
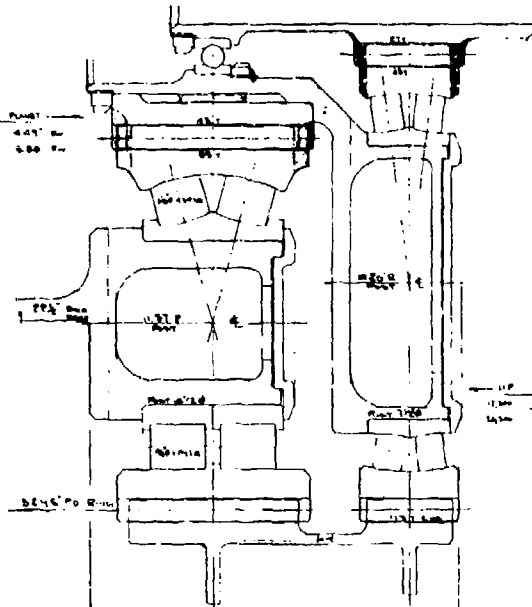
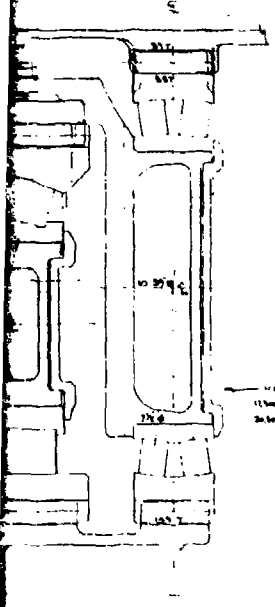
C-STANDARD TOOTH FORM (INVOLUTE)
 SHAPE DATA 0.6315
 17.3mm HP 0.182mm HP
 20 45,940 psi 10 44,000 psi
 25 107,100 psi 15 107,100 psi

D-HIGH CONTACT RATIO TOOTH FORM (INVOLUTE)
 SHAPE DATA 0.6315
 17.3mm HP 0.182mm HP
 20 45,940 psi 10 44,000 psi
 25 107,100 psi 15 107,100 psi

2nd STAGE (4 PLANETS)
 RATIO 4.62/1
 (M₂₅ 17.3/1)

2nd STAGE (4 PLANETS)
 RATIO 4.62/1
 (M₂₅ 17.3/1)

2nd STAGE (4 PLANETS)
 RATIO 4.62/1
 (M₂₅ 17.3/1)



1500 psi
 1000 psi
 500 psi

9.58" dia
 10.12" dia
 10.12" dia

144 PLANTING 25000 GWT									
PL	PITCH 0.627		D. PITCH 0.624		R. PITCH 0.622		D. PITCH 0.622		
STAGE	1"	2"	1"	2"	1"	2"	1"	2"	
W. T.	0.447	2207	494	814	245	244	070	2747	
M. H.	0.26	559	606	906	0.07	973	7.40	2260	
M. G.	C. 0.10		D. H. C. 0.		A. 0.10		D. H. C. 0.		

point) plots shows both the 3.429 standard and the 4.522 HCR to be equally suitable. Similarly, the lubricant film thickness and scoring probability are sufficient to meet the design objectives with either design.

The 4.522-pitch HCR configuration was chosen over the 3.429-pitch standard configuration because of lower contact stresses, a slight weight advantage, and because of its relatively finer pitch. The use of the finer-pitch design will provide better tooth contact conditions with lower dynamic loads and lower resultant noise levels.

A summary of planetary system weights is shown below:

4.522 DP HCR	1369 pounds
3.429 DP Standard	1390 pounds
4.522 DP Standard	1570 pounds
3.429 DP HCR	1184 pounds

ROTOR SHAFT MATERIAL STUDY

Design comparisons of the titanium and steel rotor shafts were made, Figure A-9, to define minimum weight designs for each. As indicated on the layout, the bearing journals and adjacent thrust faces on the titanium shaft will be hard coated to eliminate wear and fretting. Materials such as plasma or D-gun sprayed tungsten carbide will be evaluated. This material is applied and then ground to finish size. The splines will be coated with Nylon 11 to finish size without subsequent machining. Nylon is currently being evaluated on CH-47C cross-shafting splines.

Allowables used in these designs are shown in Table A-2.

TABLE A-2. SHAFT DESIGN ALLOWABLES		
	Steel* AISI 9310	Titanium 6AL-4V
Threads and Fillets	36,000 PSI	20,000 PSI
Thread Relief	27,000 PSI	20,000 PSI
Other Areas	25,000 PSI	20,000 PSI
Hard Coated Areas	N/A	15,000 PSI
*Values from previous rotor shaft fatigue tests.		

The study showed a 200-pound-per-shaft weight reduction using titanium as compared to the steel design. A titanium forging

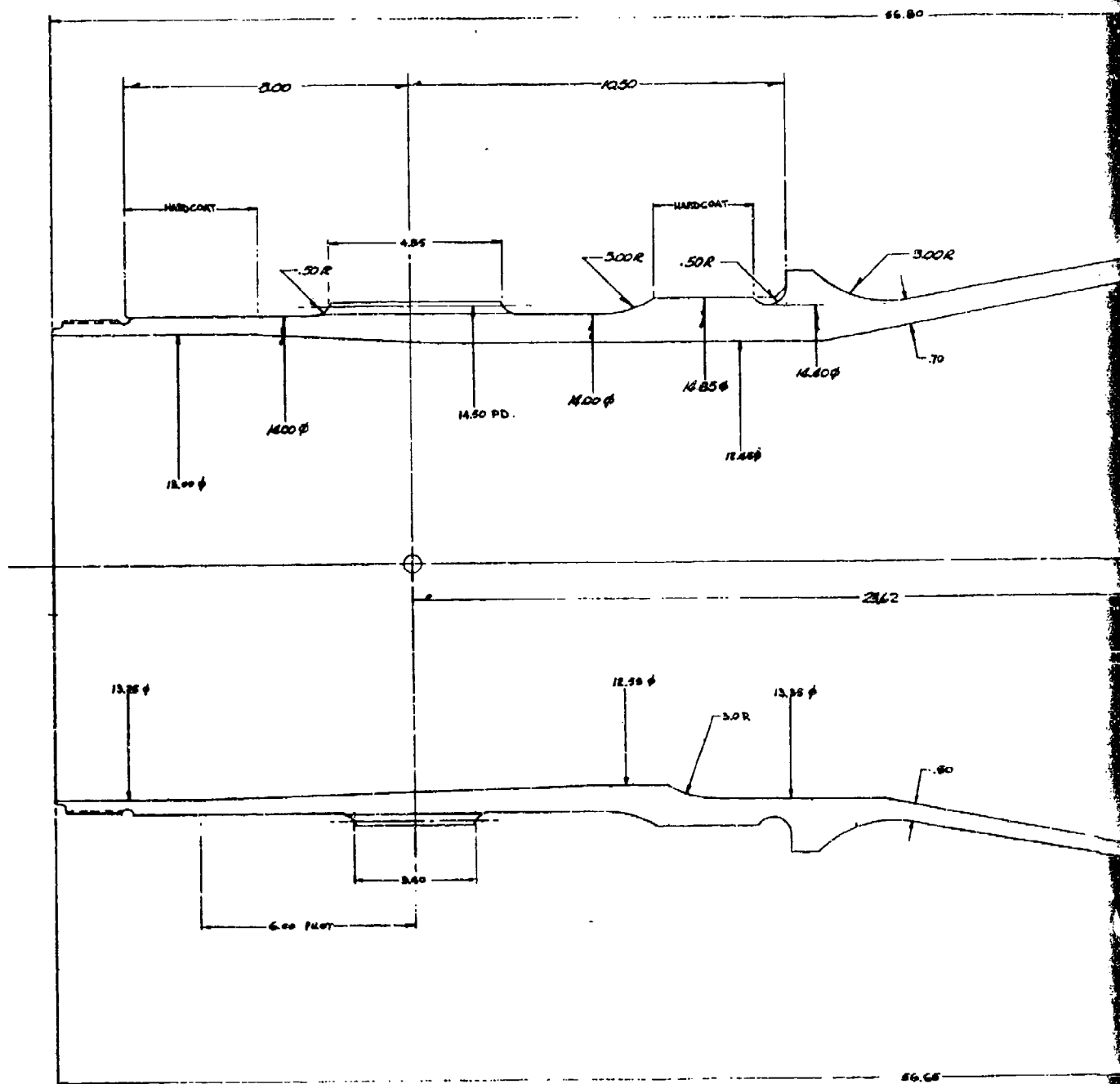


Figure A-9. Rotor Shaft Comparison, Steel - Titanium.

requirements document (D210-10409-1) was prepared to support the procurement of the titanium shaft.

ALUMINUM/GRAPHITE COMPOSITE TRADE STUDIES

Aluminum and graphite composite synchronizing and engine drive shafts were designed and analyzed using cost and weight criteria.

The initial study was based upon the torque and stiffness requirements of the synchronizing shafting, without consideration of possible design changes required to meet damage criteria. The results indicated approximately 25 percent weight reduction in favor of the graphite composite synchronizing shaft installation. This weight savings was primarily a result of the reduction in the total number of drive shaft sections required (eight sections of graphite shafting as compared to twelve sections of aluminum). However, the engine drive shaft installation showed very little weight differences for graphite versus aluminum, since the aircraft configuration required two sections of shafting for each engine installation. Weight differences exist in tubing weight only, since the end fittings and hardware remain basically constant.

The cost comparison study (Figure A-10) used best current estimates of costs to develop conclusions as to the cost effectiveness of graphite composite shafting. The conclusions were summarized as follows:

- There is a small cost savings (\$2,750 per aircraft) most likely to be derived from a composite engine-shaft tube. Because current design shows an equivalent number of parts for both composite and aluminum tubes, there is no added benefit beyond a reduction in tube weight.
- Cost savings most likely to be derived from composite tubes in the synchronizing shaft system are larger (\$41,200 per aircraft). The composite tube design permits fewer parts; therefore, there is additional advantage to be gained in maintainability and fabrication costs of bearings, couplings, and adapters.

The weight growth factor of two refers to the expected ratio of subsystem weight delta to aircraft empty weight delta.

On the basis of this study, further efforts were made to define the tube configuration which would meet the ballistic and handling damage requirements which are necessary considerations to the design of military helicopters. These efforts comprised analysis of over 25 composite shaft designs and fabrication of subscale shaft test specimens. Some results of these tests are reported in Reference 15.

- (1) PRODUCTION TOOLING
 (2) NO R&D COSTS
 (3) PRODUCTION IN 1978 - 82 PERIOD
 (4) R&M ARE CONSIDERED CONSTANT

(4) Items are considered constant.												
A	B	C	D	E	F	G	H	I		J	REMARKS	
								Δ FAB COST				
								PER TUBE	PER S/S			
WEIGHT Δ		TOTAL	\$ / LB OF WT	\$ Δ (COST Δ FROM WT)	\$ / LB MAT (Δ OVER AL)	LB TUBE MAT. AND \$ (COMPOSITE)	PER TUBE	PER S/S	MAT. & FAF S COST Δ (G + I)			
TUBE	ADAPTER											
-30#	0#	-30#	\$300	-\$18,000	\$ 40	(24#) \$960	5x20 \$100	\$ 600	\$1,560	-\$ 10,400	MOST OPTIMISTIC	
-30#	0#	-30#	\$130	-\$ 7,800	\$ 60	(24#) \$1,450	30x20 \$600	\$3,600	\$5,050	-\$ 2,750	MOST LIKELY	
-30#	* 0#	-30#	\$ 40	-\$ 2,400	\$120	(24#) \$2,080	40x20 \$800	\$4,800	\$7,880	+\$ 5,280	MOST PESSIMISTIC	
-80#	-126#	-206#	\$300	-\$172,600	\$ 40	(130#) \$5,200	\$100	\$ 800	\$6,000	-\$117,600	MOST OPTIMISTIC	
-80#	-126#	-206#	\$130	-\$ 53,800	\$ 60	(130#) \$7,800	\$600	\$4,800	\$12,600	-\$ 41,200	MOST LIKELY	
-80#	-126#	-206#	\$ 40	-\$ 16,500	\$120	(130#) \$15,600	\$800	\$6,400	\$22,000	+\$ 5,500	MOST PESSIMISTIC	

ENGINE SHAFT SYSTEM

ALUMINUM 6 SECTIONS
COMPOSITE 6 SECTIONS

(7,600 HP @ 12,000 RPM)

SYNC SHAFT SYSTEM

ALUMINUM 11 SECTIONS
COMPOSITE 8 SECTIONS

(60% X 17,300 HP @
8,000 RPM)

ENGINE SHAFT SYSTEM
 ALUMINUM 6 SECTIONS
 COMPOSITE 6 SECTIONS
 (7,600 HP @ 12,000 RPM)

SYNC SHAFT SYSTEM
 ALUMINUM 11 SECTIONS
 COMPOSITE 8 SECTIONS
 (60% X 17,300 HP @
 8,000 RPM)

*INCLUDES WEIGHT GROWTH FACTOR OF 2: E=2 (CxD)

Figure A-10. Cost Effectiveness of Graphite Composite Shafting.

Test results indicated that a design that is considerably different from that which was first considered would be required to sustain the impact and ballistic damage. A comparison of the first and last shaft designs is shown below.

<u>First</u>		<u>Last</u>
2-Ply Graphite (90°)	OD	1-Ply Dry Nylon
4-Ply Graphite (45°)		6-Ply 1002S Glass (45°)
11-Ply Graphite (0°)		26-Ply HM-S Graphite (0°)
	ID	<u>1-Ply</u> XP251-S Glass
17 Plies with $t = 0.116$ inch and $W = 0.183$ pound/inch		34 Plies with $t = 0.203$ inch and $W = 0.339$ pound/inch

The last design showed a weight saving of 75 pounds compared to an aluminum tube design. The cost of this graphite composite tube assembly was estimated to be \$18,000 more per aircraft than that of the aluminum, using the most likely assumptions of the methodology shown in Figure A-10. On this basis, the value (K column) of the composite tube assembly results in a relatively insignificant savings of \$1,000 per aircraft. The uncertainty of the material cost, and other unknowns, indicated that the immediate plan should be to revert to aluminum shafting.

Design criteria for impact and ballistic tolerance is as follows:

Impact: Sustain 125,400* inch-pounds after being struck by a 9.3 pound wrench** dropped 6 feet.

Ballistic: Sustain 125,400* inch-pounds after being struck by a fully tumbled 12.7 mm round impact at the tube centerline.

*Limit torque. (1.5 x design torque, corresponding to 1.5 x 0.60 x 17,300 HP at 8,000 RPM.)

**Corresponding to a standard wrench suitable for coupling-bolt torquing.

APPENDIX B
SUMMARY OF LOADS, ALLOWABLES AND STRESS ANALYSIS,
AFT AND COMBINER TRANSMISSIONS, ADVANCED
TECHNOLOGY COMPONENT CONFIGURATION

LOADS

Hub Loads

Noseup Pitching Limit Loads

Noseup pitching limit loads are given below. Figure B-1 shows the symbols and signs used. For these calculations, a gross weight of 118,000 pounds is used with a 2.5g force and a 60- to 40-percent split between thrust and torque.

FZF	198,000 lb
FXF	33,900 lb
MYF	3.03×10^6 in.-lb
MZF	6.44×10^6 in.-lb
FyF	2,550 lb
MXF	-158,000 in.-lb

Forward rotor head loads are critical and are used for the aft transmission.

Fatigue Rotor Loads

Steady Loads

MZF	4.29×10^6 in.-lb
FZF	66,000 Lb
MyF	1.23×10^6 in.-lb
FXF	13,780 Lb
Basis	aircraft parameters with an 8-degree flap angle

Alternating Loads

MZF	$\pm 0.515 \times 10^6$ in.-lb
FZF	$\pm 6,600$ lb
MyF	$\pm 0.246 \times 10^6$ in.-lb
FXF	$\pm 2,755$ lb
Basis	Shear and Moment = ± 20 percent of steady Thrust = ± 10 percent of steady Torque = ± 12 percent of steady

Bearing Loads

All gear shaft and planetary bearings are sized for the cubic mean power calculated in Table B-1. The corresponding cubic mean torques are shown in Table B-2. The mission profile used is shown in Table 1.

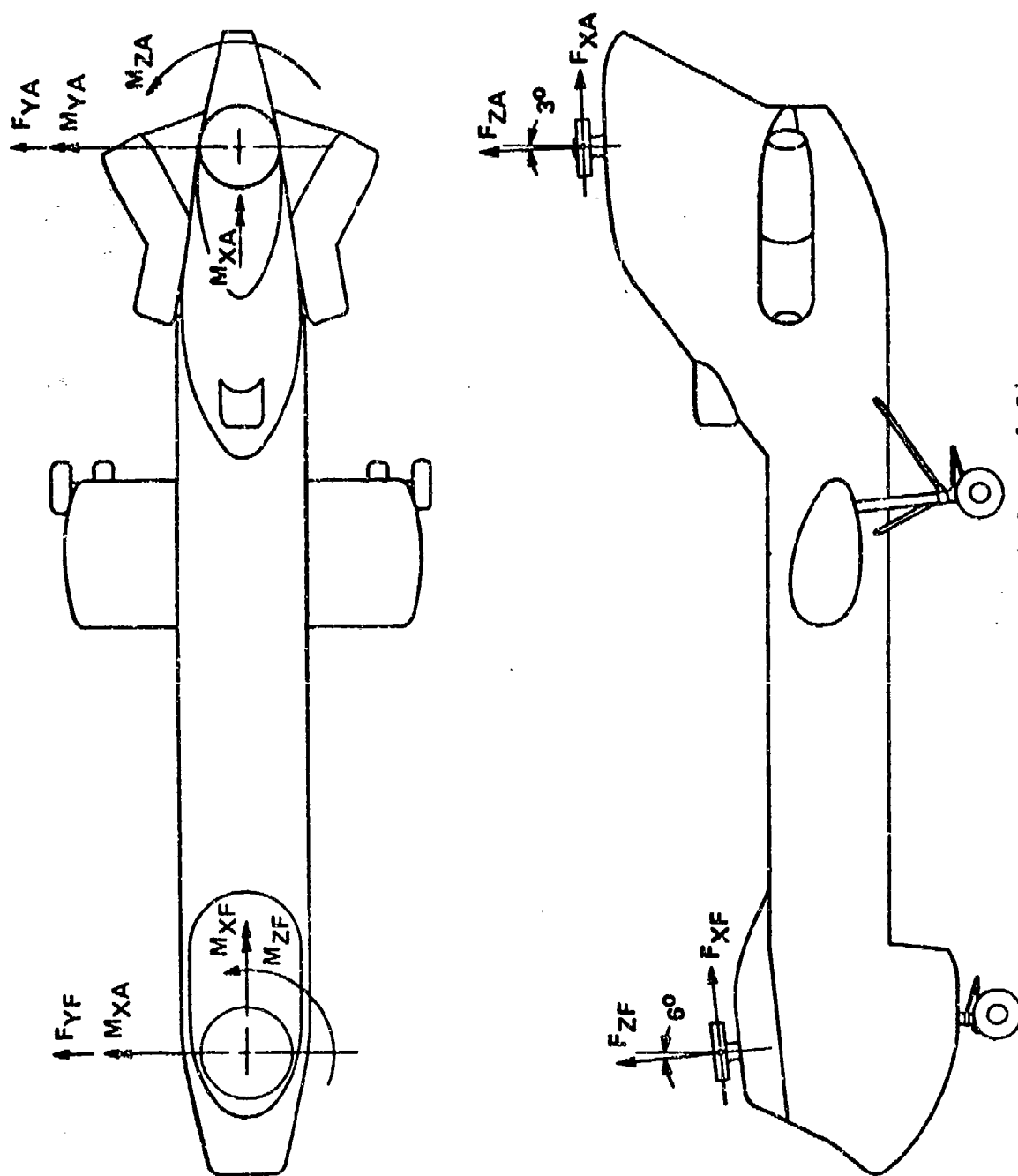


Figure B-1. Hub Loads Symbols and Signs.

TABLE B-1. CUBIC MEAN POWER									
78,000 POUNDS				118,000 POUNDS			147,500 POUNDS		
CONDITION	t	A/S	HP $\times 10^{-3}$	HP ³ $\times 10^{-9}$	A/S	HP $\times 10^{-3}$	HP ³ $\times 10^{-9}$	A/S	HP $\times 10^{-3}$
GROUND	.010		5.15	1.37		6.65	2.94		8.37
HOVER	.300		8.35	174.65		15.30	1074.40		17.70
SIDE	.020		8.04	10.30		15.10	69.85		17.70
REAR	.010		8.04	5.15		15.10	34.42		17.70
FWD, % VH									
20	.050	34	7.64	22.29	29	13.10	112.40	28	16.28
40	.020	68	7.00	6.86	58	10.90	25.90	56	14.80
50	.020	85	7.00	6.86	73	10.20	21.21	69	13.60
60	.050	103	7.50	21.10	87	10.25	53.81	83	13.10
70	.090	120	8.60	57.30	102	10.90	116.50	96	13.30
80	.115	137	10.60	136.90	117	12.10	204.00	110	14.00
90	.180	154	13.40	433.09	131	14.30	526.35	124	15.30
100	.010	171	17.70	55.45	146	17.70	55.45	138	17.70
115	.010	197	17.70	55.45	168	17.70	55.45	159	17.70
T-O PWR.CL	.030		17.70	166.35		17.70	166.35		17.70
FULL PWR.									
CL.	.040		8.13	21.50		11.99	69.00		15.37
POWER DIVE	.025		16.52	110.00		15.91	101.00		15.46
AUTOROTA.	.020		0	0		0	0		0
1.0				1284.62			2688.03		
									3985.47

$$CMP = [1284.6 \times .45 + 2688. \times .5 + 3985. \times .05]^{1/3} \times 10^3 = 12850 \text{ HP}$$

- NOTES: (1) Takeoff power climb at transmission rating.
 (2) Full power climb based on minimum power forward flight and 500 FPM rate of climb.
 (3) Transient conditions are redistributed to fwd flight and autorotation for power calculations.
 (4) Power dive based on transmission rating and 500 FPM rate of descent.

TABLE B-2. SPEED/TORQUE SUMMARY FOR GEAR AND DRIVE SHAFTING LOADS

TABLE B-2. SPEED/TORQUE SUMMARY FOR GEAR AND DRIVE SHAFTING LOADS						
LOCATION	SPEED	FATIGUE, IN.-LB (1)		FATIGUE, IN.-LB (2)		CUBIC (3) MEAN IN.-LB
		AEO		OEI		
		STEADY	ALTERNATING	STEADY	ALTERNATING	
Engine	11,500	± 32320	3880	± 44250	5300	23450
Sync Shaft	7,986	± 83800	10060			60800
1st Sun Gear	2,788	± 240000	28800			174000
2nd Sun Gear	578	± 1.159 x 10 ⁶	139000			840000
Rotor	155.9	± 4.29 x 10 ⁶	515000			3.015 x 10 ⁶

1st Post Load	-	27850 lb	3340 lb			20200 lb
1st Planet Bearing	1,570					
2nd Post Load	-	63500 lb	7620 lb			46100 lb
2nd Planet Bearing	495					

NOTES:						
1. 17700 HP @ 155.9RPM, 60/40 Rotor Distribution						
2. 8075 HP per engine @ 155.9RPM, 60/40 Rotor Distribution						
3. 12850 HP @ 155.9RPM, 60/40 Rotor Distribution (72.5% Rating)						

NOTES:

1. 17700 HP @ 155.9RPM, 60/40 Rotor Distribution
2. 8075 HP per engine @ 155.9RPM, 60/40 Rotor Distribution
3. 12850 HP @ 155.9RPM, 60/40 Rotor Distribution (72.5% Rating)

Clutch support (duplex ball) bearings are sized to operate under a continuous misalignment of 1/4 degree.

Rotor shaft bearings are sized for loads obtained by flapping angles and Table 1. The resulting equivalent radial loads are:

Upper Bearing	54,600 pounds
Lower Bearing	64,700 pounds

Accessory drive bearings are sized for the cubic mean loads shown under Accessory Loads.

Drive shaft support bearings are loaded only by the shaft weight and are sized by the required shaft section.

Rotor brake bearings are sized for the rotor brake torque given below:

Rotor Brake Loads

Rotor brake torque is 30,000 in.-lb at the brake disk. This is based on a drive system inertia of 170,000 ft-lb-sec² and a total rotor drag constant of 355 ft-lb-sec².

Accessory Loads

Accessory drive components are sized for the loads listed below:

<u>Transmission</u>	<u>Accessory</u>	<u>Rating</u>		<u>Cubic Mean</u>	
		<u>HP</u>	<u>Speed</u>	<u>HP</u>	<u>Speed</u>
Aft	Hydraulic Pump (2)	60	5,966	31.5	5,966
	Main Lube Pump	10	5,737	10.0	5,737
	Auxiliary Lube Pump	2	5,737	2.0	5,737
	Alternator (2)	97	8,062	60.0	8,062
	Blower	60	8,287	60.0	8,287
Combiner	Main Lube Pump	10	5,750	10.0	5,750
	Auxiliary Lube Pump	2	5,152	2.0	5,152
	Blower	60	8,200	60.0	8,200

Control Loads

Loads imposed upon the transmission upper cover by the rotor control system are as follows:

Actuator Loads

<u>Condition</u>	<u>Fatigue Load (pounds)</u>	<u>Ultimate Load (pounds)</u>
Normal Operation	3,700 \pm 3,700	39,500
One Actuator Failed	3,700 \pm 3,700	39,500

Stationary Scissor Loads

Stationary scissor loads, expressed as a torque about the rotor shaft centerline, are:

Fatigue	1,290 \pm 1,350 in-lb
Ultimate	13,500 in-lb

Gear and Drive Shafting Loads

A gear and drive shafting loads speed/torque summary is given in Table B-2.

DERIVATION OF ALLOWABLES

Derivation of BMS 7-223 (Vasco X-2) Design Allowables

The purpose is to provide a summary of experience including experimental gear test data and a gear analysis which establishes a data base for the HLH/ATC drive system gear design criteria.

The testing summarized in Figures B-2 and B-3 indicates that Vasco X-2 steel has a 20-percent higher bending strength than the air-melted AISI 9310 gear steel (AMS 6160) (Reference 16).

The data summarized in Figures B-4 and B-5 show a 34-percent increase in allowable contact stress (80-percent increase in load capacity) for Vasco X-2 steel when compared with the AISI 9310 data (AMS 6260) (Reference 17).

During scoring evaluation tests, the BMS 7-223 gears demonstrated an increased load carrying ability compared to the AISI 9310 gears of identical tooth form (Figure B-6). When tested in the high contact ratio tooth form, BMS 7-223 survived loadings equivalent to flash temperatures achieved in excess of the HLH requirement (shown in Figure B-6) with the exception of one test where very light scoring occurred at 380°F. Testing of bevel gears (Reference 18) indicates comparable superiority of BMS 7-223 over AISI 9310.

With the above test data as a base and qualitatively considering the effect of various influencing parameters such as the relationship between a rigid test stand and relatively flexible aircraft housing, the following index values have been established as design allowables for the HLH drive system power gearing.

Bending Stress	Spur and Helical	47,000 psi
	Spiral Bevel	47,000 psi
Contact Stress	Spur and Helical	188,000 psi
	Spiral Bevel	260,000 psi
Flash Temperature	Spur and Helical	395°F
	Spiral Bevel	550°F

The results of R.R. Moore fatigue testing conducted at Boeing Vertol are shown in Figure B-7. Figure B-7 indicates that the mean fatigue strength of smooth BMS 7-223 specimens is 50% of the ultimate tensile strength. The design allowable is derived from this by considering that the mean strength of full-size components is lower than laboratory specimens by a factor of 1.75, which accounts for such items as manufacturing techniques, size, and configuration. In addition, the mean fatigue strength is reduced to a mean -3σ level by considering that full-size components exhibit a log-normal fatigue strength distribution with a coefficient of variation of 13%, for which mean -3σ is 65.8 percent of mean. The design fatigue allowable for components other than gear teeth then becomes:

$$\frac{160,000}{2} \times \frac{.658}{1.75} = 30100 \Rightarrow +30000 \text{ psi}$$

(nonfretted, $k_t = 1.0$, $R = -1$)

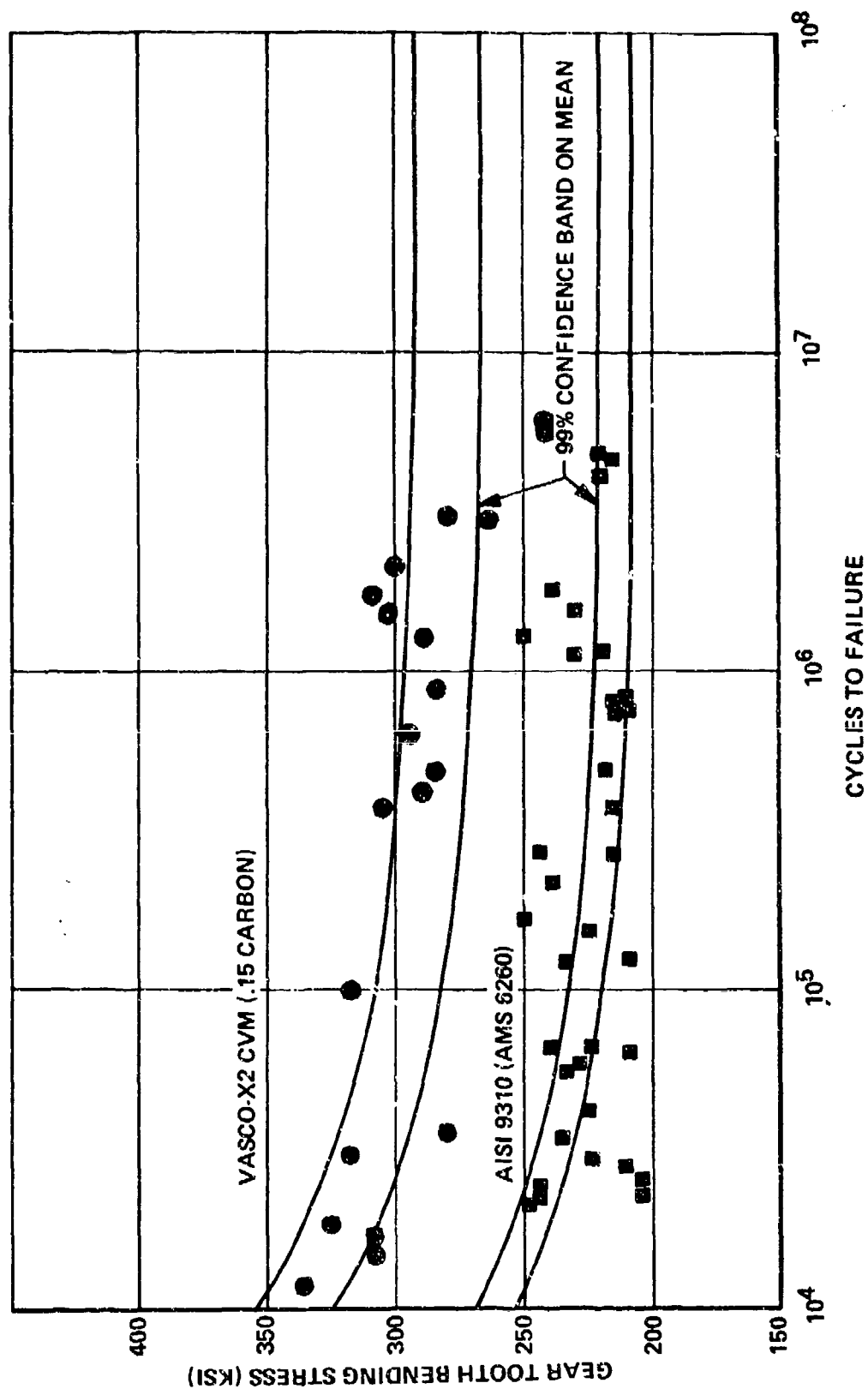


Figure B-2. Single-Tooth Bending Fatigue Test Data.

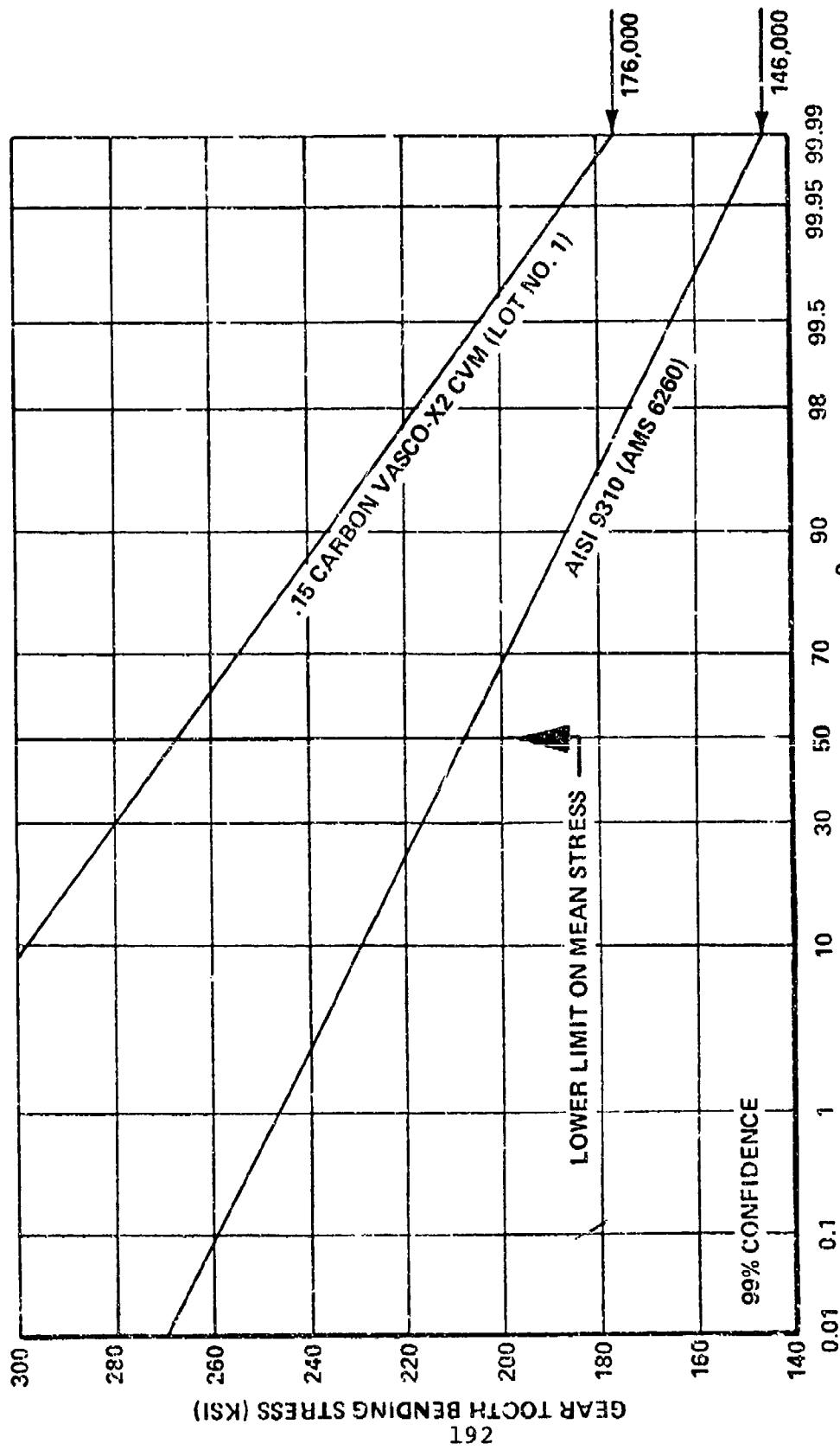
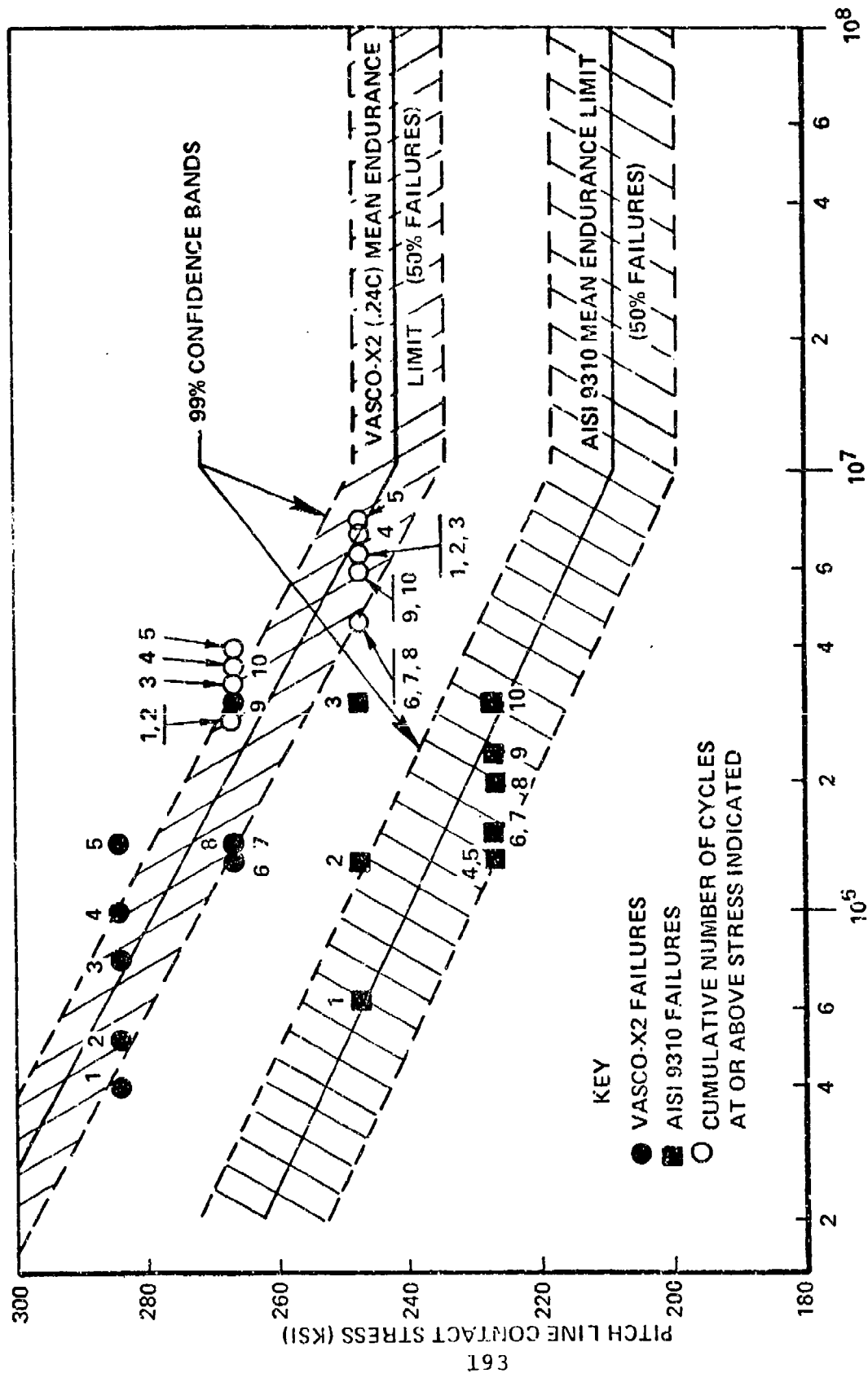


Figure B-3. Single-Tooth Bending Fatigue Test Data
(Probability of Survival).



NOTE: FAILURE OCCURRED AT HIGHEST STRESS INDICATED

Figure B-4. Contact Stress Test Data.

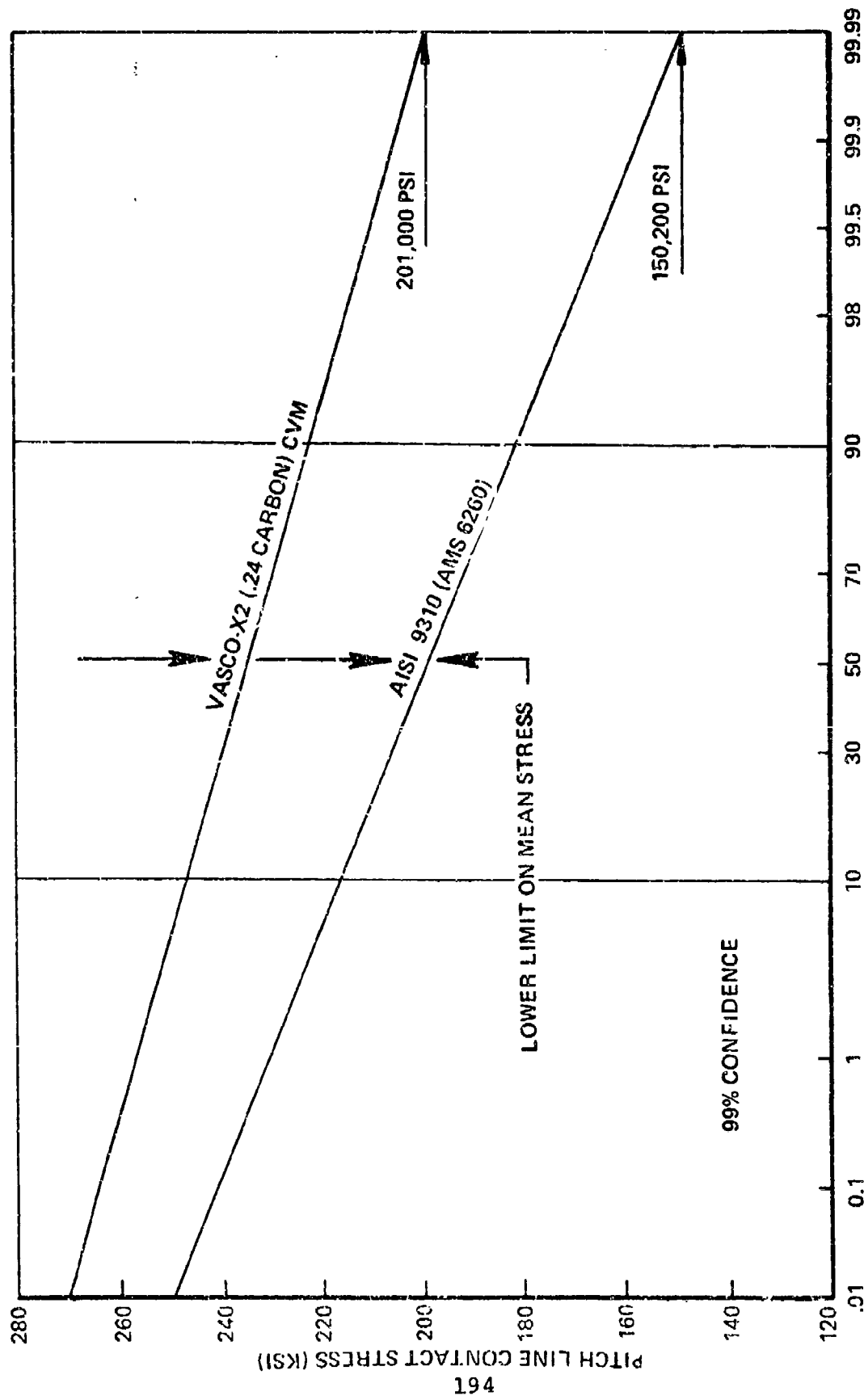


Figure B-5. Contact Stress Test Data (Probability of Survival).

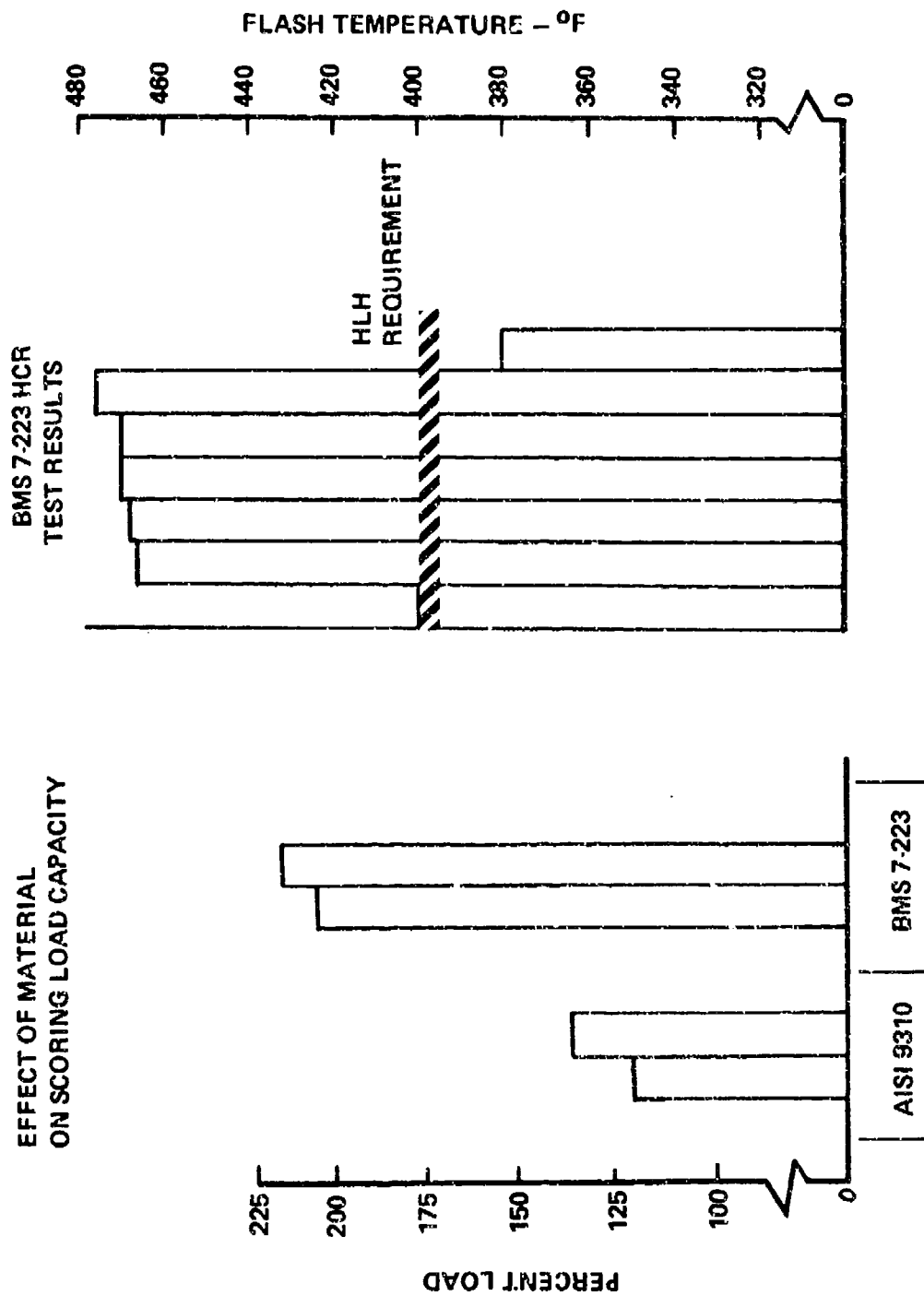


Figure B-6. HLH/ATC Gear Tooth Form Test Results.

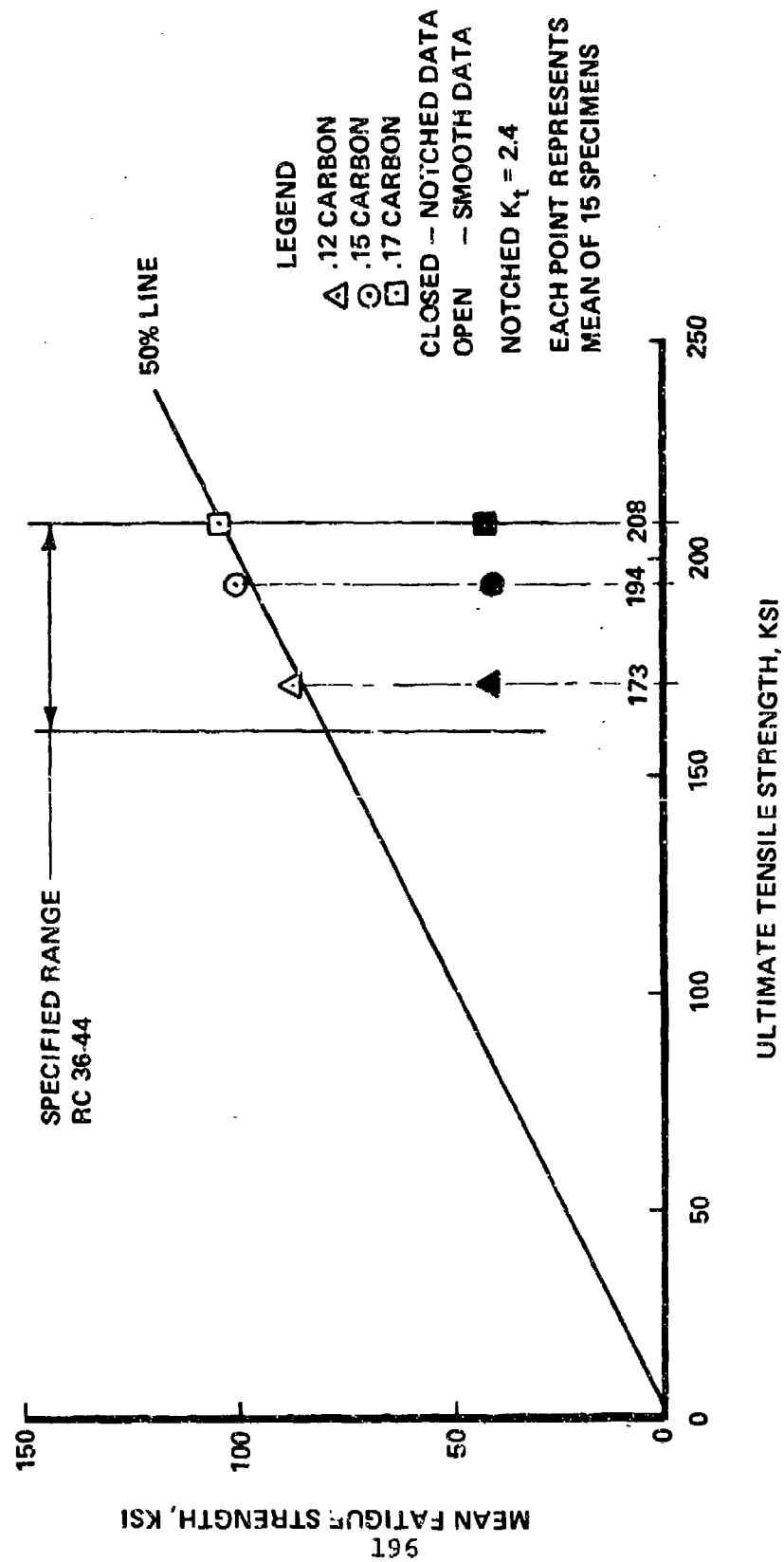


Figure B-7. BMS 7-223 Steel Rotating Beam Data.

TUNGSTEN CARBIDE COATING ON TITANIUM

Fatigue test results of coated titanium have been obtained by Union Carbide Corp. Testing was conducted on 12 uncoated, shot-peened specimens, and on 15 for each of two process variations for tungsten carbide coating. Both processes include shotpeening prior to coating; coating application is by detonation gun. Process designation LW-IN40 and LW5 test results indicate strength reductions of 13.5% and 25.8% relative to the uncoated baseline specimens. S-N curves resulting from these tests are shown in Figure B-8. The 301-10401 rotor shaft utilizes LW-IN40 coating for which a conservative bending strength reduction of 25% is assumed, resulting in an allowable of $\pm 115,000$ psi.

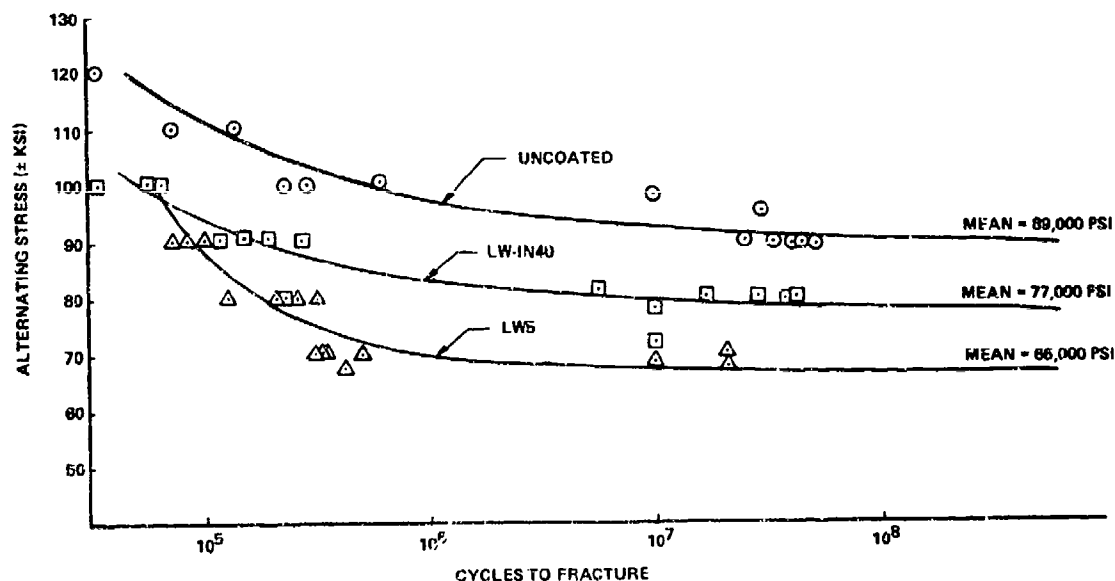


Figure B-8. Detonation Gun Coating on 6AL-4V Rotating Beam Fatigue Test Results.

ANALYSIS OF COMPONENTS

Tables B-3 through B-14 and Figures B-9 through B-22 summarize the analysis of the ATC Components.

TABLE B-3. MINIMUM MARGINS OF SAFETY			
PART NUMBER	PART NAME	CONDITION	M S
301-10401	Rotor Shaft	Fatigue	0.0
301-10610	Slant Gear	Fatigue	.25
301-10654	Helical Input Pinion	Fatigue	2.0
301-10677	Spiral Bevel Input Pinion	Fatigue	.25
301-10629	Clutch Shaft	Fatigue	3.0
301-10650	Clutch Hsg.	Ultimate	10.
301-10625	Rotor Brake Gear	Fatigue	.05
301-10601	Collector Gear	Fatigue	.60
301-10428	Spiral Bevel Pinion	Fatigue	.06
301-10419	Spiral Bevel Gear	Fatigue	.58
301-10413	First-Stage Planet Carrier	Fatigue	.10
301-11000	Sync Shaft Tube	Ultimate	.05
301-11001	Engine Shaft Tube	Ultimate	.39
301-10463	Adapter - Sync. Shaft	Ultimate	.09
301-11023	Adapter - Engine Shaft	Ultimate	.11
301-10456	Upper Cover	Ultimate (Fail-Safe)	.01

TABLE B-4. HELICAL AND SPUR GEAR TOOTH STRESS SUMMARY

Location			Part Number	No. Teeth	Trans. PD	DP	Trans. Press Angle Deg	H. Am. Deg
COMBINER	Center Engine	Pinion	301-10654	50	6.87915*	7.2683*	24.6757*	*10
		Gear	301-10601	72		10.4664*		
	Rotor Brake	Pinion	301-10601	20	4.8750	4.1026	28	J
		Gear	301-10625	31		6.3590		
AFT TRANSMISSION	First-Stage Planet 3	Sun	301-10419	39	4.522	8.6245	22	J
		Planet	301-10466	55		12.1628		
		Planet	301-10466	55	4.522	12.1628	22	J
		Ring	301-10412	149		32.9500		
	Second-Stage Planet 4	Sun	301-10459	55	4.522	12.1628	22	J
		Planet	301-10468 ① 301-10469	47		10.3936		
		Planet	301-10469 ① 301-10468	47	4.522	10.3936	22	J
		Ring	301-10412	149		32.9500		

NOTES

- ① 301-10468 - Spherical Bearing
 301-10469 - Cylindrical Bearing - Gears are identical. ③ 4 Equally
 ② Torque Values Per Mesh. ④ 6 Equally

TABLE B-5. SPIRAL BEVEL GEAR TOOTH STRESS SUMMARY

Location			Part Number	No. Teeth	PD	Dp	Press Angle Deg	Spiral Angle Deg
COMBINER	Engine LH & RH	Pinion	301-10677	50	6.25	8.000	25.	20.
		Gear	301-10601	72		11.520		
	Slant Shaft	Pinion	301-10601	72	6.25	11.520	25.	20.
		Gear	301-10610	72		11.520		
AFT	Input	Pinion	301-10428	37	4.00	9.25	25.	23.
		Gear	301-10419	106		26.50		

ESS SUMMARY

ns. D	DP	Trans. Press Angle Deg	Helix Angle Deg	Speed RPM	Face Width In	Flash Temp. Deg F	J	I	Torque (in-lb)	fb PSI
7915*	7.2683*	24.6757*	*10.*	11,500	2.75	374.	.6362	0.1399	44,250	46,50
	10.4664*			7,986	2.75		.6625		63,780	44,63
750	4.1026	28	3.0	4,495 (6)	2.00	397.	.4781	0.1260	19,355	48,1
	6.3590			2,900	2.00		.4914		30,000	46,8
22	8.6245	22	3.0	2,788	2.12	394.	.4200	0.1016	60,185	45.0
	12.1628			1,570 (5)	1.917		.4596		84,876	45.5
22	12.1628	22	3.0	1,570 (5)	1.917	253.	.4596	0.2753	84,876	45.5
	32.9500			0.0	1.60		.5954		229,936	41.9
22	12.1628	22	3.0	578.	4.35	285.	.4589	0.0936	193,414	45.8
	10.3936			495 (5)	4.528		.4430		165,281	45.4
22	10.3936	22	3.0	495 (5)	4.528	235.	.4430	0.2537	165,281	45.4
	32.9500			0.0	3.45		.5954		523,975	44.3

*As Manufactured

identical. (3) 4 Equally spaced, sequentially loaded
(4) 6 Equally spaced, sequentially loaded

(5) Effective Speed (about
(6) At Brake Application.
(7) Based upon Tooth Finis
(8) Based upon Tooth Finis

STRESS SUMMARY

	Dp	Press Angle Deg	Spiral Angle Deg	Speed RPM	Shaft Angle Deg	Face Width In	J	I	Hand & Direct	Torque (in-lb)	fb PSI	
5	8.000	25.	20.	11,500	28.50	2.850	.4864	0.0823	LH-CW	44,250	34,704	22
	11.000			7,986		2.850	.6201		RH-CCW	63,780	27,211	
5	11.520	25.	20.	7,986	33.75	2.850	.5592	0.0712	RH-CCW	83,810	39,690	23
	11.520			7,986		2.850	.5592		LH-CW	83,810	39,690	
0	9.25	25.	23.	7,986	59.25	3.00	.4400	0.1095	RH-CCW	83,810	42,800	23
	26.50			2,788		3.00	.6022		LH-CW	240,073	31,200	

3

J	I	Torque (in-lb)	f _b PSI	f _c PSI
.6362	0.1399	44,250	46,500.	149,537
.6625		63,780	44,630	
.4781	0.1260	19,355	48,109	219,744
.4914		30,000	46,801	
.4200	0.1016	60,185	45,006	167,097
.4596		84,876	45,507	
.4596	0.2753	84,876	45,507	93,453
.5954		229,936	41,980	
.4589	0.0936	193,414	45,885	159,089
.4430		165,281	45,486	
.4430	0.2537	165,281	45,486	108,259
.5954		523,975	44,363	

- ⑤ Effective Speed (about post).
 ⑥ At Brake Application.
 ⑦ Based upon Tooth Finish of 16RMS
 ⑧ Based upon Tooth Finish of 23RMS

I	Hand & Direct	Torque (in-lb)	f _b PSI	f _c PSI	Flash Temp. Deg F ⑧
0.0823	LH-CW	44,250	34,704	226,726	322.
	RH-CCW	63,780	27,211		
0.0712	RH-CCW	83,810	39,690	233,300	298.
	LH-CW	83,810	39,690		
0.1095	RH-CCW	83,810	42,800	231,000	529.
	LH-CW	240,073	31,200		

TABLE B-6. TAPERED ROLLER BEARING GEOMETRY

	LOCATION		PAFT NO.	SPEED (RPM)	CONT- ACT ANGLE	NO. OF ROLLERS	RIB LOAD (LB)
COMBINE TRANSMISSION	S. B. Engine	Inboard	301-10676	11500	15°	24	32
	Input Pinion	Outboard	301-10671		12.5°	24	11
	Slant Shaft	Inner	301-10612	7986	10°	21	36
		Outer	301-10616		22.5°	33	15
	Rotor Brake Shaft	Inboard	301-10627	2900	16.6°	22	14
		Outboard	301-10630	(1)	16.6°	25	5
AFT TRANSMISSION	Clutch Shaft	Inboard	301-10644	11500	15°24'	42	7
		Outboard	301-10651		17°5'	34	4
	S. B. Input Pinion	Inner	301-10420	7986	25°	21	90
		Outer	301-10424		20°	25	17
	S.B. Gear/Sun	Lower	301-10443	2788	15°	48	6
		Upper	301-10440		15°	71	1
	Rotor Shaft	Upper	301-10406	155.9	35°	66	21
		Lower	301-10409		45°	56	40

- (1) Speed at beginning of rotor brake application
- (2) Rib loads evaluated at fatigue torque from Table 3
- (3) All fits are tight

ENTRY

SPEED (FPM)	CONT- ACT ANGLE	NO. OF ROLLERS	RIB LOAD (2) (LB)	RIB SPEED FPM	NO. OF RIB LUBE HOLES	BORE (IN.)	FIT (10 ⁻⁴ IN.) (3)	
							O. D.	I. D.
1500	15°	24	328	20,473	40	5.5118	23 - 43	48 - 65
	12.5°	24	111	19,293	32	5.4331	20 - 40	47 - 64
7986	10°	21	368	18,225	28	7.2835	35 - 57	66 - 83
	22.5°	33	151	17,951	44	7.2047	29 - 61	65 - 82
900 (1)	16.6°	22	140	4000	0	3.3858	13 - 28	29 - 44
	16.6°	25	52	4000	0	3.3071	13 - 28	28 - 43
1500	15°24'	42	7.4	15,656	36	4.5200	25 - 31	60 - 120
	17°5'	34	4.5	11,116	28	2.7500	15 - 30	13 - 27
7986	25°	21	904	16,966	36	5.9055	31 - 53	52 - 69
	20°	25	172	15,091	28	5.8268	23 - 45	49 - 66
2788	15°	48	68	9,616	32	12.1260	42 - 74	111 - 122
	15°	71	13	99,373	44	11.9685	83 - 70	111 - 130
155.9	35°	66	211	970	0	21.339	119 - 137	119 - 159
	45°	56	408	1020	0	21.496	112 - 154	119 - 159

tion

m Table 3

TABLE B-6. Continued

LOCATION	PART NO.	SPEED (RPM)	EFFECTIVE RADIAL LOAD (1)	BASIC RADIAL RATING	LIFE (HOURS) (2)
S.B. Engine Input Pinion	In 'bd	11500	10548 5539	22700 15800	5040 13443
	Out 'bd				
Slant Shaft	Inner	7986	20832 10562	36300 19600	3585 4425
	Outer				
Rotor Brake Shaft	In 'bd	2900 (3)	11030 8768	9450 7100	>10000 >10000
	Out 'bd				
Clutch Shaft	In 'bd	11500		3310	>10000 >10000
	Out 'bd				
S.B. Input Pinion	Inner	7986	18660 9666	32300 19600	3507 5946
	Outer				
S.B. Gear/Sun	Lower	2788	14207 7572	20900 13300	4116 4038
	Upper				
Rotor Shaft	Upper	155.9	54600 64700	31400 36400	4560 4250
	Lower				

- (1) Effective radial load includes correction for CF.
- (2) Material factor of 3.0 included in life.
- (3) Speed at beginning of rotor brake application.

TABLE B-5. Continued

LOCATION & TYPE		PART NO.	SPEED (RPM)	RADIAL LOAD (LBS.)	THRUST LOAD (LBS.)	CAPACITY DYNAMIC (LBS.)	LIFE (HOURS)
COMBINER TRANSMISSION	Center Engine Shaft	Ball In'bd Out'bd roller roller	301-10643 301-10656 301-10640	11500 11500 11500	-- 3520 3700	11200 30000 36400	14500 4600 5300
	Collector Shaft	Ball Out'bd roller In'bd roller	301-10667 301-10666 301-10638	7986 7986 7986	-- 9480 8450	10300 83866 61050	3620 7800 3280
	Clutch Support	Duplex Ball	301-10635	11500	100	13400	3350
	1st Stage Planets	Spherical Roller	301-10414	1570	26200	--	2900 ^①
PT1 TRANSMISSION	2nd Stage Planets	Cylindrical Roller	301-10467	495	59600	--	3400 ^①
	2nd Stage Planets (Alternate)	Spherical Roller	301-10460	495	59600	--	2000 ^①

① 3.06 Factor, Life Per Planet I Program

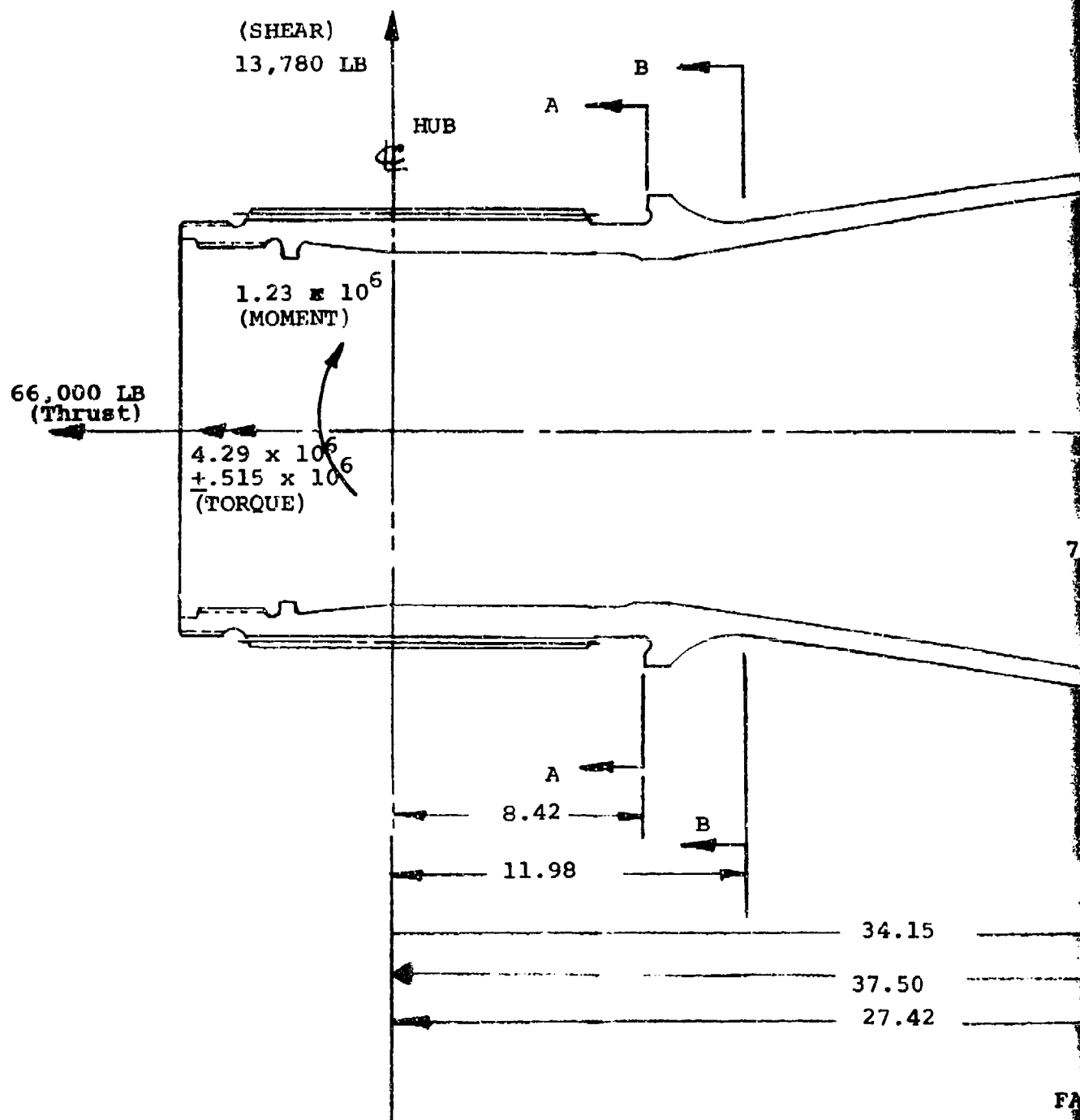
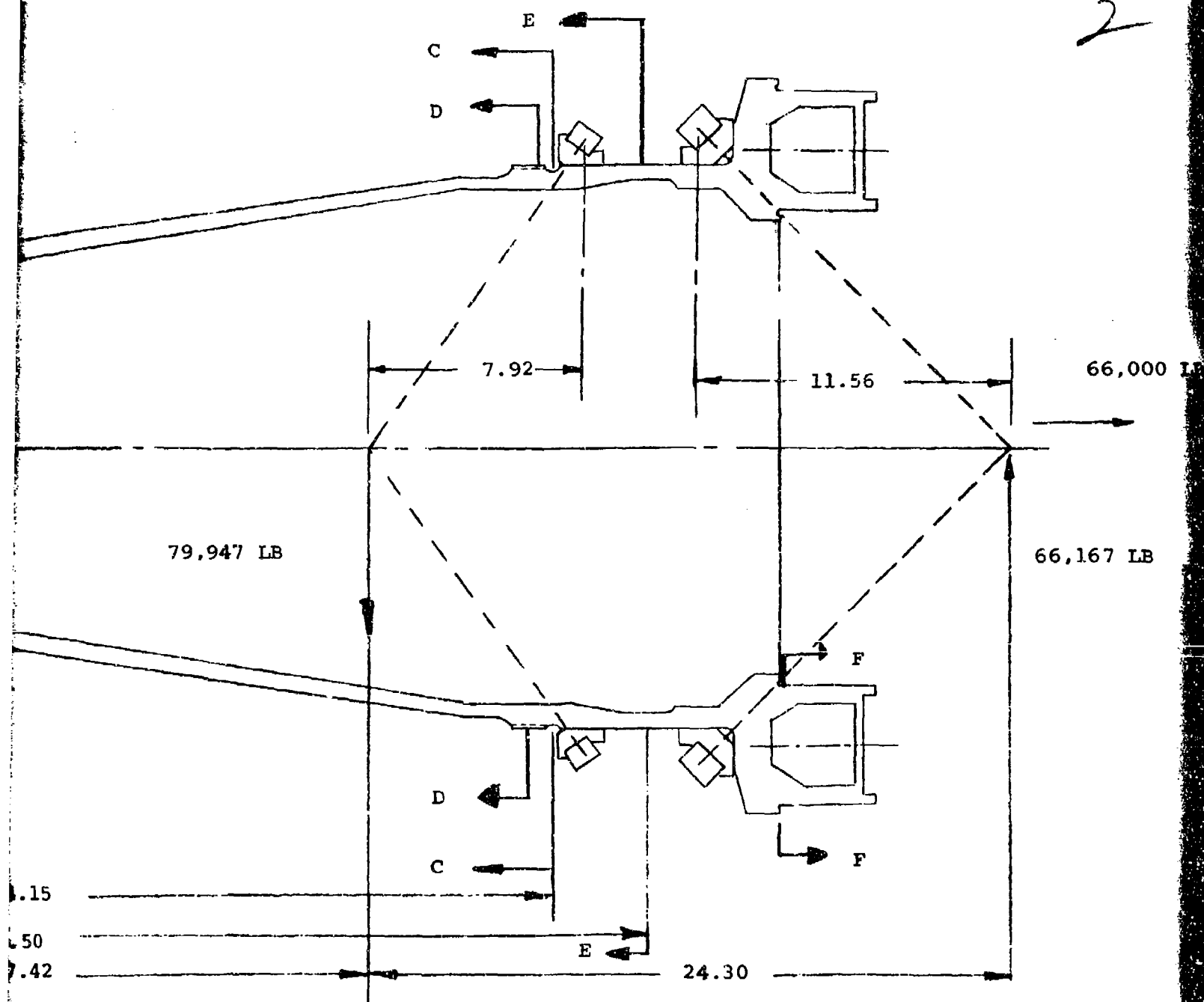


Figure B-9. Rotor Shaft/Aft Transmission.

2



FATIGUE CONDITION SHOWN

TABLE B-7. ROTOR SHAFT 301-10401

FATIGUE ANALYSIS (1) (2)

SECTION	O.D. IN.	I.D. IN	TENSION LBS	MOMENT IN-LBS	SHEAR LBS	TORQUE IN-LBS
A-A	13.93	12.0	66000	$\pm 1.346 \times 10^6$	± 13780	4.29×10^6 $\pm .515 \times 10^6$
C-C	20.89	19.50	212500	$\pm 1.70 \times 10^6$	↓	↓
D-D ⁽³⁾	21.09	19.50	212500	$\pm 1.69 \times 10^6$		

ULTIMATE ANALYSIS

SECTION	O.D. IN.	I.D. IN.	TENSION LBS	MOMENT LBS	SHEAR LBS	TORQUE LBS
A-A	13.93	12.0	297000	4.97×10^6	50800	9.66×10^6
B-B	14.12	12.72	297000	5.15×10^6	50800	↓
E-E	21.35	20.32	625500	3.47×10^6	244000	

(1) Endurance Limit = ± 20000 psi

(2) Alternating Stresses Include Stress Concentration

(3) Tab Washer Slot

TORQUE IN-LBS	K_{tb}	K_{ts}	f_t PSI	f_b PSI	f_s PSI	f_{st} PSI	MS
4.29×10^6 $\pm .515 \times 10^6$ ↓	1.486	1.375	1680	± 16780	± 960	18000 ± 2970	+ .06
	2.16	1.26	4823	± 17050	± 750	9960 ± 1510	+ .03
	1.0	5.0	4190	± 6820	± 2700	8650 ± 5200	.00

TORQUE LBS	f_t PSI	f_b PSI	f_s PSI	f_{st} PSI	F_{bu} PSI	F_{stu} PSI	MS
9.66×10^6 ↓	7560	41700	2575	40500	165000	80000	+ .61
	10070	54600	3450	51200	156000	78000	+ .22
	18570	20250	14450	28200	137000	76000	+ .61

PRECEDING PAGE BLANK FILE

TABLE B-8. GEAR SHAFT ANALYSIS-FATIGUE

PART NUMBER	LOCATION	SEC- TION	O.D. IN.	I.D. IN.	TENSION LBS	MOMENT IN-LBS
301-10610	SLANT GEAR	A-A	7.231	6.50	11960	+49860
		B-B	7.291	6.50	11960	+57870
		C-C	4.934	4.19	-	-
301-10654	HELICAL INPUT PINION	A-A	5.379	4.72	-2115	+3959
		B-B	6.995	6.30	-2115	+19168
		C-C	3.540	3.02	-	+4627
301-10677	SPIRAL BEVEL INPUT PINION	A-A	5.457	4.75	3450	+29700
		B-B	5.517	4.75	3450	+29840
		C-C	5.230	4.92	17986	+3426
301-10629	CLUTCH SHAFT	A-A	4.30	3.89	-	-
		B-B	4.464	3.89	-	-
		C-C	4.524	3.89	-	-
301-10650	CLUTCH HOUSING	A-A	5.69	5.19	-	-
		B-B	5.54	5.02	-	-
301-10625	ROTOR BRAKE GEAR	A-A	3.486	2.35	3944	+12400
		B-B	2.44	1.66	-	+10320
301-10601	COLLECTOR GEAR	AA	5.576	4.50	2491	+18200
		BB	4.740	4.08	-	+13200
		CC	7.200	6.74	2110	+62900
301-10419	SPIRAL BEVEL GEAR, AFT TRANSMISSION	AA	12.078	11.500	8340	+11700
		BB	12.138	11.500	8340	+15200
301-10428	SPIRAL BEVEL PINION AFT TRANSMISSION	AA	5.851	5.00	9428	+49800
		BB	5.911	5.00	9428	+55000
		CC	5.630	5.00	-	-
		DD	4.934	4.30	-	-
		EE	4.315	3.49	-	-

MOMENT IN-LBS	SHEAR LBS	TORQUE IN-LBS	KT _B	KT _S	f _t PSI	f _b PSI	f _s PSI	f _{st} PSI	M.S.
+49860	+18120	83800	2.25	1.5	1520	+8720	+6900	3260+586	.86
+57870	+18120	83800	2.95	3.85	1400	+12200	+16200	2990+1380	.25
-	-	83800	-	1.80	-	-	-	7390+1597	9.
+3959	+6945	44250	1.55	1.42	-	+955	+3640	3440+586	2.9
+19168	+6945	44250	-	-	-	+1670	+1906	1927+231	6.3
+4627	+6610	-	1.47	1.12	-	+3318	+5484	-	2.0
29700	+12915	44250	2.8	2.0	610	+12250	+9110	3260+783	.39
29840	+12915	44250	2.95	3.90	560	+11900	+16450	2990+1400	.25
+3426	-	-	2.41	-	7311	+2716	-	-	9.5
-	-	44250	-	3.96	-	-	-	8600+4090	3.0
-	-	44250	-	2.0	-	-	-	6000+1440	10.6
-	-	44250	-	3.75	-	-	-	5400+2419	5.9
-	-	44250	-	1.90	-	-	-	3980+910	17.
-	-	44250	-	1.60	-	-	-	4070+780	20.7
12400	+10690	30000	2.63	2.07	760	+9880	+8500	4550+1130	+ .49
10320	+4115	30000	2.40	1.88	-	+22200	+5980	13400+3020	+ .05
18200	+20100	51000	2.70	1.85	292	+5000	+8620	2601+577	+ .85
13200	+15100	-	2.32	1.63	-	+6517	+10730	-	+ .60
62900	+10500	63700	1.45	1.13	420	+10700	+4720	3750+510	+ 1.77
11700	+23600	240100	3.00	2.20	780	+1140	+9650	3900+1030	+ .58
15200	+23600	240100	3.00	3.97	704	+1340	+15740	3500+1700	+ .64
49800	+21100	83800	3.00	2.45	1300	+16280	+14198	4570+1340	+ .06
55000	+21100	83800	3.05	3.95	1210	+16870	+21279	4240+2010	+ .07
-	-	83800	-	1.55	-	-	-	6330+1180	12.7
-	-	83800	-	1.80	-	-	-	8400+1800	7.8
-	-	83800	-	1.84	-	-	-	9250+2040	6.7

TABLE B-8. Continued

PART NUMBER	NAME	SEC- TION	O.D. IN.	I.D. IN.	THRUST LB	MOMENT IN-LB
301-10610	GEAR, S.B. SLANT SHAFT	AA BB	7.231 7.291	6.500 6.500	26900 26900	112200 130000
301-10654	GEAR, HELICAL PINION	AA BB	5.379 6.995	4.720 6.300	-4759 -4759	8908 43128
301-10677	GEAR, S.B. PINION ENG. INPUT	AA BB	5.457 5.517	4.750 4.750	7769 7769	66825 67131
301-10428	GEAR, S.B. PINION, AFT TRANSMISSION	AA BB	5.851 5.911	5.000 5.000	21213 21213	112073 123750
301-10419	GEAR, S.B. AFT TRANSMISSION	AA BB	12.078 12.138	11.500 11.500	18767 18767	26384 34272
301-10629	SHAFT, CLUTCH INNER, COMB. TRANSMISSION	AA	4.464	3.890	-	-
301-10650	HOUSING, CLUTCH-ENG. SHAFT, COMB. TRANSMISSION	AA	5.540	5.020	-	-
301-10625	GEAR, SPUR ROTOR BRAKE COMB. TRANS- MISSION	AA BB	3.486 2.440	2.350 1.660	11832 -	37200 30960
301-10601	GEAR, S.B. ENGINE DRIVE, COMB. TRANSMISSION	AA BB CC	5.576 4.740 7.200	4.499 4.080 6.740	5605 - 4759	40865 29768 141503

MOMENT IN-LB	SHEAR LB	TORQUE IN-LB	f_t PSI	f_b PSI	f_s PSI	f_{st} PSI	F_{STU} PSI	F_{BU} PSI	M.S.
112200 130000	41000 41000	188600 188600	3420 3140	8720 9290	10365 9530	7330 6740	100,000 100,000	190,000 190,000	+4.31 +4.69
8908 43128	15626 15626	99574 99574	- -	1390 3760	5770 4290	7740 4340	100,000 100,000	195,000 190,000	+6.42 +10.35
66825 67131	29054 29054	99574 99574	1370 1270	9840 9070	10200 9430	7330 6730	100,000 102,000	197,000 200,000	+4.44 +4.95
112073 123750	47504 47504	188577 188577	2925 2720	12210 12510	13040 12120	10270 9530	102,000 103,000	200,000 200,000	+3.11 +3.41
26384 34272	53069 53069	540167 540167	1750 1585	857 1005	9895 8920	8770 7920	97,000 97,000	168,000 170,000	+4.29 +4.86
-	-	99574	-	-	-	19300	100,000	-	+4.18
-	-	99574	-	-	-	8955	99,000	-	+10.06
37200 30960	32070 12345	90000 90000	2275 -	11270 27640	12025 9650	13640 40180	110,000 105,000	220,000 210,000	+2.97 +1.02
40865 29768 141503	45128 34020 23699	114710 - 143386	658 - 946	4170 6320 16650	10490 14810 9380	5850 - 8430	105,000 - 97,000	207,000 200,000 180,000	+4.81 +5.67 +3.88

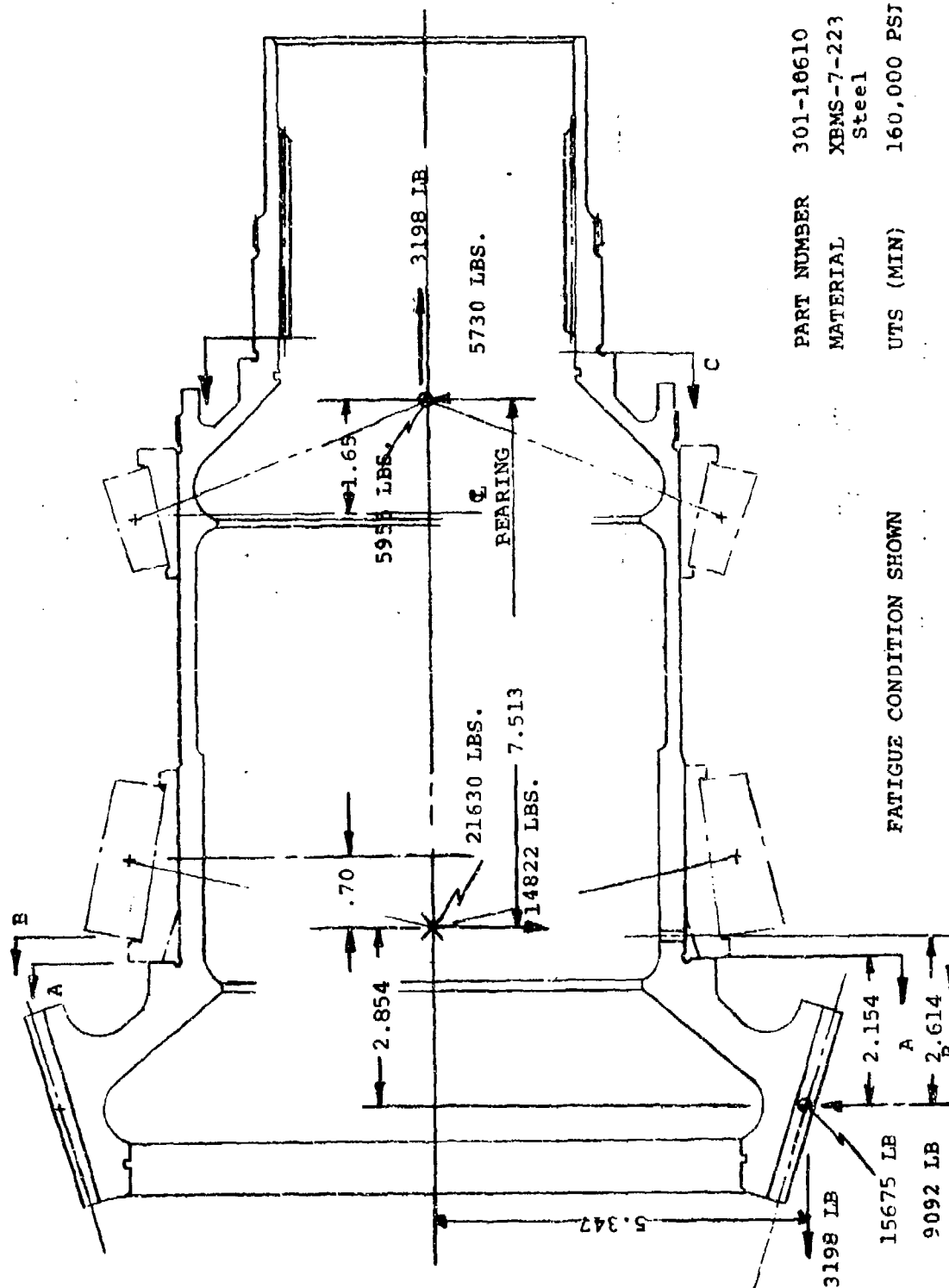
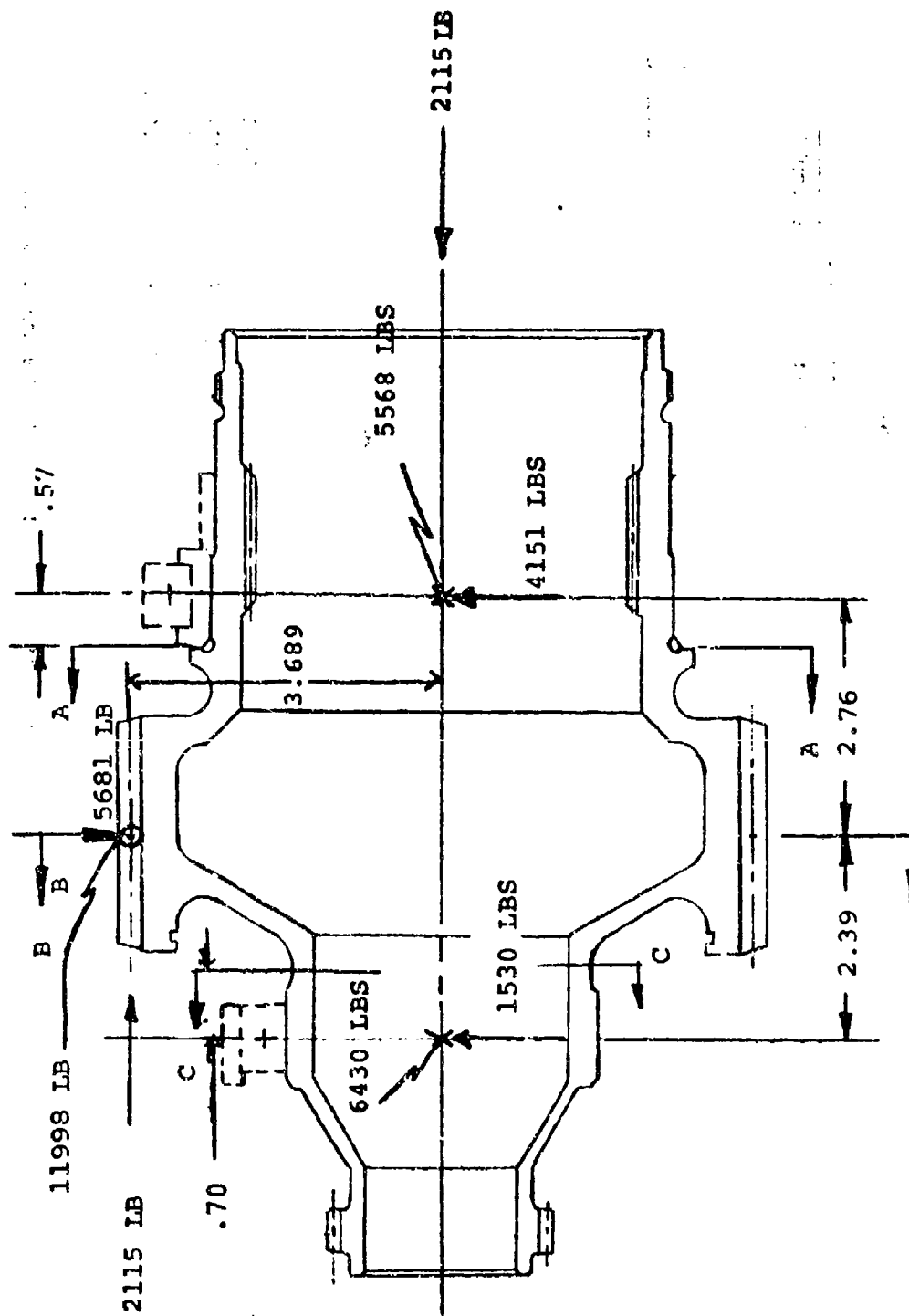
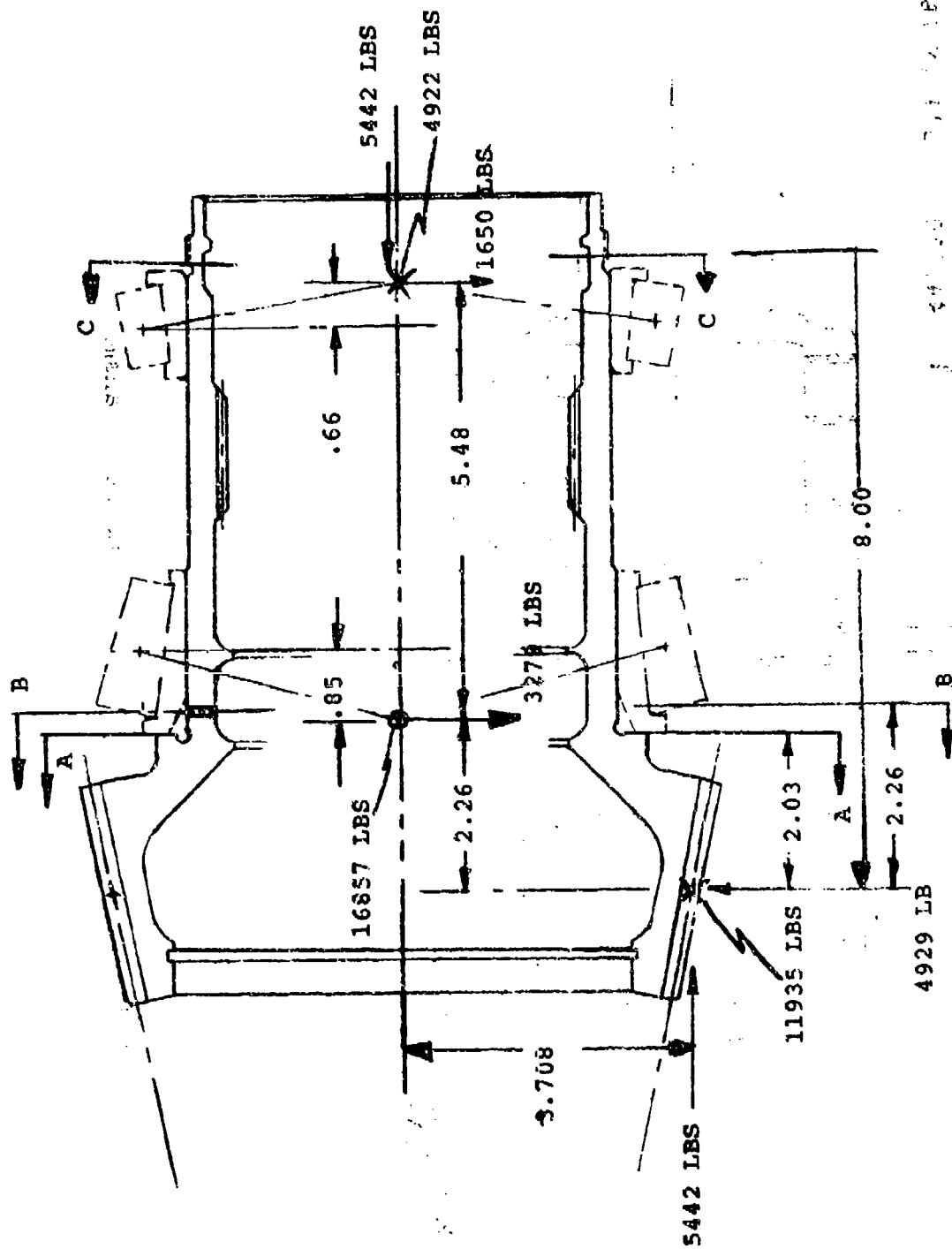


Figure B-10. Gear Spiral Bevel Slant Shaft, Combiner Transmission.



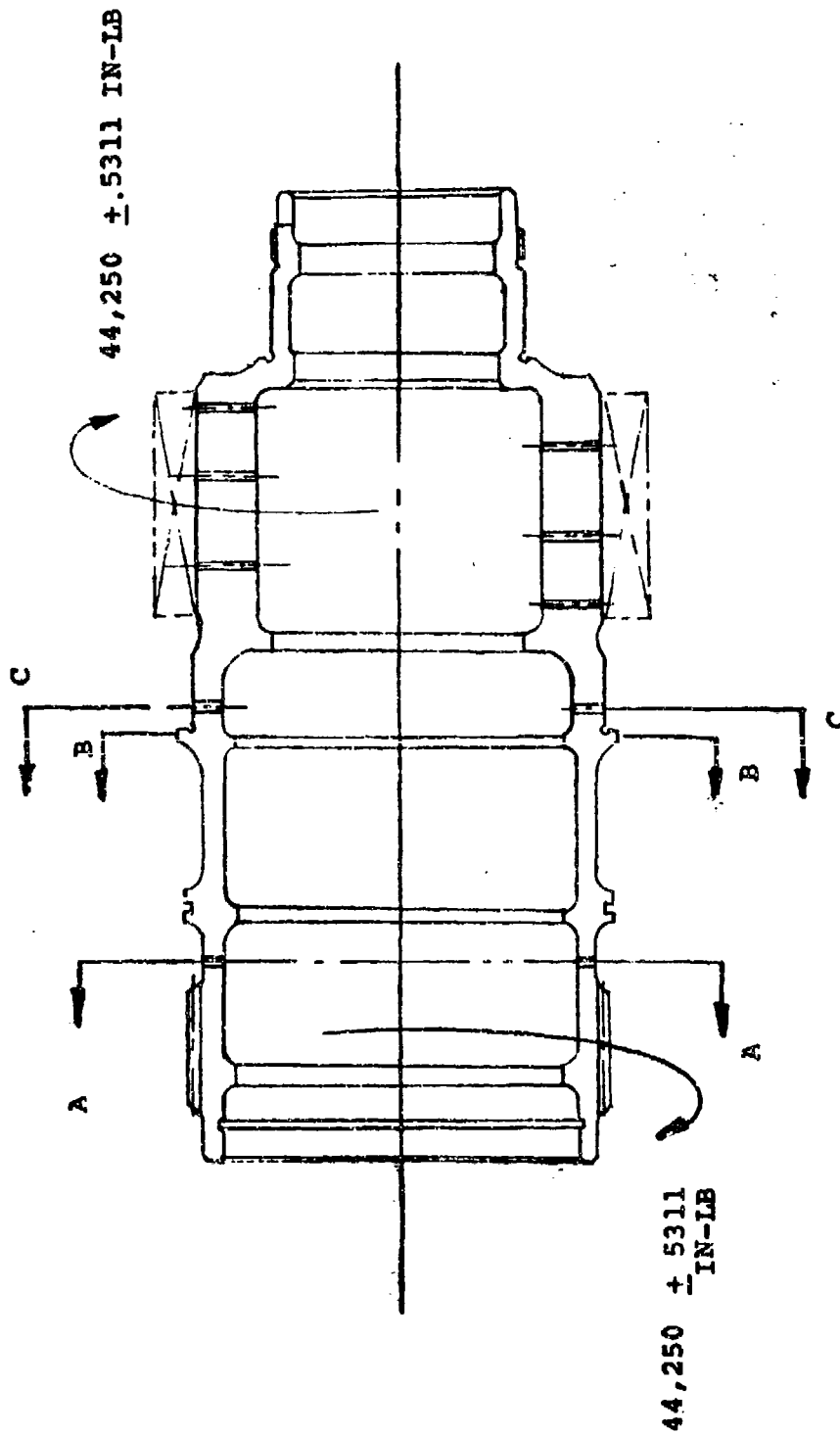
FATIGUE (OEI) CONDITION SHOWN

Figure B-11. Gear Helical Pinion - Central Engine
Shaft Combiner Transmission.



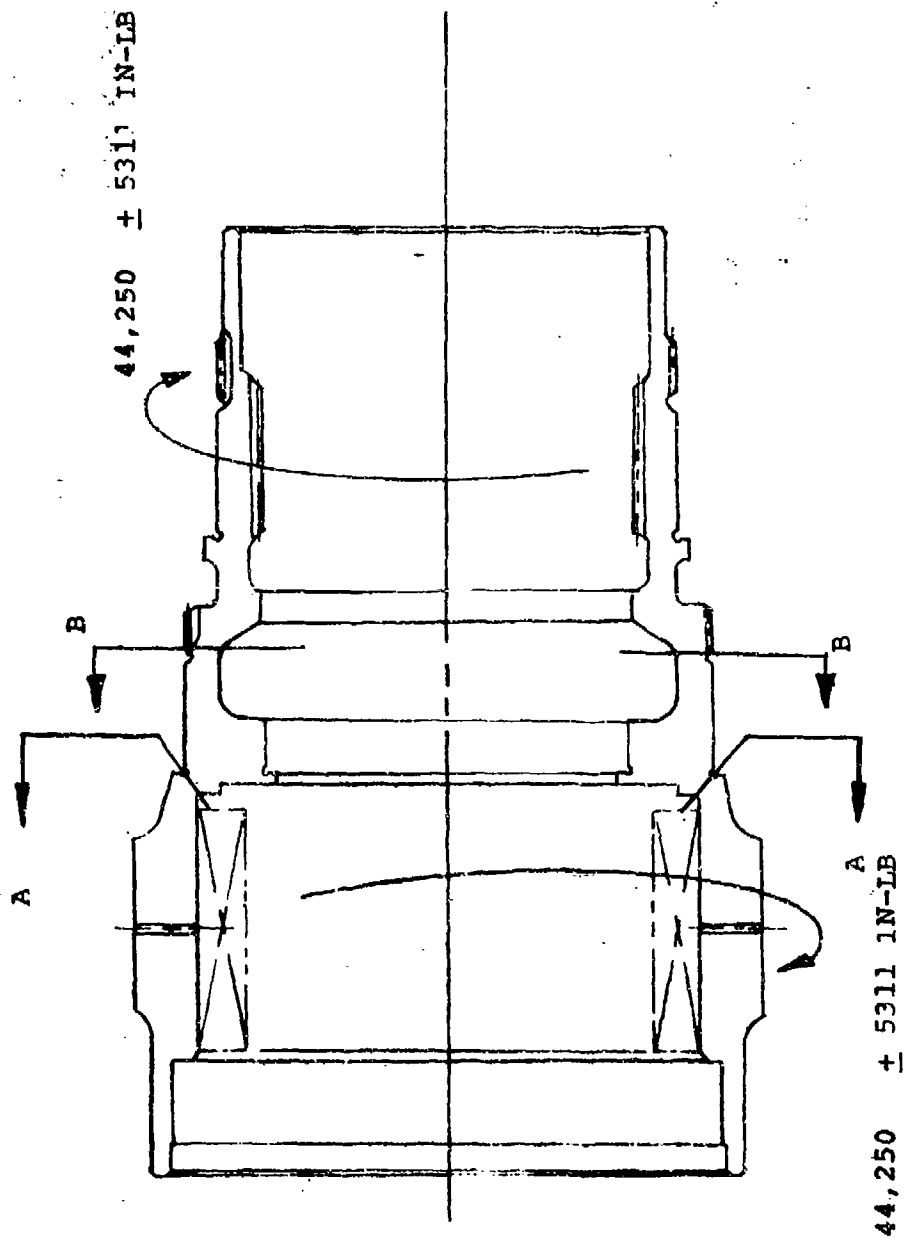
FATIGUE (OEI) CONDITION SHOWN
FOR R/H ENGINE

Figure B-12. Gear, Spiral Bevel Pinion - Engine Input
Shaft Combiner Transmission.



FATIGUE (OEI) CONDITION SHOWN

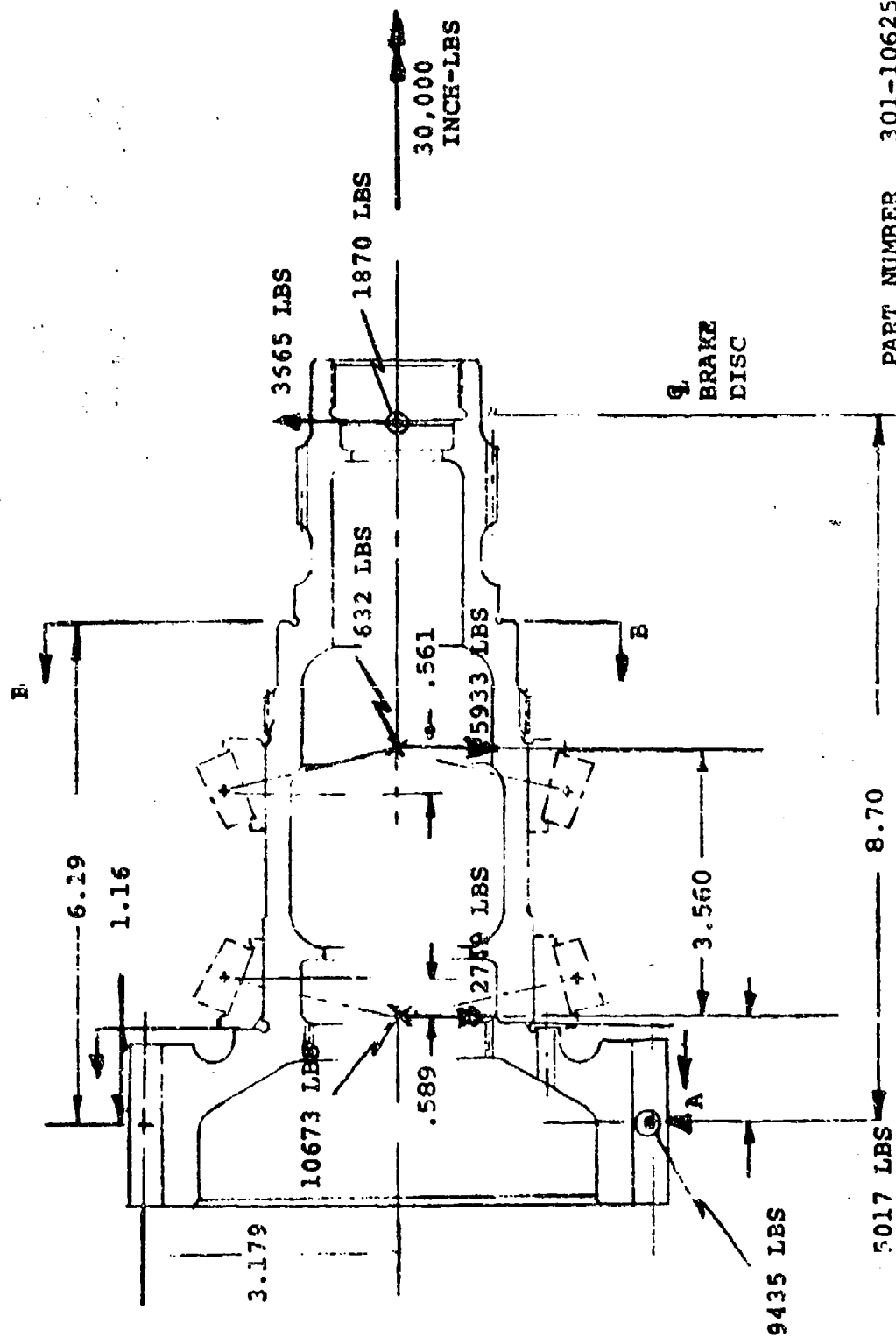
Figure B-13. Shaft, Clutch - Inner, Combiner Transmission.



FATIGUE (OEI) CONDITION SHOWN

PART NUMBER	301-10650
MATERIAL	XBMS-7-223 Steel
UTS (MIN)	160,000 PSI

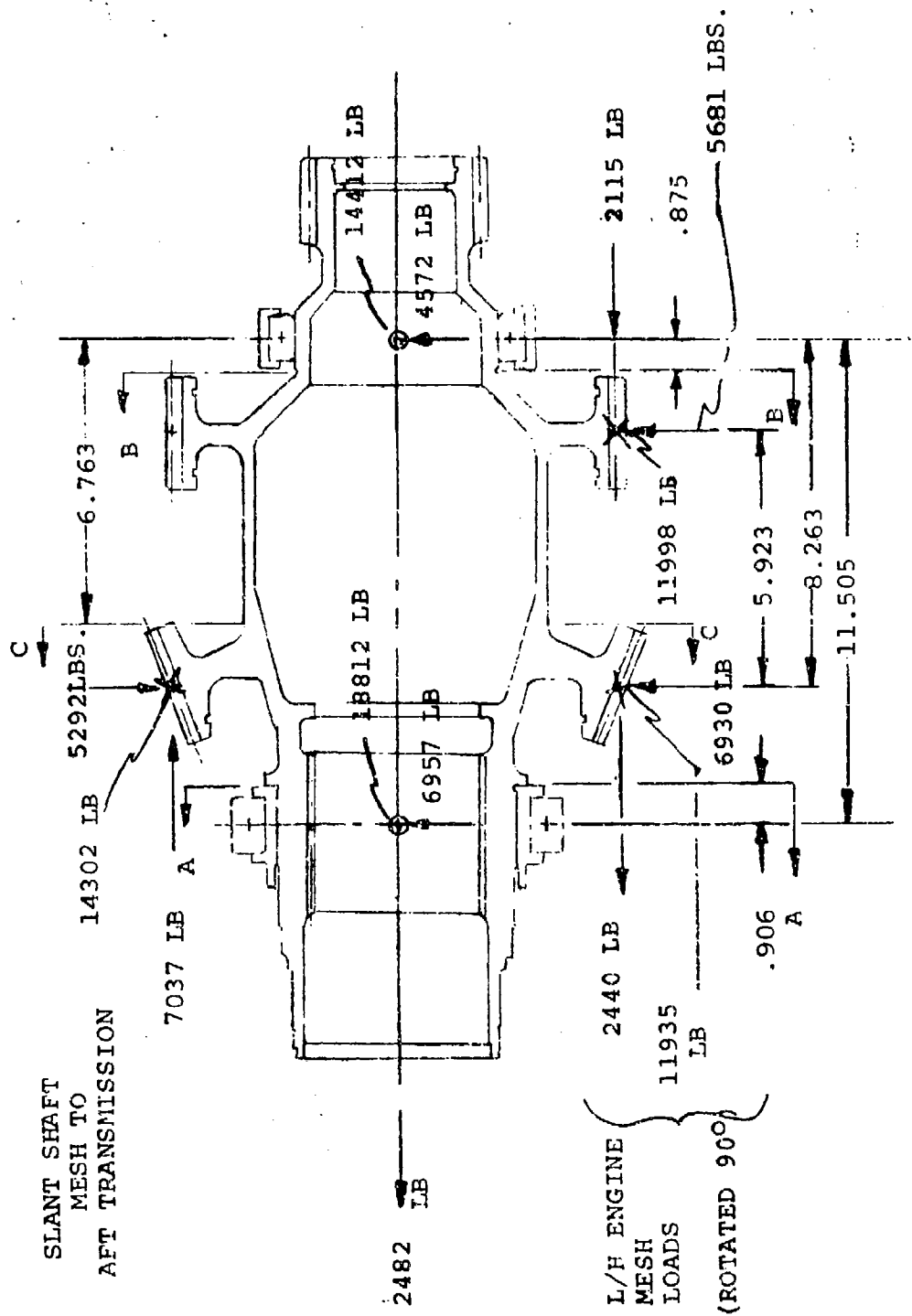
Figure B-14. Housing, Clutch-Engine Shaft, Combiner Transmission.



PART NUMBER	MATERIAL	UTS (MIN)
301-10625	XBMS-7-223	160,000 PSI
	Steel	

FATIGUE CONDITION SHOWN

Figure B-15. Gear, Spur - Rotor Brake, Combiner Transmission.



219

CRITICAL CONDITION

- 1) O.E.I. (R/H ENGINE OUT)
- 2) 60% POWER TO AFT TRANSMISSION

PART NUMBER 301-10601
MATERIAL XBMS-7-223
Steel
UTS (MIN.) 160,000 PSI

Figure B-16. Gear, Spiral Bevel Engine Drive, Combiner Transmission.

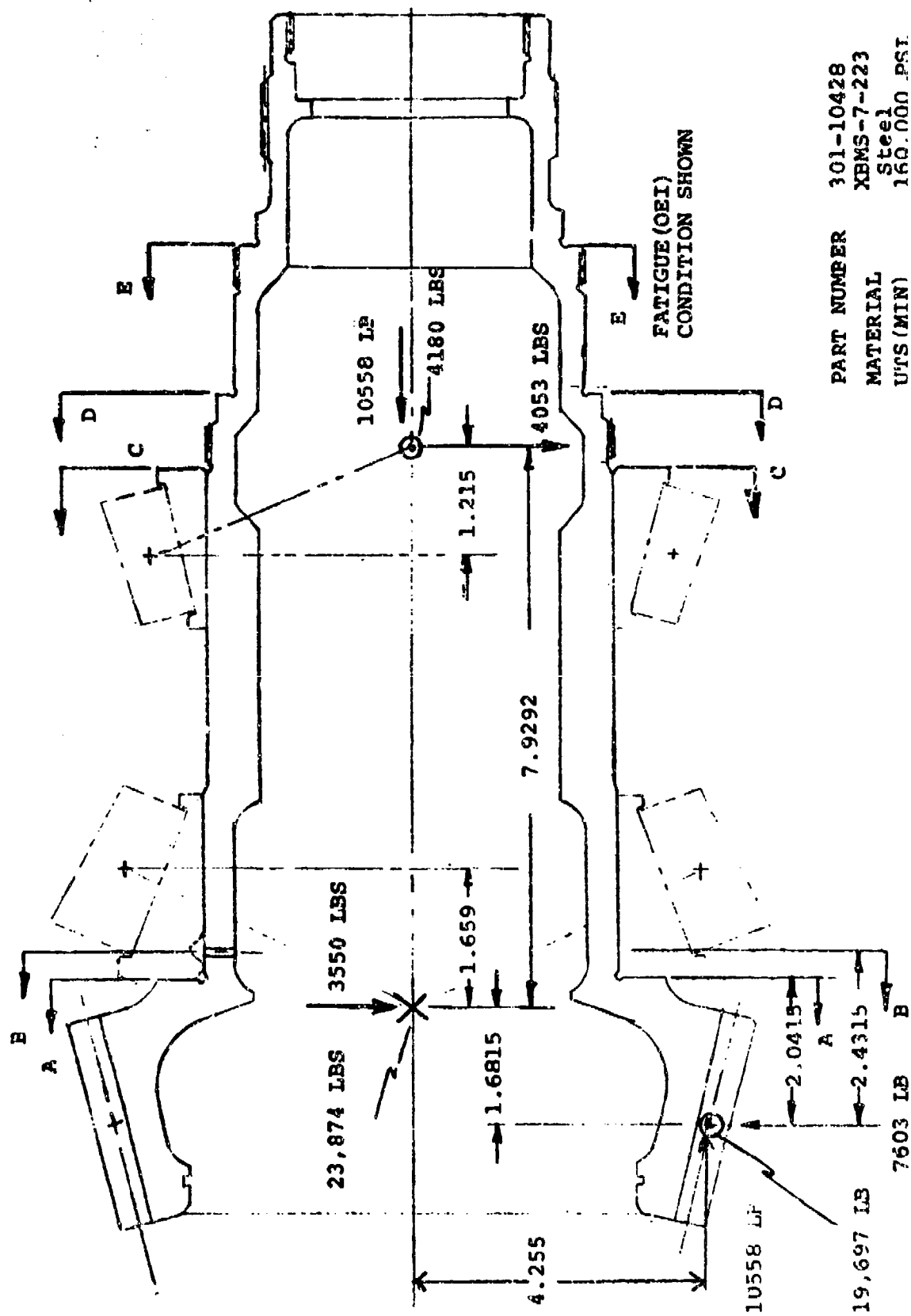


Figure B-17. Gear, Spiral Bevel Pinion, Aft Transmission.

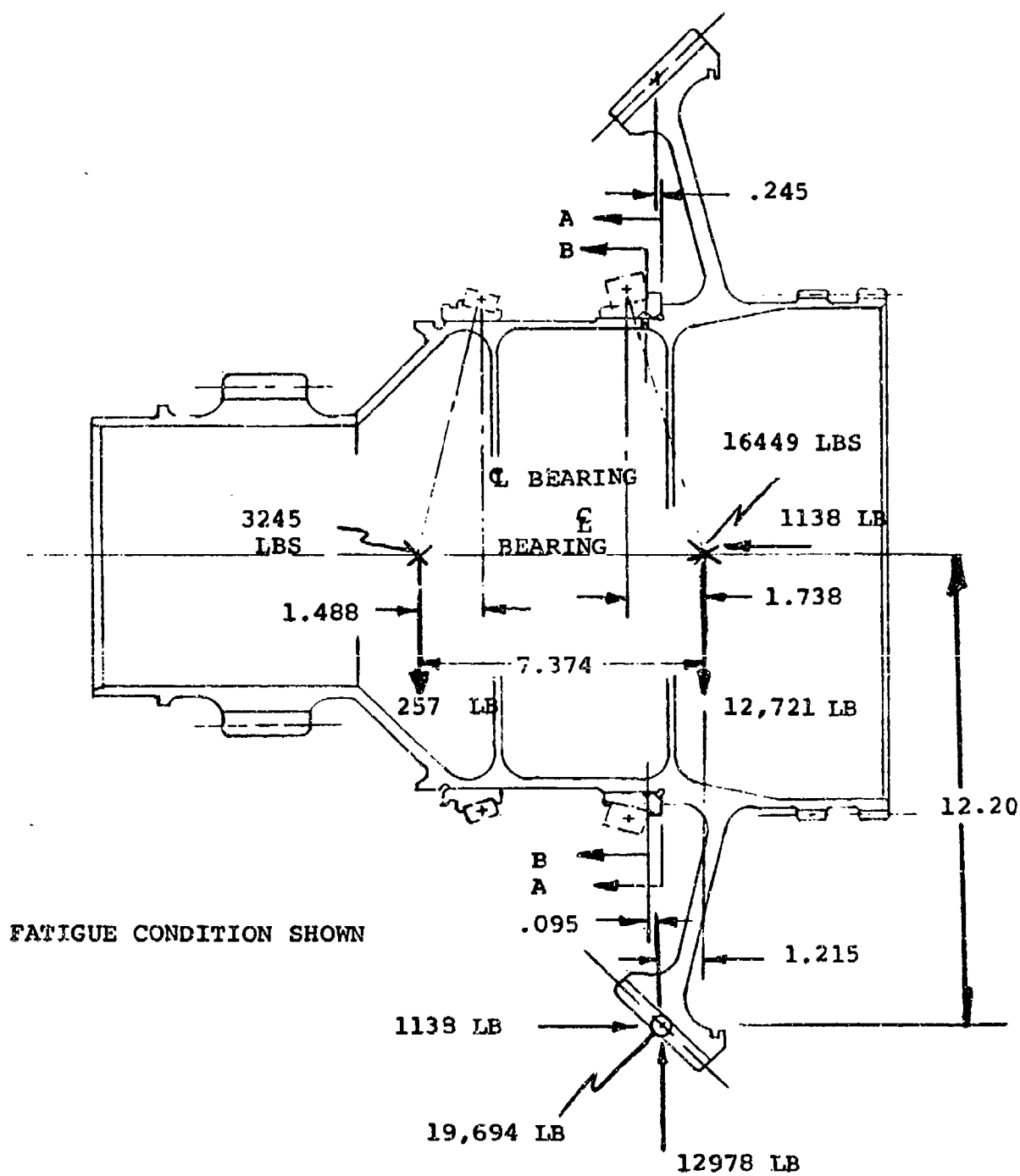


Figure B-18. Gear, Spiral Level, Aft Transmission.

TABLE B-9. FIRST-STAGE PLANET CARRIER 301-10413								
FATIGUE ANALYSIS								
SECTION	SECTION SHAPE	O.D. IN.	I.D. IN.	WIDTH IN.	THICKNESS IN.	K_{t_b}	$K_{t_{se}}$	
A-A	Circular	5.215	4.20	--	--	1.807	--	
B-B	Rectangular	--	--	9.35	.81	--	--	
C-C	Circular	9.84	9.11	--	--	--	3.0	
ULTIMATE ANALYSIS								
SECTION	SECTION SHAPE	O.D. IN.	I.D. IN.	WIDTH IN.	THICKNESS IN.			
A-A	Circular	5.215	4.20	--	--			
B-B	Rectangular	--	--	9.35	.81			
C-C	Circular	9.84	9.11	--	--			

t_{se}		MOMENT IN-LBS	TORQUE IN-LBS	f_b PSI	f_{st} PSI	M.S.
--		31200	---	7000	--	.10
--		121000 \pm 14500	52400 \pm 6280	12740 \pm 1910	33950 \pm 4070	1.20
.0		--	1.159×10^6	--	21600 \pm 9720	.14

		MOMENT IN-LBS	TORQUE IN-LBS	f_b PSI	f_{st} PSI	M.S.
		70200	---	8770	--	Large
		272000	118000	28700	76400	.21
		--	2.61×10^6	--	48600	.95

Preceding Page Blown - Fit

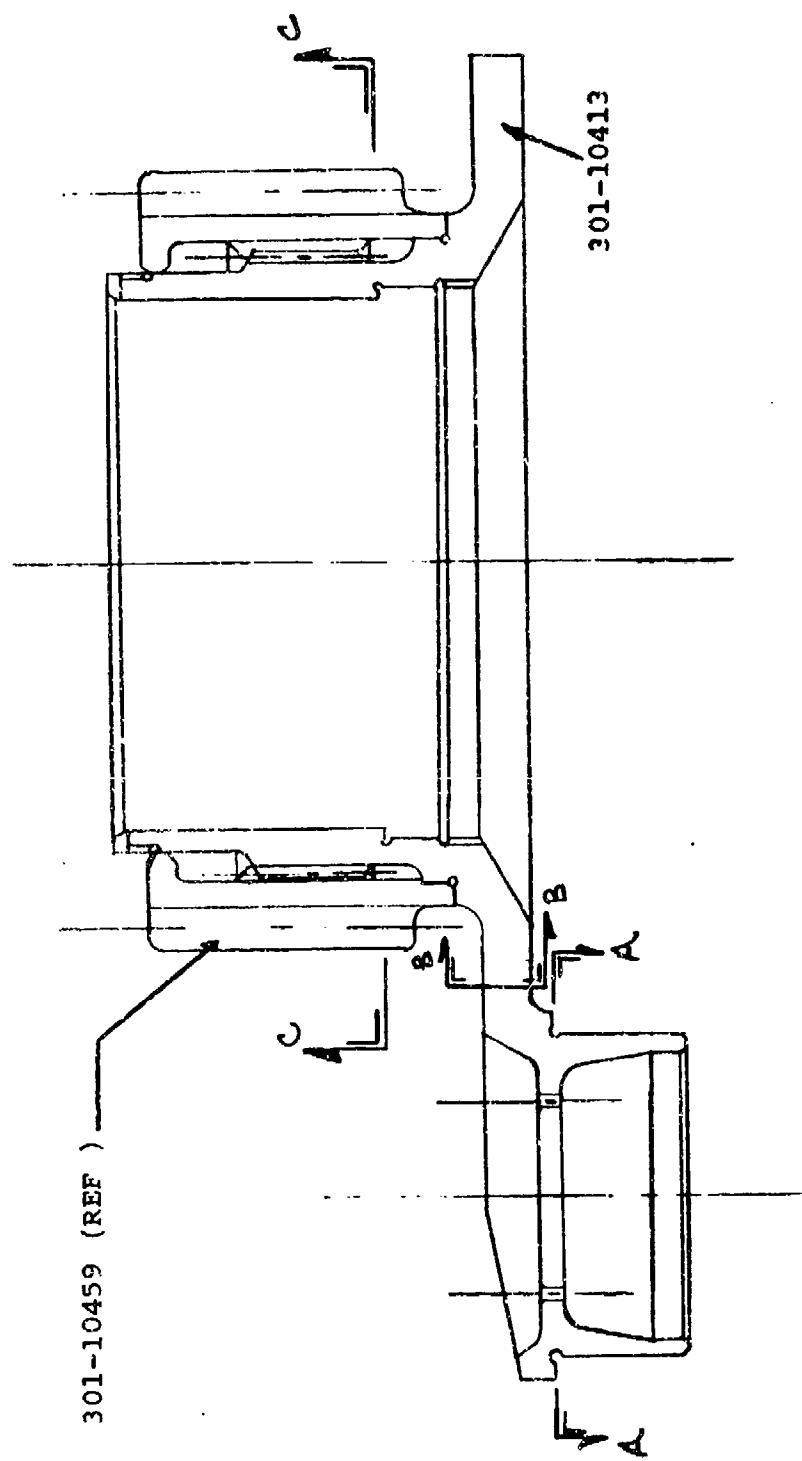


Figure B-19. Planet Carrier - 1st Stage Aft Transmission.

TABLE B-10. DRIVE SHAFT TUBES

FATIGUE ANALYSIS

LOCATION	P/N	SECTION	TORQUE IN-LB	O.D. IN.	WALL THICKNE
SYNC. SHAFT	301-11000-5 and 301-11000-25	H-H	83,800 +10060	7.25	.12
ENGINE SHAFT	301-11001-2 and 301-11001-25	H-H	44,250 + 5300	6.00	.10

ULTIMATE ANALYSIS

LOCATION	P/N	SECTION	TORQUE IN-LB	J/C IN. ³	fst psi
SYNC. SHAFT	301-11000-5 and 301-11000-25	G-G	188,600	7.81 ^①	24,200
		H-H		9.43 ^②	20,000
	RIVETS	-		-	1,740
ENGINE SHAFT	301-11001-2 and 301-11001-25	G-G	99,600	4.62 ^①	21,600
		H-H		5.53 ^②	18,000
	RIVETS	-		-	1,385

- ① NET TUBE SECTION PROPERTY
- ② GROSS TUBE SECTION PROPERTY
- ③ RIVET LOAD - LBS.
- ④ BASED ON THE LONGER (-5) TUBE
- ⑤ BASED ON THE LONGER (-2) TUBE

2

O.D. IN.	WALL THICKNESS (IN.)	J/C IN. ³	fst psi	fst psi	M.S.
7.25	.120	7.81 ^①	10720 \pm 1290	\pm 2000	.55
6.00	.102	4.62 ^①	9600 \pm 1150	\pm 2000	.74

J/C IN. ³	fst psi	fst psi	M.S.
7.81 ^①	24,200	39,000	.61
9.43 ^②	20,000	21,000	.05 ^④
-	1,740 ^③	2,170 ^③	.25
4.62 ^①	21,600	39,000	.80
5.53 ^②	18,000	25,000	.39 ^⑤
-	1,385 ^③	2,170 ^③	.57

TABLE B-11. DRIVE SHAFT ADAPTERS
FATIGUE ANALYSIS

LOCATION	ADAPTER P/N	SECTION	MATERIAL (1)	TORQUE (IN. - LB.)	P _T (4) (LB)	P _R (2) (4) (LB)	P _X (3) (4) (LB)
SYNC SHAFTS	301-10463	AA	Steel	83800 ± 10060	6540 ± 784	6044	+35.0
	301-11003	AA	Steel	83800 ± 10060	6540 ± 784	6044	+35.0
	301-11003	CC		83800 ± 10060	-	-	-
	301-11004	AA	Steel	83800 ± 10060	6540 ± 784	6044	+35.0
	301-11004	CC		83800 ± 10060	-	-	-
	301-11007	FF	Aluminum	83800 ± 10060	6540 ± 784	4964	+35.0
	301-11008	DD	Steel	83800 ± 10060	-	-	-
	301-11008	EE		83800 ± 10060	-	-	-
	301-11009	AA	Steel	83800 ± 10060	6540 ± 784	6044	+35.0
ENGINE SHAFTS	301-11005	AA	Steel	44250 ± 5300	5250 ± 630	4870	+35.0
	301-11023	AA	Aluminum	44250 ± 5300	5250 ± 630	4510	+35.0
	301-11002	AA	Steel	44250 ± 5300	5250 ± 630	7719	+35.0
	301-11021	DD	Steel	44250 ± 5300	-	-	-
	301-11022	EE AA	Aluminum	44250 ± 5300	5250 ± 630	6670	+35.0

(1) Steel - 4340 150 KSI DTS
Aluminum - 7075-T73 66 KSI UTS

(2) Includes Thomas Coupling Pack, Bolt & Nut C.F.

(3) Due to Thomas Coupling Misalignment

(4) Refer to sketch for load locations

2

P _T (LB)	(4)	P _R ⁽²⁾ (LB)	P _X ⁽³⁾ (LB)	e ⁽⁴⁾ (IN)	I.D. (IN)	O.D. (IN)	THICK- NESS (IN)	WIDTH (IN)	K St	f _t	f _{st}	f _b
40 ± 784	6044	+35.0	.681	-	-	.38	2.25	-	7500	29000 ± 3490	43950	+
40 ± 784	6044	+35.0	.681	-	-	.38	2.12	-	7500	29000 ± 3490	43950	+
-	-	-	-	3.40	3.84	-	-	1.42	-	19500 ± 3330		
40 ± 784	6044	+35.0	.681	-	-	.38	2.12	-	7500	29000 ± 3490	43950	+
-	-	-	-	3.80	4.22	-	-	1.65	-	16600 ± 3280		
40 ± 784	4964	+35.0	.80	-	-	.66	3.60	-	2086	8781 ± 915	9255	+
-	-	-	-	2.15	2.66	-	-	1.25	-	39500 ± 5030		
-	-	-	-	2.50	2.96	-	-	1.42	-	33800 ± 5760		
40 ± 784	6044	+35.0	.681	-	-	.38	2.12	-	7500	29000 ± 3490	43950	+
50 ± 630	4870	+35.0	.620	-	-	.39	2.06	-	6060	38700 ± 5800	18990	+
50 ± 630	4510	+35.0	.751	-	-	.53	2.60	-	3270	10770 ± 1290	15840	+
50 ± 630	7719	+35.0	.712	-	-	.56	2.60	-	5290	7000 ± 899	20810	+
-	-	-	-	.93	1.84	-	-	1.29	-	38600 ± 5960		
50 ± 630	6670	+35.0	.88	1.53	2.17	.38	2.54	1.42	6910	29500 ± 5017	35200	+
										18100 ± 2170		

23

WIMM (IN)	K St	f_t	f_{st}	f_b	M.S.
2.25	=	7500	29000 \pm 3490	43950 \pm 4350	+1.32
2.12	=	7500	29000 \pm 3490	43950 \pm 4350	+1.32
-	1.42	=	19500 \pm 3330	=	+2.40
2.12	=	7500	29000 \pm 3490	43950 \pm 4350	+1.32
-	1.65	=	16600 \pm 3280	=	+2.58
2.60	=	2080	8781 \pm 915	9255 \pm 547	+1.79
-	1.25	=	39500 \pm 5930	=	+ :35
-	1.42	=	33800 \pm 5760	=	+ :56
2.12	=	7500	29000 \pm 3490	43950 \pm 4350	+1.32
2.06	=	6060	38700 \pm 5800	18990 \pm 1813	+ :48
2.60	=	5270	10770 \pm 1290	15840 \pm 1900	+ :47
2.60	=	5290	7000 \pm 899	20810 \pm 1356	+10.9
-	1.25	=	38600 \pm 5960	=	+ :48
-	1.42	=	29500 \pm 5017	=	+ :83
2.54	=	6910	18100 \pm 2170	39200 \pm 1914	+4.38

TABLE B-11. Continued
ULTIMATE ANALYSIS

LOCATION	ADAPTER P/N	SECTION	MATERIAL (1)	TORQUE (IN-LBS)	P _T (LB)
SYNC. SHAFTS	301-10463	AA	Steel	188550	1472
	301-11003	AA	Steel	188550	1472
	301-11003	CC	Steel	188550	1472
	301-11004	AA	Steel	188550	1472
	301-11004	CC	Steel	188550	1472
	301-11007	FF	Aluminum	188550	1472
	301-11008	DD	Steel	188550	1472
	301-11008	EE	Steel	188550	1472
	301-11009	AA	Steel	188550	1472
	301-11005	AA	Steel	99560	1181
ENGINE SHAFTS	301-11023	AA	Aluminum	99560	1181
	301-11002	AA	Steel	99560	1181
	301-11021	DD	Steel	99560	1181
	301-11021	EE	Steel	99560	1181
	301-11022	AA	Aluminum	99560	1181

(1) STEEL - 4340 AT 150 KSI UTS

ALUMINUM - .7075-T73 AT 66 KSI VTS

(2) Includes T.C. and Bolt and Nut C.F.

(3) Due to T.C. Misalignment

(4) Refer to sketch for Load Locations

WGT (LBS)	P _T (4) (LB)	P _R (2) (4) (LB)	P _X (3) (4) (LB)	e (4) (IN)	I.D. (IN)	O.D. (IN)	THICKNESS (IN)	WIDTH (IN)	M.S. (MIN)
550	14720	9066	52.5	.681	--	--	.38	2.25	+ .09
550	14720	9066	52.5	.681	--	--	.38	2.12	+ .09
550	14720	--	--	--	3.40	3.84	---	--	+1.04
550	14720	9066	52.5	.681	--	--	.38	2.12	+ .09
550	14720	--	--	--	3.80	4.22	--	--	+1.40
550	14720	7446	52.5	.80	--	--	.66	3.60	+ .74
550	14720	--	--	--	2.15	2.66	--	--	+ .10
550	14720	--	--	--	2.50	2.96	--	--	+ .27
550	14720	9066	52.5	.681	--	--	.38	2.12	+ .09
660	11810	7305	52.5	.620	--	--	.48	2.06	+1.60
660	11810	6765	52.5	.751	--	--	.53	2.60	+ .11
660	11810	11579	--	.712	--	--	.56	2.60	+2.15
660	11810	--	--	--	.93	1.84	--	--	+ .14
660	11810	--	--	--	1.53	2.17	--	--	+ .41
660	11810	10000	52.5	.88	--	--	.38	2.54	+ .29

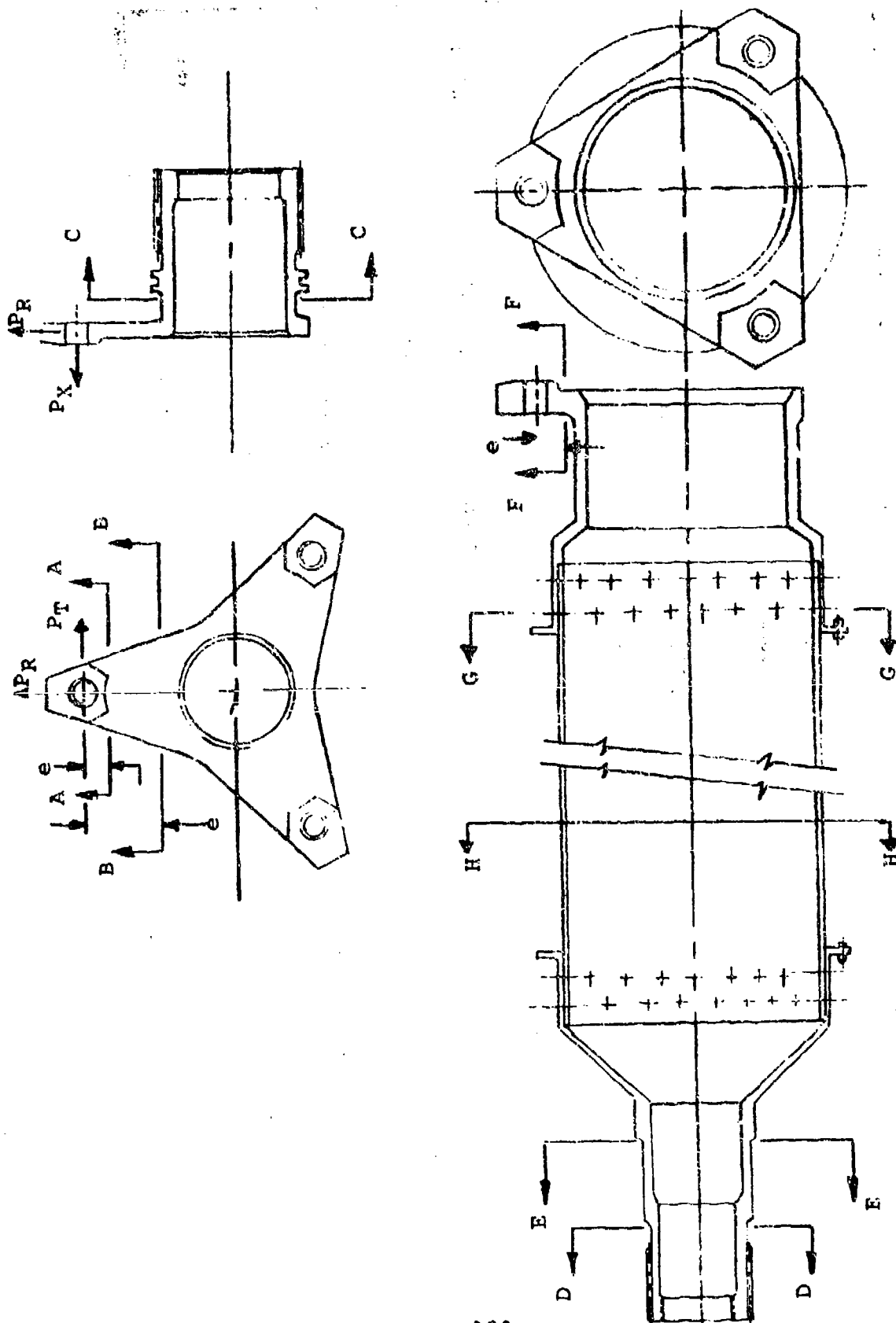


Figure B-20. Drive Shafts and Adapters, Typical Sections.

TABLE B-12. DRIVE SHAFT CRITICAL SPEEDS

	Max. Operational Speed	1st Critical Speed	Percent Margin
o <u>SYNCHRONIZING SHAFTS</u>			
FWD. (9 SECTION)	9,073 (Power Off)	10,050	11.0
	7,986 (Power On)		26.0
AFT (3 SECTION)	9,073 (Power Off)	10,240	13.0
	7,986 (Power On)		29.0
o <u>ENGINE SHAFTING</u>			
ENGINE POWER TURBINE	11,500 (Power On)	14,300	24.3
ENGINE SHAFTING (3 SECTION)	11,500 (Power On)	24,800	115.0
o CONFIGURATION: As Defined in Dwg. 301-11099, "Shafting Instl., Sync and Eng."			
o METHOD OF ANALYSIS: Engine Power Turbine: Detroit Diesel Allison Prog. BB60			
All Other Shafts: Boeing Vertol Prog. D-82 (Distributed mass and stiffness; finite element analysis)			

TABLE B-13. SPLINE STRESS SUMMARY

	LOCATION	PART NUMBER	FINITY	INTERNAL OR EXTERNAL	SURFACE TREATMENT	LN
AFT TRANSMISSION	Rotor Shaft (Hub)	301-10401	Fixed	Ext.	Nylon II Coating	
	Second Stage Sun	301-10459	Fixed	Int.	Carb.	
	First Stage Carrier	301-10413	Fixed	Ext.	--	
	Spiral Bevel Pinion	301-10428	Fixed	Ext.	Carb.	
	Adapter, S.B. Pinion	301-10463	Fixed	Int.	--	
	Alternator Drive	301-10451	Working	Int.	Carb.	
	Fan Drive	301-10445	Working	Int.	Carb.	
	Hyd Pump Drive	301-10442	Working	Int.	Carb.	
COMBINER TRANSMISSION	Lubrication Pump Drive	301-10447	Working	Int.	Carb.	
	Adapter, Clutch Hsg.	301-11002	Working	Ext.	--	
	Hsg. Clutch	301-10650	Working	Int.	Carb.	
	Clutch, Inner	301-10629	Working	Ext.	Carb.	
	S.B. Pinion	301-10677	Working	Int.	Carb.	
	Helical Pinion	301-10654	Working	Int.	Carb.	
	Adapter, Sync	301-11004	Working	Ext.	--	
	Collector Gear	301-10601	Working	Int.	Carb.	
	Adapter, Slant	301-11003	Working	Ext.	--	
	Slant Shaft	301-10610	Working	Int.	Carb.	
	Adapter, Rotor Brake	301-10682	Fixed	Int.	--	
	Gear, Rotor Brake	301-10625	Fixed	Ext.	Carb.	
	Gear, Rotor Brake	301-10625	Working	Int.	Carb.	
	Quill Aux. Lube	301-10621	Working	Ext.	Carb.	
	Quill Aux. Lub	301-10621	Working	Int.	Carb.	
	Gear, Fan Drive	301-10657	Working	Int.	Carb.	
	Quill, Fan Drive	301-10665	Working	Ext.	Carb.	
	Gear, Lube Pump	301-10659	Working	Int.	Carb.	
	Quill, Lube Pump	301-10668	Working	Ext.	Carb.	
	Quill, Lube Pump	301-10668	Working	Int.	Carb.	
ENGINE & ENG SHAFT	Adapter, Brg.	301-11021	Fixed	Ext.	--	
	Adapter, Eng. Shaft	301-11022	Fixed	Int.	--	
	Adapter, Eng. Output	301-11005	Fixed	Int.	--	
SYNC SHAFT	Adapter, Brg.	301-11008	Fixed	Ext.	--	
	Adapter, Sync Shaft	301-11009	Fixed	Int.	--	

① Lube: D - Dry
J - Jet

OA - Oil Atmosphere
G - Grease

	SURFACE TREATMENT	LUBE ①	NO. OF TEETH	P _D (inches)	D _P	NOMINAL ENGAGEMENT LENGTH (inches)	TORQUE (OPERATING) (In-Lbs.)	fbr (PSI)	fsu (PSI)
	Nylon II Coating	D	58	14.500	4/8	8.21	4.290X10 ⁶	4950	39600
	Carb.	D	81	10.125	8/16	2.08	1.159X10 ⁶	10900	31500
	--	D	81	10.125	8/16	2.08	1.159X10 ⁶	10900	36600
	Carb.	D	66	4.125	16/32	1.00	83800	9890	34400
	--	D	66	4.125	16/32	1.00	83800	9890	18800
	Carb.	OA	16	.800	20/40	.95	467	1540	2140
	Carb.	OA	16	1.000	16/32	1.00	457	914	1721
	Carb.	OA	19	1.188	16/32	1.00	635	1270	2955
	Carb.	OA	18	.750	24/48	1.06	305	1030	2850
	--	G	68	4.250	16/32	1.56	44250	3140	19490
	Carb.	J	68	4.250	16/32	1.56	44250	3140	9870
	Carb.	J	72	4.500	16/32	1.25	44250	3496	16270
	Carb.	J	72	4.500	16/32	1.25	44250	3496	6600
	Carb.	J	72	4.500	16/32	1.25	44250	3496	6600
	--	G	70	4.375	16/32	3.10	83800	2825	35590
	Carb.	G	70	4.375	16/32	3.10	83800	2825	9410
	--	G	64	4.000	16/32	2.25	83800	4656	41560
	Carb.	G	64	4.000	16/32	2.25	83800	4656	14370
	--	D	38	2.375	16/32	1.00	30000	10640	30830
	Carb.	D	38	2.375	16/32	1.00	30000	10640	58520
	Carb.	J	36	2.250	16/32	.29	25	36	--
	Carb.	J	36	2.250	16/32	.29	25	36	80
	Carb.	OA	12	.600	20/40	.38	25	365	500
	Carb.	G	16	1.000	16/32	.60	461	1537	1370
	Carb.	G	16	1.000	16/32	.60	461	1537	10660
	Carb.	J	43	2.688	16/32	.42	110	95	120
	Carb.	J	43	2.688	16/32	.42	110	95	--
	Carb.	OA	18	.750	24/48	.62	110	631	1100
	--	D	32	2.000	16/32	2.31	44250	9578	83470
	--	D	32	2.000	16/32	2.31	44250	9578	51980
	--	D	38	2.375	15/32	1.56	44250	10060	36190
	--	D	45	2.813	16/32	2.06	83800	10285	85820
	--	D	45	2.813	16/32	2.06	83800	10285	44370

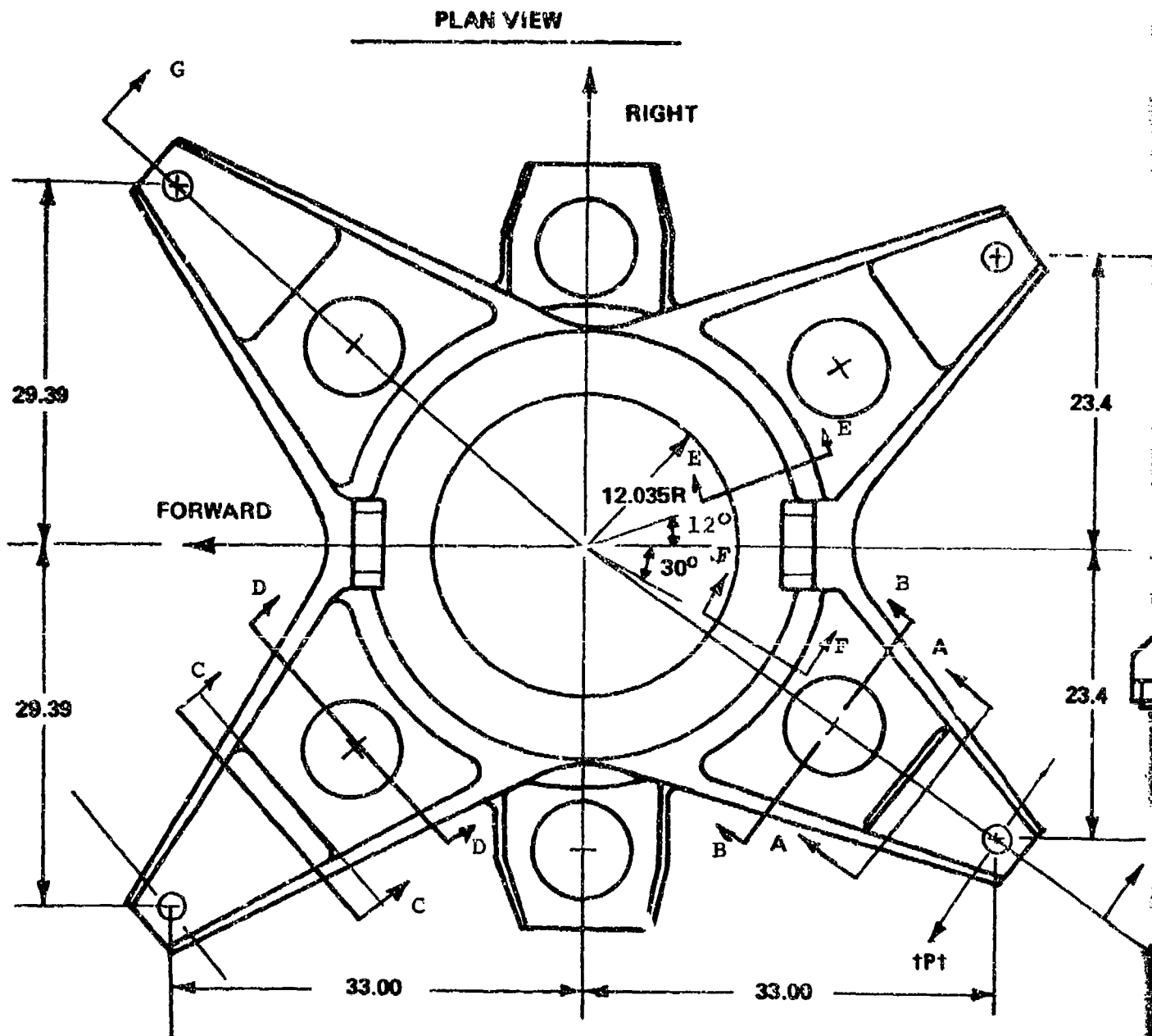


Figure B-21. Transmission Cover Analysis.

ELEVATION VIEW

SECTION G-G

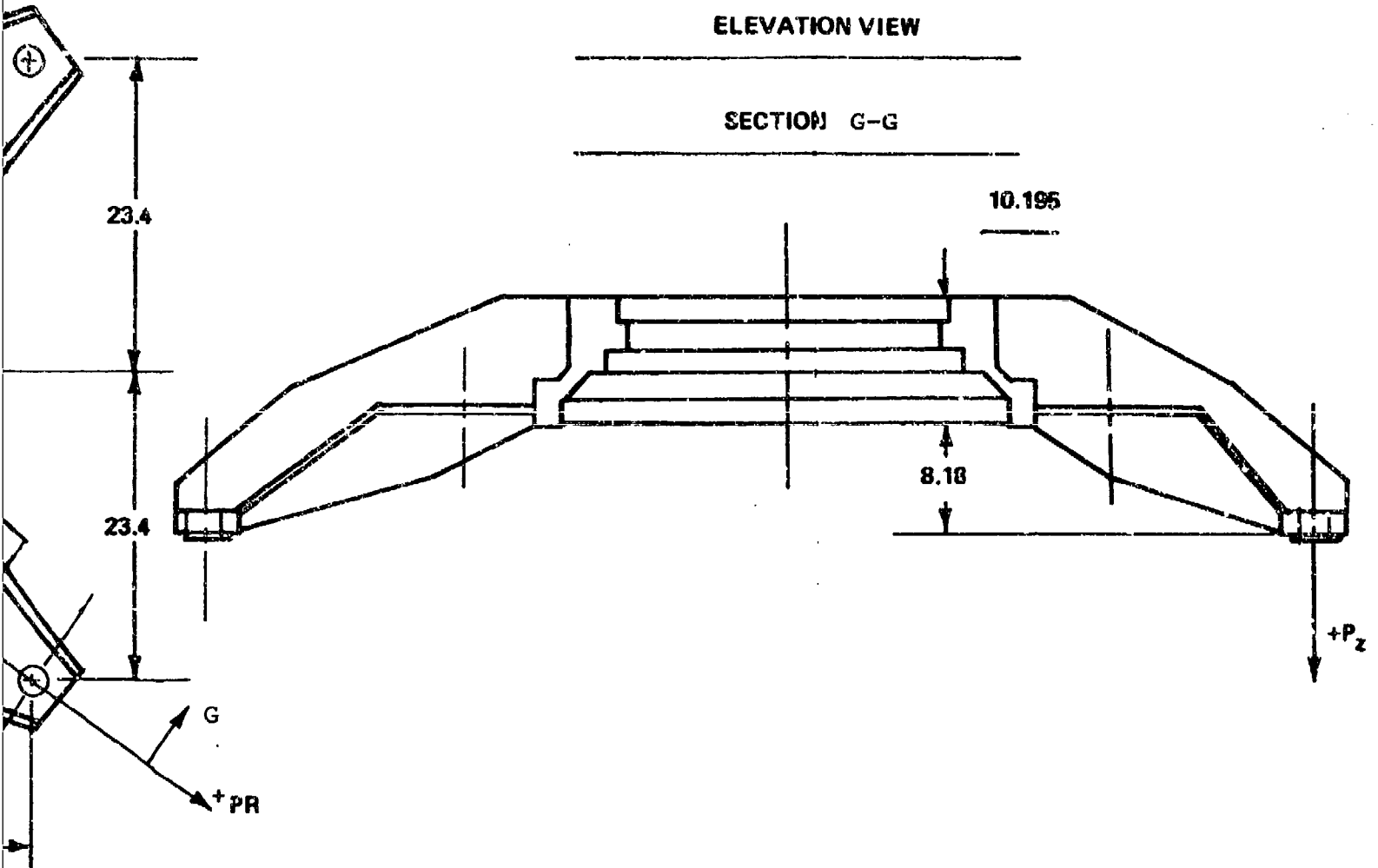


TABLE B-14. ROTOR TRANSMISSION UPPER COVER - 301-10456

FATIGUE ANALYSIS

SECTION	PR LB	PZ LB	PT LB	Mx In-LB	Mx' IN-LB	My IN-LB	Vx LB
A-A	4028 +806	34948 +5216	26971 +3471	290000 +53100	22305 +2870	307500 +39600	2697 +347
B-B	4028 +806	34948 +5216	26971 +3471	547520 +96770	66540 +8560	539420 +69420	2697 +347
C-C	3687 +738	34948 +5216	29630 +3816	272300 +50220	18000 +2320	324000 +41600	2963 +381
D-D	3687 +738	34948 +5216	29630 +3816	692600 +11900	14600 +1880	724420 +93300	2963 +381

ULTIMATE ANALYSIS

CONDITION	SECTION	PR LB	Pz LB	PT LB	Mx IN-LB	Mx' IN-LB	My IN-LB
Normal	A-A	14447	136350	71057	1.14×10^6	58700	.810x
(4 Legs	B-B	14447	136350	71057	2.14×10^6	175000	1.42x
Intact)	C-C	14450	136350	71060	1.063×10^6	43062	.774x
	D-D	11450	136350	71060	2.701×10^6	35032	1.737x
Failsafe	C-C	-10268	143990	67962	1.304×10^6	41000	.740x
(Fwd. R/H	D-D	-10268	143990	67962	3.162×10^6	33512	1.661x
Leg Out)							

Refer to cover sketch for Lug Load Directions

Refer to section sketch for Load Sign Convention

LEG SECTIONS

	Vx LB	Vy LB	Vy LB	Pz LB	Zx IN ³	Zy IN ³	AREA IN ²	fb psi	fs psi	M.S.
	26971 +3471	14452 +2344	22857 +3419	19677 +3100	21.95	81.5	17.2	20350 +3360	8720 +1230	.02
	26971 +3471	14452 +2344	1834 +236	19677 +3100	51.5	208.	31.75	16420 +2430	2420 +360	.73
	29630 +3816	14800 +2470	7410 +960	19642 +3097	22.0	77.0	17.0	19450 +3230	5670 +900	.15
	29630 +3816	14800 +2470	8450 +1090	19642 +3097	67.0	288.	36.6	13480 +2340	5876 +210	.68

Mx IN-LB	My IN-LB	Vx LB	Vy LB	Vy LB	Pz LB	fbx psi	fbv psi	ft psi	fs psi	M.S.
58700	.810x10 ⁶	71057	56600	22200	76693	52054	9936	3792	17874	+.06
175000	1.42x10 ⁶	71057	56600	4850	76693	41553	6926	2054	3219	+.49
43062	.774x10 ⁶	71060	56240	17772	76693	48500	10000	4500	20677	+.04
35032	1.737x10 ⁶	71060	56240	20275	76693	40000	6050	2090	7236	+.70
41000	.740x10 ⁶	67962	65400	17000	58474	59407	9585	3439	18691.	+.01
33512	1.661x10 ⁶	67962	65400	19395	58474	47149	5767	1590	6329.	+.54

TABLE B-14. Continued

FATIGUE ANALYSIS

SECTION	Mx IN-LB	My IN-LB	Mz IN-LB	Pz IN-LB	
E-E, Point 1	-398500 +85000	-211850 +30800	70410 +14040	36350 +4170	1
Point 2					
F-F, Point 1	-369300 +74960	2343 +8219	16880 +15150	69410 +12920	1
Point 2					
Point 3					

ULTIMATE ANALYSIS

CONDITION	SECTION	Mxp ⁽⁴⁾ IN-LB	Myp ⁽⁴⁾ IN-LB	Mz IN-LB	Pz LB
Normal	E-E	-1.129 x10 ⁶	1.136 x10 ⁶	-170150	132880
	F-F	.7x10 ⁶	.575x10 ⁶	130000	309950

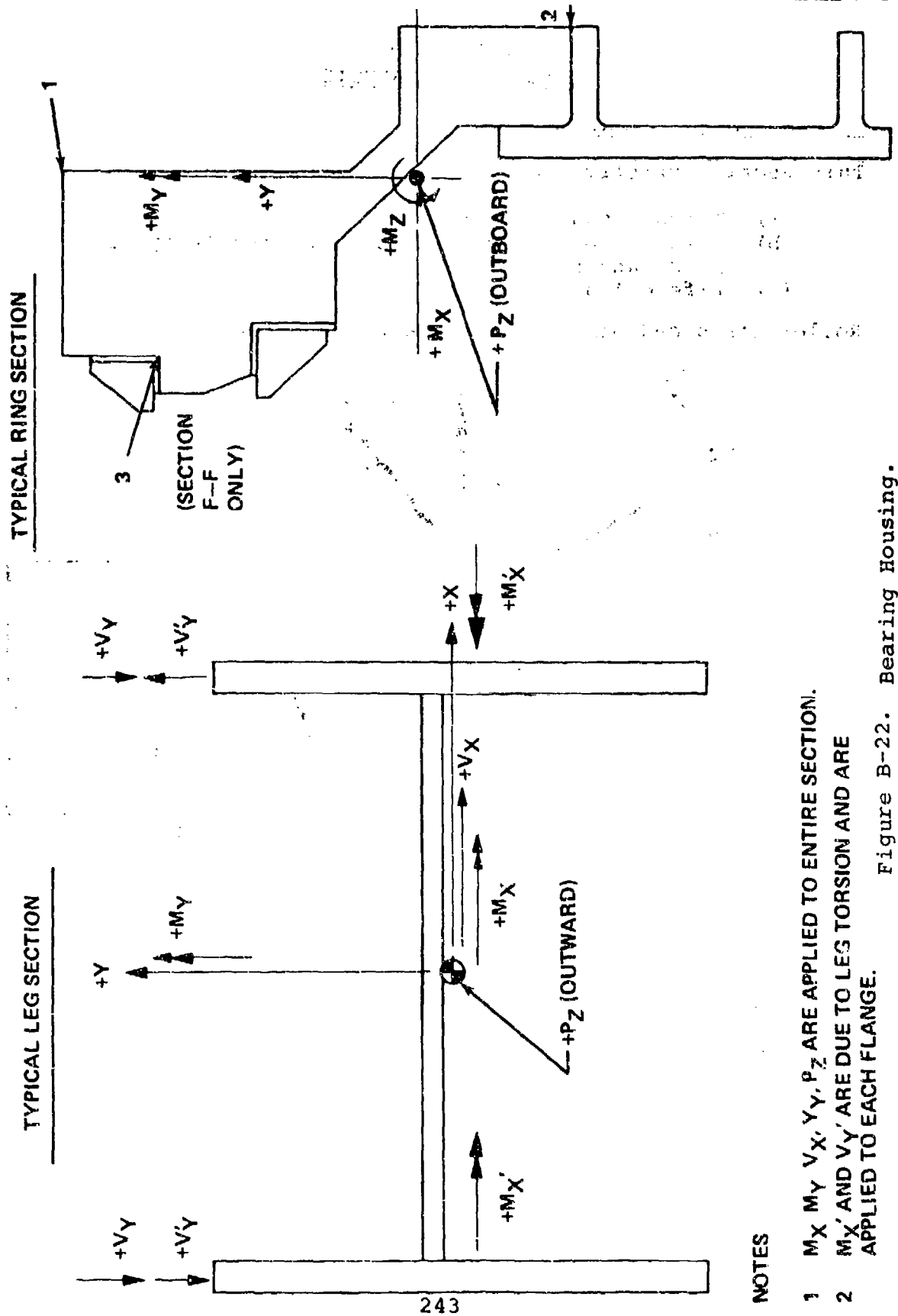
- (1) Alternating Stresses include stress concentration
- (2) Fretted point, $F_e = \pm 2000$ psi
- (3) Lubrication Jet Hole
- (4) About Principal Axes

BEARING HOUSING SECTIONS

	Pz IN-LB	Ix IN ⁴	Iy IN ⁴	Ixy IN ⁴	AREA IN ²	fb ^① psi	Kt	M.S.
	36350 +4170	1076.	161.	-300.8	45.7	13000 +2640	--	.76
						8520 +1400	②	.21
	69410 +12920	1043.	137.	-237.	40.9	6430 +1510	--	2.5
						2455 +1510	②	.26
						-510 +2340	2.5 ③	.02

	Pz LB	Mxup ^④ IN-LB	Myup ^④ IN-LB	Mzu IN-LB	Pzu LB	M.S.
	132880	12.5x10 ⁶	1.92x10 ⁶	18.5x10 ⁶	2.55x10 ⁶	.36
	309950	12.5x10 ⁶	1.92x10 ⁶	18.5x10 ⁶	2.28x10 ⁶	1.01

concentration



NOTES

- 1 M_X M_Y V_X V_Y P_Z ARE APPLIED TO ENTIRE SECTION.
- 2 M'_X AND V'_Y ARE DUE TO LEG TORSION AND ARE APPLIED TO EACH FLANGE.

Figure B-22. Bearing Housing.

APPENDIX C

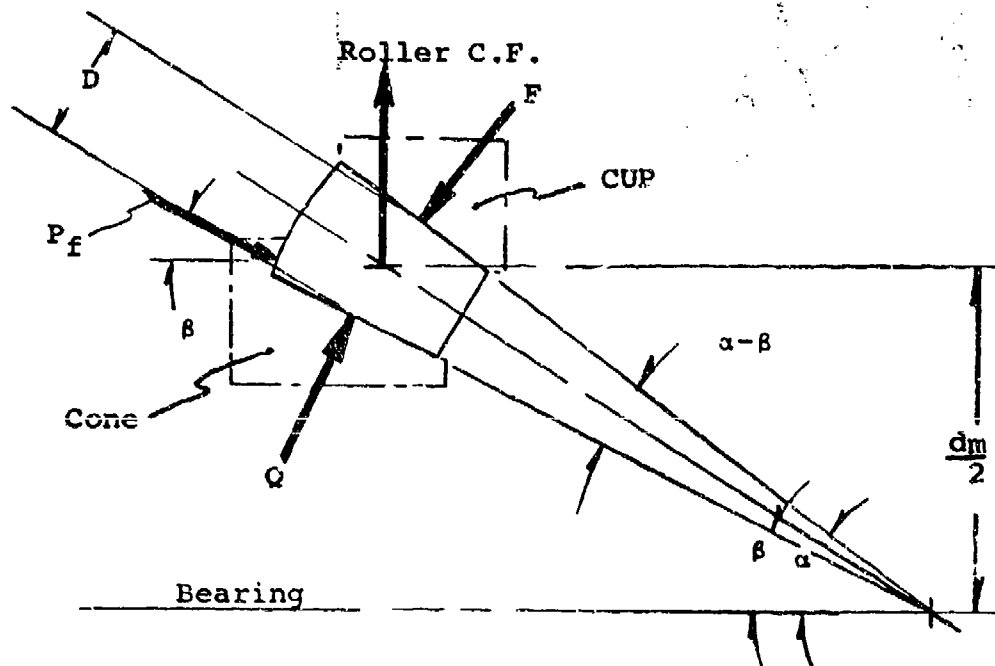
METHODS OF ANALYSIS

TAPERED ROLLER BEARINGS

This section briefly presents the development of:

- (a) Thrust induced by roller C.F.
- (b) Roller/rib load considering externally applied loads and roller C.F.
- (c) Life calculations

Roller loads and nomenclature are shown below.



Symbols not shown above:

ψ = Roller azimuth location; maximum loaded roller is at $\psi = 0^\circ$

C_b = Stribeck's constant, normally taken as 5.

B = Number of rollers

$K = .389 / \tan \alpha$

J = Correction factor for outer race load. Based on a comparison of hand and computer calculated lives of cylindrical roller bearings.

N = Bearing cone speed, rpm.

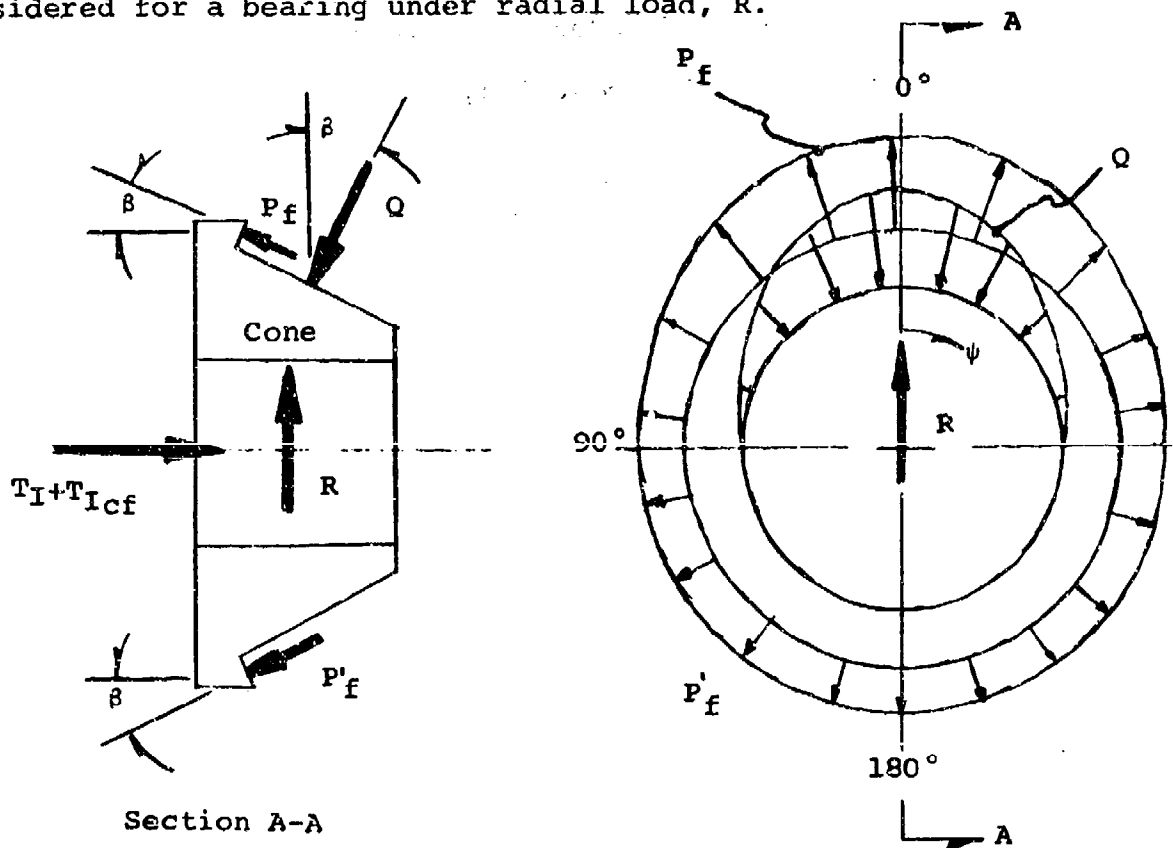
From summation of forces in the radial and axial directions, F and P_f may be written in terms of Q and C.F.

$$P_f = \frac{Q \times \sin(\alpha - \beta) + C.F. \times \sin \alpha}{\cos(\alpha - \beta)}$$

$$F = \frac{Q + C.F. \times \cos \beta}{\cos(\alpha - \beta)}$$

Moment equilibrium is accomplished by nonuniform distributions of F and Q . This, however, is not considered in the following analyses.

The following figure shows the cone loads and distribution considered for a bearing under radial load, R .



It is assumed that roller loads, Q , are distributed in some unspecified manner over the azimuth range of -90° to $+90^\circ$. Rib loads, P_f , are likewise distributed in some unspecified manner over the same azimuth range. Since the external radial load causes the cone to shift radially relative to the cup (both of which are considered to be rigid), there is no roller-to-cone contact in the 90° to 270° azimuth range. Thus, in this range, P'_f must react the thrust component of roller centrifugal force.

By summing forces on the cone in the axial and radial directions, it is established that:

- (a) the roller-to-cone load distribution is
 $Q = Q_{\max} \times \cos \psi$
- (b) the maximum roller load, Q_{\max} , and thus all roller-to-cone loads are independent of roller centrifugal force.

(c) $Q_{\max} = \frac{R \times C_b}{B \times \cos \beta}$

- (d) two components of induced thrust exist

- (1) Due to roller centrifugal force

$$T_{Icf} = \frac{B \times C.F. \times \cos \beta \times \sin \alpha}{\cos (\alpha - \beta)}$$

- (2) Due to external radial load

$$T_I = \frac{.47 \times R}{K}$$

- (e) Cone life can be calculated by standard methods presented in Reference 12.

Cup life is calculated by considering the probability of non-failure of the most heavily loaded point on the cup, including roller centrifugal force, and by defining an equivalent external radial load which, when applied without roller centrifugal force, will produce the same life as the actual conditions.

This results in the following:

$$R_e = R \left[1 + \frac{C.F. \times B}{C_b \times R} \times \cos^2 \alpha \times J \right]$$

Next, it is established that the Basic Radial Rating (which is really the cone's rating) and the cup's rating are related approximately by

$$\text{Cup Rating} = \left(\frac{\sin \alpha}{\sin \beta} \right)^{1.324} \times \text{BRR}$$

The cup and cone lives are combined as follows to produce the net bearing life.

$$\text{Net Bearing Life} = \left[\left(\frac{1}{\text{Cone Life}} \right)^{9/8} \times \left(\frac{1}{\text{Cup Life}} \right)^{9/8} \right]^{-8/9}$$

Substituting cup and cone loads and ratings yields the following, which define the Effective Radial Load to be used in bearing in life calculations.

$$R_{\text{eff}} = R \left[\frac{1 + \left(\frac{\sin \beta}{\sin \alpha} \right)^{4.95} \times \left(1 + J \times \frac{\text{C.F.} \times S \times \cos^2 \alpha}{5 \times R} \right)^{3.74}}{1 + \left(\frac{\sin \beta}{\sin \alpha} \right)^{4.95}} \right]^{.268}, \text{LBS}$$

and

$$\text{Bearing } L_{10} = \left(\frac{\text{BRR}}{R_{\text{eff}}} \right)^{10/3} \times \frac{90 \times 10^6}{60 \times N} \text{ Hours}$$

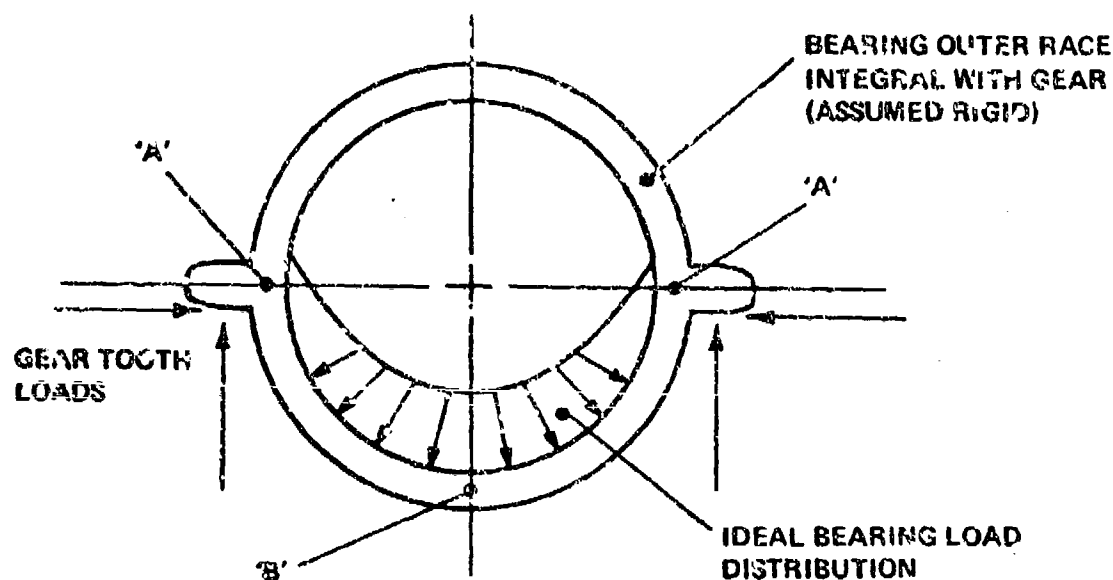
Rib load and contact stress is significant in the preservation of an adequate oil film thickness. Table C-1 defines parameters that influence tapered bearing performance at high speed. The test bearing varied by a factor of two in cone rib stresses. Tests showed that an adequate hydrodynamic film was formed at the cone rib of the 6500 series, while the HM 926700 series was characterized by intermittent scuffing in that area. The HLH bearings, with one exception, run at or below the 36,133 psi of the 6500 series and are therefore expected to maintain an adequate EHD film. The aft input pinion bearing (-10420) is above the test-proven limit. A lower contact angle bearing with decreased loads and stresses and increased EHD film thickness will be available as a backup. Decreasing the contact angle and other internal changes reduces the calculated life of this bearing from approximately 3500 hours B-10 to 1800 hours.

TABLE C-1. SUMMARY OF HLH TRANSMISSION BEARINGS									
Part Number	TEST BEARINGS		HLH COMBINDER TRANSMISSION			HLH AFT TRANSMISSION			
	6,500	HM926700	301-10676	-10671	-10612	-10616	-10420	-10424	-10443 -10440
Shaft Speed (RPM)	16,000	11,500	11,500	11,500	7,986	7,986	7,986	-7,986	2,788 2,788
Cone Rib Velocity (FPM)	20,200	20,264	20,474	18,666	18,397	17,978	17,143	15,261	9,671 9,340
Max Rib Load ((LB)	236	915	328	111	398	170	904 (497)	172 (220)	68 13.2
Max Cone Rib Stress (PSI)	36,133	64,147	32,773	19,653	20,962	28,106	52,148 (32,600)	28,880 (33,300)	12,246 7,357
Gyroscopic Moment (In-Lb)	24	88	29	13.6	52.7	17.3	87 (50)	17.8 (17.8)	2.0 .4
Contact Angle	15°	26.2°	15°	12.5°	10°	22.5°	25°	20°	15° 15°
NOTES:									
1. All conditions based on 100% power rating for each location.									
2. Values shown in () are for the aft input pinion when the 301-10420 bearing is replaced with a EE1070C series tapered roller bearing.									

PLANET BEARING LIFE

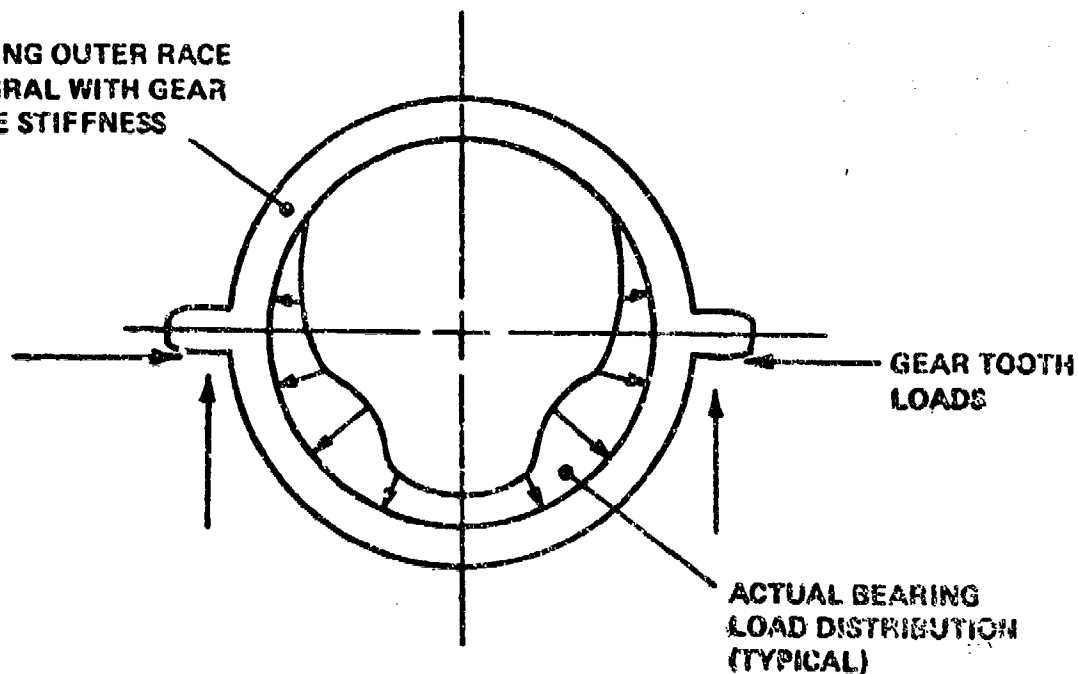
Planet bearing lives are calculated by the method presented in Reference 11. This appendix presents a brief discussion of this method and the derivation of a life experience factor for the planet bearings.

Planet gear loading is shown in the figure below together with the planet bearing roller load generally assumed. This ideal roller load distribution is based on the assumption that both the inner and outer races are rigid.



While the assumption of a rigid inner race is reasonable (because of the planet post), the assumption of a rigid outer race leads to considerable inaccuracy. Note that the effect of the gear tooth loads and roller loads as shown is to deflect the gear ring inward at points 'A' and outward at point 'B', thus altering the roller load distribution. The actual load distribution is typically oriented as shown in the following figure, when the finite gear stiffness is included as in Reference 11. The analysis has been incorporated into computer program PLANET I.

BEARING OUTER RACE
INTEGRAL WITH GEAR
FINITE STIFFNESS



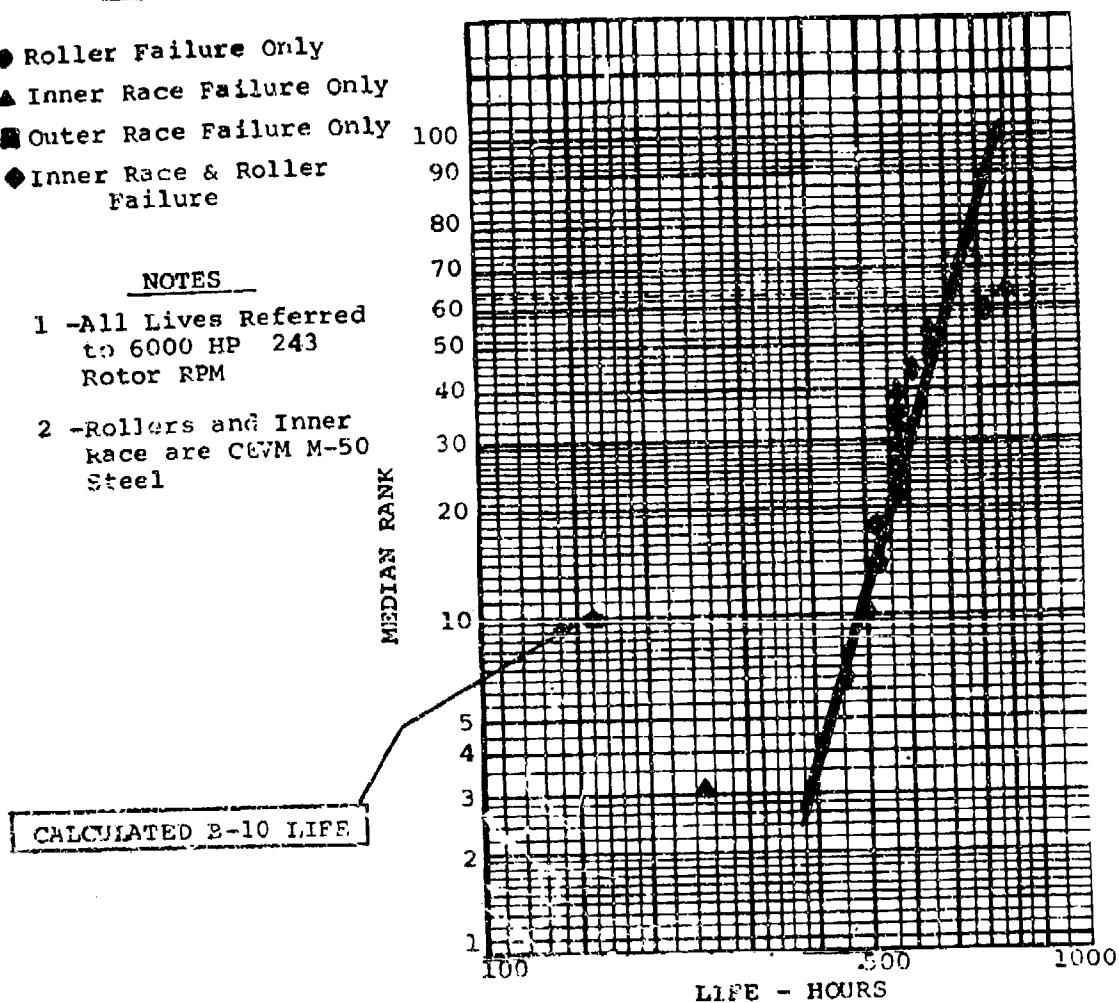
The experience factor is based on testing of the CH-47C second-stage planet bearing, primarily from failures in the test program of Reference 19. The test results are presented in Weibull plot form in Figure C-1 and indicate a B-10 life of 490 hours. The calculated life of this bearing, per PLANET I, is 160 hours, thus indicating that a factor of 3.06 may be applied to calculated lives to predict actual lives.

LEGEND

- Roller Failure Only
- ▲ Inner Race Failure Only
- Outer Race Failure Only
- ◆ Inner Race & Roller Failure

NOTES

- 1 -All Lives Referred to 6000 HP 243 Rotor RPM
- 2 -Rollers and Inner Race are CEVM M-50 Steel



WEIBULL PROBABILITY PAPER

n = 100 Specimens
16 Failures

$$K = \frac{490}{160} = 3.06$$

Figure C-1. CH-4C 2nd-Stage Planet Bearings.

COMPLIANT ROLLER ANALYSIS BASED ON TESTING BETWEEN PLATES

This section presents a brief discussion of the techniques used in the compliant roller analysis. A detailed discussion is presented in Reference 20.

Planet bearing sizing for B-10 fatigue life requirements has a direct influence on the pitch diameter size of the planetary ring gear. To minimize the size and weight of the ring gear, the capacity of the planet bearings must be improved. Boeing-Vertol's current design practice is to use self-aligning spherical roller bearings to accommodate planet bearing post deflection. For the HLH 2nd-stage planetary system, studies were conducted to determine methods of providing improved bearing capacity at reduced weight and size.

These studies have shown that cylindrical roller bearings could provide increased capacity compared to spherical roller bearings and thus provide higher fatigue life. The objection to cylindrical roller bearings is their inability to accommodate misalignments on the order of .003 inch/inch slope. Field experience and testing of cylindrical roller bearings, even with special crowned rollers under misaligned condition show a drastic reduction in fatigue life. Therefore, to take advantage of the higher capacity, a significant improvement in misalignment capability must be incorporated into the cylindrical roller bearing.

The results of the above studies showed that a cylindrical roller bearing design using a .25-inch-diameter roller and a length of 1.50 inches provided a required B-10 life in excess of 2,000 hours while meeting all the design objectives.

To reduce the influence on fatigue life of an asymmetrically loaded cylindrical roller bearing, compliant (hollow-ended) cylindrical rollers were used to supplement the standard crown modification. The unique hollow-ended roller design was developed by the Rollway Bearing Company, Syracuse, New York. Rollway was subcontracted to investigate the use of such a design in the HLH rotor transmission planetary system and to provide a method of analysis.

The "Footprint" technique is the key to accurately determining the static contact areas from which comparisons may be made to select a bore/crown relationship yielding the best load distribution for the specified operating conditions. Permanent recording of the contact area is made possible by using chemically etched steel plates.

This accurate description of loading on the rolling element is of great importance, as it serves as the basis for the determination of the stress distribution in the body. The contact stresses in a solid roller due to the deformation of a local area from the applied load contact are determined in a straightforward manner using classical equations. However, analyzing the stress distribution in a hollow-ended roller is not a routine problem; additional stresses are involved due to rim deflection, which must be combined with the contact stress state to yield an accurate stress determination. A three-dimensional finite element elasticity study was used to determine the stress state in the flexible rim section due to deflection. This computer program provides a numerical solution for the stresses induced in a conical shell elastically supported at one end and under the influence of an asymmetrical self-equilibrating line load. The results of the finite element analysis when properly combined with the local Hertzian contact stress yield an accurate description of the subsurface shear stress state in the hollow-ended roller which may be compared to the subsurface shear stress state existing in a solid type roller subjected to identical operating conditions. Knowledge of the peak bore stress and maximum subsurface shear stress allows a decision on roller feasibility to be made.

The planet bearing design procedure began with the basic sizing, using the PLANET I analysis described on page 249. As discussed there, this analysis includes the effect of a flexible outer race and a material correction. However, it does not have the capability of including misalignment, or compliant rollers.

This defined the bearing containing 1.25-inch diameter x 1.5-inch length rollers described above.

To include the effect of misalignment, i.e., roller edge loading, computer program S-04 was used to estimate the peak roller stress and reduction in life due to misalignment on a bearing containing solid rollers. The techniques used by the Rollway Co., as described above, provided the reduction in peak roller stress to be expected when the solid rollers are replaced by hollow-ended compliant rollers operated at similar misalignments. Since life is related to roller stress, the life improvement resulting from compliancy can be estimated.

TRANSMISSION NOISE

The internal noise criterion is that production aircraft noise levels shall not exceed MIL-A-8806A Tables I, II, and IV in the cockpit and troop compartment, at design gross weight, and during the HLH mission profile. Figure C-2 shows the predicted sound pressure levels from untreated and treated transmissions and transmission enclosures compared to the specification.

From this chart, it can be seen that tuned shafts and ring gear are predicted to reduce SPL by 17 dB. Tuned transmission shafts have been adjusted in mass and stiffness characteristics to minimize vibratory amplitude at the bearing supports and gear meshing points. During the ATC design program, experimental verification was obtained that these vibrations can be analytically predicted. Further, it was shown that predominate noise frequencies coincided with the shaft excitations, supporting the theory that the noise is generated by gear mesh irregularities transferred from bearings to the exterior.

During the bench test program, comparisons will be made of SPL output from transmission components which have been designed to minimize vibratory response and from components similar in function but designed without this consideration.

Coatings of viscoelastic materials are shown to provide a further 10-dB reduction. Acoustics laboratory tests performed in the ATC program gave evidence that these coatings are effective in suppressing noise. The methods of application and areas to be covered depend upon the effectiveness of the third element of the noise reduction program: the 27-dB enclosure which forms the transmission compartment. Trade-offs between applying the coating to the transmission case or to the enclosure will be developed in future testing and in design studies.

While the noise level reduction required in the HLH is greater than it is in lower-powered helicopter transmission systems, the ATC program has defined several areas whereby this reduction can be attained at weights less than predicted by conventional approaches.

CALCULATED NOISE LEVELS FOR CUBIC MEAN TORQUE FULL OCTAVE ANALYSIS

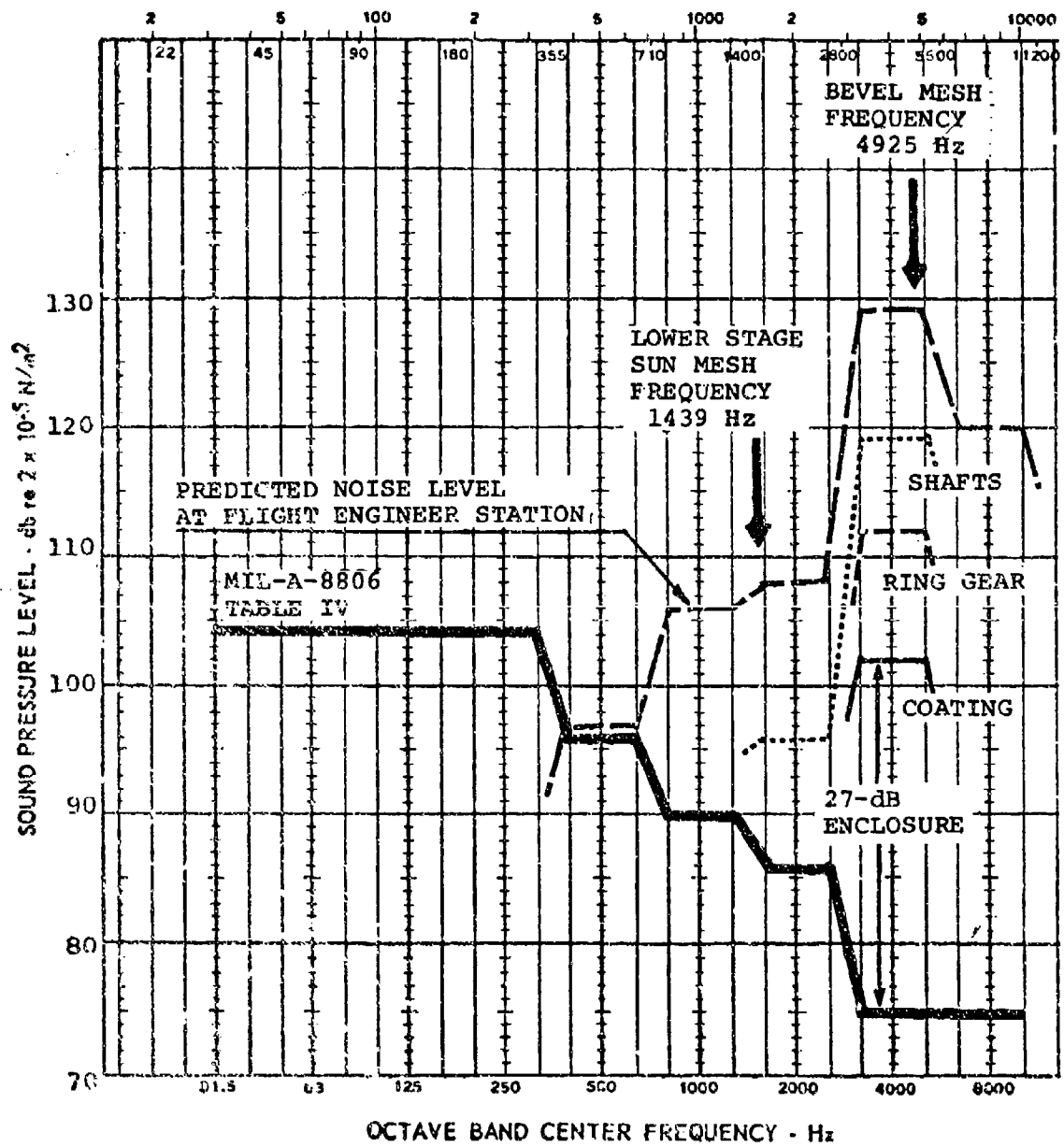


Figure C-2. Comparison of Predicted Baseline Transmission Sound Spectrum to Mil-Spec.

FINITE ELEMENT STRESS ANALYSIS OF GEARING

Finite element stress analyses were conducted to determine the state of stress for the HLH aft input pinion. Loading conditions were imposed on the finite element models to simulate the influence of applied input torque as the pinion teeth roll through mesh.

Finite Element Method

The Gleason method of finite element analysis is based on the FEABL program,* which was developed by M.I.T. under Air Force Contract F44620-70-C-0020. FEABL has recently been expanded by a cooperative effort between the Gleason Works and M.I.T. to include out-of-core storage capabilities and substructuring by static condensation.

The analysis reported here incorporates solid element Hex 24, which is a quasi-linear, 24-degree-of-freedom element, and models the pinion as four distinct substructures as shown in Figure C-3. Three of the substructures represent three neighboring pinion teeth and portions of the pinion blank beneath the teeth; the fourth substructure represents the continuation of the pinion blank minus the teeth. Deletion of the remaining pinion teeth, normally associated with the fourth substructure, is done to reduce model sizes and to reduce computer run times. It is felt that teeth more distant than one tooth away from the loaded tooth do not significantly affect the stress distribution in the vicinity of the loaded tooth.

The primary advantage of substructuring the pinion as shown in Figure C-3 is that the assembled pinion (the global system) represents the same total number of degrees of freedom as the assemblage of four substructures but contains a reduced number of global degrees of freedom to be solved. Consequently, the reduced number of degrees of freedom represents significantly reduced solution times. Coupled with one or more runs of the same assembled global system, but with different applied loads, a considerable savings in computer time can be realized.

*FEABL (Finite Element Analysis Basic Library), O. Orringer and S. French, ASRL, Dept. of Aeronautics and Astronautics, M.I.T., Cambridge, Mass., August 1974.

TOTAL GLOBAL NODES = 190

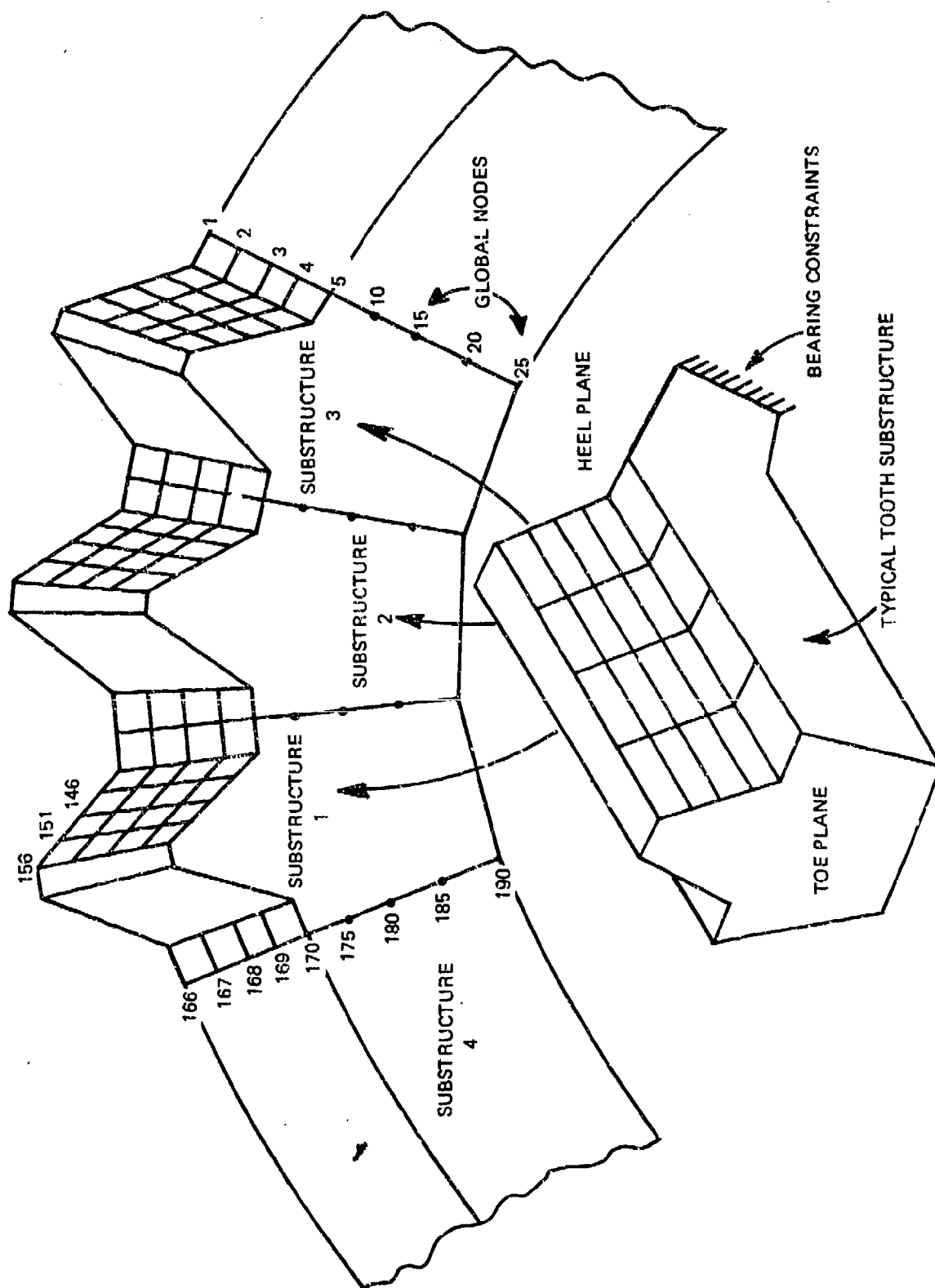


Figure C-3. Finite Element Model of HLH Aft Input Pinion.

A secondary advantage of substructuring is that individual substructures can be updated or modified without the expense of rerunning all other substructures in the model.

Significance of Stress Numbers Obtained from Finite Element Analysis

Because of the accuracy problems inherent with any numerical stress method, such as Finite Element, the magnitudes of the stress numbers should be assumed to be no more accurate than about 75% of the true stress values. The relative changes in stress numbers, however, as pinion design parameters are changed, may be as accurate as 90%, or more. These accuracy limits should be considered as rough guidelines in interpreting the stress numbers, as isolated portions of the tooth model may significantly deviate from these estimates.

Pinion Model Description

The general shape of the pinion model is equivalent to the spiral bevel parameters listed on Gleason dimension sheets. However, one exception is that the spiral bevel tooth form has been replaced by a straight bevel tooth form with the same general tooth depth and taper. This simplification understates the modified contact ratio and eliminates tooth curvature as an influence. It is felt, however, that for the purposes of initial analysis, the simplifications listed above will not greatly affect the stress numbers. Further developments of FEABL now have included tooth curvatures.

Tooth loading, as the pinion model simulates a rotation through mesh, is shown in Figure C-4. The tooth form shown in Figure C-4 is the projected layout of the pinion tooth at the mean section of the tooth. Contact between the pinion and gear teeth is assumed to occur where the surfaces of the teeth intersect the line of action as defined in conventional bevel gear theory.

Four distinct load positions are shown in Figure C-4 representing four rotated positions of the pinion and gear tooth. A total of seven stresses representing a roll-through mesh can be obtained from these four load positions. As an example, to calculate the points for the full contact root stresses, the stresses could be taken from point B_T (Figure C-4) for load positions 1 through 7. However, due to symmetry, it is noted that the stresses at B_T caused by loads at positions 5 through

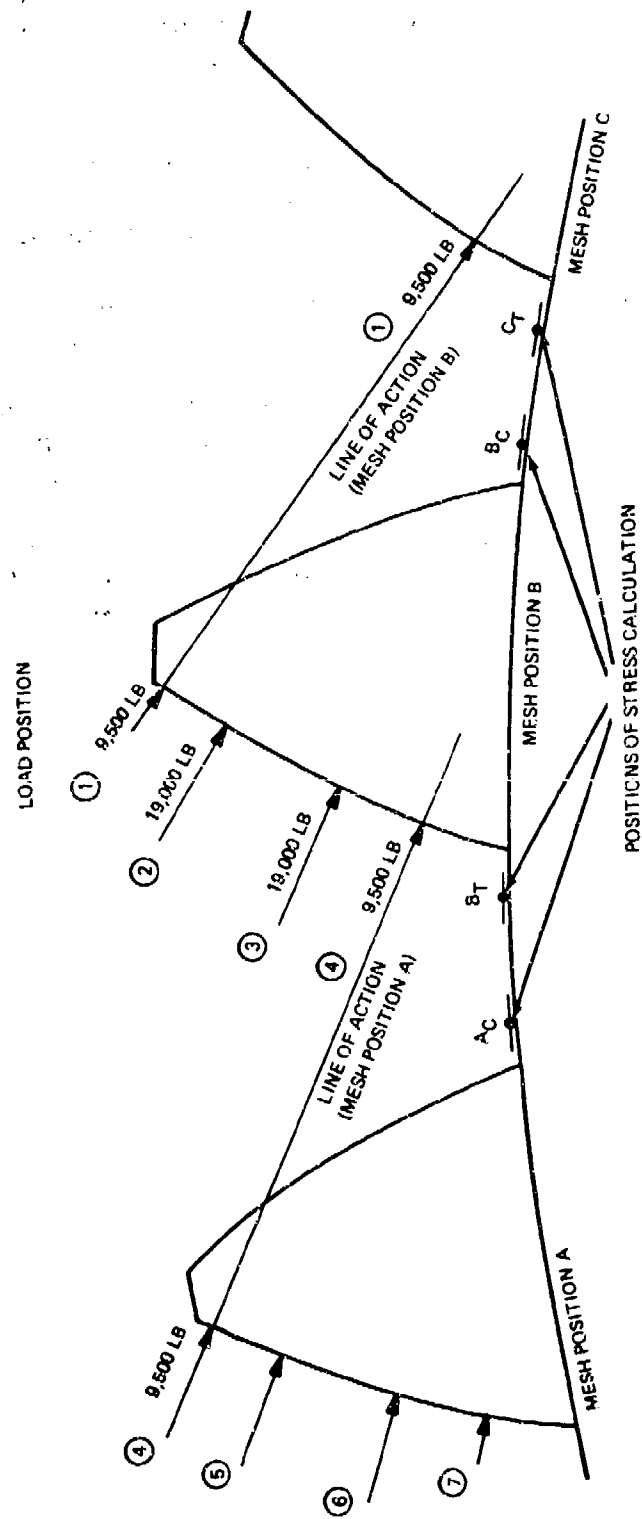


Figure C-4. Tooth Loading as a Function of Tooth Mesh Position (Mean Normal Plane).

7 are the same as stresses at C_T caused by loads at positions 2 through 4. Therefore, the four load positions give all the information necessary to plot the stresses resulting from a roll-through mesh.

Total pinion tooth loading is assumed to be statically equivalent to a transmitted torque of 84,000 lb-in. Assuming an average pinion tooth radius of 4.433: at the pitch point, the average load per tooth is approximately 19,000 pounds. It is further assumed that when two teeth are in contact, the total load of 19,000 pounds is divided evenly between the two teeth.

In general, the finite element model load points are positioned such that the height of the loads above the pinion axis are in agreement with the tooth rollout of Figure 76. In the case of loads along the face of the tooth, when there is less than full-width tooth contact, the load values have been weighted according to the reduced area of contact and in keeping with consistent loading methods of the finite element technique. Actual loading patterns used in HLH analysis are shown in Figures C-5 and C-6.

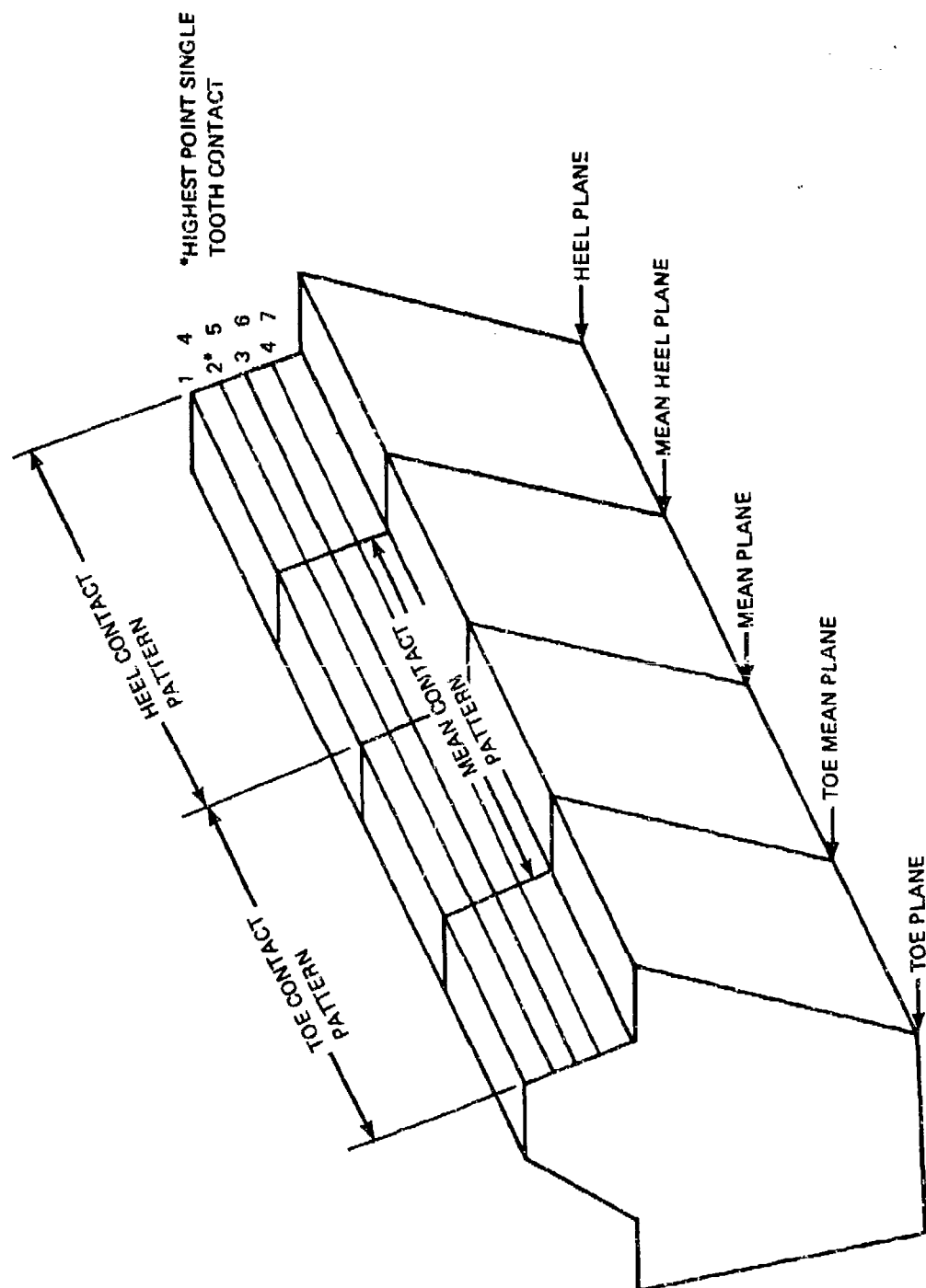
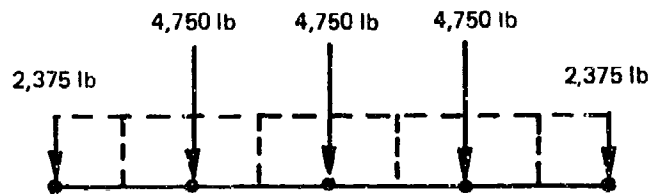


Figure C-5. Schematic Showing Location of Finite Element Loads.

FULL CONTACT



19,000 Pounds Evenly Distributed

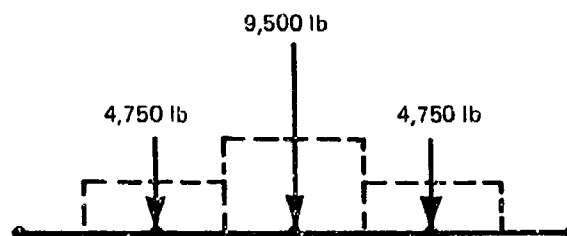


Finite Element Equivalent

MEAN CONTACT



19,000 Pounds Elliptically Distributed



Finite Element Equivalent

Figure C-6. Finite Element Modeling of Distributed Loads.

HIGH CONTACT RATIO GEARING

The methods of analysis utilized in the design of HCR gearing are essentially the same as those used for standard gearing. The major difference occurs in the magnitude and location of the maximum tooth loads. The maximum load on a standard contact ratio gear tooth occurs at the highest point of single tooth contact. In addition, the full transmitted load is carried by a single tooth pair over much of the tooth flank. In contrast, the maximum load on a high-contact-ratio gear tooth occurs in the vicinity of the pitch line. The full transmitted load is never applied to a single tooth pair. In fact, due to the alternate 2 and 3 pair contact, the maximum load applied to a single tooth pair is less than 65% of the total transmitted load.

HCR gearing utilizes a basic involute form but changes are made to the addendum area, tooth root, whole depth, pressure angle, etc., to increase the profile contact ratio from 1.2 - 1.35, which is typical of standard involute gearing to over 2.1. Thus for a high contact ratio gear set three pairs of teeth share the load during entrance and exit and in the vicinity of the pitch line, while for standard gears two pairs of teeth carry the load for a short time at entrance and exit and a single pair of teeth carry the full load during the remainder of the mesh cycle. The mesh action of the HCR and standard designs are shown in Figure C-7. The alternate two- and three-pair load sharing for HCR gears has been verified experimentally (in a prior Navy funded program) as shown in Figure C-8 by a strain survey

The advantages of HCR gearing include lower stress levels per unit load (thus permitting greater loads to be carried without exceeding basic stress limits), lower noise and vibration levels, improved reliability, and generally smoother mesh action. During an HCR test program conducted by Boeing Vertol, noise and vibration measurements were taken for both HCR and standard baseline gear sets of equivalent configuration. Although noise measurements made during the test program were not absolutely definitive, a significant reduction in noise level resulted. The vibration level of the HCR gears, as measured by an accelerometer attached to the test gear case and monitored on an oscilloscope, was only 1/2 to 2/3 that observed for the standard gears operating at the same loads and speeds.

The increased load capacity of HCR gearing is, of course, its most significant advantage. By increasing the number of teeth in contact, the maximum load which must be carried by any single tooth is reduced, thus for a constant stress level, the HCR design will carry more load. Conversely, for a given load, the HCR set may be made with a smaller face width and

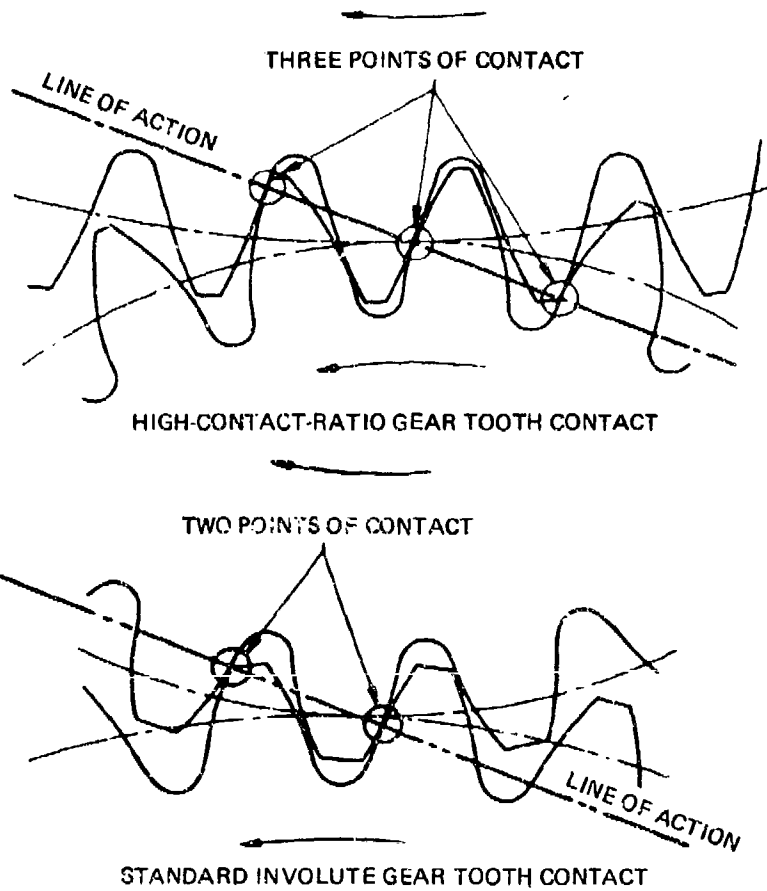


Figure C-7. Basic Meshing Principles of Standard Involute and High-Contact-Ratio Gearing.

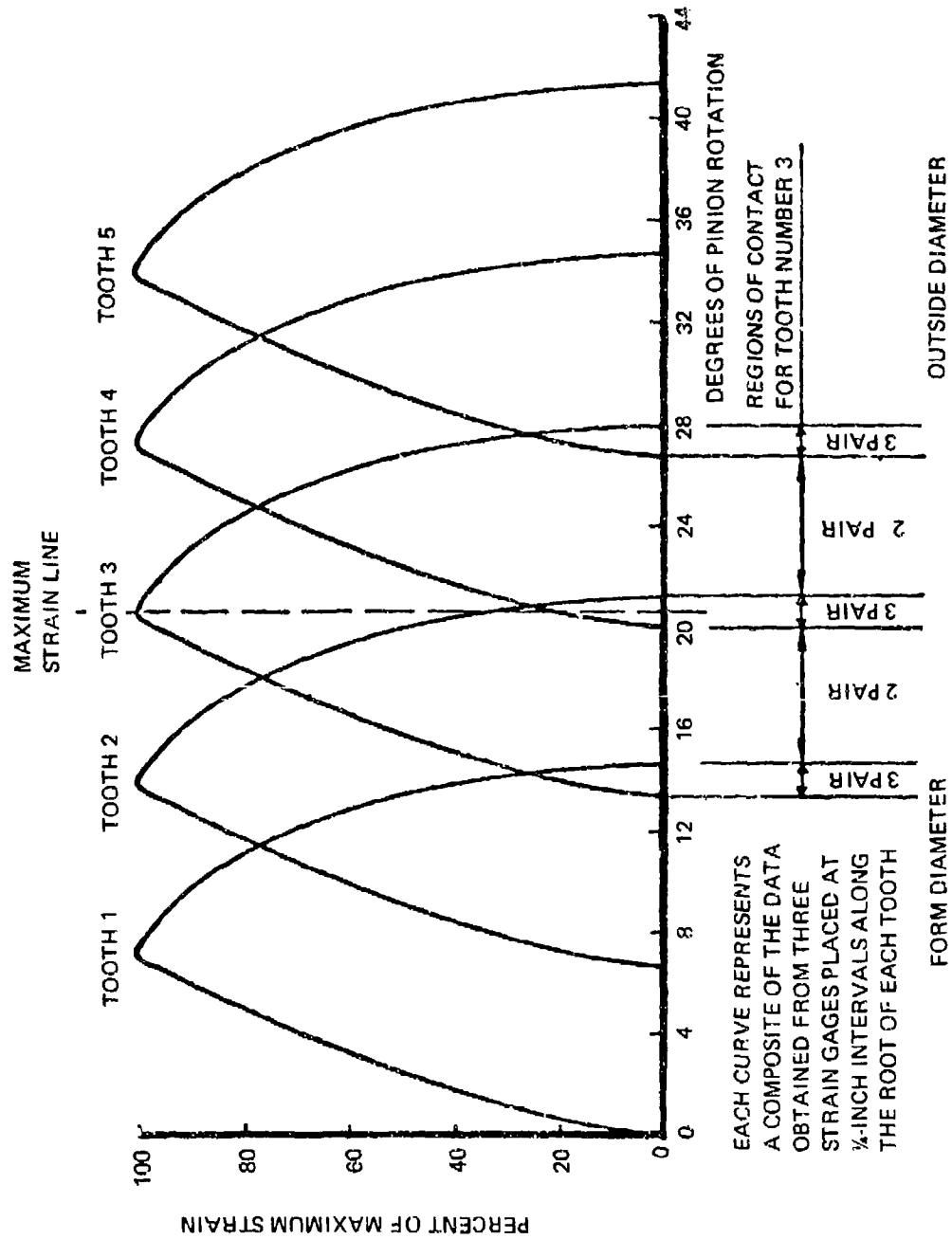


Figure C-8. Five-Tooth Plot of Strain Survey of High-Contact-Ratio Spur Gear.

thus be lighter in weight. The data obtained from the strain survey shown in Figure C-9 was also utilized to develop the tangential tooth load distributions shown in Figure C-9. The maximum load applied to any single HCR tooth can thus be seen to be only about 63% as great as the maximum load carried by any single standard tooth of equivalent design. This sharing of load also reduces the magnitude of the dynamic engagement and disengagement loads to provide quieter, smoother action. Helical gears are often used at high speeds to provide smooth action. This smoothness of action is obtained by the face overlap obtained from the helical tooth shape. Typical aircraft helical gears have face contact (overlap) ratios in the range of 1.5 to 2.0 yielding a net total contact ratio in the range of 1.6 to 1.5. HCR spur gears provide similar high speed characteristics without the disadvantage of thrust loading, however, the HCR concept can also be applied to helical gears to further improve their contact ratio while minimizing the thrust loading.

In addition to a reduction in the magnitude of the maximum load, the location of this maximum load along the profile is different on an HCR design. Unlike the standard gear which sees maximum load at the highest point of single tooth contact, the maximum load on an HCR gear tooth occurs very near (just below) the pitch diameter, as shown in Figure C-10. The combination of lower tooth loading and load repositioning produces root bending stresses approximately 20% less than an equivalent standard gear.

Similarly, the reduced load spectrum along the profile results in a substantial reduction in contact stress. The relative load capabilities of a typical set of standard and HCR involute gears is shown in Figure C-11.

As might be expected, there are limitations on the design and application of HCR gearing systems. The primary problem area is in the somewhat higher sliding velocities and slip ratios which occur, particularly in the pinion dedendum area, due to the extended contact length. In many cases, this does not cause a significant problem. In other applications, such as the Heavy Lift Helicopter drive system, HCR gearing is coupled with the added benefits of an advanced gear material to yield a substantial net improvement in system capacity. The advanced gear material (BMS7-223 developed by Boeing Vertol) provided the increased surface durability required to allow the HCR gears to operate at slightly increased sliding velocities.

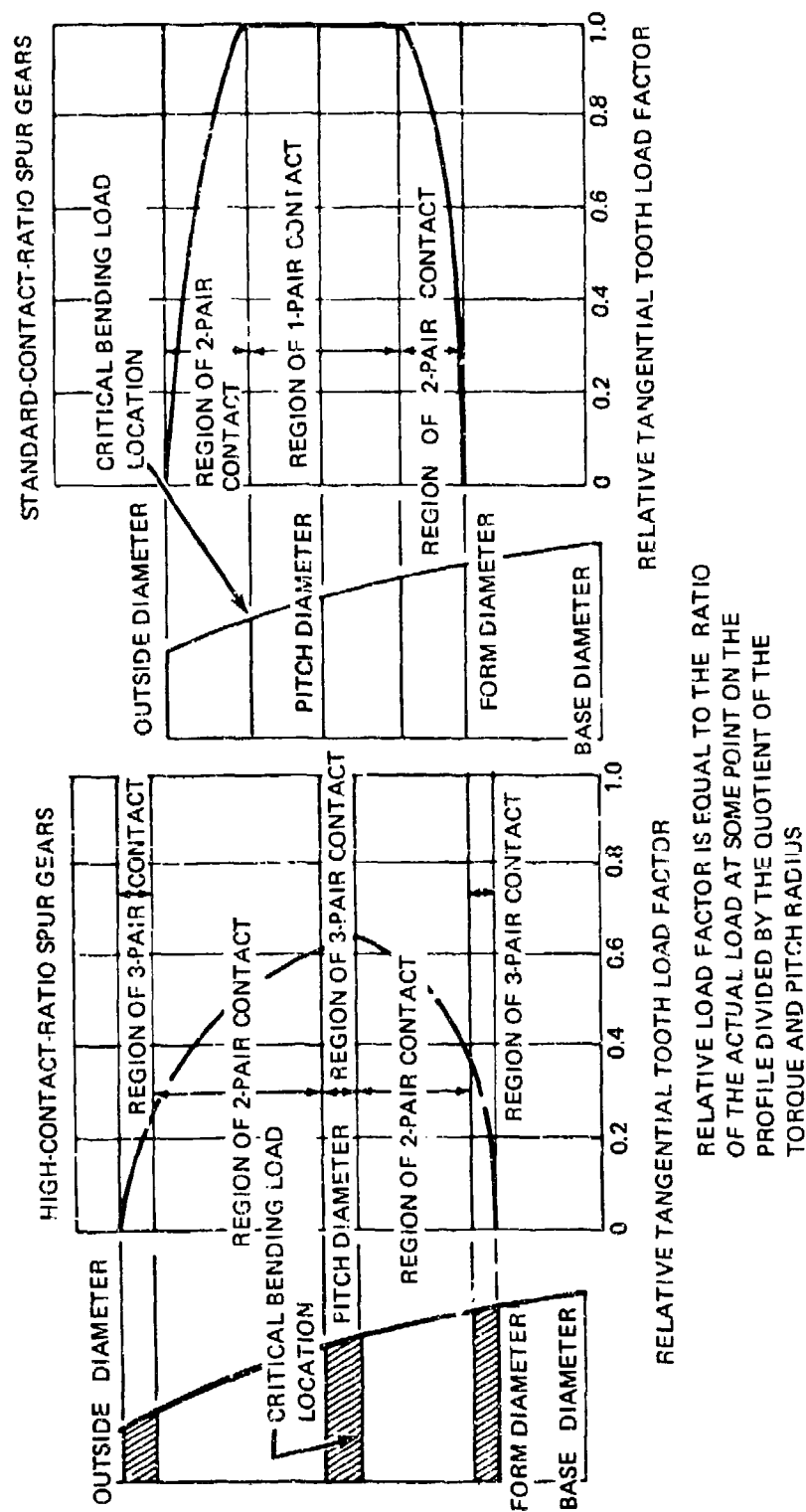


Figure C-9. Comparison of Standard and High-Contact-Ratio Tooth Loading.

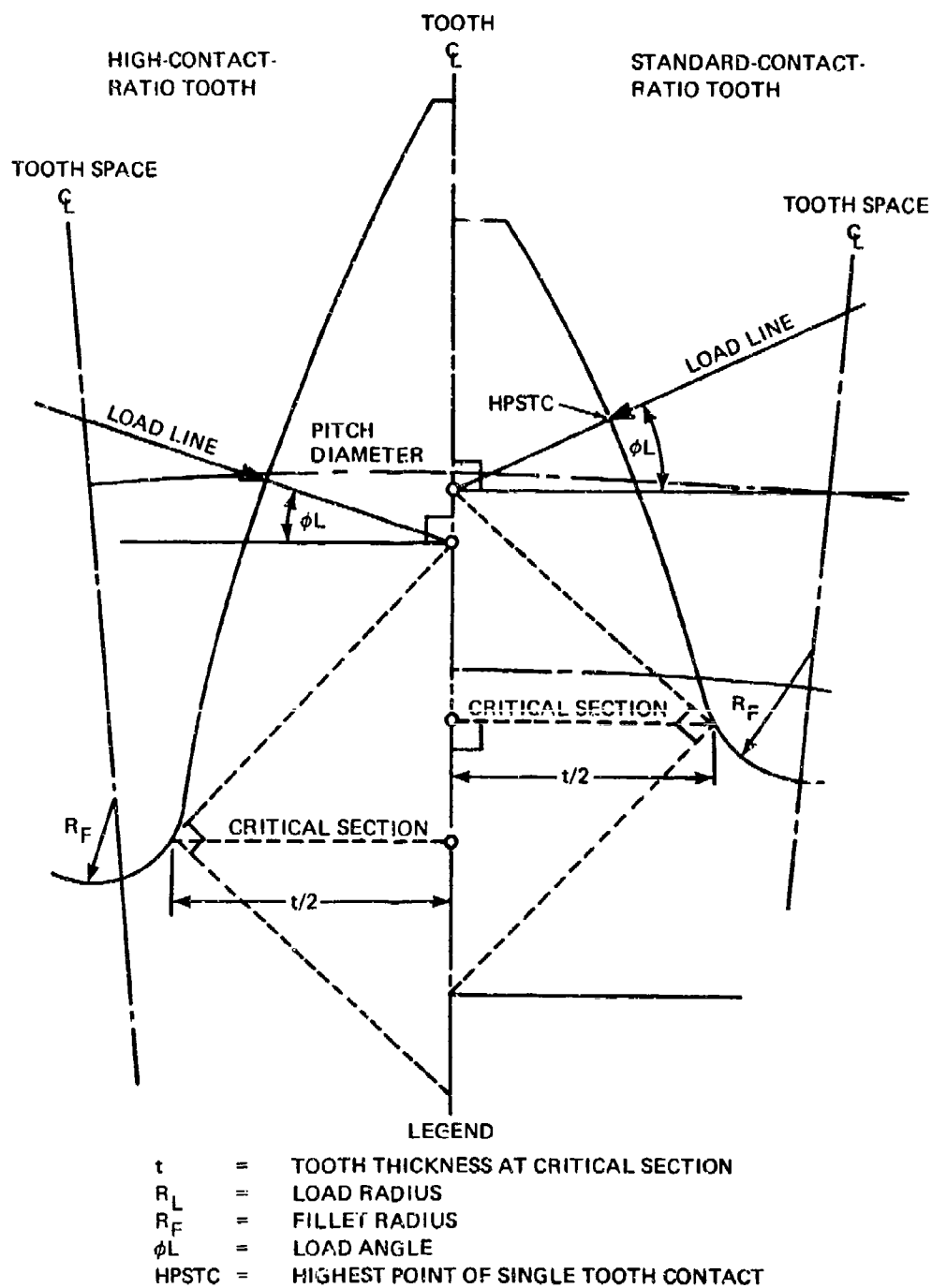
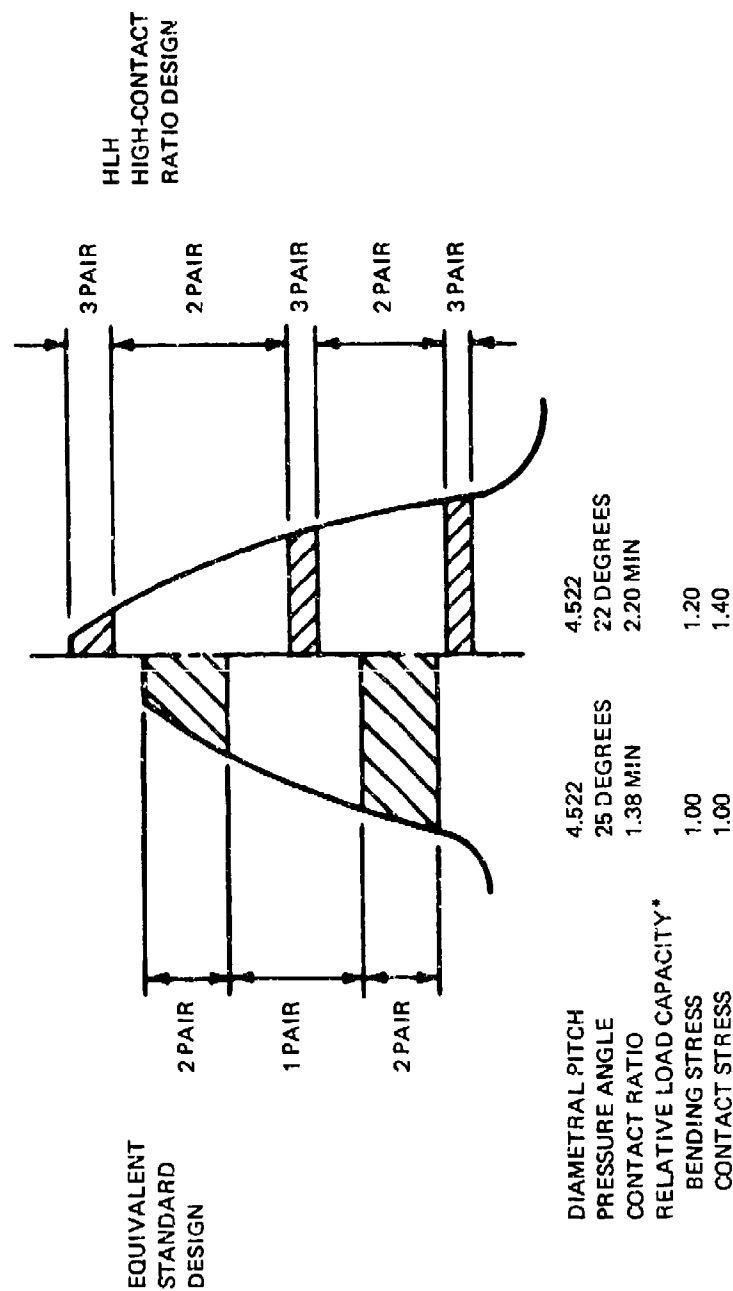


Figure C-10. Comparison of Standard and High-Contact-Ratio Bending Stress Layouts.



*Relative load capacity is the factor by which a given basic load must be multiplied when applied to the HCR gear set to produce the same stress as when the basic load is applied to the standard gearing.

Figure C-11. Comparison of Load Capacity of Heavy-Lift Helicopter (HLH) High-Contact-Ratio Spur Planetary Gearing and Equivalent Standard Design Gearing.

APPENDIX D
DESIGN SUPPORT TEST SUMMARIES

The following pages summarize the various test programs conducted in support of the drive system design and presents conclusions based on the results.

HIGH-SPEED TAPERED ROLLER BEARINGS

Background and Purpose

An initial high-speed tapered roller bearing development program, undertaken by Boeing Vertol Company and Timken Company, indicated the feasibility of the use of tapered roller bearings in a high-speed helicopter transmission. This program proved that a 3.5-inch bore modified tapered roller bearing can be operated at approximately 20,000 fpm cone rib velocity (16,000 rpm). At the conclusion of this initial development program, it was determined that additional work was needed to optimize the bearing design and lubrication system parameters. A Government contract was obtained to further evaluate the performance of tapered roller bearings analytically and experimentally. This work was reported in Reference 21.

Although the high-speed and load capability of tapered roller bearings has been demonstrated, additional test work was necessary to evaluate larger tapered roller bearings for application in the HLH Drive System. The increase in bearing sizes, increase in loads, higher speeds, and the steep-angled HM926700 series bearing were to be evaluated under HLH operating conditions.

The objective of this program was to develop a tapered roller bearing for an HLH application by testing and evaluating the HM926700 series tapered roller bearing at the loads and speed of the HLH combining transmission input pinion gear. The basic tapered roller bearing design parameters, oil-flow rates, initial test machine bearing adjustment, and emergency self-lubrication feasibility were to be determined.

The test program was organized to investigate and evaluate the following objectives:

- Design and build a high-speed tapered roller bearing test machine capable of testing 9-inch to 20-inch OD bearings at speeds up to 14,000 rpm with a maximum applied radial load of 25,000 pounds and a maximum applied thrust load of 10,000 pounds.
- Determine the number and size of radial lubrication oil holes required in the HM926700 series bearing.
- Develop the HM926700 series steep-angle ($26^{\circ}9'$) bearing to run at 14,000 rpm. The 14,000 rpm speed is an overspeed condition and was changed during the program to 11,500 rpm, corresponding to the in-flight cruising speed.

- Evaluate selected materials that could be used in a fail-safe bearing design. The evaluation of these materials was to be performed in a Timken lubricant and wear test machine.
- Evaluate two fail-safe bearing designs and determine the wear characteristics of the better of these two designs when operating in oil.
- Run a repeat fail-safe test on four previously tested fail-safe bearings.
- Test additional modified HM926700 series bearings to determine an optimum bearing setting (end-play adjustment) and an optimum oil-flow rate both to the large and small end of the bearing.
- Conduct a tapered roller bearing cone-flange oil distribution spin test to evaluate the effect of the angle and length of the radial lube holes in the cone which will, in turn, provide adequate oil distribution to the cone rib/roller end contact area.
- Manufacture and test the XC11439 series bearing (Boeing Vertol P/N 301-10676) in the high-speed test machine. This bearing represented the actual bearing used in the HLH/ATC combining transmission.
- Test four XC11439 series bearings (Boeing Vertol P/N 301-10676) for 150 hours or until damage occurs.

The results of these tests were used to establish the final design and installation requirements to be used in the high-speed tapered roller bearings in the HLH/ATC aft and combining transmissions.

Summary

The data derived from this program show that modified high-speed, steep-angle, HM926700 series bearings and shallow-angle, XC11439 series bearings can be successfully run at 14,000 rpm and 11,500 rpm, respectively, under a wide range of loading and can also withstand relatively high acceleration rates. Certain design, adjustment, and metallurgical considerations were found to be necessary and are covered in the detailed conclusions which follow.

Current technology and materials have not been developed to a point where it is possible to make a fail-safe (30-minute operation without oil) bearing for operation at these speeds (20,000 fpm tangential cone rib velocity). Length of operation without oil varies exponentially with speed dropping off sharply from 30 minutes above 6000 fpm cone rib velocity.

An alternate source of lubricating oil for fail-safe operation is the best approach to this problem. Previous work has shown that the tapered roller bearing can operate with small quantities of oil, thus making an alternate source practical.

Design and Build a High-Speed Tapered Roller Bearing Test Machine (Figure D-1)

A high-speed tapered roller bearing test machine was designed and built for this program to specifically test the HM926700 series bearing (9-inch OD). In the latter portion of the test program, the machine was modified to test the 8-5/8-inch OD XC11439 series bearing (Boeing Vertol P/N 301-10676). This machine is also capable of testing up to a 20-inch OD bearing with the proper modifications. Some minor machine shortcomings were discovered and corrected during testing. Basically, this machine performed satisfactorily throughout this test program.

Determination of Number and Size of Radial Lubrication Oil Holes in the HM926700 Series Bearing

Forty 0.040-inch-diameter radial lubrication oil holes were needed to adequately lubricate the roller end/cone rib contact. The size of the holes could be substantially smaller than 0.040-inch diameter; however, the size was set at a minimum of 0.040 inch to prevent foreign matter from clogging the holes and restricting oil flow.



Figure D-1. HLH High-Speed Tapered Roller Bearing Test Machine,
Shown Driven by 700-HP Drive System.

Development tests - Modified HM 926700 Series Bearings

The modified HM926700 series bearing can be operated at 14,000 rpm (25,000 fpm) under 15,619 pounds radial load and 4394 pounds thrust load and 195°F oil inlet temperature. The bearing cup OD temperatures, when tested under these conditions, ranged from 325°F to 335°F. Some of the bearings had spalls on the cone races after the test as a result of geometry distortion due to the temperatures exceeding 300°F.

The modified HM926700 series bearings can be accelerated from 0 to 10,000 rpm in less than 30 seconds and from 10,000 to 11,500 rpm in less than 5 seconds under 10 percent load (1230 pounds radial and 440 pounds thrust load applied to housings) from a room temperature oil or preheated oil start. After running at 11,500 rpm under 100 percent load (12,300 pounds radial and 4394 pounds thrust load), the bearings can be accelerated to 14,000 rpm in less than 5 seconds under 75 percent thrust loads.

Evaluation of Fail-Safe Wear-Resistant Bearing Materials

Tests in the Timken lubricant and wear test machine showed that Borkote materials show the least amount of wear during the oil-off tests. Tests also showed that the LP alloys gave the best overall life with a reasonable amount of wear. The LPA 404 alloy with 40 percent 4600 steel binder was the best of the LP alloys tested.

Evaluation of Two Fail-Safe Bearing Designs

Bearings with LPA 404 with 40 percent 4600 steel binder applied to the cone large end rib performed better than Borkote applied to the rib under fully lubricated conditions. The bearings with LP alloy applied to the rib were run for 24 hours with no abnormal wear. At the end of 24 hours, the oil was shut off, and the bearings continued to run for 8-1/2 seconds. The goal was 30 minutes operation without lubricating oil.

Repeat Fail-Safe Test

A repeat fail-safe test was run with four bearings with LP alloy that had been previously tested. This test was run for 3 hours before the oil was shut off. The bearings continued to rotate for 10 seconds. A suitable wear-resistant fail-safe material and a method of attaching this material to the bearing has not been reached with our present technology. An alternate source of lubricating oil should be considered as a fail-safe lubrication system.

Additional HM926700 Series Bearing Tests (See Figure D-2)

These tests showed the best bearing adjustment to be between 0.001 inch and 0.0035 inch end play. Bearing damage occurred when the end play was reduced to less than 0.001 inch and increased above 0.0035 inch.

The only significant difference from bearing sets appeared to be the level of retained austenite. Higher levels of retained austenite were less resistant to scuffing damage between the roller end and cone rib at the higher stress levels in steep-angle bearings. More work is needed to verify this conclusion, since the data obtained in these tests is very limited.

Tapered Roller Bearing Cone Flange Oil Distribution Spin Test

Results show that there is good correlation between the high-speed strobe light photographs showing the oil distribution from the radial oil lubrication holes and the computer program used to determine the percent of adequate lubrication at the cone rib interface.

Testing of XC11439 Series Bearings

Testing of the XC11439 series bearing was successful. Seventeen bearings in eight test setups were tested during this phase of the program. The duration of testing ranged from 1 hour to 126 hours. Three of the bearings had accumulated 150 hours.

As was expected, the bearing end-play adjustment had to be increased slightly with this shallow-angle bearing over that for the steep-angle, HM926700 series bearing. Successful tests were run with bench bearing end-play adjustments ranging from 0.0035 inch to 0.005 inch. A bench bearing end-play adjustment of 0.0025 inch resulted in premature bearing damage in one of the tests.

A mathematical approach to predicting start-up bearing adjustment (running approximately 5 minutes) and level off condition bearing adjustment (running several hours) has been developed. It shows that under the successful bench end-play bearing adjustments that were tested, the bearings were actually slightly preloaded under level-off test conditions.

Based upon the data generated, the design HLH/ATC high-speed tapered roller bearing used in the aft and compiner transmission has finalized. A total of 10 different size tapered roller bearings will be tested by Boeing Vertol in both bench transmission and DSTR test stands prior to installation into the prototype HLH.

A complete report on the test program is presented in Reference 22.

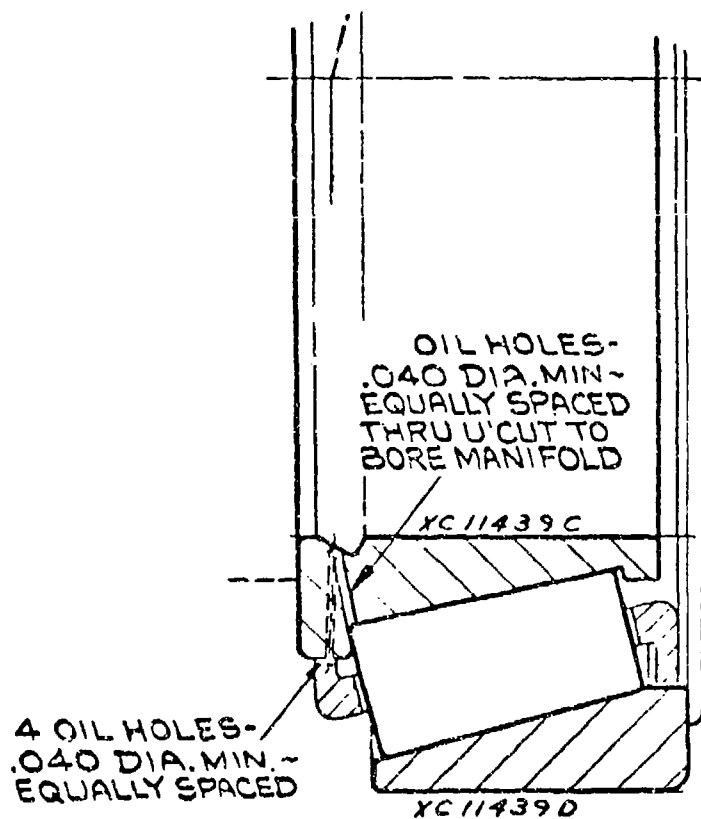


Figure D-2. Modified HM926700-Series Bearing With 17 Radial Holes to the Rib Face - Z Type Machined Cage

COMPLIANT ROLLER BEARINGS

Background and Purpose

The main gearbox of current Vertol helicopter power transfer systems use spherical roller bearings in their planetary gear system. With ever increasing power requirements, the use of this type of bearing severely restricts the use of optimum gear sizes and the potential weight reduction in this area. Spherical roller bearings have been mainly used for their ability to accommodate post deflections and misalignments which are experienced in the planetary gear system.

Trade studies have shown that cylindrical roller bearings could provide greater capacity in the same size bearing and thus provide higher fatigue life. The only objection to cylindrical roller bearings is their inability to accommodate severe misalignments. Field experience and testing of cylindrical roller bearings, even with special crowned rollers, under misalign condition show a drastic reduction in fatigue life. Therefore, to take advantage of the higher capacity ratio, a significant improvement in misalignment capability must be incorporated into the cylindrical roller bearing.

The primary objective of this program was to determine the feasibility of using a tandem cylindrical roller bearing with modified hollow-ended rollers (Figure D-3) to function under severe operating conditions in the HLH rotor transmission's 2nd-stage planetary system (Figure D-4). Static roller tests were performed to establish the optimum roller crown and hollow-end configuration which is capable of supporting high loads and misalignments. The test loads were established by bearing computer analysis of the HLH rotor transmission's 2nd-stage planet bearing which accounted for internal load distribution, internal clearance and flexibility of the planet gear. Testing was conducted between tandem hollow-ended rollers and flat plates to determine the load distribution on most heavily loaded rollers under the following specified load and deflection conditions:

- Load Condition - 18,000 pounds (equivalent to 10,400 hp to rotor transmissions)
12,000 pounds (equivalent to cubic mean load of 7200 hp to rotor transmissions)
8,000 pounds (lower power rating)
- Misalignment - .003 inch/inch

The results of these tests determined the feasibility of using a bearing with tandem hollow-ended cylindrical rollers operating at high loads and misalignment.

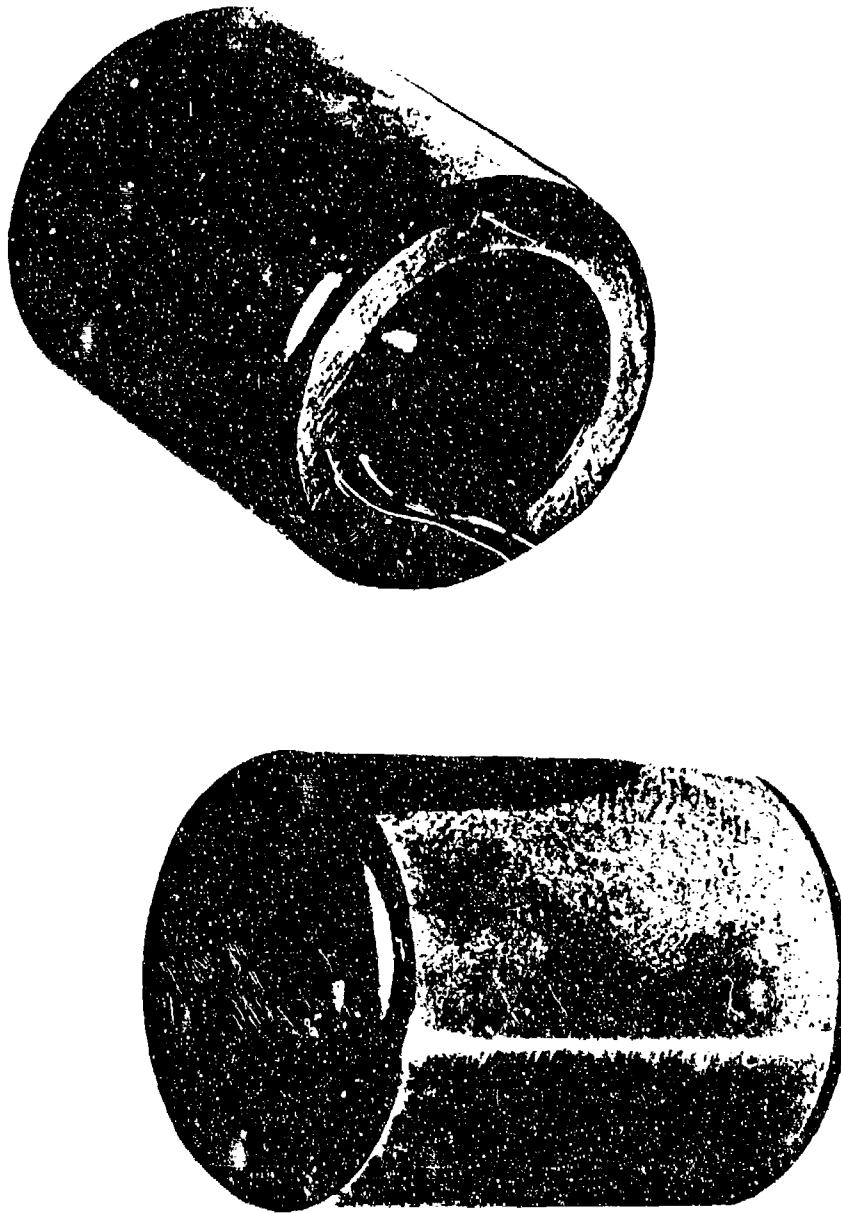


Figure D-3. Illustration of Hollow-Ended Roller Design.

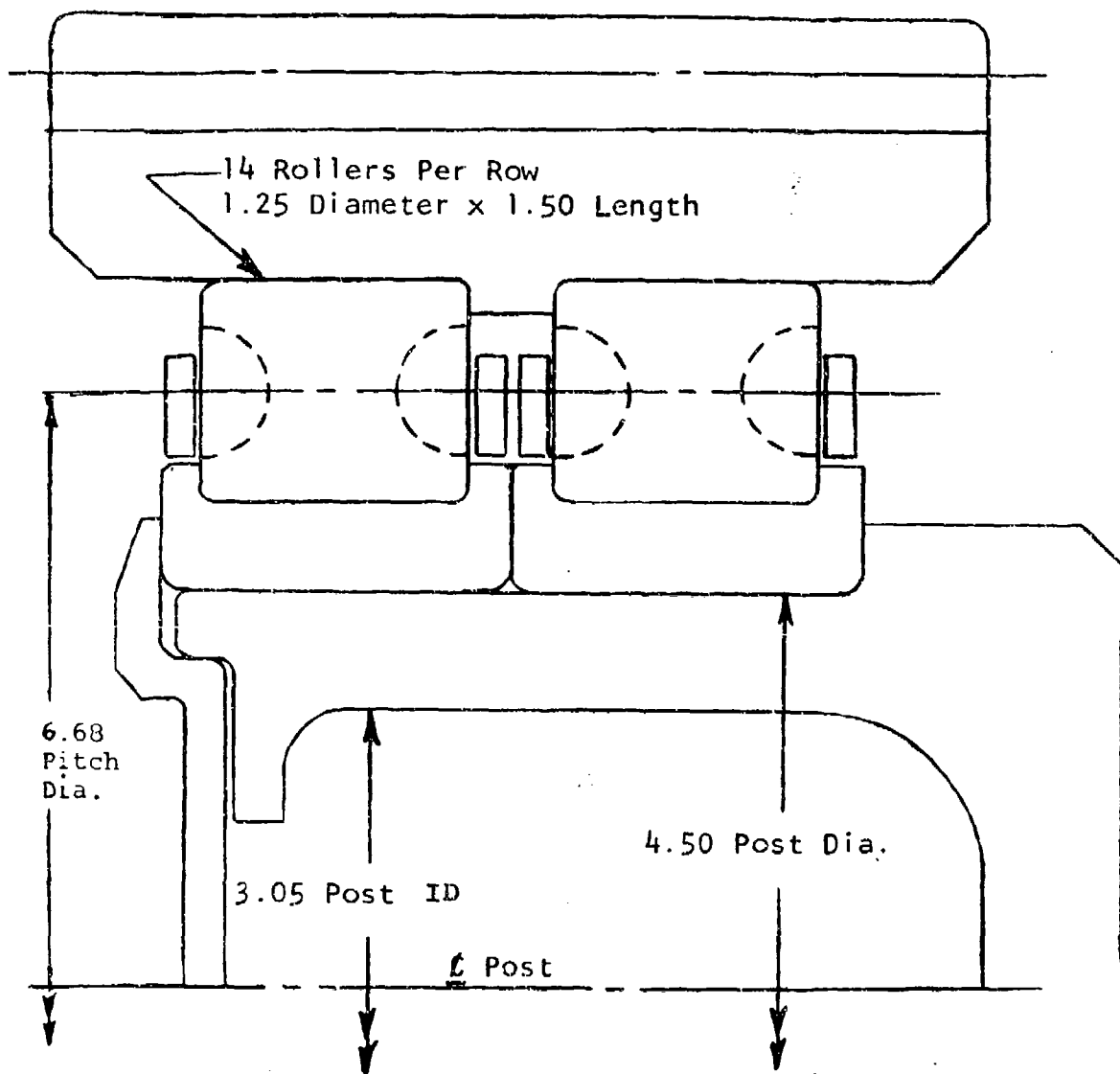


Figure D-4. HLH Design Study - Planetary Bearing (Second-Stage Planet).

Conclusions

The following sequential descriptions, with appropriate conclusions, logically include all conclusions reached as a result of the various investigations in this development program.

1. The conclusion resulting from a "Footprint" study to determine the influence of roller crowning on solid roller load distributions for 18,000 pounds applied load per roller set and .0005 inch/inch misalignment is as follows:

The solid roller with crown geometry #10, Table D-1, produces the best "Footprint" considering end of contact shape.

2. Crown #10 was applied to various hollow-ended roller configurations which were then subjected to an 18,000 pound load and .003 inch/inch misalignment. The following conclusion was made with respect to bore shape selection:

The roller with bore configuration 3 (Figure D-5) was responsible for the best "Footprint", considering both end of contact shape and maximum contact width.

3. A "Footprint" analysis was performed on this contact area yielding the load distribution on the roller. These results provided input data for a comprehensive stress analysis on the hollow-ended roller rim. Specific conclusions regarding the stress state existing in the rim of the most heavily loaded roller in the tandem set are as follows:

- a. The maximum shear stress located just inside the bore surface is 40,000 psi and is well within acceptable limits.

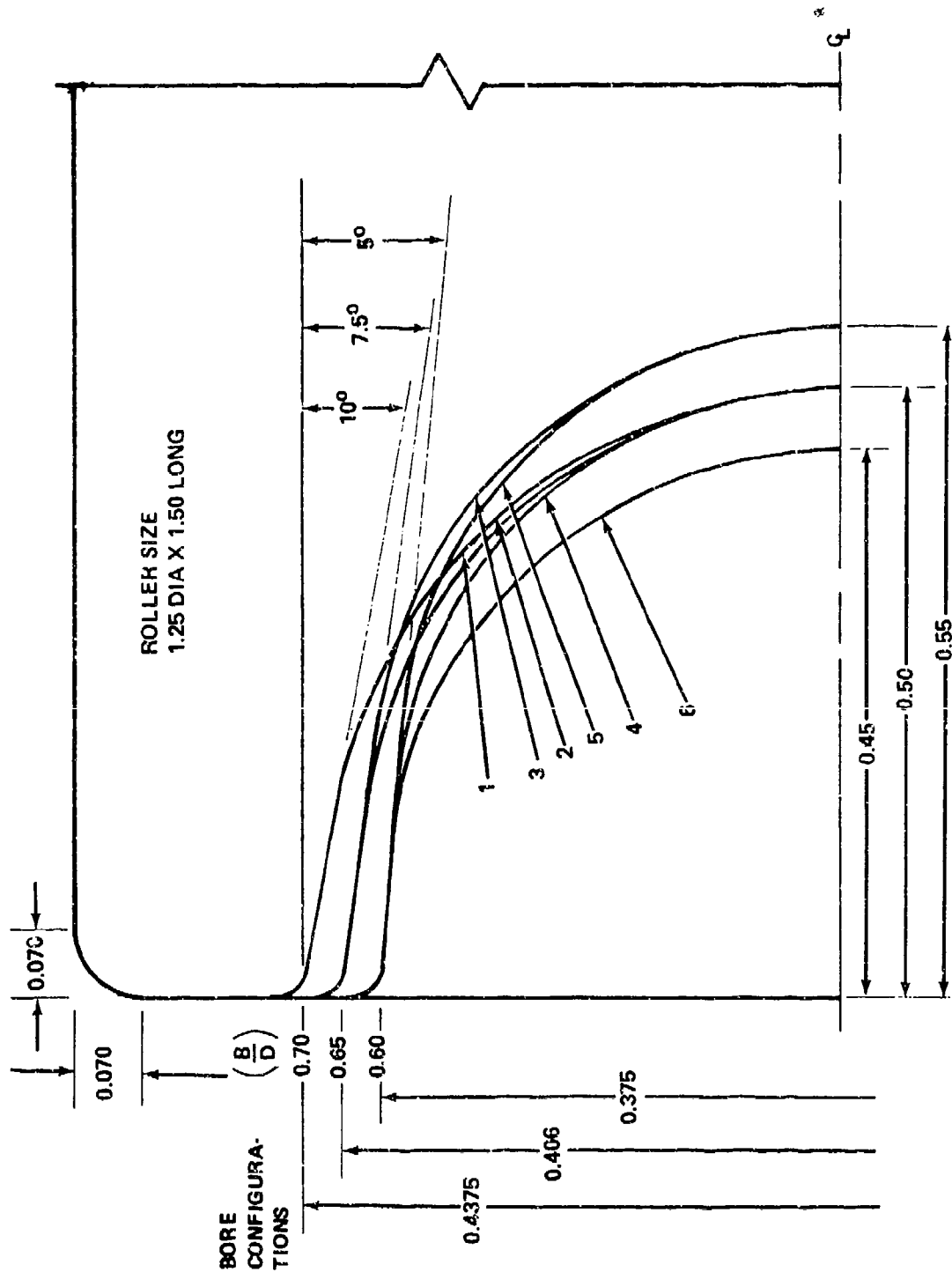


Figure D-5. Prototype Hollow-Ended Bore Shape Comparator

- b. The maximum subsurface shear stress (resulting from combining the Hertzian contact stresses with those induced from rim deflection) found near the surface of the roller, directly under the plane of the load, is 102,000 psi and is a reasonable static stress level.
 - c. As the significant shear stress at the outside diameter is substantially greater than that found in the bore, and assuming a good bore finish, the failure mode in the hollow-ended roller will be conventional outside diameter fatigue spalling, which is normal and predictable.
4. Tailored crowning was considered for the hollow-ended roller for operating conditions of 18,000 pounds load per roller set and .003 inch/inch misalignment. Conclusions from this investigation are:
- a. The best bore/crown relationship for the above specific conditions is bore 3 (selected previously) with crown #11 (Table D-1).
 - b. A reduction in the previously established maximum shear stress level (102,000 psi) is possible employing the above bore/crown combination.
 - c. "Footprints" created at 12,000 pounds and 8000 pounds with .003 inch/inch misalignment also exhibit satisfactory contact shapes.
5. Comparing a hollow-ended roller "Footprint" set to a respective solid roller set for the same application (18,000 pounds and .003 inch/inch), the following conclusions apply:
- a. The applied load is shared more favorably by the two hollow-ended rollers (heaviest loaded solid roller supports 16,029 pounds while the respective hollow-ended roller supports 14,938 pounds).
 - b. A 20% decrease in the subsurface maximum shear stress level found when comparing a hollow-ended roller to a conventional solid roller results in a significantly greater L_{10} fatigue life for the hollow-ended type.
 - c. The maximum Hertzian contact stress of the hollow-ended roller is 350,000 psi compared to a stress of approximately 400,000 psi for the solid roller configuration under identical load conditions.

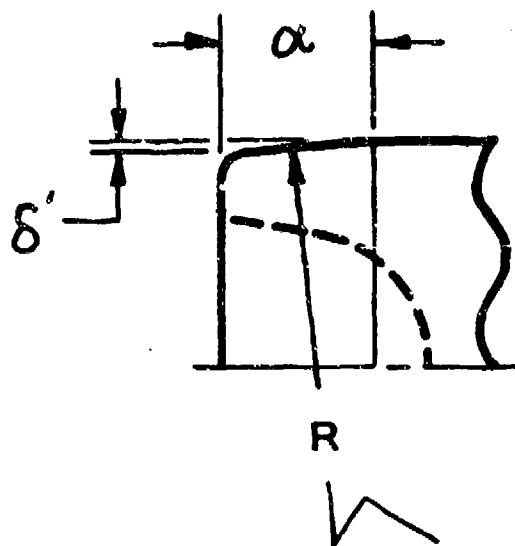


TABLE D-1. TEST ROLLER CROWN GEOMETRIES

CROWN NO.	CROWN RAD (R)-IN.	CROWN LENGTH (α)-IN.	CROWN DROOP (δ')-IN.
1	200	0.200	0.0004
2	200	0.280	0.0006
3	150	0.220	0.0006
4	120	0.170	0.0006
5	260	0.360	0.0006
6	110	0.204	0.0008
7	70	0.175	0.0010
8	110	0.740	0.0021
9	110	0.259	0.0010
10	70	0.197	0.0010
11	53	0.185	0.0013

- d. Life comparison based upon these conclusions for various HLH planet bearing configurations is shown in Figure D-6. These results show that the hollow-ended cylindrical roller bearing configuration provides the best life performance under the expected HLH operating conditions.

Although the data generated in this development program is of a conclusive nature as far as design feasibility is concerned with the assumed operating misalignment, it does not prove whether the proposed bearing, which includes hollow-ended rollers, will function with maximum benefit under the actual misalignment conditions which may be more or less severe than anticipated. In this application, because of the complicated nature of deflections involved in components other than bearings, it is very difficult to analytically determine the precise deflection expected to exist at the bearing locations. If the misalignments are found to be not as expected, the roller geometry may need further refinement to result in a more favorable load distribution, hence increasing reliability and life. The basic "Footprint" method may be extended to include evaluation of whole bearings.

A complete report on the test program is presented in Reference 20.

1. Bearing B-10 lives are based on cubic mean power of 7200 hp at 156 rotor rpm.
2. Bearing B-10 lives at .003 inch/inch misalignment were calculated based on test data of this report.

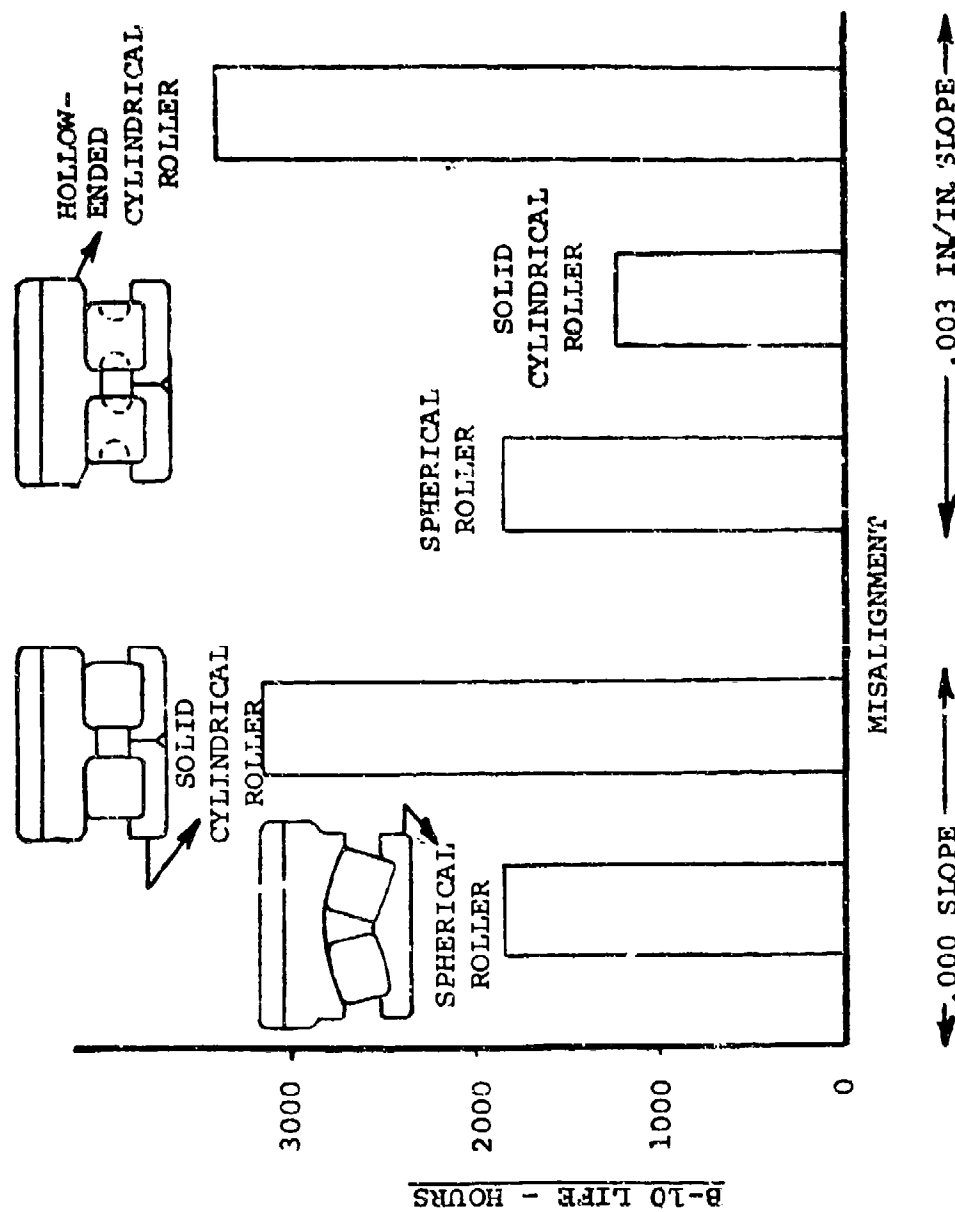


Figure D-6. Life Comparison-HLH Planet Bearing Candidates.

ROTOR SHAFT BEARINGS

The HLH rotor shaft support bearing requirements are directly influenced by the rotor head loads and the type of bearing configuration used to react these loads. To minimize the size and weight of these rotor shaft support bearings, the highest capacity bearing configuration must be used. Trade studies were conducted to determine the most efficient method of reacting the HLH rotor loads. The design study was conducted using the following ground rules:

1. Bearings to react rotor loads based on 118,000 pound gross weight and 6° flap angle
2. Rotor head loads for the above condition are:

Thrust	70,800 pounds
Drag	15,030 pounds
Moment	872,000 inch-pounds
Speed	156 rpm
3. Minimum bearing B-10 life of 2000 hours under these conditions
4. Bearing pitch diameter to be approximately 24 inches

The bearing configuration which meets the above criteria was duplex-mounted tapered roller bearings (Figure D-7) which had pitch diameters of 23.5 and 24.0 inches and contact angles of 35 and 45 degrees. In addition, these bearings were designed with pin-type cages which provided for maximum capacity within a given cross-sectional area. The pin-type cage allows for the rollers to be guided by pins through a hole in the center of each roller and allows for minimum space between rollers so that the maximum roller complement can be achieved.

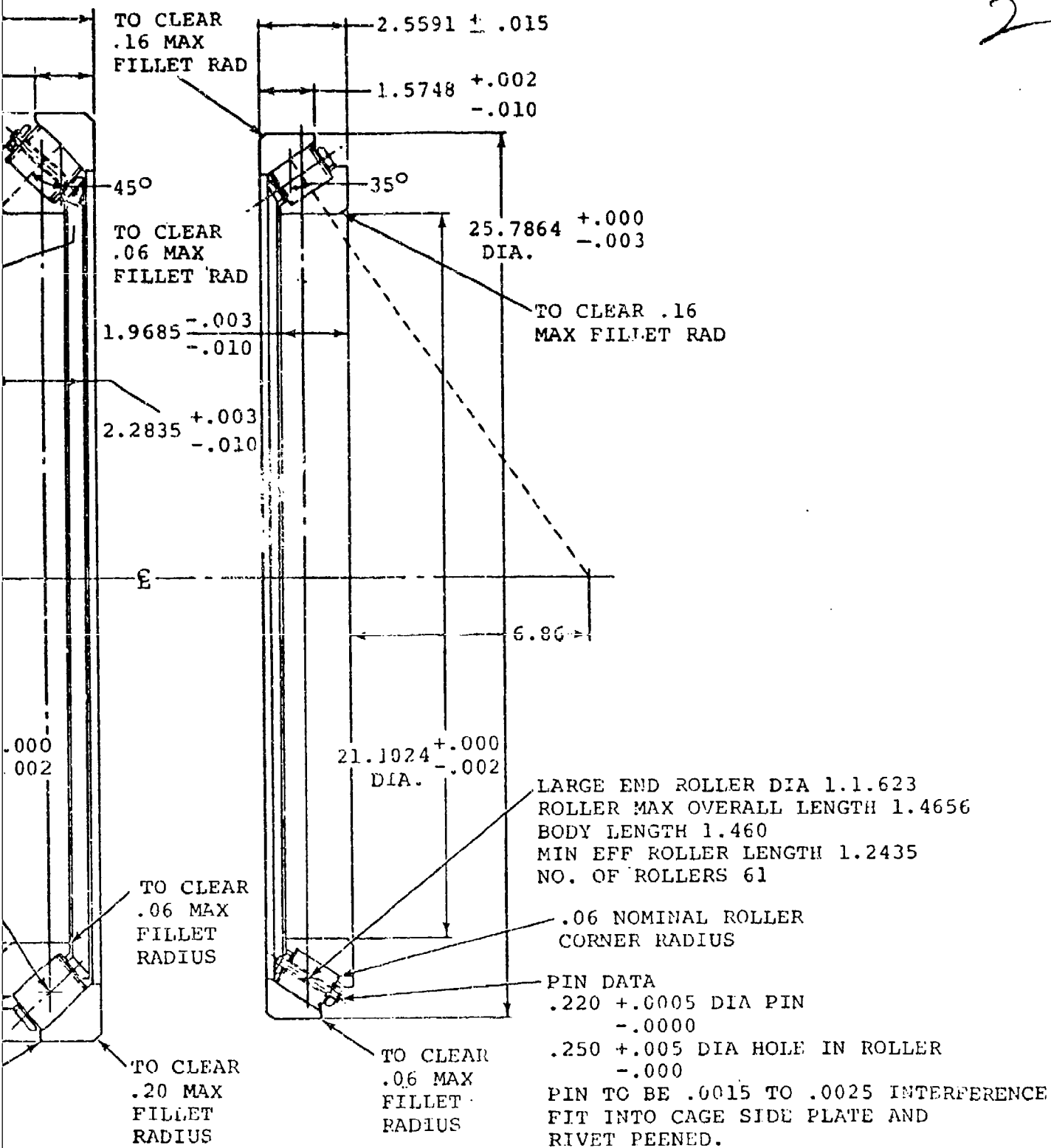
The use of tapered roller bearings to support combined thrust, radial, and moment loads is not new; but because of several departures from conventional bearing size and geometry configuration, a test program was conducted to evaluate the effect of the following critical parameters:

1. Effects of high contact angle on bearing performance
2. Effects of azimuth variations in stiffness of the bearing housing on the internal load distribution of the bearings
3. Effects of various preloads on bearing performance



-2 UFF

2



R BRG
and Description.

-2 UPPER BRG

4. Effects of low oil film thickness on bearing life
5. Effects of pin-type cage on bearing performance and life

The above parameters were evaluated in a back-to-back test rig which was designed to simulate the expected loading, lubrication system, housing stiffness, and preload of the HLH aft rotor shaft bearing application.

Three sets of bearings were designed and fabricated at the Timken Company, Canton, Ohio, to the specifications defined by Boeing Vertol.

After completion of the design and fabrication of the test bearings, several design changes were made concerning the HLH transmission bearings which resulted in dimensional changes to the rotor shaft bearings. A comparison of the test bearings and the actual transmission bearing is shown in Table D-2. These changes basically were the results of weight savings effort and design load changes. The test bearings used in this program simulated all the major design factors and therefore were tested to evaluate the HLH rotor shaft bearing application.

Accelerated-life testing was conducted with ratios from .28 to .36 between calculated test life and calculated service life. The service life calculation was based upon the thrust and moment conditions previously defined.

Summary of Testing

After 47.0 hours, a test rig failure necessitated replacement of upper housing bearings. The second set of bearings in the upper housing assembly accumulated 1093.0 total hours. Of this time, 693.0 hours was at a loading condition of 70.83×10^3 pounds thrust load and a moment of 2.16×10^6 inch-pounds. The remaining 400 hours was run at a 57.50×10^3 pound thrust load and a moment of 1.96×10^6 inch-pounds (Table D-3).

The bearings in the lower assembly had a total test time of 1140.0 hours. Of this time, 719.5 hours was at a thrust load of 70.83×10^3 pounds and a moment of 2.16×10^6 inch-pounds. A total of 400 hours was run under a thrust load of 57.50×10^3 pounds and a moment of 1.96×10^6 inch-pounds. The initial 16 hours was run under a "no-load" condition followed by a 6.5-hour interval during which the thrust load was increased in approximately 10 percent intervals.

During the break-in period, a temperature rise of 20°F was measured under no-load conditions and 40°F under full loading

TABLE D-2. COMPARISON OF TEST BEARINGS AND ACTUAL HLH TRANSMISSION BEARINGS

Bearing Location	Upper Bearing		Lower Bearing	
	Test Rig	HLH Transmission	Test Rig	HLH Transmission
Boeing Vertol P/N	SK301-10257-2	301-10406-1	SK301-10257-1	301-10409-1
Contact Angle, deg	35	35	45	45
Pitch Diameter, in.	23.5	23.4	24.0	24.08
Number of Rollers	61	66	52	56
Roller Diameter, in.	1.162	1.052	1.435	1.325
Roller Length, in.	1.460	1.120	1.829	1.423
Radial Capacity, lb	44,000	31,400	50,000	36,400
Thrust Capacity, lb	78,500	56,000	128,000	93,500
Cage Design	Pin Type	Pin Type	Pin Type	Pin Type
Roller Spherical End Radius, pct	80	80	80	80
Weight, lb	87.7	60	137.5	98

TABLE D-3. TEST BEARING LIFE SUMMARY

Bearing Location	Bearing Part No.	Cubic Mean Equivalent Radial Test Load, lb	(1) L ₁₀ , hr	Test Time, hr	Ratio = $\frac{\text{Test } L_{10}}{\text{Test Results}}$	Test Results
Upper Bearing Upper Housing	SK301-10257-2	80,500	3855	1090	0.283	No Failure
Lower Bearing Upper Housing	SK301-10257-1	95,000	3407	1090	0.334	Spalled
Lower Bearing Lower Housing	SK301-10257-1	95,200	3385	1138	0.336	No Failure
Upper Bearing Lower Housing	SK301-10257-2	80,600	3840	1138	0.296	No Failure
(1) Includes a material life improvement factor of 3.0						

conditions without preheating the oil. During testing under the prescribed operating conditions, the peak "g" levels were between 1.0 and 2.0. The test assembly power consumption was approximately 1.5 kw under steady-state conditions. Total lubricant flow was 3.0 gpm.

The first indication of a possible bearing failure occurred at 899.5 total hours test time on the upper assembly bearings.

Inspection of the bearings at the conclusion of the test program (1093.0 total hours on the upper assembly and 1140 total hours on the lower assembly) revealed that the lower bearing in the upper assembly had failed. The fatigue failure (spall) may have been influenced by the numerous failures of the preload bolts and edge loading of the rollers caused by the lateral growth of the bearing cone when the preload plate deflected. The failed bearing had 38 spalled rollers and the cup had several spalls in the area of the highest load application and greatest housing stiffness.

The tungsten-carbide bearing seats exhibited excellent wear properties in spite of the severe conditions imposed on them during the test program. From the experience of many assemblies and disassemblies, it appeared that the hard (Rc-72) and smooth surface (3-12 in. rms) of the tungsten-carbide material is very beneficial for installing and removing the bearings from the shaft, as was the inclusion of an oil groove in the bearing seats. The use of 440C stainless steel deposited by a spray welding process for bearing seats does not appear to be suitable for this application.

Post-test visual hardware inspection indicated that the alkaline copper plating on the bearing cone bores, combined with an increase in interference fits, contributed to the improved surface conditions at the bearing and shaft interface.

Of the analytical and experimental methods investigated to determine bearing preload spacer lengths, the experimental method was more successful in that it was easier, more reliable, and required fewer regrinding operations to establish the desired preload setting.

Conclusions

1. The use of large-diameter, steep-contact-angle tapered roller bearings to support the HLH rotor shaft provides good performance and adequate fatigue life.
2. Azimuth variation in stiffness of the bearing support housing does affect the internal load distribution of the bearing. Initiation of spall failures is associated with the mounting arms of the housing which produce local concentrated peak loads.

3. Various preloads from line-to-line to 0.0015 inch appear to be adequate and practical for the HLH rotor shaft bearings. This preload range is sufficient to provide good performance without excessive heat generation.
4. Low oil film thickness does not appear to affect bearing performance or fatigue life. There was no evidence of surface distress on the raceways and roller spherical end surfaces.
5. The pin-type cage used in the HLH rotor shaft bearings is adequate and allows maximum bearing capacity. There was no evidence of cage distress or pin wear at completion of testing.
6. Copper plating the cup outer diameter, cone bore, and cone back face appeared to minimize fretting damage during operation.
7. The type of preload clamp-up plate used in this test program had a significant effect on reducing bearing performance and life.
8. Based upon the results obtained from this test program, it is expected that the actual HLH aft rotor shaft bearing performance should be adequate and a life of more than 1300 hours should be achieved. (Table D-4).

A complete report on the test program is presented in Reference 23.

TABLE D-4. HLH ROTOR SHAFT BEARING LIFE SUMMARY

Bearing Part No.	Location	Equivalent Radial Load, lb	L ₁₀ Life, hr	Fatigue Life Ratio From Test	Aircraft Flight Time Equivalent To Total Test Time, hr
301-10406	Upper Bearing	54600	4560	0.283 0.296	1290 1352
301-10409	Lower Bearing	64700	4250	0.334 0.336	1420 1428
*L ₁₀ Life Includes a Material Life Improvement Factor of 3.0					

ENGINE SHAFT SUPPORT BEARING

This bearing development program was directed toward the development of a grease-lubricated ball bearing to operate at 632,500 DN (DN is the product of the bearing bore diameter in millimeters times the bearing speed in rpm) in a simulated HLH engine shaft support bearing housing. The bearing chosen for testing was the MRC 111-KS deep-groove ball bearing with a 55 mm bore. The operating conditions for this test program simulated a combination of the HLH engine and synchronization shaft support applications, and were as follows:

Shaft Speed	11,500 rpm (engine shaft)
Shaft Misalignment	0° 15'
Shaft Inclination	34° (synchronization shaft)
Shaft Weight	80 pounds
Shaft Unbalance	0.10 + 0.02 inch-ounce
Lubrication	Grease
Ambient Temperature	180°F
Duration	300 hours without regreasing

Prior to actual full-size bearing testing, preliminary screening tests were conducted to establish the type of grease to be used. Testing was conducted on 204 size ball bearings operated at 32,000 rpm (640,000 DN). These tests indicated that Aeroshell 22 grease, meeting Government specification MIL-G-81322, gave satisfactory performance as a lubricant under these test conditions.

To accomplish the full-scale objectives, four cage designs and two housing designs were initially proposed and put into test. As testing was performed, the need for additional bearing and housing modifications became apparent. The program was expanded until a final bearing and housing configuration was obtained to achieve a 300-hour regreasing interval.

After the completion of this program, additional testing of the final bearing and housing configuration was conducted as authorized by Contract DAAJ01-73-A-0017. This testing demonstrated the ability of high-speed grease-lubricated ball bearings to operate satisfactorily through a number of regreasing intervals (300 hours).

Preliminary Grease Evaluation Test Rig

Preliminary grease screening testing was conducted using a MRC 1000°F grease test spindle whose basic use is to evaluate the high temperature performance requirements of most military grease specifications. The test method employs two 204-K Conrad-type bearings on a belt-driven spindle (Figure D-8). The unit can be used for testing lubricants at temperatures up to 1000°F, with applied bearing thrust loads from 0 to more than 1000 pounds and at speeds up to 35,000 rpm. All spindle parts are fabricated from stabilized high temperature die steel, and all critical surfaces are hard chrome plated to prevent high temperature oxidation. This test unit meets the requirements for the apparatus specified in the Coordinating Research Council L-54 Research Technique.

The test rig was set up with a high-speed drive to evaluate the performance and capabilities of candidate greases to lubricate the 204 test bearing at a DN of 640,000. The operating conditions of the test rig were:

Speed	32,000 rpm
Bearing	MRC 204-S-17
Thrust Load	50 pounds
Lubrication	Candidate greases
Temperature	180°F or higher, no heat added

These tests showed that Aeroshell 22 grease, meeting specification MIL-G-81322, gave the best performance of all the greases tested.

Full-Scale Bearing Test Rig

Two test machines were fabricated to conduct full-scale bearing tests. The test machines were designed to operate under the following conditions:

Shaft Speed	11,500 rpm
Shaft Incline Angle	34°
Shaft Misalignment	15 minutes
Ambient Temperature	180°F
Shaft Weight	80 pounds
Shaft Unbalance	0.10 \pm 0.02 inch-ounce

In addition, the bearing housings were required to match a specified external configuration and the housings were mounted on elastomeric mounts. These mounts are similar to those presently used on helicopters to reduce shaft misalignments and improper positioning of the shaft and bearing.

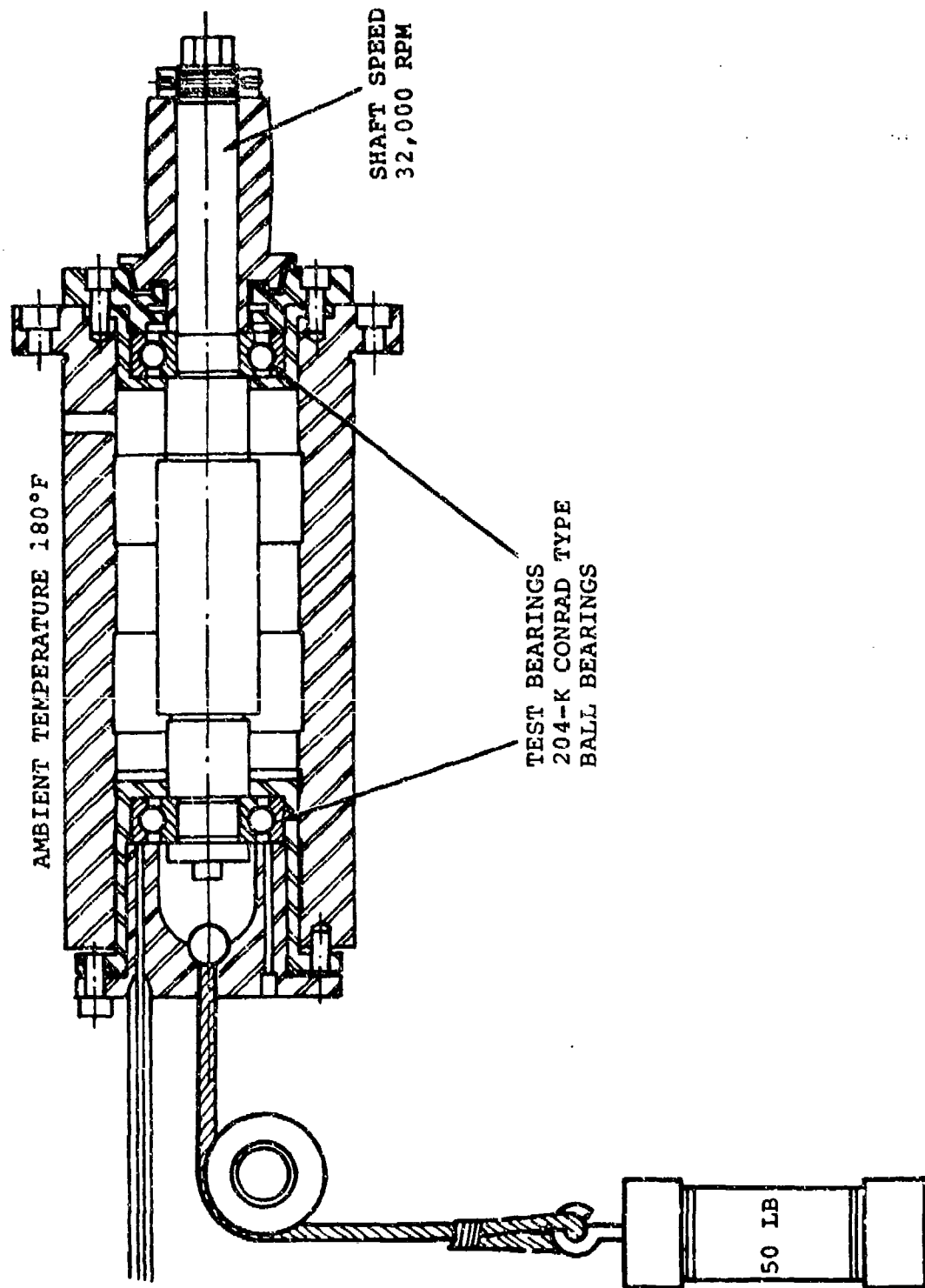


Figure D-8. MRC High-Temperature Grease Test Spindle.

Each test spindle tested two bearings and was driven by a 10 horsepower alternating-current electric motor. Shaft speed was essentially constant and was reached soon after start-up.

Two spindles were fabricated for this test program. A plain housing was installed on the drive end of the rig, and a grease-circulating device was installed on the outboard end. After the first test on each spindle, the grease circulating devices were changed from the "uphill" side of the outboard housing to the "downhill" side. At the same time, labyrinth seals with 0.10 inch diametral clearance were installed on both sides of each housing.

Three tests ran with no grease circulating or flinging device in either housing. Final testing was done with washer-type grease flingers on both sides of each test bearing to retard grease migration, as shown in Figure D-9.

Summary of Testing

Of the several cage designs initially tested, only the machined inner-land-riding S-Monel cages consistently ran the scheduled 300 hours. All specimens of the inner-land-riding S-Monel cage designs suffered objectionable wear, and bearings which operated on the drive end of the test rig consistently experienced greater wear than those on the outboard location. The Design 3 cage, incorporating silver-plate, experienced the least wear or damage of the cages tested prior to test 16.

Performance of pressed-steel cages, both with and without Teflon-S coating, was somewhat erratic. Two bearings ran until the 300-hour scheduled suspension; one cage failed at 110 hours; another cage failed at 246 hours. One bearing which ran the scheduled 300 hours showed overheated ball pockets. While the pressed-steel cage has the advantage of minimum bulk and permits a maximum grease fill, it does not have the reliability which the application demands. The control of manufacturing tolerances of this type of cage design appears to be the major disadvantage.

The fail-safe cage with DuPont Vespel SP-21 inserts appeared to be too bulky and too difficult to lubricate for this application. A basic problem was the small section of the MRC 111-KS ball bearing. Machining operations on SP-21 material require some minimum section for structural stability. When space within the bearing package is limited, the supporting frame or the space for lubricant is seriously reduced. The original design did not permit adequate lubrication. When this design was modified by removing sufficient stock from the frame to significantly improve lubricability, the

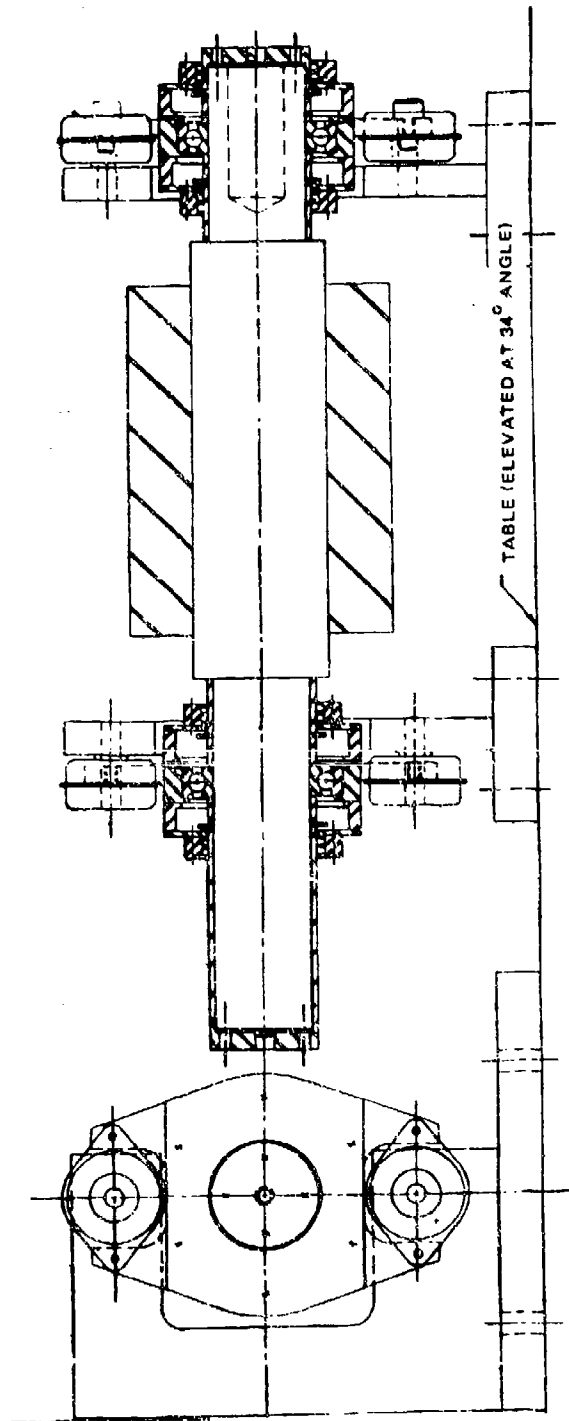


Figure D-9. Test Rig, Version 4.

structural strength was impaired and cage failure occurred. In a heavier section bearing this fail-safe concept could be quite satisfactory.

The steel cage and the outer-land-riding S-Monel cage designs did not have sufficient structural strength for the application and failed during its testing.

At the completion of test 15, a review of all the test data was conducted to determine what changes could be made to eliminate the serious cage wear problem. A review of each of the bearing temperatures, both unheated and heated, was conducted. This review showed that an increase in race curvature resulted in lower operating temperatures and that the ball-riding, pressed-steel cage also provides good operating characteristics. Therefore, the final bearing configuration tested (Figure D-10) included increased race curvatures and a machined ball-riding S-Monel silver-plated cage. Very little cage wear occurred during 300 hours of testing this design; therefore this design satisfied the HLH/ATC design criteria.

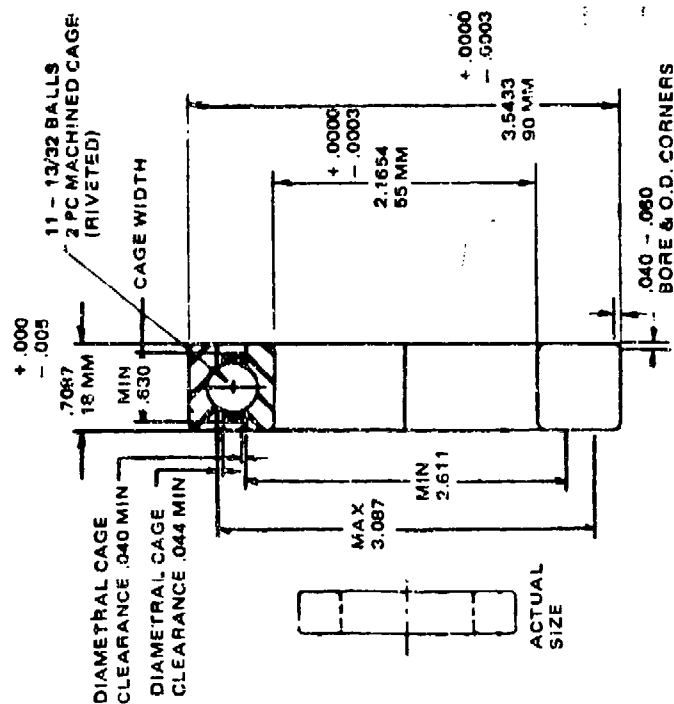
The final housing configuration (Figure D-11) that provided adequate grease retention was a combination of labyrinth seals plus shaft flingers.

Conclusions

This test program established that a Conrad type ball bearing operation at 632,000 DN with grease lubrication is entirely within the state-of-the-art. However, housing design, bearing geometry, and cage design are very critical and greatly influence the performance of the bearing.

The following design criteria were established for the successful operation of the HLH/ATC engine shaft support bearing for 300 hours without regreasing:

1. Aeroshell 22 grease conforming to military specification MIL-G-81322 is a satisfactory lubricant for the HLH application. Later work indicated Mobile-28 grease conforming to MIL-G-81322, as also satisfactory lubricant.
2. Misalignment presented the greatest hazard to successful bearing operation in this program; consequently, the bearing raceway curvatures were modified (increased to 53% on the inner surface and 54% on the outer surface) to reduce the effects of misalignment on cage wear, raceway distress, and reduced friction losses.



- (1) ABEC - 5 GRADE
- (2) MATERIAL:
RINGS - VACUUM CONSUMABLE
ELECTRODE PROCESS M-50
STEEL R_C 60 MIN.
BALLS - VACUUM CONSUMABLE
ELECTRODE PROCESS M-50
STEEL R_C 60 MIN.
CAGE - S-MONEL
RIVETS - SAE 1010 STEEL
- (3) RADIAL CLEARANCE .0016 - .0020
MEASURED UNDER 11 LBS GAGE LOAD
- (4) SURFACE FINISH:
BALLS - 2 RMS
RACEWAYS - 8 RMS
O.D. - 16 RMS
BORE - 16 RMS
RING FACES - 16 RMS
O.D. OF INNER - 16 RMS
BORE OF OUTER - 16 RMS
- (5) RACE DEPTH:
INNER 22% OF BALL DIA NOM
OUTER 20.5% OF BALL DIA NOM
- (6) RINGS TO BE 100% MAGNETIC PARTICLE
INSPECTED PER ES-105
- (7) BEARINGS TO BE 100% VISUAL INSPECTED
PER ES-139
- (8) CAGE MUST BE 100% FLUORESCENT PENETRANT
INSPECTED PER ES-106
- (9) RINGS & BALLS TO BE 100% NITAL ETCH
INSPECTED PER ES-109
- (10) RIVET SHANK DIA .068
- (11) CAGE POCKET CLEARANCE .031 - .036
- (12) CAGE SILVER PLATED .001 - .002 THICK
PER AMS 2412
- (13) CAGE TO BE BALANCED TO 3 GRAM CENTI-
METER MAX.
- (14) INNER RACE RADIUS 53% OF BALL DIA NOM
OUTER RACE RADIUS 54% OF BALL DIA NOM

Figure D-10. Modified Test Bearings, Cage Design 6.

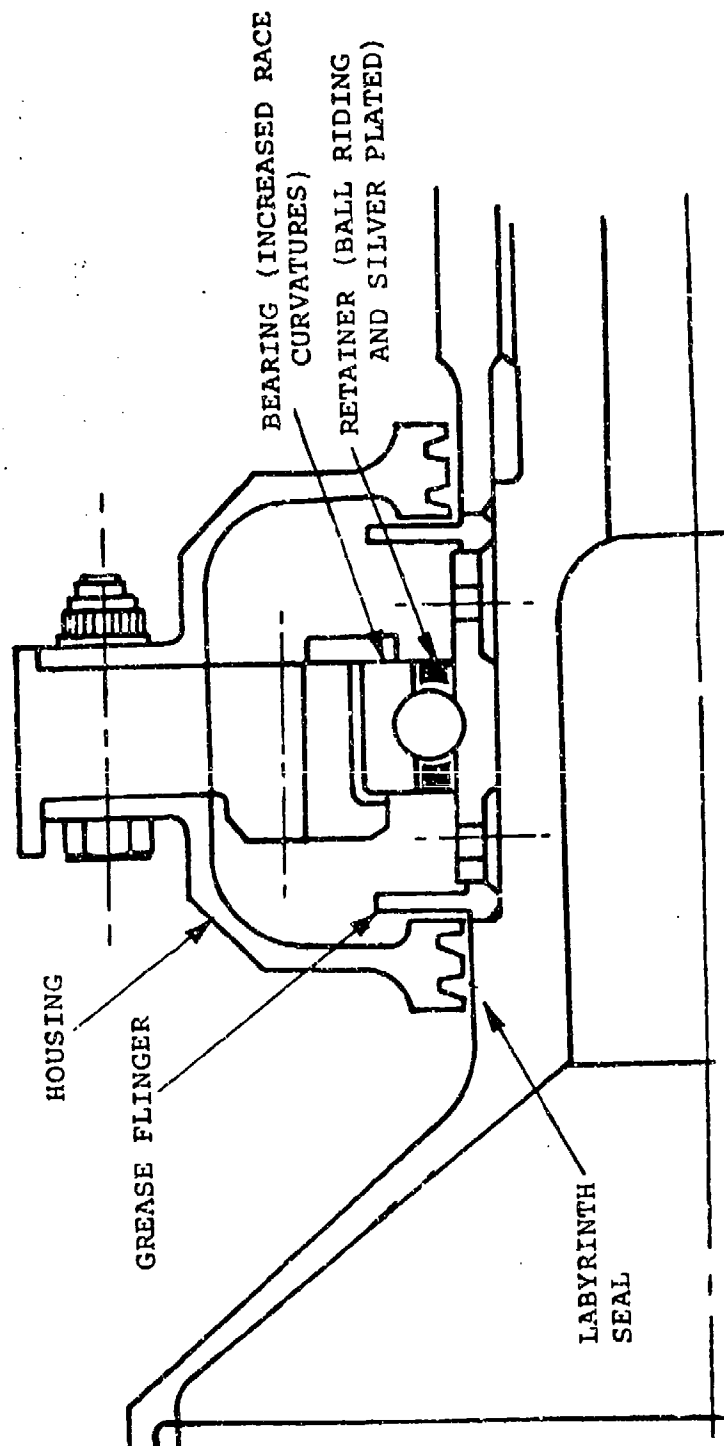


Figure D-11. Final HLH/ATC Engine Shaft Support Bearing Configuration.

3. The use of shaft flingers and labyrinth seals provides adequate grease retention within the bearing housing cavity. However, excessive vibration or temperature may cause some migration of grease past the flingers and seals.
4. The use of standard regreasing procedures, such as pumping grease through a grease fitting until grease is purged through seals, is a satisfactory method of regreasing the bearing. Brief temperature excursions do occur after regreasing, but temperature stabilization is achieved after a short period of operation.
5. The best cage configuration is a silver-plated, machined, ball-riding S-Monel cage. The cage should be balanced prior to assembly to insure satisfactory operation.

Based upon the above design criteria, the HLH/ATC engine shaft support bearing and housing shown in Figure D-11 were designed. A complete report on the test program is presented in Reference 24.

GEAR MATERIAL EVALUATION

Vasco X2 steel, a low carbon version of H12 tool steel, has exhibited excellent hot hardness and scoring resistance. Previous IR&D and R&D programs resulted in the selection of this material for the HLH/ATC transmission components.

The specific objectives of this program were to develop proper understanding of the metallurgical and mechanical properties of this material by determination of the following:

- Crack propagation rates in both air and corrosive environments.
- Impact strength.
- Surface contact fatigue strength and its relationship to various heat treat parameters.
- Effect of the duplex microstructure on the endurance limit of the core material.
- Hardenability.
- Effects of hardening and tempering temperatures and time, on both case and core materials.
- Fatigue strength of decarburized core material.
- The surface oxidation mechanism which permits carburization to occur uniformly.

The material used in the investigation was procured to Vertol Specification BMS 7-223 and Vasco Specification MB-X2 (Appendixes A and B). The material was consumable vacuum remelted and was produced by Vasco, a Teledyne Company, Latrobe, Pa. Throughout this report, the Vasco X2 (0.15% carbon) material is designated "X2". The contractor procurement specification for X2 is BMS 7-223.

The individual elements of this test program with the significant results are listed below and summarized in Table D-5.

Fatigue Crack Propagation Rates

Sixteen crack propagation test specimens were tested in several environments at stress levels which might be experienced by

TAF TABLE D-5. SUMMARY OF TEST ELEMENTS AND RESULTS

<u>TEST</u>	<u>RESULTS</u>
Crack Propagation Test	Crack growth rates typical of other gear steels.
Charpy Impact Test	Material is capable of operation at -65°F while retaining ductility (20 ft.-lbs.).
Gear Roller Test (Surface) Contact Fatigue Resistance)	No significant effect on surface contact fatigue when varying hardening temperature from 1750°F to 1900°F and/or surface carbon from 0.9% to 1.5%. Carbides, whether heavy or light, did not affect surface contact fatigue life.
R.R. Moore Fatigue Test - Effect of Duplex Micro- structure	Ferrite, up to 5.4 percent, did not affect the fatigue life.
Jominy End Quench Test	Material exhibits excellent hardenability. Five inch rounds can be completely through-hardened.
Hardening and Tempering Effects on Carburized Case and Core Material	Optimum heat treatment and hardness response on samples hardened at 1850°F and tempered at 600°F. Increasing hardening temperature results in decreased percent ferrite. However, decreasing percent ferrite is not necessarily desirable.
Fatigue Life Determination of Decarburized Core Material	Fatigue life decreased by decarburized surface, even when shot-peened.
Determination of the Mechanism which Permits Uniform Carburization of BMS 7-223 Steel	1800°F preoxidation temperature reconfirmed as optimum. Mechanism was not determined.

the transmission system components. Nine specimens were manufactured in the longitudinal grain direction and the other seven in the transverse grain direction. Stress ratios employed were -0.50, +0.05, +0.33 and +0.67; the environments evaluated were room temperature air, water and MIL-L-23699 oil. The test conditions were developed to evaluate their influence on fatigue crack propagation rates.

Neither environment nor grain orientation had a major effect on propagation rate. No significant variations were noted between the crack propagation rate of X2 steel and other gear steels.

Charpy Impact Tests

Twelve Charpy impact test specimens were tested in order to obtain data on the mechanical behavior of the material regarding its tendency to behave in a brittle manner. Testing was accomplished in accordance with ASTM E23.64 requirements. The data obtained indicated that the 0.15% carbon material exhibited good impact toughness even at temperatures below 0°F. The fracture impact curve indicated a smooth ductile-to-brittle transition with no evidence of a sharp reduction in impact strength with decreasing temperature.

Geared Roller Test Evaluation

The primary objective of this evaluation was to optimize the surface contact fatigue resistance of the material by varying certain heat treat parameters of the test specimens. Variables evaluated included both surface carbon percentage (obtained by varying the carbon potential of the carbonaceous atmosphere during carburizing) and hardening temperature. One hundred and two test specimens were machined and heat treated utilizing seven combinations of these variables. Testing was conducted in a Caterpillar geared roller test machine which imparted both rolling and sliding contact to the test specimens. All testing was accomplished at a constant Hertz compressive stress of 450,000 psi.

Approximately 75% of the tests were considered to be valid. Evaluation of the data revealed no significant increase or decrease in B10 fatigue life as a function of heat treat parameters. Metallurgical determination of the surface carbon and the amount of visual carbides present in various test samples disclosed no direct relationship between these parameters and surface contact fatigue life.

R. R. Moore Fatigue Tests

The X2 core material exhibits a duplex microstructure consisting of highly alloyed ferrite interspersed in a tempered martensite matrix. The percentage of ferrite in the core microstructure is inversely related to the nominal carbon content of the alloy. The purpose of the R. R. Moore fatigue tests was to determine the effects of duplex microstructure on the fatigue life of the material. Three mill heats of steel with carbon contents of 0.12, 0.15 and 0.17 percent were procured. After heat treating, 30 fatigue test specimens (15 notched and 15 smooth) were obtained from each mill heat. Each heat contained a different percentage of ferrite.

Test results indicated that increasing the percentage of duplex microstructure by decreasing the nominal carbon content had no significant effect on the fatigue life of the alloy.

Jominy End-Quench Tests

The objective of the Jominy end-quench tests was to determine the hardenability of X2 steel. Four specimens were machined and tested per ASTM A255-62T requirements. The data obtained revealed that the material possessed excellent hardenability, i.e., sections up to 5 inches in diameter can be fully hardened with a resultant hardness loss of approximately three Rockwell C points from the surface to the center of the section.

Hardening and Tempering Effects on Carburized Case and Core

The objective of this test was to determine the effects of hardening and tempering temperatures versus time on the surface hardness and microstructural features of both carburized case and core material. Thirty specimens were prepared by carburizing per the contractor developed heat treatment. Hardening and tempering were accomplished utilizing various temperatures and times. Metallurgical evaluation of all samples was done after final heat treatment. The data obtained revealed the following:

- The percentage of ferrite in the core microstructure decreased with increased hardening temperature. The ferrite contents after hardening at 1750°F and 1900°F were 9.0% and 0.5%, respectively.
- The X2 exhibited excellent temper resistance. Tempering at 1000°F resulted in a surface hardness on the case material of R/C 59.0 (1850°F hardening temperature) and a hardness of R/C 44.0 on the core material.

- The X2 exhibited a secondary hardening effect, i.e.; with increasing tempering temperature, a slight increase in hardness was observed. This effect was noted in the core material only and resulted in a maximum increase of 2 to 4 Rockwell C points.

Endurance Fatigue Life Determination of Decarburized Core Material

The thermal processing of the X2 alloy requires a special oxidation treatment in order to insure uniform diffusion of carbon into the surface of the steel. This oxidation results in a decarburized layer on the surface of the steel prior to carburizing. Manufacturing requirements for the HLH/ATC components do not allow decarburized areas on finished parts. The purpose of this evaluation was to determine what effect the decarburized core material has on the endurance fatigue life of the base material. The effect of shot peening the layer was also studied.

Seventy-five R. R. Moore fatigue test specimens were prepared in groups of 15 each. Two of the five groups were pre-oxidized and tested; two other groups were preoxidized, shot peened and tested. The fifth group of specimens was not preoxidized, but hardened and tempered only in order to provide baseline data.

After testing, the data disclosed the following:

- The endurance limit of the as-preoxidized specimens was decreased from 34% to 43% when compared with those specimens which were hardened and tempered.
- Shotpeening the preoxidized surface resulted in increasing the endurance fatigue life of the material but not sufficiently to attain base material levels.

Determination of the Mechanism which Permits the Uniform Carburization of X2

X2 requires special processing in that a unique preoxidation treatment of all components must be accomplished prior to carburization in order to insure a uniformly carburized surface. The objective of this test was to determine the mechanism; i.e., what does preoxidation actually do to the surface which permits uniform carburization of the steel.

Ninety specimens were produced by various machining methods, (i.e., milling, shaping and grinding) and preoxidized utilizing several variations of temperature and time. Forty-two of the specimens were preoxidized, carburized, and hardened

(Group I); 42 (Group II) were preoxidized only; and the remaining six samples (Group III) were not heat treated, but were used as test standards. For each Group I sample, there was a corresponding Group II sample. Metallurgical evaluation of all Group I samples indicated which preoxidation treatment resulted in a uniformly carburized surface. Results confirmed the 1800°F preoxidation temperature as optimum. X-ray diffraction fluorescent analysis of Group II (samples which were processed by preoxidation only) indicated that various oxides were being formed at the steel surface-oxide interface. Characterization of these oxides was not accomplished. A complete report on this program is presented in Boeing Vertol Report D301-10036-2.

Additional Gear Material Evaluations

Subsequent to the tasks reported by D301-10036-2, the following evaluations were made.

- **Fracture Toughness of Vasco X-2 with Various Heat Treatments**

A test program to understand the effects of heat treatment on the fracture toughness of VASCO X-2 steel was defined.

Fracture toughness testing has been standardized in order to obtain meaningful test data. ASTM E399-72 specifies the procedure and data requirements for determining valid fracture toughness values.

Fracture toughness tests were conducted on twelve (12) specimens according to ASTM E399-72. The results of the testing are presented in Table D-6. The testing conducted is summarized in Table D-7. These data indicate that the baseline heat treatments provided the best fracture toughness. The average fracture toughness of the baseline heat treat specimens fell slightly below that previously measured for VASCO X-2. This difference in the baseline heat treat results is considered to be within the expected scatter.

- **Bending Fatigue Strength of Vasco and 9310 Steels**

The testing conducted is summarized in Table D-7.

TABLE D-6. FRACTURE TOUGHNESS (K_{IC}) TEST RESULTS VASCO
X-2 HOT HARDNESS STEEL ROOM TEMPERATURE

HEAT TREATMENT SPECIFIED	SPECIMEN NUMBER	FRACTURE TOUGHNESS K_{IC} PSI \sqrt{IN}	AVERAGE FRACTURE TOUGHNESS K_{IC} PSI \sqrt{IN}
BASLINE SPECIMENS (ORIGINAL X-2) 1850°F FOR 45 MIN., OIL QUENCH, 600°F FOR 4 HRS., AIR COOL	10 11 12	41334 45397 44883	43871 (1)
1750° FOR 45 MIN., OIL QUENCH, 950°F FOR 4 HRS., AIR COOL	1 2 3	Pre-crack Failure* Pre-crack Failure* 35994	35994
1800°F FOR 45 MIN., OIL QUENCH, 950°F FOR 4 HRS., AIR COOL	4 5 6	38312 34362 36215	36296
1850°F FOR 45 MIN., OIL QUENCH, 950°F FOR 4 HRS., AIR COOL	7** 8 9	33718** 35477 34406	34534
<p>* NO MEASUREMENT POSSIBLE</p> <p>** FATIGUE PRE-CRACK SLIGHTLY SHORTER THAN REQUIRED; DOES NOT MEET ASTM REQUIREMENT FOR VALID MEASUREMENT.</p> <p>(1) NOTE: THE AVERAGE FRACTURE TOUGHNESS, K_{IC}, MEASURED PREVIOUSLY FOR VASCO X-2 IS 48647 PSI \sqrt{IN}.</p>			

TABLE D-7. SUMMARY OF CANTILEVER BENDING FATIGUE TESTS OF VASCO AND 9310 STEELS

TEST CONDITION			NUMBER OF SPECIMENS TESTED			
NO.	TYPE OF TEST	TEMP.	STRESS RATIO, R	VASCO STEEL BMS7-223		9310 STEEL BMS 7.6
				HEAT LOT 3273A	HEAT LOT 3413A	
I	Basic Bending Fatigue	Room	-1.0	3	3	6
II	Basic Bending Fatigue	350°F	-1.0	5	5	8

Conditions I and II are shown in Figures D-12 and D-13 respectively. This data is considered to be preliminary since the metallurgical examinations have not been completed. These examinations could result in certain of the data points being deleted. The preliminary data indicates that the bending fatigue strengths of Vasco and 9310 steels are similar and that there is no significant difference in fatigue performance between heat lots of this Vasco steel.

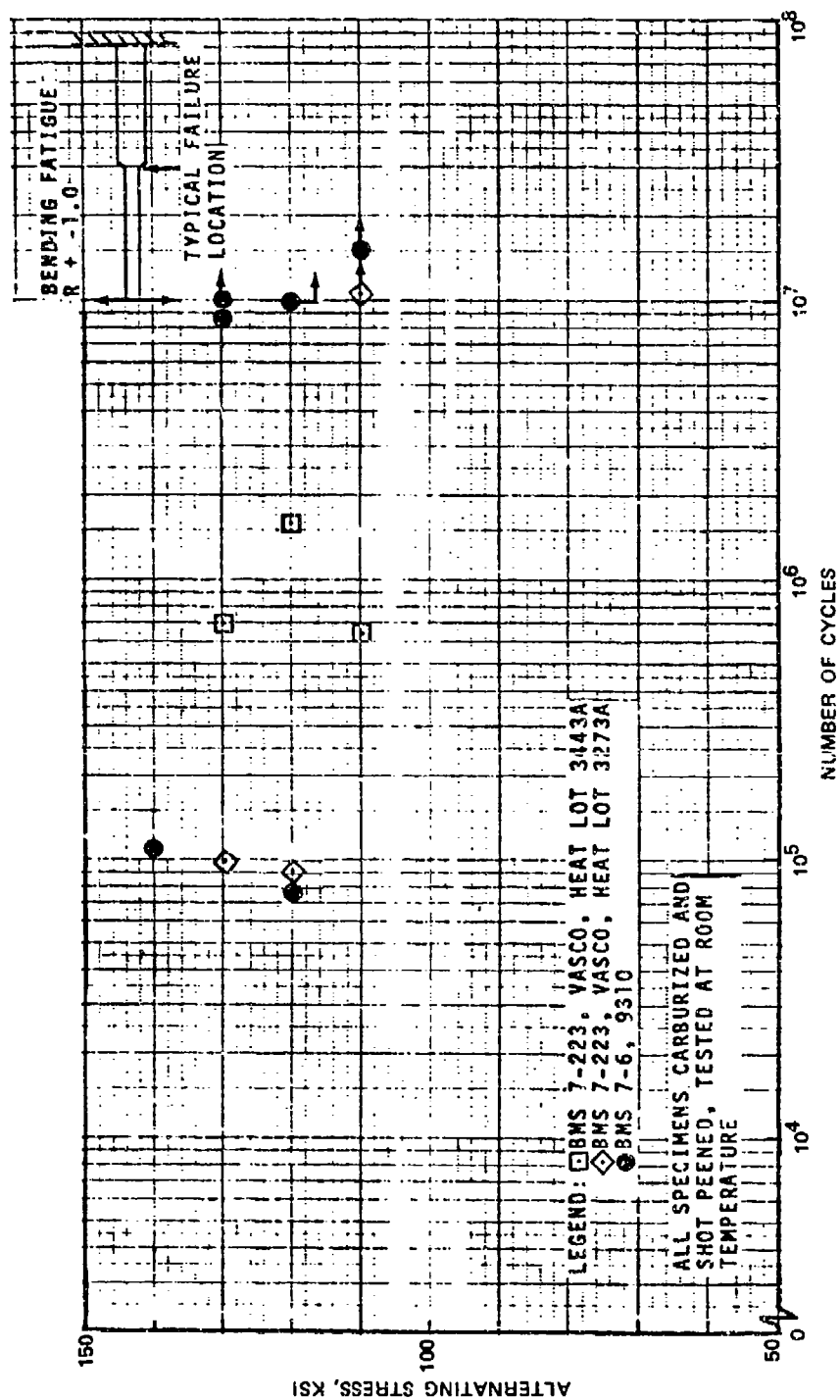


Figure D-12. S-N Data Gear Materials Evaluation, Room Temperature

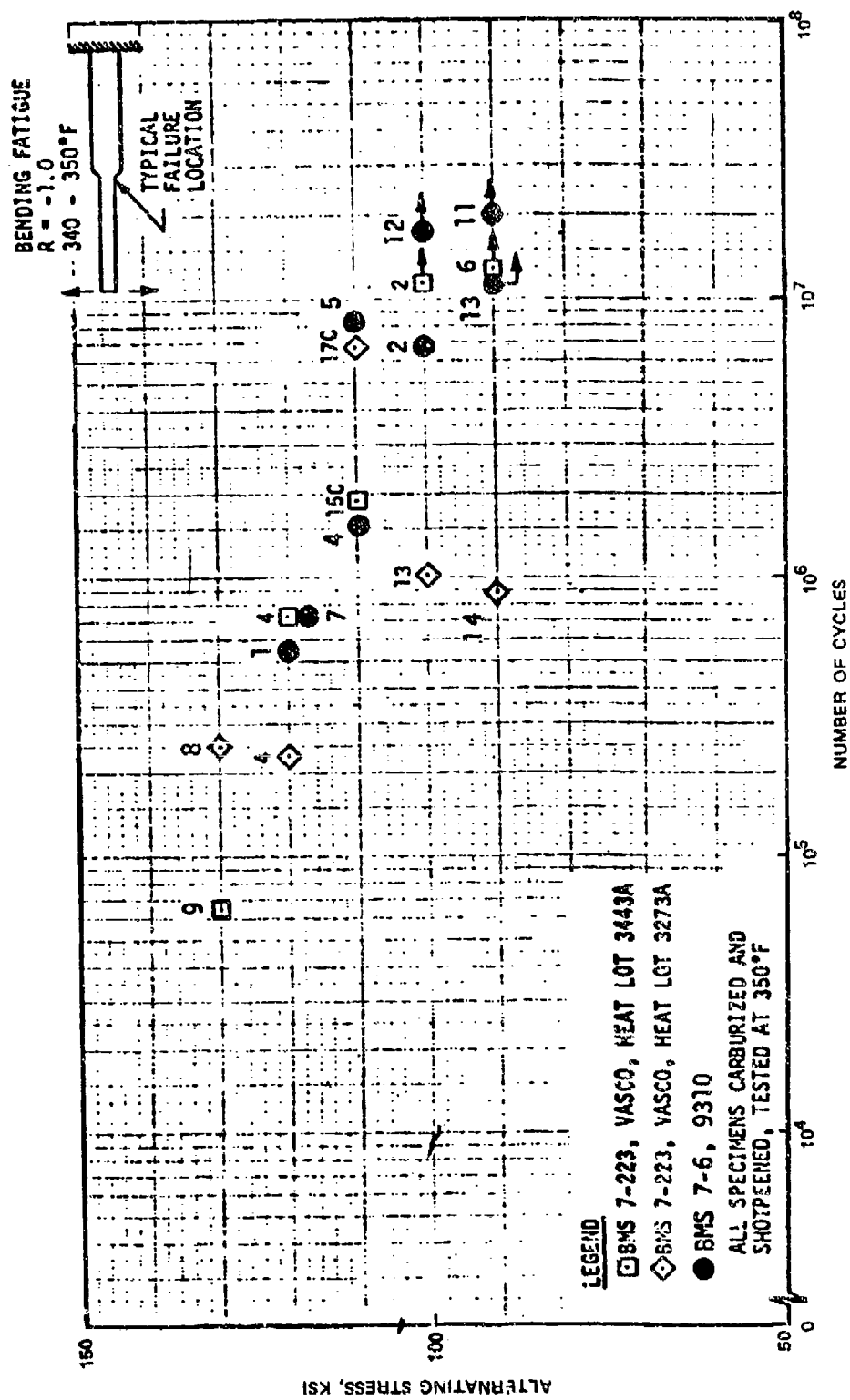


Figure D-13. S-N Data Gear Materials Evaluation - 350°F

GEAR TOOTH FORM

Background

The proposed HLH/ATC design combines two recent gear technology advances: high-contact-ratio tooth geometry and VASCO-X2 material.

Boeing Vertol has conducted several individual test programs to evaluate the bending strength, surface durability, and scoring hazard of both high-contact-ratio 9310 gearing and conventional contact ratio VASCO-X2 gearing. Testing of several high-contact-ratio gear tooth configurations demonstrated the potential for reduced tooth stress and noise levels from improved load sharing. The alternate two- and three-pair load sharing was demonstrated by testing programs employing strain gages.

An analytical investigation verified the effect of load sharing on the stress levels. One phase of this testing measured noise generation. The effective noise level of the high-contact-ratio gearing was approximately 3 db below that of the standard baseline gear set. In addition, the vibration level, as measured by an accelerometer located on the test gearbox, was one-half to one-third the standard baseline test set.

In light of previous experience and the design stress levels, the most likely problem area in the HLH spur gearing system is scoring. The most critical mesh, based on a flash temperature analysis of the system, is the first-stage sun-planet mesh. In order to validate the flash temperature levels of the HLH/ATC spur gearing, a test program was designed and conducted.

Methodology

In order to validate the HLH/ATC flash temperature design levels, a test program was undertaken employing specimens which closely simulate the first-stage sun-planet mesh (the spur gear set with the highest scoring hazard). Three test gear configurations were developed. First, an AISI 9310 (AMS6265) standard contact ratio design was developed to provide baseline data. Second, a configuration which was geometrically identical to the AISI 9310 design but which used VASCO gear material was developed to evaluate the merits of this material. The third configuration was developed to evaluate the combined effects of high-contact-ratio teeth and VASCO material (Figure D-14).

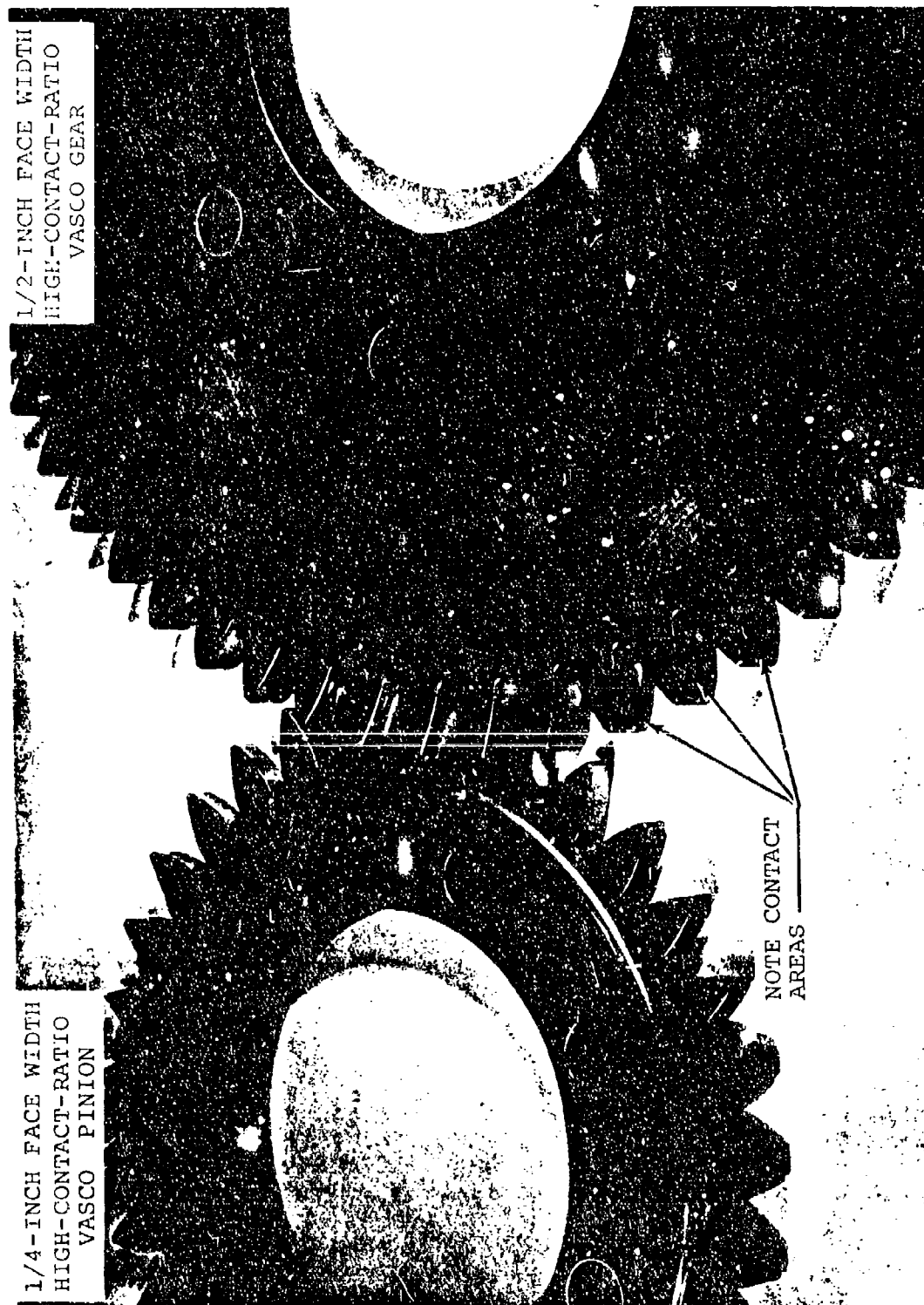


Figure D-14. Final High-Contact-Ratio Gear Configurations.

All three test configurations were designed to be run in the Boeing Vertol gear research test stand, in the 10-inch center distance overhung configuration. In this configuration, the test gears may be changed quickly and without any stand disassembly. In addition, the entire coverplate may be removed for thorough visual inspection of the test set.

Specimen Metallurgical Evaluation

A destructive metallurgical examination was conducted on a baseline AISI 9310 gear (SK 24275-1, serial number P103) and a VASCO-X2 gear (SK 24279-1, serial number P113) in order to determine their conformance with the respective Boeing Vertol specifications. Both gears conformed to all their respective specification requirements, except that the case depth was below the requirement at a single point in the root of one tooth on the 9310 gear. This discrepancy did not occur along the active profile and did not exert any influence on the test results. The silicon content of the Vasco pinion was slightly above the maximum required, but this had no effect on the test results.

Table D-8 contains a representative listing of the actual and required values of the parameters evaluated during this examination.

Test Apparatus

The experimental test program was conducted on the Boeing Vertol Gear Research Test Stand (Figure D-15), which is specifically designed for spur, helical, and bevel gear research and development. The design incorporates provisions for controlling center distance, speed, oil temperature, torque, and oil flow. The system is a regenerative (four-square) design using one gearbox as the slave unit and one gearbox as the test unit. Gear mountings were designed to be rigid and stable under all loading conditions, with through-bored housings for maximum accuracy.

Test Data and Results

Initial test results indicated the presence of a misalignment problem in the test setup, which led to the generation of invalid test data. A program of correction was undertaken, leading to a modified test specimen configuration and a revised testing technique, so that valid data could be obtained. In the course of researching the problem, a

TABLE D-8. METALLURGICAL EVALUATION RESULTS

Parameter	Value (9310)		Value (Vasco X-2)	
	Observed	Required	Observed	Required
<u>Inspection</u>				
<u>Nital Etch</u>	No Ind.	-	No Ind.	-
Magnetic Particle	No Ind.	-	No Ind.	-
<u>Hardness</u>				
Core	Rc 37	Rc 36-40	Rc 39	Rc 50 max
Surface - Flank	Rc 62	Rc 60-64	Rc 63	Rc 60-64
Surface - Root	Rc 62	Rc 60-64	Rc 63	Rc 50-64
<u>Chemistry</u>				
Carbon	.11	.07- .13	.14	.13- .16
Manganese	.66	.40- .70	.32	.20- .40
Silicon	.27	.20- .35	1.05	.80-1.00
Nickel	3.10	3.00-3.50	-	-
Molybdenum	.11	.08-.18	1.36	1.30-1.50
Copper	.07	.35 max	-	-
Chromium	1.30	1.06-1.40	5.10	4.75-5.25
Vanadium	-	-	.46	.40-.50
Tungsten	-	-	1.20	1.20-1.50
<u>Microstructure</u>				
Grain Size	-	-	8	5 or finer
Retained Austenite (Case)	<10% acceptable	-	<10% acceptable	-
Carbide Network	Class A acceptable	-	Class B acceptable	-

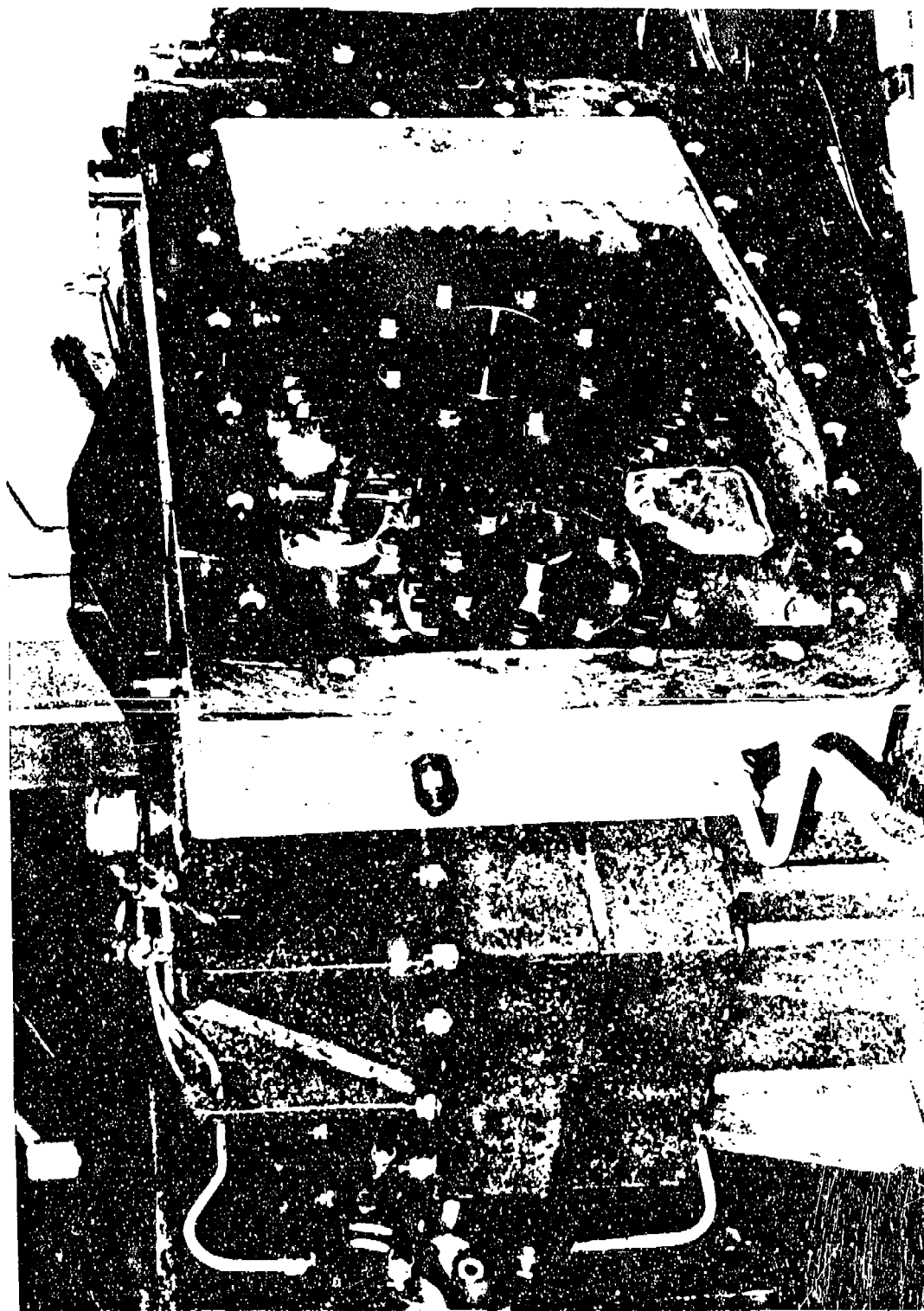


Figure D-15. Gear Tooth Form Test Rig.

ground gear set (about 16 RMS finish) was run. The load levels attained by the ground gear runs were not significantly different from those obtained with similar honed (about 10 RMS finish) sets; therefore, the honing requirement was eliminated from both the test gears and the HLH gears. Although the honing process does, in general, lead to improved load capacity, a development program to define the optimum honing technique for a particular gear set is usually required to obtain maximum benefit. Since the scoring threshold obtained with the ground test gears was well above the HLH operating level, no useful purpose would be served by developing the honing process at this point in the program. Development of the honing process may accompany future growth capability requirements.

After the shaft-induced misalignment problem was resolved, testing of 10 high-contact-ratio Vasco gear sets (reworked to the final configuration) was undertaken. This testing yielded 34 data points, including 10 failure points and 24 nonfailure data points. This testing included two gear sets - which were manufactured and run in accordance with a Government-authorized modification to the original program. In order to provide some basis for comparison, a set of standard 9310 gears and a set of standard Vasco gears were also reworked to the final configuration and run to yield 15 data points (six standard 9310 and nine standard Vasco), including two failure points each.

The results of this testing are summarized in Figure D-16. No significant operational problems were encountered during the final configuration testing. The standard 9310 test specimens were incrementally loaded through their expected (330° to 360°F) flash temperature failure range and both experienced scoring failures at the high end of this range to yield an average scoring threshold flash temperature of 357°F.

In order to clearly define the scoring threshold, testing was halted at the first sign of scoring. Generally, scoring had progressed over less than 10% of the available face contact area. However, in some cases, scoring progressed up to 15% during the 15-minute run.

Since the expected failure range of the Vasco material was not known with certainty, and in order to insure maximum utilization of the modified test specimens, the first standard contact ratio test specimen was incrementally loaded in relatively small increments until its scoring threshold was

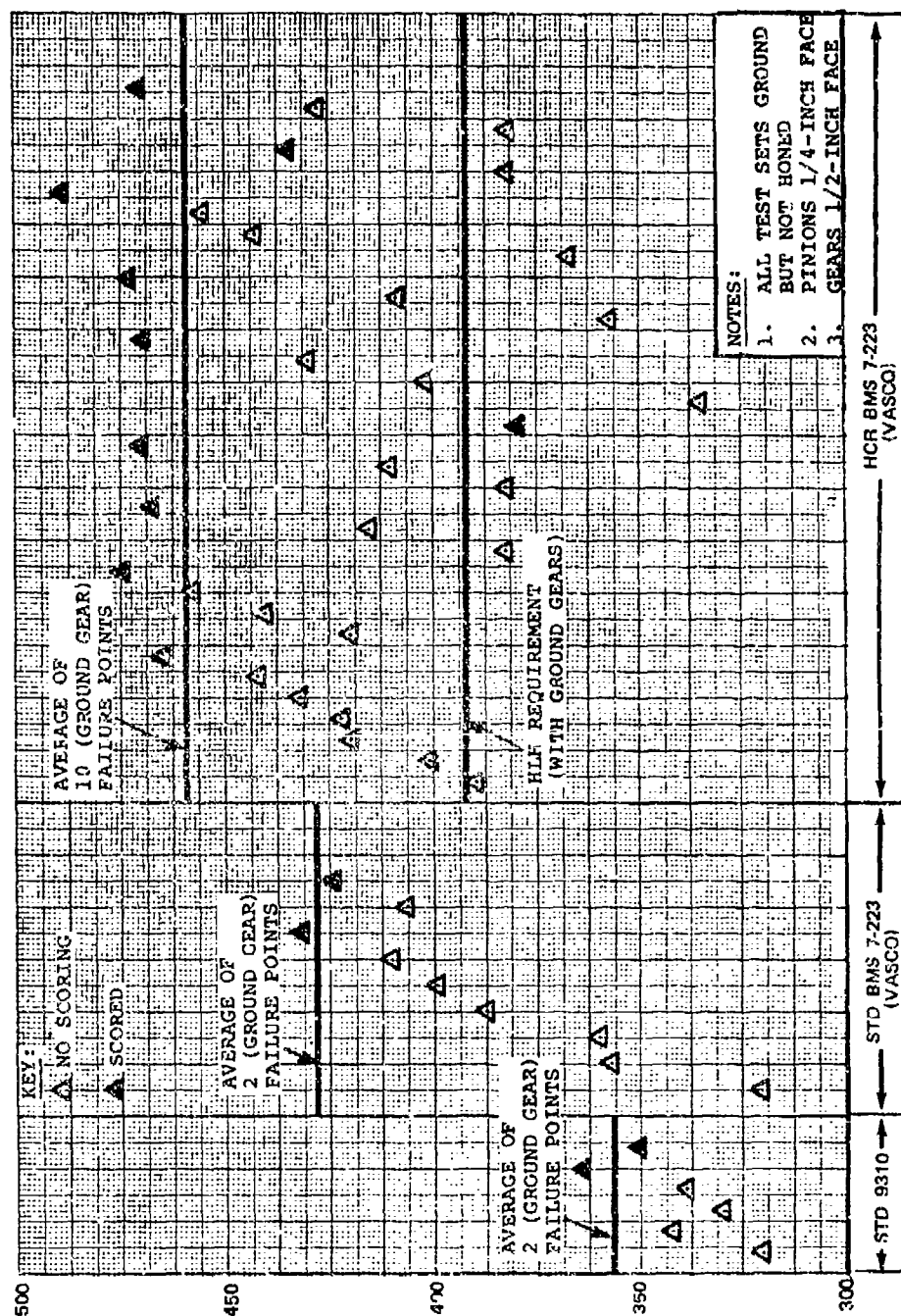


Figure D-16. Graphic Summary of Final Configuration Test Data.

reached (432°F flash temperature). The second specimen was loaded in steps to failure, to yield an average scoring threshold of 428°F flash temperature. In terms of load capacity testing, Vasco has demonstrated a 66% improvement over AISI 9310, as shown in Figure D-17.

Although the increased load capacity demonstrated by the standard Vasco gears over that of the standard 9310 gears is of interest, the relationship between the scoring threshold of the high-contact-ratio Vasco test gears and the HLH high-contact-ratio planetary gears is of even greater interest. The average scoring threshold derived from the ten high-contact-ratio Vasco failure points, 459°F, exceeds the HLB requirements of 394°F by 17%. A statistical analysis of the ten high-contact-ratio Vasco failure points, as summarized in Table D-9, shows that the 1/2 of 1% scoring hazard level will occur at a flash temperature of 427°F, well above the HLH Critical value of 394°F.

Based on the results of this testing, the scoring probability of the most critical spur gear mesh on the HLH system (the first-stage sun-planet) is less than 1/10 of 1% at design power and speed.

All test results were quite consistent and repeatable, with the exception of two high-contact-ratio Vasco points. The first of these points, pair number HV 17, failed at a flash temperature of 380°F, well below the average failure point. Pair number HV 18, simply pair number HV 17 reversed, failed within the expected flash temperature range. In order to find a reason for the poor performance of HV 17, an extensive metallurgical and geometric investigation was undertaken. No explanation of this premature failure was found. At the time the point was run in the test stand, an immediate check of the torque, temperature, and flow control systems revealed no problems. Pair number HV 21 failed at 434°F, slightly below the expected range. However, examination of the involute profile charts for this set revealed a mild discrepancy in the profile (a step below the pitch line), which would account for this slightly lower load capacity.

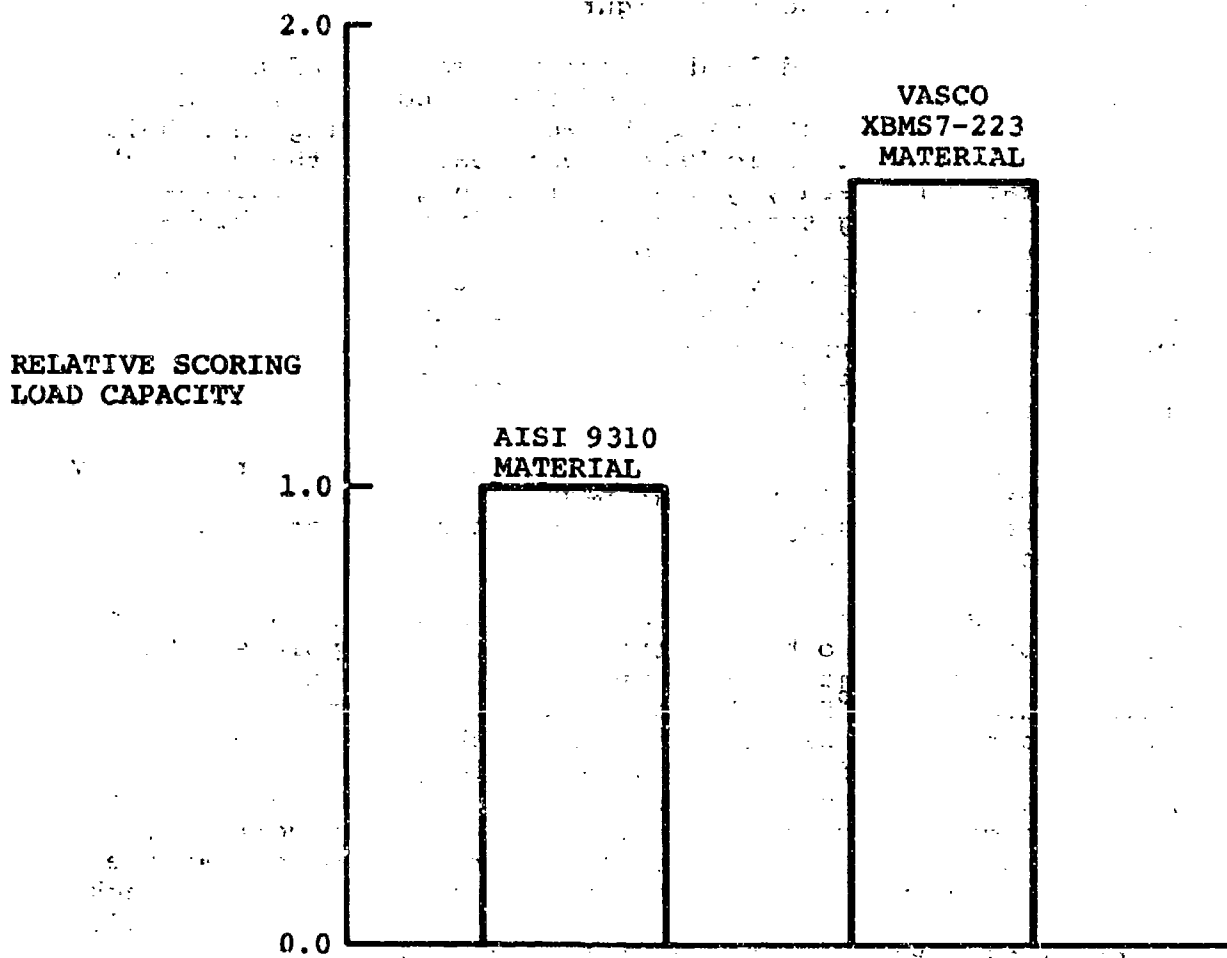


Figure D-17. Relative Scoring Load Capacity of AISI 9310 Gear Material Compared to VASCO XBMS7-223 Material.

TABLE D-9. SUMMARY OF STATISTICAL ANALYSIS OF
HCR VASCO SCORING DATA*

Number of Points	10
Sample Mean	459
Sample Standard Deviation	31
Sample Variance	961
Lower Limit on Mean	
At 99.0% Confidence	431
At 99.5% Confidence	427
At 99.9% Confidence	417
*Final Configuration Only	

The noise level of the HLR transmission, while not specifically within the scope of this investigation, is of great importance to the overall design effort. With this in mind, some significant observations were made during the test program.

An accelerometer was mounted on the test gear housing so that, as a safety measure, general case vibration could be monitored. The amplitude of the signal generated by the accelerometer was constantly monitored on an oscilloscope so that an immediate shutdown could be made in the event of a catastrophic failure. Although the magnitude of the vibration signature thus observed is of no significance by itself, it is interesting to note that the signature recorded for the high contact ratio test gears was, in general, about half that of the standard contact ratio gears at the same conditions. Since the most significant cause of noise in the aircraft is case vibration due to dynamic tooth forces, this reduction in vibration through the use of high-contact-ratio gears indicates that a significant reduction in noise levels will also be obtained.

TITANIUM ROTOR SHAFT PROXIMITY COUPON TESTS

Fatigue testing, fatigue crack propagation rate testing, and mechanical properties testing of β STOA 6Al-4V titanium alloy forging was undertaken to provide data for predicting the performance of a β STOA 6Al-4V titanium HLH rotorshaft.

Fatigue Testing of Goodman Specimens

The specimen geometry for fatigue specimens is similar to that used for the HLH ATC program for evaluation of ($\alpha + \beta$) STOA 6Al-4V titanium forging. Specimens are obtained from the planet post flange as shown in Figure D-18.

Of the 57 specimens available (36 smooth; 21 notched), a total of 20 specimens were tested. The rotorshaft post proximity coupons demonstrate that improved fatigue performance is achieved with a β Solution Treated and Overaged (STOA) forging. Fatigue data shown in Figure D-19 demonstrates that at room temperature the β STOA post coupons exhibit a significantly higher endurance limit at 5×10^7 cycles than the HLH/ATC program ($\alpha + \beta$) STOA coupons.

The endurance limit for β STOA rotorshaft post material at 250°F is lower than the endurance limit for room temperature, as expected; however, it is important to note that the endurance limit at 250°F for β rotorshaft post material is still greater than the room temperature value for the HLH/ATC program ($\alpha + \beta$) STOA 6Al-4V titanium forging.

Notched fatigue results, shown in Figure D-20, demonstrates the same trends. The fatigue strength of the β STOA coupons at 250°F is equal to the $\alpha + \beta$ STOA fatigue strength at room temperature at 5×10^7 cycles, indicating a significant improvement in fatigue strength.

Fatigue Crack Propagation Rate Testing

To verify β STOA titanium forging crack propagation rates, a series of four tests were conducted for conditions identical to those used in the HLH ATC program on ($\alpha + \beta$) STOA titanium forging. As shown in Figure D-21, the crack growth rates for both materials for stress ratio $R = 0.1111$ and in room temperatures air are the same, thereby demonstrating that β STOA material crack rates are not detrimental for this application.

Mechanical Properties Testing

To check static properties of the HLH ($\alpha + \beta$) STOA + β STOA rotorshaft material, two standard tensile specimens were fabricated and tested. Table D-10 is a comparison between the test results obtained and the average values for ($\alpha + \beta$) STOA forging measured in one HLH/ATC program.

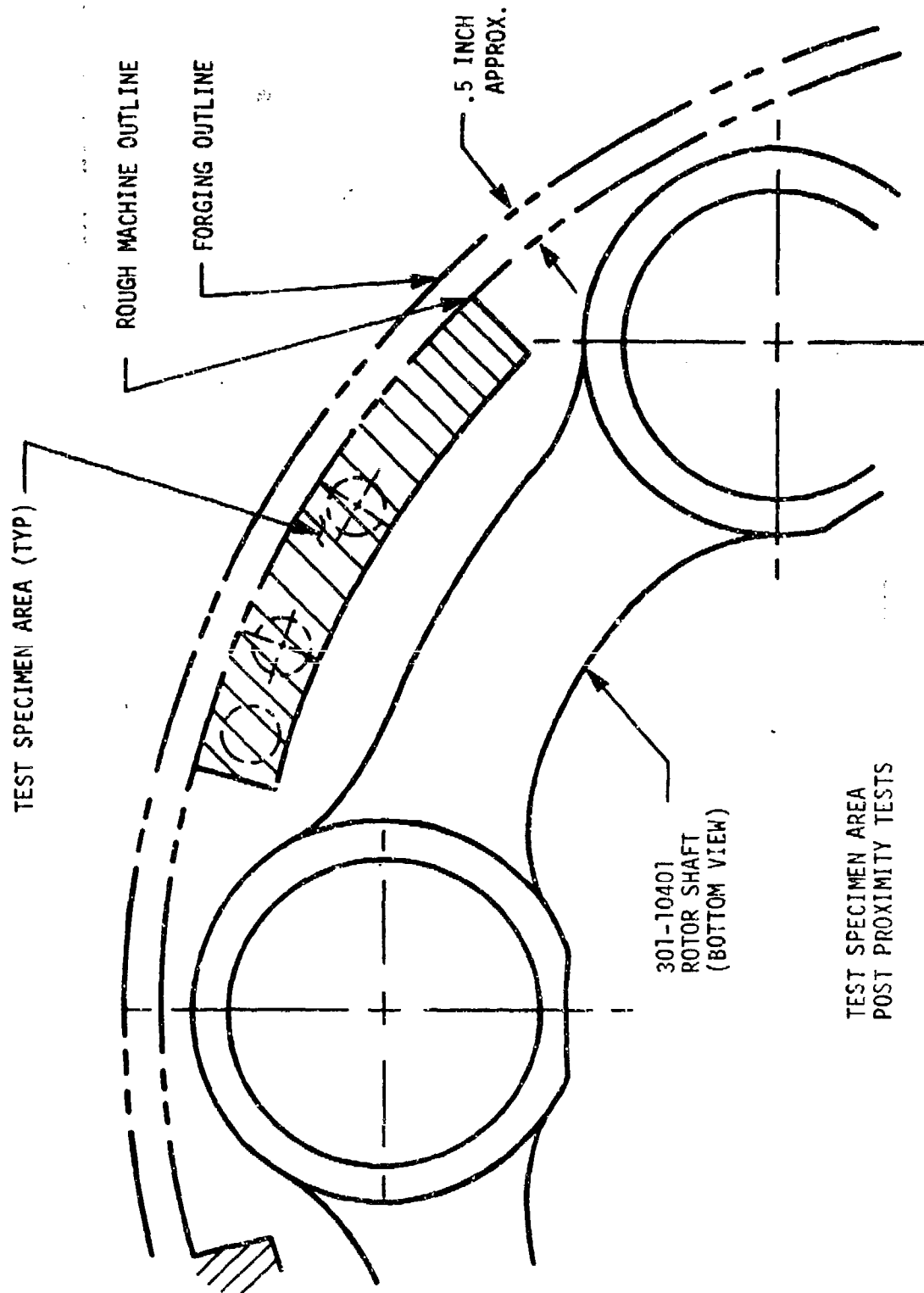


Figure D-18. Test Specimen Area Post Proximity Tests.

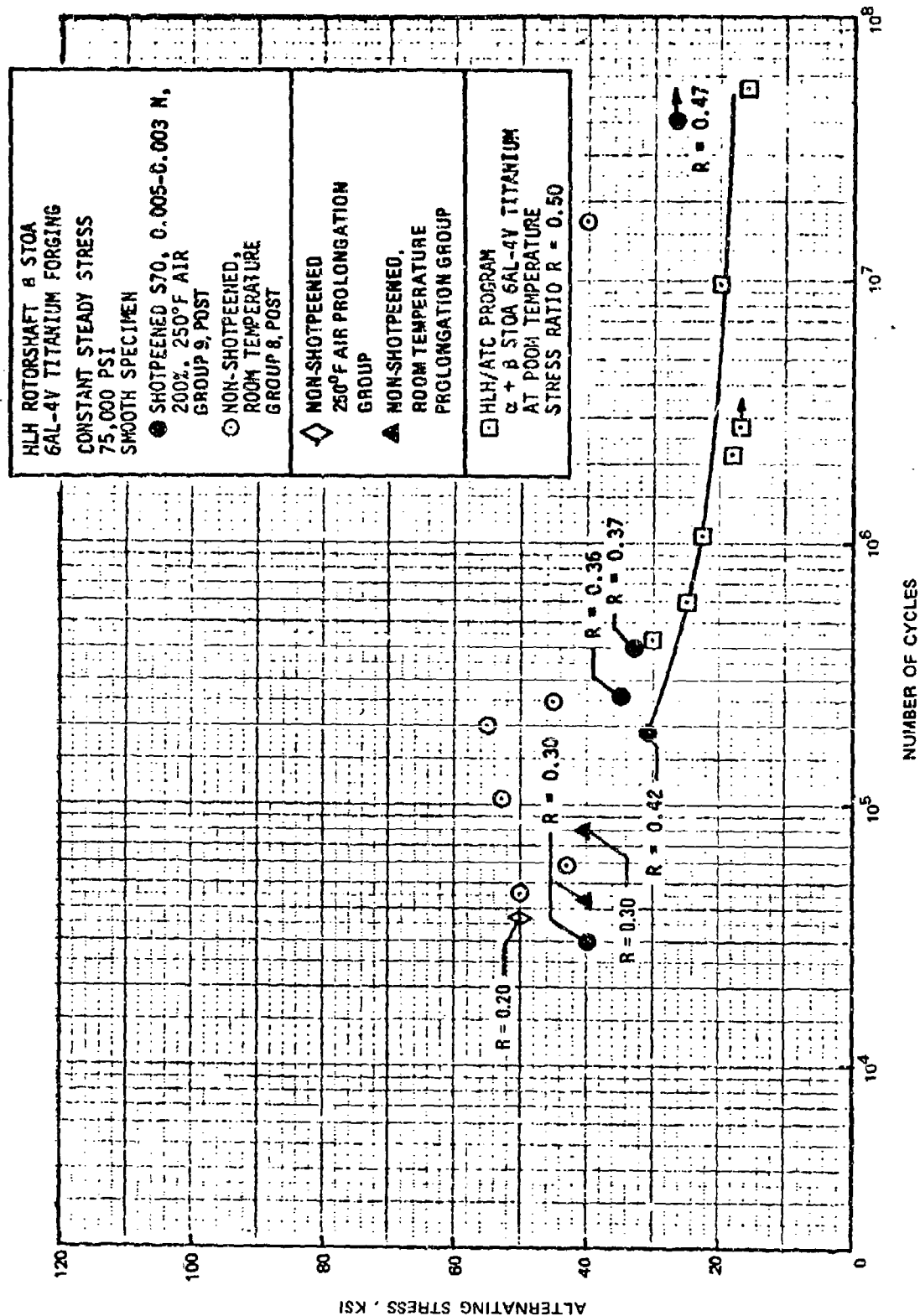


Figure D-19. Titanium Smooth Specimen Results.

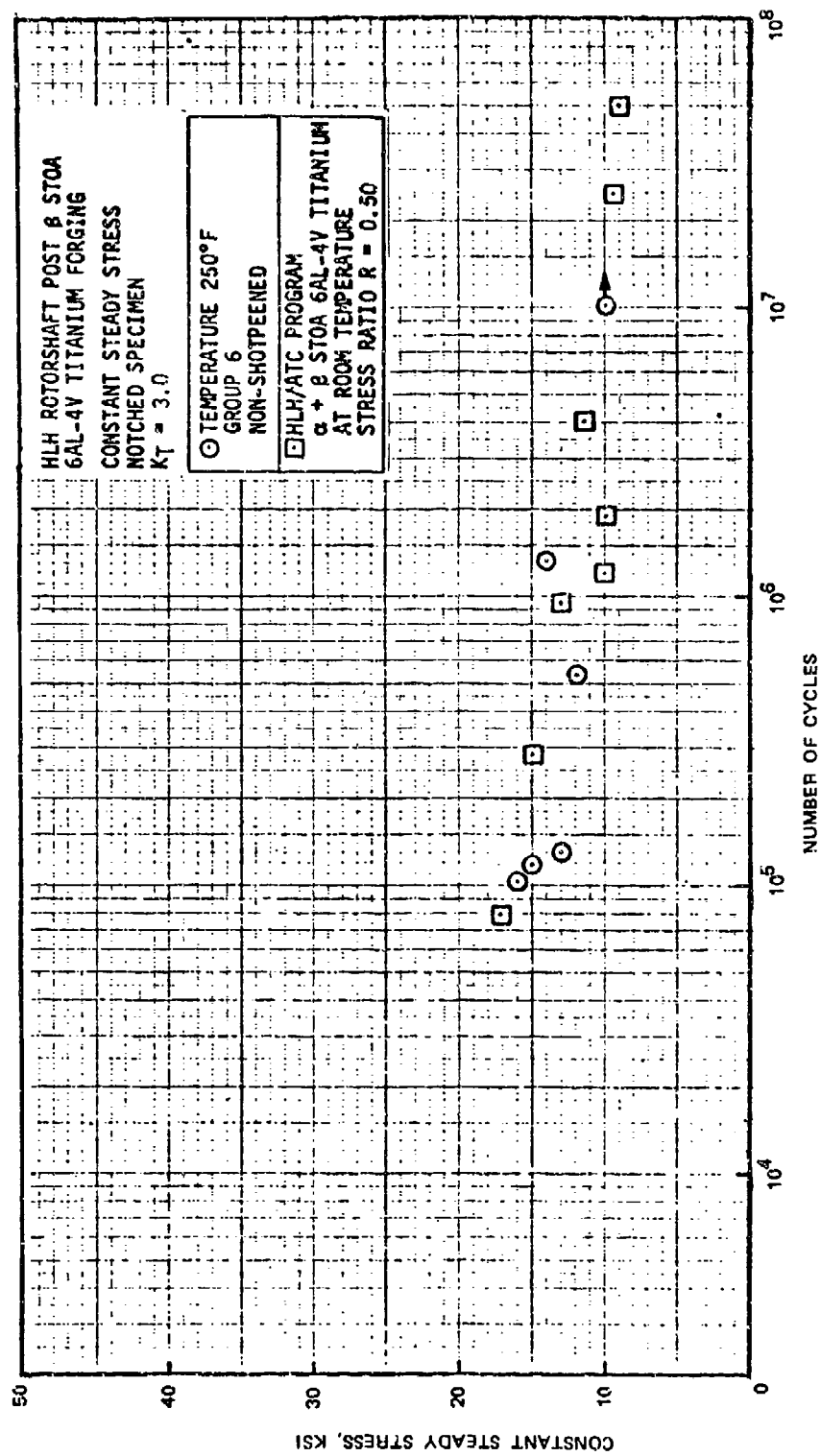


Figure D-20. Titanium Notched Specimen Results.

LEGEND

\square $(\alpha + \beta)$ STOA + β STOA FORGING, PROLONGATION
 \circ $(\alpha + \beta)$ STOA FORGING, HLH ATC PROGRAM
 Δ $(\alpha + \beta)$ STOA FORGING, HLH ATC PROGRAM

STRESS RATIO $R = 0.1111$
 ENVIRONMENT: ROOM TEMPERATURE AIR
 LOAD FREQUENCY: 5 Hz

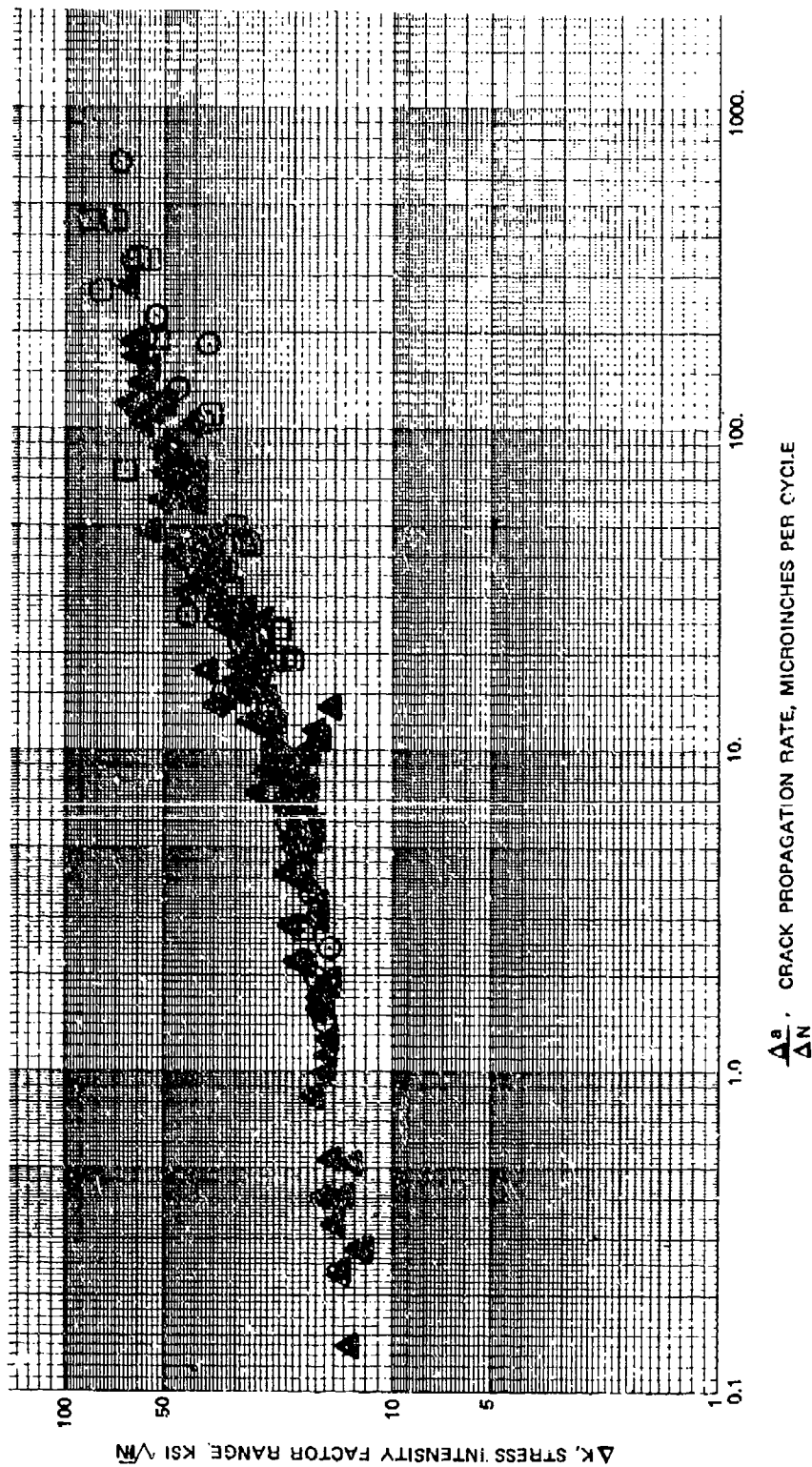


Figure D-21. Comparison of Fatigue Crack Growth Rates in 6Al-4V Titanium Alloy Forgings.

TABLE D-10. TENSILE TEST RESULTS				
SPECIMEN	YIELD STRENGTH (PSI)	ULTIMATE STRENGTH (PSI)	% ELONGATION	% REDUCTION IN AREA
β -1	135437	145162	4	8.6
β -2	INVALID - SLIPPED IN GRIPS DURING TEST			
HLH ATC (α + β) STOA FORGING	122642	135821	11	20.5

TITANIUM HARD-COAT TESTING

Testing was conducted to determine the influence of a tungsten carbide hardcoat on the fatigue strength of shotpeened 6Al-4V titanium alloy. A summary of the testing is shown below.

SPECIMEN DESIGNATION SK301-10434	TYPE OF COATING AND COATING THICKNESS	NUMBER OF SPECIMENS
-1	Bare Titanium, No Coating	12
-2	0.002-Inch Coating, As Ground	12
-3	0.008-Inch Coating, As Ground	12
-4	0.008-Inch Coating, Abusively Ground	11
-5	0.008-Inch Coating, Simulated Repair	6
	Total	53

Figure D-22 is an S-N plot of the data obtained. Initial analysis of the data and metallurgical examination of specimens have been completed. Conclusions based on these studies include the following:

- (1) A properly processed hard coat does not significantly degrade the fatigue strength of shot-peened titanium. Nominally, the -2, -3, and -5 groups represent specimens with proper processing of the hard coat. There is a tendency for the specimens with the thicker coating to fall toward the bottom of the scatterband. It was also noted that of the properly processed specimens, those simulating a repair (-5 group) fell toward the bottom of the scatterband in the high-cycle region of the plot.
- (2) An improperly processed hard coat can significantly degrade the fatigue strength of titanium. In this program, this effect was seen with specimens having an abusively ground coating and with a specimen having a porous coating.

In the case of the specimens with the abusively ground coating (-4 group), the fatigue life tends to exhibit a very large scatter, ranging from the same life to less than one tenth the life of a specimen with a properly processed coating. A dye penetrant inspection

method provides a means for determining possible abusive grinding damage.

Coating porosity was found to be a factor in the low fatigue life exhibited by specimen no. 12 of the -2 group. Before the testing of -2 no. 12 began, it was subjected to a dye-penetrant inspection by the Materials Engineering Laboratory. No cracks were observed, but one edge of the coating had a discrete area of small dye check spots. After testing was completed, dye-penetrant inspection revealed cracks in the coating on only one side, the side from which the fatigue emanated. All previously failed specimens had a uniform distribution of coating cracks.

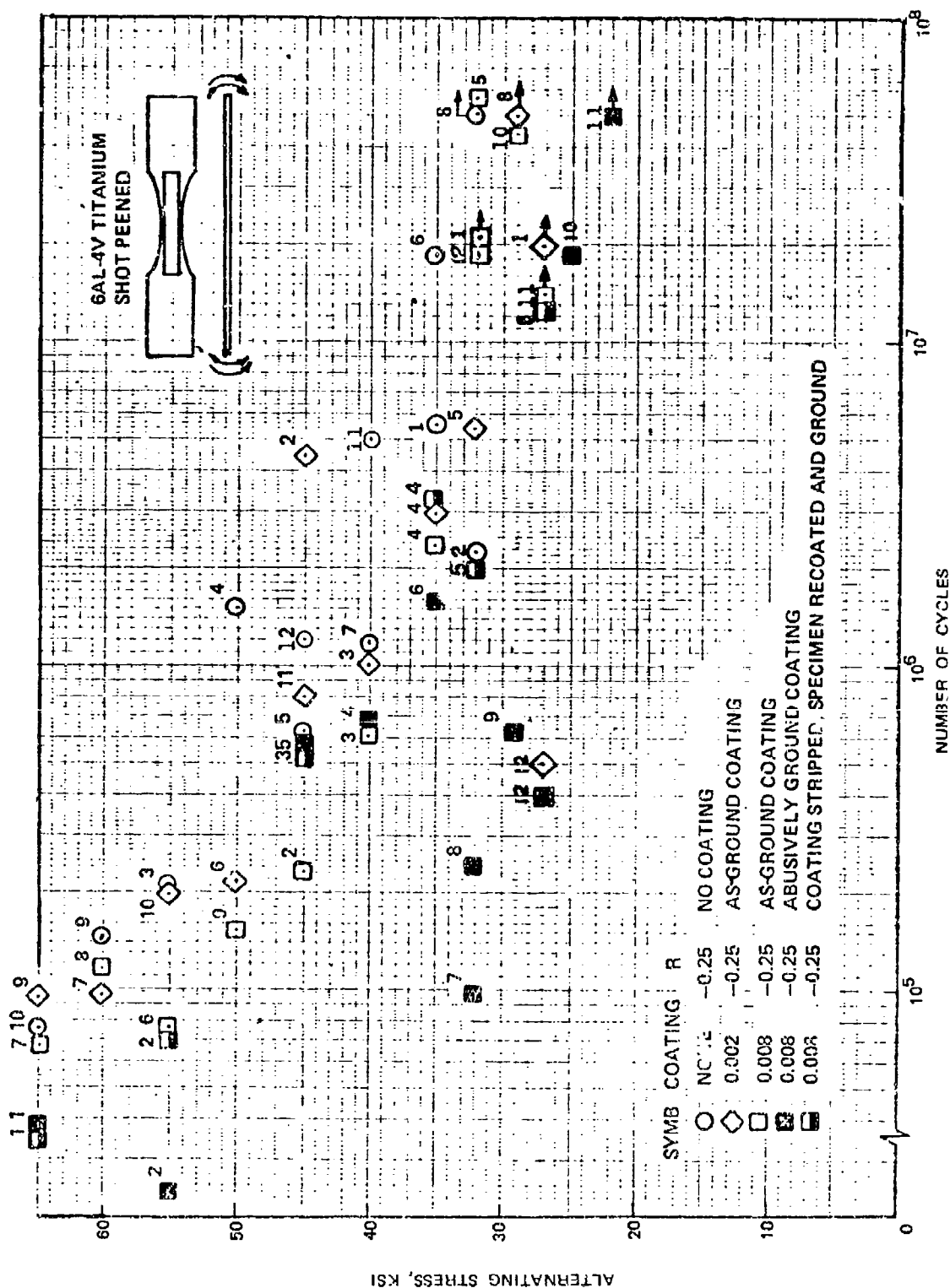


Figure D-22. Fatigue Strength Hard Coated Titanium.

TRANSMISSION HOUSING MATERIAL EVALUATION

Background and Purpose

The ZE41A-T5 magnesium sand casting alloy is reported by aircraft users in both the United Kingdom and Europe to be cost-effective due to virtual elimination of the microporosity problem which severely affected component deliveries of AZ91C-T6 alloy castings. Magnesium alloys containing rare earths, such as cerium in ZE41A-T5 (Table D-11) are rated above the aluminum zinc alloys for general castability. Due to improved castability and minimal microporosity, mechanical properties should have improved uniformity.

With the proposed use of ZE41A magnesium for the HLH transmission housings, it became necessary to develop static and fatigue strength properties prior to fabrication and testing of full-scale transmission components.

To evaluate thickness effect on properties such as fatigue strength, specimens were fabricated from both thick (3.0 inches) and thin (0.38 inch) areas of the test castings.

Weld repair of foundry-produced defects invariably occurs in production castings. To evaluate the effect of welds on fatigue strength, tensile strength, and fatigue crack propagation rates, welds were made in a number of the test casting coupons.

TABLE D-11. CHEMICAL ANALYSES FROM VENDOR CERTIFICATION							
Alloy	Melt Number	Heat Treat Batch Number	Composition - Percent				
			Aluminum	Zinc	Total Rare Earth Cerium	Zirconium	Magnesium
ZE41A	J2011M	M008	---	4.3	1.4	.75	Balance
ZE41A	J2211M	M008	---	4.2	1.1	.71	Balance
ZE41A	L3011M	1122-5	---	4.3	1.2	.74	Balance
AZ91C	L2917R	1102-6	8.6	.80	---	---	Balance
AMS 4439 Requirement (ZE41A)				3.5 5.0	.75 1.75	.4 1.0	Balance
QQ-M-56 Requirement (AZ91C)			8.1 9.3	.4 1.0	---	---	Balance

Test Results

The majority of the tensile, fatigue, and crack propagation test results were obtained from ZE41A magnesium sand castings which were subjected to a one-stage precipitation heat treatment cycle of 480°F for 24 hours. This treatment was developed by experiment at the vendor's facility and involved the testing of 108 separately cast tensile test coupons after exposure to four different thermal cycles including the two-stage treatment recommended by Magnesium Elektron of England who introduced and developed this alloy. Mechanical test results of thin and thick material from all castings of ZE41A-T5 given the one-stage treatment met or exceeded AMS 4439 requirements. Similar tests on ZE41A-T5 casting which was given a two-stage thermal treatment exhibited average yield strength values below AMS requirements.

Tensile tests of all the nonwelded ZE41A-T5 specimens, even those removed from 3-inch-thick sections, indicated strengths and elongations in excess of AMS 4439 requirements (Figure D-23). All the welded specimens, with the exception of those removed from the thickest section, exhibited mechanical properties exceeding the requirements for nonwelded material. Maximum thickness of the HLH transmission housings is 1.5 to 2.0 inches.

Bending fatigue tests of the "as-cast" surface of nonwelded ZE41A-T5 specimens indicated that those from the thin (3/8 inch) section of the casting had an average fatigue strength approximately 20 percent higher than those from the thick (3 inch) section of the casting (Figure D-24). This difference in fatigue performance is attributed to the surface condition and microstructural factors. This fatigue testing conducted on the ZE41A-T5 material indicates that the current fatigue design allowable stress currently used for AZ91C-T6 transmission housings is applicable and is conservative for ZE41A-T5.

The thick sections revealed a problem of surface finish and microstructure associated with the geometry of the casting which is similar to an ingot of magnesium 16 inches x 14 inches x 30 inches. Chill bars used for cooling this mass of metal could only be located on the drag surface (bottom) since the cope half of the mold contained several risers. In actual production of transmission housings, this particular problem would not occur. Due to the geometry of thick sections, such as transmission mounting pad areas, it is possible to place chills on three or four sides of the pad. This permits optimum cooling rates and should limit the degree of segregation in the microstructure. The optimum test casting for this type of evaluation should have an irregular profile with 3-inch-wide bars having variable heights. This shape would permit the foundry to chill the casting in a manner more representative of good casting technology.

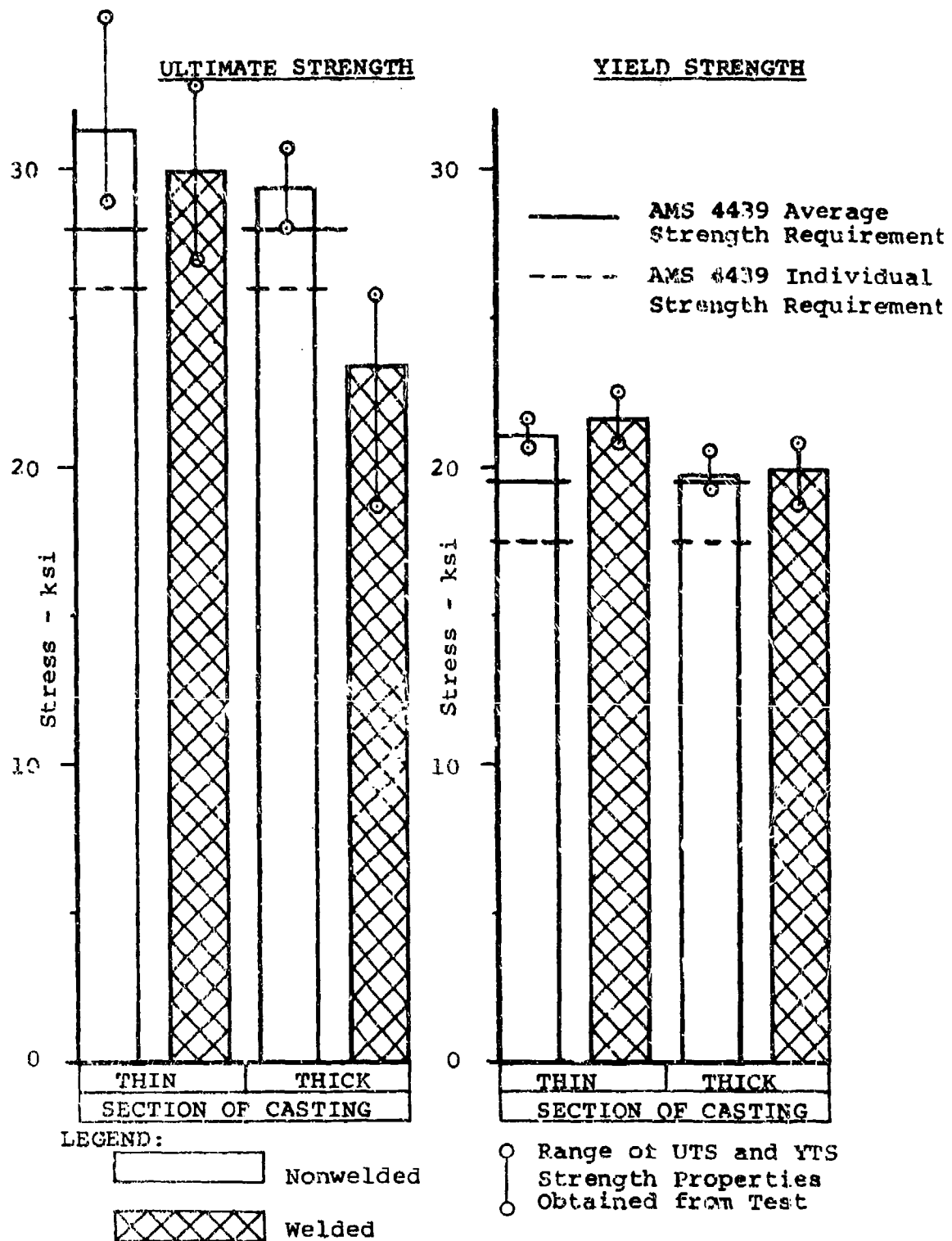
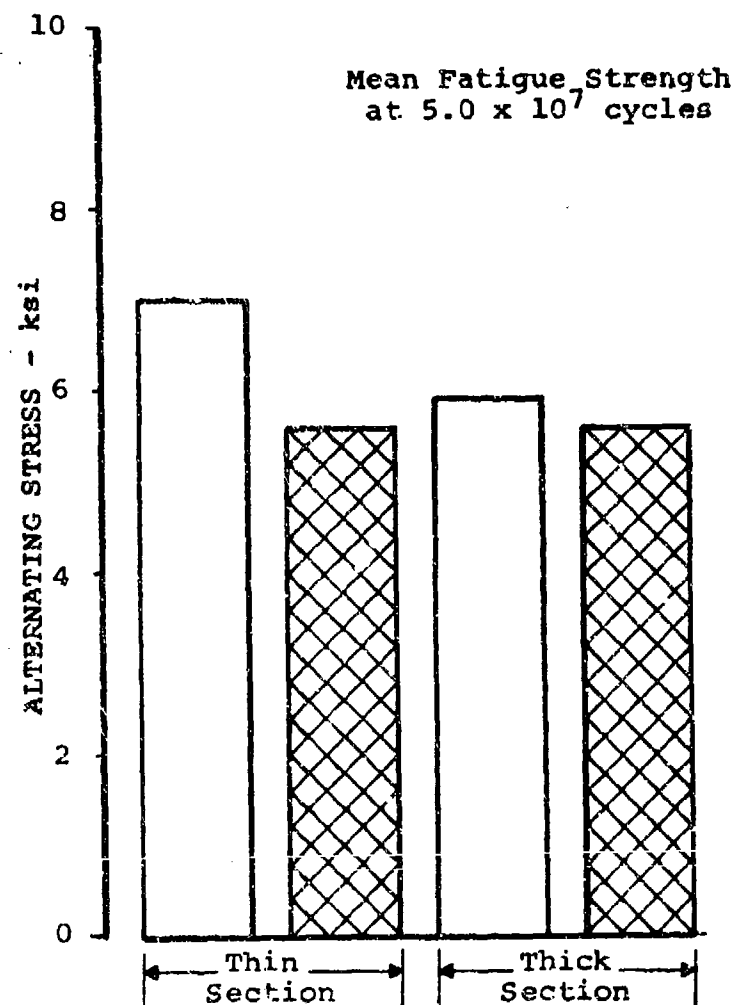


Figure D-23. Average Tensile Properties for ZE41A-T5 Magnesium.



LEGEND:

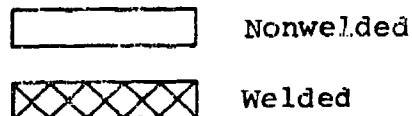


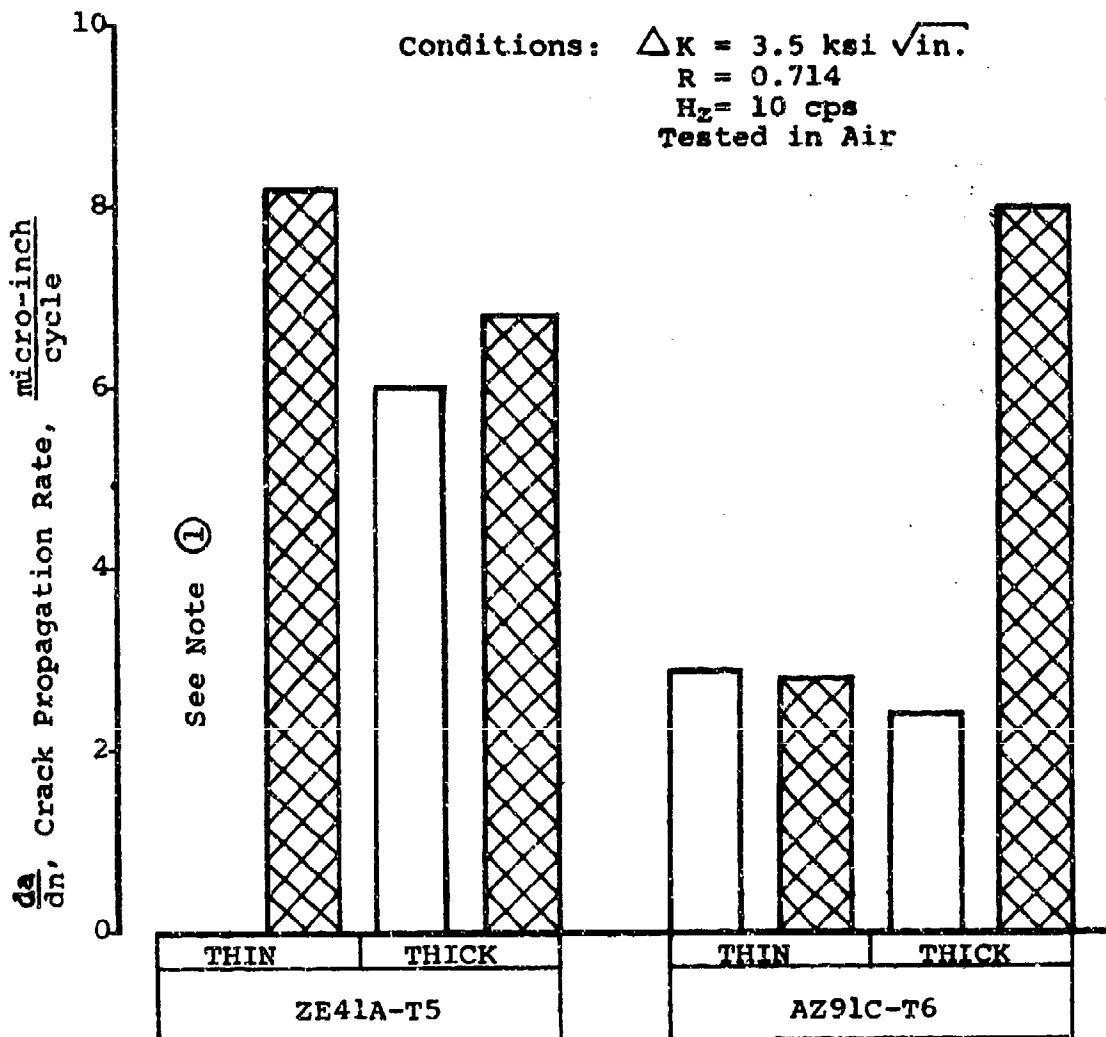
Figure D-24. Mean Fatigue Strength for ZE154A-T5 at a Stress Ratio of Zero.

Welding proved detrimental to the fatigue strength of ZE41A-T5 magnesium. Welded specimens from both thin and thick sections of the casting showed a 10 to 20 percent lower fatigue strength than nonwelded specimens from corresponding sections. It should be noted, however, that currently weld repair is permitted only in the low stress, noncritical areas of a helicopter transmission housing. Under this condition, weld repair offers an effective economic means of salvaging many castings without compromising structural integrity. The testing described herein indicates that this approach could also be utilized with HLH transmission housings of ZE41A-T5.

Fatigue crack propagation testing of ZE41A-T5 material conducted in air at 10 Hz indicated essentially the same crack growth rate characteristics for welded and unwelded specimens utilizing material from thick or thin sections of the casting (Figure D-25). Tests conducted to compare the fatigue crack growth characteristics of ZE41A-T5 and AZ91C-T6 indicated that the AZ91C-T6 material had a crack growth rate which, on the average, was two to three times slower than that of the ZE41A-T5 material. While this difference is primarily attributed to microstructural differences and is considered significant, there is a question as to how well the AZ91C-T6 material used in this program represented yield strength and elongation properties of actual transmission housing castings. The low yield strength and high elongation of the material are not considered representative of typical properties determined from tests on material removed from actual housings.

Since minimum wall thickness and stiffness requirements, rather than strength requirements, control the design of a typical helicopter transmission housing, small differences in strength properties from alloy to alloy are generally not significant. The previous successful structural performance of AZ91C-T6 housings is an indication that ZE41A-T5 housings having similar mechanical properties will also perform satisfactorily. In addition, ZE41A's superior castability, resulting in less scrapage, will provide a more cost-effective design.

A complete report on the test program is presented in Boeing Vertol Technical Report T301-10147-1.



NOTE ①: Limited data at this condition does not warrant a comparison

LEGEND:

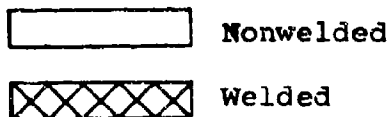


Figure D-25. Crack Growth Comparisons for Magnesium Alloys at a Constant Stress Intensity Value.

OVERRUNNING CLUTCH

Description of Test Clutches

Three clutch configurations were given a preliminary evaluation. These designs were designated as clutch designs A, B, and C and are shown in Figure D-26. As a result of these preliminary tests, Design B was judged to have the best performance. The selected configuration was then optimized to eliminate the discrepancies which occurred during the preliminary evaluation and designated as optimized Design D. Finally, the optimized Design D underwent an extensive test program which demonstrated satisfactory performance in meeting HLH design requirements.

Design A, Borg-Warner X137661, is a two-row sprag-clutch assembly with tandem inner and outer cages incorporating two inner and two outer drag strips and a central energizing ribbon.

Design B, Borg-Warner X137675, is a two-row sprag-clutch assembly with a tandem inner and outer cage incorporating two outer drag strips but no inner drag strip. Silver-plated lands on the inner cage pilot closely to the inner shaft and use viscous drag to actuate the cage.

The function of the drag strips in all cases is to create frictional drag between the sprag assembly and the adjacent inner and/or outer races, thereby aiding in the assembly cage actuation.

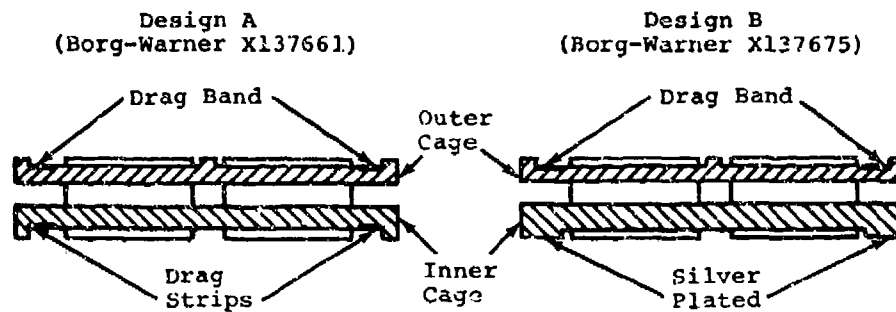
Design C, Formsprag CL-41802, consists of two single-row sprag-clutch assemblies, each having a cage and two garter springs to locate and actuate the sprags. The sprags have interlocking surfaces which prevent rollover when an overload condition occurs.

Optimized Design D, Borg-Warner X137920, is similar to Design A in appearance and Design B in configuration except for optimization to eliminate minor discrepancies which occurred during the preliminary evaluation. The design consists of a two-row sprag-clutch assembly with a tandem inner and outer cage incorporating two inner and two outer drag strips. Silver-plated lands on the inner cage pilot closely to the inner shaft. The race-contact surface of the outer drag strips were increased to minimize wear.

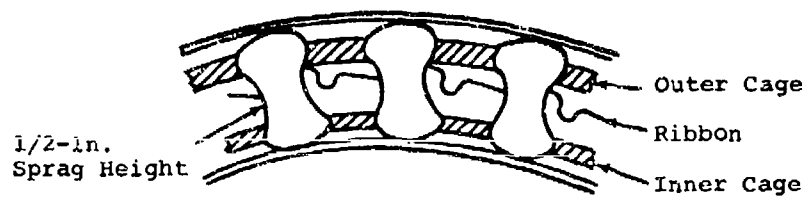
Lubrication to the clutch designs tested was provided centrifugally via holes drilled through the inner shaft (race).

The final HLH/ATC parts are identical to the optimum Design D tested.

OVERRUNNING CLUTCH



Borg-Warner Sprag Clutch



Design C (Formsprag CL-41802)

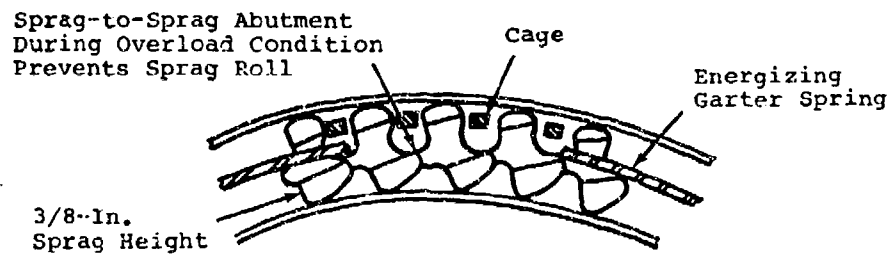


Figure D-26. HLH/ATC Sprag Clutch Designs.

Test Discussion and Results

Initial Checkout of Fixture

The clutch test facility is shown in Figure D-27. The specimen clutch was housed between two tapered-roller bearings. During the initial assembly of the test-specimen cartridge, the bearings were installed with 0.005 to 0.001 inch of axial float. At the completion of a pretest run it was noted that there was light circumferential scoring on the tapered rollers and at the completion of the first 5-hour run, the bearing cage had failed. Analysis of the failure indicated that it was the result of the axial float and marginal lubrication. The assembly was modified to allow a greater oil flow through the bearings. The axial float was eliminated, and the bearings were preloaded from 1 to 5 in.-lb. of running torque. In addition to these steps, the bearing cages were glass peened and silver-plated to increase their marginal lubrication capability. No further difficulties were experienced with the tapered-roller bearings.

Testing of Optimized Design D

Full and Differential Speed Overrunning

The optimum Design D (Borg-Warner X137920), which is similar to Design B (Borg-Warner X137675), except for the addition of inner drag at strips as included in Design A (X137661), was configured after analysis of the data from the previously tested clutches and consideration of the HLH aircraft requirements. The best features of each clutch with modifications and additions as required were incorporated into Design D. The bend radii of the inner and outer drag strips were increased to improve the wear characteristics in this area. The flattened bend radii showed no measurable wear at the completion of the 50-hour endurance test. Design D successfully completed the entire series of the full- and differential-speed overrun tests. The differential-speed overrun tests were run with a 4-gpm oil flow in accordance with the conclusions reached during the disengagement testing of the clutch B which showed lower oil flows to be marginal. This represents 100-percent of the final design oil flow to the clutch. No discrepancies were noted throughout the entire test series.

Endurance Testing

A 50-hour 75-percent differential-speed endurance test with a 3 gpm oil flow was conducted on this clutch. An oil flow rate of 3 gpm was chosen in lieu of the final design oil pump output of 4 gpm in order to evaluate and determine if there

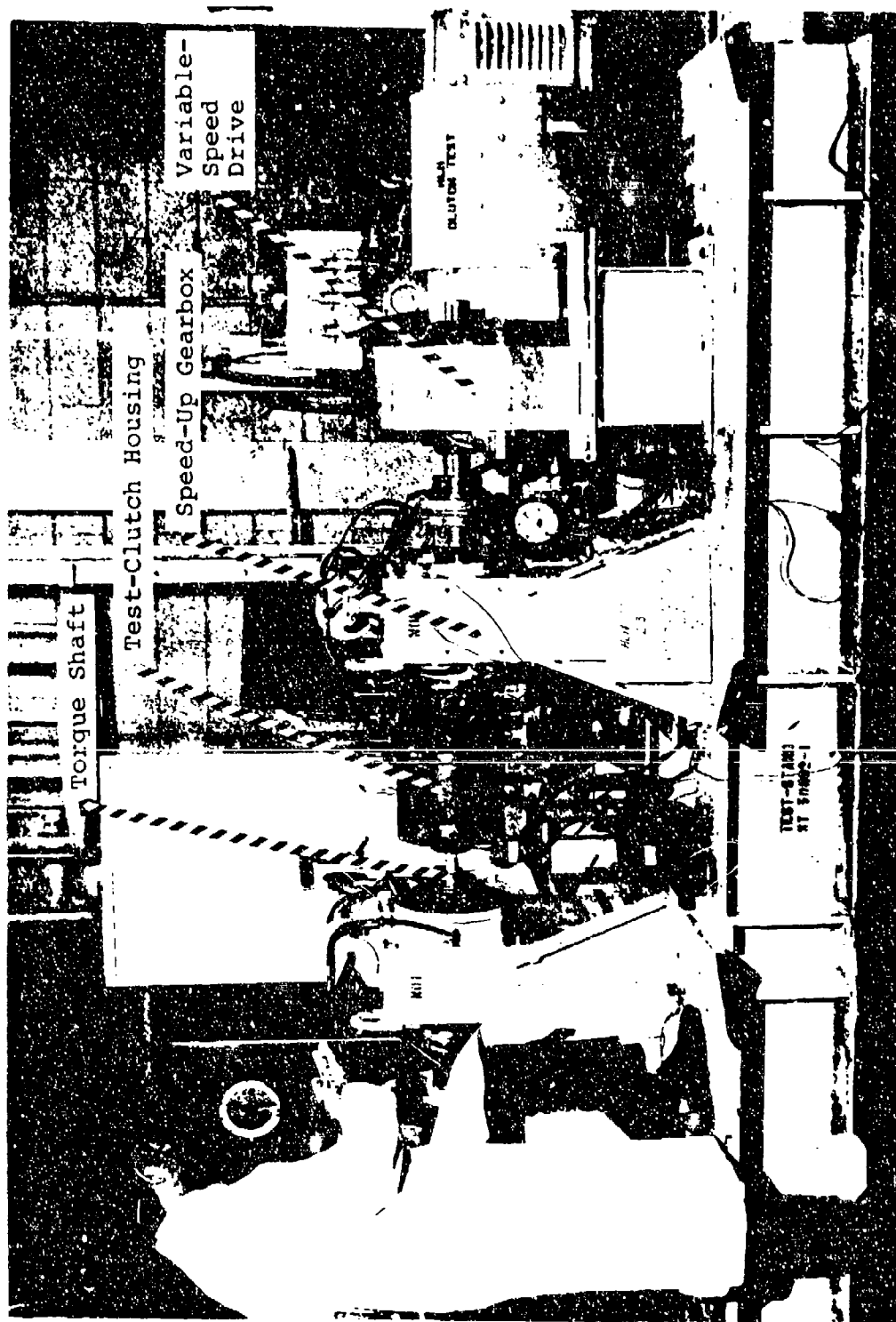


Figure D-27. Dynamic Clutch-Test Facility.

is a sufficient margin of lubrication. At the completion of the endurance test, inspection of the clutch revealed:

- A 0.0002-inch wear path on the inside diameter of the sprags.
- Several breaks in the energizing ribbons.
- No wear on the clutch inner race

The indexing of the energizing ribbons and inner and outer cage pockets was checked and found to be within tolerance. The energizing ribbon radii were checked and found to be undersize. This condition was corrected for production parts.

Cyclic Testing

Because Design D was not available for test at this time and the geometric configuration of the cages, sprags, energizing ribbons, and drag strips of clutch Design A were similar to those ordered for Design D, static testing was performed on Design A. Slip rates are shown in Figure D-28.

A frequency sweep from 10 Hz to 30 Hz with 90,000 in-lb steady and +9,000 in-lb. alternating torque applied was performed to determine if a resonant condition existed, thereby causing the slippage. No angular displacement between the inner and outer races was indicated. There was no amplitude or phase shifts throughout the entire sweep indicating that no detrimental resonance was present within the limits checked.

Fatigue testing was performed at a mean 91,000 in-lb and an alternating torque of +13,600 in-lb. It was noted that the slip rate decreased as the cyclic count increased beyond 250,000. At 500,000 cycles, slippage stopped (Figure D-29). The clutch completed 10 million cycles with no further slippage and no indication of distress.

A continuation of the nonrotating slippage test was performed at a steady load of 45,500 in-lb and an alternating load of +3,000 in-lb. The alternating load was increased in increments of 3,000 in-lb. The clutch assembly was then subjected to a 5-minute test at each incremental load level. At the +18,000 in-lb alternating load level, the clutch began to slip at the rate of 6 deg/min. Inspection at the completion of cyclic fatigue and slippage testing revealed several fatigue-induced cracks emanating from pocket radii below drawing tolerance in both the inner and outer clutch cages. There was light fretting on the spray contact area and pronounced fretting on approximately 180 degrees of the silver-plated pilot surface of the inner cage.

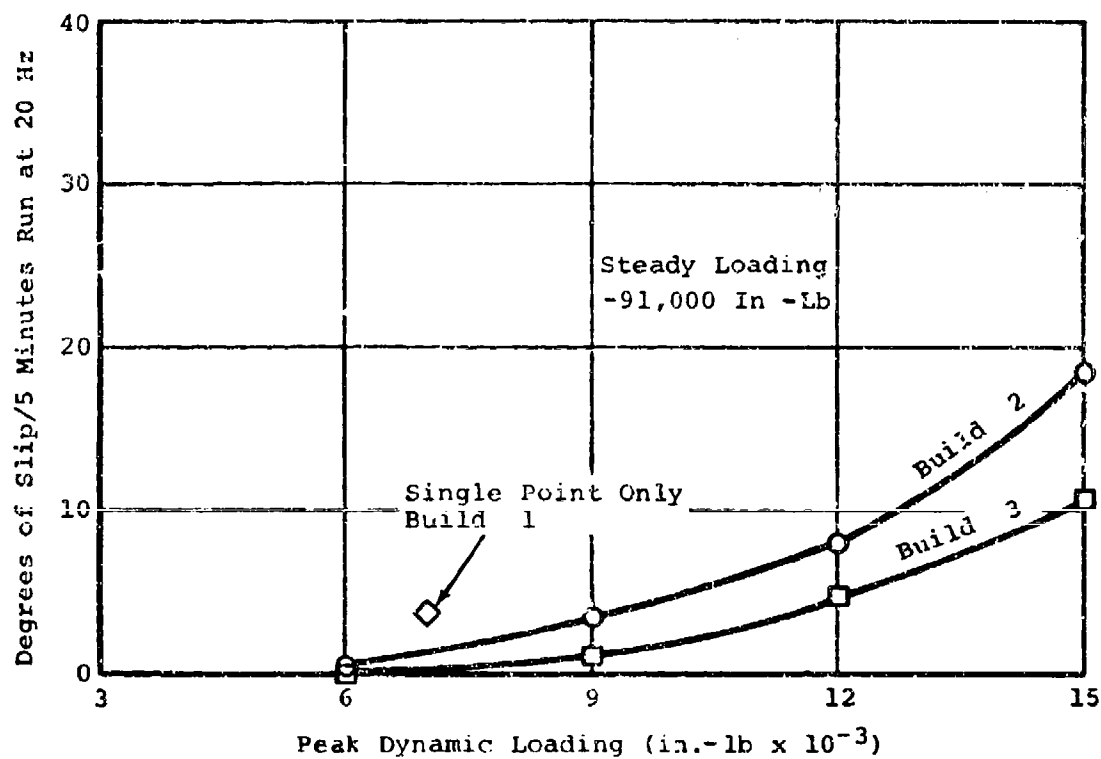


Figure D-28. Results of Slip Test.

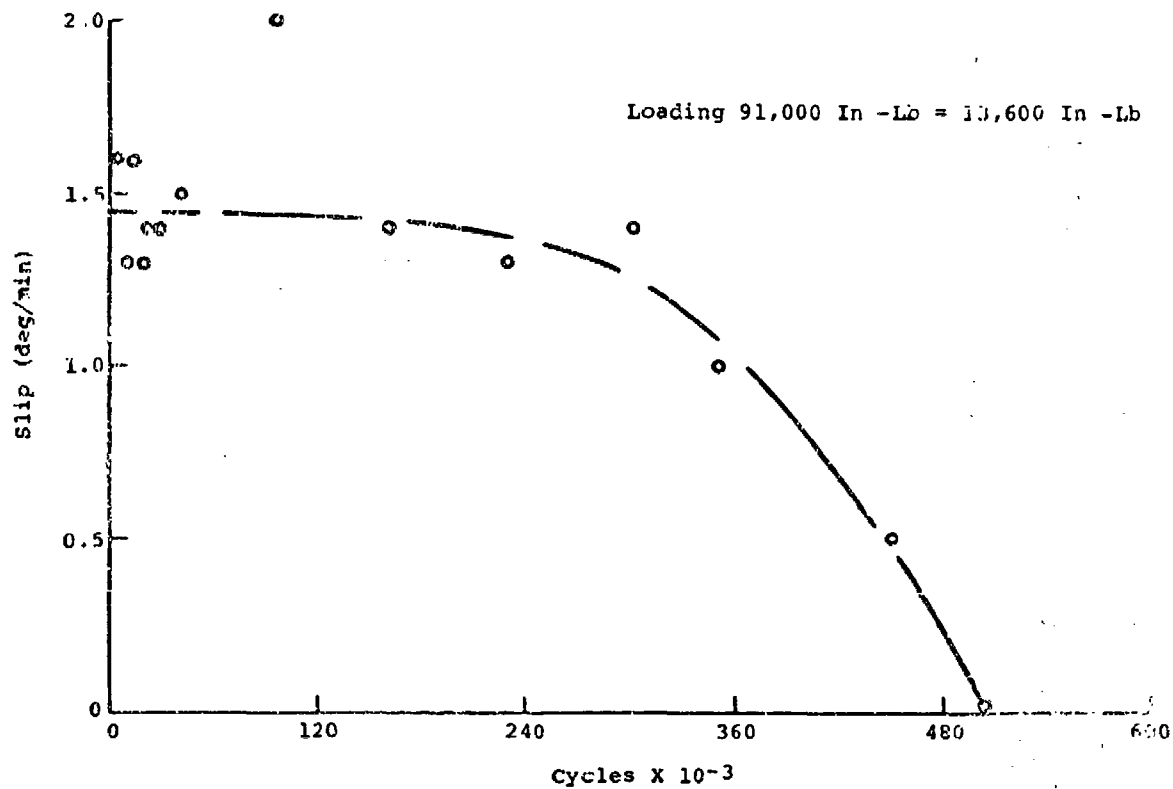


Figure D-29. Results of the Nonrotating Cyclic Torque Fatigue Test.

Static Overload Test

This test was conducted on one optimum clutch Design D only. The purpose of the test was to determine the clutch ultimate capacity.

Failure was defined as rollover, slippage, or component fracture. All clutch parts including bearings were coated with grease (MIL-G-81322).

The following data were recorded at each torque setting:

- | | |
|--|---------|
| • Torque, ft-lb | ±10 |
| • Angular Displacement, deg | ±0.5 |
| • Outer-Shaft Deflection over each
Row of Sprags - 8 Places Total, in | ±0.0005 |
| • Load Sharing Between Rows of Sprags, pct | ±20 |

Failure occurred at a torque level of 206,900 in-lb or 17,240 ft-lb, which is equivalent to 468 percent of one-engine design torque.

The failure was sprag rollover. All sprag preload spring tabs but one were broken off. Also, several sprags had sheared "coffin corner" edges. Shaft and housing showed some brinelling. Unaided visual examination of the inner and outer cages revealed no damage.

Table D-12 shows the results of the load-sharing test and indicates that on the average, each row carries approximately 50 percent of the torque.

Conclusions

Table D-13 presents the results as compared to the design criteria. The expected rollover torque for the aircraft clutch based on the test is also shown. Although this is slightly less than 450 percent torque, a problem with the aircraft clutch is not expected since the drive system ultimate torque is equivalent to 225 percent. Also, the outer-race hoop stress in the aircraft clutch is 3.5 percent above the criteria at 200 percent torque. However, since the test clutch completed 10 million cycles during the fatigue test at a torque level equivalent to 206 percent, ±39.8 percent, of aircraft single-engine torque without indication of outer race distress, and since the aircraft clutch operating condition is equivalent to 100 percent, ±12 percent, of single-engine torque, the slightly higher calculated hoop stress does not indicate an objectionable condition. Note also that at clutch rollover, the outer-race hoop stress is less than the race ultimate tensile strength.

TABLE D-12. SUMMARY OF LOAD-SHARING TEST RESULTS

Position*	Torque Through Row 1** (pct)	
	Torque Bridge 1	Torque Bridge 2
1	61.4	56.3
2	49.8	47.9
3	53.7	44.3
4	43.2	46.5
Average	52.0	48.8

*Any random position

**In the assembled position, row 1 is the first sprag-clutch row, looking from the engine end.

TABLE D-13. COMPARISON OF DESIGN D AND AIRCRAFT CLUTCH
PARAMETERS WITH DESIGN CRITERIA

Parameter	Design Criteria	Design D	HLH Clutch
Contact Stress at 200 Percent of Torque, psi	$\leq 450,000$	435,000	433,000
Contact Stress at 300 Percent of Torque, psi	$\leq 600,000$	510,000	504,000
No Failure (Rollover), pct of torque	≥ 450	489* 469**	466* 447***
Outer-Race Hoop Stress at 200 Per- cent of Torque, psi	$\leq 71,200$	68,400	73,600
Cam Rise at 200 Percent of Torque, pct	≤ 80	49.8	51.7
*Calculated **Test ***Estimated from test			

OIL SEALS

Oil seals are a potential risk area due to the combination of size and shaft speed. Seal rubbing speeds of up to 17,100 ft/min. are desired for optimum design configuration so that seal diameters do not limit shaft diameters.

Conventional elastomer type seals using Viton or silicone materials are limited to rubbing speeds below 4,000 ft/min. Carbon face type seals are available with ratings up to 20,000 ft/min. However, conventional face type seals are relatively expensive and are easily damaged during transmission assembly or teardown.

Three seal vendors (Gits, Koppers, and Stein) have been selected to develop seal designs incorporating features to overcome some of the hazards and limitations of current state-of-the-art seals. Figure D-30 shows the configurations to be tested by each company.

Results of Program

The Gits Brothers Manufacturing Company tested two seal design concepts:

- A floating carbon type seal (P/N 02531-1100) completed the twelve-hour dynamic run and twelve-hour static check within the 2 cc/hr leakage limit. The 1000-hour test was completed within the 2 cc/hr limit; however, the required oil flow of one GPM was not met. At zero pressure, the flow was reduced to 0.72 GPM and at 0.375 psi the flow was reduced to 0.31 GPM in order to keep within 2 cc/hr leakage limit. This seal should be satisfactory for HLH transmission application except in area of clutches. Approximately 1412 hours of testing were accumulated on this design.
- An elastomer type seal (P/N 02531-3000) was also tested by Gits. This seal was not successful due to the breakdown of the ebolon packing elastomer at the rubbing speed of 21,000 FPM. Their prior experience with this type seal was only up to one-half of this rubbing speed. The seal was also apparently too stiff to respond to low operating seal cavity pressure. Approximately 89 hours of testing were accumulated on this design.

The Stein Seal Company tested two design concepts:

- A segmented circumferential carbon type seal (P/N 4376) was tested. This seal, coupled with a screw thread wind back and windage screen, was successful in meeting all conditions of the test plan. Average oil leakage was only 0.1 cc/hour. The carbon wear rate extrapolates to over 14,000 hours expected seal life.

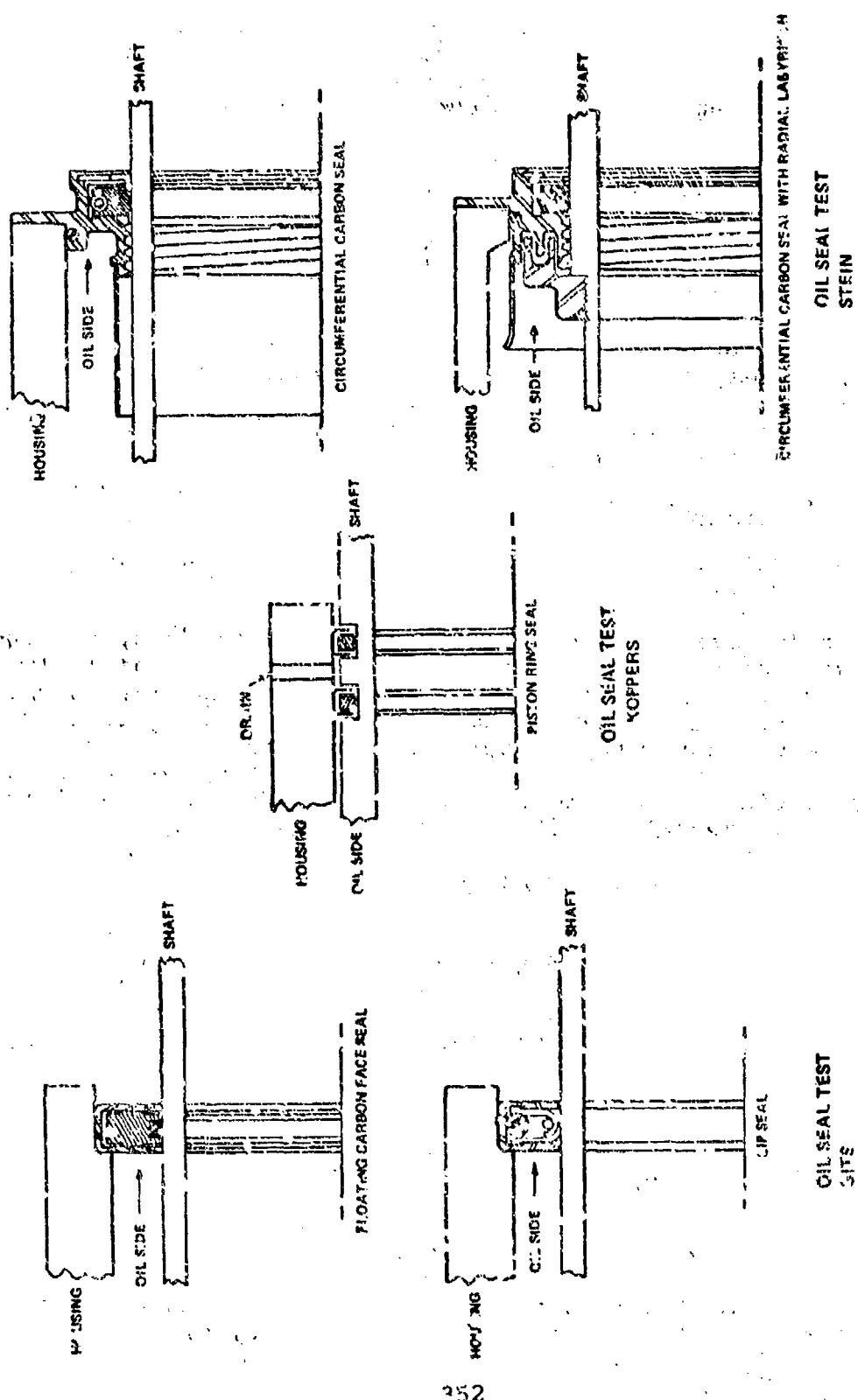


Figure D-30. Test Configurations.

- A second design (P/N 4375) is similar to the above but includes an additional radial labyrinth. This design was not successful in meeting 2 cc/hour leakage limit and was therefore stopped in favor of developing the simpler first design.

The piston ring type design submitted by The Koppers Company may be successful under oil mist conditions but was not satisfactory under the oil flow requirements imposed in the test plan which simulated HLH transmission conditions at the overrunning clutches. Approximately 15 hours of testing were accumulated on this design.

Conclusions

- The Stein seal design (P/N 4376) met the test conditions and test leakage limits. Seal application unlimited.
- The Gits seal design P/N 02531-1100) nearly met the test conditions and met leakage limits.
- The Koppers design was not successful except at 10% required oil flow conditions.
- The Stein seal has been selected as prime in the transmission test program. The Gits seal will also be evaluated in certain locations.

ROTOR BRAKE DEVELOPMENT

The extraordinary rotor stopping and rotor holding requirements occasioned by the size of the HLH rotor system made a brake development program necessary. Two major objectives of this program were weight reduction and increased stop life before disc or liner replacement. These objectives were achieved.

The development program was subdivided into three phases. Phase I was a design study program to select test candidates for Phase II. Phase II evaluated full-scale disc and lining specimens and selected one design for further evaluation and qualification in Phase III. Design, fabrication and testing for all phases was performed by B. F. Goodrich Aerospace and Defense Products, Troy, Ohio.

Phase I

In Phase I, preliminary design parameters were as defined in Table D-14. A steel disk was selected as the baseline for evaluation of the candidate designs. Other disc candidates were described as follows:

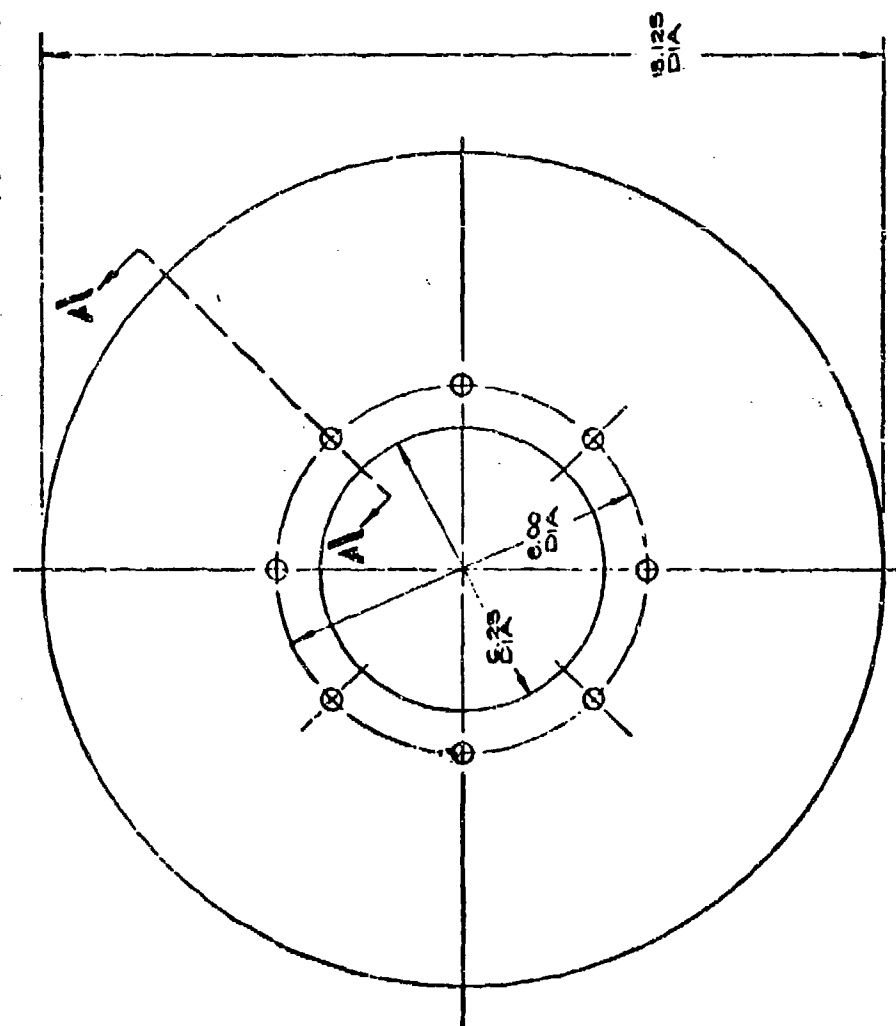
- Structural graphite (Figure D-31). The lining material would also be structural graphite.
- Structural beryllium with sintered metallic lining plates (Figure D-32).
- Structural beryllium with graphite wear pads (Figure D-33).

Disc and lining material properties are compared in Table D-15.

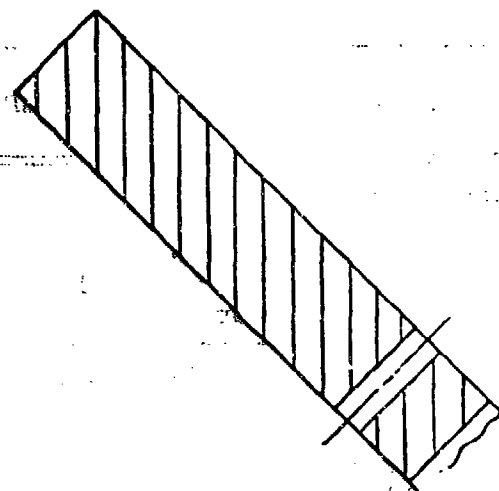
A comparison of the rotor brake disc designs is shown in Table D-16. Four stop times are defined - 30, 35, 40, and 45 seconds. From this chart it can be concluded that the advanced designs show increasing benefits as the duty cycle becomes more severe (stop time decreases). At the 30-second stop time the weight decrement for disc and head can be as much as 90 pounds. It was also estimated that the increased stop life of the advanced designs could nearly cancel the greater cost of the advanced material, to achieve a parity in life-cycle costs compared to the baseline steel disc. Of the advanced designs, the graphite/graphite lining concept was favored because of its inherent design simplicity as compared to the beryllium with attached wear pads.

TABLE D-14. PRELIMINARY HLH ROTOR BRAKE DESIGN PARAMETERS.

<u>Operating Conditions</u>	
Total Stopping Time	30 seconds (desired)
Rotor Speed Decay Time	As optimized by sub-contractor
Brake Stopping Time	-----
Normal Design Service Life Between Overhauls	1000 Stops (Desired)
Normal Rotor Speed	156 RPM
Rotor Blade Diameter	92 feet
Rotor Inertia (Both Heads)	115,500 ft/lb/sec ²
Total System Inertia	127,000 ft/lb/sec ²
Rotor Drag Constant	294 ft/lb/sec ²
Operating Ambient Temperature Range	-65°F to 250°F
Maximum Allowable Brk. Disk Temperature	1500°F
Normal Brk. Disk Speed	4000 - 5500 RPM (Max. Range)
(Optimum normal speed to be selected within this range by subcontractor)	
Normal Engine Speed	11,500 RPM
Maximum Brake Disk Overspeed	25% above normal disk speed
Total Engine Stall Torque (3 Engine)	1500 ft/lb
Hydraulic System Operating Pressure	2900 PSI Minimum 3000 PSI Maximum
Emergency Operating Requirement	1-stop capability from a rotor speed of 156 RPM
<u>Physical Size Limits</u>	
Maximum Brake Disk Outside Dia.	18.0 In
Minimum Inside Dia. Mounting Bolt Circle	6.0 In
Maximum Inside Dia. Mounting Bolt Circle	8.0 In
Maximum Brake Disk Thickness	1.5 In
Maximum Radial Brake Lining Width	5.0 In
Maximum Brake Lining Angular Sweep	100 Deg



356



SECTION A-A
SCALE 1/1

Figure D-31. Layout-Structural Graphite Disk and Steel Disk.

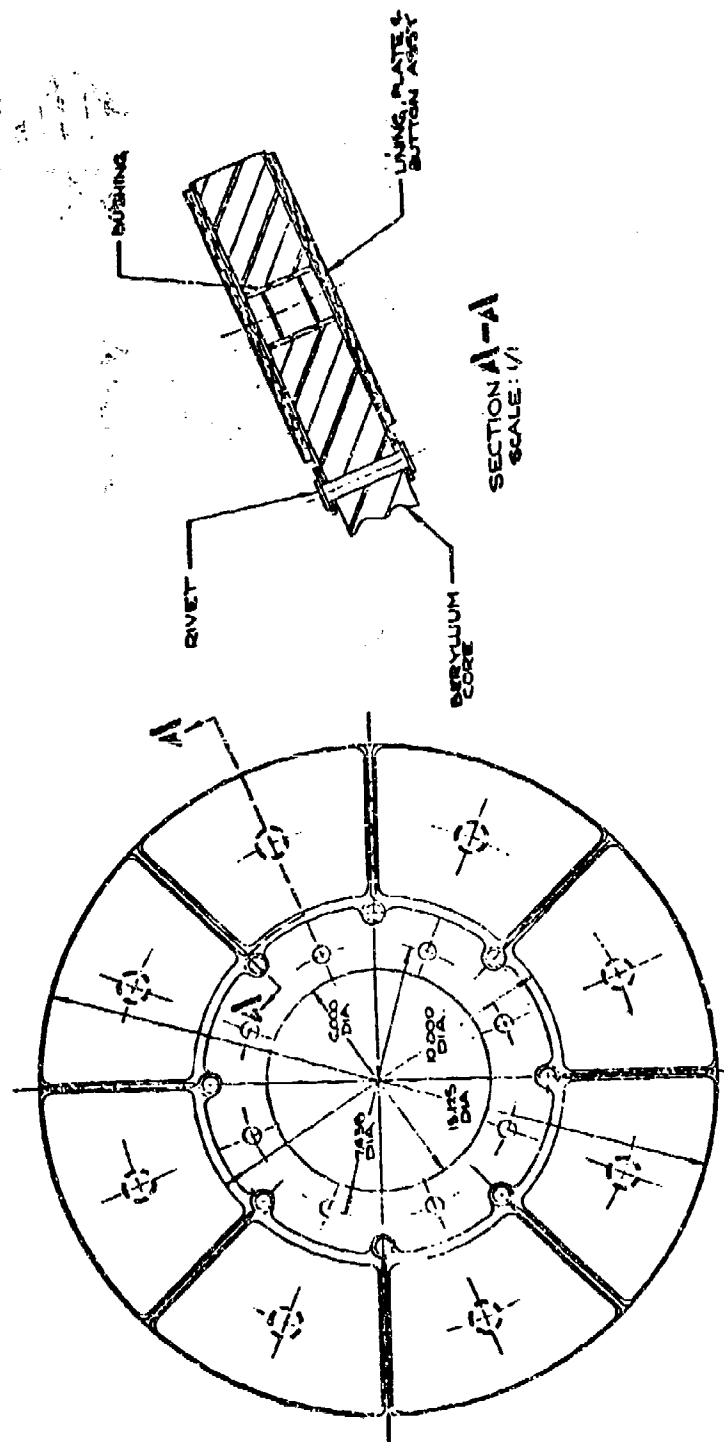


Figure D-32. Layout-Structural Beryllium Disk with Metallic Linings.

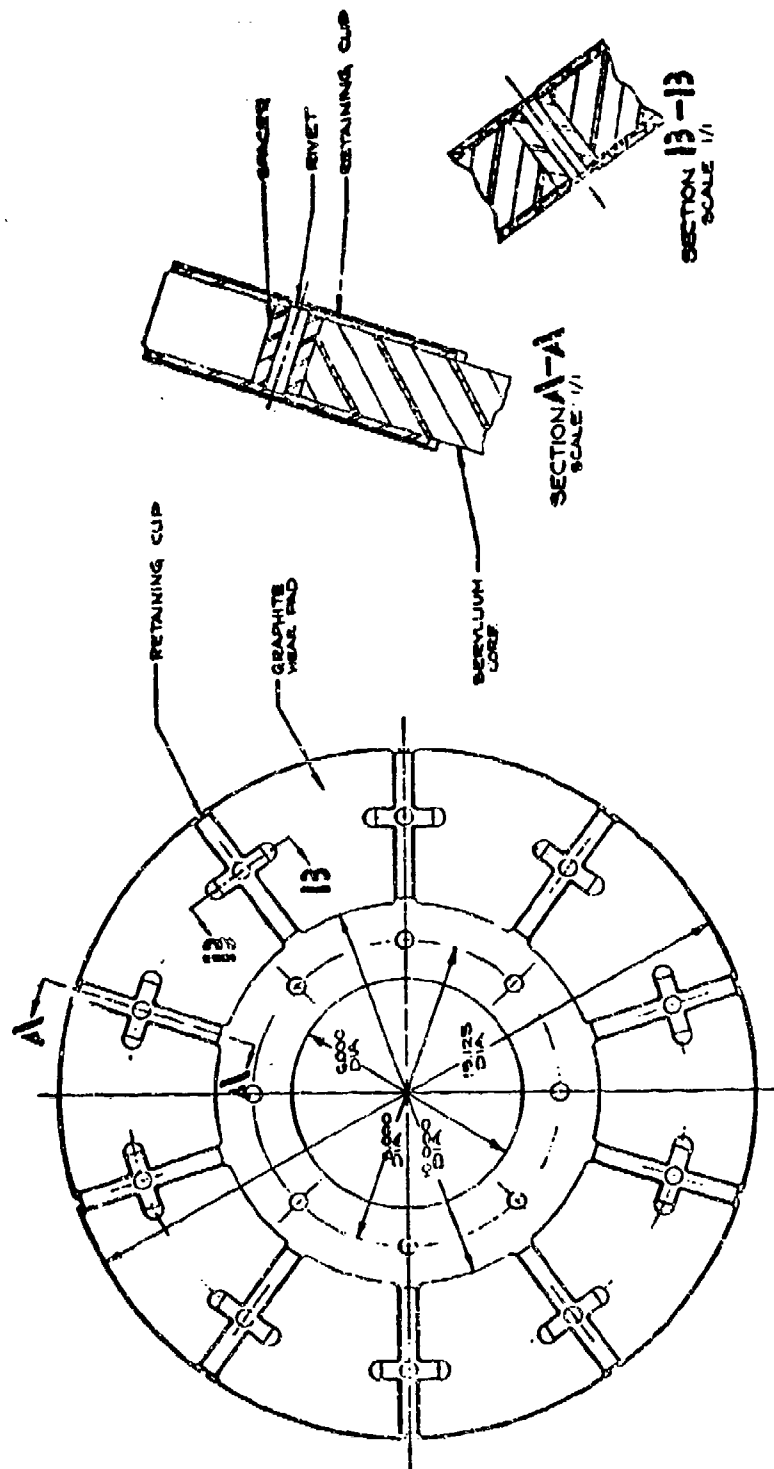


Figure D-33. Layout-Structural Beryllium Disk with Graphite Linings.

TABLE D-15. HEAT SINK MATERIAL COMPARISON				
PROPERTY OR CHARACTERISTIC	ISOPRESSED			PYROLYTIC GRAPHITE
	LOW ALLOY STEEL	BERYLLIUM	& SINTERED BERYLLIUM	
Density, LB/IN ³ (ρ)	.283	.066		.055-.060
Thermal Conductivity, BTU/HR-FT ² -F° (k)	70°F 25 600°F 23 1000°F 21	275 105 140 69 90		
Specific Heat, BTU/LB-F° (c)	70°F .10 600°F .14 1000°F .17	.43 .62 .65		.23 .33 .38
Thermal Diffusivity, k/c ρ FT ² /HR	70°F .51 600°F .34 1000°F .25	12.03 2.14 4.27 .98 2.38		
Mean Coefficient of Thermal Expansion, IN/IN/°F x 10 ⁻⁶	70°F to 7.0 1000°F	7.5		1.8
Modulus of Elasticity PSI	29 x 10 ⁶	42 x 10 ⁶		4.3 x 10 ⁶ (Edgewise)
Ultimate Tensile Strength, KSI	70°F 180 600°F 160 1000°F 104	37 25.5 20.		11 11 11
Melting Point	°F 2795	2340		6330
Maximum Design Bulk Operating Temperature for Brake Design	800	800		1300

TABLE D-16. COMPARISON CHART-ROTOR BRAKE DESIGNS, BOEING VERTOL HLH.

12-17-71

Heat Sink Mat'l.	Total Stop Time (sec.)	Disk Size (Inches) O.D.	Disk Size (Inches) T	Disk Wt. (Lb.)	Brake Head Wt (Lb.)	Total Brake Wt (Lb.)	Estimated Service Life (stops)	Est. Prod. Unit Cost (\$)	Est. Material Overhaul Costs (\$)	Est. Life Cycle Costs (\$)	Heat Sink Loading (Ft. Lb.) Lb.	Power Rate (Ft. Lb.) Sec.	Rolling Speed (FPM) (3)
Steel - Metallic Linings	30	18.12	1.37	89.0	55.5	144.5	290	1,700	17,500	19,200	60,000	386,700	11,389
Beryllium - Metallic Linings	30	18.12	1.34	22.4	38.6	61.0	345	5,300	17,835	23,135	65,000 STL 360,000 BE	386,700	11,389
Graphite - Graphite Linings	30	18.12	1.23	17.1	35.3	52.4	1,000	4,850	16,820	21,670	295,100	417,700	11,386
Beryllium - Graphite Linings	30	18.12	1.32	17.7	36.6	54.3	1,000	4,750	16,000	20,750	140,000 C 360,000 BE	417,700	11,386
Steel - Metallic Linings	35	18.12	1.29	84.0	52.5	139.5	360	1,675	13,300	14,975	60,000	272,400	11,385
Beryllium - Metallic Linings	35	18.12	1.26	21.3	38.6	59.9	440	5,000	15,640	20,640	65,000 STL 360,000 BE	272,400	11,389
Graphite - Graphite Linings	35	18.12	0.93	12.8	35.3	48.1	1,000	3,900	13,460	17,360	295,650	408,000	10,699
Beryllium - Graphite Linings	35	18.12	1.02	13.7	36.6	50.3	1,000	3,800	13,000	16,800	140,000 C 360,000 BE	408,000	10,699
Steel - Metallic Linings	40	18.12	0.73	47.5	55.5	103.0	460	1,600	8,800	10,400	60,000	270,700	10,501
Beryllium - Metallic Linings	40	18.12	0.86	16.1	38.6	54.7	500	3,600	10,800	14,400	65,000 STL 360,000 BE	283,000	10,253
Graphite - Graphite Linings	40	18.12	0.78	10.8	35.3	46.1	1,000	3,600	12,600	16,200	294,980	341,000	9,754
Beryllium - Graphite Linings	40	18.12	0.87	11.7	36.6	48.3	1,000	3,450	11,500	14,950	140,000 C 360,000 BE	341,000	9,754
Steel - Metallic Linings	45	18.12	0.49	31.8	55.5	87.3	490	1,450	5,250	5,700	60,000	253,300	9,259
Beryllium - Metallic Linings	45	18.12	0.71	14.2	38.6	52.8	545	3,000	8,640	11,640	65,000 STL 360,000 BE	253,300	9,259
Graphite - Graphite Linings	40	18.12	0.74	10.2	35.3	45.5	1,000	3,150	12,190	15,340	293,640	403,750	9,419
Beryllium - Graphite Linings	40	18.12	0.83	11.1	36.6	47.7	1,000	3,200	10,750	13,950	140,000 C 360,000 BE	403,750	9,419

NOTES: (1) Estimated service lives for graphite and graphite lined beryllium are minimum projections based on a minimum amount of available data. These estimates to be verified during Phase II.

(2) Overhaul and life cycle costs are based on 1,000 stops per year for 10 years.

(3) Rubbing speed at brake application.

Phase II

The objective of Phase II was to design, fabricate, and evaluate, by testing, four separate rotor brake concepts. The differences among the concepts were in the heat sink materials. The heat sink consisted primarily of a rotating disk/disk assembly and stationary lining segments. The four concepts were as described under Phase I.

An existing rotor brake head assembly was utilized for all concept testing. Various linings and disks/disk assemblies were designed for use with the head assembly.

The following parameters apply to the head assembly as used for the HLH Phase I testing:

Piston Area	- 25.02 in ² total
Brake Radius	- 7.078 inches
Back Pressure Capability	- 25 psi
Head Assembly Weight (less linings and pressure plates)	- 21.5 lb

Figure D-34 illustrates a cross-sectional view of the brake head assembly.

Conventional Steel Disk Design -

The steel disk was fabricated from 4140 steel and heat treated to a Brinell Hardness of 372-426. The physical size was 18.062 inches outside diameter with a .940-inch thickness in the rubbing area. Through normal wear and occasional grinding of the disk to return it to parallelism, the final thickness upon completion of the last test averaged .783 inch.

The area around the bolt holes was reduced to .375 inch thick, primarily for weight reduction. The total disk weight in the new condition was 51.7 pounds. Eight 1/2-inch bolt holes were used. The disk temperature was monitored by a single thermocouple inserted 1-5/16 inches from the inside diameter, approximately 1/8 inch into the friction area.

Several types of linings were evaluated in conjunction with the steel disk for the best possible wear life. These included iron-copper base, iron base, copper base, and organic linings. Various sizes, thicknesses, and energy ratings were also evaluated.

All lining materials except the organic were sintered onto a steel lining carrier. This lining carrier acts as a base for

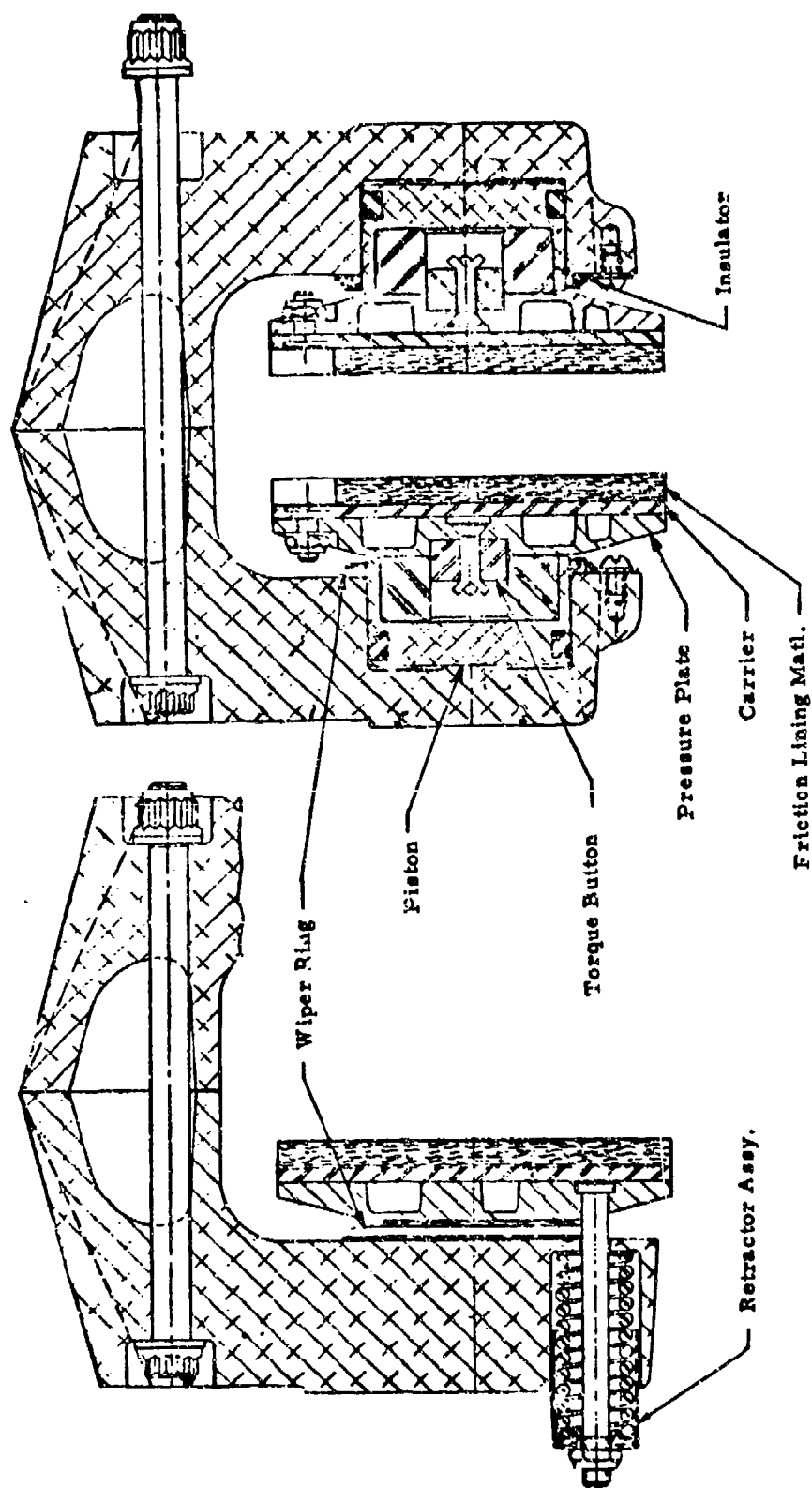


Figure D-34. Cross Sections of Piston Housing Assembly.

the friction material, additional heat sink material, and provides the means of attachment onto the pressure plate. The organic lining was epoxied and riveted onto the lining carrier.

Beryllium Disk/Metallic Lining Design —

The rotating disk assembly (Figure D-35) consists of a structural beryllium core with steel backed lining segments attached to both surfaces. These wear segments had .100-inch-thick iron base lining material sintered onto a steel backing. The wear segments were attached at three points: through the disk mounting bolt holes, and through two torque removal slots on the disk periphery. The beryllium core incorporates expansion slots beneath the area where two adjacent wear segments meet. The disk assembly was 18.062 inches in diameter with a thickness in the rubbing area (with wear segments) of .880 inch. Eight 1/2 inch bolts were used for mounting and the disk assembly weighed 17.75 pounds.

The disk temperature was monitored by a single thermocouple inserted 1-5/16 inches from the inside diameter, approximately 1/8 inch into the friction area.

The linings used were of a sintered iron based friction material, designed identical to those used on the steel brake concept. Lining temperatures were monitored as before on the steel disk concept. This design concept has been utilized successfully in full circle brakes on several aircraft wheel brakes in production today.

Beryllium Disk/Graphite Lining Design —

The rotating disk assembly (Figure D-36) consisted of a structural beryllium core with structural graphite wear segments attached to both surfaces. Attachment was achieved by an overlapping of the graphite segments with steel retainers which were in turn riveted to the beryllium. The overall assembly size was 18.062 inches outside diameter with a .868 inch total thickness. Eight 1/2-inch bolts were used and the assembly weight was 12.42 pounds. Temperature was monitored by a thermocouple inserted 1.31 inches into the material center from the inside diameter. The wear segments provided a total of .040 inch of allowable wear.

Graphite Disk and Lining Design —

The structural graphite disk (see Figure D-37) had an outside diameter of 18.083 inches and a thickness of .824 inch. Eight 1/2-inch bolt holes were originally specified, but eight additional 3/8-inch bolt holes were added prior to testing, to allow a lower bolt preload. The total disk weight was 9.47 pounds. A thermocouple was inserted 1-1/4 inches from the inside diameter and axially centered.

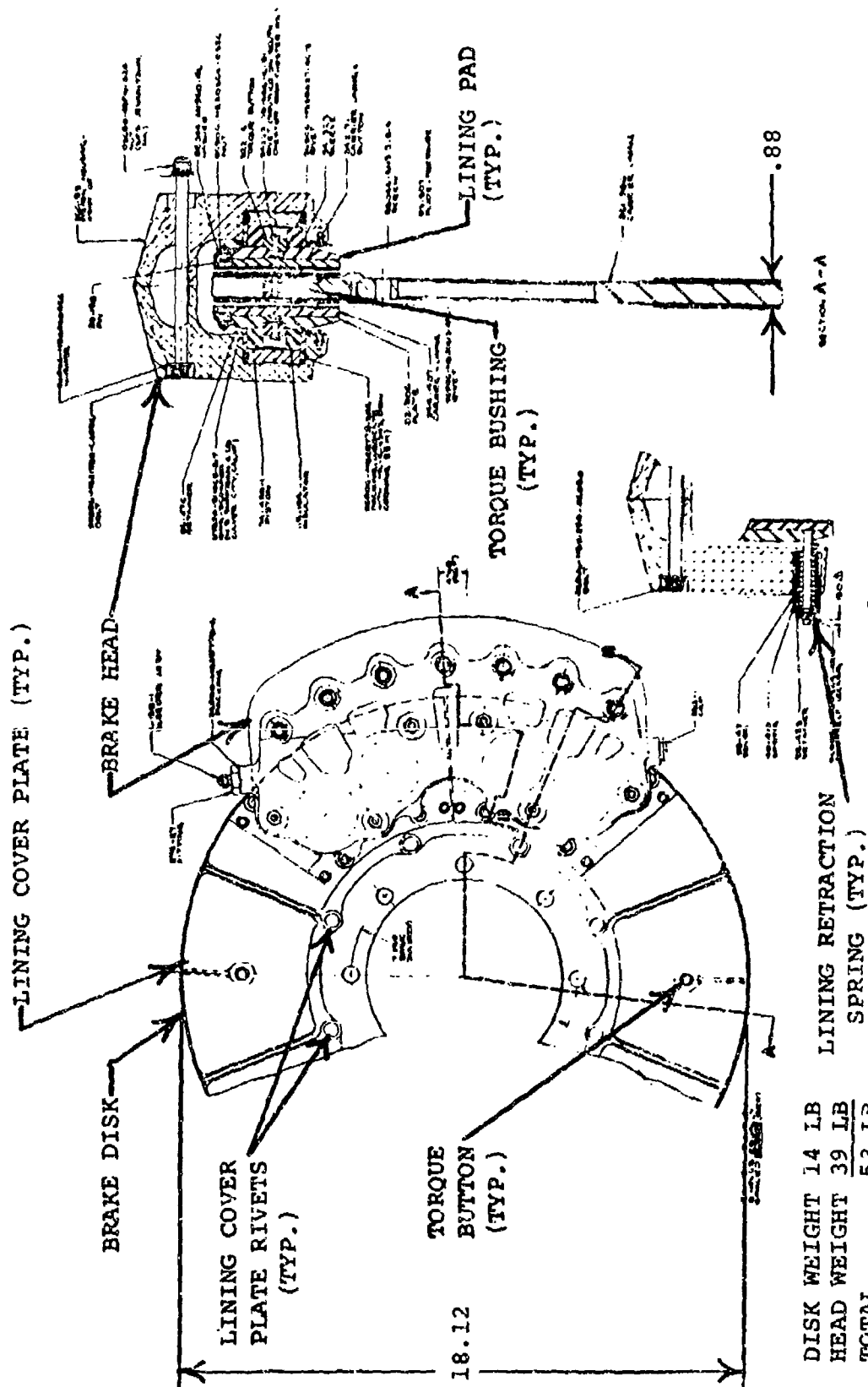


Figure D-35. Metallic Lined Beryllium Brake Disk Assembly.

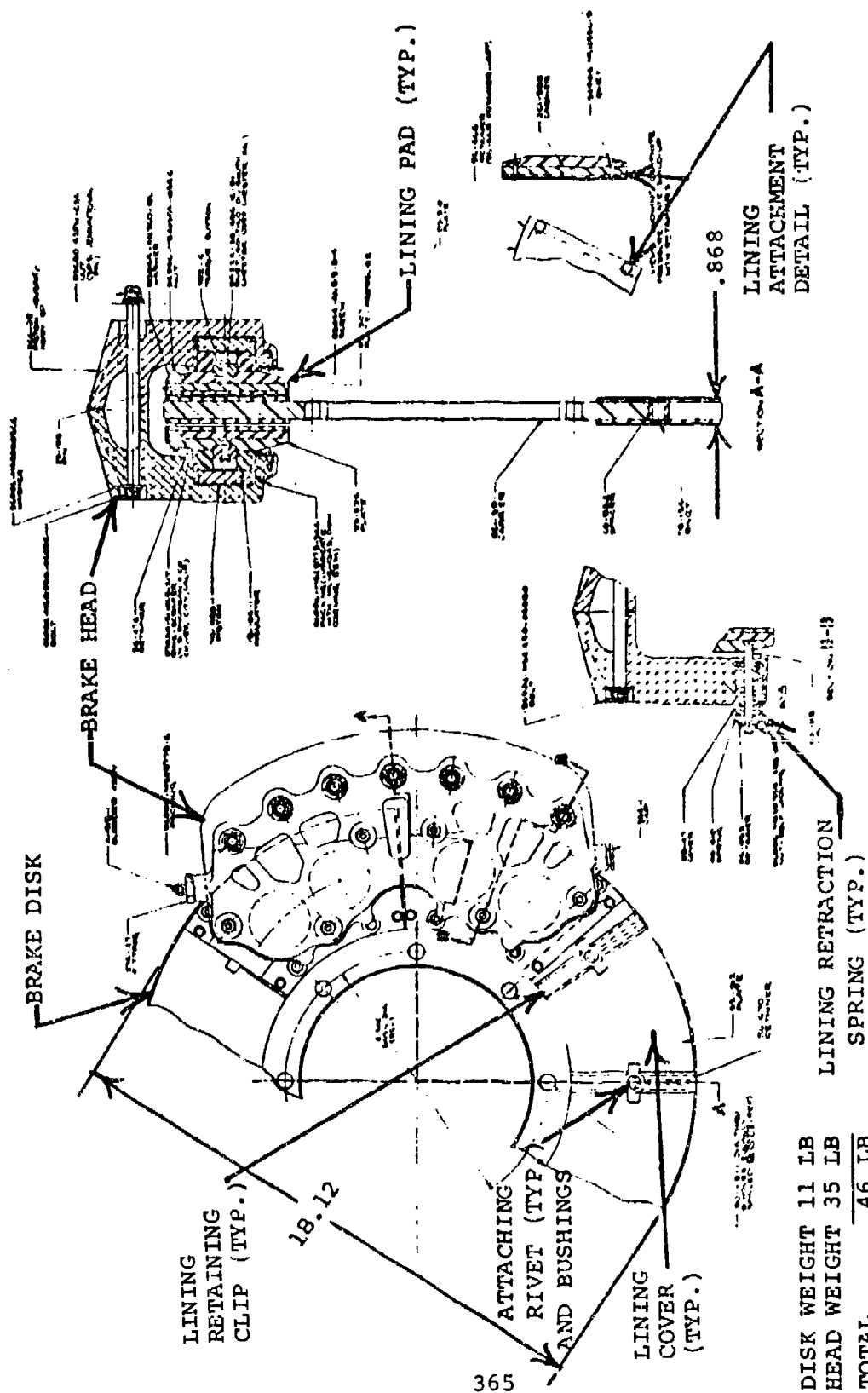


Figure D-36. Carbon/Graphite Lined Beryllium Brake Disk Assembly.

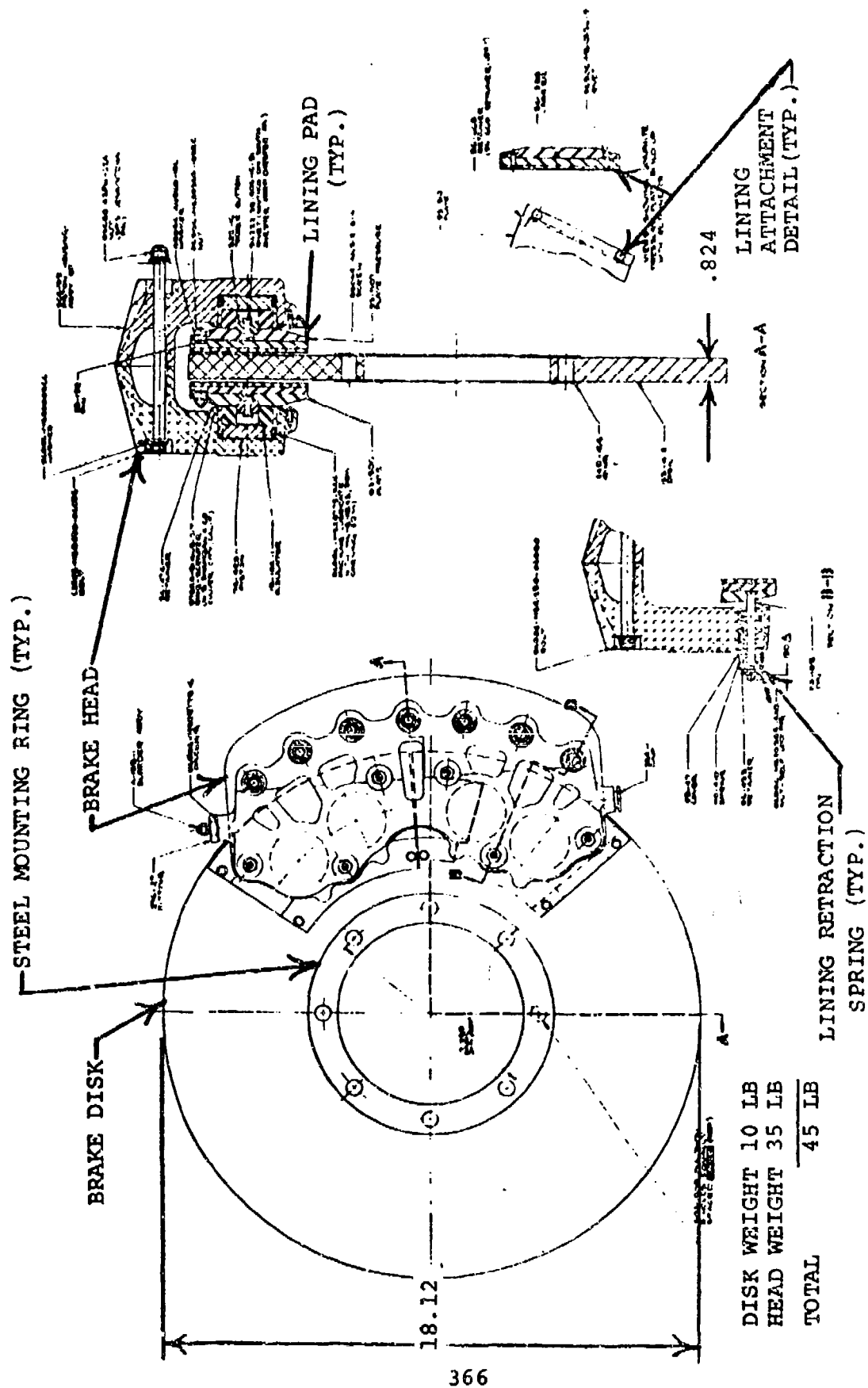


Figure D-37. Structural Carbon/Graphite Brake Disk Assembly.

The linings were also constructed of graphite. Due to the higher temperature associated with a graphite brake, mechanical retention of graphite linings becomes more difficult than conventional linings. The method developed for this test worked very well due to the effort put forth in locating the rubbing surface as far from the steel retainers as possible. In addition, an attempt to partially shield the retainers from the heat was made. No lining carriers were required for this concept; the linings were mounted directly to the pressure plate. No thermocouple was inserted into the lining.

Test Apparatus/Equipment —

All dynamic and static torque evaluations were performed on the B. F. Goodrich 48 Inch Shaft Dynamometer. In addition to its standard panel recording instruments, an instrumentation room is equipped to monitor all of the necessary brake parameters.

Brake test parameters monitored on selected dynamic torque stops were as follows:

Brake Torque, ft-lb	Lining Temperatures (4)
Disk Speed, rpm	Pressure Plate Temperatures (2)
Stop Time, sec	Piston Housing Temperature
Brake Pressure, psi	Disk Mounting Fixture Temperature
Disk Temperature	(All Temperatures were in °F)

A variable speed (Vari-Drive) unit was incorporated to conduct disk strength and endurance tests. The unit was equipped with a magnetic pick-up to monitor speed.

During the disk strength testing of the beryllium disk with metallic wear plates, a catastrophic failure occurred which rendered the drive unit useless. A second, smaller unit was incorporated in conjunction with a pulley and drive shaft arrangement which separated the disk/disk assembly from the drive unit.

Test Procedures

Dynamic Torque Tests —

Once the number of inertial disks were engaged so that the particular test condition kinetic energy was produced at the desired brake application RPM, the following test procedure was utilized: Rotate disk up to speed, apply predetermined hydraulic pressure to the brake head pistons, record the various key parameters during actual brake stopping. The hydraulic pressure varied for the first several test stops until the desired test condition brake stopping time was obtained. Once the correct brake head hydraulic pressure had been determined, the

test procedure was repeated until the required 250 test stops or a failure had occurred.

Wet Stop Dynamic Torque Tests —

A wet disk dynamic torque test was conducted on each of the two advanced material disk concepts which utilized graphite friction surfaces. These tests were performed on brake disk/lining assemblies which had been subjected to a 24-hour water soak. The test conditions and procedures were the same as those for a normal dynamic stop.

Static Torque Tests --

A static torque, equivalent to that torque produced by the engines at 65°F O.A.T. idle power, was applied to the brake. The brake was required to demonstrate the ability to prevent rotation with a normal operating pressure applied. This test also determined the maximum holding torque of the brake at normal operating pressure. The normal operating pressure was determined from the dynamic torque tests conducted for each configuration.

Disk Endurance Tests —

Each disk (less brake head assembly) to be tested was mounted on the output shaft of a vari-drive unit and cycle tested from stationary, up to speed, and return to a stationary condition for 1100 cycles. The first 1,000 cycles were at the normal operating speed of 5,150 rpm and the final 100 cycles were at 6,440 rpm (25% overspeed condition). The disk assemblies were then inspected for any visual signs of fretting or fatigue damage.

Disk Strength Tests —

Each disk (less brake head assembly) to be tested was mounted on the output shaft of a vari-drive unit and tested by driving it 1.25 times the normal operating speed for a period of 30 minutes. The disk was then driven at 1.37 times the normal operating speed for a period of 30 seconds (normal operating speed is 5150 rpm). The disk assemblies were then visually inspected for any fretting, fatigue, or ultimate damage.

Test Results

Steel Disc: A total of 197 stops were completed on various lining materials. Table D-17 summarizes the results.

Metallic Lined Beryllium Disc: A total of 38 stops were made under two dynamic conditions. During the disc strength test, 3 sets of cover plates separated from the disc and the resultant unbalance created a catastrophic failure of the disc

TABLE D-17. CONVENTIONAL STEEL DISK DYNAMIC TORQUE TEST RESULTS.

Test No.	Lining Material & Code	Area/Thickness	Average Kinetic Energy/Absorbed by Brake (ft-lb) x 10 ⁶	No. of Stops	Average Stop Time (sec)	Average Torque (ft-lb)	Average Pres. (psi)	Average Disk Peak Temp. (°F)	Average Lining Leading Edge Temp. (°F)	Average Lining Trailing Edge Temp. (°F)	Average Pressure Plate Temp. (°F)	Average Piston Housing Temp. (°F)	Average Lining Wear (in/ft) ^A	Average Disk Wear (in/ft) ^A	Maximum Lining Wear (in/ft) ^A	Projected Stop Life at 40 Stps Total A/C Stop Time
T-3778	Fe Cu (E)	24.0/0.080	4.0	8	14.7	1,925	797	278	1,138	1,108	511	134	0.00401	N/A	0.00600	30-40 Stops
T-3778	Fe (C)	84.0/0.100	4.23	10	14.8	2,043	843	347	1,074	1,030	536	133	0.00538	N/A	0.00850	Insufficient Data
T-3821	Cu (A)	66.9/0.260	3.83	23	13.8	1,964	601	529	1,077	978	549	110	0.00519	0.00018	0.00848	Insufficient Data
T-3821	Organic (F)	86.9/0.260	3.85	9	13.8	1,960	525	848	288	258	233	95	0.01155	0.00015	0.0217	30 Stops
T-3837	Cu (A)	94.0/0.200	2.9	15	11.3	2,111	705	339	781	758	363	115	0.00799	N/A	0.00467	95 Stops
T-3837	Cu (A)	94.0/0.155 ^B	3.27	15	12.4	2,040	683	403	909	846	470	136	0.00247	N/A	0.00347	95 Stops
T-3837	Cu (A)	94.0/0.115 ^B	3.7	20	14.2	1,892	677	430	1,026	898	378	136	0.00378	0.00118	0.00800	95 Stops
T-3800	Cu (A)	94.0/0.300	3.03	95	11.5	2,829	598	338	841	815	467	118	0.00181	0.000217	0.00210	96 Stops

(A) In./ft. Inches Per Stop Per Surface
 (B) These values are averages since all 3 conditions of T-3837 were conducted on 1 set of Brakes.
 (C) Based on 0.300 in. Min. Lining Thickness, Max. Wear Rate and 3.2 x 10⁶ ft-lb Kinetic Energy

assembly. Previously, warpage and poor heat transfer characteristics had shown this design to be improper for a caliper type brake. In aircraft wheel brakes, where uniform pressure around the entire disc exists, this design has shown excellent characteristics.

Structural Graphite Disc: A total of 363 stops were completed. Table D-18 summarizes the results. In addition, disk endurance and overspeed tests were accomplished satisfactorily. The disc was cycled from zero to 5150 rpm for 1000 cycles, to 6440 rpm for 120 cycles, and rotated at over 8800 rpm for 15 seconds.

Conclusions

1. Conventional Steel Disk Design

- a. The design will work in the intended application; however, the lining service life will be extremely low.
- b. The unit weight will be very high.
- c. Any steel disk configuration utilizing metallic linings will throw off sparks when stopping at the lining surface speeds encountered in the HLH design; however, the fire hazard presented by these low-density, short-duration sparks is felt to be very low.

2. Beryllium Disk/Metallic Lining Design

- a. This design will not work in the intended application due to severe disk lining warpage, retention problems and poor lining/disk heat transfer.

3. Beryllium Disk/Graphite Lining Design

- a. This design will not work in the intended application due to poor disk lining/disk heat transfer, high lining wear rates due to the high rubbing speeds and potential long-term disk lining retention problems.

4. Graphite Disk and Lining Design

- a. This design will work in the intended application; however, the lining/disk wear rate will be approximately 67% higher than originally predicted.
- b. The unit weight will be approximately 60% of a conventional steel disk/metallic lining design.

TABLE D-18. STRUCTURAL GRAPHITE DYNAMIC TORQUE TEST RESULTS.

Test No.	Area Thickness at Start (1)	Avg. KE Absorbed by Brake (ft-lb x 10 ³)	Avg. Speed at Appli. (RPM/FPM)	No. of Stops	Avg. Stop Time (sec)	Avg. Torque (ft-lb)	Avg. Press. (psi)	Avg. Disk Temp. (°F)	Avg. Leading Edge Temp. (°F)	Avg. Trailing Edge Temp. (°F)	Avg. Piston Housing Temp. (°F)	Avg. Lining Wear (in/s/s)	Avg. Disk Wear (in/s/s)	Max. Lining Wear (in/s/s)	Avg. Revs.	Avg.
T-3873	78.0/.887	3.27	2551	200	8.3	2947	882	776	462	491	139	.000774	.000511	.001264	181.5	.233
T-3873 Wet Stop	78.0/---	3.265	2550	1	8.6	2844	930	640	382	406	136	----	----	----	183.8	.213
T-3962	78.0/.833	2.999	2444	25	7.77	3016	854	1170	444	483	147	.000403	.000418	.000622	155.0	.239
T-3962	78.0/---	3.255	2546	2	8.1	3014	880	1197	462	509	129	----	----	----	175.8	.222
T-3962	78.0/.858	3.893	2588	30	10.17	2825	924	1222	539	569	125	.000874	.000600	.001057	223.0	.207
T-3962	78.0/.822	4.500	2566	20	11.83	2831	890	1317	614	660	175	.001200	.000820	.001685	243.7	.216
T-4019	78.0/.813	3.09	2050	85	14.22	2025	478	1207	526	551	150	.000603	.000600	.000908	245	.306

(1) Includes Pressure Plate Thickness
(2) Dynamic Friction Coefficient

- c. The unit life should be 600% to 800% greater than that of a conventional steel disk/metallic lining design.

General Conclusions

1. Any helicopter rotor brake assembly operating in the speed and energy range required by an HLH type aircraft should employ a single homogeneous material disk design.
2. Advanced material (graphite and beryllium) helicopter rotor designs offer a potential weight savings over a conventional steel disk brake assembly in the order of 40% to 60%.

Phase III

Technical Approach

Phases I and II of this program showed that the optimum rotor brake configuration for the HLH helicopter would consist of a structural graphite brake disk in conjunction with a conventional aluminum caliper housing utilizing structural graphite linings. Phase III testing was performed on a structural graphite brake assembly designed specifically for the HLH helicopter in accordance with Boeing Vertol HLH Rotor Brake Procurement Specification S301-10045. The Phase III test program was intended to subject the graphite rotor brake assembly to all of the qualification type testing normally required of a production helicopter rotor brake. The testing included functional, dynamic torque, static torque, wear, pressure, low temperature and vibration.

Test Specimen Design —

The following paragraphs are pertinent excerpts from the HLH Rotor Brake Design Specification which governed the design and test of the structural graphite rotor brake assembly?

- 1) All components of the brake shall operate satisfactorily for the number of cycles specified herein without failure due to thermal expansion, corrosion, decrease in strength at elevated temperature, vibration, wear, acceleration, fatigue, or any combination of these causes. The brake shall be capable of satisfactory operation under the environmental conditions specified herein and must satisfactorily pass all performance and environmental tests specified in Section 4.0 of this specification.

2) Operating Conditions

	<u>Condition #1</u>	<u>Condition #2</u>
Total Stopping Time	45 sec	60 sec
Rotor Speed Decay Time	28-29 sec	47-48 sec
Brake Stopping Time	16-17 sec	12-13 sec
Normal Design Service Life Between Overhauls	400 stops	600 stops
Normal Brake Disk Speed	5152 rpm	
Disk Speed at Brake Application	2609 rpm	1982 rpm
Kinetic Energy to be Absorbed by Brake	$5.1 \times 10^6 \text{ ft-lb}$	$3.1 \times 10^6 \text{ ft-lb}$
Disk Stopping Torque	30,000 in-lb $\pm 5\%$	
Minimum Disk Static Holding Torque	36,000 in-lb	
System Inertia at the Brake Disk	155.9 ft-lb-sec ²	
Emergency Operation Require- ment	One stop capability (Minimum) throughout the service life from normal disc speed (5152 rpm) within 30 seconds	

3) Environmental Conditions

All components of the brake shall be designed for satisfactory operation under the following environmental conditions:

- a. Fluid temperature range from -65°F to $+275^\circ\text{F}$.
Ambient temperature range from -65°F to 250°F .
- b. 100% relative humidity over full ambient temperature range.
- c. Fungi encountered in tropical and semi-tropical climates.
- d. Exposure to airborne sand and dust particles.

- e. Exposure to atmosphere containing salt laden moisture.
- f. Pressure altitudes from sea level to 20,000 feet.
- g. Vibration and Acceleration: The brake must withstand and function under the vibrations and accelerations encountered in helicopter operation. The design shall preclude resonant vibrational modes within +20% of the following frequencies: 2.6 Hz, 10.4 Hz, 20.8 Hz, 133 Hz, 192 Hz, 2662 Hz, and 9583 Hz when mounted in a manner similar to the aircraft installation. In addition, any springs utilized in the design shall not have fundamental modes at any of the above frequencies.

Design Life—

The brake shall be designed to operate with optimum performance without adjustment or replacement of parts for not less than 400 stops (Condition #1) or 600 stops (Condition #2). The total operation life of the brake head assembly shall be no less than 10,000 stops (equivalent to approximately 7200 flight hours).

The brake assembly as tested in Phase III is shown in Figure D-38.

Test Requirements and Results

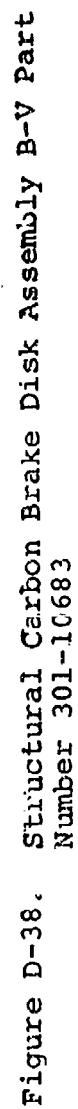
(The following is abstracted from B.F. Goodrich report Q-6099, "Qualification of the B. F. Goodrich P/N 2-1314 Single Disk Rotor Brake for the Boeing Vertol Heavy Lift Helicopter.)

Dynamic Torque Test

Requirements —

A total of 250 brake stops shall be conducted as follows:

Kinetic Energy - ft-lb x 10 ⁶	3.1
Inertia - slug ft ²	135.06
Disk Velocity - rpm	2125
Stop Time - seconds	12 to 14
Maximum allowable av. ft-lb torque	2500
Cooling fans	Off until at least 60 seconds after stop
Wear measurements	Approximately every 50 stops
X-Y plots	Approximately every 10 stops



Results -

Two hundred and fifty dynamic brake stops were accomplished as specified. Average results are listed below.

	<u>Stops 0-125</u>	<u>Stops 126-250</u>	<u>Stops 0-250</u>
Number of stops	125	125	250
Kinetic energy - ft-lb	3.094	3.096	3.095
Inertia - slug ft	135.06	135.06	135.06
Disk velocity - rpm	2124.04	2125.0	2124.52
Stop time - sec	12.3	11.9	12.1
Brake pressure - psi	930	959	944
Brake torque - ft-lb	2261.1	2338.3	2299.4
Stop distance - revs	220.47	217.56	219.02

Average Peak Temperature - °F *

	<u>Stops 0-125</u>	<u>Stops 126-250</u>	<u>Stops 0-250</u>
Disk	749	768	759
Leading inboard lining carrier	393	415	406
Trailing inboard lining carrier	401	422	412
Leading outboard lining carrier	391	407	399
Trailing outboard lining carrier	372	383	378
Piston housing	140	137	139
Disk mounting fixture	368	375	372

The cooling fan was off during the stop and until 60 seconds after the stop except for cooling profile stops 10, 50, 100, 150, 200 and 250. On the cooling profile stops, the cooling fan was off during the stop and until 5 minutes after the stop.

Wear measurements were taken after stops 25, 75, 125, 175 and 250. Average wear rates for 250 stops (inches per stop per surface are shown on the following page).

*Average peak temperatures were taken from cooling profile stops only. On the other stops, the cooling fan was turned on before the temperatures were all peaked.

	<u>Wear Rate</u>	<u>Max. Useable</u>	<u>Projected Life</u>
Leading inboard lining	.0004376	.300	754
Trailing inboard lining	.0006432		513
Leading outboard lining	.0004100		804
Trailing outboard lining	.0006196		532
Disk	.0003322	.300	452

Twenty-five stops were recorded on X-Y plots during the test.

A series of stop tests were conducted with a disk of 1.2 inches thickness. The wear life of this disk, based on a minimum allowable thickness of .7 inch, is approximately 755 stops.

Static Torque Test

Requirements —

Using the average actuation pressure required for dynamic torque stops, an increasing torque load shall be applied until slippage occurs. The actuation pressure shall then be increased until 3000 ft-lb of static torque is attained without slippage for a minimum of 60 seconds.

Results —

A static torque survey was performed by actuating the brake with various pressures and applying an increasing torque load until slippage occurred. Then, using an actuation pressure of 2160 psi, a torque load of 3,150 ft-lbs was applied and maintained for 30 minutes without slippage. Results of the torque survey are as follows:

<u>Actuation Pressure, psi</u>	<u>Torque - ft-lb</u>
300	500
625	1000
925	1450
1230	1850
1540	2250
1835	2750
2140	3150
2425	3600
2740	4000
2825	4100
2930	4200
3010	4350

Disk Strength Test

Requirements —

A new disk assembly shall be driven at 6440 rpm for 30 minutes. No failure or permanent deformation is to occur. This disk is then to be driven at 7060 rpm for 30 seconds without structural failure.

The same tests shall be accomplished on a fully worn disk.

Results are to be recorded on an X-Y plot.

Results —

A new 134-73 disk assembly was driven at 6440 rpm for 30 minutes and at 7060 rpm for 40 seconds.

A 134-73 disk assembly, which had previously been used for 250 dynamic torque stops, was driven at 6440 rpm for 30 minutes and at 7060 rpm for 30 seconds.

There was no deformation or failure of either disk assembly.

Disk Endurance Test

Requirements —

A new disk assembly shall be cycle tested from stationary, up to speed, and return to a stationary condition for 1100 cycles. The first 1000 cycles shall be at 5150 rpm, and the remaining 100 cycles shall be at 6440 rpm.

Results —

A new 134-73 disk assembly was cycle tested to 5150 rpm for 1012 cycles and to 6440 rpm for 100 cycles without failure.

Proof Pressure Test

Requirements —

A proof pressure of 3150 ± 50 psi shall be applied to the piston housing assembly for a period of five minutes. No permanent deformation or measurable leakage shall occur. The pressure shall then be reduced to 5 psi and held for five minutes with no resultant leakage.

Results —

A pressure of 3150 psi was applied to the piston housing assembly and held for 15 minutes. The pressure was then reduced to 5 psi and held for 5 minutes. There was no permanent deformation and there was no leakage.

Note: Brake head assembly for this test had the 27-560 graphite lining segments replaced with ones made of aluminum.

Brake Endurance

Requirements —

With the brake head assembly temperature maintained at 225° - 250°F, 50,000 pressure cycles shall be applied. Fifty percent of these cycles are to be at the normal operating pressure and the remaining fifty percent are to be at the pressure required to achieve 3000 ft-lb of static torque. Additionally, each 25,000 cycles shall be divided into four conditions simulating various worn lining configurations. These configurations are to be 25%, 50%, 75% and 100%. Positive actuation and retraction shall be monitored by an indicator light connected to the pressure plate limit switches.

Results —

With the brake head assembly temperature maintained at 250°F, 50,000 pressure cycles were performed as follows:

<u>Condition</u>	<u>Brake Pressure</u>	<u>Cycles</u>
25% worn	1000	6250
25% worn	2100	6250
50% worn	1000	6250
50% worn	2100	6250
75% worn	1000	6250
75% worn	2100	6250
100% worn	1000	6250
100% worn	2100	6250

Actuation and retraction was monitored by an indicator light connected to the limit switches.

Note: Brake head assembly for this test had hard coated piston bores, four pistons hard anodized, and the 27-560 graphite lining segments replaced with ones made of aluminum.

Functional Check

Requirements —

With the brake head assembly and a disk mounted in their proper relative positions, perform the following operations:

Determine pressure required for initial piston movement.

Determine pressure at initial lining - disk contact.

Determine pressure at which linings break contact with the disk.

Determine approximate time for full lining retraction.

Determine housing deflection at varying pressures from 0 - 3000 psi.

Results —

With the brake head assembly mounted on a test fixture, the required operations were performed satisfactorily and the data recorded.

Low Temperature

Requirements —

After allowing the brake assembly to cold soak for eight hours minimum at -65°F, functionally check the brake by cycling at the normal pressure for 25 cycles, followed immediately by 5 cycles at the static torque pressure. Positive retraction shall be established between cycles by monitoring an indicator light connected electrically to the retractor limit switches.

Results —

After 64 hours at -65°F, the brake was cycled 25 times with 1050 psi and 5 times at 2150 psi. Positive retraction was indicated between each cycle by the light connected to the retractor limit switches. There was no leakage.

Note: In the brake head assembly, the tops of the piston bores were chamfered, the piston bores were hard coated, four pistons were coated with Nituff, the 27-560 graphite lining segments were replaced with ones made of aluminum, the 40-560 and 40-561 springs were replaced with 40-570 springs, the 80-624 washers were replaced with 80-647 washers, and the MS 28774-220 and 68-923 packings were replaced with "T" type packings (Greene, Tweed and Co.).

Vibration

Requirements —

One brake head assembly shall be subjected to vibration in accordance with MIL-STD-810B, Paragraph 4.6, Procedure I, Section 4.6.1, Part 1, utilizing test curve AT as shown in Figure 514.1-1. In addition, the brake shall be vibrated specifically at 2.6, 10.4, 20.8, 133, 192, 2662, 9583 Hz to ascertain the absence of any fundamental modes at these frequencies.

Results —

The vibration test was conducted at the Bowser-Morner Testing Laboratories, Dayton, Ohio. As a result of vibration test experience, the 55-113 aluminum spring covers on the test brake were replaced with steel ones, the 38-606-20-91 rivets were replaced with MS 20427-6F12 rivets, the 80-624 washers were replaced with 80-647 washers, the 40-560 and 40-561 springs were replaced with 40-570 springs, and the 5HMI Micro-Switches were replaced with 1SE1 Micro-Switches. There were no failures in the brake assembly so equipped.

Disk Balance Check

Requirements —

One disk assembly shall be statically balance checked to determine compliance with the maximum assembly radial unbalance limit of .30 oz-in.

Results —

The balance test was conducted at The Balancing Company, Dayton, Ohio. Two new disk assemblies were statically balance checked and found to have an unbalance in excess of .30 oz-in. These two disk assemblies were then balanced by drilling holes in the 245-172 spacer rings. After balancing, they were rechecked and found to be within the unbalance limit of .30 oz-in.

Salt-Spray Corrosion

Requirements --

Sufficient test results will be made available on a similarity basis to delete the requirement for conducting this test on a complete brake assembly. In addition, samples of graphite will be salt spray tested in accordance with Procedure I of Spec. MIL-STD-810B for a period of 48 hours.

Results —

Test results from prior salt spray corrosion tests were submitted to and accepted by Boeing Vertol. Samples of graphite were tested per Procedure I of Spec. MIL-STD-810B for a period of 212 hours. The testing had no effect on the graphite.

Conclusions

The B.F. Goodrich 2-1314 rotor brake assembly has demonstrated full compliance to the test requirements and conditions specified for the Boeing Vertol Heavy Lift Helicopter (HLH) by the Boeing Company Design Procurement Specification No. S301-10045.

TRANSMISSION COVER PHOTOELASTIC MODEL STRESS AND DEFLECTION TEST

The HLH aft transmission upper cover or rotor shaft support housing is relatively large and represents a significant portion of the HLH drive system weight due to the magnitude of the applied rotor loads. Thus, in order to limit total drive system weight, it is necessary to control the weight of the upper cover. On the other hand, because of the critical rotor support function of the cover, it is also necessary to insure that the design incorporates sufficient strength and stiffness to meet all of the structural design criteria.

The conflicting nature of these requirements makes an accurate stress and deflection analysis essential to the design of an upper cover that is not only lightweight, but also has the necessary strength and rigidity. However, the upper cover is a relatively complex structure as a result of the multiple functions which it must perform. The HLH upper cover acts as the rotor mounting and support structure, as a part of the gearbox housing, as the gearbox mounting structure, as the support for the rotor control actuators and as the rotor shaft bearing housing. This complexity, in turn, makes the accurate determination of stresses and deflections very difficult using only analytical methods.

The epoxy model technique has several advantages as a procedure which can be used to alleviate the above difficulties and contribute to the design of an optimum upper cover. These advantages include a relatively short model fabrication time span which permits an optimization program to be conducted prior to the finalizing of the actual design, the ability to easily modify the model which permits the configuration to be successively evaluated and improved, and a compatibility with birefringent coatings which can be used for experimental stress analysis.

The objective of this program was to obtain a minimum weight rotor shaft support housing consistent with an unlimited fatigue life and acceptable bearing deflection. This was accomplished by determining and evaluating areas of stress concentration and minimizing their effects by successive model modification. Geometry improvements were also investigated to minimize bearing outer race warping due to external loads. This was accomplished by modifications to the model.

Technical Approach

The various functions of the upper cover were segregated in order to obtain an insight into their contribution to the

combined stresses and deflections. The segregation chosen for this testing was (a) rotor torque, (b) rotor hub loads, and (c) rotor control actuator loads. A combined load condition was imposed after completion of these three load conditions. Deflections were measured for 25%, 50%, 75%, and 100% of the loads as defined in the Reference 1 test plan for the model as initially configured. After modification, the deflections were measured at 50% and 100% of the combined loading for comparison with previous results. Photoelastic stress measurements were made at 100% load levels for both the initial and modified configurations.

Test Method

Test Specimen Design

The test specimen utilized for this program was a one-half size model of the HLH rotor shaft support housing. The specimen assembly also included simulations of the rotor shaft bearings, a segment of the rotor shaft, and the planetary ring gear. (See Figure D-39.)

The rotor shaft support housing model was essentially a one-half scale copy of the housing being designed for the HLH aft transmission. During manufacture, several modifications were made to the model configuration in order to facilitate fabrication. These included changing the shape of the horizontal webs of the mounting legs from conical to flat, reducing the draft angle on the vertical ribs of the mounting legs and changing the shape of the support ribs for the actuator mounting pads.

The bearings used in the test specimen assembly were simulated tapered roller bearings. The outer races were similar to actual bearing races but the inner races and rollers were combined into single-piece units. The models were designed to include the pertinent elements of the rotor shaft bearing geometry such as race and roller diameters, contact angles and number of rollers.

The portion of the rotor shaft that is within the transmission was included in the test specimen. The model shaft was a straight, circular cylinder that simulated the diameter and wall thickness of the actual shaft in the area of the bearings. The upper end of the model shaft was designed to provide for application of the rotor loads.

For simplicity, the model ring gear had a rectangular cross-section rather than the "tee" section of the actual part. However, the model was designed to simulate the radial stiffness of the actual ring gear.

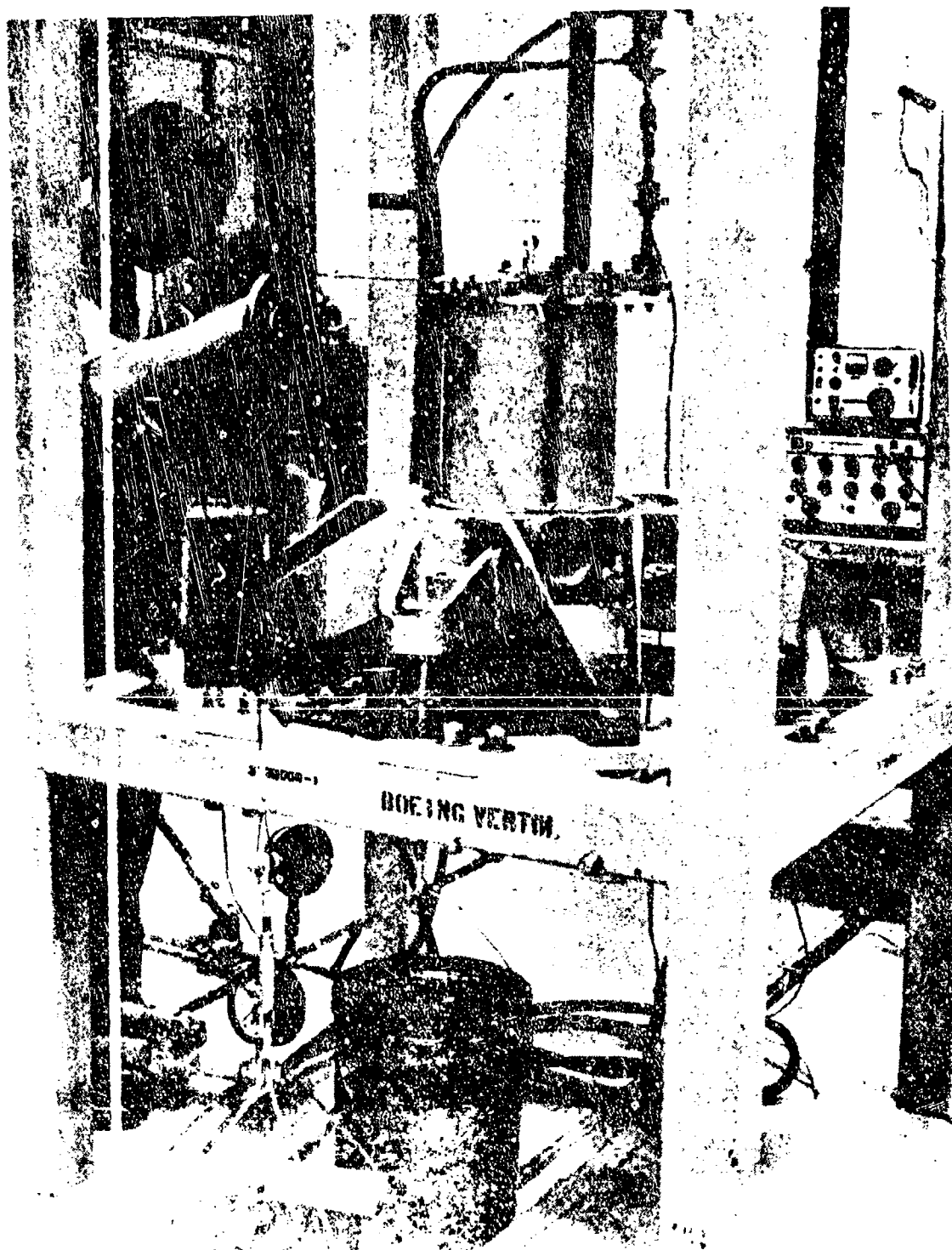


Figure D-39. Rotor Shaft Support Housing Model.

The rotor shaft, inner bearings, outer bearings, and ring gear models simulated steel components and were fabricated with a high modulus epoxy ($1,370,000 \text{ lb/in}^2$). The rotor shaft support housing model simulated an aluminum component and was fabricated with a low modulus epoxy ($560,000 \text{ lb/in}^2$). This modulus ratio for the models approximates the modulus ratio that will exist for the components.

Conclusions

The photoelastic analysis provided data with which to evaluate the relative magnitude of known stress concentrations. This permits the selective reduction of the observed stress concentrations. Significant reductions were obtained for those data points at which a modification was incorporated. At the maximum stress concentration point, the maximum reduction of 40.5% of the initial concentrated shear stress measurement was obtained.

Due to a change in the basic design configuration, caused by the change in the swashplate actuator system, there was no attempt to obtain a complete optimization. Several successive modifications such as the one described in this report would provide such an optimization.

In addition to defining the reduction in stress concentration, the modified configuration provided an insight into the effectiveness of the ring portion below the rotor shaft support bearings. It can be concluded from a comparison of deflection measurements before and after modification that the material below the bearing support area is effective for the ring section analyses of the housing. This increase in the effective section will permit a reduction of ring thickness in the immediate proximity of the bearing support resulting in a corresponding reduction in weight.

TRANSMISSION NOISE REDUCTION

Background

The arguments for reasonably low noise levels in military aircraft are generally well understood. They encompass requirements for an environment which will not be medically damaging to hearing, will not cause undue fatigue, and will permit reliable communication. To meet these requirements, the military services generally include MIL-A-8806 as part of the specification for aircraft procurement.

Rotor transmissions generate the highest levels of internal noise in most helicopters, and they are generally located near the flight crew or passengers. If no preventive measures are taken, the gearboxes produce an environment which does not permit reliable speech communication, produces undue fatigue of crew and passengers, causes temporary hearing threshold shifts, and possibly (after repeated extended exposure) permanent hearing loss. Therefore, the question of acoustical treatment of transmissions is not whether it shall be done, but how much and in what manner.

In order to ensure compliance with MIL-A-8806 as the best compromise between an optimum acoustical environment and the penalties imposed on an aircraft by the inclusion of a sound-reducing treatment (e.g., weight, cost, maintenance, and incompatibility with other operational requirements), methods of predicting noise levels and tools to perform trade studies (i.e., source noise reduction versus enclosures) are being developed.

The method used to calculate and reduce noise levels was developed as part of the HLH/ATC Noise Reduction Program. In addition, several other AMRDL funded programs directed towards transmission noise prediction and noise reduction at its source have been incorporated in this analysis. However, the methods that were evolved are somewhat incompatible - the method of predicting noise being dependent on cycled energy at the gear mesh, while the method of reducing source noise is dependent on the reduction of displacements at the shaft supporting bearings. Because of this, a company IR&D program was conducted to develop a semiempirical method relating changes in sound pressure level to changes in the dynamic response of the gear shafts. Existing test data, obtained from the HLH/ATC Noise Reduction Program, was utilized to determine empirical constants.

The noise producing mechanism has been investigated under contracts funded by USAAMRDL. The hypothesis is that noise is generated by the transmission case as a result of nonuniform

transfer of torque from pinion to gear due to tooth profile errors and the elastic deformation of gear teeth under load. This nonuniform transfer of torque produces a dynamic force at the gear mesh frequency, and its multiples, resulting in a coupled torsion/lateral vibration response of the gear shaft. The lateral vibration (or bending) produces displacements at the bearings, which in turn cause the case to vibrate, thus producing noise. This noise-producing mechanism and methods of predicting lateral response were experimentally verified for a CH-47 transmission, as a result of this HLH/ATC program. Using the lateral response analysis, modification to shafts can be analyzed to design the shaft with reduced response and therefore reduce the noise.

Noise Prediction

The method of calculating sound pressure level (SPL) is based on a scheme developed by Mechanical Technology Incorporated. This scheme assumes that some fraction (α) of the cycled energy leaves the gear mesh as acoustic energy. The case is initially assumed to be spherical in geometry and then in geometry correction factor (β) is employed. These constants are found as factors and the product $\alpha\beta = 2.06 \times 10^{-3}$ was experimentally determined to correlate with the CH-47C transmission test. The SPL is then calculated by the following equation:

$$L_f = 10 \log \left[\frac{4.94 \times 10^4 \alpha \beta f \Sigma e_o F_o}{r^2} \right]$$

where:

- L = SPL in dB
- α = energy conversion factor
- β = housing geometry factor
- f = frequency of excitation - Hz
- e_o = peak value of sinusoidal excitation - μ inches
- F_o = dynamic tooth force at each excitation point - lbs
- r = radial distance to center of sound - radiating surface - ft

The peak values of the sinusoidal excitation (e_o) are calculated by the computer program GEARO (R-33) and the dynamic tooth force (F_o) is calculated using the computer

program TORRP (R-32). The TORRP model used for the pretest predictions of the aft transmission installed in the test stand is shown in Figure D-40. The sound pressure level (SPL) of the baseline transmissions is shown in Figure D-41 for the thin walled shafts (-1 shafts) and ring gear but with a stiffening ring installed in the pinion shaft.

Noise Reduction

To reduce the noise, the shaft displacements at the shaft supporting bearings are reduced. This is accomplished by predicting the damped forced response (DFR) of the gear shafts using a computer program DFR (D-82). The shafts are then mathematically modified and a new response is determined. A change in noise levels is then associated to the change in displacements. The DFR model used for this analysis is shown in Figure D-42. The predicted responses for the baseline shafts are shown in Figures D-43 and D-44 for the sun mesh frequency and in Figures D-45 and D-46 for the bevel mesh frequency.

The relation of the resultant noise reduction to the change in shaft displacement is very complex. If a single shaft were supported by a single bearing, the resultant noise reduction would behave approximately as below:

$$\Delta \text{ SPL} = 20 \log \left[\frac{(kx) \text{ New}}{(kx) \text{ Baseline}} \right] \quad (1)$$

where $F = kx$ is the dynamic force at the bearing station. However, real transmissions have two primary shafts (excluding the rotor shaft) and several supporting bearings. This results in considerable difficulty in estimating the noise reduction.

A method which evolved as a result of the HLH/ATC program which is currently being used, is outlined below

- Establish a dB level for each bearing dynamic force, using the largest force as the reference force.
- Logarithmically sum the referred noise levels.
- Using equation (1) calculate the $\Delta \text{ SPL}$ for each bearing and add to the referred noise levels.
- The difference between the log sum of the referred noise levels and the log sum of the referred modification noise levels is the most probable SPL reduction.
- Repeat above for each mesh frequency.

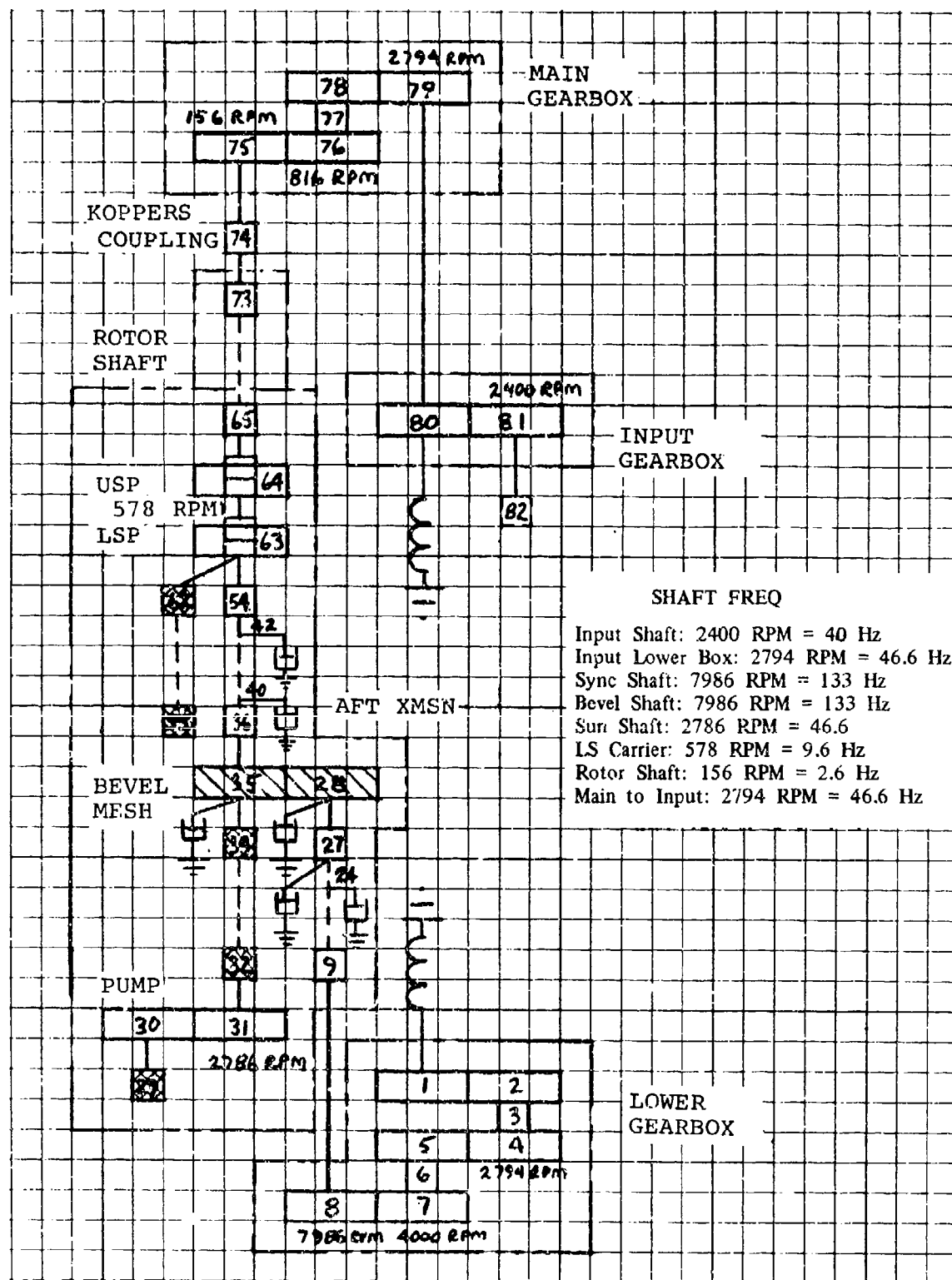


Figure D-40. TORRP (R-32) Model of Closed Loop Test Stand.

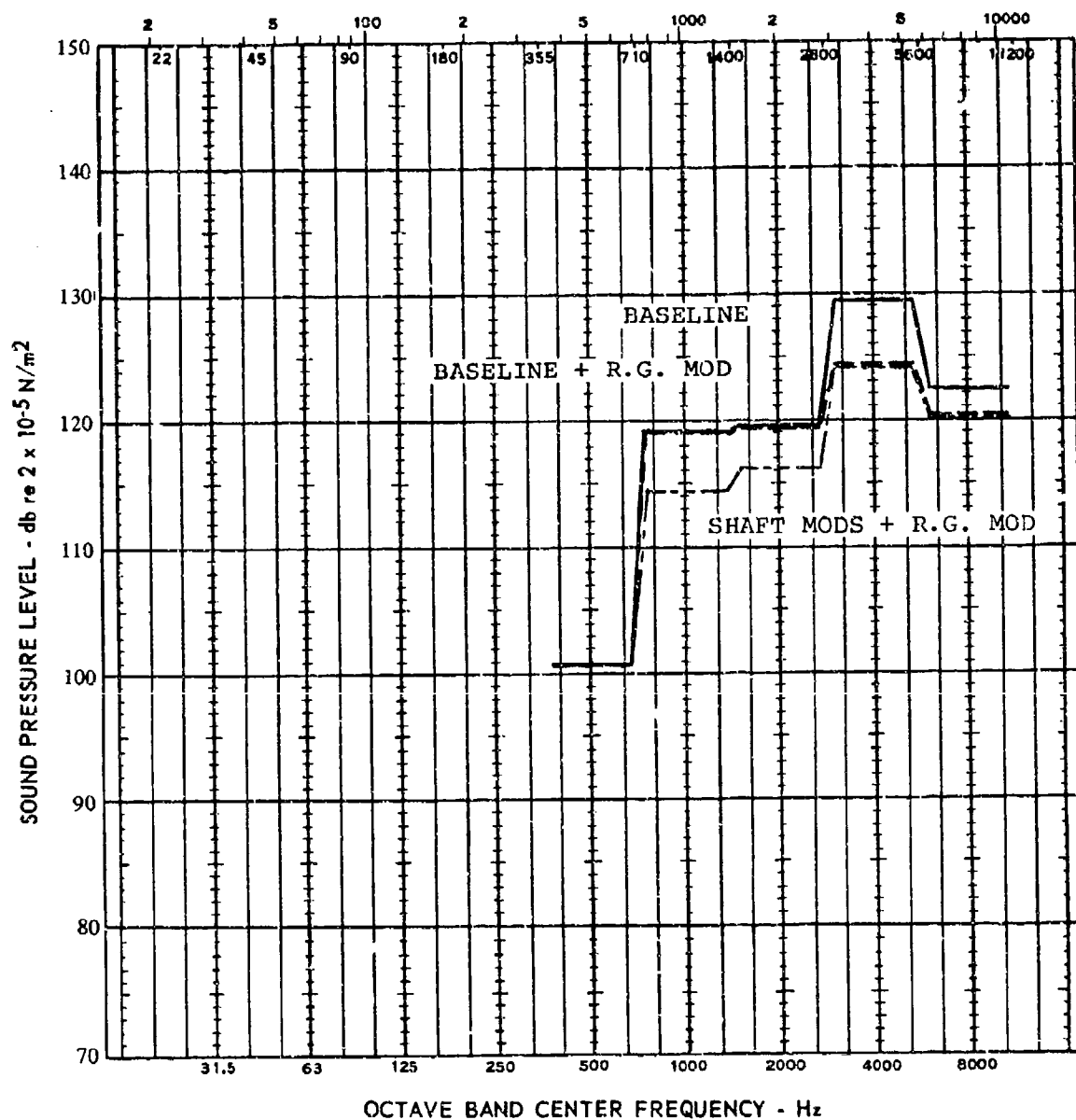


Figure D-41. Noise Spectrum - HLH-ATC Transmission Installed in Closed Loop Test Stand.

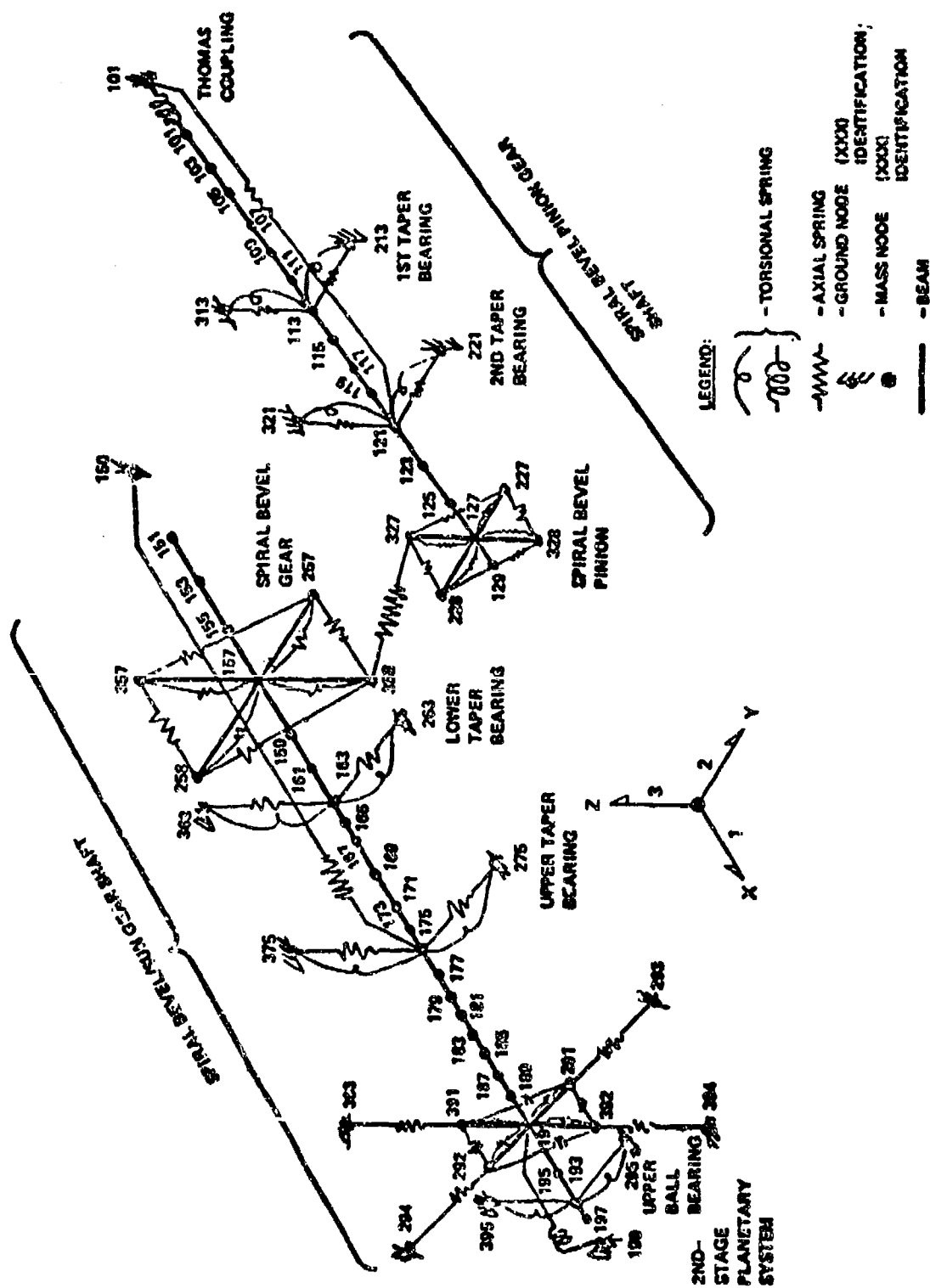


Figure D-42. Coupled Bevel Gear and Sun Gear HLH/ATC Transmission Model.

The approach outlined above provided correlation with the measured dynamic forces at the bearing. This correlation, however, was considered unsatisfactory for design trade-off utilization. Therefore, an empirical correction factor B was experimentally developed and incorporated into the analysis as:

$$\Delta \text{ SPL}_{\text{corrected}} = (1 + B) \Delta \text{ SPL}_{\text{predicted}} \quad (3)$$

where $B = -6.5539 + 6.394 \times 10^{-3} f - 1.338 \times 10^{-6} f^2$ and f = mesh frequency.

using this correction factor and the change in shaft displacement at the bearings as shown in Figures D-43 through D-46, a reduction in SPL at the sun mesh frequency was calculated while no net change was noted for the bevel mesh frequency. This change in SPL spectrum is also shown in Figure D-41 along with an additional reduction for increasing the wall thickness of the stationary ring gear. As the final part of the HLH/ATC Noise Reduction Program, the transmission will be tested with baseline and modified components to validate the analytical methodology. The test approach is described in detail in section 11.d of this report.

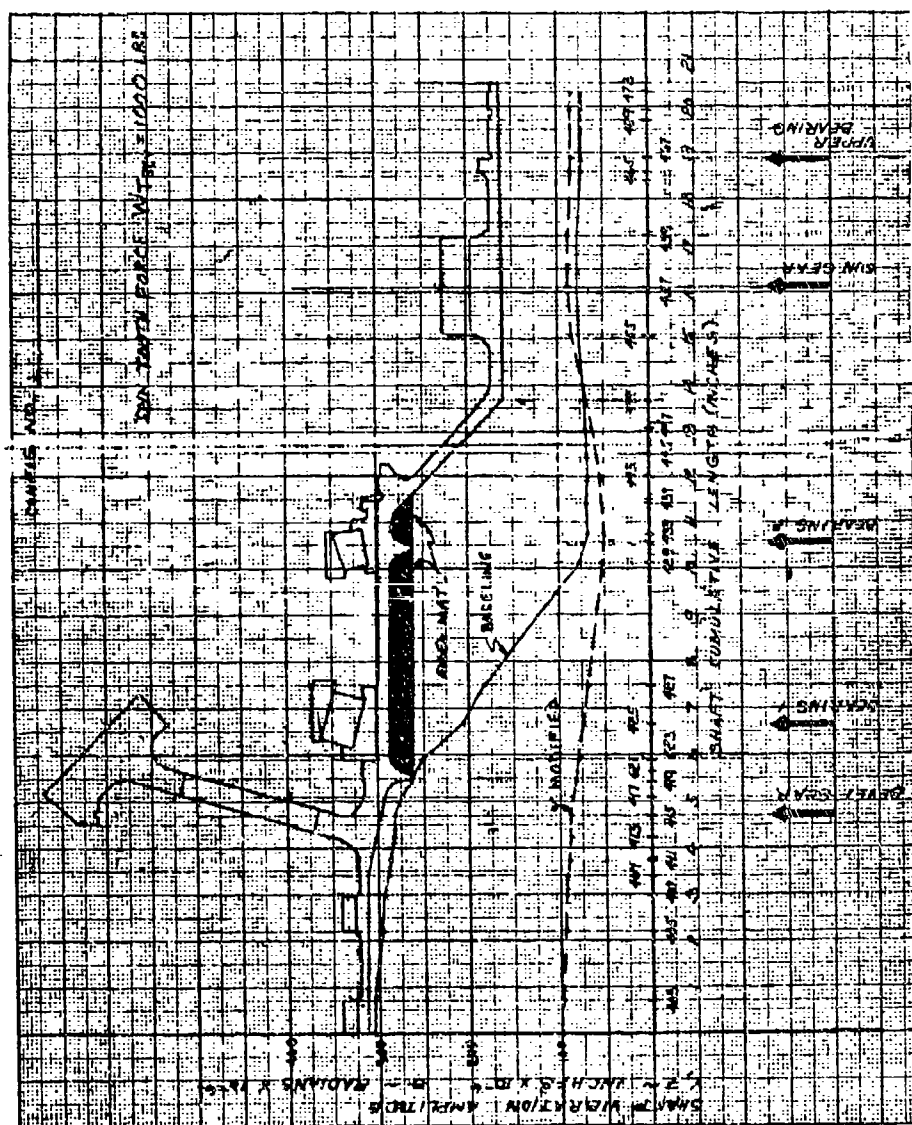
Dynamic Analysis of HLH Combiner Transmission

Although noise is not of primary concern with regard to this box, the beneficial effects of reducing shaft displacements at the bearings was felt sufficient reason to perform a dynamic analysis. The Boeing Vertol D-82 Computer Program was again used to determine the damped forced response of the box components.

The mathematical model of the HLH combiner box is shown in Figure D-47. The coupled response of the six main components (center shaft, right- and left-hand engine shafts, slant shaft, center engine shaft, and rotor brake) were analyzed for the three primary frequencies (idler mesh frequency, pump mesh frequency, and rotor brake mesh frequency).

With six shafts responding to three frequencies, and sixteen supporting bearings, the optimum configuration is at best a compromise. The modification which provided the best overall response is seen in Figure D-48. For the 18 conditions analyzed (six shafts at three frequencies), this modification was determined to be "better than" the baseline for eight cases, "equal to" for seven cases, and "worse than" for three cases.

This modification was designed as a removable slug inserted in the spur gear end of the center shaft. This will allow for a "with" and "without" comparison as a further verification of this type of dynamic analysis.



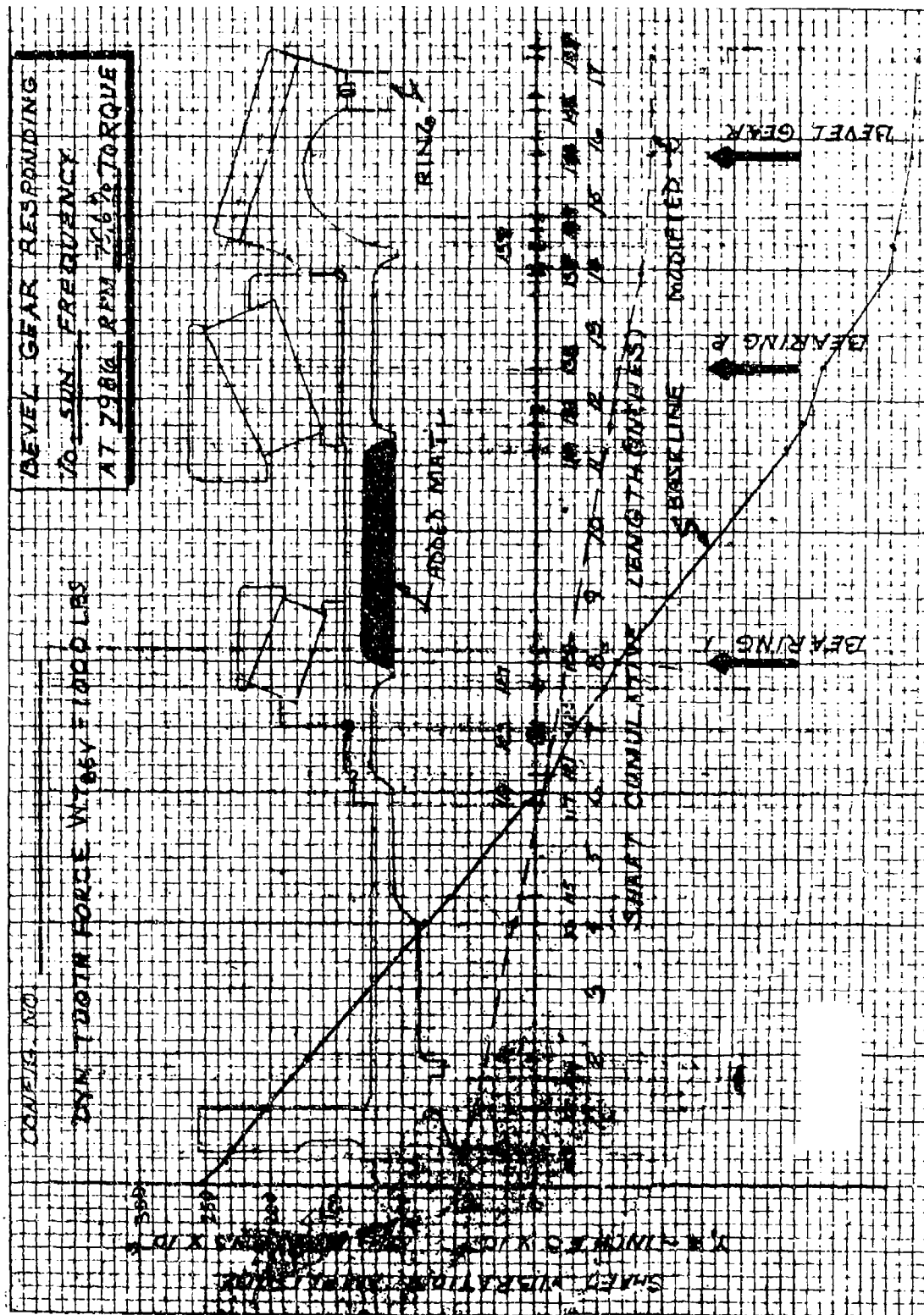


Figure D-44. Bevel Gear Responding to Sun Frequency, 7,986 rpm, 75.6% Torque.

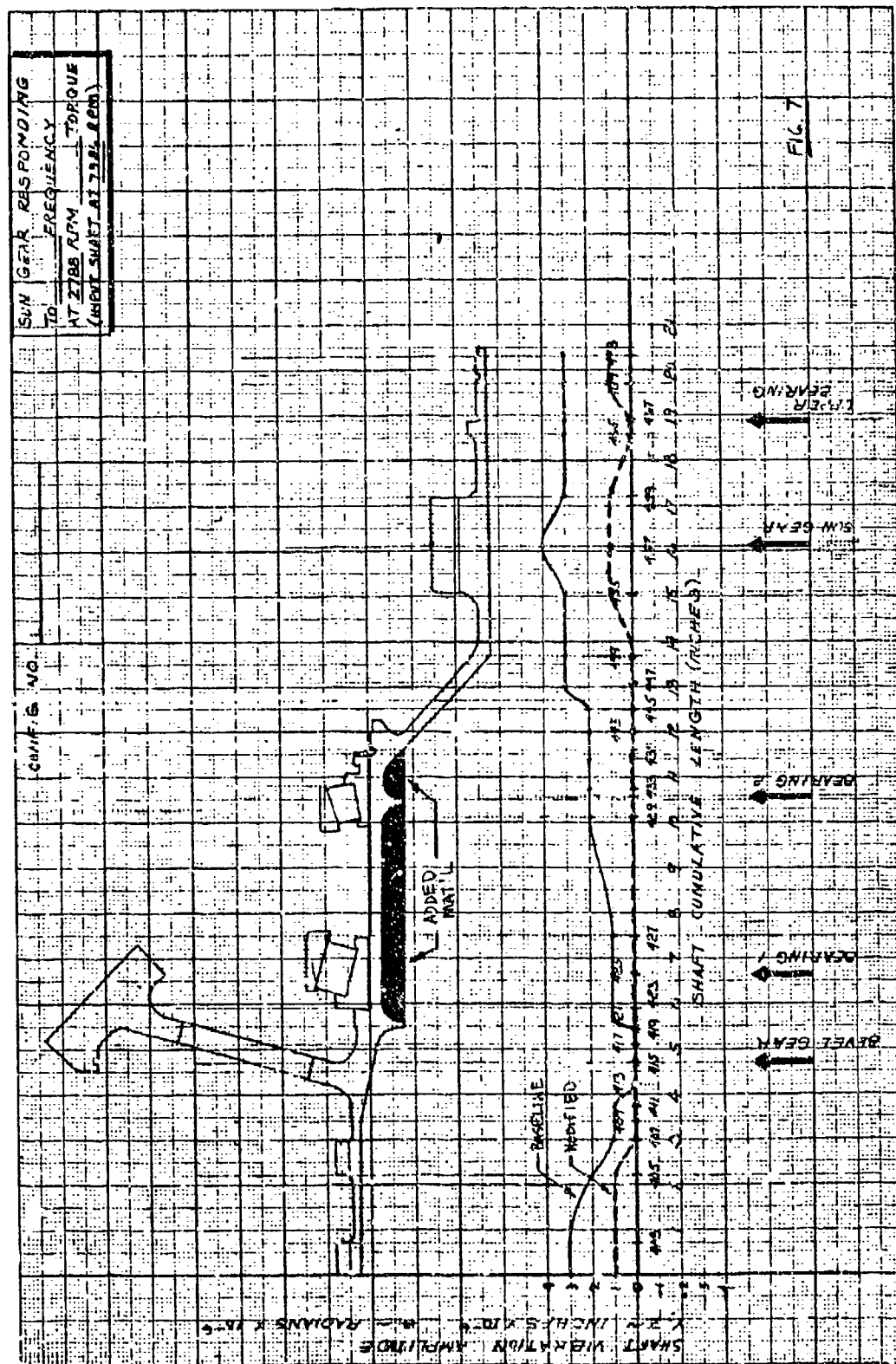


Figure D-46. Sun Gear Responding to Sun Frequency, 2,788 rpm, 75.6% Torque (Input Shaft at 7,986 rpm).

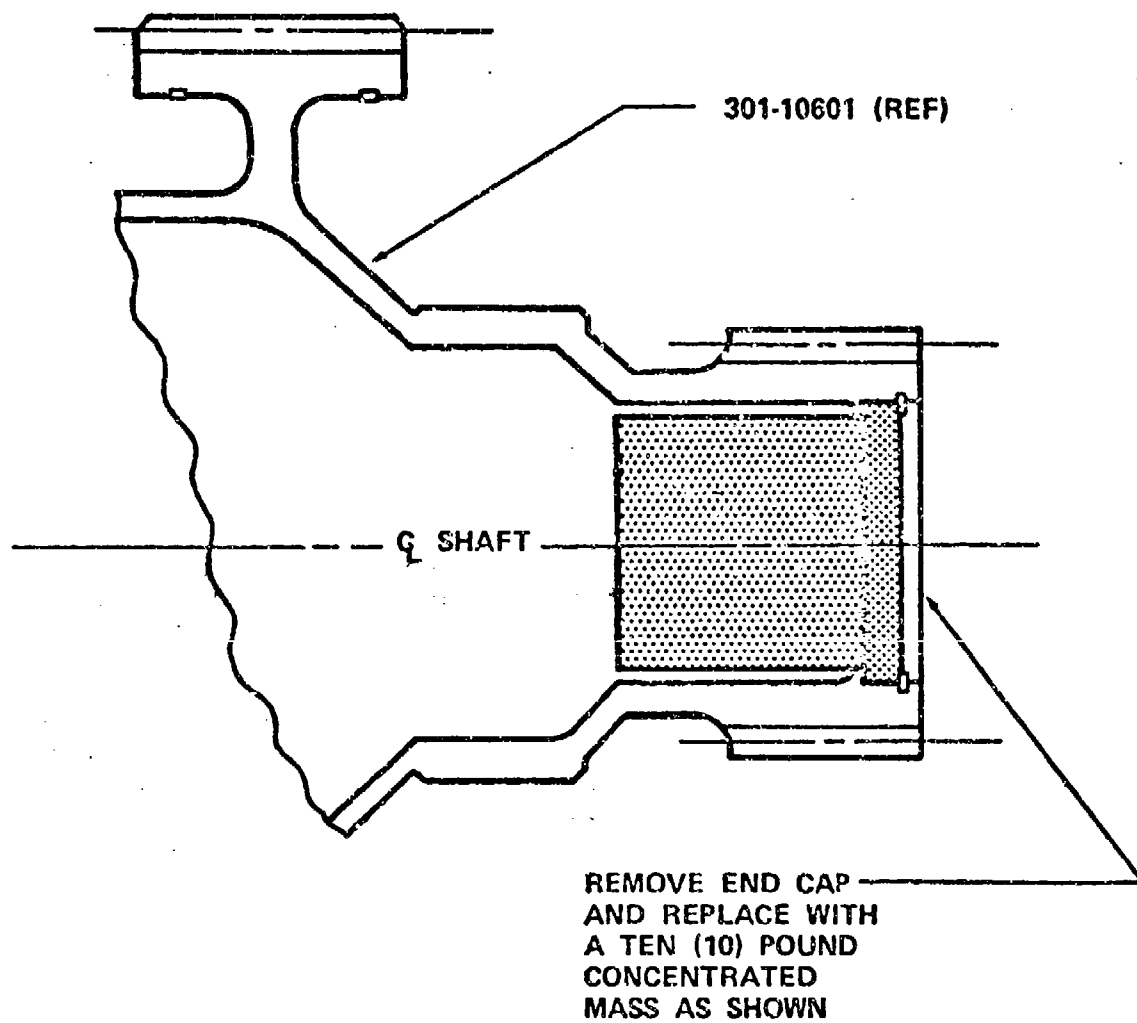


Figure D-48. Modification to HLH Mix Box Center Shaft.

Preliminary Noise Data

The aft transmission contained modified input bevel and sun gear shafts with an unmodified stationary ring gear. The noise was measured at two microphone locations: 1 foot directly below the sump, and 2.5 feet from the case at the HLH flight engineer's approximate location. The preliminary data was obtained without the benefit of the acoustic enclosure and is possibly 3 to 6 dB higher than the levels generated by the rotor transmission alone.

Narrow and one-third octave frequency analysis revealed the major noise contributors as: the upper-stage planetary system mesh frequency 388 Hz (f_1) and its second harmonic 776 Hz (f_2), lower-stage planetary system mesh frequency - 1,438 Hz (f_1) and its second and third harmonics 2,876 Hz (f_2), and 4,314 Hz (f_3), and input pinion mesh-frequency 4,933 Hz (f_1).

Comparing the measured noise at the two microphone locations, 1 and 2.5 feet, indicated an approximate 8-dB difference, which was expected due to the spherical spreading of sound with distance.

Noise levels compared on an input torque basis show little difference with changes in torque (Figure D-49), while the noise generated at the upper stage planetary mesh frequency (388 Hz) is reduced a significant twelve decibels when simulated rotor loads were applied.

The preliminary noise measurements of the HLH rotor transmission with rotor load show the levels to be nearly those predicted for the transmission with tuned shafts, and within the range of noise reduction that can be achieved with available noise attenuating transmission case coatings and aircraft interior acoustic barriers.

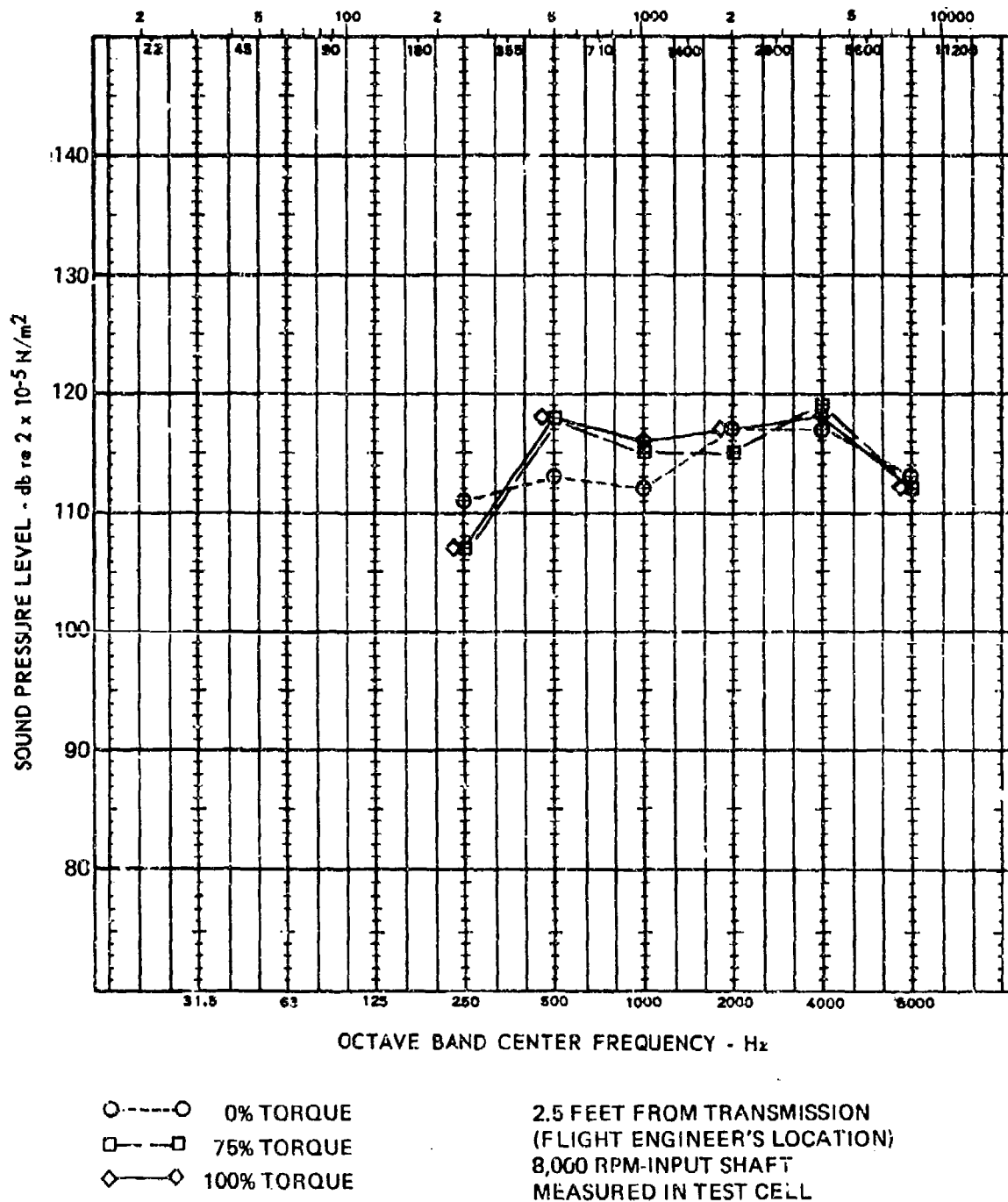


Figure D-49. HLH/ATC Aft Transmission Noise Levels.

TRANSMISSION NOISE ATTENUATION MATERIALS

A test program was conducted to evaluate materials for transmission case vibration damping and isolation, and airborne noise attenuation. Damping materials applied directly to the case reduce the vibration and prevent the generation of objectionable structureborne and airborne noise. Damping comparisons were made of the constrained and unconstrained viscoelastic materials, tuned mechanical absorbers, an antiballistic compound, and a magnetostrictive damping material. Materials with good noise attenuation qualities can be used as acoustical barriers enclosing transmission cases to reduce airborne noise radiation. Noise attenuation comparisons were made between the viscoelastic materials and the leaded foam material.

All testing was conducted using the Boeing Vertol Acoustical Material Test Laboratory, a 1/2-inch magnesium plate to represent the HLH transmission case material, and a 50-pound dynamic shaker for excitation.

Figure D-50 summarizes the measured reduction in vibration and noise attenuation at 1400 Hz along with a comparison on a weight basis. Some of the major conclusions were:

Damping

- A bonded viscoelastic material in a constrained configuration was required to achieve the goal of 18 dB vibration reduction. An 18-dB reduction at 1400 Hz was required to limit amplification of the panel resonance to a maximum of 5 dB.
- A bonded viscoelastic material in an unconstrained configuration approaches the 18-dB reduction goal and is more effective on a weight basis.
- The antiballistic self-sealing compound approaches the reduction goal, but is less effective on a weight basis than either a constrained or an unconstrained viscoelastic material. However, it has the potential to improve survivability.
- Magnetostrictive damping, using copper-manganese inserts, approached the reduction goal but it is not known whether this reduction was due to the mass or the behavior of the inserts when subjected to vibration.
- Tuned mechanical absorbers were found to be ineffective in damping heavy panels with multiple resonances.

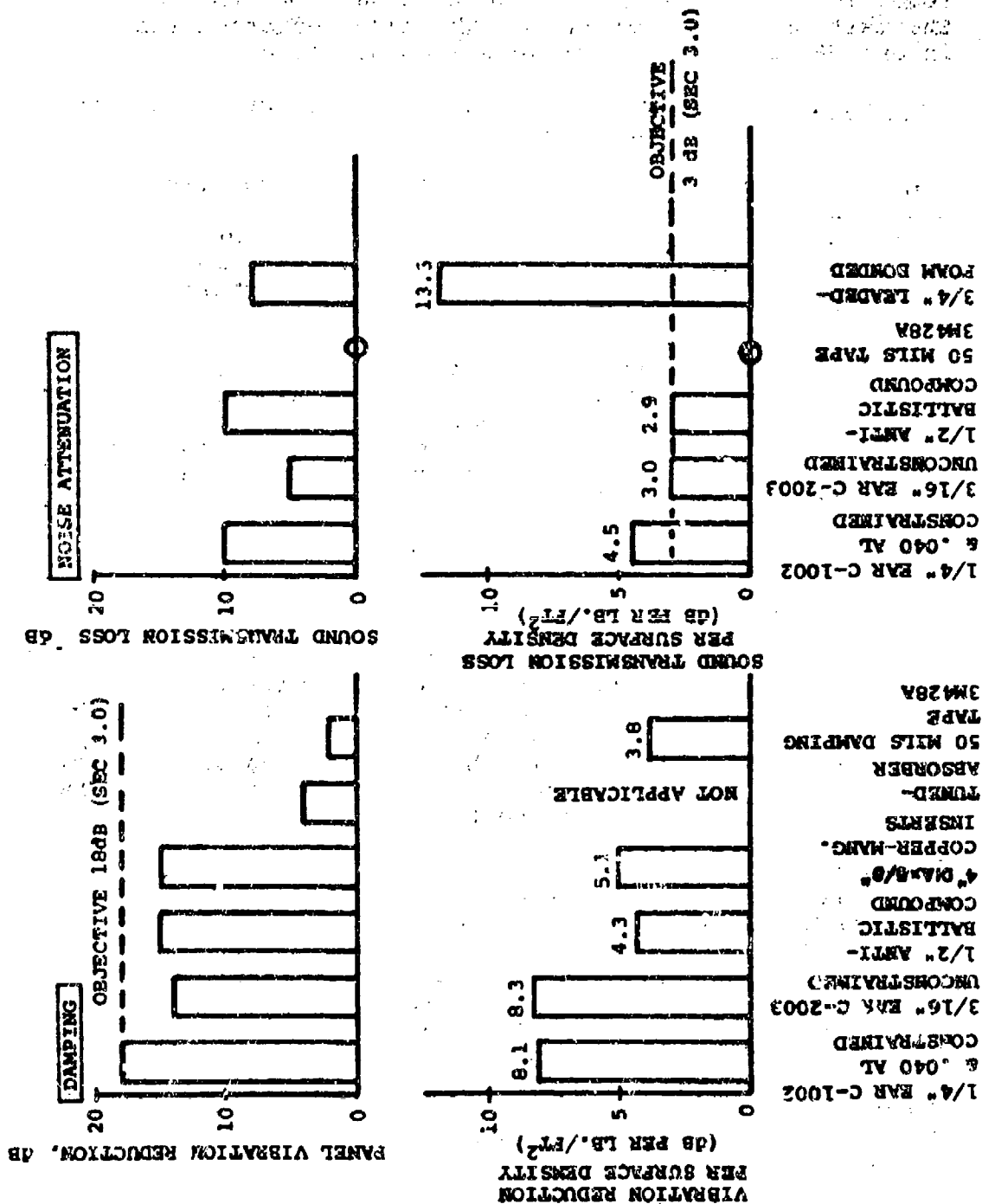


Figure D-50. HLH/ATC Transmission Noise - Case Damping and Attenuation Evaluation Summary - 1,400 Hz.

- Damping tape is inadequate for damping large vibrating masses.
- A direct 1/1 dB relationship between the vibration level reduction and sound level reduction was confirmed during the test program. One dB of vibration reduction results in one dB reduction of structure-borne noise.

Noise Attenuation (Material used as an acoustical enclosure around the case.)

- The noise attenuation properties of the better viscoelastic materials met the 3 dB per lb/ft² objective on a weight efficiency basis, with the constrained configuration substantially exceeding it. Therefore, these materials can provide a combination of case damping and airborne noise attenuation.
- The leaded foam material which had been selected as a candidate damping material actually provided little damping but very good noise attenuation. Therefore, if transmission airborne noise is a major contributor, this material could be used as an acoustical enclosure though still not as efficiently as fiberglass. Furthermore, some way of improving its serviceability characteristics over present installations would be necessary.

Recommendations

The large reduction in transmission noise required for the HLH to meet the levels specified in MIL-A-8806A will necessitate the use of many noise reduction methods and techniques. The subject test program disclosed that the better materials evaluated provided substantial vibration damping and acoustical attenuation, and should definitely be considered for HLH transmission noise reduction treatment.

- The best viscoelastic materials constrained and unconstrained, and the antiballistic compound, are recommended with the final selection to be based on compatibility with the environment, manufacturing methods required, and cost. Although all the materials evaluated were intended for damping application up to 150°F, discussions with the manufacturers revealed that similar materials with equivalent damping in the higher temperature range, 200°-250°F (estimated HLH case temperature), are being developed. These materials are to be available in time for evaluation on an HLH transmission case during the ATC program.
- Areas to be treated will be determined from actual transmission case vibration measurements scheduled to be obtained during the ATC program.

ALUMINUM/GRAPHITE COMPOSITE DRIVE SHAFT TRADE STUDIES

COMPOSITE SHAFT TEST PROGRAM

A test program using subscale tubes (4.5-inch diameter) was completed. The purpose of this program was to optimize the composite tube configuration for ballistic survivability and impact resistance. A tube configuration of high-modulus graphite and S-glass has been developed using the material properties of each material in the manner for which they are particularly qualified.

Five half-scale diameter and nominally half-scale wall thickness tubes were fabricated and tested. The number of plies and ply orientation were as follows:

SPEC	PLIES			
	INNER 90°	± 5°	± 45°	OUTER SCUFF CLOTH
#1	-	8 HT (FIBERITE)	4 1002S	1 DRY 120 CLOTH (.004)
#2	-	8 HT (FIBERITE)	4 1002S	1 DRY NYLON CLOTH (.007)
#3	1 XP251S	8 HM (HERCULES)	4 1002S	1 DRY NYLON CLOTH (.007)
#4	-	8 HT (FIBERITE)	4 1002S	1 DRY NYLON CLOTH (.007)
#5	-	8 HT (FIBERITE)	4 1002S	1 DRY NYLON CLCTH (.007)

The design torque values (sub-scale) were as follows:

Operating torque = 14,700 ± 2205 in-lb

Limit torque = 22,050 in-lb

Ultimate torque = 33,070 in-lb

It was predicted that both specimen configurations would be critical in buckling at 150°F. The predicted torsional strengths were:

Specimens #1, #2, #4, #5: T = 35,300 in-lbs.

Specimen #3: T = 51,000 in-lbs.

The five specimens were tested at Ft. Eustis and Boeing Vertol, according to the following schedule:

(see Figure D-51).

Specimen #1

Types of Test(s): a. Impact
b. Torque

Temperature: Room temperature

Results:

- a. Debonding between glass and graphite occurred at 10% of design impact. Graphite cracked longitudinally. No cracking of glass at 100% impact. Tube went .10 out of round.
- b. After impact testing, specimen was torqued and failed in buckling at 26,000 in-lbs.

Specimen #2

Type of Test: Ballistic

Temperature: 150°F

Results:

Specimen withstood .30 caliber tumbled hit on center of mid-span with steady design torque load applied. Specimen then torqued to failure between 26,000 and 30,000 in-lbs. Failure mode was buckling.

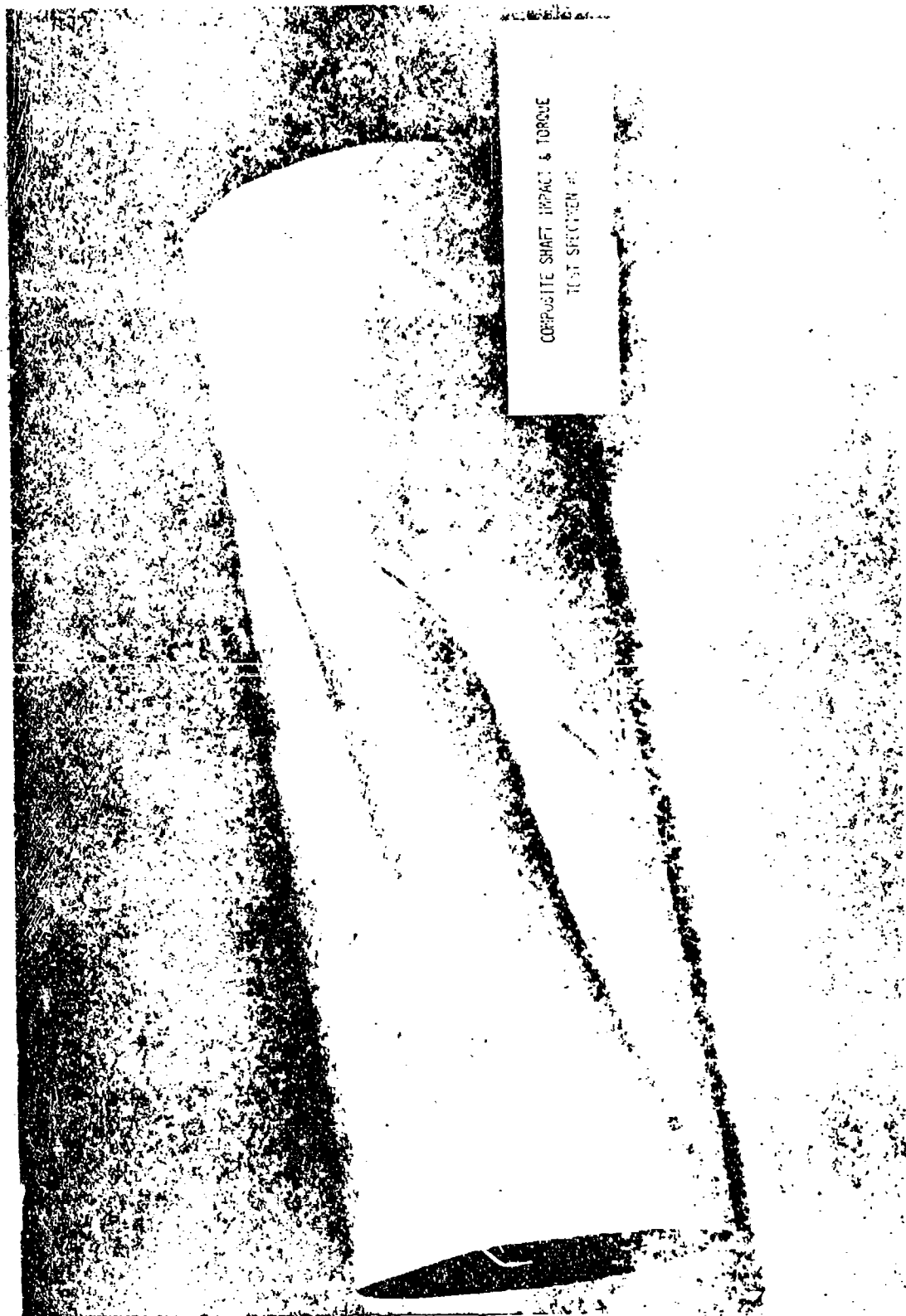


Figure D-51. Composite Shaft Ultimate Torque Test (Sheet 1 of 5).



Figure D-51. Composite Shaft Ultimate Torque Test (Sheet 2 of 5).



Figure D-51. Composite Shaft Ultimate Torque Test (Sheet 3 of 5).



Figure D-51. Composite Shaft Ultimate Torque Test (Sheet 4 of 5).

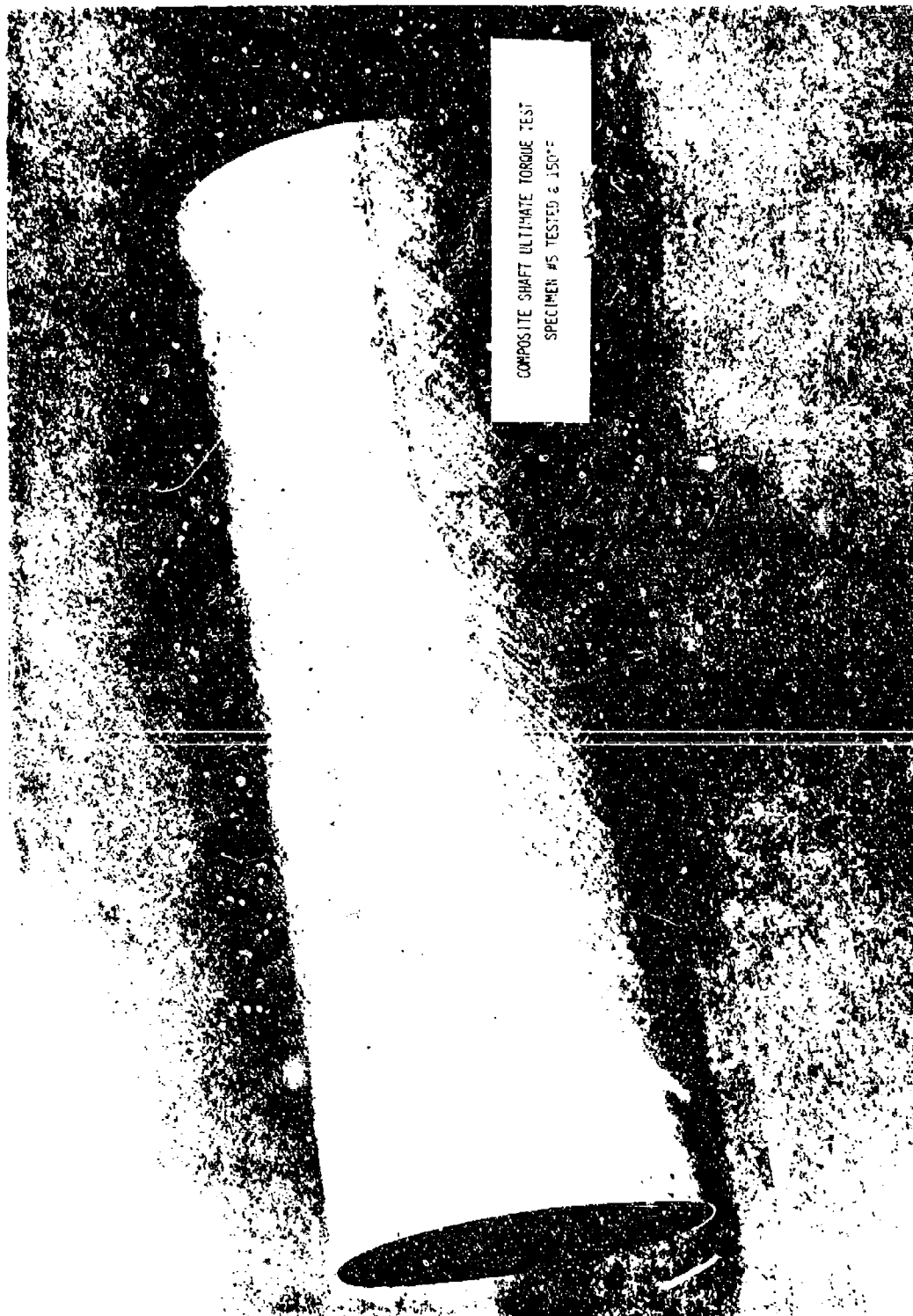


Figure D-51. Composite Shaft Ultimate Torque Test (Sheet 5 of 5).

Specimen #3

Type of Test: Ultimate/Impact

Temperature: Room

Results:

Specimen torqued to 90% (49,000 in-lbs) of predicted ultimate torque without mishap; then impacted at 120% design impact load. Inner ply of glass and graphite failed and broke away from cross-plyed glass. No out of roundness noted. Specimen then retorqued and buckling occurred at about 24,000 in-lbs. Buckling originated at point of impact.

Specimen #4

Type of Test(s): a. Scuffing
b. Torque

Temperature: a. Room
b. 150°F

Results:

- a. Both a 1-inch steel bar and a plastic screwdriver handle were hand-held against the specimen for two minutes. The shaft was rotated at 1000 rpm. No signs of wear apparent in scuff cloth, but resin was "smudged".
- b. Tested with objective of attaining 90% of predicted ultimate before ballistic test. Failed at 36,000 in-lbs.

Specimen #5

Type of Test: Torque

Temperature: 150° ± 10°F

Results:

Specimen buckled at 48,000 in-lbs. Shaft was holding torque at 48,000 in-lbs.

CONCLUSIONS

The subscale test program indicated that the basic configuration (Specimens #1, #2, #4, and #5) would meet the impact and ballistic criterion of transmitting limit torque after damage. A full-diameter, full-length tube of this configuration, however, would not be adequate from a buckling standpoint (135,000 in-lbs. vs. a required 188,100 in-lbs). The full-scale tube test configuration then would be derived from subscale test specimen #3, with the following layup:

Plies

1 ply dry nylon (.005)	Outer
6 plies 1002S glass at $+5^{\circ}$ (.060)	
26 plies HM-5 graphite at $+45^{\circ}$ (.130)	
1 ply x P251-S glass at 90° (.0078)	Inner

The sync shaft system weight, with a composite tube of this configuration would be 597 pounds, resulting in a weight savings of 75 pounds per aircraft, when compared to an aluminum tube sync shaft system.

ALUMINUM SYNCHRONIZING SHAFT ULTIMATE AND FATIGUE TESTS

The aluminum synchronizing shaft utilized in the HLH/ATC drive system represents a critical link in the rotor synchronization path. Testing of this shaft is required to verify structural design and fabrication technique. A further reason for testing is that this shaft represents a significant increase in tube diameter to wall thickness ratio compared to past experience.

Test Objective

The objectives of this test were to establish the torsional fatigue strength, the ultimate strength, the mode of failure, and a failure progression rate for the aluminum synchronizing shafts, including their end connections. The shafts' ultimate torsional requirement is 188,000 in-lb and the operating torsional requirement is 83,000 \pm 10,100 in-lb.

Specimen Design

The test specimens were fabricated in accordance with Figure D-52, and consist of the 2024-T3 aluminum tube having an outside diameter of 7.25 inches and a wall thickness of .125 inch with a 7075-T73 adapter riveted to one end and an adapter assembly fabricated from 4340 steel riveted to the other end. A Thomas Coupling was included at each end of the specimen assembly. The ultimate load specimen (-2) was full length (approximately 69 inches) while the fatigue specimens (-3) were reduced to 33 inches overall to accommodate the test machine amplitude limitations.

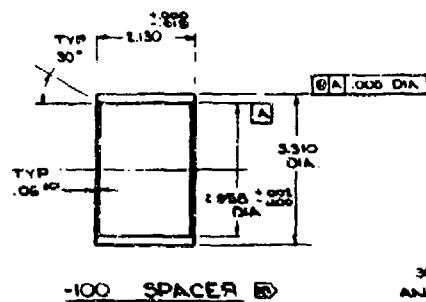
Fixture Design

Torsional fatigue testing was conducted utilizing a Baldwin-Lima-Hamilton Model IV-20 fatigue machine operating at 20 Hz. A Sonntag Scientific Model SF-10 torsion fixture was used to convert the force produced by the IV-20 into a torque and to apply this torque to one end of the specimen. The torque was reacted at the opposite end of the specimen by a weldment bolted to the bed of the IV-20.

The ultimate test was conducted using a rotary hydraulic actuator for load application and the fatigue weldment for the reaction.

Test Instrumentation

Each of the four test specimens was strain gaged with a single four arm torque bridge in the central section of the shaft. The three fatigue specimens also had crack wires installed on the shaft adjacent to both end fittings to



DIA

ANA-11A BOLT
— AN960-41G WASHER

RIVET DR
 MIN. OF
 OPPOSE

301-11010-1 (REF.)
AND 80-41GL WARMER.

SECTION C7
TYP (4) PLACES

801-11000-B (-2 ASS'Y.) } REF
801-11000-C (-3 ASS'Y.) }

MARK BOEN
CODE IDENT
NO. SERIAL

301-14C

MA5K 75

→ BG

VIEW A3

Figure D-52. Rotary Wing Drive Shaft Assembly (Sheet 1 of 2).

2 1

A BOLT
NO. 415 WASHER

OS 2.10
OS 2.05

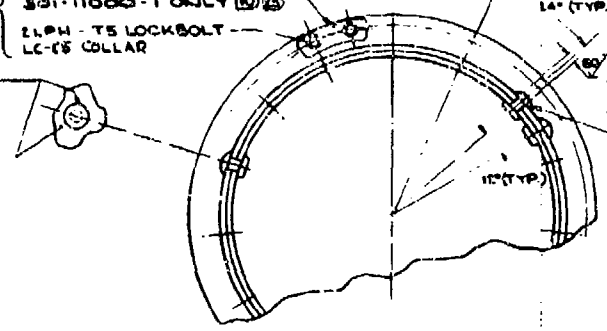
MS21045-4 WLT 5
301-11015-1 (REF.)

ON C7
PLACES

TYP. BOTH ENDS

VS40702-1 & -2 WEIGHTS
AS REQ'D. FOR BALANCING
301-11000-1 ONLY 55
2LPH - TS LOCKBOLT
LC-15 COLLAR

RIVET HEADS MUST BE SEATED AT A
MIN. OF TWO DIAMETRICALLY
OPPOSITE POINTS



1.25 DIA - 10 HOLE (1 ROWS OF
EQUALLY SPACED - ROWS STAGGERED
FOR 301-11000-1, -2 & -3)

MS 20410008-0 (30 RIVETS)
WPD. HEAD OUTSIDE
(FOR 301-11000-1, -2 & -3)

SECTION 33

(REF)
VS40702-1 & -2 WEIGHTS

MARK BOEING VERTOL
CODE IDENT NO., PART
NO., SERIAL NO. 55

301-11015-1

301-11007-1

.120 (REF)

STENCIL IN GLOSS BLACK LETTERS
{ 1/8" HIGH ON OUTSIDE OF TUBE

BALANCED ASSY. S/N
DO NOT CHANGE ADAPTER
INDEXING OR INTERCHANGE
ADAPTERS

1.25 DIA
(REF.)

MARK NO. 1
HERE 55
OS 2.10 x .45"
TYP. BOTH ENDS

MASK 55

BG_M

301-11000-5 TUBE (-1 & -2 ASSY.)
301-11000-6 TUBE (-3 ASSY.)

9.43

.81

A TUBE LENGTH

2.09 (A)

C REF.

FINISH 55

SECTION 36

SEE VIEW 21
STUD. 55

(A5)

SHAFT ASSY.	THICK	A	BS. 03	C (INCH)
-1	.5	54.78	62.75	67.81
-2	.5	54.78	61.73	67.81
-3	.6	55.55	58.55	58.65

(Sheet 1 of 2).

301-11000 A/2

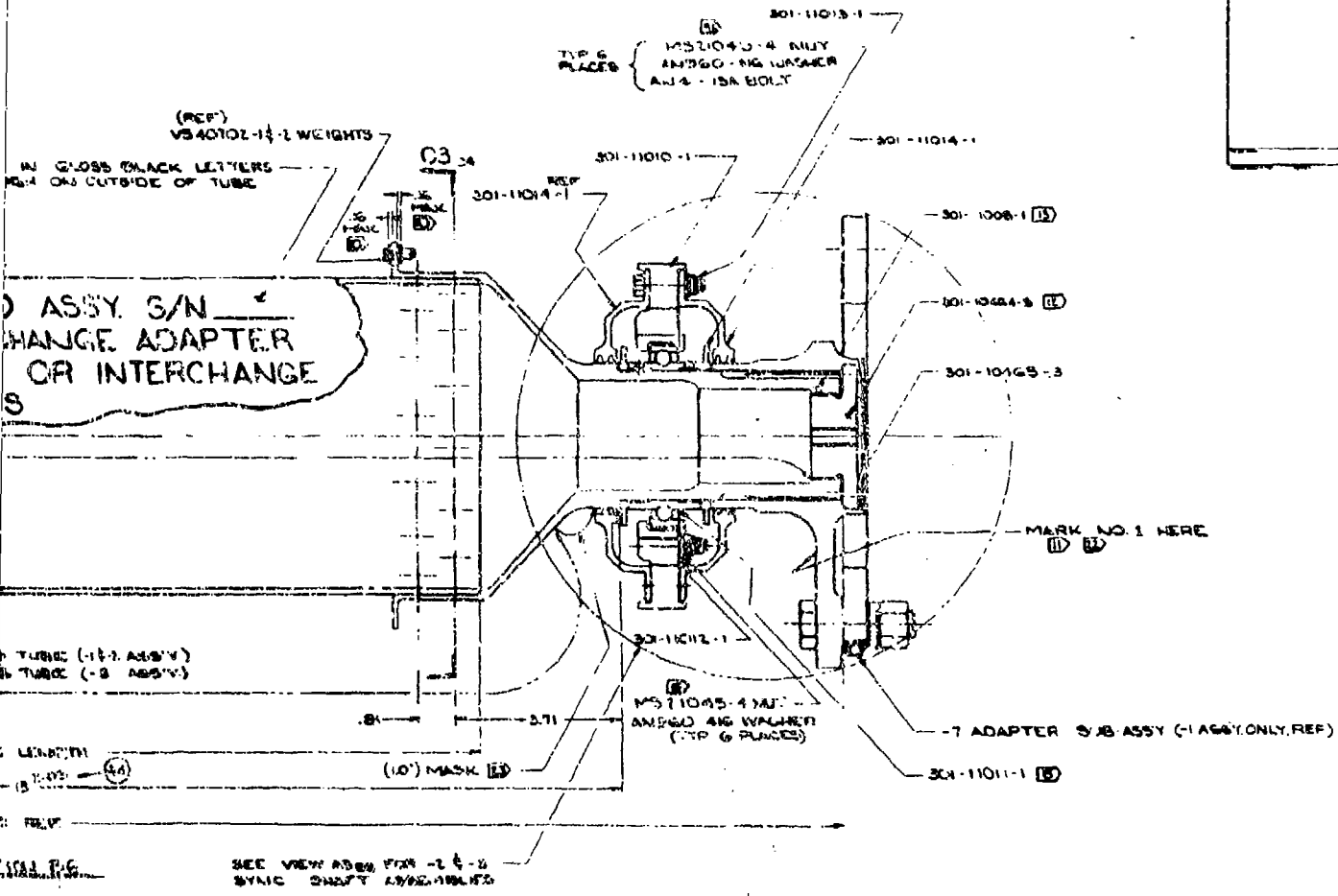
3

A REVISE

1. 25 1/2" DIA. 30 HULLS (1 ROWS OF 15 EACH) (1) } TYP. BOTH ENDS
EQUALLY SPACED - RINGS STAGGERED AS SHOWN
(FOR 301-11000-1, 2 & 3)

2. 10 1/2" DIA. 10 (30 RIVETS) WITH } TYP. BOTH ENDS
MFG. WELD OUTSIDE
(FOR 301-11000-1, 2 & 3)

ITEM	QUANTITY	DESCRIPTION
1	1	301-11013-1
2	1	301-11014-1
3	1	301-11010-1
4	1	301-11011-1
5	1	301-11012-1
6	1	301-11015-1
7	1	301-11016-1
8	1	301-11017-1
9	1	301-11018-1
10	1	301-11019-1
11	1	301-11020-1
12	1	301-11021-1
13	1	301-11022-1
14	1	301-11023-1
15	1	301-11024-1
16	1	301-11025-1
17	1	301-11026-1
18	1	301-11027-1
19	1	301-11028-1
20	1	301-11029-1
21	1	301-11030-1
22	1	301-11031-1
23	1	301-11032-1
24	1	301-11033-1
25	1	301-11034-1
26	1	301-11035-1
27	1	301-11036-1
28	1	301-11037-1
29	1	301-11038-1
30	1	301-11039-1
31	1	301-11040-1
32	1	301-11041-1
33	1	301-11042-1
34	1	301-11043-1
35	1	301-11044-1
36	1	301-11045-1
37	1	301-11046-1
38	1	301-11047-1
39	1	301-11048-1
40	1	301-11049-1
41	1	301-11050-1
42	1	301-11051-1
43	1	301-11052-1
44	1	301-11053-1
45	1	301-11054-1
46	1	301-11055-1
47	1	301-11056-1
48	1	301-11057-1
49	1	301-11058-1
50	1	301-11059-1
51	1	301-11060-1
52	1	301-11061-1
53	1	301-11062-1
54	1	301-11063-1
55	1	301-11064-1
56	1	301-11065-1
57	1	301-11066-1
58	1	301-11067-1
59	1	301-11068-1
60	1	301-11069-1
61	1	301-11070-1
62	1	301-11071-1
63	1	301-11072-1
64	1	301-11073-1
65	1	301-11074-1
66	1	301-11075-1
67	1	301-11076-1
68	1	301-11077-1
69	1	301-11078-1
70	1	301-11079-1
71	1	301-11080-1
72	1	301-11081-1
73	1	301-11082-1
74	1	301-11083-1
75	1	301-11084-1
76	1	301-11085-1
77	1	301-11086-1
78	1	301-11087-1
79	1	301-11088-1
80	1	301-11089-1
81	1	301-11090-1
82	1	301-11091-1
83	1	301-11092-1
84	1	301-11093-1
85	1	301-11094-1
86	1	301-11095-1
87	1	301-11096-1
88	1	301-11097-1
89	1	301-11098-1
90	1	301-11099-1
91	1	301-11100-1
92	1	301-11101-1
93	1	301-11102-1
94	1	301-11103-1
95	1	301-11104-1
96	1	301-11105-1
97	1	301-11106-1
98	1	301-11107-1
99	1	301-11108-1
100	1	301-11109-1



1	2	3	4	5	6	7	8	9	10	11	12	13	14	15	16	17	18	19	20	21	22	23	24	25	26	27	28	29	30	31	32	33	34	35	36	37	38	39	40	41	42	43	44	45	46	47	48	49	50	51	52	53	54	55	56	57	58	59	60	61	62	63	64	65	66	67	68	69	70	71	72	73	74	75	76	77	78	79	80	81	82	83	84	85	86	87	88	89	90	91	92	93	94	95	96	97	98	99	100
---	---	---	---	---	---	---	---	---	----	----	----	----	----	----	----	----	----	----	----	----	----	----	----	----	----	----	----	----	----	----	----	----	----	----	----	----	----	----	----	----	----	----	----	----	----	----	----	----	----	----	----	----	----	----	----	----	----	----	----	----	----	----	----	----	----	----	----	----	----	----	----	----	----	----	----	----	----	----	----	----	----	----	----	----	----	----	----	----	----	----	----	----	----	----	----	----	----	----	-----

- 1 SYNC SHAFT ASSY.
- 2 SYNC SHAFT ASSY. SAME TO 1 EXCEPT AS SHOWN
- 3 SYNC SHAFT ASSY. SAME TO 1 EXCEPT AS SHOWN

31301-11000

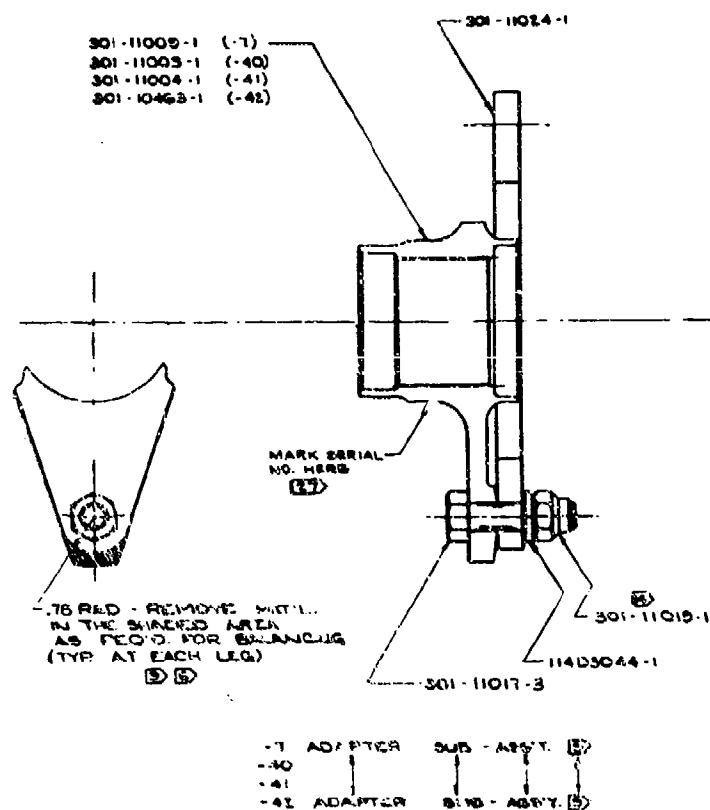


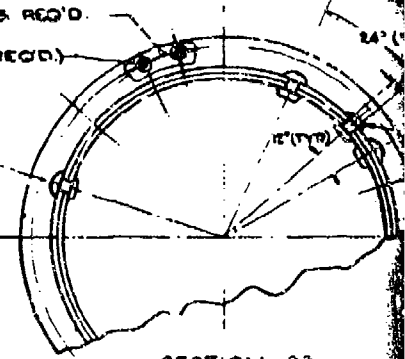
Figure D-52. Rotary Wing Drive Shaft Assembly (Sheet 2 of 2).

2

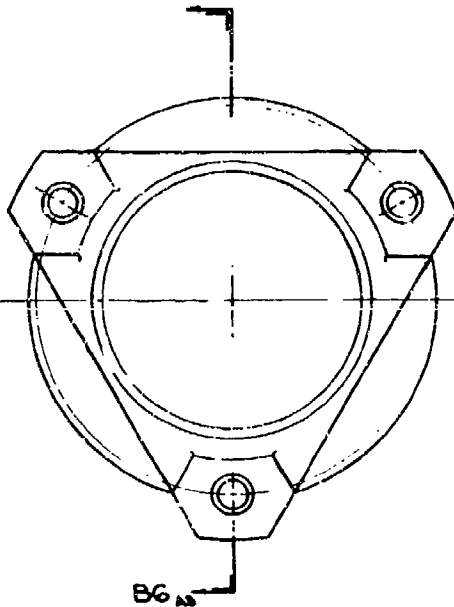
TYP. BOTH ENDS

{ V240702-16-2 WEIGHTS AS REQ'D.
FOR BALANCING (2) (2)
2 LPH-TS LOCKBOLT (AS REQ'D.)
LC-C5 COLLAR (AS REQ'D.)

RIVET HEADS MUST BE SEATED
AT A MIN. OF TWO
DIAMETRICALLY OPPOSITE
POINTS

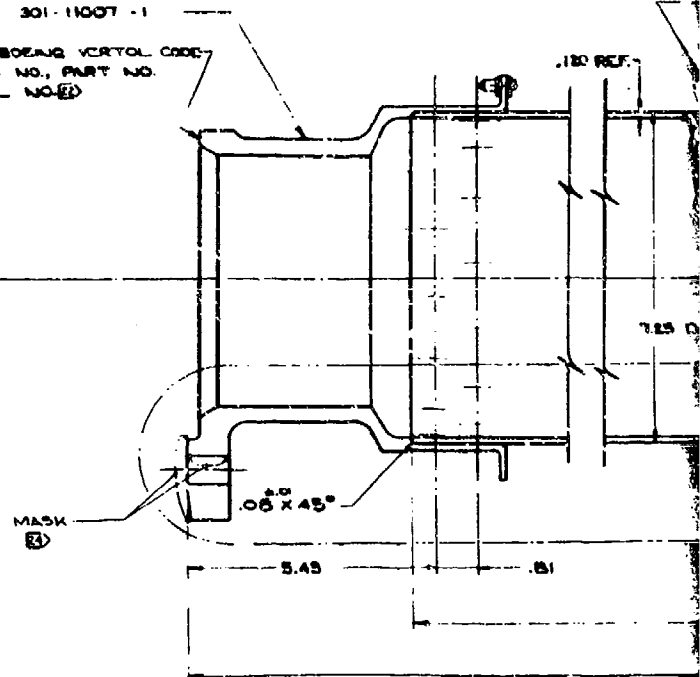


SECTION C3



301-11007 -1

MARK: BOEING VERTOL CODE
IDENT. NO., PART NO.
SERIAL NO (2)



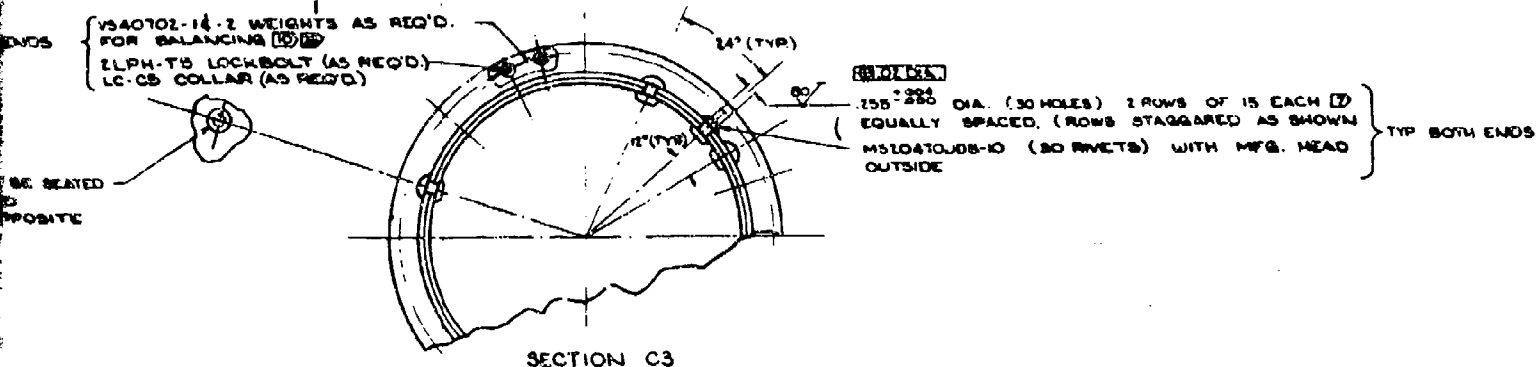
301-11015-1
44-1

(20)

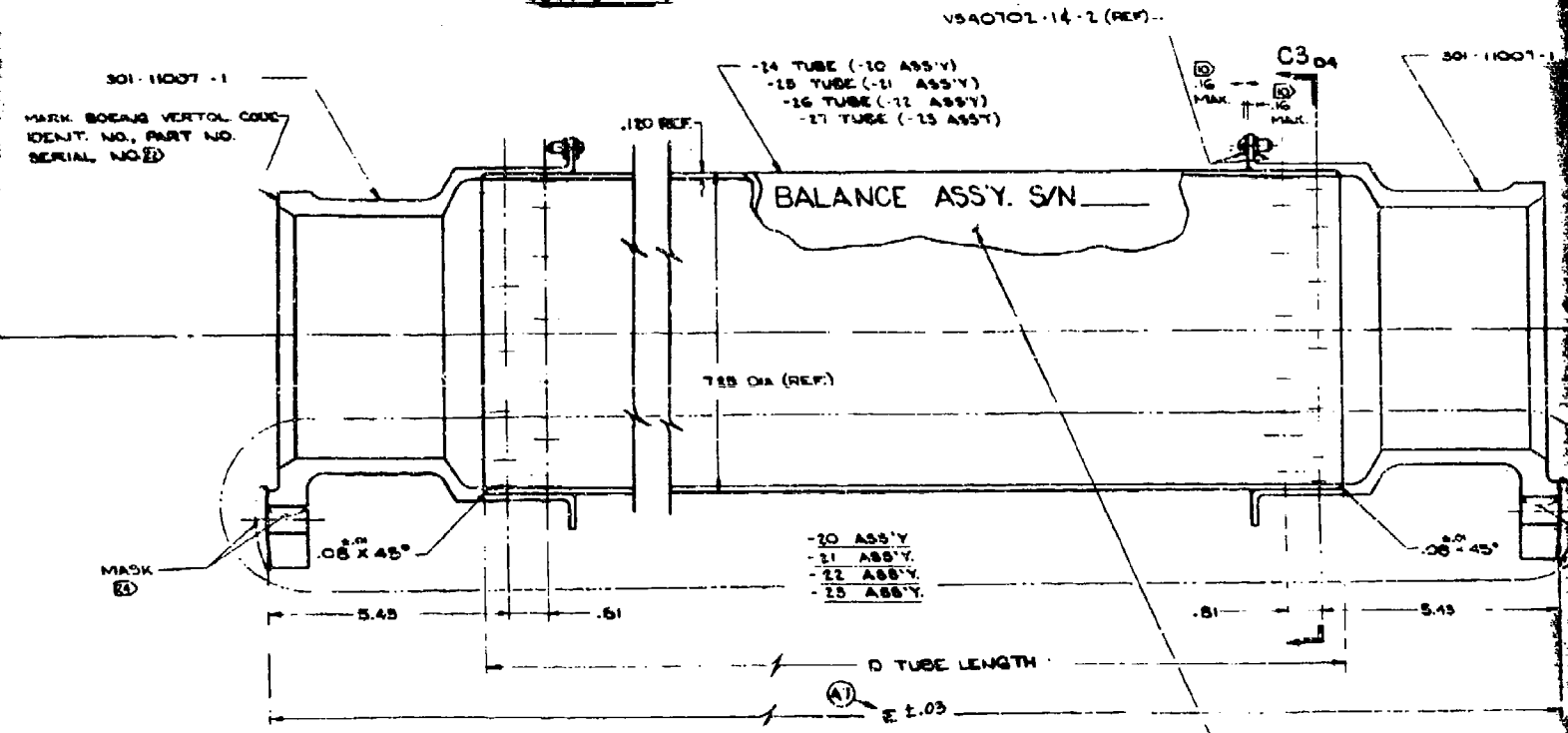
ly (Sheet 2 of 2).

301-11000 A13

3



SECTION C3



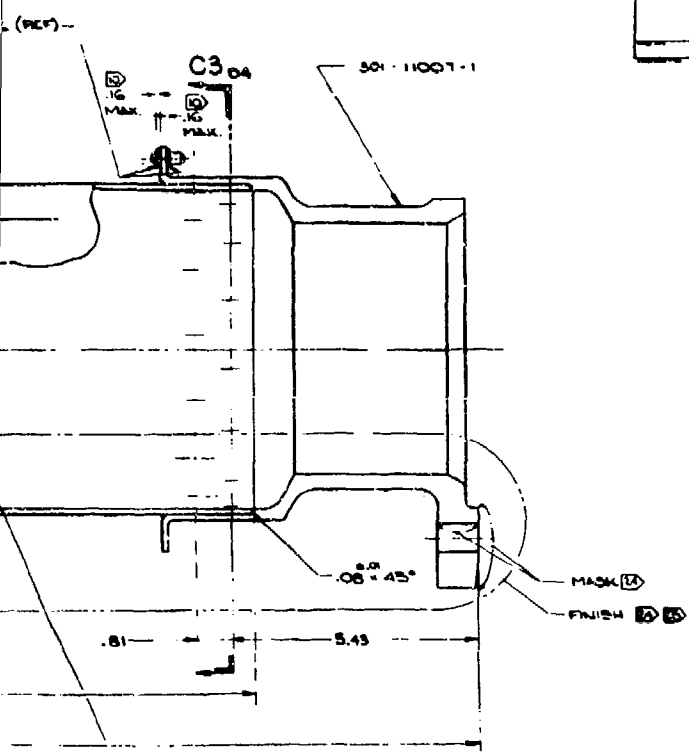
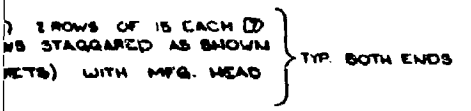
SECTION C6

(A0)

ITEM	QTY	D	A.OL	E ±.03
-20	-24	41.5	51.21	
-21	-25	33.58	48.24	
-22	-26	23.58	38.24	
-23	-27	16.53	25.99	

301-11000 A3

1	2	3	4	5	6	7	8	9	10	11	12	13	14	15	16	17	18	19	20	21	22	23	24	25	26	27	28	29	30	31	32	33	34	35	36	37	38	39	40	41	42	43	44	45	46	47	48	49	50	51	52	53	54	55	56	57	58	59	60	61	62	63	64	65	66	67	68	69	70	71	72	73	74	75	76	77	78	79	80	81	82	83	84	85	86	87	88	89	90	91	92	93	94	95	96	97	98	99	100	101	102	103	104	105	106	107	108	109	110	111	112	113	114	115	116	117	118	119	120	121	122	123	124	125	126	127	128	129	130	131	132	133	134	135	136	137	138	139	140	141	142	143	144	145	146	147	148	149	150	151	152	153	154	155	156	157	158	159	160	161	162	163	164	165	166	167	168	169	170	171	172	173	174	175	176	177	178	179	180	181	182	183	184	185	186	187	188	189	190	191	192	193	194	195	196	197	198	199	200	201	202	203	204	205	206	207	208	209	210	211	212	213	214	215	216	217	218	219	220	221	222	223	224	225	226	227	228	229	230	231	232	233	234	235	236	237	238	239	240	241	242	243	244	245	246	247	248	249	250	251	252	253	254	255	256	257	258	259	260	261	262	263	264	265	266	267	268	269	270	271	272	273	274	275	276	277	278	279	280	281	282	283	284	285	286	287	288	289	290	291	292	293	294	295	296	297	298	299	300	301	302	303	304	305	306	307	308	309	310	311	312	313	314	315	316	317	318	319	320	321	322	323	324	325	326	327	328	329	330	331	332	333	334	335	336	337	338	339	340	341	342	343	344	345	346	347	348	349	350	351	352	353	354	355	356	357	358	359	360	361	362	363	364	365	366	367	368	369	370	371	372	373	374	375	376	377	378	379	380	381	382	383	384	385	386	387	388	389	390	391	392	393	394	395	396	397	398	399	400	401	402	403	404	405	406	407	408	409	410	411	412	413	414	415	416	417	418	419	420	421	422	423	424	425	426	427	428	429	430	431	432	433	434	435	436	437	438	439	440	441	442	443	444	445	446	447	448	449	450	451	452	453	454	455	456	457	458	459	460	461	462	463	464	465	466
---	---	---	---	---	---	---	---	---	----	----	----	----	----	----	----	----	----	----	----	----	----	----	----	----	----	----	----	----	----	----	----	----	----	----	----	----	----	----	----	----	----	----	----	----	----	----	----	----	----	----	----	----	----	----	----	----	----	----	----	----	----	----	----	----	----	----	----	----	----	----	----	----	----	----	----	----	----	----	----	----	----	----	----	----	----	----	----	----	----	----	----	----	----	----	----	----	----	----	-----	-----	-----	-----	-----	-----	-----	-----	-----	-----	-----	-----	-----	-----	-----	-----	-----	-----	-----	-----	-----	-----	-----	-----	-----	-----	-----	-----	-----	-----	-----	-----	-----	-----	-----	-----	-----	-----	-----	-----	-----	-----	-----	-----	-----	-----	-----	-----	-----	-----	-----	-----	-----	-----	-----	-----	-----	-----	-----	-----	-----	-----	-----	-----	-----	-----	-----	-----	-----	-----	-----	-----	-----	-----	-----	-----	-----	-----	-----	-----	-----	-----	-----	-----	-----	-----	-----	-----	-----	-----	-----	-----	-----	-----	-----	-----	-----	-----	-----	-----	-----	-----	-----	-----	-----	-----	-----	-----	-----	-----	-----	-----	-----	-----	-----	-----	-----	-----	-----	-----	-----	-----	-----	-----	-----	-----	-----	-----	-----	-----	-----	-----	-----	-----	-----	-----	-----	-----	-----	-----	-----	-----	-----	-----	-----	-----	-----	-----	-----	-----	-----	-----	-----	-----	-----	-----	-----	-----	-----	-----	-----	-----	-----	-----	-----	-----	-----	-----	-----	-----	-----	-----	-----	-----	-----	-----	-----	-----	-----	-----	-----	-----	-----	-----	-----	-----	-----	-----	-----	-----	-----	-----	-----	-----	-----	-----	-----	-----	-----	-----	-----	-----	-----	-----	-----	-----	-----	-----	-----	-----	-----	-----	-----	-----	-----	-----	-----	-----	-----	-----	-----	-----	-----	-----	-----	-----	-----	-----	-----	-----	-----	-----	-----	-----	-----	-----	-----	-----	-----	-----	-----	-----	-----	-----	-----	-----	-----	-----	-----	-----	-----	-----	-----	-----	-----	-----	-----	-----	-----	-----	-----	-----	-----	-----	-----	-----	-----	-----	-----	-----	-----	-----	-----	-----	-----	-----	-----	-----	-----	-----	-----	-----	-----	-----	-----	-----	-----	-----	-----	-----	-----	-----	-----	-----	-----	-----	-----	-----	-----	-----	-----	-----	-----	-----	-----	-----	-----	-----	-----	-----	-----	-----	-----	-----	-----	-----	-----	-----	-----	-----	-----	-----	-----	-----	-----	-----	-----	-----	-----	-----	-----	-----	-----	-----	-----	-----	-----	-----	-----	-----	-----	-----	-----	-----	-----	-----	-----	-----	-----	-----	-----	-----	-----	-----	-----	-----	-----	-----	-----	-----	-----	-----	-----	-----	-----	-----	-----

[illegible]

STENCIL IN GLOSS BLACK LETTERS 1
IN. HIGH ON OUTSIDE OF TUBE

3301-1000	301-1000	3A
-----------	----------	----

establish a baseline for crack propagation studies.

Dynamic forces were measured from standard strain gage amplifiers and an oscilloscope. Static force was applied by a rotary actuator and monitored by a pressure transducer.

The force measuring systems were accurate to within 2% full scale. Test measuring and recording instrumentation were in current calibration in accordance with MIL-C-45662A and traceable to the National Bureau of Standards.

Test Results

Fatigue Results

Specimen No. A106 was tested with an initial load of 83,800 in-lb. + 10,100 in-lb. This load was maintained until runout occurred at 2.0 million cycles.

The fatigue test was resumed with the 301-11017-1 bolts in the specimen adapter torqued to 800-1000 in-lb. (dry). This run was made with a load of 83,800 in-lb. + 12,600 in-lb. and runout occurred at 2.635 million cycles.

The load was increased to 83,800 in-lb. + 15,300 in-lb. and this was maintained until runout at 2.02 million occurred.

The load was increased again to 83,800 in-lb. + 21,000 in-lb. and at 4.07 million cycles the 301-11000-6 tube cracked.

This crack emanated from under the 301-11008-1 adapter and had progressed to .25 inch beyond the edge of the adapter where the crack detection wire was broken stopping the test.

With the crack closely monitored, the test was restarted, maintaining the same load. Complete failure of the tube occurred at 4.374 million cycles. During this time a crack-growth was recorded and is shown in Table D-19.

Specimen No. A108 was used for the next series of runs.

This specimen ran at a load of 83,800 in-lb. + 21,000 in-lb. for 10.363 million cycles. At this time a crack tripped the crack circuit and the test was stopped.

The visible portion of the crack was approximately 3.3 inches long, starting from under the 301-11008-1 adapter. No crack was visible at the previous inspection period at 10.193 million cycles.

TABLE D-19. HLH/ATC SYNCHRONIZING SHAFT - FAILURE
PROGRESSION RATE.
P/N 301-11000-3

S/N A-106

LOAD - IN-LB.	CYCLES X 10 ⁶	
83,800 \pm 10,100	2.009	RUNOUT
83,800 \pm 12,600	2.635	RUNOUT
83,800 \pm 15,300	2.020	RUNOUT
83,800 \pm 21,000 ↓	4.070	CRACK IN TUBE .25 INCH LONG FROM EDGE OF 11008-1 ADAPTER VISIBLE CRACK LENGTH .30"
	4.080	.33
	4.090	.33
	4.100	.36
	4.110	.40
	4.120	.42
	4.130	.42
	4.140	.45
	4.150	.45
	4.160	.47
	4.180	.55
	4.190	.58
	4.200	.62
	4.210	.62
	4.230	.75
	4.250	.83
	4.270	.92
	4.296	1.05
	4.310	1.22
	4.320	1.28
	4.331	1.50
	4.340	1.58
	4.350	1.85
	4.360	2.10
	4.370	2.83
	4.374	COMPLETE FAILURE
SN A-107		
83,800 \pm 23,000	5.396	CRACK LENGTH .50 INCH
\pm 10,100	.967	.65 INCH
	3.637	2.40 INCH

The test was resumed at a reduced load of 83,800 in-lb. + 10,100 in-lb. until the tube ruptured at .021 million cycles.

Specimen No. A107 was subjected to a fatigue loading of 83,800 in-lb. + 23,000 in-lb. After 5.396 million cycles a crack developed in the 301-11006-6 tube, emanating from under the 301-11008-1 adapter. The length of the crack at the time of discovery was .5 inch.

The load was reduced to 83,800 in-lb. + 10,100 in-lb. and after .967 million cycles the crack had progressed to .65 inch long.

At 3.637 million cycles the 301-11007-1 adapter failed, terminating the test. The crack in the tube had grown to 2.4 inches long.

Reviewing the results of the three fatigue tests it is concluded that in each case the typical mode of failure is tube cracking starting at rivet holes where the 301-11008-1 adapter is secured. In each specimen the crack occurred at the same end of the tube.

By plotting the three points of failure and by applying a standard curve shape for riveted aluminum structures, the value of the mean fatigue strength was determined to be 83,800 in-lb. + 19,190 in-lb at 50 million cycles.

By applying the mean minus three standard deviations an endurance limit of 14,000 in -lb is indicated. (Figure D-53.)

Ultimate Results

A full size specimen was used for this test, serial no. A105. A torsional load was applied in increments until the MS20470DD8-10 rivets failed at the joint between the 301-11000-5 tube and the 301-11008-1 adapter.

The failing load was 212,700 in-lb.

After teardown for inspection it was found that the 301-11017-1 and the -3 bolts had yielded. This would account for the observed offset in the plot of load vs. deflection.

Based on the results of this test the ultimate strength of the 301-11000-2 sync shaft is 212,700 in-lb. The mode of failure is attributed to overloading of the MS20470DD8-10 rivets.

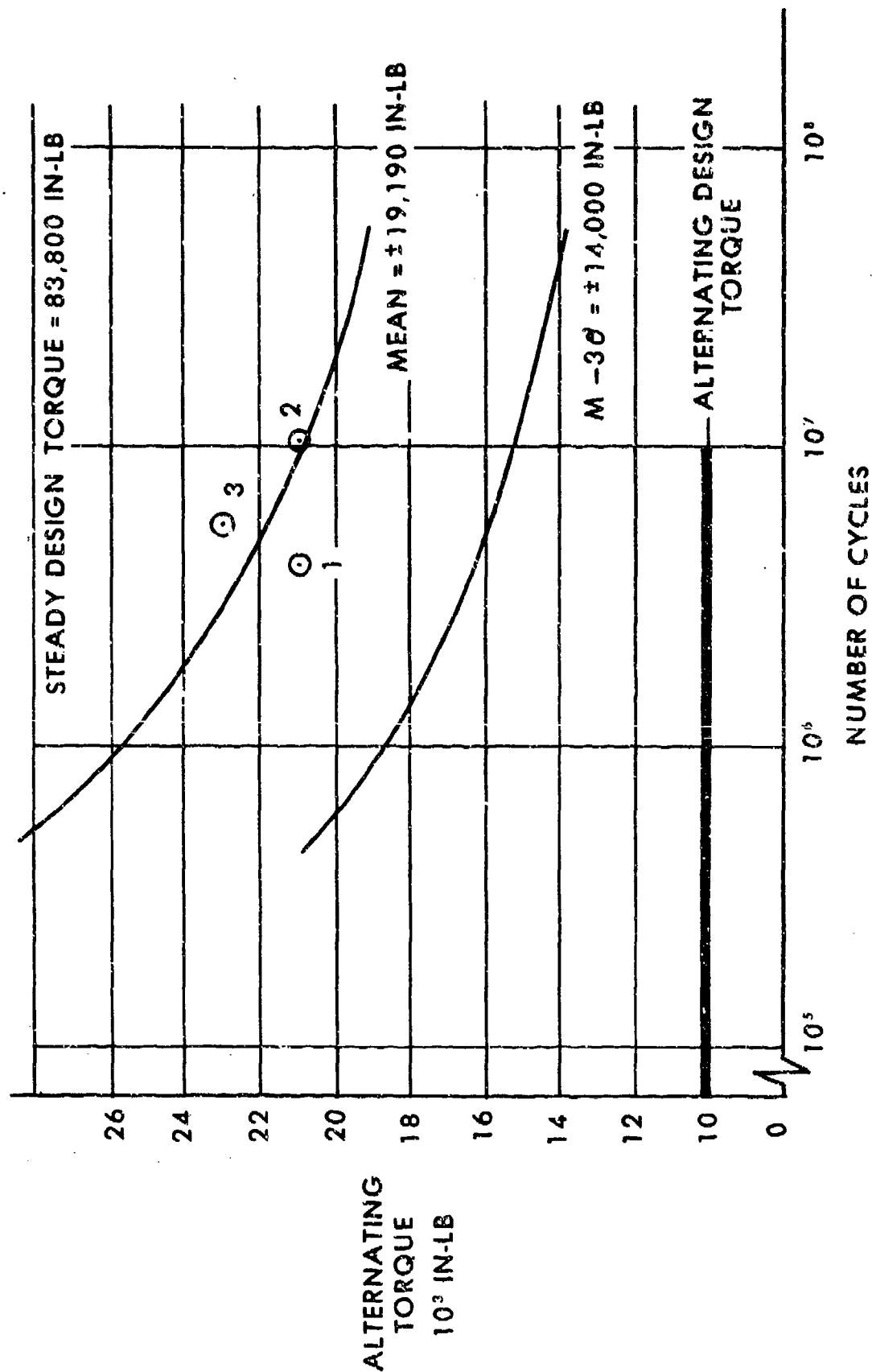


Figure D-53. HLH Synch Shaft Fatigue Test.

Conclusions

The results of these tests verify the structural design of the synchronizing shaft. The endurance limit (taken as the mean minus three times the standard deviation) is 83,000 inch-pounds \pm 14,000 inch-pounds. This represents a 38% margin of safety over the design torque of 83,800 \pm 10,100 inch-pounds. The predominant mode of failure is tube cracking with some adapter cracks also occurring, both at the rivet holes. Burrs at the rivet holes and fretting at the tube/adapter interface were contributing factors to the fatigue failures.

The torsional design ultimate strength of 189,000 inch-pounds has been exceeded by 13.1%. Ultimate failure occurred at 212,700 inch-pounds due to shearing of the rivets.

A complete report on the test program is presented in Loening Vertol Report T301-10265-1.

LIST OF SYMBOLS

Ft (ft)	feet
g	acceleration of gravity
°F	degrees fahrenheit
ft/min	feet per minute
HP (hp)	horsepower
C.G.	center of gravity
Lb (lb)	pound(s)
rpm	revolutions per minute
T	torque
psi	pounds per square inch
psig	pounds per square inch gage
psia	pounds per square inch absolute
lb/min	pounds per minute
sq in	square inch
%	percent
R	radius
Rad	radius
TYP	typical
Dia	diameter
gal	gallon
cu in	cubic inch
min	minute
rev	revolution
GPM	gallons per minute

BTU	British thermal unit
W	weight
mV	millivolts
mA	milliampere
uA	microampere
Hz	Hertz, cycles per second
<u>S</u>	centerline
<u>M</u>	maintainability
<u>R</u>	reliability
t	thickness
Rc	Rockwell hardness c scale
u	coefficient of friction
AC	alternating current
DC	direct current
TPI	threads per inch